THE SIMULATION OF A TRANSIENT LEACHING CIRCUIT

JOHAN ANDRIES MÜLLER RADEMAN

Dissertation presented for the Degree of

Doctor of Philosophy

in Engineering

at the University of Stellenbosch.

Promoters: Prof. L. Lorenzen

Prof. J.S.J. van Deventer

September 1995

Aan my Ouers,

vir alles wat hulle vir my beteken

Volume I

Declaration

I the undersigned hereby declare that the work contained in this dissertation is my own original work and has not previously in its entirety or in part been submitted at any university for a degree.

J. A. M. Rademan

September 1995

Synopsis

The hydrometallurgical leaching of sulphide concentrates was introduced in the 1950's. Generally the leaching mechanisms of these processes are not understood fundamentally. The reasons for this are the inherently complex nature of sulphide chemistry and that the sulphide concentrates usually consist of highly intergrown sulphide minerals. The leaching kinetics of sulphide concentrates where only one metal-sulphide mineral occurs have been investigated intensively, but not for sulphide concentrates with more than one metal-sulphide mineral. The behaviour of these mixed metal-sulphide minerals has mostly been investigated on plant scale to qualitatively determine the leaching trends of the process. The consequence of the relatively unknown leaching mechanism and kinetics is that these processes are not controlled efficiently.

This study was conducted on the acid-oxygen pressure leaching of Ni-Cu matte (the first stage leach process at the Ni-Cu refinery of Impala Platinum Ltd.). As a first step to improve the control efficiency of the process, the process must be stabilised. Therefore, an off line computer simulation program is proposed to control the repulping section of the plant that has previously been controlled solely by an operator. Controlling the repulping section is very important, because conditions exist in the repulping tanks for leaching to occur. This causes perturbations in the pulp entering the pressure leach autoclave. Due to the fast reaction kinetics of the matte in the pressure leach autoclave the perturbations entering the autoclave will influence the performance of the acid-oxygen pressure leach process. The simulation program was tested on the plant and indicated that considerable improvement in the stability of the operation could be achieved.

In obtaining a better understanding of the behaviour of this process, it is essential that key variables and trends are identified. A methodology is proposed to analyse and model this ill-defined and poorly understood process from historical data by

artificial neural networks (ANN), inductive learning by decision trees and statistical techniques. The back propagation neural network, learning vector quantization neural network and the decision trees yielded comparable classification rates between 73% and 84%, and could serve as a basis for the adjustment of operating conditions to improve the efficiency of the process. The relative importance of the process variables is determined by a method of sensitivity analysis and together with the statistical mean, the effect of an increase or decrease in the variable on the process is quantified. These results are substantiated by experimental findings.

A leaching mechanism for the acid-oxygen pressure leach of Ni-Cu matte is postulated. The leaching sequence of the nickel and copper sulphides is Ni_3S_2-Ni_7S_6-NiS-Ni_3S_4, and Cu_2S-$Cu_{31}S_{16}$-$Cu_{1.8}S$-CuS, respectively. Ni_7S_6 and $Cu_{31}S_{16}$ are intermediate nickel and copper sulphide phases that form during the leaching process. Ni alloy has a galvanic effect on the sulphide minerals which inhibits the overall leaching rate and results in the formation of H_2S and the intermediate nickel and copper sulphides (Ni_7S_6 and $Cu_{31}S_{16}$). A semi-empirical kinetic model was developed based on the chemical reaction rate expressions of the leaching mechanism. This model can accurately simulate the batch leaching process for variations in the oxygen partial pressure, oxygen flowrate, temperature, particle size, initial acid concentration and pulp density. A sensitivity analysis on the model indicated that for a matte with a lower initial Ni alloy content the leaching rate of nickel is much faster.

Opsomming

Die hidrometallurgiese loging van sulfied konsentrate is bekend sedert die 1950's. In die algemeen word die logings meganismes van die prosesse nie fundamenteel goed verstaan nie. Die redes hiervoor is die komplekse aard van sulfied chemie en dat die sulfied konsentrate gewoonlik uit hoogs vergroeide sulfied minerale bestaan. Die logingskinetika van sulfied konsentrate waar net een metaal-sulfied mineraal in voorkom is al intensief ondersoek, maar nie vir sulfied konsentrate met meer as een metaal-sulfied mineraal nie. Die gedrag van die gemengde metaal-sulfied minerale was meestal ondersoek op aanleg skaal om kwalitatief die logings tendense van die proses vas te stel. Die gevolg van die relatiewe onbekende logingsmeganisme en kinetika is dat die prosesse nie so effektief beheer word nie.

Hierdie studie was uitgevoer op die suur-suurstof druk-loging van Ni-Cu swawelmetaal (die eerste stadium logingsproses van die Ni-Cu rafinadery van Impala Platinum Bpk.). As 'n eerste stap om die prosesbeheer te verbeter moet die proses gestabiliseer word. Daarom is 'n "off-line" rekenaar program voorgestel om die herpulpingseksie van die aanleg te beheer wat voorheen alleenlik deur een operateur beheer is. Die beheer van die herpulpingseksie is baie belangrik omdat toestande in die herpulping tenks bestaan vir loging om plaas te vind, wat dan veranderings in die pulp wat die druk-logingsreaktor binnekom, veroorsaak. Die vinnige reaksies van die swawelmetaal in die druk-logingsreaktor sal dan tot gevolg hê dat die veranderende pulp wat die reaktor betree, die effektiwiteit van die suur-suurstof druk-logingsproses beïnvloed. Die simulasie program is op die aanleg getoets en het aangedui dat 'n beduidende verbetering in die stabiliteit van die proses bereikbaar is.

Om die proses werking beter te verstaan is dit noodsaaklik dat die belangrikste veranderlikes en proses tendense geïdentifiseer moet word. 'n Metodologie word voorgestel om die swak gedefinieerde en swak verstaande proses te analiseer en te

modelleer vanaf historiese proses data met kunsmatige neural netwerke, die induktiewe leer proses met besluitnemings bome en statistiese metodes. Die "back propagation" neurale netwerk, "learning vector quantization" neurale netwerk en die besluitnemings bome het vergelykbare klassifikasie resultate gelewer, tussen 73% en 84% wat as 'n basis gebruik kan word om die bedryfskondisies aan te pas en die effektiwiteit van die proses te verbeter. Die relatiewe belangrikheid van die proses veranderlikes is bepaal deur 'n metode van sensitiwiteits analises en saam met die statistiese gemiddeld is die effek wat 'n verhoging of verlaging in die veranderlike veroorsaak in die proses, gekwantifiseer. Hierdie resultate word gesubstansieer deur die eksperimentele bevindinge.

'n Logingsmeganisme vir die suur-suurstof druk-loogproses vir Ni-Cu swawelmetaal word gepostuleer. Die logings volgorde van die nikkel en koper sulfiedes is Ni_3S_2-Ni_7S_6-NiS-Ni_3S_4, *en* Cu_2S-$Cu_{31}S_{16}$-$Cu_{1.8}S$-CuS, *onderskeidelik.* Ni_7S_6 *en* $Cu_{31}S_{16}$ *is intermediêre nikkel en koper fases wat vorm gedurende die logingsproses. Ni allooi het 'n galvaniese effek op die sulfied minerale wat die algemene logingstempo inhibeer en veroorsaak dat* H_2S *en die intermediêre nikkel en koper sulfiedes gevorm word (*Ni_7S_6 *en* $Cu_{31}S_{16}$*). 'n Semi-empiriese kinetiese model is ontwikkel, gebaseer op die chemiese reaksie tempo vergelykings van die logingsmeganisme. Die model kan die variasies in die suurstof parsiële druk, suurstof vloeitempo, temperatuur, partikel grootte, begin suur konsentrasie en pulp digtheid akkuraat simuleer vir die enkellading logingsproses. Sensitiwiteits analises met die model het aangedui dat vir 'n swawelmetaal met 'n laer begin Ni allooi inhoud, die logingstempo van nikkel baie vinniger is.*

Acknowledgements

The work described in this dissertation was carried out in the Department of Chemical Engineering at the University of Stellenbosch as well as at the Nickel-Copper Refinery of Impala Platinum Ltd. in Springs, South Africa.

I wish to express my sincere appreciation to:

- Prof Leon Lorenzen and Prof Jannie van Deventer for their encouragement and support throughout this investigation.

- Mr Derick Moolman and Dr Chris Aldrich for their helpful discussions on artificial intelligence techniques, as well as the staff at the Department of Chemical Engineering who helped with all the administrative tasks.

- The personnel at the Nickel-Copper Refinery of Impala for their patience and assistance with my experimental work.

- Gratitude is expressed to Mr Peter Gaylard and Impala Platinum Ltd. whose generous financial support made this research possible.

- My family and friends for their encouragement and understanding during the completion of this dissertation.

- Finally to the Almighty God who creates opportunities like this for me and then gives me the ability to complete them.

Contents

VOLUME II

List of Figures

Chapter 5:

Chapter 6:

Chapter 7:

Chapter 8:

Chapter 9:

List of Tables

Chapter 6:

Chapter 7:

Chapter 8:

Chapter 9:

Chapter 1

INTRODUCTION

The extraction of metals by chemical dissolution, i.e. hydrometallurgy, has become one of the most important means of recovering metals from its ores. The principal objective of hydrometallurgical processes is to leach the desired elements selectively into an aqueous phase so as to separate them from the bulk of unwanted material. Hydrometallurgy is a specialised branch of extractive metallurgy dealing with metal recovery from ores, concentrates and other intermediate products. Modern hydrometallurgy can be traced back to the end of the nineteenth century, dating back to 1887 when two important processes were invented, the cyanidation process for treating gold ores and the Bayer process for the production of alumina. Since 1940 it has been advancing progressively and even replacing some pyrometallurgical processes. In the 1950's, pressure hydrometallurgy was introduced for leaching sulphide concentrates, laterites, tungsten ores, as well as for direct precipitation of metals from solution. In general, hydrometallurgy involves two distinct steps: the selective dissolution of the metal values from an ore, i.e. *leaching* and the selective recovery of the metal values from the solution, i.e. *precipitation*.

1.1 MATTE LEACHING

In this dissertation the selective leaching of base metal sulphides, specifically nickel and copper sulphides, is investigated. The term "leaching" involves both the dissolution of metals in solution as well as the precipitation of the metals out of the solution, called cementation. This dissertation was conducted for a specific process, viz. the acid-oxygen pressure leaching of Ni-Cu matte. Matte refers to the intermediate product that was produced in a furnace (converter), after concentrating of the primary ore. The matte consists mainly of nickel, copper, iron, cobalt, sulphur and platinum group metals (PGM). The acid solution used in the leaching process is spent electrolyte that is recycled from the copper electrowinning section, further

down stream in the process. The spent electrolyte solution contains a high concentration of H_2SO_4 and dissolved nickel, copper, iron, cobalt and ammonium.

The Ni-Cu matte leaching process under investigation is the first stage leach process of Impala Platinum Ltd. based on the Sherritt Gordon technology for H_2SO_4-O_2 pressure leach (see Fig. 1.1). This section includes a milling operation, from where the pulp is pumped to a repulping tank where the pulp density is adjusted with spent electrolyte solution. The pulp is then pumped to another tank where the pulp density is again adjusted with spent electrolyte solution. From this tank the pulp is pumped to the pressure autoclave. Modern control equipment in this process section is almost non-existent, because the control of the two repulping tanks is not considered to be important and the knowledge of the chemistry, reaction mechanisms and kinetics of the process, is virtually unknown. Furthermore, this part of the process is controlled by one operator. The factors that contribute to the complexity of the leaching mechanism in the process are, (i) various mineral species that exist in the solid phase during the leaching process, with each mineral species having different leaching characteristics and kinetics, (ii) unknown interaction of the various mineral species with each other and with the acid, nickel, copper and iron in the solution, and (iii) the inherently complex nature of sulphide chemistry.

Only two references in the literature which investigated the Sherritt Gordon first stage acid-oxygen pressure leach process were found. One was by Plasket and Romanchuk (1978) who performed laboratory and pilot plant experiments for the commissioning of this process technology by Impala Platinum Ltd. and the other one was by Dutrizac and Chen (1987) who performed a systematic analysis of the actual plant process. The work by Dutrizac and Chen (1987) was slightly different from the work of Plasket and Romanchuk (1978), and possibly more reliable and up to date. Dutrizac and Chen did not investigate the leaching process systematically under a variety of possible process conditions (as batch experiments), therefore, the finer intrinsic behaviour of the leaching mechanism was not identified. Published papers on the matte leaching at atmospheric pressure, as well as literature on the general base metal sulphide leaching were used selectively to verify different observations on the reaction mechanism. Due to the presence and the formation of various mineral phases, a background on the mineralogical characteristics is necessary. No

literature was found on the leaching kinetics for the acid-oxygen pressure leach process of Ni-Cu matte.

1.1.1 Process control

The major problem experienced in the first stage leaching process of Impala Platinum is that the process cannot be controlled efficiently. This is because the operators are not always able to cope adequately with the vagaries of the complex process (see Chapter 3) and can fail to develop a feel for anticipating and rectifying situations that could have an adverse effect on the performance of the plant. There has been a long-standing awareness that these control practices are far from ideal, and the dramatic increase in personnel turnover on industrial plants has only exacerbated the problem. Intensifying this problem is the fact that this process is the first stage in the refining of the Ni-Cu matte to produce a high grade PGM (platinum group metals) concentrate. Therefore, small improvements will have a significant effect on the production efficiency of a high grade PGM concentrate.

The principal cause of the control problem for this process is the ill-defined and complex nature of the reaction mechanisms, as well as the inability of the operators and process engineers to relate the multi-variable process to basic operating procedures. The control problem could originate from perturbations caused in the repulping (two feed tanks) section. The perturbations from the repulping section will then cause perturbations in the leaching in the pressure autoclave. These perturbations can occur because the extent of reactions in the repulping tanks is unknown (and possibly ignored) or by the inability of the operators to control the tank levels and pulp densities in these two tanks (the different operators have different control procedures). Controlling tank levels and pulp densities of tanks are no trivial task that could be performed effectively by any human being. Furthermore, the importance of controlling tank levels is that it will determine the residence time of the pulp in that tank, which is important because conditions exist for leaching reactions to occur, therefore, the leaching obtained in these tanks will vary. The same argument applies for controlling the pulp densities. A simple and cheap control

system is developed, i.e. an off-line computer simulation program, that will help the operator to significantly improve the control of the process (Chapter 5).

1.1.2 Extracting process knowledge from historical data

It is long known that historical data contain a wealth of information and until a few years ago the only method of extracting knowledge from data was by means of statistical evaluations. Any chemical or metallurgical plant has a vast amount of historical data that could effectively be used to extract knowledge and characterise process trends. The analysis of the historical data can also qualitatively characterise the behaviour of the process under various operating conditions. Recently the field of artificial intelligence has virtually exploded and a variety of techniques are now available to model and analyse process data for any ill-defined and poorly understood process. The main advantage of these artificial intelligence techniques is that they do not need any *a priori* information of a process. The artificial intelligence techniques that will be focussed on in this study are artificial neural networks and the inductive learning by decision trees. These artificial intelligence techniques do not substitute statistics, because statistical calculations produce valuable information that can be used in conjunction with the artificial intelligence techniques to efficiently analyse data. Therefore, these techniques are used to model and analyse the process to obtain explicit knowledge of the behaviour of the leaching process from the measured variables on the plant (Chapter 6).

1.1.3 Reaction kinetics

The complex nature of the leaching mechanism, as well as the fundamentally unknown behaviour of the leaching process, necessitated the experimental investigation into the mechanism, and kinetics of the leaching reactions (Chapter 4). The complex leaching mechanism involves the successive leaching and formation of various sulphide minerals, which are influenced by the reaction conditions (oxygen pressure, temperature, copper concentration in solution, etc.) and the interacting effects of the minerals on each other (Chapter 7). A kinetic model is developed from this knowledge of the leaching mechanism to simulate the kinetics of the complex

leaching process (Chapter 8 & 9). The future importance of the kinetic model is that it can be used in sensitivity analyses to determine the effect on the leaching efficiency for a variation in a process parameter (that cannot be experimentally tested or is difficult to test).

1.2 OBJECTIVES

The objectives of this study are (see Fig. 1.2 for a schematic presentation):

(i) improving the efficiency and the control of the process through the stabilisation of the repulping (preleach) section of the first stage leach process by means of an inexpensive tool, i.e. an off-line computer simulation program,

(ii) developing robust process models with artificial neural networks and inductive learning by decision trees to obtain process knowledge from historical data,

(iii) determining the leaching mechanism of the acid-oxygen pressure leach process of Ni-Cu matte with spent electrolyte solution, and

(iv) developing a fundamental kinetic model that can simulate the leaching process under varying conditions.

The final objective of this study is to present a better understanding of the intrinsic behaviour of the process to the process engineers. The implementation of the knowledge and kinetic model into the plant to improve the efficiency and control thereof falls outside the scope of this dissertation.

1.3 THEORETICAL CONTRIBUTIONS OF THIS STUDY

- The general concept of an off-line computer simulation program to stabilise the performance of a repulping section in any plant is presented.

- A methodology is proposed to model and analyse ill-defined and poorly understood processes from historical data with artificial neural networks and inductive learning by decision trees.

- The leaching mechanism of the acid-oxygen pressure leaching of Ni-Cu matte with spent electrolyte solution is postulated from experimental results.

- A semi-empirical kinetic model based on the leaching mechanism is developed to simulate the behaviour of the process for varying conditions.

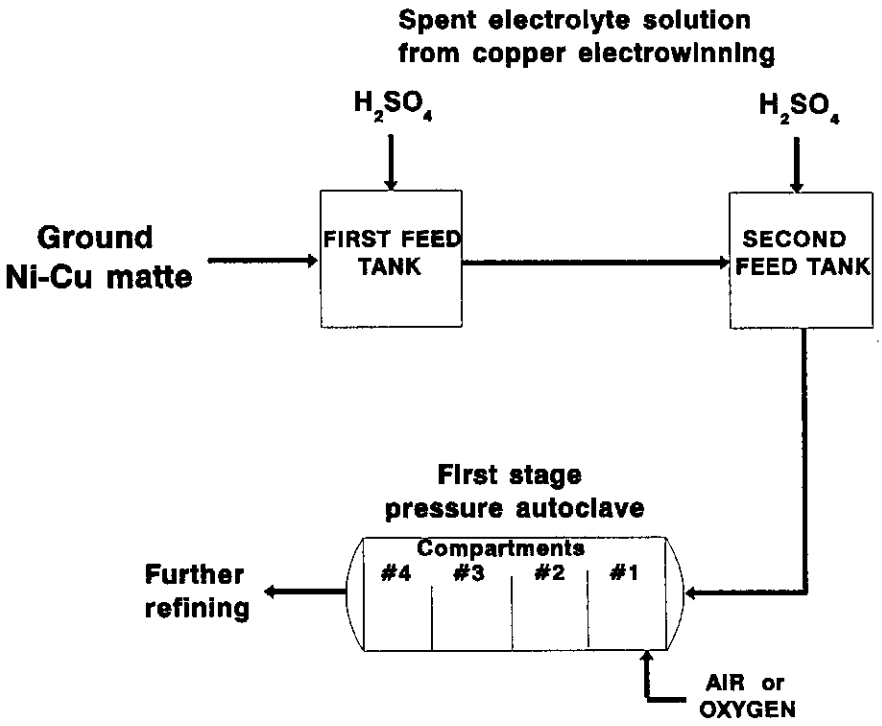

Figure 1.1 - Schematic flowsheet of the first stage leach process for the Ni-Cu matte leaching circuit

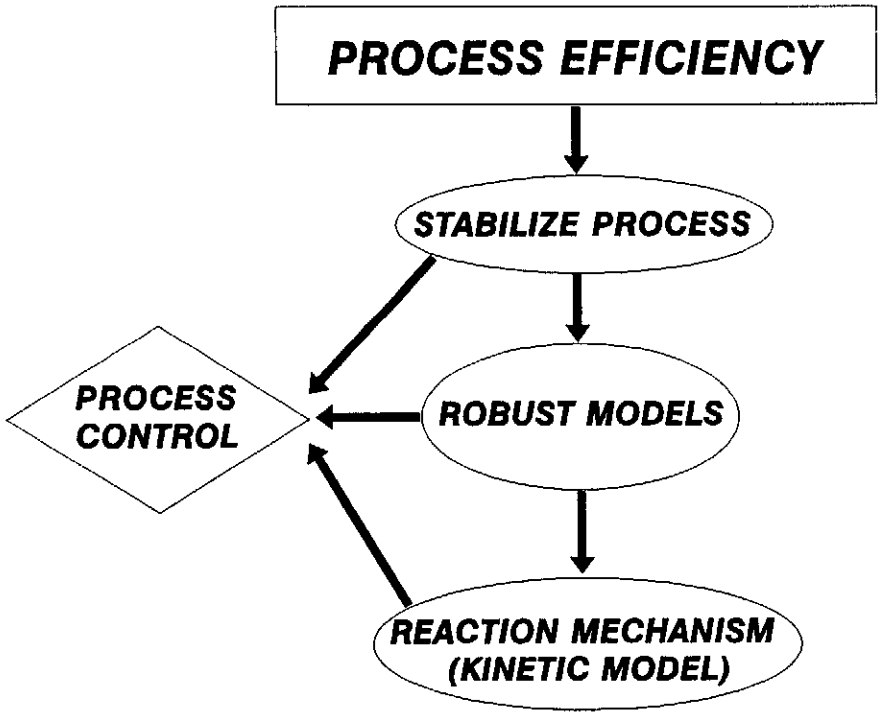

Figure 1.2 - Schematic diagram of the objective of this project

Chapter 2

LITERATURE REVIEW

The literature study was conducted to obtain as much information as possible on the leaching reactions and kinetics of base metal sulphides and more specifically of the Sherritt Gordon acid-oxygen pressure leach process (the leaching of nickel and copper from converter matte). No substantial, up to date, literature is available that describes the Sherritt Gordon acid-oxygen pressure leach process (only published work by Plasket and Romanchuk, 1978 and by Dutrizac and Chen, !987). It was, therefore necessary to study literature that discussed the leaching of base metal sulphides in general. It was also determined that the mineralogy of the matte plays an important role in the extent and course of the leaching of the cation metals out of the sulphide lattice. Thus a summarised background on basic mineralogy and more specifically the aspects that will be used in the discussion of the leaching mechanism is presented here.

Short literature reviews of the modelling and data analysis techniques used in Chapter 6 (i.e. artificial neural networks (ANN), inductive learning by decision trees and statistical evaluations) will be presented and explained in Chapter 6.

2.1 REACTION MECHANISM FOR THE LEACHING OF Ni-Cu MATTE

Various chemical reactions have been proposed by different authors for the leaching of Ni-Cu matte with spent electrolyte solution. These reaction mechanisms are for two types of Sherritt Gordon processes, namely where a (i) first stage acid-oxygen pressure leach process, or (ii) atmospheric leach process is used (with successive pressure leach stages).

2.1.1 Sherritt Gordon acid-oxygen pressure leach process

The leaching mechanism proposed in the paper of Plasket and Romanchuk (1978) is based on laboratory and pilot plant test work by Sherritt Gordon Mines Limited. This was before the Ni-Cu refinery of Impala Platinum was commissioned. The main objective of the first stage leach (part of the process which will be concentrated on in this dissertation) was to achieve as high a nickel extraction as possible and at the same time produce a solution low in copper. For simplicity, it was considered that the matte composition can be represented by Ni_3S_2 and Cu_2S. The first stage leach can be considered to proceed in three separate steps according to the equations given below:

Step 1: Copper cementation by the matte

$$Ni_3S_2 + CuSO_4 \rightarrow NiSO_4 + 2NiS + Cu \qquad (2.1)$$

Step 2: Metal dissolution by H_2SO_4 and O_2

$$Ni_3S_2 + H_2SO_4 + {}^1/_2O_2 \rightarrow NiSO_4 + 2NiS + H_2O \qquad (2.2)$$

$$Cu_2S + H_2SO_4 + {}^1/_2O_2 \rightarrow CuSO_4 + CuS + H_2O \qquad (2.3)$$

Step 3: Copper replacement by nickel in the leach residue

$$NiS + CuSO_4 \rightarrow CuS + NiSO_4 \qquad (2.4)$$

Step 3 is needed to be carried out in the absence of O_2 to help prevent the following oxidation reactions:

$$NiS + 2O_2 \rightarrow NiSO_4 \qquad (2.5)$$

$$CuS + 2O_2 \rightarrow CuSO_4 \qquad (2.6)$$

The oxidation reaction (2.6) is undesirable in that it contributes to a high copper content in the leach solution. Nickel powder was initially used for the cementation of copper from the solution, as shown by the following equation:

$$Ni + CuSO_4 \rightarrow Cu + NiSO_4 \qquad (2.7)$$

The reactions suggested by Plasket and Romanchuk (1978) occurring during the second stage leach are reactions (2.5), (2.6), (2.8), (2.9) and (2.10).

$$Cu + H_2SO_4 + {}^1/_2O_2 \rightarrow CuSO_4 + H_2O \qquad (2.8)$$

$$Ni + H_2SO_4 + {}^1/_2O_2 \rightarrow NiSO_4 + H_2O \qquad (2.9)$$

$$FeS + 2O_2 \rightarrow FeSO_4 \qquad (2.10)$$

The objective of the second stage leach was to extract as much of the soluble nickel, copper and cobalt metal values as possible from the first stage leach residue.

Dutrizac and Chen (1987) carried out a mineralogical study to identify the changes occurring in the sulphide phases during the leaching of Ni-Cu matte in $CuSO_4$-H_2SO_4-O_2 solutions (Sherritt Gordon process). This study was conducted by taking samples from the actual plant process. The matte composition consisted of major amounts of heazlewoodite (Ni_3S_2), nickel (Ni), chalcocite (Cu_2S) and/or chalcocite-Q ($Cu_{1.96}S$), and traces of magnetite. No significant changes of the matte occur in the preleach (mixing) tanks in contrast to the changes occurring in the autoclave. The solids that were already in contact with the spent electrolyte ($CuSO_4$-H_2SO_4) solution, consist of a matrix of Ni_3S_2 and Cu_2S containing finely dispersed Ni alloy particles. It is presumed that the platinum group metals, PGM's, are preferentially associated with the Ni alloy phase. Small inclusions of various oxide phases such as nickel oxide (possibly NiO) containing minor amounts of Cu, Fe, Co, and S, iron oxide (Fe_3O_4) and iron-nickel oxide (possibly $NiFe_2O_4$) were observed. A schematic flowsheet of the first stage leach process for the Ni-Cu matte leaching circuit is presented in Fig. 1.1.

First compartment of the autoclave: The leaching reaction greatly accelerates in the first compartment of the autoclave (from the preleach tank), with the decline in nickel content and a corresponding increase in the copper (in the solids). Traces of covellite (CuS) were seen, and the trace quantities of iron oxide, iron-nickel oxide and nickel oxide persisted. The principal difference between the pulp in the first compartment and the pulp in the tank before entering the autoclave is the higher degree of dissolution of the pure nickel and the nickel alloy phases in the pulp of the first compartment.

Second compartment of the autoclave: In the second compartment all the Cu_2S (or $Cu_{1.96}S$) had been converted to digenite ($Cu_{1.8}S$) and covellite (CuS) is now present in major amounts. Heazlewoodite (Ni_3S_2) has vanished and polydymite (Ni_3S_4) is now the major phase. A trace of Ni alloy was still present and the oxide phases were readily detectable. The amount of sulphate increased significantly in this compartment, indicating the precipitation of hydroxy-sulphate species. The absence of iron in the sulphates precludes ammonium jarosite in the first and second compartments of the autoclave. Furthermore, virtually all the metallic phases have dissolved.

Third compartment of the autoclave: The trends observed in the first and second compartment are only intensified in the third compartment. In this compartment digenite ($Cu_{1.8}S$), covellite (CuS), polydymite (Ni_3S_4) and traces of magnetite (Fe_3O_4) are present. The amount of nickel sulphide seems to decrease, and traces of ammonium jarosite were detected. All the Ni_3S_2 had been dissolved and/or transformed, and all the metallic phases had been leached. The oxide phases present in the leach do not seem to have been attacked extensively during the leaching process, so far.

Fourth compartment of the autoclave: The composition of the pulp in this compartment is similar to that in the third compartment, except that no ammonium jarosite was detected in this compartment. The oxide and silicate phases are still evident as unaltered particles, and Cu-Ni sulphides were detected ($Cu_{1.8}S$ spheroids in a matrix of CuS and Ni_3S_4; the Ni alloy phase is absent).

A mineralogical study conducted by Lourens (1993) on the first stage leach process of Impala Platinum Limited obtained similar results to those obtained by Dutrizac and Chen (1987). Lourens (1993) states that the matte consists of large particles with Ni_3S_2 matrix in which rounded inclusions of Cu_2S occur. Furthermore, small inclusions of predominantly Ni alloy are randomly distributed throughout the Ni_3S_2 matrix. Nickel ferrite is also present in small quantities. The PGM's are closely associated and probably alloyed with nickel. The samples taken from the preleach tanks are very similar to those of the matte. The matrix still consists of Ni_3S_2 with rounded inclusions of Cu_2S, and the Ni alloy containing the PGM's are visible (scanning electron microscope, SEM). No Cu metal was detected in these samples.

Compartments no. 1 and 4 of the autoclave: The XRD analysis for the samples taken from the first compartment shows the presence of $Cu_{1.8}S$ and Ni_3S_4 as the major phases and vaesite (NiS_2) as a minor phase. Covellite (CuS) is present in trace quantities in this compartment. In samples from the fourth compartment more CuS is present. Samples from both the first and fourth compartment have a Ni_3S_4 matrix with minor quantities of NiS_2. The fourth compartment has more CuS in the matrix with relatively large inclusions of $Cu_{1.8}S$.

Autoclave leach residue (first stage leach): A dramatic change in the mineralogical composition of the samples from the preleach section compared with the samples taken from the leach residue was detected. The Cu_2S has been completely converted to $Cu_{1.8}S$ and CuS, and CuS is now present as the major phase. Minor amounts of Ni_3S_2 remain in the matrix and some Ni_3S_4 may be present. Furthermore, the Ni alloy has almost totally disappeared, exposing the PGM particles. The other phases that have been observed are nickel ferrite, quartz, potassium-alumina silicate and lead sulphide.

The leaching mechanism suggested by Dutrizac and Chen (1987) was thus as follows:

In the two preleach tanks before the autoclave vessel, sulphuric acid and copper sulphate are added together with recycled Cu-Ni cement product. Both the Ni alloy in

the matte and the cemented copper react rapidly in the preleach tanks according to equations (2.7), (2.8) and (2.9).

A minor amount of Ni_3S_2 may react in the preleach tanks, but this is not evident from either the microscopic or X-ray diffraction results. The Ni alloy continues to be leached rapidly according to equations (2.7) and (2.9), and no Ni alloy is present in the third compartment of the autoclave. Therefore, the Cu_2S and $Cu_{1.96}S$ originally present in the matte begin to be oxidised to digenite ($Cu_{1.8}S$). (For the sake of simple stoichiometric coefficients, the $Cu_{1.96}S$ formula has been substituted with Cu_2S in the reaction equations.)

$$5Cu_2S + {}^1/_2O_2 + H_2SO_4 \rightarrow 5Cu_{1.8}S + CuSO_4 + H_2O \qquad (2.11)$$

The conversion of Cu_2S to $Cu_{1.8}S$ is nearly completed in the second tank of the first stage leach. The reaction between the Ni_3S_2 and $CuSO_4$-H_2SO_4-O_2 begins in the first compartment of the autoclave, although the extent of the reaction is hard to gauge because of similarities in the powder diffraction patterns of Ni_3S_2 and Ni_3S_4.

$$2Ni_3S_2 + {}^3/_2O_2 + 3H_2SO_4 \rightarrow 3NiSO_4 + Ni_3S_4 + 3H_2O \qquad (2.12)$$

$$3Ni_3S_2 + 2CuSO_4 + 2O_2 + 4H_2SO_4 \rightarrow 6NiSO_4 + Ni_3S_4 + 2CuS + 4H_2O \qquad (2.13)$$

The fact that covellite (CuS) is present in only modest amounts in the first compartment suggests that equation (2.12) is initially more important than equation (2.13). In the second compartment Ni_3S_2 has entirely disappeared and covellite (CuS) is present as the major phase. This suggests that equation (2.13) has become more important and that $Cu_{1.8}S$ is being attacked to some extent.

$$5Cu_{1.8}S + 2O_2 + 4H_2SO_4 \rightarrow 5CuS + 4CuSO_4 + 4H_2O \qquad (2.14)$$

Nevertheless, Plasket and Romanchuk (1978) suggested that the leaching of Ni_3S_2 proceeds through NiS rather than through Ni_3S_4. A careful and systematic study of

the various X-ray diffraction patterns by Dutrizac and Chen (1987) of the residues failed to detect any of the crystallographic forms of NiS. The discharge from the autoclave consists of $Cu_{1.8}S$, CuS and Ni_3S_4 together with various oxide and silicate phases. The sulphides are further attacked by H_2SO_4-O_2 in the second stage leach, where both CuS and Ni_3S_4 are further oxidised to soluble sulphates. $Cu_{1.8}S$ is leached to CuS according to equation (2.16), and CuS is oxidised to $CuSO_4$ by reaction (2.5). Ni_3S_4 is oxidised according to the following reaction:

$$Ni_3S_4 + H_2O + {}^{15}/_2O_2 \rightarrow 3NiSO_4 + H_2SO_4 \qquad (2.15)$$

Although iron consists of only a fraction of a percent of the original matte, the behaviour of this element during processing is worthy of comment. Part of the iron is present as magnetite and nickel ferrite, which may dissolve. However, the fluctuating content of the iron in the residues suggests that the iron is precipitated and redissolved in a variety of ways. Limited evidence suggests that the iron is precipitated mostly as ammonium jarosite (Dutrizac and Chen, 1987).

$$(NH_4)_2SO_4 + 3Fe_2(SO_4)_3 + 12H_2O \leftrightarrow 2NH_4Fe_3(SO_4)_2(OH)_6 + 6H_2SO_4 \qquad (2.16)$$

At the points in the circuit where fresh acid is added, dissolution of the ammonium jarosite occurs and reaction equation (2.16) proceeds in reverse, therefore releasing iron to the solution.

Plasket and Dunn (1986) suggested that with the acidic conditions in the first stage leach and redox potentials varying from oxidising to mixed across the four compartments, iron is leached from the matte possibly according to the following equations:

$$Ni_3S_2.FeS + H_2SO_4 + {}^1/_2O_2 \rightarrow 3NiS + FeSO_4 + H_2O \qquad (2.17)$$

$$2FeSO_4 + H_2SO_4 + {}^1/_2O_2 \rightarrow Fe_2(SO_4)_3 + H_2O \qquad (2.18)$$

Because of the dynamic behaviour of the system some of the iron reprecipitates as a jarosite-type compound, as shown by equation (2.16).

2.1.2 Sherritt Gordon process with a first stage atmospheric leach

Hofirek and Kerfoot (1992) described the chemistry for the nickel-copper matte leach process of Rustenburg Base Metals Refineries, situated at Rustenburg, South Africa. The major differences of this process (compared with the Impala process) are that the converter matte is initially separated into a PGM-containing metallic fraction and a non-magnetic sulphide fraction, as well as the fact that the first stage leach is an atmospheric leach. The non-magnetic sulphide fraction of the converter matte is leached in a series of continuous stirred tank reactors under atmospheric pressure. The resulting residue is then subjected to a two stage pressure leach in copper-spent electrolyte in Sherritt Gordon horizontal autoclaves at temperatures in excess of 130°C.

The chemical reactions described by Hofirek and Kerfoot (1992) are similar to equations derived by Llanos *et al.* (1974) and Symens *et al.* (1979). The reaction mechanism proposed by Hofirek and Kerfoot (1992) is as follows:

Atmospheric leach: The ability of nickel-copper matte to precipitate Cu^{2+} ions is a historically known fact ascribed in the older literature to the special metallic character of one nickel atom in the Ni_3S_2 lattice. The general consensus in the modern literature is on the overall reaction (metathesis):

$$Ni_3S_2 + 2CuSO_4 \rightarrow Cu_2S + NiS + 2NiSO_4 \qquad (2.19)$$

which is supported by the formation of Cu_2S and intergrowths of NiS with Ni_3S_2. An excess of acid in the reaction system is consumed by the decomposition of Ni_3S_2 (eq. 2.2). Work carried out by Sherritt Gordon has indicated that the reaction in

equation (2.2) proceeds stepwise through the initial formation of godlevskite (Ni_7S_6) as follows:

$$3Ni_3S_2 + 2H_2SO_4 + O_2 \rightarrow 2NiSO_4 + Ni_7S_6 + 2H_2O \quad (2.20)$$

$$Ni_7S_6 + H_2SO_4 + {}^1/_2O_2 \rightarrow NiSO_4 + 6NiS + H_2O \quad (2.21)$$

During the decomposition of heazlewoodite, a substantial quantity of ferrous ion is released into solution. Any ferric ion present in the feed solution is rapidly reduced to the ferrous state. As in many leaching systems, it is assumed that the dissolved iron acts as an electron carrier and enhances the leaching rate.

$$Ni_3S_2 + 2Fe^{3+} \rightarrow 2Fe^{2+} + 2NiS + Ni^{2+} \quad (2.22)$$

$$\uparrow \qquad \downarrow$$

$$H_2O + 2Fe^{3+} \leftarrow 2Fe^{2+} + 2H^+ + {}^1/_2O_2 \quad (2.23)$$

At pH values above 2 - 2.5 the reactions of iron dissolution and its reduction to the ferrous state appear to cease and the ferrous ion is oxidised to the ferric ion by the oxygen according to reaction (2.18).

Pressure leach: The major reactions during the initial phase of the oxidising period are dissolution of nickel from NiS (millerite):

$$4NiS + H_2SO_4 + {}^1/_2O_2 \rightarrow Ni_3S_4 + NiSO_4 + H_2O \quad (2.24)$$

and copper from Cu_2S by reaction (2.3). These reactions are supported by the appearance of two totally new species in the leach residue, i.e. polydymite (Ni_3S_4) and covellite (CuS). A substantial part of the nickel is dissolved by direct oxidation of NiS to $NiSO_4$ (eq. 2.5). A large quantity of copper can be precipitated from solution as a sulphide by metathesis according to equation (2.4).

Optical microscopic examinations of residues showed that the particles of Ni_3S_4, formed rapidly from NiS during the oxidising leach, were pitted with cracks or veins

which became predominantly filled by a copper sulphide. Electron microscopy revealed that the copper sulphide was predominantly $Cu_{1.8}S$ with a minor amount of CuS. As the leach progressed, $Cu_{1.8}S$ spread rapidly until significant areas in the interior of the Ni_3S_4 grains were filled with $Cu_{1.8}S$. While the indications are that the mechanism of the reaction between Ni_3S_4 and the cupric ion involves a range of non-stoichiometric metal sulphides, the overall reaction can be conveniently represented by the equation:

$$4Ni_3S_4 + 9CuSO_4 + 8H_2O \rightarrow 5Cu_{1.8}S + 9NiS + 3NiSO_4 + 8H_2SO_4 \qquad (2.25)$$

There is also strong evidence of free acid formation (a drop in the pH of the reaction slurry), and iron redissolution occurs (acid formation indicated by reaction in eq. 2.25). The acid decomposition of $Cu_{1.8}S$ results in the formation of CuS (eq. 2.14). The generated CuS is either directly oxidised to copper sulphate (eq. 2.6) or can be decomposed,to elemental sulphur by the leaching of copper from the CuS lattice:

$$CuS + H_2SO_4 + {}^1/_2O_2 \rightarrow CuSO_4 + S^0 + H_2O \qquad (2.26)$$

The reaction sequence for the dissolution of Ni_3S_4 is obscure, but the overall stoichiometry can be described by reaction (2.15). At this high temperature (140-145°C) the ferric ion hydrolysis commences at a moderate acid concentration (~30g/l). Depending on the conditions, iron precipitates either as jarosite (eq. 2.16) or as haematite:

$$Fe_2(SO_4)_3 + 3H_2O \rightarrow Fe_2O_3 + 3H_2SO_4 \qquad (2.27)$$

Both reactions release a considerable quantity of acid which is either consumed or results in an increase in acid concentration.

Another reaction mechanism was described by Brugman and Kerfoot (1986) for the nickel-copper matte leach process at Western Platinum Limited situated at Rustenburg, South Africa. This process differs from the process employed at Impala, with the first stage pressure leach being replaced by an atmospheric leach, carried

out in a train of agitated tanks, followed by a single pressure leach stage. The Western Platinum matte consists mainly of heazlewoodite (Ni_3S_2), synthetic chalcocite ($Cu_{1.96}S$) and a significant amount of nickel is present in the form of a magnetic nickel-copper-iron alloy. Iron is also present in oxide form as haematite and magnetite.

Atmospheric leach: The principal reactions occurring in the initial stages of the first stage atmospheric leach are reactions of nickel-copper alloy and Ni_3S_2 with sulphuric acid in the presence of oxygen to form nickel sulphate. The alloy dissolves totally, according to the reaction in equation (2.8) while Ni_3S_2 is converted to NiS (eq. 2.2). The leaching of nickel can continue in the presence of oxygen, with the conversion of NiS to Ni_3S_4 (eq. 2.24). In the latter stages of the leach the principal reaction is the precipitation of copper by the interaction of the cupric ion with the nickel sulphides. Both Ni_3S_2 and NiS apparently react with cupric sulphate to precipitate copper as a sulphide by metathesis reactions of the type shown in equations (2.19) and (2.28).

$$5NiS + 2CuSO_4 \rightarrow Cu_2S + 2NiSO_4 + Ni_3S_4 \qquad (2.28)$$

The copper sulphide precipitated in these reactions is believed to be largely $Cu_{1.8}S$, which has been identified, together with $Cu_{1.96}S$ in the first stage leach residue. The metallic iron in the nickel-copper alloy dissolves together with the metallic nickel in the initial stage of the leach, to form ferrous sulphate:

$$Fe^0 + H_2SO_4 + {}^1/_2O_2 \rightarrow FeSO_4 + H_2O \qquad (2.29)$$

The dissolved iron remains largely in the ferrous state, but rapid oxidation to the ferric state can occur with the precipitation of hydrated ferric oxide by hydrolysis (eqs. 2.18 and 2.27).

Pressure leach: The base metal sulphides undergo total oxidation to the corresponding sulphates in the pressure leach. The first stage leach residue consists essentially of NiS and the two copper sulphides, $Cu_{1.96}S$ and $Cu_{1.8}S$. The principal overall reactions are shown in equations (2.5), (2.3) and (2.6). X-ray

diffraction analysis of the pressure leach residue indicated that the major components were magnetite and ferroplatinum, with lesser amounts of CuS.

2.2 KINETIC INFLUENCES IN THE LEACHING OF BASE METALS

A literature study was conducted on the effects of different conditions on the kinetic behaviour of the leaching of base metals. This study includes papers which varies from leaching experiments with Ni-Cu mattes to synthetic base metal sulphides being leached by sulphuric acid, nitric acid, hydrochloric acid, oxygen, ferric ions, etc., or a combination thereof. Whenever a mixture of minerals is leached, galvanic interactions are possible between these minerals. The possible galvanic interactions and their effect on the leaching process are also briefly discussed.

2.2.1 Ni-Cu mattes

The work by Llanos *et al.* (1974) examined the atmospheric leaching response of mattes with varying conditions in the Port Nickel refinery. Detailed information about the effects of matte composition, matte particle size, solution composition, solution temperature and pulp density was obtained after the reaction chemistry was determined. It was concluded that only slightly higher initial rates of nickel extraction were observed when leaching the finer ground mattes as compared to the coarser mattes. However, during later stages, considerably more nickel was solubilised after finer grinding. The time needed to leach these mattes is inversely proportional to the sulphur content in the matte, but almost insensitive to the matte Ni/Cu ratio. The rate of nickel dissolution is apparently controlled by the rate of cementation of copper on nickel during the first few minutes of leaching. The ratio of Cu^{2+}/H_2SO_4 of the spent electrolyte has little effect on the total nickel solubilised from the matte. Higher iron concentration in either the matte or the spent electrolyte solution resulted in considerable deviations from these results. The higher the molar ratio $Cu^{2+} + H_2SO_4$ to nickel in the matte, the longer the leaching time and the greater the nickel extraction. An optimum pulp density exists for the processing of individual mattes, allowing maximum nickel extraction in the shortest possible time. Leaching at 85°C

increases the leaching time needed to reject the copper and acid from solution, but results in somewhat higher nickel extractions than at 75°C.

Symens *et al.* (1979) developed and demonstrated the technology, at plant scale, for leaching high iron (>0.5%) Ni-Cu matte with spent electrolyte at atmospheric pressure to solubilise over half of the matte's nickel values while maintaining near complete rejection of the spent electrolyte acid, copper and iron content. Copper rejection is faster the higher the ratio of acid-to-copper in the electrolyte feed, and at the same time nickel extraction is maximised. When the sulphur content of the matte was decreased, copper rejection accelerated and iron removal became more difficult, because copper catalyses iron oxidation which accelerates its hydrolysis. Too little oxygen retards iron oxidation and its subsequent rejection from solution, whereas too much oxygen interferes with copper rejection. Furthermore, a high reaction temperature (90°C) retards iron rejection, but improves copper rejection.

Plasket and Dunn (1986) developed a high temperature jarosite process which achieved near complete rejection of iron, arsenic and lead from pre-neutralised leach solutions. It incorporates the jarosite process upstream of the traditional process such that high-iron bearing solutions can be readily accommodated while maintaining the specifications for the nickel purification liquor. Precipitation of jarosite occurred between 96°C and 170°C with the pH between 1.3 and 2.5. As the pH increased above 2.5, haematite and goethite became the predominant species. The oxidation of ferrous sulphate to ferric sulphate was examined at a temperature of 140°C under differing partial pressures of oxygen. The rate of reaction was found to be first order with respect to oxygen pressure and second order with respect to ferrous concentration. It also became apparent that the free acid concentration, not the pH, should be the measured parameter, because sulphuric acid is released by the precipitation of iron (eqs. 2.16 and 2.27).

Hofirek and Kerfoot (1992) stated that in the absence of cupric ions the oxidation of ferrous ions becomes the rate limiting step. The catalytic effect of cupric ions on ferrous ion oxidation was first suggested by Burkin (1966) and since confirmed by various authors. The data (Hofirek and Kerfoot, 1992) indicated that high

temperature (150°C) and low acidity (<5 g/l) at the initiation of precipitation favour haematite formation, while lower temperature (130°C) and increased acidity leads to jarosite formation. The experimental data also indicated that the acid concentration plays a very important role in the direct oxidation, a fact which is not implied by the reaction of equation (2.6). This suggests the possible involvement of iron in the oxidation mechanism, acting as an electron carrier from the sulphide phase to the dissolved oxygen. Dobrokhotov (1959), in the study of the pressure oxidation of base metal monosulphides in the presence of iron, suggested the following mechanism:

$$MeS \leftrightarrow MeS_{act} \leftrightarrow Me^{2+} + S^{2-} \quad (2.30)$$

$$S^{2-} + 2Fe^{3+} \rightarrow S^{0} + 2Fe^{2+} \quad (2.31)$$

$$S^{0} + 6Fe^{3+} + 4H_2O \rightarrow SO_4^{2-} + 6Fe^{2+} + 8H^{+} \quad (2.32)$$

$$S^{2-} + 8Fe^{3+} + 4H_2O \rightarrow SO_4^{2-} + 8Fe^{2+} + 8H^{+} \quad (2.33)$$

$$4Fe^{2+} + 4H^{+} + O_2 \rightarrow 4Fe^{3+} + 2H_2O \quad (2.34)$$

Thermodynamic analysis of the reactions (2.30 - 2.34) shows that high acidity, low temperature and low oxygen partial pressure will favour reaction (2.31), while changing these factors in the opposite direction will shift the reaction mechanism in favour of the direct oxidation of the sulphide ion to the sulphate ion (eq. 2.33). Although oxidation of elemental sulphur (eq. 2.32) is thermodynamically favourable, practical experience shows that the generated sulphur does not undergo any further change. Therefore, Hofirek and Kerfoot (1992) suggested that high initial acid excess should be avoided, maintaining maximum aeration rate and correct temperature, so that the formation of elemental sulphur will generally be suppressed to manageable limits.

A process for the reduction leaching of manganese nodules using nickel-copper matte in dilute hydrochloric acid solution was investigated by Chen *et al.* (1992). It

was determined that Cu^{2+} acts as a catalyst together with MnO_2 to oxidise the Ni_3S_2 when the temperature is higher than approximately 70°C.

2.2.2 Synthetic nickel sulphides

Mulak (1987) investigated the kinetics of dissolution of synthetic Ni_3S_2 in nitric acid solution in the presence of cupric and ferric ions. The effects of stirring, particle size, temperature and concentration of cupric and ferric ions were examined. A constant dissolution rate of Ni_3S_2 was obtained which can be attributed to the electrochemical reactions occurring on the surface of the particles. Chemical analysis indicated that in the presence of Fe^{3+}, the sulphide ions are almost completely oxidised to sulphate, whereas in the presence of cupric ions, 70% of the initial sulphide ions are oxidised to sulphate and 30% to elemental sulphur (at temperature of 80°C). In previous work by Mulak (1985) it was demonstrated that during the leaching of Ni_3S_2 in nitric acid solutions containing $\leq$ 2.0 mol/L HNO_3, generation of H_2S is faster than its oxidation and the dissolution rate is completely inhibited after the first 30 minutes of leaching. Pawlek (1969) proved experimentally that adding H_2S at a pressure of 200 kPa can completely suppress the reaction. According to thermodynamic calculations Ni_3S_2 is unstable in acid oxidising solutions and evolution of H_2S takes place spontaneously (eq. 2.35). Addition of silver, cupric or ferric ions eliminates the evolution of H_2S in nitric acid solutions and considerably accelerates the dissolution rate.

$$Ni_3S_2 + 2H^+ \leftrightarrow NiS + 2Ni^{2+} + H_2S + 2e^- \qquad (2.35)$$

Cupric or ferric ions accept electrons from the evolved H_2S more rapidly than gaseous oxygen and intermediate products are formed which are oxidised by oxygen, so that catalytic ions are produced again. Therefore it was suggested that H_2S is oxidised by the ions rather than directly by oxygen.

Mulak (1992) also investigated the dissolution of Ni_3S_2 in sulphuric acid solutions containing potassium dichromate ($K_2Cr_2O_7$). This work indicated that a sulphur layer

was formed in a temperature range of 30-60°C, thus the leaching kinetics is controlled by a product layer diffusion process.

Kanome *et al.* (1987) leached Ni_3S_2 prepared by a wet process at a temperature of 110°C, oxygen partial pressure of 1.0 MPa and a sulphuric acid concentration of 0.1-0.15 mol/L. The oxidative leaching of Ni_3S_2 proceeds through a fast phase-transformation reaction to NiS followed by slow dissolution of the latter. The formation of elemental sulphur in the leaching process seems to be a side reaction. Furthermore, the diffusion of oxygen through a thin sulphur layer formed on the surface of the sulphide appears to be the rate determining step.

2.2.3 Copper sulphides

Mao and Peters (1982) determined that the conversion of chalcocite (Cu_2S) resolves into two distinguishable steps which may be explained by the intermediate conversion of chalcocite to digenite ($Cu_{1.8}S$), shown in equation (2.11), followed by the conversion of digenite to covellite (CuS), shown in equation (2.14). It was also found that the leaching kinetics changed twice, with the probable explanation lying in the formation of $Cu_{1.8}S$ as the major mineral species and then later the formation of CuS as the major mineral species. The morphology of the copper sulphide particle changes during the leaching process from a solid particle to a porous particle and finally the particle crumbles. They interpreted that ferric (Fe^{3+}) ions may play the role of either being regenerated heterogeneously, or it is a surface active agent that catalyses the reduction of oxygen.

The kinetics of leaching chalcocite and covellite in acidic oxygenated sulphate and chloride solutions were investigated by Chu Yong Cheng and Lawson (1991a,b). It was found that the higher the oxygen partial pressure the faster the reaction rate for Cu_2S and CuS, under the experimental conditions. The reaction rate also increases when the acid concentration increases from 0.2 *M* to 0.5 *M*. The increase in the acid concentration results in the reduced solubility of oxygen which decreases the leaching rate of copper. However, for CuS there is a significant decrease when the acid concentration is higher than 2.0 *M* (Chu Yong Cheng and Lawson, 1991b). It

was clear that ferric ions had a very marked influence and increased the leaching rate of Cu_2S appreciably (Chu Yong Cheng and Lawson, 1991a). The copper dissolution rate in the solution containing Fe^{3+} ions is much higher than that of the solution without Fe^{3+} ions. The specific behaviour of Fe^{3+} ions with respect to the leaching of Cu_2S is not entirely clear, although they almost certainly increase the redox potential of the leach solution.

Experiments were conducted by Grewal, *et al.* (1992) at INCO's Copper Cliff Refinery, where a copper sulphide residue containing precious metals was subjected to a pressure leach at 115°C. Copper occurs predominantly as Cu_2S and $Cu_{1.96}S$ with minor occurrences of Cu^0 and Cu_2O. The reaction of Cu_2S and $Cu_{1.96}S$ to $Cu_{1.8}S$ and then to CuS is partially sequential. It was found that the leaching of Cu_2S, $Cu_{1.96}S$ and $Cu_{1.8}S$ is very fast compared to the leaching of CuS. The comparison of the leaching rate of experiments done with and without iron in solution, shows that the presence of iron in solution increases the leaching rate. A net increase in the cupric (Cu^{2+}) and ferric (Fe^{3+}) ion concentration increased the mixed potential and as a result increased the leaching rate. This observation is significant since it indicates that the levels of copper and iron in solution are important as catalysts.

Nicol (1984) stated that it is generally believed that activation occurs as a result of ion exchange between copper and the cation of the mineral as follows:

$$MS + Cu^{2+} \rightarrow CuS + M^{2+} \qquad (2.36)$$

The driving force for this reaction is the lower solubility of the heavy-metal sulphide product and predictions based on this premise have been confirmed by several authors.

Peters (1984) confirmed that the most extensive electrochemical studies on minerals have been performed on copper sulphides. It was stated that the E_h-pH diagrams do not express the electrochemistry that is commonly observed in the laboratory, for example that sulphate ions are virtually kinetically inert. Peters (1984) also described processes that consume H_2S and generate sulphides under anodic conditions, or decompose sulphides and produce H_2S under cathodic conditions.

Copper sulphides anodised in absence of H_2S in acid solution follow the sequence Cu_2S-$Cu_{1.8}S$-CuS-S^0 and when anodised in the presence of H_2S the sequence is almost the same, Cu-Cu_2S-$Cu_{1.8}S$-CuS-S^0.

Oktaybas *et al.* (1994) studied the kinetics of copper precipitation from sulphate solutions by H_2S. Precipitation by H_2S is often applied due to its selectivity to precipitate copper. It is possible to precipitate copper selectively at around a pH of 0-1 and to separate it from solution containing Co^{2+}, Ni^{2+}, Fe^{2+} and Mn^{2+} ions.

2.2.4 Leaching of sulphide minerals

A study on the direct leaching of sphalerite in sulphuric acid solution was conducted by Haung and Bernal (1984) which stated that for electrochemical reactions to take place, the solid must exhibit a certain electronic conductivity in order to transfer electrons from the anodic to cathodic sites. In the experiments it was found that copper ions accelerate the leaching reaction and prevent the formation of H_2S, which may inhibit the reaction rate because of its adsorption on the cathode surface, therefore blocking the reaction path. Generally high temperatures cause the formation of H_2S, especially at oxygen pressures less than 10 bar. The leaching rate also increased with the increase in the ferrous sulphate concentration. The reason for the catalytic behaviour is due to the slow oxidation of gaseous oxygen directly onto the particle surface, with the ferric-ferrous ion couple acting as the intermediate species to carry out the leaching cycle.

Barriga Mateos *et al.* (1987) investigated the leaching of chalcopyrite ($CuFeS_2$) in ferric sulphate solution, as well as the effect of reactivation of the $CuFeS_2$ surface with metal sulphides. The reactivation effect of some of the metal sulphides can be explained by an electrochemical mechanism based on the formation of metal-sulphide/$CuFeS_2$ galvanic cell.

Habashi (1992) stated that the leaching of solids in an aqueous medium depends on the nature of the solid (i.e. ionic, covalent or metallic bond), because this will determine the leaching process, which may be physical, chemical, electrochemical,

reduction or electrolytic in nature. The kinetics of electrochemical reactions may be influenced by the presence of lattice defects in the solid or by trace impurities which may increase or decrease the electrical conductivity of the solid. Furthermore, a metal in contact with a sulphide mineral may promote the formation of a galvanic cell.

2.2.5 Galvanic interactions

The interaction between two sulphide minerals resulting from their electrochemical reactivities is called galvanic interaction. Such interaction occurs when two or more sulphide minerals are in contact. The electrochemical reactivity is indicated by the rest potential of the sulphide mineral, i.e. the higher the rest potential, the nobler it is and the least reactive in thermodynamic sense (Subrahmanyam and Forssberg, 1993). The same observation was made by Rao and Finch (1988) who investigated the galvanic' effect between pyrite, chalcopyrite, galena and sphalerite and by Nakazawa and Iwasaki (1986) in investigating the galvanic contact between nickel arsenide and pyrrhotite.

Mehta and Murr (1983) conducted a systematic study to understand the role of galvanic interactions in the leaching of sulphide minerals (chalcopyrite, pyrite and sphalerite). It was also found that fine mixed solids of the minerals in comparison with single large specimens of the minerals showed improved metal dissolution during the leaching process. Dutrizac and MacDonald (1973) made the following noteworthy observations: (i) concentrated slurries are more amenable to galvanic interactions, (ii) locked particles (e.g. rounded inclusions of Cu_2S in a Ni_3S_2 matrix) demonstrate the galvanic mechanism better than individual particles, and (iii) agitation of slurries removes oxidation products from particles, which may hinder the process.

2.3 MINERALOGY

The science of mineralogy concerns itself with the study of the elements and their compounds which occur naturally and synthetically on earth. It is recognised that every property of matter (the location of atoms in the crystal framework and how they are attached to each other) is due to its atoms, their arrangement within the matter, and the nature and strength of the attractive forces which keep them together (Sinkankas, 1966). Minerals are crystals with regular stacking of atoms in three dimensions, following the rules set by the atoms. From a structural point of view the atomic bonds of minerals may be classified as (Habashi, 1992, Frye, 1974, Sinkankas, 1966):

(i) *metallic bonds* - positive ions bathed in a sea of electrons,

(ii) *ionic bonds* - valence electron is transferred completely from anion to cation,

(iii) *covalent bonds* - electron is shared by the atoms, and

(iv) *mixed bonds - metallic-ionic*, *covalent-ionic* and *metallic-covalent*.

The kinds of bonds present in the minerals are nearly as important in their influence on the appearance and properties of minerals as the atoms themselves.

The study of crystals and crystal structures has led to a series of observations known as Pauling's rules (Frye, 1974). Real minerals display these characteristics and hypothetically conceived structures that do not, are usually found to be non-existent and impossible to create.

Pauling's rules:

(i) A co-ordination polyhedron of anions is formed around each cation. The cation-anion distance is determined by the sum of the respective radii and the co-ordination number is determined by the radius ratio.

(ii) In a stable ionic structure, the valence of each anion, with changed sign, is exactly or nearly equal to the sum of the strengths of the electrostatic bonds to it from the adjacent cations. Electrostatic neutrality must be maintained to have a stable structure.

(iii) The presence of shared edges and especially of shared faces in a co-ordination structure decreases its stability. This effect is large for cations with

large valence and small co-ordination numbers. Two cations with large repulsive forces tend to be as far apart as possible in a crystal structure.

(iv) In a crystal containing different cations those with large valence and small co-ordination numbers tend not to share polyhedron elements with each other. This may be thought of as cations trying to shield themselves as completely as possible with anions.

The structure of the ionic lattices is determined mainly by the packing of the large anions, while the smaller sized cations of higher valences are situated in the interstices of the anionic lattice. For simplicity sake it could be visualised that mineral structures are composed of close packed layers of spherical ions (anions). The layers can then be placed in two different ways on top of each other, i.e. hexagonal close packing (HCP) and cubic close packing (CCP), which is well documented in the literature (Sinkankas, 1966, Frye, 1974). The smaller cations will then fill some of the gaps left by the HCP or CCP which will determine the actual crystal structure of the mineral in question.

It is important to discuss some of the physical characteristics of the minerals when mineralogical change is combined with the chemical reactions in the minerals. These will include the geometry of the crystal, the specific gravity and the electrical properties of the mineral species. The different types of symmetry in crystal structures, in the order from high symmetry to low symmetry (Rao and Rao 1978), are:

(1) isometric (cubic),
(2) tetragonal,
(3) hexagonal (rhombohedral),
(4) orthorhombic,
(5) monoclinic, and
(6) triclinic.

The specific gravity of minerals vary because of the structure of the mineral and due to the individual specific gravities of the ions (anions are usually bigger and lighter than cations or metal ions), as well as the difference in mass of the different metal ions. A few crystals have electrical properties such that they conduct electrical

current. These crystals are mostly crystals with metallic bonds, as in native metals and some of the sulphide minerals. The electrical properties of the minerals were identified to be important because the leaching reactions that occur are electrochemical in nature, and galvanic interactions between the different minerals are possible. Although the electrical conductivity was not measured or determined for the different minerals (in the experiments), the possible effect that these variations can have on the leaching kinetics will be discussed briefly. Fleet (1977) argued that the Ni-Ni distances in Ni_3S_2 are similar to that in metallic Ni, therefore it indicates a significant degree of metallic bonding in Ni_3S_2. This in effect implies that Ni_3S_2 will exhibit good electrical conductivity properties. Náray-Szabó (1969) stated that the electrical conductivity of pure phases is normally higher than that of intermediate phases. Pure phases can be defined as stable phases, i.e. the phases that are the most stable are the phases with the highest type of symmetry (highest resistance to the leaching reactions).

2.3.1 Mineral phase transition in solids

A given assembly of atoms or molecules may be homogeneous or non-homogeneous. The homogeneous parts of such an assembly, called phases, are characterised by thermodynamic properties like volume, pressure, temperature and energy. An isolated phase is stable when its energy, or free energy is a minimum for specified thermodynamic conditions. As the temperature, pressure or any other variable like an electrical current or chemical solutions acting on the system is varied, the free energy of the system changes smoothly and continuously (a solid undergoes a phase transition when a particular phase of the solid becomes unstable under a set of thermodynamic and chemical conditions). The variation in free energy at the transition is associated with structural changes (atomic and electronic configuration) and mainly compositional changes for this specific system under investigation. It is suggested by Rao and Rao (1978) that during phase transitions the free energy change of the system remains continuous, whereas the thermodynamic quantities like entropy, volume and heat capacity undergo discontinuous changes. The reactivity of many solids is high in the neighbourhood of

phase transitions. A solid phase has a uniform structure and composition, and is separated from other phases by sharp boundaries.

Thermodynamic treatment of the mineral phases only give a macroscopic picture of phase transitions. While the thermodynamics of phase transitions can be correlated with structural changes accompanying phase transitions, it does not provide information on specific structural features of the transition (Rao and Rao, 1978). Burkin (1966) stated that the thermodynamic considerations are of secondary importance in leaching studies, because the combination of reagents and their concentrations are chosen in such a way to obtain favourable free energy changes. Therefore, the rate of reaction is of far greater importance.

It is well recognised today that a knowledge of crystal chemistry in terms of atomic arrangements and bonding in crystals is essential for understanding properties of solids (Rao and Rao, 1978). Although phase transitions are usually identified by means of changes in crystal structure, detailed structural implications are not often examined. However, if crystal-chemical principles are borne in mind, the study of phase transitions becomes more interesting. Crystal chemistry can provide a basis for classification and prediction of the nature of phase transitions. Relations between the structures of the initial and transformed phases yield valuable information on the mechanism of transformation.

2.4 LEACHING KINETICS

The dissolution of low-grade Fe-Ni-Cu-Co matte in acidic ferric sulphate solution was studied by Dry and Bryson (1987). The mathematical (electrochemical) model assumed that the matte particles were leached by a shrinking-particle mechanism, and that the surface reaction was rate-limiting and electrochemical in nature. The rate of dissolution of "simple" sulphides (MS) seems, in most cases, to be controlled by chemical reaction rather than diffusional processes (quoted from Dutrizac, 1974). Dry and Bryson (1987) stated that when a particle containing alloy and troilite is placed in an oxidising environment such as ferric solution, galvanic interaction between the metal and sulphide phases will inhibit the dissolution of FeS until the

metallic phase has dissolved completely. The reason is that the standard reduction potentials of metallic nickel and iron are appreciably more negative than that of FeS. Obviously, if the particle does not contain any alloy phase this will not occur.

Ma and Ek (1991) developed a mathematical model for the acid leaching of manganese carbonate ore. The effects of the variation in the particle size, pulp density and initial acid concentration were investigated. The test results showed that decreasing the particle size or pulp density increased the leaching rate, but increasing the initial acid concentration has only a limited influence on leaching kinetics.

The solubility of oxygen in a number of aqueous electrolyte solutions was determined by Narita *et al.* (1983). The effects of changes in electrolyte concentration, temperature and partial pressure of oxygen were investigated. The ratio of the solubility of oxygen in the electrolyte solutions to that in pure water decreases as the concentration of the electrolyte increases but is essentially independent of both temperature (over the range 298 - 348 K) and the oxygen partial pressure (over the range 0.1 - 1.0 atm).

Verbaan and Crundwell (1986) described the leaching of a sphaleritic flotation concentrate in an acidic ferric sulphate solution by an electrochemical charge-transfer model in which the mineral surface potential is approximated by the solution redox potential for the ferrous-ferric redox couple. The oxidation of ferrous ions by dissolved oxygen is described by a model consistent with previously reported models (eq. 2.37).

$$\frac{d[Fe(III)]}{dt} = k\frac{[Fe(II)]^2[O_2]}{[H^+]^{0.35}}\exp\left(\frac{-68.6}{RT}\right) \qquad (2.37)$$

Chmielewski and Charewicz (1984) investigated the oxidation of Fe(II) in aqueous sulphuric acid solutions under oxygen pressure. The effects of partial oxygen pressure, temperature and initial concentrations of H_2SO_4 and Cu(II) on the oxidation rate have been determined.

It was determined that the rate of pressure oxidation of Fe(II) in H_2SO_4 solution was dependent on Fe(II) concentration according to the second-order kinetic equation (2.38) at Fe(II) concentrations above 3-8 g/L, but according to a first-order equation at lower concentrations.

$$\frac{d[Fe(III)]}{dt} = k[Fe(II)]^2 p_{O_2} \exp\left(\frac{-56.9}{RT}\right) \qquad (2.38)$$

2.5 SUMMARY

Few references in the literature discuss the mechanism of leaching for the acid-oxygen pressure leach process of Ni-Cu matte. Slightly more literature is available on the matte leaching process at atmospheric pressure, which can be used as a basis for the determination of the leaching mechanism of the pressure leach process.

A significant body of literature discusses the leaching of separate or synthetic base metal sulphides. This information is used selectively to clarify certain aspects in the discussion of the leaching mechanism (Chapters 7 and 8). It was concluded that the atmospheric leaching of finer ground Ni-Cu mattes is initially slightly faster when compared to coarser mattes, but during the later stages of the leach considerably more nickel is solubilised. Copper (Cu^{2+} ions) catalyses iron (Fe^{2+} ions) oxidation and its subsequent hydrolysis. Too little oxygen retards iron rejection while too much oxygen interferes with copper rejection. It is also suggested that iron is involved in the oxidation mechanism, acting as an electron carrier from the sulphide phase to the dissolved oxygen. A high reaction temperature (90°C) retards iron rejection, but improves copper rejection. Iron precipitates as either jarosite (NH^+ present in solution) or haematite at temperatures between 96°C and 170°C with the pH between 1.3 and 2.5, haematite more prominent if the pH is above 2.5. It was demonstrated that during the pressure leaching of Ni_3S_2 in oxidising solutions the formation H_2S takes place spontaneously, which can inhibit any further reaction. It was found that the leaching rate of sphalerite in sulphuric acid solutions is increased by copper ions in the solution, and the formation of H_2S is prevented. Generally high

temperatures cause the formation of H_2S, especially at oxygen pressures less than 10 bar.

It is evident from the available literature that leaching of the base metal sulphides occurs through a mechanism of phase transitions. The mineral transformations that occur in the solid phase and the effect of its structural changes are aspects of heterogeneous (solid-liquid) reactions that are often neglected. Therefore, the brief discussion of the mineralogy was necessary because crystal chemistry can provide a basis to define relations between the structure of initial and transformed phases, yielding valuable information on the mechanism of transformation and its kinetics. Also, whenever a mixture of minerals exists, galvanic interactions are possible that will subsequently influence the leaching kinetics.

Chapter 3

PROCESS DESCRIPTION

Impala Platinum Limited is one of the largest producers of platinum in the Western World today. The Company has established a completely integrated operation, from the mining of the Merensky Reef near Rustenburg, South Africa, to the refining of the platinum group metals, nickel and copper (Plasket and Romanchuk, 1978) at Springs.

The ore is concentrated and smelted to matte containing about 50% nickel, 28% copper and a small quantity of platinum group metals. Further refining of the matte takes place at Springs, Gauteng, where nickel is produced in powder and briquette form and copper is recovered by electrowinning. From the Nickel-Copper Refinery the concentrated platinum group metals are sent to the Platinum Metals Refinery, at the same site, where the platinum group metals(PGM) and small quantities of gold and silver are refined.

3.1 MINERALOGICAL CHARACTERISTICS

The occurrence of PGM (platinum, palladium, osmium, ruthenium, iridium and rhodium as well as small amounts of gold and silver) in the ores of the Merensky and UG-2 reef is most complex, and apart from the multitude of platinum group minerals present, their association is also diverse. By far the greater part of the platinum group elements associate as complex sulphides within base metal sulphides. The three principal base metal sulphides present in the Merensky Reef ore are chalcopyrite ($CuFeS_2$), pentlandite ((Fe,Ni)S) and pyrrhotite (FeS) (Hochreiter, *et al.*, 1985). The platinum group minerals can occur as associations with any of these minerals, or as discrete particles within the gangue minerals. Research indicated that PGM's can occur within the lattice of the gangue minerals which, with present extraction techniques, renders them non-recoverable (Hochreiter *et al.*, 1985).

The proportional percentages of the six PGM's and gold are presented below (Hochreiter *et al.*, 1985):

Pt - 57%	Ru - 8%
Pd - 25%	Ir - 1%
Os - 1%	Rh - 4%
Au - 4%	

3.2 METALLURGICAL EXTRACTION OF PGM's

Currently, the extraction process can be divided into several different stages:

(1) crushing and grinding of the ore to 60-90% minus 44 μm (325 mesh),

(2) concentration by physical techniques such as gravity concentration and flotation,

(3) pyrometallurgical concentration which produces nickel-copper sulphide mattes,

(4) hydrometallurgical separation of the base metals and the concentration of the PGM product, and

(5) final refining to produce the individual PGM's.

3.2.1 The production of the converter matte (stages 1 to 3)

Impala Platinum Limited is mining the ore of the Merensky reef and the UG-2 reef near Rustenburg in South Africa. The mined ore is concentrated at the mineral processing plant of Impala on the mine site. The ore is concentrated to the base metal sulphides and platinum group metals (PGM's) in the form of converter matte.

The difference between the Merensky reef and the UG-2 reef is that the Merensky reef contains more sulphide than the UG-2 reef and is found in a silicate substrate. The UG-2 reef contains approximately the same precious metals content as the Merensky reef, but it has a higher Cr_2O_3 level. In the concentrating process the minerals of the Merensky reef and the UG-2 reef are combined with a ratio of 53% Merensky reef and 47% UG-2 reef. This ratio is chosen to cause the least disturbance to the existing process when the UG-2 reef ore is added to the process.

A simple flow diagram of the concentrating process is presented in Fig. 3.1. The concentrating process entails the separating of the sulphide minerals from the silicate minerals by flotation, the flotation product is dried and then smelted in an electric arc furnaces to remove some of the entrained silicates and oxides (to the furnace slag). The furnace matte consists mainly of iron, nickel and copper sulphides (FeS, Ni_3S_2, Cu_2S) with some cobalt sulphide (CoS) and very small amounts of PGM's. In the Pierce Smith converters, iron sulphide, from the furnace matte is preferentially oxidised. The most important reaction taking place in the converter is as follows:

$$2FeS + 3O_2 + SiO_2 \leftrightarrow (FeO)_2.SiO_2 + 2SO_2 \quad (3.1)$$

The iron oxidation reaction greatly simplifies the reactions taking place in the converter. Apart from oxidising the FeS and FeO, obviously a certain degree of oxidation of the other metals will take place, i.e.:

$$2Cu_2S + 3O_2 \leftrightarrow 2Cu_2O + 2SO_2 \quad (3.2)$$

$$2Ni_3S_2 + 7O_2 \leftrightarrow 6NiO + 4SO_2 \quad (3.3)$$

$$CoS + {}^3/_2O_2 \leftrightarrow CoO + SO_2 \quad (3.4)$$

However, due to the principle of selective oxidation, the metals are resulphidised by the existing FeS from the furnace matte as follows:

$$Cu_2O + FeS \leftrightarrow Cu_2S + FeO \quad (3.5)$$

$$NiO + FeS \leftrightarrow NiS + FeO \quad (3.6)$$

$$CoO + FeS \leftrightarrow CoS + FeO \quad (3.7)$$

It should be noted that the resulphidisation of Co is not as favourable as the resulphidisation of Ni and Cu. The converter slag is recycled to the furnace and the

converter matte produced is sent to Impala Platinum Refineries. The converter matte mainly consists of nickel and copper sulphides (Ni alloy, Ni_3S_2 and Cu_2S) with smaller amounts of iron and cobalt sulphides and very small amounts of PGM's.

3.2.2 Hydrometallurgy - Sherritt Gordon process

Until the 1940's pyrometallurgy was essentially the only means utilised for the primary extraction of nickel and copper from its ores (Boldt, 1967). Since that time hydrometallurgy has become an important means of recovering nickel from its ores. The principal objective of wet chemical extractive processes is to leach the desired elements selectively into an aqueous phase so as to separate them from the bulk of the unwanted material. The advantage of hydrometallurgical treatment of the Ni-Cu smelter matte is that it results in high purity products, avoids SO_2 emissions during refining, and significantly reduces hold-up time of both the principal base metals and the associated precious metal by-products.

Impala decided on the Sherritt Gordon acid pressure-leaching process. The plant was put into commercial practice in 1969 (Veltman and Weir, 1981). The Sherritt Gordon pressure-leaching process involves successive stages of acid-oxidation leaching. Nickel is removed in the first stage and the solution is reduced with hydrogen under pressure to produce a nickel powder. Copper is removed in the second stage and recovered by electrowinning. The residue from the second stage is leached further under acid conditions, and the final residue, rich in PGM's, constitutes the feed to the platinum metals refinery.

An overview of the hydrometallurgical refining of the matte is given in this chapter, but more emphasis will be placed on the first stage leach, because this is the part of the process which will be investigated further in this dissertation. The first stage leach is viewed as the most important part of the base metal refining process, as well as the PGM concentrating process, because most of the reactions occur in the first stage leach process, as well as the fact that the efficiency of the first stage leach plays the cardinal role in the quality of the final product. A simplified flow sheet of the Sherritt Gordon acid-oxygen pressure leach process (Plasket and Romanchuk,

1978, Plasket and Dunn, 1986, Veltman and Weir, 1981) is shown in Fig. 3.2. In the process five stages of leaching are practised.

A typical analysis of the converter matte feeding the first stage leaching process of the Nickel-Copper Refinery is as follows:

Nickel (Ni)	47.0 - 51.0%
Cobalt (Co)	0.2 - 0.5%
Copper (Cu)	26.5 - 31.2%
Iron (Fe)	0.2 - 1.4%
Sulphur (S)	19.8 - 22.0%

The objective of the first stage leach is to achieve as high as possible nickel extraction, while at the same time producing a solution low in copper (precipitating copper out of the solution as copper sulphide). Following liquid-solid separation, the thickener overflow is treated with fresh matte (and sodium hydrosulphide) to precipitate the remaining copper. The remaining copper-free nickel solution is treated for the recovery of nickel. The solution is first treated in the jarosite plant where most of the iron and other impurities are precipitated. The solution is then treated with NH_3 and sparged with air to precipitate the remaining iron and arsenic. The solution is then treated with barium sulphide (BaS) for lead removal. Next, the solution is treated with ammonia and ammonium sulphate in the solution adjustment step. The adjusted solution is fed to an autoclave, in which the nickel in the solution is reduced with hydrogen under pressure and precipitated as nickel powder. The remaining nickel reduction end solution is treated with ammonium sulphate and sent to the cobalt plant to recover cobalt as a powder product. The residue solution from the cobalt plant goes to the ammonium sulphate plant to recover and recycle ammonium sulphate.

The thickener underflow after the first stage leach passes to a surge tank where the pulp density is adjusted prior to the second stage leach. The second stage leach extracts approximately all of the copper and residual nickel values from the first stage leach residue (the pulp reacts with O_2 and H_2SO_4 to dissolve the copper sulphides and residual nickel sulphides). The solids discharged from the second stage leach are transferred to the PGM concentrating circuit (third, fourth and fifth

stages). The solution from the second stage is treated for impurity removal before going to the copper electrowinning section where the copper solution is electrolysed to recover cathode copper as a product. The spent electrolyte is recycled to the first stage leach.

The third to fifth stage leach extracts the remaining small amounts of nickel, copper and iron from the second stage leach residue, and recycle this solution. Therefore it leaves a residue with a high concentration of platinum group metals which are sent to the platinum metals refinery.

3.2.2.1 First stage leach

The matte coming from Impala Platinum Mines at Rustenburg is milled before entering the hydrometallurgical process. In the first stage leach the ground matte are repulped with return electrolyte from the copper electrowinning process. The typical analysis of the spent electrolyte is:

H_2SO_4	90 - 110 g/L
Ni^{2+}	30 - 35 g/L
Cu^{2+}	20 - 23 g/L
Co^{2+}	0.2 - 0.3 g/L
Fe^{3+}	0.4 - 0.7 g/L

The required pulp density for the first stage leach is approximately 1.35-1.50 kg/L. The sulphuric acid content of the return electrolyte is dependent on the operation of the copper electrowinning circuit. The pulp is then pumped to an autoclave. The temperature of the autoclave is regulated at approximately 140°C and the total pressure of approximately 5.0 bar (500 kPa) is maintained by sparging oxygen into the autoclave.

The first stage pressure leach autoclave (see Fig. 3.3) is a four-compartment, horizontal cylinder with dished ends. Each compartment are equipped with an agitator. The pulp flows from compartment no. 1 to 2 through a U-notch in the separating walls. The pulp flows from compartment no. 2 to 3, and from compartment

no. 3 to 4 through a "hole" beneath the level of the pulp in the separating walls to prevent the free flow of oxygen from compartment no. 1 or 2 to enter compartment no. 3 and 4. A balancing line connects compartment no. 2 and 3 to prevent the build-up of gases in compartment no. 3. Vent lines are situated in compartment no. 1, 2 and 4 to prevent the excessive build-up of pressure and dangerous gases inside the autoclave.

The first stage leach is carried out initially under oxidising conditions in the presence of oxygen or air (in the first and second compartment). Finally under non-oxidising conditions (in the third and fourth compartment) it enables some of the dissolved copper to precipitate or to exchange with unleached nickel sulphide. The discharge slurry is treated with sodium hydrosulphide and fresh matte to precipitate the remaining copper values.

The principal reactions occurring in the initial stages of the first stage leach are the reactions of nickel alloy (Ni) and heazlewoodite (Ni_3S_2) with sulphuric acid (H_2SO_4) and Cu^{2+} in solution in the presence of oxygen (O_2) to form copper sulphide and nickel sulphate. A few chemical reaction mechanisms have been proposed in the literature (see Chapter 2).

The residue discharged from the first stage leach consists of $Cu_{1.8}S$, CuS and Ni_3S_4, together with various oxides and silicate phases.

3.2.2.2 Second stage leach

In the second stage leach the objective is to extract as much of the soluble nickel, copper and cobalt metal from the first stage leach residue. (Typical standard conditions for the second stage leach are: 135°C, 1.38 bar (138 kPa) partial pressure of oxygen, and four hours retention time.) The target copper concentration in solution of 70 g/L dictated the pulp density of the feed. Sulphuric acid is added to the charge to give a specified S/(Ni+Co+Cu) molar ratio (where S = sulphur in solids and solution). The slurry is then treated in the second stage leach circuit where the sulphides are further attacked by O_2-H_2SO_4 (see Chapter 2).

Most of the remaining nickel and copper are dissolved under oxidising conditions in the presence of sulphuric acid and oxygen in the second stage leach. After liquid-solid separation, the second stage leach residue is repulped and leached in the third, fourth and fifth stage autoclaves.

Based on the feed matte, the extractions obtained at the end of the second stage leach are supposed to be as follows:
Nickel - 99.9%,
Cobalt - 99.0%,
Copper - 98.0%, and
Iron - 93.0%.

The filtrate of the second stage leach, containing dissolved nickel and copper, is treated in the copper electrowinning circuit for the recovery of copper. The return electrolyte, which is depleted in copper and also containing nickel, is recycled to the first stage leach.

Treatment of the copper solution

Following liquid-solids separation, the copper solution from the second stage leach is treated for the recovery of copper by electrowinning. At this stage the solution contains about 75 g/L copper, 25 g/L nickel and 2 g/L iron. If a 25 g/L nickel and 70 g/L copper solution is fed to the copper electrowinning step, 50 g/L copper will be depleted resulting in a return electrolyte solution containing about 25 g/L nickel, 20 g/L copper and a high concentration sulphuric acid. The return electrolyte is recycled to the first stage leach.

3.2.2.3 Third, fourth and fifth stage leach

The objective of the third, fourth and fifth stage leaches are to obtain a final leach residue that will serve as feed for the platinum refinery with a useable concentration of platinum group metals. In order to achieve a high concentration of platinum group metals, essentially all of the nickel, cobalt, copper and iron would have to be

extracted from the filtered second stage leach residue. The final stage leach residue, containing a high concentration of platinum group metals, is sent to the platinum metals refinery for recovery of the precious metals.

This was in short a general overview of the whole process up to the concentrating of the PGM's. The refining of the PGM's will not be discussed as it is not significant for the purpose of this dissertation.

3.3 PHYSICAL DESCRIPTION OF THE FIRST STAGE LEACH PROCESS

A simplified flow sheet of the first stage leach process is shown in Fig. 3.4. The fresh matte is fed into a ball mill together with demineralised water. Sometimes nickel sulphate, drainage water from the plant, cobalt hydroxide and products from the process that do not meet specifications are also recycled to the mill.

The slurry from the mill is pumped to tank 1506 (until recently tank 1100, which had been taken off line for repairs) where the pulp density is adjusted with spent electrolyte solution. The solids (matte) recycled from the Cu cementation circuit (press 1407) is added to tank 1506. From tank 1506 the slurry is pumped through a splitter box to tank 1102 where the pulp density is again adjusted with spent electrolyte solution. Tanks 1506 and 1102 can be described as preleach or repulping tanks.

The spent electrolyte solution is return solution from the copper electrowinning section. The spent electrolyte solution is stored in tank 313 (in the copper electrowinning section) from where it is pumped to tanks 1506, 1102 and 1107. Tank 1107 is the storage or buffer tank for the spent electrolyte solution used in the autoclave.

The slurry from tank 1102 is pumped with an air pump to the first compartment of the autoclave. The air pump is a single action pump where the pump cylinder is filled with pulp from a centrifugal pump before compressed air is used to empty the cylinder again. The cylinder volume is 74 litres. Steam and oxygen are added to the

first compartment to maintain the temperature and pressure in the autoclave, respectively. Spent electrolyte solution is also added to the first compartment of the autoclave to maintain the desired pH in the autoclave. The discharge from the autoclave goes to a liquid-solid separation step in the form of a thickener. The solution is then sent to the Cu cementation circuit and a few impurity removal stages before nickel is recovered in a powder or briquette form to be sold. The solids then go to the second stage leach process.

3.3.1 Control strategy and equipment

3.3.1.1 Milling

The matte feedrate to the ball mill is controlled by a weightometer on the conveyor belt and the demineralised water flowrate is set by hand with a valve. By observing the power draw of the mill and by hearing, balls are periodically added by the milling operator. Furthermore, the ball mill is operated on a start/stop basis which is determined by the level in tank 1506, so that milling starts when the level is below 50% and stops after it is full.

The mill product is controlled by measuring the pulp density on a pulp density scale at regular intervals while milling. The efficiency of the milling will therefore greatly depend on the skill and experience of the mill operator.

3.3.1.2 Preleach tanks

Tanks 1506 and 1102 have an approximate total volume of 10 m^3 with slight conical bottoms. Both tanks 1506 and 1102 are equipped with level indicators which are connected to the programmable logic controller (PLC) system in the control room. The pulp is pumped from tank 1506 to tank 1102 through a splitter box (see Fig. 3.5) which controls the slurry flowrate to tank 1102. The splitter box as well as the spent electrolyte flowrate to tanks 1506 and 1102 are set manually by the operator. These settings are made according to the pulp densities in these tanks and the operator's

The autoclave is vented at constant intervals to prevent the unnecessary build-up of gases and to ensure a thorough flow of oxygen through the pulp.

Samples are taken regularly from compartment no. 1 and 4 of the autoclave for analysis of the metals content (Ni, Cu and Fe) and more samples are taken at shorter intervals to determine the pH of the pulp in these two compartments. The pH values are the most important controlling parameter for the autoclave. Depending on the pH, the operator will vary the spent electrolyte flowrate from tank 1107 to the autoclave or adjust the pulp flowrate to the autoclave.

3.3.2 Process control

The problem experienced at this plant is that the process must be controlled by operators, who are not always able to cope efficiently with the apparently capricious behaviour of the process. The process is not understood sufficiently well for the operators to enable regulated and consistent control of the process. This is because the operators control the process on experience and not on knowledge of the process, which inherently means that different operators will control the process differently. Therefore, this causes an unstable process from the one shift to the next. The project described in this dissertation is aimed at improving the first stage leach process and enabling better process control than previously possible.

Each parameter and its effect on the process are briefly discussed below:

(i) Matte composition

The variation in the composition (amounts of the different elements) in the feed matte will have an effect on the leaching process to a varying degree, depending on the actual increase or decrease of a specific element. For example, if the feed matte contains a higher concentration of iron(Fe) it will result in a higher concentration of iron, in either the leach discharge solution or in the solids.

(ii) Spent electrolyte solution composition

Variations occur in the acid concentration of the spent electrolyte solution coming from the copper electrowinning section (tank 313), as well as in the concentration of other ionic species (Ni, Cu, Fe, Co, etc.). The variation in the acid concentration will influence the rate of chemical reactions taking place in tanks 1506 and 1102, as well as in the autoclave. The variation in the ionic species will have the same effect on the leaching process as does the variation in the matte composition. Furthermore, it is possible that ammonium ions (NH_4^+) in the spent electrolyte solution will form jarosite precipitates under the right conditions.

(iii) Particle size distribution of the milled matte

The particle size of the milled matte is controlled to the extent that the operating conditions are specified (pulp density of the slurry leaving the mill) so that the desired particle size distribution could be obtained. The results of the samples taken for the particle size classification analysis are only available at a later stage rendering these samples useless for the effective control of the milling circuit. The fact that the milling operation is conducted on a stop-start basis further increases the difficulty of efficiently controlling the particle size distribution of the matte. The size distribution of the matte will affect the leaching reaction in that the finer the grind, the larger is the contact area and the better is the liberation of the Ni, Cu, Co and Fe.

(iv) Pulp density

The pulp density is an important factor in the reaction kinetics of the pulp, because for lower or higher pulp densities the leaching will either be more, or less efficient. The reason why the pulp densities in the preleach or repulping tanks must be maintained is: (i) to have constant reaction kinetics in the two tanks, and (ii) to be able to obtain the desired pulp density when the pulp is fed from one tank to the next and to the autoclave. Theoretically this implies that when the slurry is pumped from one vessel to the next a calculated amount of spent electrolyte could be added to obtain the desired pulp density in that vessel.

(v) Solids recycled from the Cu cementation circuit

The solids (from the Cu cementation circuit) that are recycled from press 1407 to tank 1506 contain higher amounts of copper in the solids than the matte coming from the mill. Furthermore, the solids recycled from the copper cementation circuit will affect the pulp density of the slurry in tank 1506 and it will also influence the leaching reactions in this tank. No monitoring of the amount or composition of the recycled solids is conducted, so this procedure is an unknown disturbance from a control point of view.

(vi) Temperature

The temperature in the preleach/mixing tanks is not recorded or controlled, which leads to temperature variations in these tanks which will affect the leaching kinetics of the pulp in these tanks. The temperature in the autoclave is obtained by sparging steam at 1100 kPaG pressure directly into the autoclave and the temperature is automatically controlled by the PLC system.

(vii) pH

The pH in the preleach tanks will affect the reactions taking place in the preleach tanks. The pH in the first compartment of the autoclave is controlled by the addition of spent electrolyte solution to the autoclave. Furthermore, it is assumed that if the pH in the first compartment is correct and the standard process conditions exist, the pH in the fourth compartment will be correct.

A problem experienced in the plant is that the acid concentration of the spent electrolyte solution (original source tank 313) does vary. This variations will cause variances in the pH values of the pulp and when this disturbance is corrected it will cause variations in the pulp density.

(viii) Spent electrolyte flowrate

The spent electrolyte solution (from tank 313) feeds both tanks 1506 and 1102 as well as tank 1107. The spent electrolyte is added to tank 1506 and 1102 on the operator's judgement to maintain the desired pulp densities. The spent electrolyte flowrate to the autoclave (from tank 1107) is also adjusted by the operator to achieve the desired pH in the first compartment of the autoclave.

(ix) Pressure

The importance of maintaining the oxygen pressure in the reactor is directly linked to the reaction kinetics as well as the temperature of the autoclave. The addition of oxygen enriches the autoclave for better oxidising conditions, therefore higher leaching rates and a higher throughput of matte. The pressure in the autoclave is maintained automatically (with the PLC) by sparging pure pressurised oxygen into the autoclave.

(x) Oxygen flowrate

The oxygen flowrate is determined by the ventilation times in compartment 1 and 2, because the vent valves open for 5 seconds every 30 seconds and for 10 seconds every 60 seconds, respectively. It could also be influenced by the number of samples taken and the time used to withdraw each of the samples. Therefore, this parameter will also cause some perturbations in the process.

(xi) Pulp feedrate

The feedrate of the pulp from tank 1102 to the autoclave is usually set at a setting that is believed to be the optimum for the maximum throughput while obtaining the desired degree of leaching. The feedrate is sometimes varied by the operator, to increase the throughput or to change the operating conditions.

3.4 SUMMARY

In this chapter an overview of the metallurgical extraction of PGM's (up to the production of concentrate for the platinum refinery) is briefly discussed. However, the emphasis is on the hydrometallurgical extraction of the base metals from the converter matte by means of the Sherritt Gordon process. A physical and operating description of the process is also provided for a better understanding of the variables influencing the actual process. These above mentioned factors clearly shows that it is impossible for the operator (one operator) to control the process in a steady state operation, considering all the parameters.

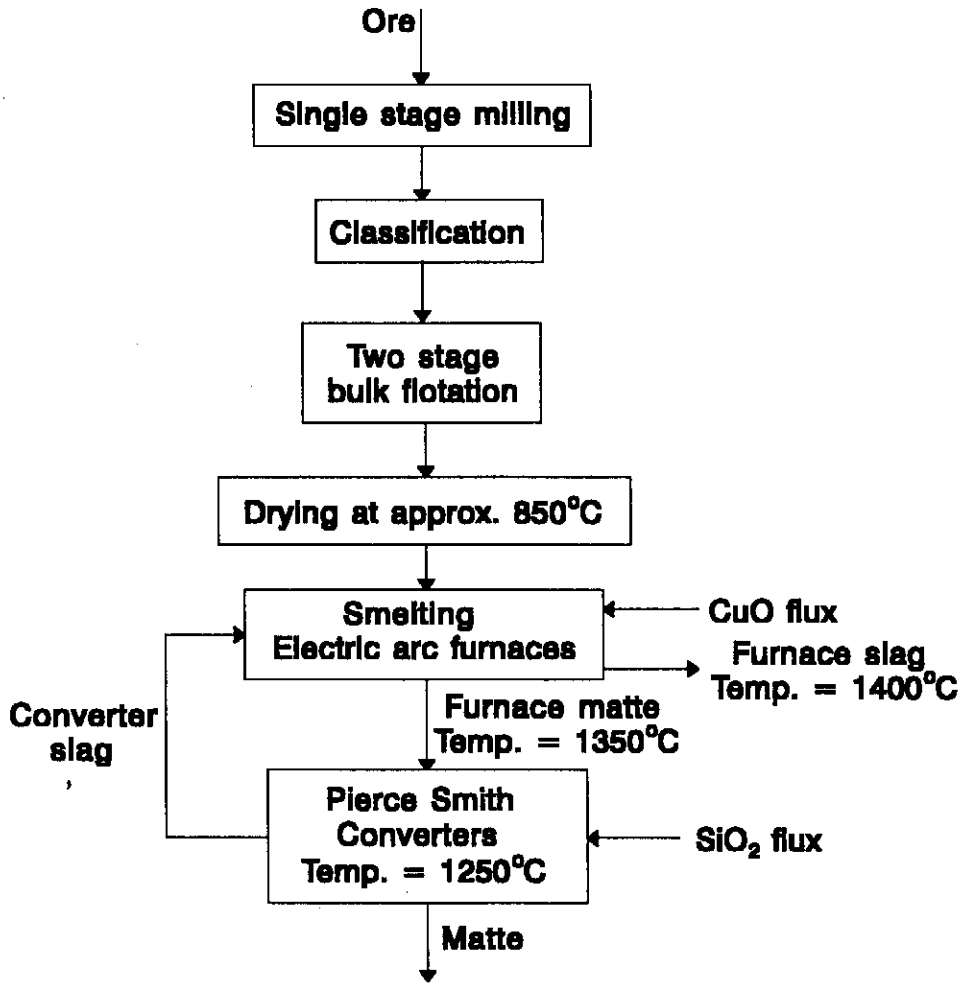

Figure 3.1 - Simplified flow diagram of the concentrating process at the mineral processing plant of Impala Platinum Limited.

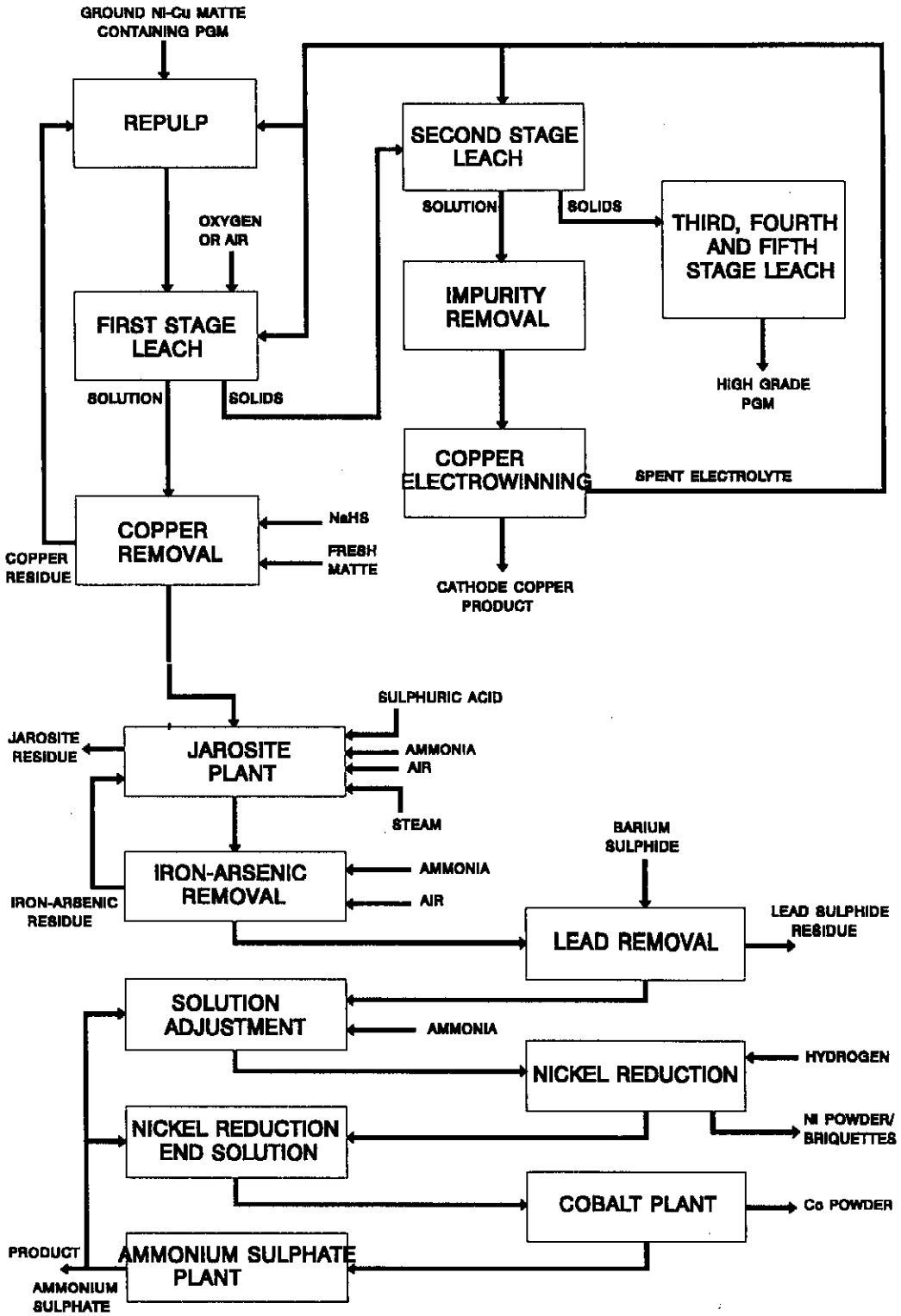

Figure 3.2 - Simplified flow diagram of the Sherritt Gordon acid-oxygen pressure leach process

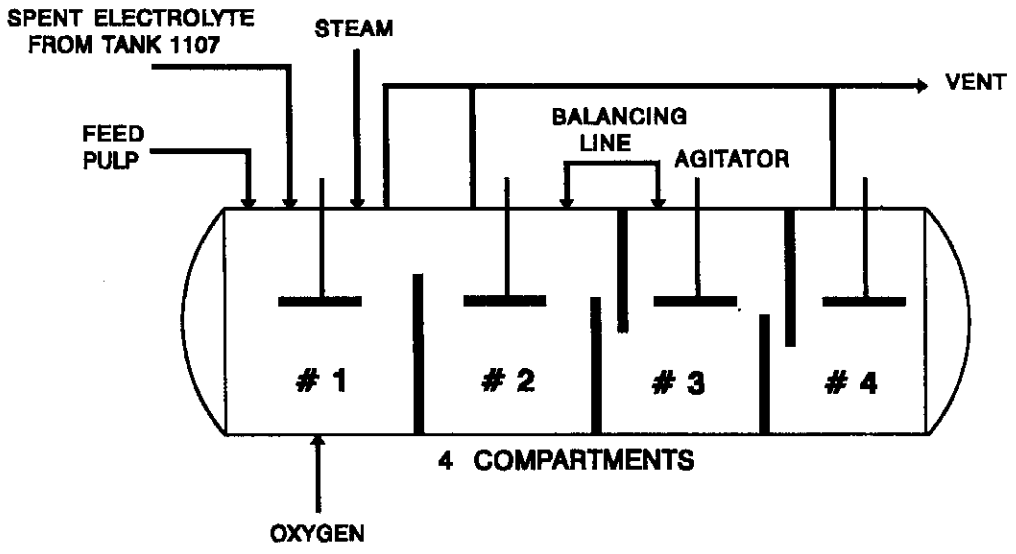

Figure 3.3 - First stage (Sherritt Gordon) acid-oxygen pressure leach autoclave

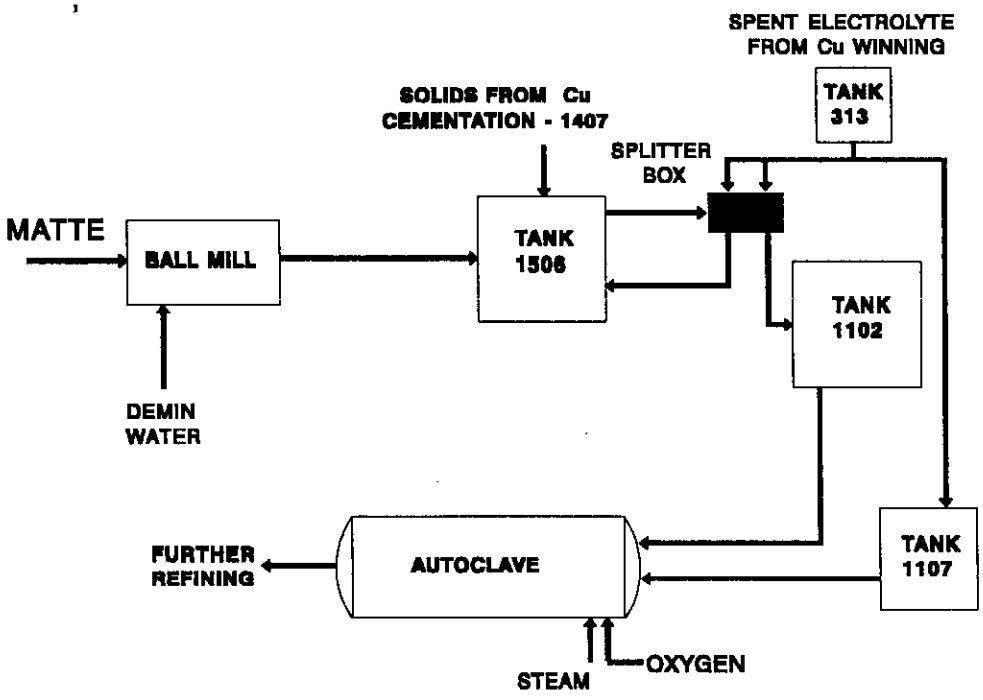

Figure 3.4 - Simplified flow diagram of the first stage leach process

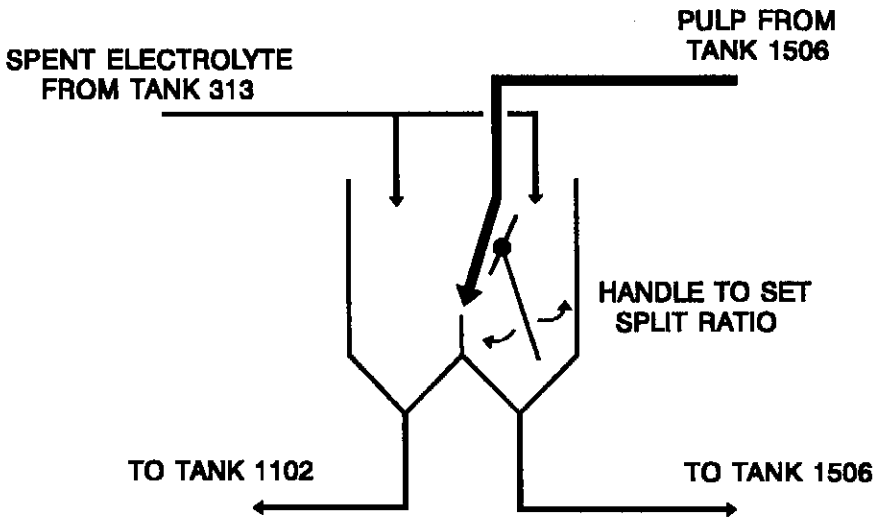

Figure 3.5 - Drawing of the Splitter box

Chapter 4

EXPERIMENTAL

Experiments were conducted to investigate the behaviour of the process under various operating conditions and to determine the reaction mechanisms and kinetics of the process. The experiments were aimed at simulating the operating conditions in the plant. The most important parameters in this leaching process have been identified in Chapter 3. Furthermore, the effect of the variations of these parameters on the leaching efficiency, was determined in the experiments. This information will be used to learn more about the reaction mechanisms of the process, and at the same time, develop a reaction model for the process.

The experimental work was conducted at Impala Platinum Refineries in their pilot plant/laboratory scale autoclave.

4.1 EXPERIMENTAL EQUIPMENT

The experimental autoclave is a pressure vessel with a 316L stainless steel shell and a total volume of 82 litres. The autoclave has a feed chute, dip pipe for bubbling gas through, sample point, drain, thermocouple, two vent valves, agitator and internal coil for heating with steam or cooling with water. See the simplified drawing in Fig. 4.1.

The temperature in the autoclave is controlled by a thermocouple that is connected to a temperature controller, which sends an air signal to a valtex control valve that controls the steam flow through the steam coil. The pressure in the autoclave is controlled by hand by setting the pressure on the regulator of the oxygen bottle and then by monitoring the pressure on the autoclave itself and on the oxygen line. The

pressure vessel is ventilated by opening the valve on the 'constant vent' line (Fig. 4.1); this setting was also adjusted by hand. The stirring speed of the agitator was kept constant for all the experiments.

4.2 MATERIAL PREPARATION

A bulk sample of matte, approximately 388 kg (dry weight), was taken from the plant. The sample was taken after the milling section in the form of a slurry, which was dried, crushed and mixed. The approximate density of the matte was determined by weighing 100 grams of matte and measuring the volumetric displacement in water. The average matte density was calculated as 5.70 kg/L.

The particle size distribution (see Table 4.1) of the matte was used as the standard particle size distribution for all the experiments. Due to the relatively large scale of the experiments (±8 kg of matte per experiment) it will be too time consuming to separate the matte into the various particle size fractions. However, the effect of the variation in the particle size distribution on the leaching reactions was tested for. Therefore it was necessary to screen part of the bulk sample into specific particle size fractions to be used in these tests. This resulted in 51.2 kg of the bulk sample being screened into particle size fractions of +300, -300 +150, -150 +106, -106 +75, -75 +45, -45 μm. These particle size fractions (Table 4.2), differ from the particle size fractions measured in the plant (Table 4.1) in order to obtain a more evenly spread mass distribution in the particle size fractions, so that enough sample is available in each size fraction to conduct an experiment with. Some discrepancies may be present in the screening process due to the fact that the matte was dry screened. This caused some of the fine powder to be retained in the larger particle size fractions (due to the fineness of the matte). Moreover, the fine powder particles started clinging together due to static electricity being created when the matte was vibrating on the screens.

The sum of the mass of the +45 and -45 μm size fraction from Tables 4.1 and 4.2 represents 45.6% and 40.1% respectively of the mass of matte of the bulk sample (388 kg) and that of the batch (51.2 kg) that was screened. This indicates that

approximately 5.5% (of fine matte) of the batch that was screened was retained in the other particle size fractions.

A bulk sample (approximately 1000 litres) of the spent electrolyte solution was also taken from the plant (tank 313 in the Cu electrowinning section), and was stored in five two hundred litre drums. All the experiments were conducted using the spent electrolyte solution from the bulk sample, except for the last five experiments where the spent electrolyte from a new batch was used.

4.3 EXPERIMENTAL SET-UP

4.3.1 Standard conditions

The standard conditions for the experiments were aimed at simulating the actual conditions of the autoclave in the plant (see Table 4.3).

One of the most important questions was what the standard pulp density must be, because no clear knowledge existed of what the optimum pulp density is for the actual process. From plant logsheets the average spent electrolyte flowrate to the autoclave was approximately 80 L/min. The flowrate of the pulp from tank 1102 to the autoclave was 42 L/min with a pulp density of 1.60 kg/L. This calculated to a pulp density of 1.34 kg/L of the pulp in the autoclave. Thus, the standard pulp density were taken as 1.35 kg/L.

The actual process could not be simulated by the batch experiment in one run. The part of the process that the experiment could not simulate, together with the oxygen pressure leach, was the preleach of the pulp. The preleach takes place in tank 1506 and then in tank 1102 before entering the autoclave (see Table 4.4). It was assumed that with the more extreme conditions (higher temperature and the oxygen pressure), the degree of leaching that occurred in the preleach section would be reached quickly in the experiment. Therefore, the point where the composition of the experimental sample was the same as that of the solids before entering the autoclave in the plant was reached far more quickly in the experimental reactor.

The reaction volume for the experiments was decided on the basis that the reactor must be full enough so that it could be agitated and heated sufficiently (pulp in the reactor is heated by an internal steam coil). Secondly, it was important for the reaction that a space above the pulp was available to form an atmosphere with an excess of oxygen. Lastly, the minimum reaction volume was chosen so that the maximum number of experiments could be conducted with this batch of matte. The total volume of the autoclave was 82 litres and the design operating volume ranged between 40 and 50 litres. Therefore, with the given reasons explained above, 40 litres was chosen to be the reaction volume for all the experiments.

One aspect of the autoclave leaching process in the plant that was not repeated in the experimental autoclave was the non-oxidising leach occurring in compartments no. 3 and 4 of the plant autoclave. There are two reasons why it was decided that this procedure will not be repeated in the experiments:

(i) More than 95% of the reactions occur in the first two compartments of the plant autoclave. Furthermore a reasonable amount of dissolved oxygen will enter compartments no. 3 and 4 of the plant autoclave, especially because of the slow reaction rates in these two compartments.

(ii) Tests were conducted where the oxygen flow to the experimental autoclave was shut-off but the pressure in the autoclave dropped quickly, therefore varying the desired reaction conditions for the experiment. Tests were also performed (for the non-oxidising leach) where the oxygen pressure was applied every 30 minutes to maintain the correct reaction pressure, but these tests produced unstable results.

The leaching time for the experiment was another problem that had to be solved. The rationale for determining the leaching time was that it must be sufficient so that the point of leaching of the matte in the experiment sufficiently exceeds that of the first stage leach in the plant. After a few experiments were conducted it was evident that five hours (300 minutes) would be more than sufficient.

Another significant parameter was the oxygen flowrate through the pulp. From the logsheet the approximate average oxygen flowrate to the first stage leach in the plant is 240 kg/h, which implies 1.3 kg/h per 40 litres. The standard oxygen flowrate

for all the experiments was taken as approximately 0.6 kg/h, mainly to cut the cost of the excessive use of pure oxygen. The significance of the oxygen flowrate made it important that the time and procedure of sample taking for each experiment should be constant. The other factors that necessitated that a constant number of samples must be taken were: (i) if too many samples are taken the reaction volume will be reduced considerably, and (ii) the cost involved in taking more samples will also be quite significant, for example, the 27 experiments that were conducted generated 330 solid samples that had to be analysed. Therefore, the sampling time was determined by taking the samples at such intervals that it will characterise the whole leaching process by taking as few as possible samples. Samples were taken at the following times for all the experiments: 0 (original sample), 5, 10, 20, 40, 80, 120, 160, 200, 240, 300 min.

The volume for each sample that was taken was approximately 350 ml. For each 350 ml sample approximately 40 g of solids were retained. Of this 40 g solid sample, 15 g was needed for the solid analysis and 25 g was needed for SEM-EDX (scanning electron microscope) analysis. This resulted in approximately 8.8% of the original reaction volume being withdrawn as samples at the end of the experiment.

A computer program was compiled to calculate the variations in experimental conditions (see Appendix A), i.e. for a change in the pulp density the various ratios of matte, spent electrolyte and demineralized water had to be calculated.

4.3.2 Start-up procedure

The start-up procedure for the experiments was important because small variations in the start-up conditions could influence the initial kinetics of the process. Therefore it was very important to create a start-up procedure that would be easy and relatively stable to reproduce.

The following steps were taken for each experiment that was conducted:

1. The amounts of demineralized water, spent electrolyte solution and matte were weighed off (a separate matte sample was taken for analysis purposes,

time = 0 min). Because of the low metal concentration (<100 ppm) and the small amount of the demineralized water being used, no sample was taken of the demineralized water for any of the experiments.

2. The spent electrolyte solution was added first and heated to approximately 89°C, which is just below its boiling point at the altitude in Springs (atmospheric pressure ± 85 kPa or 0.85 bar). When this temperature was reached a sample of the spent electrolyte was taken and the matte and demineralized water were added. After charging the autoclave the charge valve and the vent valve were closed and the temperature was increased. This is the point where the actual timing of the experiment started, i.e. Time = 0 minutes. (From this point the process took approximately 20 minutes to reach its desired conditions.)
3. Another sample was taken after 5 minutes from the time when the matte and demineralized water were added. The sample was filtered and the filter cake washed with water. The filtrate was stored in a sample bottle (to be analysed later) and the washed filter cake was dried in a oven. At this stage the temperature ranged between 110 to 115°C and the pressure between 1.0 to 1.5 bar.
4. The next sample was taken after 10 minutes. The sample was filtered, washed, etc. The temperature now ranged between 130 to 134°C and the pressure between 2.0 to 2.6 bar. This was the point where the oxygen pressure was applied on the reaction mixture.
5. If the start-up procedure ran smoothly up to this stage the experiment reached the desired conditions after 20 minutes from the start of the actual experiment, which was a temperature of 140°C and a pressure of 5.5 bar.

Certain instabilities in the start-up of the experiments were due to the fact that the temperature controller overshot if it was not incrementally adjusted to the required temperature. Another factor was that the oxygen pressure was set by hand on the oxygen regulator, therefore, making it difficult to obtain the desired pressure immediately.

After completion of the start-up procedure, the experiment was stable and it was only necessary to take the required samples at the specified times (the times of sample taking have been mentioned above).

4.3.3 Reproducibility of tests

Two similar tests were conducted to establish the consistency of the experimental procedure. From Fig. 4.2 and Fig. 4.3 it is evident that the leaching kinetics (for the solution and solids) for these two experiments are for practical purposes exactly similar. Therefore if the experimental start-up procedure and the materials stay consistent, the tests could be repeated quite accurately. This indicates that the influence of the different parameters could be compared with each other, with good certainty.

4.4 PARAMETERS

4.4.1 Experiments conducted

The variations in the parameters that have been tested for in the experiments were mostly such that one had a higher value and one had a lower value than the standard conditions. This gave a minimum of three variations for each one of the parameters tested.

Experiments were conducted for each of the variations indicated by the settings (Table 4.5). This means that an experiment was conducted with the set of standard conditions of all the parameters (the standard experiment). Experiments were then conducted for each variation of a specific parameter, while keeping the other parameters the same as that of the standard conditions. For example, in the experiment with the oxygen flowrate at 3.12 kg/h (Test 1) the pulp density is 1.35 kg/L, the temperature is 140 °C, the oxygen partial pressure is 1.8 bar, etc.

Three experiments on the conditions of the two preleach tanks (tank 1506 and 1102) were also conducted (Table 4.6). These experiments were conducted to determine what the extent of the reaction was in these two tanks. The two experiments for tank 1102 were done with, (i) fresh matte from the original batch sample and (ii) with pulp obtained from tank 1506 in the plant. These two experiments conducted on the conditions in tank 1102 were necessary to compare the effect of the leaching of fresh matte directly in tank 1102 to that of leaching matte coming from tank 1506, as is the sequence in the plant (see Appendix B).

The acid concentration of the spent electrolyte in all the tables refers to the acid concentration of the spent electrolyte solution and not the initial acid concentration of the pulp.

4.4.2 Plant sampling

Before the experiments were conducted it was decided to undertake a thorough sampling of the whole first stage acid-oxygen leach in order to obtain the conditions, as well as the material compositions in all the parts of this process section. These results will help to verify the conditions for the experiments so that the process could be simulated exactly by the experiment. These results will also be used to compare it with the results obtained from the experiments which will then indicate if the experiments as a whole simulate the plant process.

The samples in Table 4.7 were taken over a period of eleven hours, at the beginning of each hour. The ranges in the compositions and conditions are given because these are the kind of values that could be expected. These results could not be described as representative of the minimum or maximum variations in the parameters, due to the constant variation in the parameters, the influence of the different parameters on each other, as well as the fact that these results are just for the test samples taken over a period of eleven hours. These results will therefore only give a good idea of the ranges of compositions to be expected in the experiments.

4.5 ANALYSES AND PRELIMINARY RESULTS

All the solid samples are analysed for their nickel(Ni), copper(Cu), iron(Fe), cobalt(Co) and total sulphur(S) content. These elements were chosen because they are the main components of the matte, accounting for more than 99 mass %. The PGM's, Au, As, Pb, Se, Te and other elements consist of less than 1 mass % of the total composition of the matte. The solids were analysed for Ni, Cu, Fe and Co with an ICP and for S a LECO analyser was used.

The solutions were analysed for free acid (which is sulphuric acid), total metals(TM), Cu, Fe, Co and S. The Fe, Co and some of the Cu analyses (when concentration is low) were done on the atomic absorption (AA) analyser. The free acid, Cu and S values were determined by titration and the TM were also determined by titration with an auto titrator (see Appendix C).

The solutions were analysed for TM instead of Ni (to analyse for Ni on the AA a dilution of at least 1:50 000 is needed, due to the high concentration, where on the other hand a 1:10 dilution is used for the TM titration, which will most certainly minimise possible dilution errors). The TM concentration value that was determined by titration includes all the metals in the solution (Ni, Cu, Fe, Co, PGM's, Au, etc.), which implies that to determine the Ni concentration of the solution the Cu, Fe and Co concentration should be subtracted. This method of determining the Ni concentration in the solution is possible because Ni, Cu, Fe and Co are the major metal components in the spent electrolyte (as well as in the matte). Therefore, the only element that will have a significant influence on the TM concentration other than the Ni concentration is the concentration of Cu.

4.5.1 Material composition

The analysis of the matte and the spent electrolyte solution compositions were done regularly before starting an experiment. Most of the variations in the matte composition in Table 4.8 could be ascribed to the fact that the sample used for analysis (0.2g) was not representative of the whole matte sample used in the

experiment, or to analysis errors. This is said because the mass balance of the Ni, Cu, Fe, Co and S for especially the matte samples with a high Ni concentration, ranges from approximately 103 - 111%, where it should in actual fact be just less than 100%.

4.5.2 Data smoothing

From the mass balance of the solids analyses results it was evident that the data were not very accurate, because the mass balances varied from approximately 91% - 111%. The concentrations of Ni, Cu, Fe and Co were analysed on an ICP after 0.2g of the solid sample had been fused and redissolved. Looking at the data it seems that the error in the data for each sample is consistent in the sense that when the mass balance is over 100% all the elements seem to be analysed too high, and conversely when the mass balance is below 100%.

Table 4.9 shows the comparison of the coefficient of variance of the adjusted data in relation to the original data. It also shows that the coefficient of variance for sulphur is smaller in comparison with Ni and Cu. Therefore, the sulphur analyses results were assumed to be the more stable data. The results of Table 4.9 indicate that the smoothing on the data produced an improvement. With these adjustments it was possible to obtain better mass balances for the solids and more acceptable concentrations of the different metals (see Table 4.10).

4.6 SUMMARY

This chapter showed that experiments could simulate the plant process and that the experiments can also be reproduced accuraretly. The experiments for the preleach tanks and the plant sampling that was conducted will be used in the discussion of Chapter 5 for improving the control of the preleach section. Experiment or test 9 is used to develop the leaching mechanism (Chapter 7) and kinetic model (Chapter 8), and the other experiments are used to validate the kinetic model (Chapter 9).

Table 4.1 - The average particle size distribution of the bulk sample of matte

Particle size	Distribution
+300 μm	7.0%
-300 +212 μm	10.0%
-212 +150 μm	14.0%
-150 +75 μm	24.4%
-75 +45 μm	11.8%
-45 μm	32.8%.

Table 4.2 - The final particle size distribution of the 51.2 kg batch of matte that was screened

Particle size	Mass	Distribution
+300 μm	4.08 kg	8.0 %
-300 +150 μm	11.06 kg	21.6%
-150 +106 μm	7.37 kg	14.4%
-106 +75 μm	8.16 kg	15.9%
-75 +45 μm	10.81 kg	21.1%
-45 μm	9.73 kg	19.0%

Table 4.3 - Comparison between conditions on plant autoclave and the standard conditions for the experiments

Parameter	Plant condition	Experiment condition (Test 10)
Particle size (Table 4.1)	Plant distribution	Plant distribution
Temperature	140 °C	140 °C
Pressure	4.9 - 5.0 bar	5.5 bar
Oxygen flowrate (per 40 l)	1.3 kg/h	0.59 kg/h
Pulp density	1.340 kg/L	1.35 kg/L
Acid concentration of spent electrolyte	90 - 100 g/L	101 - 105 g/L
Residence time	± 90 min	300 min (5 hours)

Table 4.4 - Conditions in the repulping/preleach tanks

	Tank 1506	Tank 1102
Pulp density	1.90 - 2.10 kg/L	1.50 - 1.65 kg/L
Temperature	71 - 78 °C	57 - 58 °C
Residence time	230 - 460 min	±180 min

Table 4.5 - Experimental conditions for the acid oxygen pressure leach tests (kinetic experiments)

Parameter	Standard (Test 10)	Variations on parameters			
Oxygen flowrate	0.59 kg/h	0.30 kg/h (test 6)	3.12 kg/h (test 1)	0.48 kg/h (test 9)	0.96 kg/h (test 27)
Pulp density Weight/weight %	1.35 kg/L 14.7%	1.30 kg/L 10.2% (test 12)	1.40 kg/L 18.9% (test 13)		
Temperature	140 °C	120 °C (test 14)	158 °C (test 15)		
O_2 partial pressure Total pressure	1.8 bar 5.5 bar	0.7 bar 4.4 bar (test 16)	4.4 bar 8.0 bar (test 21)		
H_2SO_4 concentration of spent electrolyte	105 g/L	86 g/L (test 24)	76 g/L (test 25)		
Particle size (μm)	plant	-300 +150 (test 18)	-75 +45 (test 19)	-106 +75 (test 20)	-45 (test 22)
Reaction time	300 min				

Table 4.6 - Experimental conditions for the preleach tanks

Parameter	Tank 1506 (test 7)	Tank 1102 (test 8: fresh matte)	Tank 1102 (test 23: pulp from tank 1506)
Pulp density	1.90 kg/L (48.7% w/w)	1.60 kg/L (33.1% w/w)	1.60 kg/L (33.1% w/w)
Temperature	75 °C	60 °C	60 °C
Pressure	Atmospheric	Atmospheric	Atmospheric
Acid concentration of spent electrolyte	105 g/L	105 g/L	105 g/L
Particle size	plant	plant	plant
Reaction time	720 min	720 min	480 min

Table 4.7 - Conditions on the first stage acid oxygen leach section in the plant

Parameter	Tank	Tank	Press	Autoclave	
	1506	1102	1407	#1	#4
Level (%)	50 - 102	55 - 103			
Pulp density (kg/L)	1.98 - 2.18	1.51 - 1.61			
Temp(°C)	71 - 78	57 - 58		140	
pH	2.3 - 5.6	0.6 - 1.6		1.8 - 3.0	1.6 - 3.0
SOLUTION:					
Free acid (g/L)	<1	29.9 - 80.2			
Total metals (g/L)	36.0 - 52.0	52.3 - 64			110 - 121
Copper (g/L)	0.001-0.032	0.002 - 9.6		1.0 - 11.0	0.14 - 9.3
Iron (g/L)	2.9 - 5.2	2.7 - 3.5			0.15 - 1.4
SOLIDS:					
Nickel (%)	46 - 54	42-46 (62)	36 - 38		
Copper(%)	26.6 - 28.1	27.7 - 29.8	29.1 - 32.0		
Iron (%)	0.31 - 0.34	0.15 - 0.22	0.17 - 0.18		
Cobalt (%)	0.33	0.22 - 0.31	0.14 - 0.15		

The free acid concentration in tank 1107 varied between 93 - 99 g/L.

Table 4.8 - Matte and spent electrolyte solution composition

	Matte % (solids)	Spent electrolyte g/L (solution)
Acid (H_2SO_4)		103 - 109
Total metals (TM)		49.0 - 49.6
Nickel (Ni)	45.0 - 58.7	
Copper (Cu)	23.4 - 34.1	21.0 - 21.6
Iron (Fe)	0.46 - 0.73	0.51 - 0.53
Cobalt (Co)	0.32 - 0.40	0.22 - 0.23
Sulphur (S)	19.8 - 22.3	

Table 4.9 - Comparison of the coefficient of variance for Ni, Cu and total sulphur and the coefficient of variance of the adjusted sets of data

Sample time Element	0 min Original	0 min Adjusted	5 min Original	5 min Adjusted	10 min Original	10 min Adjusted
Ni	9.24 %	2.44 %	6.17 %	4.34 %	9.22 %	5.66 %
Cu	8.20 %	4.71 %	10.42 %	5.54 %	10.82 %	5.36 %
Sulphur	2.74 %	2.74 %	3.45 %	3.45 %	4.23 %	4.23 %

Table 4.10 - A comparison of the original results of the solids analyses with the adjusted results after implementing the data smoothing calculation for one specific experiment (test 9)

Sample time min	Nickel Ni %	Copper Cu %	Iron Fe %	Cobalt Co %	Sulphur S %	Mass balance 100 %
0	58.7	30.0	0.581	0.375	21.7	111.4
5	49.3	36.3	0.143	0.206	24.0	109.9
10	42.5	40.7	0.100	0.182	23.5	107.0
20	36.1	44.6	0.074	0.129	23.5	104.4
40	33.6	46.5	0.292	0.048	24.4	104.8
80	27.7	48.8	0.050	0.028	24.6	101.2
120	24.6	51.7	0.054	0.036	26.0	102.4
160	20.5	54.2	0.046	0.048	30.4	105.2
200	17.4	54.1	0.695	0.046	30.6	102.8
240	14.7	49.3	4.480	0.036	28.2	96.7
300	13.3	47.8	5.270	0.034	27.3	93.7
Adjusted data set						
0	51.3	26.2	0.507	0.327	21.7	100.0
5	43.6	32.1	0.126	0.182	24.0	100.0
10	38.9	37.3	0.091	0.166	23.5	100.0
20	34.1	42.2	0.069	0.122	23.5	100.0
40	31.6	43.7	0.274	0.045	24.4	100.0
80	27.3	48.0	0.049	0.028	24.6	100.0
120	23.8	50.1	0.052	0.035	26.0	100.0
160	19.1	50.4	0.042	0.044	30.4	100.0
200	16.7	52.0	0.668	0.044	30.6	100.0
240	15.4	51.7	4.694	0.038	28.2	100.0
300	14.6	52.3	5.769	0.037	27.3	100.0

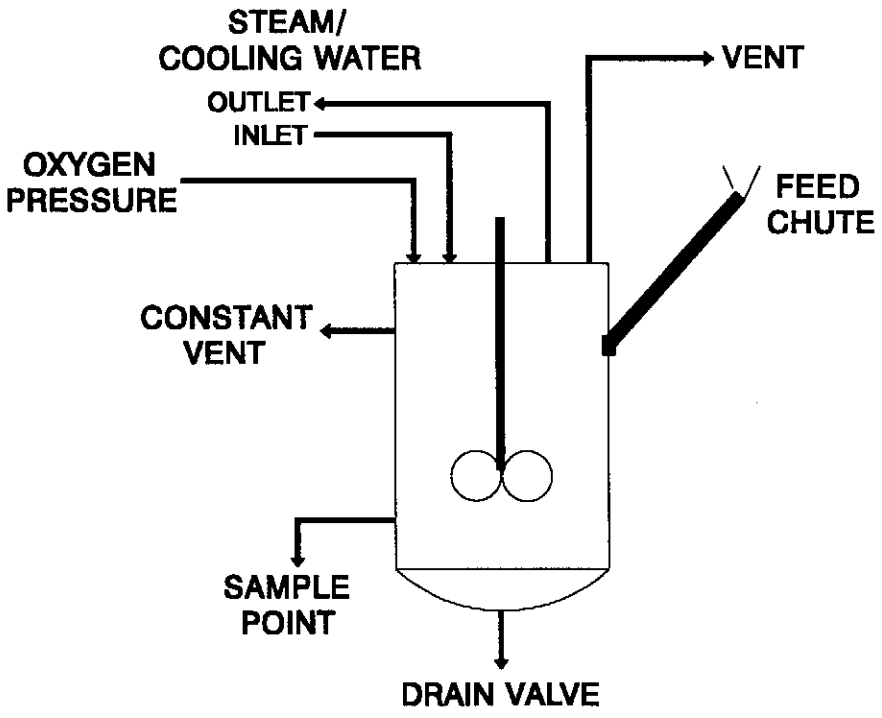

Figure 4.1 - A simplified drawing of the experimental autoclave

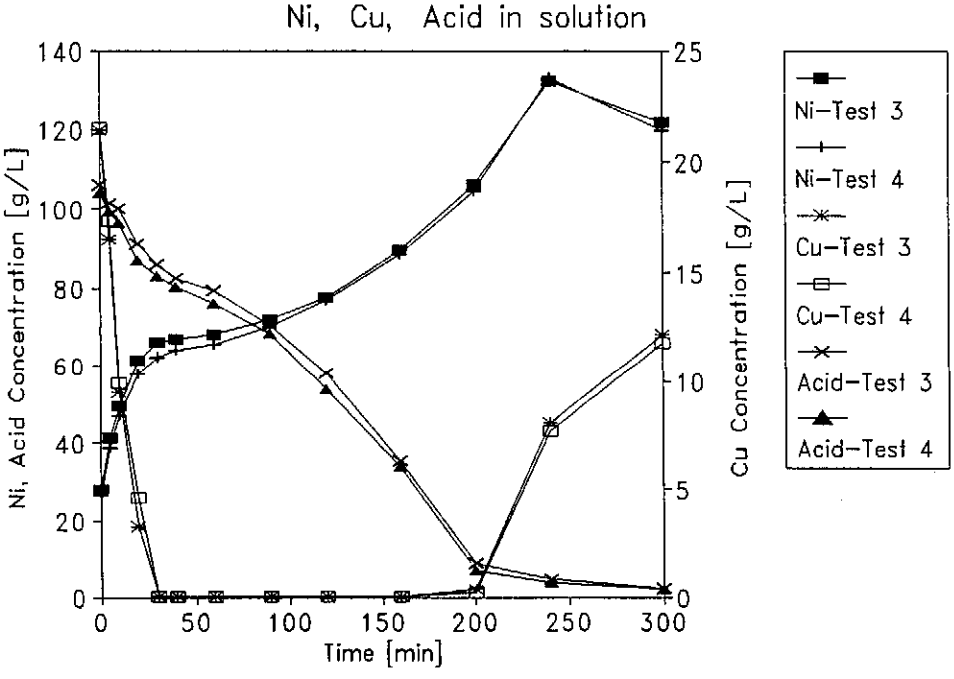

Figure 4.2 - Comparing the results of the solution analysis of tests 3 and 4 to determine the reproducibility of the experimental procedure

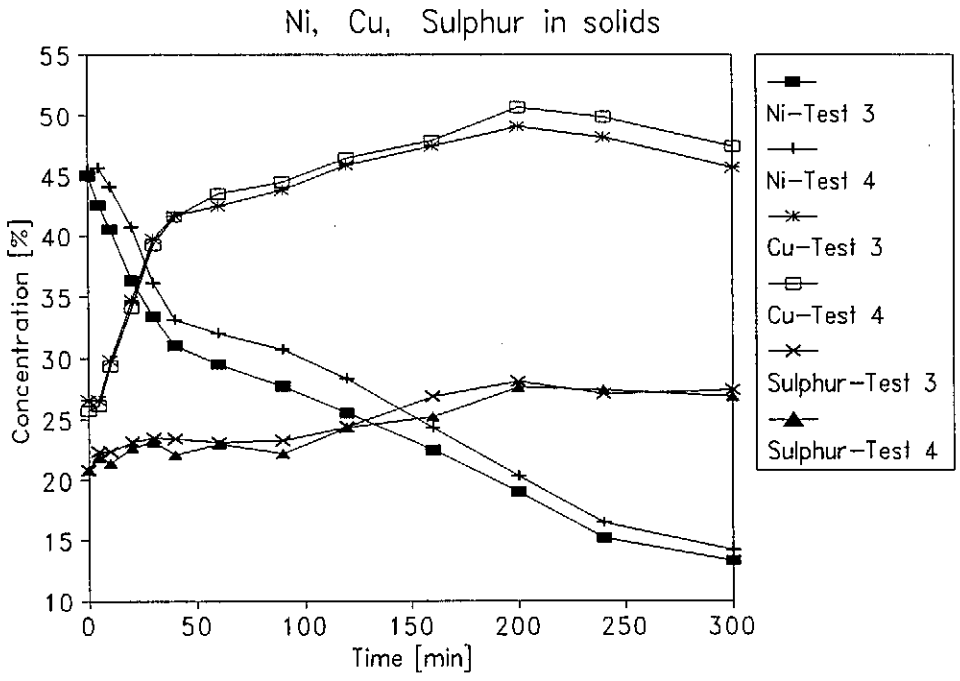

Figure 4.3 - Comparing the results of the solids analysis of tests 3 and 4 to determine the reproducibility of the experimental procedure

Chapter 5

OFF-LINE COMPUTER SIMULATION OF THE REPULP SECTION OF THE PLANT

5.1 INTRODUCTION

Problems in the repulp (preleach) section have been identified from experience on the plant as a control problem (see Chapter 3). Controlling the repulping section is of special importance in unit processes with fast kinetics which are preceded by the repulping section. The fast reaction kinetics make it essential to control the conditions of the incoming pulp to the autoclave.

The main objective of the computer simulation described in this chapter is to restrict perturbations coming from the repulping section to the leaching process, which could cause instabilities in the leaching process. The aim of the simulation program is to prevent perturbations from leaving the repulp section, rather than to rectify for these perturbations in the leaching process.

Two methods were investigated for the calculation of the mathematical model. The obvious method would be to use Laplace transforms for the calculation procedure, or the alternative method is to use a numerical method for the calculation procedure. However, to use the Runge-Kutta(RK) procedure to predict the different settings in the repulp section, an optimisation procedure was necessary. A one-dimensional region elimination method, the Golden Section Search(GSS) method was chosen due to the following: (i) it is an easy method to compile in a program, (ii) calculation and optimisation method (or time) is fast, and (iii) this method's accuracy is sufficient for this specific problem.

The repulping section which will be discussed in this investigation (see Fig. 5.1) consists of a feed stream from the mill into tank 1506. From tank 1506 the milled

pulp stream is passed through a stream splitter into tank 1102 and finally to the autoclave. Tanks 1506 and 1102 can also be described as two CSTR's (continuous stirred-tank reactors) due to the reactions that occur in these tanks, therefore the repulp section can also be called the preleach section. The basic leaching reactions occurring in the repulp section (preleach) and leaching process following the repulping section have been discussed in Chapter 2.

The purpose of the simulation is to maintain the optimum reaction conditions in these two tanks. Therefore the optimum reaction conditions for tanks 1506 and 1102 would be where the maximum leaching of Ni and maximum cementation of Cu occur. At the current operating conditions the approximate residence times in tanks 1506 and 1102 are 240-300 minutes and 150-180 minutes, respectively.

5.2 THE NEED FOR PROCESS CONTROL

Batch experiments emulating the conditions in tanks 1506 and 1102 confirmed that substantial reactions occur in these two tanks. The leaching efficiencies of Ni for tanks 1506 and 1102 with the indicated residence times are 7.2% (with a pulp density of 1.90 kg/L or 1900 kg/m^3) and 6.5% (with a pulp density of 1.60 kg/L or 1600 kg/m^3), respectively. The data for Fig. 5.2 - Fig. 5.5 were obtained from batch experiments emulating the conditions in tanks 1506 and 1102 and the leaching vessel. Figure 5.2 indicates the variation in the concentration of Ni in the solid phase, the concentration of Cu in the solution and the pH changes with time. Figure 5.3 shows the variation in the concentration of Ni in the solid phase and the concentrations of Cu and acid in the solution phase for tank 1102. From Fig. 5.2 and Fig. 5.3 the leaching rate of Ni, the cementation rate of Cu out of the solution and the pH increase (acid decrease) are evident. The results as presented in Fig. 5.2 and Fig. 5.3 emphasise the need for controlling the residence time (tank levels) in tanks 1506 and 1102.

The aim of this leaching process is to leach Ni and at the same time to keep Cu cemented in the solid state. Therefore, the problem that arises from the repulping section, is that the pulp from tank 1102 sometimes still contains a high concentration

of Cu in the solution when it arrives at the leaching vessel. In such a case the leaching process would not be able to cement Cu out of the solution in the leaching time available in the actual leaching vessel.

The need to control the repulp section is confirmed by the results in Table 5.1, which gives the assays of samples taken from tanks 1506 and 1102 on the plant. From Table 5.1, at times 8, 9 and 10 hours, the solution analyses of tank 1102 indicate a large increase in Cu and acid concentrations which will result in a perturbation to the leaching process, following the repulping of the material. This perturbation could be ascribed to the higher pulp density in tank 1506, because less acid (spent electrolyte) was added to this tank and less reaction could thus occur. When the pulp was pumped to tank 1102, more spent electrolyte solution was needed in this tank to maintain the desired pulp density, which increased the acid concentration, as well as the concentration of Cu in this tank (spent electrolyte solution contains approximately 21g/L of Cu). This inevitably led to a higher concentration of Cu in the first compartment of the autoclave.

The effect of the variation in the pulp density is most evident in the autoclave according to the batch experiments conducted, emulating the autoclave with variations in the pulp density. The results from these experiments indicate that the leaching rate of Ni (Fig. 5.4) increase with a decrease in the pulp density of the reaction mixture. Figure 5.5 indicates on the other hand that the cementation of Cu is faster and more complete at higher pulp densities. The reason for this could be that, for a lower pulp density more spent electrolyte solution is added, which means that more Cu is added, which in turn must be cemented in the leaching process. These results confirm the necessity of controlling the density of the pulp going to the autoclave in order to obtain the maximum leaching of Ni, while keeping the concentration of Cu in the solution below a certain concentration.

5.2.1 Control strategy

The simulation will be used as a tool to help the operator to control the tank levels (which in effect will mean the residence time in the tanks) and pulp densities in the

repulping section. The tank levels and pulp densities are controlled by calculating the flowrates of the pulp and spent electrolyte streams to and from tanks 1506 and 1102 so that the desired conditions could be maintained, or reached. Therefore, the rationale for developing the computer program to control the repulp section is to obtain a pulp stream flowing to the autoclave with a constant pulp density and a constant chemical composition.

One function of this model is to maintain the pulp densities in tank 1506 and especially tank 1102, at the desired pulp density. The desired pulp density in tank 1102 is achieved by changing the feedrates of the pulp from tank 1506 and the spent electrolyte feed stream. Maintaining the desired pulp density in tank 1506 is difficult because the pulp stream coming from the milling circuit is not continuous, as well as the untimely re-entering of recycled solids from the Cu cementation circuit to tank 1506. The recycle of solids to tank 1506 and the spent electrolyte solution used to wash (and repulp) the solids into tank 1506, are taken as continuous inputs (although they are actually a step input), in order to simplify the calculating procedure.

Controlling the tanks at specific pulp levels is as important as maintaining the desired pulp densities, because the variations in the tank levels will influence the residence time of the pulp in both tanks 1506 and 1102, and therefore the extent of the reaction. Because of the non-continuous pulp stream coming from the milling section to tank 1506, the level of tank 1506 cannot be controlled at a specific level. The milling operation starts when the level is below the minimum level and stops when the level reaches the maximum level. The desired level of tank 1102 is obtained by manipulating the pulp and spent electrolyte feedrates to tank 1102.

5.3 OUTLINE OF SIMULATION PROGRAM

The attraction of this control method is that it requires only a personal computer (a PC with a 386 or higher processor). An operator familiar with a computer can be used successfully to maintain the system. Furthermore, it is inexpensive to implement, because no physical changes in the process equipment are necessary

with only a computer that must be acquired. The trained operator can use the package to determine optimum conditions on the PC with plant data. This enables him to make the necessary changes to the plant process control equipment quickly and correctly, if needed.

5.3.1 Input

The user has different options to enter the input values for calculations in the input section for the simulation program, depending on what information the user wishes to obtain. Therefore, the input options for the program are divided into three sections, i.e.:

(i) calculating the flowrate settings and predicting the time when milling operation will commence and end,

(ii) calculating the flowrate settings with the milling time known, and

(iii) calculating the conditions in this section when the flowrate settings are guessed.

5.3.2 Output

The outputs of the program will include the calculated settings for the flowrates, as well as the predicted conditions in tanks 1506 and 1102 at the end of the time period. As outputs the user has the following options to view the calculated results:

1) Mill conditions, milling times and conditions for tanks 1506 and 1102
2) Mill conditions and milling times
3) Conditions in tanks 1506 and 1102
4) Graph of the pulp density change with time for tanks 1506 and 1102
5) Graph for the tank level changes with time in tanks 1506 and 1102

The computer code for the program which has been written in Borland Turbo Pascal 7.0 (Yester, 1991) is given in Appendix D.

5.4 MATHEMATICAL MODEL

Two assumptions were made during the compilation of the mathematical model to control the repulp section:

(i) all the feed streams to and from tanks 1506 and 1102 are continuous, except for the pulp stream from the mill to tank 1506,

(ii) variations of pulp densities in the tanks will not directly affect the variation in the tank levels (the volume is independent of the pulp density).

The values of the different variables for the milling process are calculated with a steady state mass balance over the mill.

The demineralised water feedrate to the mill is:

$$F_W = \frac{F_M(1 - P_3/P_M)}{(P_3 - P_W)} \tag{5.1}$$

The pulp flowrate from the mill to tank 1506 is:

$$F_3 = F_W + F_M/P_M \tag{5.2}$$

The values of the different variables for tanks 1506 and 1102 are calculated with dynamic mass balance equations over tanks 1506 and 1102, respectively.

The dynamic state equations for tank 1506 are as follows:

$$\frac{d(P_2V)}{dt} = P_1F_1 + P_3F_3 + P_4F_4 + P_5F_5 - P_2F_2 \tag{5.3}$$

$$\frac{dV}{dt} = F_1 + F_3 + F_4 + F_5 - F_2 \tag{5.4}$$

Equation (5.4) was derived from eq. (5.3) with the assumption that the change in the pulp volume is independent of a change in pulp density. This is assumed because no extensive leaching occurs in either tank 1506 or 1102, therefore the leaching would not have a noticeable effect on the pulp density of the pulp in either of the tanks. Therefore by substituting eq. (5.4) into eq. (5.3) an equation for the density changes of the pulp (due to the flowrates of the different streams entering the tank), eq. (5.5), in tank 1506 can be obtained.

$$\frac{dP_2}{dt} = \frac{F_1}{V}(P_1 - P_2) + \frac{F_3}{V}(P_3 - P_2) + \frac{F_4}{V}(P_4 - P_2) + \frac{F_5}{V}(P_5 - P_2) \qquad (5.5)$$

The dynamic state equations for tank 1102 are as follows:

$$\frac{d(P_7 V_1)}{dt} = P_2 F_2 + P_6 F_6 - P_7 F_7 \qquad (5.6)$$

$$\frac{dV_1}{dt} = F_2 + F_6 - F_7 \qquad (5.7)$$

Equation (5.7) was derived from eq. (5.6) again with the same reasoning as discussed above for tank 1506. Therefore by substituting eq. (5.7) into eq. (5.6) an equation for the density changes of the pulp in tank 1102, eq. (5.8), can be obtained.

$$\frac{dP_7}{dt} = \frac{F_2}{V_1}(P_2 - P_7) + \frac{F_6}{V_1}(P_6 - P_7) \qquad (5.8)$$

Equations (5.4), (5.5), (5.7) and (5.8) could now be solved with the fourth order Runge-Kutta procedure.

5.5 CALCULATION METHOD

5.5.1 Runge-Kutta

The numerical method that was chosen to solve the differential equations was the fourth order Runge-Kutta method. This method is also the most widely used in computer solutions to differential equations (Gerald and Wheatly, 1984).

The Runge-Kutta(RK) calculation procedure is used to calculate the pulp volume of tank 1506 (V) and tank 1102 (V_1), the pulp density in tank 1506 (P_2) and tank 1102 (P_7). (The tank level has a linear relation to the tank volume and is as follows: tank 1506, $h = \frac{V}{Volume\ of\ tank\ 1}$ and tank 1102, $h_1 = \frac{V_1}{Volume\ of\ tank\ 2}$.). However, before these variables could be calculated the optimum input settings for the manipulated variables must be determined (spent electrolyte flowrate to tank 1506 (F_1), pulp flowrate from tank 1506 to tank 1102 (F_2) and the spent electrolyte flowrate to tank 1102 (F_6)).

5.5.2 Golden Section Search

The optimum flowrate settings for the manipulated variables (F_1, F_2 and F_6) are determined through a region elimination optimisation method, called the Golden Section Search(GSS) (Edgar and Himmelblau, 1989). The strategy employed in the GSS is to locate the two interior points so that the interval eliminated on one iteration will be of the same proportion regardless of the interval length. For any particular interval L^k, a^k and b^k are the current bounds of the interval at stage k in the search and the two interior points are located at $x_1^k = a^k + X_s L^k$ and $x_2^k = b^k - X_s L^k$. Where the fraction $X_s = \frac{3-\sqrt{5}}{2} \approx 0.382$ was known in ancient times as the "golden section".

Determining the function values for $f(x_1^k)$ and $f(x_2^k)$ and seeing that $\left|f(x_1^k) - P_{T1}\right| > \left|f(x_2^k) - P_{T1}\right|$, hence for minimising, at the next step $a^{k+1} = x_1^k$ and

$b^{k+1} = b^k$. The interior point x_2^k is replaced by x_1^{k+1} and we select the new interior point as $x_2^{k+1} = b^{k+1} - X_s(b^{k+1} - a^{k+1})$.

This procedure is repeated until the difference between the calculated value ($f(x^k)$) and the desired value (P_{T1} or P_T) is less than the specified margin of error.

5.5.3 Calculation sequence

A short description of the calculation sequence in the program and the relevant rationale for the sequences which are presented in Fig. 5.6a - Fig. 5.6e, are discussed below.

Input options 1 and 2: (see Fig. 5.6a)

The whole procedure is iterative and begins where starting values for the manipulated variables are determined with the GSS method (Fig. 5.6b) in that specific range of the variable (minimum and maximum). The starting values for the pulp flowrate from tank 1506 to tank 1102 (F_2) and the spent electrolyte flowrate to tank 1102 (F_6) are calculated first (F_2 and F_6 are the manipulated variables for tank 1102), because F_2 is necessary to perform the RK calculation on tank 1506.

A value for the spent electrolyte flowrate to tank 1506 (F_1) is determined (F_1 is the manipulated variable for tank 1506) with the GSS method (Fig. 5.6d), before the RK calculation (Fig. 5.6e) for tank 1506 is conducted. The RK calculation determines the pulp density (P_2) and the level (h) of the pulp in tank 1506. The pulp density in tank 1506 (P_2) calculated from the objective function is then used as the value which is compared with the desired value. If the calculated value is not within the margin of accuracy (99.95%) which is specified, the GSS method continues to optimise for the spent electrolyte flowrate to tank 1506 (F_1). The pulp density in tank 1506 (P_2) is used as the measure of accuracy for the GSS optimisation process. The spent electrolyte flowrate to tank 1506 (F_1) is the variable to be optimised and is dependent on the level of the pulp in tank 1506 (h). The maximum flowrate of spent electrolyte to tank 1506 (F_1) is determined according to the available volume in tank

1506; $\frac{V_{TOT}-VOL}{Time}+F_2-(F_3+F_4+F_5)$. This procedure will continue until the set condition is reached or it will terminate after a specified number of iterations (C_1) was performed.

After the spent electrolyte flowrate to tank 1506 (F_1) has been calculated, the RK calculation for tank 1102 is conducted (Fig. 5.6c). Due to the fact that the pulp density in tank 1506 (P_2) is a disturbance to tank 1102 the RK calculations for both tanks 1102 and 1506 are performed simultaneously for each time step, so that the influence of the variation of the pulp density in tank 1506 (P_2) on tank 1102 could be taken into account in the calculations. The objective function in the RK calculation for tank 1102 will calculate the pulp density (P_7) and the level of the pulp (h_1) in tank 1102. The calculated value of the pulp density in tank 1102 (P_7) is used to compare with the desired value to determine if the chosen combination of F_1, F_6 and F_2 satisfies the required margin of accuracy. The flowrates of the pulp from tank 1506 to tank 1102 (F_2) and the spent electrolyte to tank 1102 (F_6) are dependent on the available volume in tank 1102, as well as the flowrate from the pulp from tank 1102 to the leaching vessel ($\frac{V_{T1}-VOL1}{Time}+F_7$). If the set condition is not met, the GSS procedure for determining the pulp flowrate from tank 1506 to tank 1102 (F_2) and the spent electrolyte flowrate to tank 1102 (F_6) will continue, therefore, repeating the whole process described thus far.

This whole procedure above will continue until the optimum values for F_1, F_2 and F_6 are obtained (specific conditions are satisfied) or until the specified number of iterations (C_2) have been completed (measure to stop the program from running *ad infinitum* if no exact solution is possible).

Input option 3: (see Fig. 5.6a)

In this section the input values for the spent electrolyte flowrate to tank 1506 (F_1), the pulp flowrate from tank 1506 to tank 1102 (F_2) and the spent electrolyte flowrate to tank 1102 (F_6) are given by the user, therefore the program will only perform the RK calculations for tanks 1506 and 1102 to determine the end conditions (pulp

densities in tanks 1506 (P_2) and 1102 (P_7) and the pulp levels in tanks 1506 (h) and 1102 (h_1)) of the process.

5.6 LAPLACE TRANSFORMS

The Laplace transformation of the mathematical model is a linear model that approximates the dynamic behaviour of a non-linear system in the neighbourhood of specified operating conditions. Linearisation is widely used in the design of control systems for the following reasons (Stephanopoulos, 1984):

(i) Closed-form, analytical solutions are possible for linear systems. This is not possible for non-linear systems, and computer simulation provides us only with the behaviour of the system at specified values of inputs and parameters.

(ii) All the significant developments toward the design of effective control systems have been limited to linear processes.

The one major disadvantage of the Laplace transform solution of the mathematical model is that the necessary accuracy cannot be obtained. Furthermore the Runge-Kutta(RK) solution (including the GSS optimisation method) of the mathematical model is more accurate than the Laplace solution, as can be seen from Table 5.2, by comparing the results of the two calculation methods for the pulp densities in tank 1102 (P_7 - highlighted columns). In almost all the cases the RK solution calculated the pulp density in the required margin of accuracy (99.95%), except for three situations where it was physically impossible to reach the desired pulp density in the specific time period. This in effect will mean that the flowrate settings (F_2 and F_6) calculated by the RK procedure are constantly more accurate than the Laplace solution.

The problem with the inaccurate solution of the mathematical model with Laplace transforms is due to the fact that the values that are used to linearise the model around the steady state conditions of the process are not close enough to the initial values. This happens in any linearisation procedure where the point at which the linearisation occurred is not close enough to the point of calculation. Therefore, the

further the initial value is from the point of linearisation the more likely it is that the inaccuracy of the calculation will increase.

5.7 PROGRAM IMPLEMENTATION

The simulation program was implemented in the plant for a period of 16 hours to determine the effectiveness of the simulator. Because little or no automatic measuring equipment is in use in this section of the plant, it was quite difficult to perform a test run with the program. The flowrates of all the streams had to be measured (with a bucket and a stopwatch) and the valves had to be calibrated manually. The valves had to be calibrated so that the settings calculated by the program could be made reasonably accurately. The experimental and simulated results for the two tanks are presented in Fig. 5.7 - Fig. 5.10.

The program gives a good simulation of the tank level changes in tank 1506 (Fig. 5.7) and a reasonable simulation of the tank level in tank 1102 (Fig. 5.8). From Fig. 5.7 it is evident that the predicted tank level of tank 1506 is for practical purposes sufficiently accurate. The predicted tank levels for tank 1102 show some variations from the actual levels of the pulp in the tank. The desired pulp level in tank 1102, which is being controlled by the simulation program, is 80.0%. The constant variation in the actual level of tank 1102 is due to the sensitive nature of the setting on the splitter box; i.e. the screen box of the pump feeding the splitter box tends to get choked, therefore decreasing the flowrate to the stream splitter. The pump is designed to pump at approximately 300 L/min. A stream with a flowrate of approximately 30 L/min is splitted from the main stream from the pump, hence a small variation in the pump flowrate will have a significant influence on the level in tank 1102. This is confirmed by the results for the predicted level of tank 1506 (Fig. 5.7) and the actual level of tank 1102 (Fig. 5.8). At 15 hours the predicted level of tank 1506 is 35.5% and the actual level 57.0% and for tank 1102 it is the opposite where the predicted level is 80.0% and the actual level is 64.0%. Practically this indicates two possibilities for these variations: (i) the calibrated settings on the valve of the spent electrolyte solution flowrate to the tank 1506 are inaccurate, and (ii) the

setting on the stream splitter did not deliver the desired flowrate to tank 1102 due to choking of the pump feeding the stream splitter.

The desired pulp densities for tanks 1506 and 1102 are 2.00 kg/L and 1.60 kg/L, respectively. For both tanks 1506 and 1102 the program gives good simulation results for the pulp density changes in the tanks. The variations in the pulp density of tank 1506 (Fig. 5.9) could be ascribed to: (i) the solids recycled from the Cu cementation circuit to tank 1506 are not recycled on a continuous basis, and (ii) the amount of spent electrolyte solution used to wash the recycled solids into tank 1506 is not always the same.

The variations of the actual pulp density values in tank 1102 (Fig. 5.10) from the predicted values are mainly due to the ineffective stream splitting of the stream splitter and to the variations of the actual pulp densities from the calculated pulp densities in tank 1506.

5.8 SUMMARY

The simulation program gives a reasonable prediction of the actual process, in spite of the influence of the practical problems. More accurate and better control with the simulation program will be obtained if the control instrumentation of the process is more advanced. The calculation of the mathematical model for simulation purposes indicated that the Runge-Kutta calculation method, which incorporates the Golden Section search optimisation procedure, is better than the Laplace transformation calculation for this specific type of control.

This chapter illustrated that the control of the preleach section is important to obtain a stable process. Furthermore, the computer simulation program showed that it could be used as a tool to help the operator in the effective control of this section of the process. The effect that variations in the pulp densities and tank levels have on the leaching efficiency of nickel, copper and iron will be determined in the next chapter (Chapter 6).

Table 5.1 - Solution samples taken from the repulp section every hour

Time hours	Tank 1506 Level %	Pulp density kg/L	Cu g/L	pH	Tank 1102 Level %	Pulp density kg/L	Cu g/L	Acid g/L
1	84	2.06	0.001	4.7	74	1.51	0.012	41.0
2	90	2.05	0.004	3.1	103	1.56	0.002	45.6
3	102	2.05	0.007	4.6	72	1.57	0.007	32.9
4	92	2.02	0.032	4.0	99	1.58	0.003	29.9
5	62	2.02	0.003	5.6	55	1.61	0.006	35.1
6	50	1.98	0.003	2.3	96	1.56	0.006	58.6
7	87	2.12	0.004	3.2	64	1.60	0.005	41.2
8	90	2.18	0.011	5.5	59	1.61	2.5	80.2
9	70	2.17	0.007	5.5	84	1.60	6.1	85.0
10	65	2.10	0.002	5.5	100	1.61	9.6	82.7

Table 5.2 - Sensitivity analysis and comparison of the Laplace transform solution and the Runge-Kutta solution on the mathematical model for tank 1102

Set conditions for calculations:	F_7 = 52 L/min
	P_2 = 1.90 kg/L
	P_6 = 1.20 kg/L
	Calculation time = 60 minutes
Desired conditions for calculations:	h_1 = 75 %
	P_7 = 1.60 kg/L
	Margin of accuracy($P7$) > 99.95%

Initial	**Initial**	**Laplace solution**				**Runge-Kutta solution**			
P_7	h_1	F_6	F_2	P_7	h_1	F_6	F_2	P_7	h_1
1.600	75	0.0223	0.0297	1.5999	75.00	0.0223	0.0297	1.5999	75.00
1.700	75	0.0335	0.0185	1.6147	75.00	0.0367	0.0153	1.6001	75.00
1.500	75	0.0110	0.0410	1.5856	75.00	0.0079	0.0442	1.6000	75.00
1.600	73	0.0209	0.0356	1.6129	75.04	0.0236	0.0317	1.6005	75.00
1.600	77	0.0237	0.0250	1.5870	75.02	0.0209	0.0278	1.6000	75.00
1.700	73	0.0321	0.0232	1.6258	74.98	0.0377	0.0176	1.6004	75.00
1.700	77	0.0350	0.0137	1.6030	75.02	0.0356	0.0131	1.6004	75.00
1.500	73	0.0096	0.0457	1.6001	74.98	0.0096	0.0457	1.6000	75.00
1.500	77	0.0125	0.0362	1.5702	75.02	0.0061	0.0426	1.6000	75.00
1.800	75	0.0448	0.0072	1.6290	75.00	0.0512	0.0008	1.5999	75.00
1.400	75	0	0.0520	1.5699	75.00	0	0.0520	1.5699	75.00
1.600	65	0.0151	0.0535	1.6637	74.96	0.0294	0.0393	1.6003	75.00
1.600	85	0.0294	0.0059	1.5329	74.98	0.0151	0.0202	1.6002	75.00
1.800	65	0.0377	0.0310	1.6759	75.02	0.0547	0.0139	1.6001	75.00
1.800	85	0.0353	0	1.6578	74.98	0.0353	0	1.6577	75.00
1.400	65	0	0.0687	1.6183	75.02	0.0041	0.0645	1.5999	75.00
1.400	85	0.0069	0.0284	1.4861	74.98	0	0.0353	1.5186	75.00

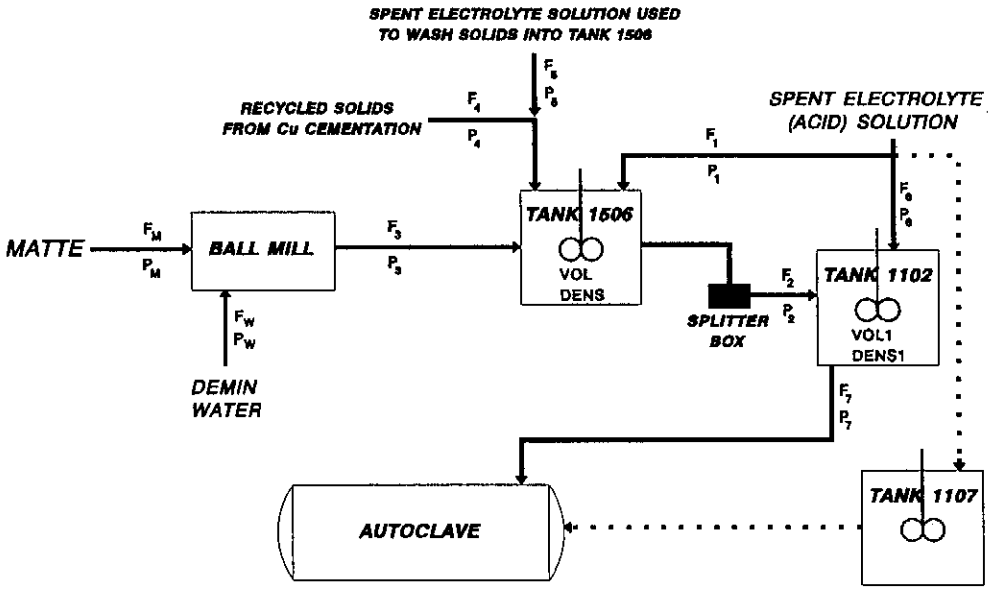

Figure 5.1 - Repulping section of the plant

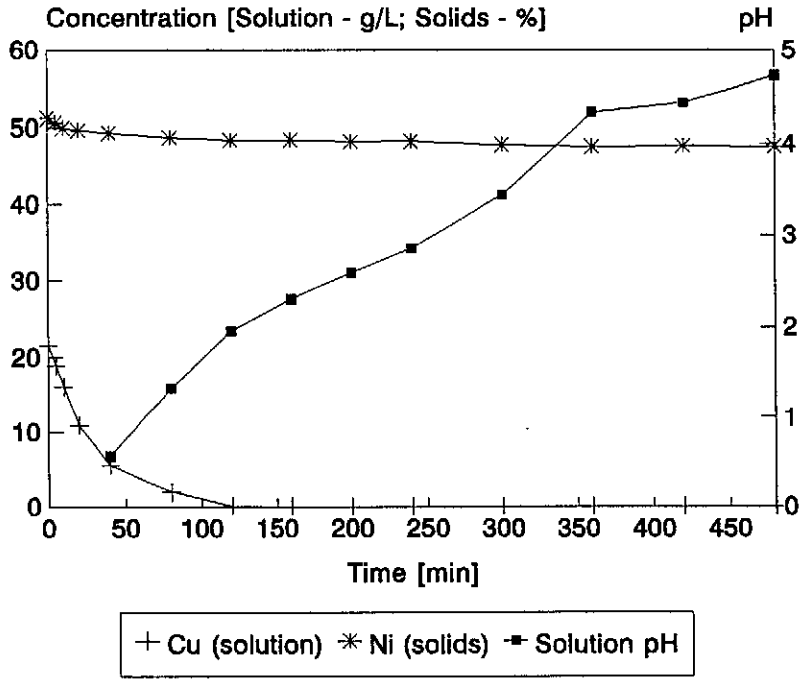

Figure 5.2 - The experimental batch emulation of **tank 1506**

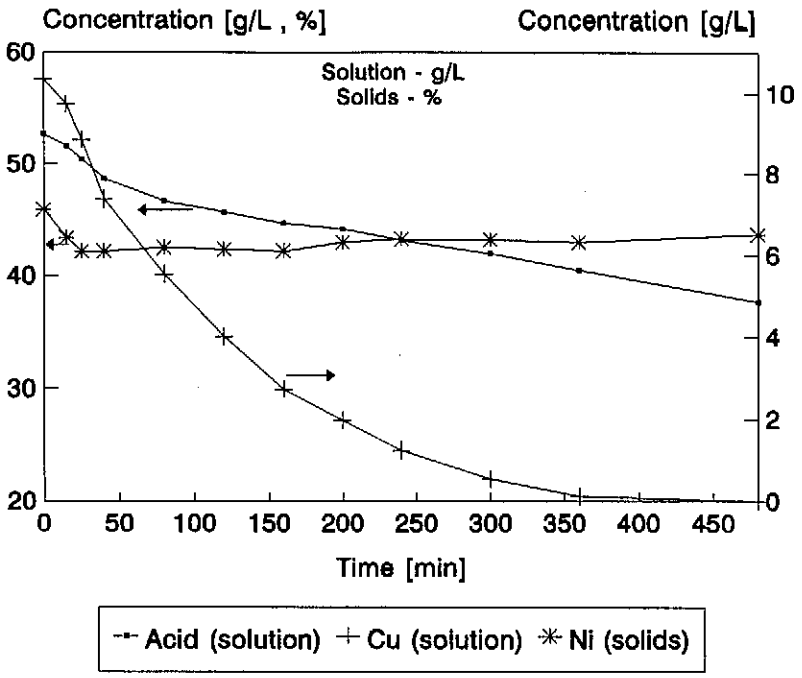

Figure 5.3 - The experimental batch emulation of **tank 1102**

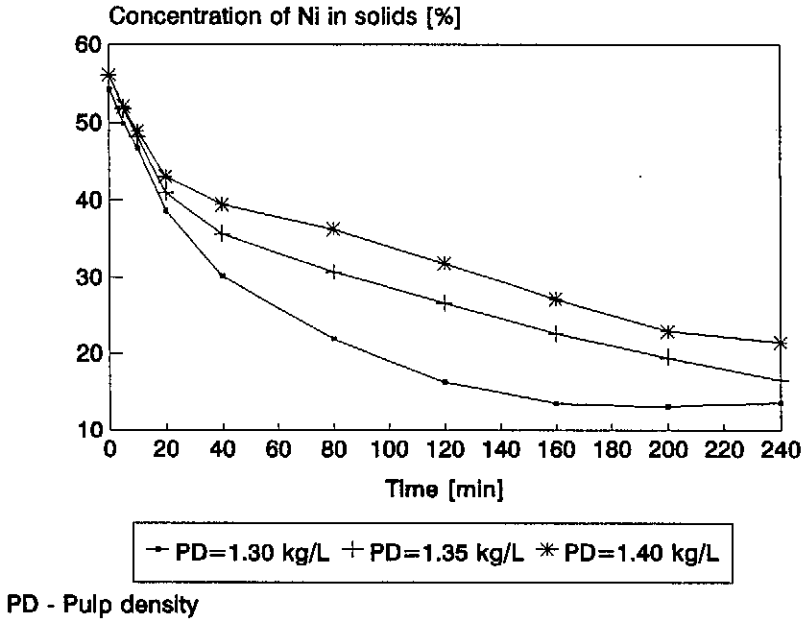

Figure 5.4 - The effect of pulp density on the leaching characteristics of Ni in the autoclave, as emulated in a batch test

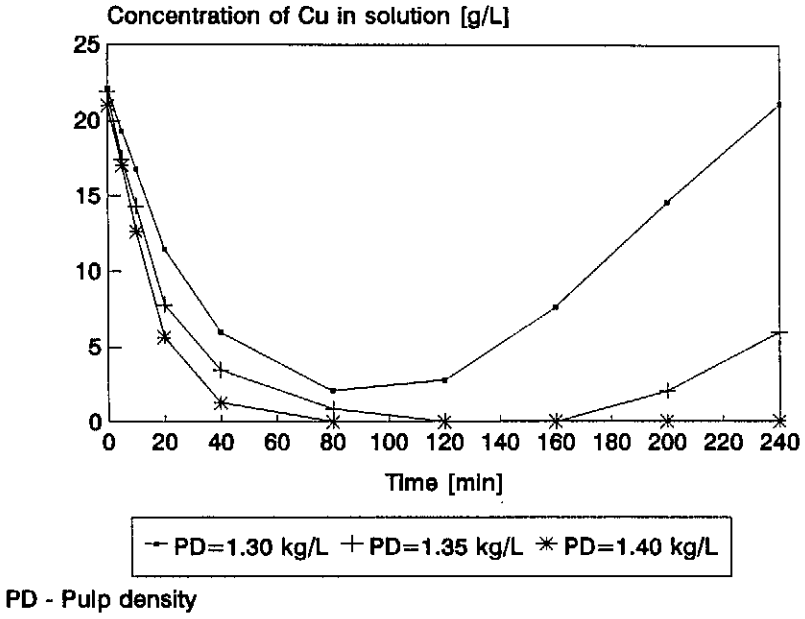

Figure 5.5 - The effect of pulp density on the cementation of Cu in the autoclave, as emulated in a batch test

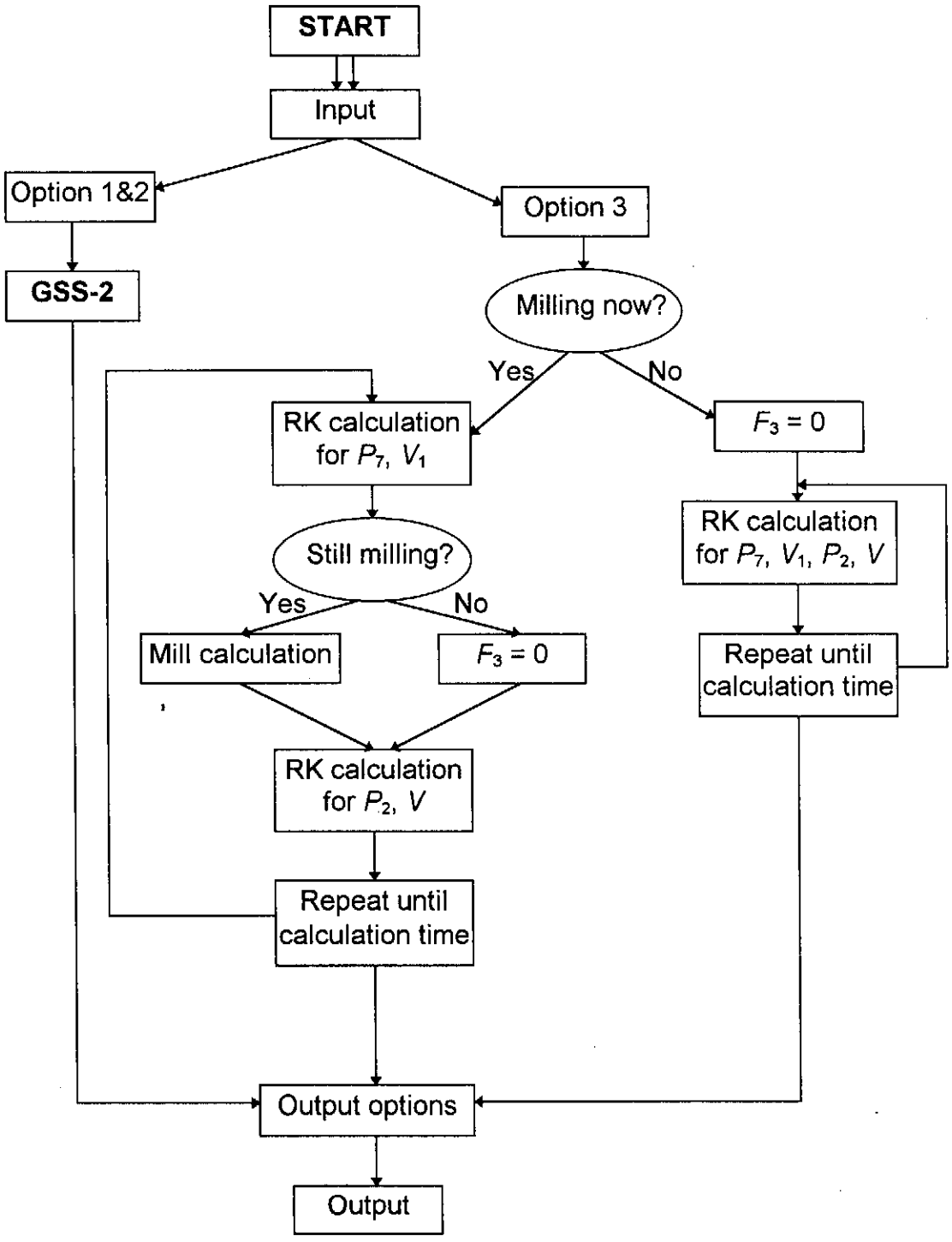

Figure 5.6a - Flow diagram of the main program of the computer simulation to control the repulping section of a plant

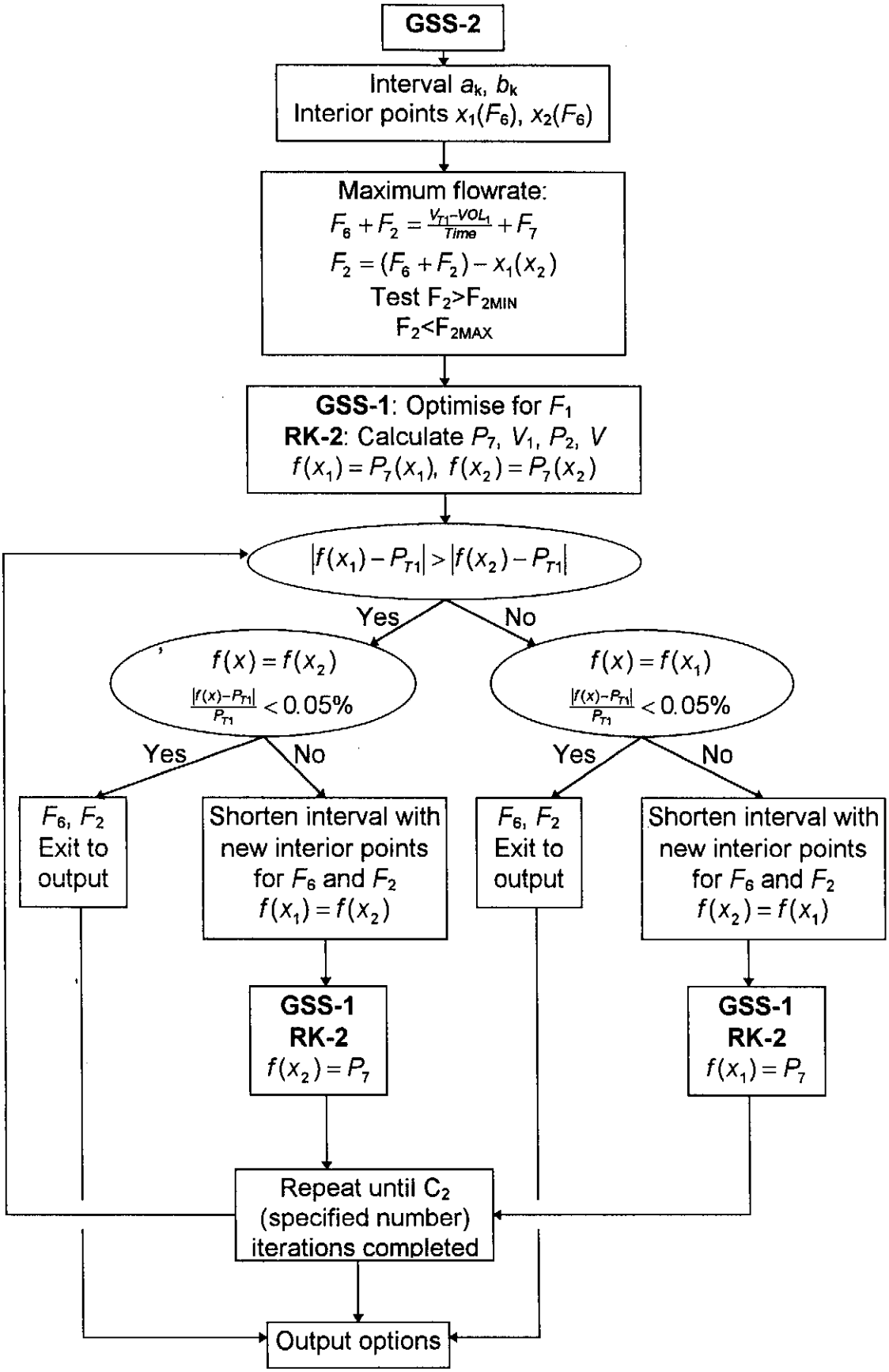

Figure 5.6b - Flow diagram of the Golden Section Search procedure 2 (GSS-2) of the computer simulation

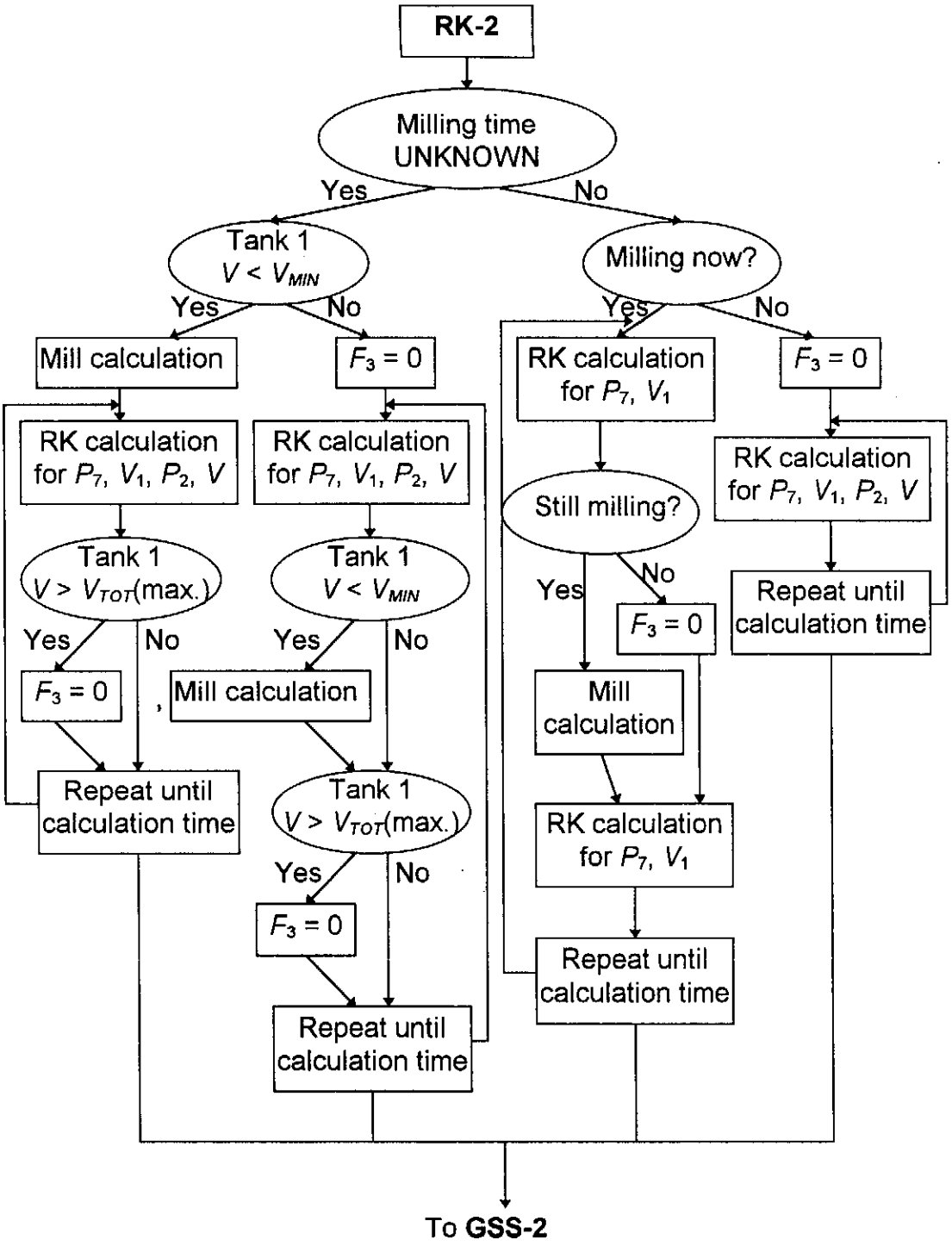

Figure 5.6c - Flow diagram of the Runge-Kutta procedure 2 (RK-2) of the computer simulation

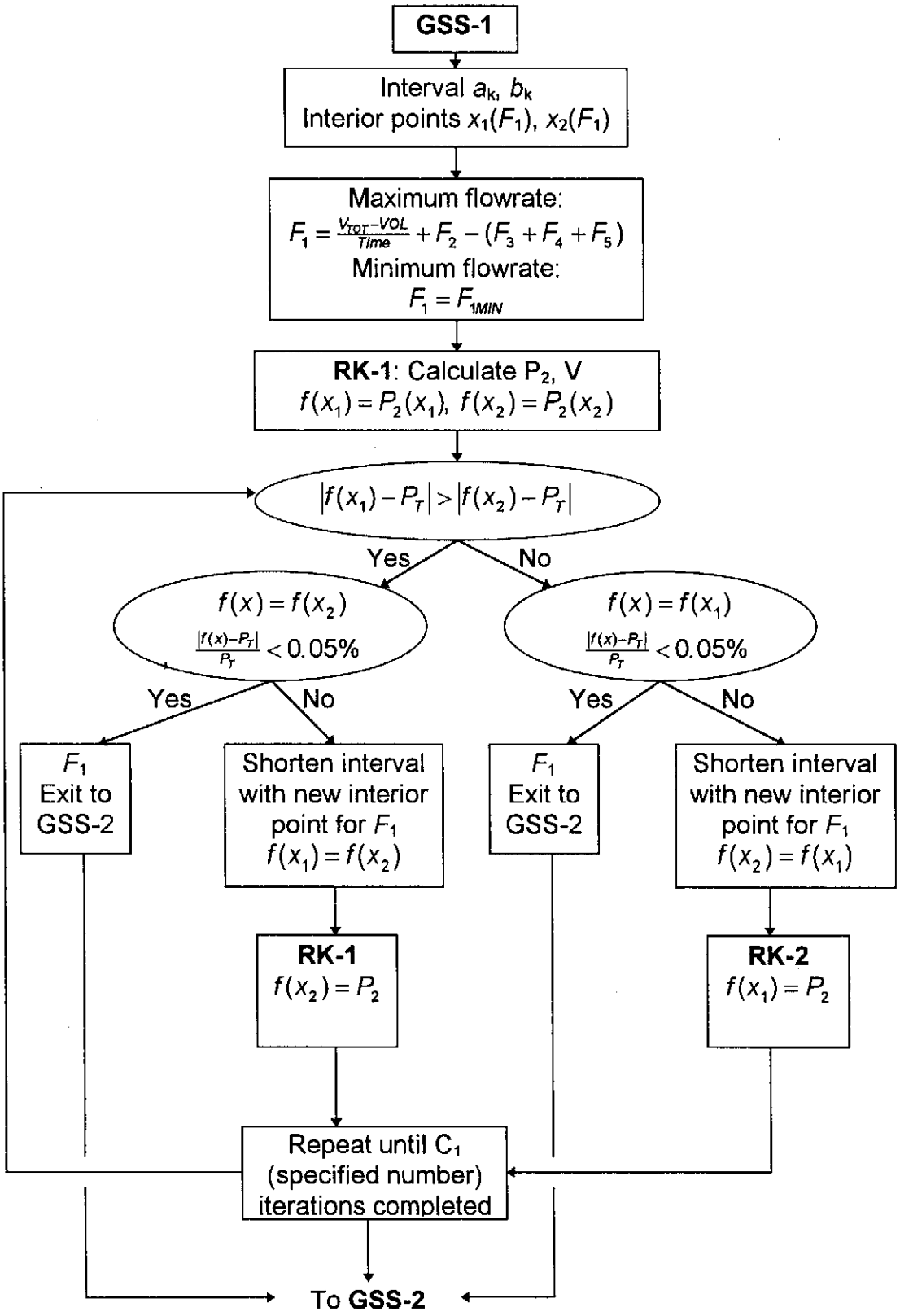

Figure 5.6d - Flow diagram of the Golden Section Search procedure 1 (GSS-1) of the computer simulation

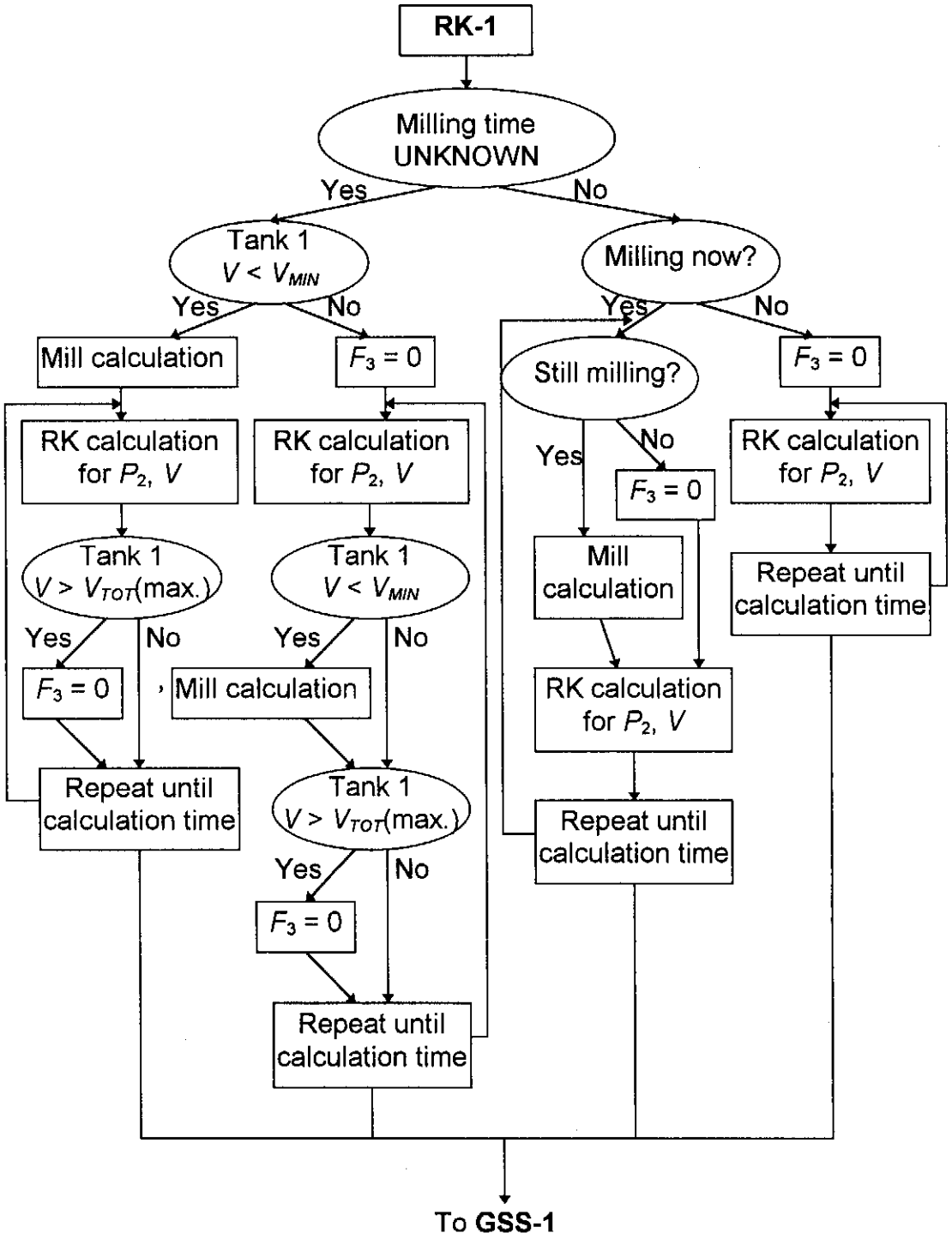

Figure 5.6e - Flow diagram of the Runge-Kutta procedure 1 (RK-1) of the computer simulation

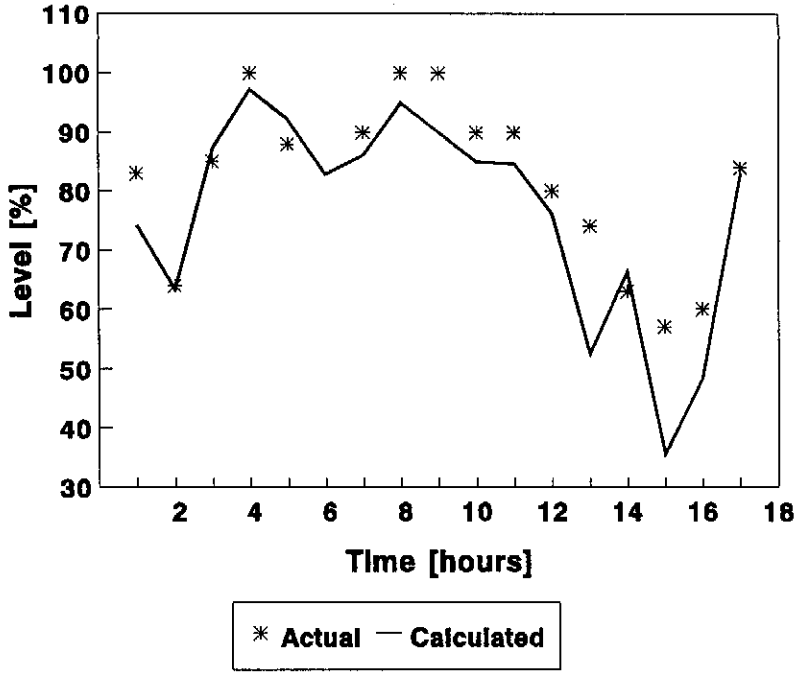

Figure 5.7 - Comparison of the predicted and actual levels in **tank 1506**

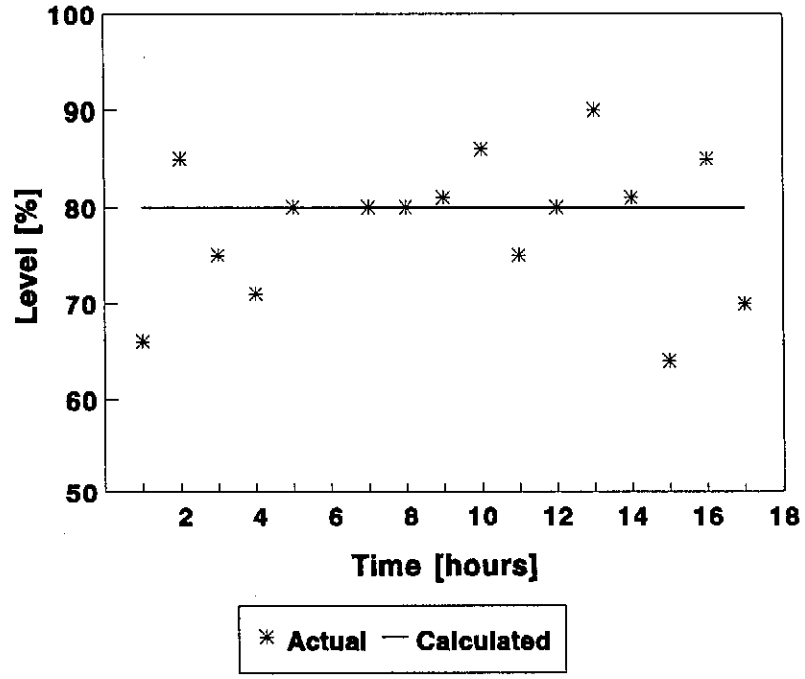

Figure 5.8 - Comparison of the predicted and actual levels in **tank 1102**

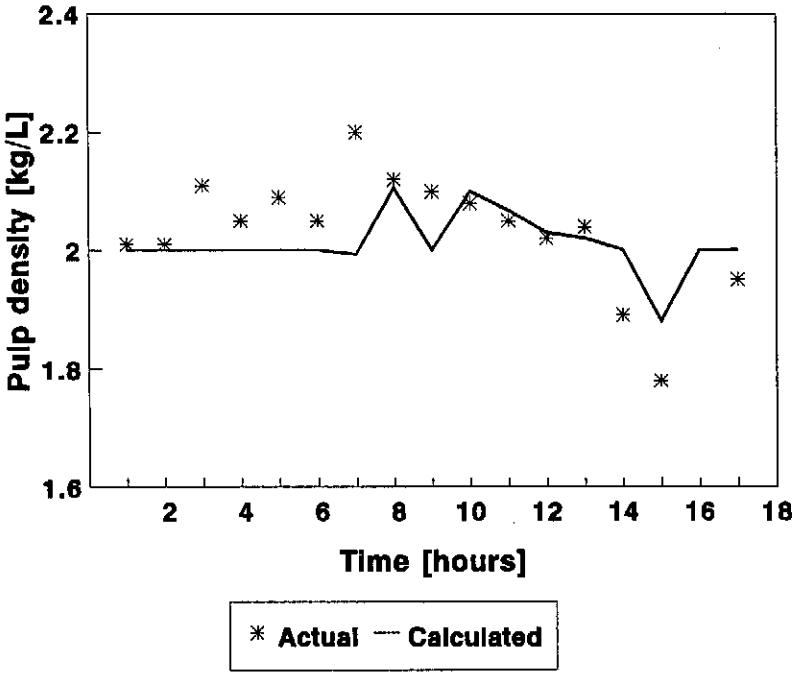

Figure 5.9 - Comparison of the predicted and actual pulp densities in **tank 1506**

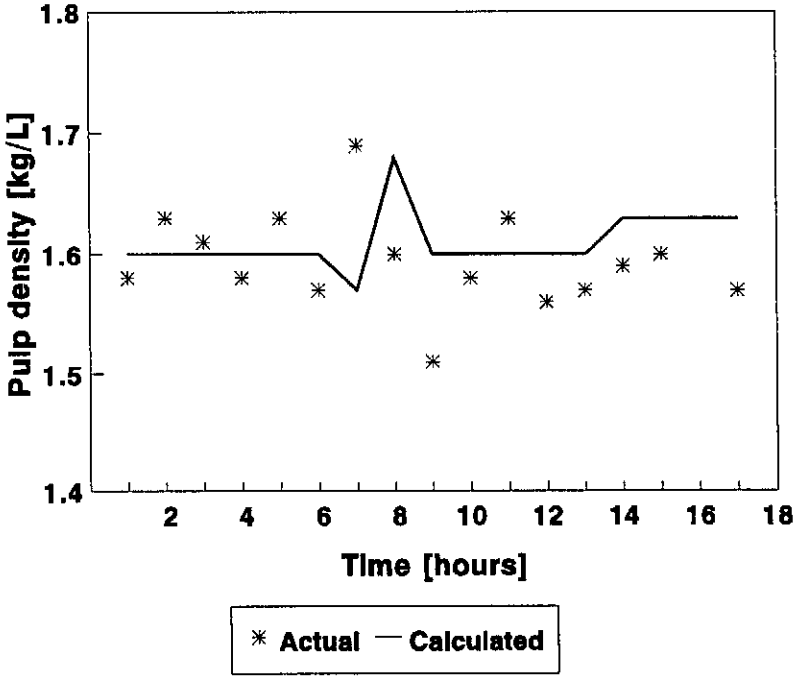

Figure 5.10 - Comparison of the predicted and actual pulp densities in **tank 1102**

Chapter 6

MODELLING AND ANALYSING THE FIRST STAGE LEACHING PROCESS FROM HISTORICAL DATA

6.1 INTRODUCTION

During the last few years there has been a significant effort towards improved control of chemical and metallurgical process plants, owing to more stringent demands from society regarding the sustainable use of resources, harsher environmental legislation and the economic production of higher quality commodities and speciality materials. The ill-defined nature of many of the chemical and metallurgical processes in the industry necessitates the quest for new modelling techniques to extract the features of processes which are poorly understood from a fundamental point of view. Most chemical and metallurgical plants have a large databank of historical process data which could be used effectively to develop a process model, and to extract process trends.

From plant experience, operators are skilled in recognising and interpreting real-time patterns from process data and in relating these patterns to process trends, which they can subsequently use to form a "mental" model of the process. As a result process operators tend to rely on their past operational experience, which takes into account many secondary factors which can affect the process. Therefore, the correct interpretation of measured process data is essential for the efficient control of chemical processes. The selective leaching of base metals with the Sherritt Gordon acid-oxygen pressure leach process is a highly complex and poorly understood process and is described in Chapter 3. The efficiency of the process is determined by the experience and the ability of the operator to interpret and diagnose patterns in the available data to make the necessary adjustments to the process. As a result the process is frequently controlled suboptimally, due to the lack of a fundamental

understanding and the inability of the operator to relate the multi-variable process to basic operating procedures.

There has been a long-standing awareness that these control practices are far from ideal, and recent macroeconomic trends which have seen a dramatic increase in personnel turnover on industrial plants have only exacerbated the problem. On the other hand, with computer control and increased use of statistical process and quality control, a wealth of sensor data stored in electronically accessible forms have been established in many industrial plants. These infrastructures allow ready implementation of machine learning techniques and it is for this reason that advances in intelligent process monitoring and control have been met with considerable enthusiasm in the process engineering community.

The techniques investigated and applied in the analysis of process data are subsequently discussed. These techniques include (i) conventional statistical methods, (ii) artificial neural networks (ANN), specifically back propagation neural networks (BPNN), self-organising map (SOM) neural networks and learning vector quantization (LVQ) neural networks, and (iii) inductive learning techniques (by decision trees).

Intelligent techniques provide a means to capture and implement the heuristic knowledge used on plants. Neural nets for example, do not require explicit process models, but can construct complicated implicit models from examples of process behaviour. As a result, they can be used very effectively to identify key trends and interactions between variables. However, the single most important drawback of neural nets in this regard is their intransparency. With neural nets pivotal relationships between variables can be discovered, but back tracking to identify underlying phenomena or to verify conclusions is difficult. Symbolic techniques such as induction methods on the other hand allow the construction of explicit rules to validate decisions in a natural and transparent manner. In this chapter the use of neural nets to analyse the behaviour of an ill-defined leaching plant is considered and compared with inductive decision trees and it is shown that these methods provide an effective means to identify key variables and relationships in the plant.

The objective of this chapter is twofold, one is to present a methodology to analyse plant data and to develop a model of a process which is highly complex and poorly understood, and two is to present examples of the different modelling and data analysis techniques for analysing a leaching process. The practical advantages of classifying the process outputs when artificial neural networks and inductive learning are used are also illustrated. Robust artificial neural network process models and induced decision trees are proposed that overcome the inherent difficulties of noisy process data. The process model together with statistical parameters are used to extract knowledge of the process. The relative importance of the different input variables in relation to the output variables is determined by means of sensitivity analyses with the process model, and the statistical parameter gives an indication whether an increase or decrease in a variable will have a positive or negative effect on the process. The classification efficiency of the neural network models and induced decision trees are compared, as well as their ability to identify the most important features of a process. At the same time, the positive and negative aspects of each analysis technique will be emphasised. The process engineer is therefore provided with a better indication of what technique should be used depending on the information required from the process.

6.2 LEACHING OF BASE METALS

The first stage leach section which is investigated (Fig. 6.1) starts with a feed stream from the mill to tank 113 (tank 113 was still in operation when historical data were gathered for this study, but due to the cost implications of the material hold-up in this tank it was later taken out of operation). From tank 113 the milled pulp stream is passed through a stream splitter into tank 1506, where it is diluted with spent electrolyte solution. From tank 1506 the pulp is passed through a stream splitter into tank 1102, where it is again diluted with spent electrolyte solution and from tank 1102 the pulp is pumped to the pressure leaching vessel (autoclave).

The matte being leached in this process consists mainly of Ni_3S_2, Cu_2S (and minor amounts of Fe) and Ni alloy. The approximate variations of the compositions of the matte and spent electrolyte solution are shown in Table 6.1. The purpose of the first

stage leaching process is to leach Ni and Fe while retaining Cu cemented in the solid state. Although Ni is the desired product, Fe also has to be extracted from the solid phase because it is an impurity in the concentrated solid product produced for further refining in the PGM recovery section.

The hydrometallurgical leaching of base metal sulphides has a very complex reaction mechanism. This is caused by the interaction between the various base metal elements and the base metal sulphides, as well as by the complex nature of sulphide chemistry. Reaction mechanisms (see Chapter 2) have been proposed for similar processes by several authors (Plasket and Romanchuk, 1978, Dutrizac and Chen, 1987, Hofirek and Kerfoot, 1992, Symens, *et al.*, 1979), but no process model has yet been developed for any of these processes. The complexity of effective process control is caused by the poor fundamental understanding of the process or the lack of a satisfactory process model (i.e. an understanding of the leaching reaction mechanisms and its interactions), as well as the fact that the preleach section is controlled manually by the operators.

6.3 DATA

In commercial chemical plants, many hundreds of variables can be measured. Direct application of data analysis techniques such as regression methods usually needs many thousands of data points. For instance, a quadratic regression analysis with 100 variables will estimate more than 5000 parameters (Shieh and Joseph, 1992), and as a rule of thumb would require between 20 000 and 100 000 data points. In many instances where plant data are difficult or expensive to obtain, these approaches are not practical. Moreover, it is known that human operators typically do not concentrate on more than a few key variables when making decisions regarding the performance of a process. Also, as far as their actions are concerned, they tend to *classify* the behaviour of a process, rather than attempting to quantify relationships. The plant is thus either performing satisfactorily or not, or the values of variables indicative of performance are too high or too low, etc.

All these factors stress (a) the importance of data screening or feature selection as a necessary first step in the analysis of plant data, and (b) the importance of a classification approach as a means towards the understanding of complex process behaviour. If the data are seen as points in hyperspace, feature selection eliminates redundant measurements (highly correlated variables) without excessive loss in information, and also reduces the dimensionality of the hyperspace, which can have a pronounced effect on the interpretation of data.

6.3.1 Principal variables

Data of the process is collected from day to day to evaluate the control performance and to analyse the efficiency of the process. All the data entered on the logsheets are not principal variables that will significantly influence the efficiency of the process. On the other hand some of the principal variables are not recorded due to cost implications (measuring equipment, etc.). The principal variables to evaluate the efficiency of the process were identified from fundamental engineering knowledge and from experience (see Chapter 3 and Appendix E) and are as follows:

(i) material composition,

(ii) particle size,

(iii) pulp densities in tanks 1506 (P_2) and 1102 (P_7),

(iv) tank levels in tanks 1506 (h) and 1102 (h_1), which in effect influences the residence times in these tanks, depending on the flowrates,

(v) pulp flowrate from tank 1102 (F_7) to the autoclave (compartment no. 1),

(vi) spent electrolyte solution flowrate (F_{Acid}) to the autoclave (compartment no. 1),

(vii) acid concentration ($[H_2SO_4]$) of spent electrolyte (SE) solution,

(viii) pressure (p_1) in the autoclave compartment no. 1,

(ix) temperature (T_1) in the autoclave compartment no. 1,

(x) oxygen flowrate (F_{ox}) to the autoclave compartment no. 1,

(xi) pH in the autoclave (pH_1) compartment no. 1,

(xii) pH in the autoclave (pH_4) compartment no. 4,

(xiii) concentration of Cu in the autoclave ($[Cu]_1$) compartment no. 1,

(xiv) concentration of Ni in the autoclave ($[Ni]_4$) compartment no. 4,

(xv) concentration of Cu in the autoclave ($[Cu]_4$) compartment no. 4, and

(xvi) concentration of Fe in the autoclave ($[Fe]_4$) compartment no. 4.

From these principal variables, the material composition and the particle size of the material were omitted in the development of the model, because the material composition is analysed per batch received at the plant and the particle size is determined per batch being milled while the other data are recorded on an hourly basis. Furthermore, the fact that the milling process is not continuous causes the freshly milled material to be mixed with the pulp already in tank 113, thus making it impossible to obtain a representative material composition and particle size distribution of the material. The pulp densities (P_2 and P_7), pulp flowrate (F_7), spent electrolyte flowrate (F_{acid}), pressure (p_1), temperature (T_1) and oxygen flowrate (F_{ox}) are the manipulated variables and the acid concentration ($[H_2SO_4]$) of the spent electrolyte solution is the measured disturbance of the process. The pH's (pH_1 and pH_4) and the Cu concentration ($[Cu]_1$) can be regarded as secondary measured outputs in the process, but for modelling purposes they are regarded as measured disturbances, because no clear knowledge exists that relates these variables to specific output conditions. The desired outputs are the concentrations $[Ni]_4$, $[Cu]_4$ and $[Fe]_4$.

6.3.2 Interpretation of the data

The correct interpretation and presentation of the data is very important for effective analysis. The different aspects of the data that had to be taken into account were: (i) the noise present in the data, (ii) the residence times of the different units in the section, and (iii) the compilation of a representative data set of the process.

(i) Noise in data

The noise in data is the biggest problem in the effective analysis of plant data, because:

(a) the operators do not always record the data entries on the hour,

(b) instrumental errors occur in the plant,
(c) different process assistants (and operators) have different sampling methods,
(d) the analysts occasionally make mistakes, and
(e) writing and typing errors are made in the databank development.

It is important that the modelling techniques investigated can cope and overcome the problem of noisy data. One of the advantages of neural networks is their ability to handle noise in data.

(ii) Residence time

The section of the process being modelled consists of various units which all have different residence times. From the principal variables identified above, it is obvious that the units that will mostly affect the development of the model are, tanks 1506 and 1102, and compartments no. 1 to 4 of the autoclave. The approximate residence times in tanks 1506 and 1102 are 240 minutes and 150 minutes, respectively and the total residence time of the pulp in the autoclave is approximately 90 minutes, corresponding with the operating conditions employed at the time the databank was accumulated. These approximate residence times cannot be incorporated in the data presentation *per se*, as the outputs have different relationships to the residence times in previous units. As a consequence a method was developed (with the model), which will be discussed later, to identify the best presentation of the data.

(iii) A representative data set

A representative data set of the process should contain sufficient data entries (data vectors) so that all the possible states of the process are included in the data. The databank for this case study has been developed from the hourly logsheet entries for 76 days (01/01/1992 to 16/04/1992), which constitutes 1824 data vectors. A successful model should be able to model the process under all possible operating conditions (excluding start-up and shut-down operations).

6.4 DATA ANALYSIS AND MODELLING TECHNIQUES

The modelling and data analysis techniques that have been investigated, are (i) conventional statistical methods, (ii) artificial neural networks (ANN), and (iii) inductive learning by means of decision trees.

6.4.1 Statistical methods

The conventional statistical modelling technique of multiple linear regression was the first attempt at modelling the data. This produced the results as shown in Fig. 6.2, where the R^2 (coefficient of multiple determination) is very low for all three of the desired outputs. This can be explained by the fact that no simple linear relation between the different inputs and outputs exists and because of the noise content of the data. Figure 6.2 also shows the comparative R^2 values obtained with the refined data sets after the optimum data presentation was determined. The refined data sets were developed, after the modelling technique which gave the best results was determined, by incorporating time delays and time series expansions for some of the variables. This indicates that by obtaining a better data presentation a slightly better fit of the multiple linear regression model could be achieved.

The multiple linear regression technique does not take into account that the inputs have different levels of importance in relation to the different outputs. Therefore, the correlation coefficients (Walpole and Myers, 1989) were determined to investigate the linear relation (or degree of linear relation) between the different inputs and outputs. The correlation coefficients of the different independent variables in relation to the dependent variables were determined according to eq. E.1 (Appendix E). The results of the correlation coefficients of the three dependent variables (outputs) are illustrated in Fig. 6.3 - Fig. 6.5. It can therefore be concluded that there are no strong linear correlations between any of the inputs in relation to the outputs. On the other hand, the correlation coefficients can give a reasonable indication of what variables can be expected to have a strong relation with the different outputs. The correlation coefficients of the variables cannot be compared directly with one another, because of the possible non-linear relationship of the variables.

Another statistical parameter that was used to investigate the data, was the autocorrelation function (Pandit and Wu, 1983) that expresses the statistical dependence in the data between successive observations. By obtaining the autocorrelation values for the variables (see Fig. 6.6) it is evident that some of the variables have a strong time series dependence, which is an important factor that has to be considered in the development of a model.

6.4.2 Artificial neural networks (ANN)

Artificial neural network models are composed of many non-linear computational elements operating in parallel and arranged in patterns reminiscent of biological neural systems (Fig. 6.7). Computational elements or nodes are connected via weights that are typically adapted during training of a data set to improve the performance of the model. The functioning of artificial neural networks has been described in detail in the literature (Lippmann, 1987, Wasserman, 1989, Maren, *et al.*, 1990) and therefore it is not repeated in this study. Existing artificial neural network software programs from NeuralWare were used in the investigations.

The application of artificial neural nets in process engineering has increased dramatically in recent years. Neural nets are essentially data driven computing devices comprised of large numbers of simple process units or nodes that are interconnected on a massively parallel scale. These (non-linear) nodes are typically arranged in layers and adjustable numerical values or weights are associated with the connections between different nodes in layers. Although back propagation neural nets have been used extensively in a large variety of applications to date, it is often necessary to preprocess the exemplars of complicated processes presented to these types of nets in order to attain optimal performance. In other types of nets, such as those with Kohonen layers, the input vectors are categorised prior to further use. This amounts to self-organised or implicit feature selection, which can lead to a significant improvement over the performance of neural nets presented with the input exemplars not subject to preprocessing. In this paper various types of networks are considered, viz. back propagation neural nets, as well as neural net systems

equipped with Kohonen layers, i.e. learning vector quantization (LVQ) and self-organising map (SOM) neural nets.

6.4.2.1 Back propagation neural networks (BPNN)

Back propagation neural networks are the most commonly used neural networks in the modelling of continuous processes and are described in the literature (Hinton, 1992, Chitra, 1993, Bhat and McAvoy, 1990, Hong-Te Su, *et al.*, 1992, Reuter, *et al.*, 1992, Van der Walt, *et al.*, 1991, Van der Walt, *et al.*, 1992, Karim and Rivera, 1992, Kramer and Leonard, 1990). It has also been shown in the literature that back propagation neural networks are superior to more traditional modelling techniques (Bhat and McAvoy, 1990).

These nets are trained by means of exemplars and the differences between the outputs of the net and the desired outputs are used as a basis to adjust the weight matrix of the net, that is

$$w_{ij}(t+1) = w_{ij}(t) + \Delta w_{ij}(t) \qquad (6.1)$$

where

$$\Delta w_{ij}(t) = -\tau.\delta_i\, z_i(t) \qquad (6.2)$$

and where τ is a learning rate parameter which defines the step size during the search (typically a gradient descent technique). Convergence can sometimes be improved by the inclusion of a momentum term, which takes the effect of previous weight changes $\Delta w_{ij}(t\text{-}1)$ into account, i.e.

$$\Delta w_{ij}(t) = -\tau.\delta_i\, z_i + \alpha\Delta w_{ij}(t\text{-}1) \qquad (6.3)$$

When training data are not sufficiently representative of the expected future behaviour of the plant, other neural networks that exploit the structure or similarity of the input data are sometimes better able to model the process (Maren *et al.*, 1990).

data and have been described in detail in the literature (Lippmann, 1987, Maren, *et al.*, 1990, Lippmann, 1989) and only a brief overview of their main characteristics is supplied.

The LVQ network assigns vectors to different classes (Maren, *et al.*, 1990) and contains an input layer composed of one process element for each input parameter, a Kohonen layer that is trained to perform the classification and an output layer containing one process element for each class (Fig. 6.9). The structure of the Kohonen layer is defined arbitrarily. During training, the distance between the input vector and each process element is computed and the nearest process element (the winner) is determined. If the winning process element is in the same class as the training vector it is moved towards the training vector, otherwise it is repulsed. As a result of training, process elements assigned to various classes migrate to the regions associated with these classes. After training, i.e. during classification, the distance of an input vector to each process element is computed and the input vector is assigned to the class of the nearest (winning) process element.

One of the most powerful and commonly used abilities of the LVQ neural network is the classification of patterns. The advantage of this network is its ability to organise the representation of categories among the input data, to correspond to the specific output classes (supervised training). Back propagation neural networks, on the other hand, have had supervised training methods in which the network was taught to recognise an exemplar pattern via adaptive weight-changing algorithms. Back propagation neural networks (BPNN) were tested for the classification of the process data and compared to LVQ neural nets (Fig. 6.10). Nearly similar classification results were obtained by both these techniques, but it was decided to concentrate on the LVQ neural network approach because it is inherently a classification network.

6.4.3 Inductive learning

Inductive learning is the most intensively explored kind of learning in artificial intelligence (Bratko, 1993). Knowledge engineers typically select one of two broad approaches when developing a knowledge base (Kattan, 1994): (i) the model driven,

or active approach where knowledge engineers interview human experts to elicit their knowledge, and (ii) the data driven, or passive approach. Recently, the data driven approach, where an induction tool or statistical technique is used to develop rules from a data set, has received much attention. The induction algorithm (Quinlan, 1986 and Quinlan, 1990) generated decision trees by recursively splitting the data set on the different attributes represented by the set. The classification power is used to determine the order in which (binary) splits on attributes are implemented. For discrete class labels the selection of the attribute to split during construction of the decision tree is based on the information content of each attribute with regard to classification. The information content is represented by the information entropy with the maximum information content corresponding to the minimum entropy, as represented by equation (6.5).

$$E = p^{+}\log_2(p^{+}) + n^{-}\log_2(n^{-}) \qquad (6.5)$$

where E is the entropy, p^{+} the probability of a positive instance and n^{-} the probability of a negative instance. A forward pruning criterion terminates splitting when it is not possible to create two branches each with a number of examples equal to or larger than a lower branching limit. The lower branching limit is the minimum number of examples that a branch in the decision tree is allowed to have. A value of two was specified in this investigation. The drawback of these types of algorithms arise when classification is based on continuous-valued attributes (such as is often the case on process plants). Under these circumstances the attributes have to be discretised and this may have a significant effect on the performance of the algorithm. Moreover, decision trees can be large and unpractical, especially as far as noisy data are concerned and can have difficulty dealing with incremental data or reconciling trees obtained with different sets of data pertaining to the same process. The main practical advantage of decision trees is that the classification knowledge is presented in a form that human decision-makers can readily understand. The software program, ExpertRule Analyser, was used in this study to develop the decision trees.

6.5 DEVELOPMENT OF PROCESS MODELS

The outputs of the data sets used for the analysis techniques were divided into classes (Hoskins and Himmelblau, 1992). The operating criteria in a plant are usually that the concentration of the desired element should either be above or below a certain concentration. The classification of the outputs into classes furthermore simplifies the construction of the discriminant surfaces characterising the various classes of operating conditions. This technique also reduces the influence of noisy data to a certain extent and therefore simplifies the classification process (predicting the output class and not an exact value).

A factor that has to be taken into account when choosing a classification boundary, especially for cases where the outputs are classified into two classes is that the process output values could have a normal distribution around the boundary point. This could make the classification inherently noisy. The only way of reducing these errors (of noisy data) made by classifying the outputs into two classes is to determine the frequency distribution of the output parameters and to choose the most appropriate boundary point while taking the process restrictions into consideration. The process requirement is the most important consideration in deciding on the classification boundaries for the output variables. Therefore, the choice of arbitrary values for the classification boundaries is unacceptable, especially with the process requirement known for the specific parameters, which is usually specified as a range of the desirable output. For this process the desirable concentration range for Ni is >100 g/L, Cu <0.6 g/L and Fe >1.0 g/L, respectively, according to the process engineers. Figures 6.11 to 6.13 illustrate the frequency distribution of the Ni, Cu and Fe concentrations, respectively.

The classification boundary for Ni was chosen as 105 g/L as seen on Fig. 6.11 where the requirement by the process engineers are 100 g/L, but this point is very close to the highest frequency of the concentration of Ni. With the classification boundary at 105 g/L, it is at a lower frequency and therefore the possibility of classifying the output as high when it is actually low and *vice versa*, is reduced. This adjustment to the specified process requirement could also be motivated by the fact

that a higher concentration of Ni is more desirable. The frequency distribution graph of the concentration of Cu (Fig. 6.12) reveals that a boundary point for classification of Cu at 1.0 g/L is far better than at 0.6 g/L where the frequency distribution is still high, but with the boundary point at 1.0 g/L it will be in a "valley" of lower frequencies. This shift in the concentration will have a negligible effect on the process, because of the logarithmic variations in the concentration of Cu. It will also have the effect of decreasing the error for the classification of data in the region of the classification boundary. Furthermore, this shift of the boundary point could be motivated by the fact that the concentration of Cu is generally, either below 0.75 g/L or above 2.75 g/L according to the frequency distribution graph (this is also an indication of the complex nature of the process reaction mechanism). Obtaining the most appropriate division point for Fe was not as simple as for the previous two parameters, because the frequency distribution of Fe has a nearly normal distribution (see Fig. 6.13). Subsequently, the division point for the classification of Fe was choşen as 1.1 g/L (1.0 g/L specified by the process) to obtain a more balanced distribution of values allocated to be classed in the high and low classes.

It was determined that a back propagation and LVQ neural network model with only one output learn the mapping between this single function and its variables more easily as opposed to neural net models with more outputs (Van der Walt, *et al.*, 1992). Therefore a separate neural network model is developed for each output. The same argument holds for induced decision trees, simplifying the tree and therefore making it easier to analyse. Furthermore, the ability of extracting process knowledge on a specific process output is simplified by developing a model for each output separately.

In developing an LVQ neural net model with the process data, the following aspects must be determined (in this order): (i) the optimum architecture of the network, (ii) the preliminary degree of importance of the input variables, and (iii) the optimum representation of the data. For the development of the LVQ models approximately 75% of the data set was used as training exemplars and approximately 25% as testing exemplars.

(i) LVQ network architecture

The network architecture was determined by trail and error. The optimum architecture for the classification of all three output parameters (with a different amount of input parameters) is an LVQ network with a Kohonen layer with 3 nodes per output node.

(ii) Degree of importance of the input variables

A method of sensitivity analysis was used to determine the relative importance of the variables (based on the leave-one-out principle). The sensitivity analyses are performed by training and developing LVQ neural network models for each new data presentation. The results obtained with the original data representation are compared with the results of the sets of data where one input variable at a time is omitted, to determine the influence of this variable on the specific output.

(iii) Representation of the data

The optimum representation of the data is obtained when the LVQ model producing the best classification is developed with the data. Two factors that will improve the data representation are the use of the relevant features (input parameters) and the correct time representation of the different features (delay times, etc.). This will produce a more appropriate description of the discriminant surfaces characterising the various classes of operating conditions. From the sensitivity analyses determining the degree of importance of the different inputs it is possible to identify the input parameters that have no influence on the performance of the model. These input parameters are then omitted in the further development of the model. The knowledge obtained with these sensitivity analyses is then used as a basis for determining the optimum data representation.

Data sets

Two related sets of data were used in the analysis. Each set was comprised of 1824 records or exemplars. The first set (data set A) consisted of raw, or the original, plant

data. The second set (data set B) was identical to the first, except that the variables were rearranged to account for the delay times and the relative importance of the different variables in the process. Mathematically a data entry is represented by $x_i(t)$, where x is the value, the subscript i is the number of the variable it represents and t is the time. The data vectors are represented as,

$$\mathbf{x}_j(t) = \{ x_1, x_2, \ldots, x_i / Class \} \qquad (6.6)$$

for developing the models from historical data. The values of variables x_1 - x_i were based on hourly measurements. The time delays in the various process units are known approximately and are used as the basis for the determination of the time representation of the data (the delay time depends on the specific process unit). Two types of time presentations of the various input parameters were investigated, i.e. a time delay of 1 hour ($x_i(t-1)$), 2 hours ($x_i(t-2)$), or more, or a time series expansion of 2 with a time delay of 1 or more hours. A time series expansion of 2 is where a specific variable is represented by two data entries of the same variable with a time delay. For example a time series expansion of 2 for variable no. 1 is presented in Table 6.2. This representation makes provision for the time dependence of the variables as determined with the autocorrelation function. The time series expansion of the parameters is not increased above 2 to prevent the further increase in the dimensionality of the input space. The parameter with the highest degree of importance is the starting point in investigating the optimum time dependence of the data by using sensitivity analyses. After the best time representation for this specific parameter has been determined, it can then be used as the basis for determining the time representation of the next parameter (second highest degree of importance). This procedure is repeated until the time representation of all the relevant parameters have been determined. The optimum data representation for development of the process models (for Ni, Cu and Fe) is shown in Tables 6.3, 6.4 and 6.5, respectively. Therefore, the LVQ neural network models developed, with these data representations are optimised, for the classification of the concentrations of Ni, Cu and Fe.

For the development of the decision trees 70% of the data set was used as training exemplars and 30% as testing exemplars. Instead of a leave-one-out method, the input variables (attributes) of the data set were ranked statistically by means of a χ^2 - test (Table 6.6). For each attribute the values were assigned to two categories so as to give the highest possible χ^2-value when the two categories are used to classify the outcomes. This ranking could be compared with those obtained with the neural nets, as well as a ranking based on the entropy of the data (the basis on which the decision trees were constructed).

6.6 DISCUSSION OF RESULTS

6.6.1 Efficiency of the models

The self-organising maps were able to produce distinct groupings of clusters for the two classes (high and low) for each output. As an example Fig. 6.14 illustrates that the self-organised mapping for Ni can be divided into two separate clusters. In order to give a better indication of the location of the clusters for the outputs, the centres of gravity for each cluster were determined (see Fig. 6.15). As can be seen from Fig. 6.14, the clusters are not sharply separated and the class containing high values for the output values appears to be more dispersed than the class containing the low values of the output variables. Moolman *et al.* (1995) stated that the advantage of using topological maps (SOM) in relation to other types of classifiers (for example LVQ nets), is that they can track the performance of a process on a continuous basis, as opposed to the identification of discrete classes by using other types of classifiers. Therefore this technique will be advantageous for on-line monitoring of processes, because it enables the early detection of a process deviation. However, to be able to successfully use this technique for on-line monitoring of a process more information of the poorly understood process is required to relate process deviations to specific operating conditions.

Both a sigmoidal back propagation neural net, as well as a learning vector quantization neural net were used to classify the data. The back propagation neural net consisted of an input layer with 13 nodes, a 3-node hidden layer, as well as a 1-node output layer for the classification of the output variable. The back propagation neural net was trained by means of the generalized delta rule. The learning vector quantization neural net consisted of an 13-node input layer, a 3-node Kohonen layer, as well as a 2-node output layer. The back propagation neural net, with data set A, was able to classify the output for Ni at 76.7%, 78.7% for Cu and 74.7% for Fe, while the LVQ neural net classified the outputs as follows: 77.6% for Ni, 78.2% for Cu and 73.4% for Fe (see Fig. 6.10). Both the LVQ neural net and back propagation neural net were able to obtain good comparable classification results, with data set A (original data).

By comparing the classification efficiency of the LVQ net models (Fig. 6.16) and the back propagation neural net models (Fig. 6.17) based on data sets A and B, it is evident that somewhat better results were obtained with data set B, for both the techniques. The refined data set (data set B) refers to the optimum representation (obtained with LVQ nets) of the data by using the relevant features and the correct time representation of these features when developing the models. The decision trees (Fig. 6.18) on the other hand did not show any significant difference between the two data sets. The decision trees also did not show any improvement when the lowest ranked attribute was omitted from data set A used to develop the decision tree. As an example the acid solution flow rate, the lowest ranked attribute for the classification of nickel (see Table 6.6), was omitted and a decision tree was developed. This decision tree produced a classification result of 78.1% which is lower than the classification of the tree where this attribute was not omitted (79.5%). The same procedure was followed for the lowest ranked attribute for the classification of copper (oxygen flowrate, F_{ox}), producing a classification result of 77.7% which is also lower than the classification of the tree where this attribute was not omitted, 78.2%. It can therefore be concluded that the decision trees are not as sensitive to variations in the data representation as the LVQ neural network models. The slightly better classification results were obtained by the LVQ models, especially for copper, than the induced decision trees (see Fig. 6.19). Another conclusion that was made from these results of the decision trees is that even when the lowest

ranked attribute is not present as a node in the pruned decision tree it is not necessarily an insignificant attribute that could be omitted in the induction of the tree.

The LVQ neural net models obtained high classification results with data set B (refined data) for classifying the outputs as either high or low as illustrated in Fig. 6.19 (79.6% for Ni, 82.0% for Cu and 75.4% for Fe). The sigmoidal back propagation neural nets performed very similar to the LVQ nets, viz. 76.3% for Ni, 84.1% for Cu and 77.9% for Fe. The results obtained are significantly better than the statistical probability of randomly predicting the nickel, copper and iron concentration as high or low, which is 50%. As an example, Fig. 6.20 illustrates the efficiency of the LVQ neural network model in simulating the actual output of the process for copper. These results are quite significant if it is taken into consideration that noisy plant data were used.

The classification results of the decision trees (Fig. 6.19 - 79.5% for Ni, 78.2% for Cu and 74.7% for Fe) were almost similar to those of the LVQ and back propagation neural net models. Examples of the induced decision trees for Ni and Cu are shown in Fig. 6.21 and 6.22, where the values underneath the outcomes indicate the probability for that outcome to be classified correctly.

6.6.2 Degree of importance of variables

The degree of importance (or ranking) of the input variables as obtained by the correlation coefficients (Fig. 6.3 - Fig. 6.5), by sensitivity analyses with the LVQ models (Fig. 6.23 - Fig. 6.25) and by the χ^2 -test employed by the inductive learning by decision trees (Table 6.6) is compared and discussed subsequently. To simplify the discussion only the results for Ni and Cu are considered, as these are the most important output parameters for the process.

The four highest ranked variables, for Ni and Cu, obtained by the different techniques are shown in Table 6.7. *Nickel:* Table 6.7 illustrates that all the techniques ranked the acid concentration ($[H_2SO_4]$) of the spent electrolyte solution

as the most important feature for predicting the Ni concentration. Furthermore, the LVQ models ranked the variables, level in tank 1506 (h) and pressure (p_1) as the second and third most important variables where the decision trees ranked them as third and second most important variables. With the correlation coefficients the variable for the level in tank 1506 (h) is ranked three. *Copper:* The three different techniques (Table 6.7) ranked the pH in compartment no. 4 (pH_4) and the Cu concentration ($[Cu]_1$) in compartment no. 1 (of the autoclave) as the two most important features for predicting the final Cu concentration ($[Cu]_4$) in the process.

It is therefore evident that the different techniques have the ability to identify the most important features for each of the output variables and could be used to confirm the most important variables in a process. At the same time it must be remembered that these three techniques do not have the same reliability. The correlation coefficients determine the linear relation between the various inputs and the output making it the least reliable, but it is still able to give a good indication of what features are the most important. The χ^2 -test is a non-linear method, therefore it is slightly more reliable than the correlation coefficients. The degree of importance of the different variables determined by sensitivity analyses with the LVQ neural network models of the process is the most accurate of these techniques, because (i) the LVQ models are inherently non-linear and (ii) the LVQ models are more sensitive to variations in the input data set than the decision trees, as well as the fact that (iii) the LVQ models obtained better classification results than the decision trees.

6.6.3 Extracting process knowledge

The fact that artificial neural networks are "black box" models of processes does not prevent the extraction of process knowledge from such models. Process knowledge can be extracted from any artificial neural network model, for example with sensitivity analyses (entering perturbations for the various input parameters and analysing the results) (Van der Walt, *et al.*, 1991). The most important variables, as obtained from the sensitivity analyses of the LVQ models for Ni, Cu and Fe and confirmed by the decision trees and correlation coefficients, can be explained in practical terms by simple statistical evaluations of the input vectors. This is performed by separating

the input vectors into two classes for the high and low concentrations of Ni, Cu and Fe and calculating the mean and variance of each variable. As examples, the statistical mean (averages) for the six most important variables for each output is presented in Table 6.8.

6.6.3.1 Nickel

The most significant information of the process (Fig. 6.23), is that the acid concentration ($[H_2SO_4]$) is by far the most important variable that will influence the leaching of Ni. This is supported by the difference in the averages (mean) for the acid concentration (see Table 6.8). It can thus be concluded that the higher the acid concentration, the more Ni will be leached. In practice this variable will be the most important parameter that must be controlled in the process to either obtain a high or a low concentration of Ni ($[Ni]_4$). All the other parameters have approximately the same level of influence on the leaching of Ni. The level in tank 1506 (h) or the pressure (p_1) in the autoclave (compartment no. 1) is the second most important variable for leaching Ni in the process. By investigating the averages of the level in tank 1506 and the pressure, the importance of these variables is confirmed by the difference in these values. These averages also indicate that for longer residence times (or higher average tank levels) in tank 1506 and higher pressure, the higher the leaching efficiency of Ni will be. The same argument applies for the oxygen flowrate (F_{ox}). From the averages of the pulp density in tanks 1506 (P_2) and 1102 (P_7) it is evident that a higher pulp density results in better leaching of Ni. These results confirm the ability of the LVQ neural network model to identify the most important variables in the process for Ni extraction.

6.6.3.2 Copper

The two most important variables identified in Fig. 6.24 for the leaching of Cu are the pH (pH_4) in the autoclave (compartment no. 4) and the concentration of Cu ($[Cu]_1$) in the autoclave (compartment no. 1). The importance of these two variables could have been expected since they are actually secondary output variables for the process (explained previously). The averages (see Table 6.8) for these two variables

indicate that a reasonable difference exists between the averages of the high and low classes. The effect of a low pH in the autoclave (compartment no. 4) and a high concentration of Cu in the autoclave (compartment no. 1) will produce a high concentration of Cu in compartment no. 4 ($[Cu]_4$) of the autoclave. The other important variables that have a considerable influence on the leaching of Cu are the level in tank 1102 (h_1) and the pulp density in tanks 1506 (P_2) and 1102 (P_7). These variables (as well as the concentration of Cu in compartment no. 1 of the autoclave) indicate in practice the importance of controlling the preleach section properly, since the residence time in the autoclave is too short to cope with possible perturbations entering from the preleach section. The averages of the level in tank 1102 indicate that a shorter residence time (or a lower average tank level) in tank 1102 results in less leaching of Cu. An interesting aspect that is evident from the average pulp densities in tanks 1506 and 1102 is that a lower pulp density in tank 1506 and a higher pulp density in tank 1102 will produce a higher leaching efficiency of Cu. This could be ascribed to different chemical reaction mechanisms occurring in these two tanks, because of the existence of different process conditions in these tanks (for example the temperatures in tank 1506 and tank 1102 are approximately 71 and 58°C, respectively).

According to the sensitivity analyses the pressure in compartment no. 1 (p_1) of the autoclave is the sixth most important variable for the leaching of Cu. For Ni pressure is the third most important variable for the leaching of Ni in comparison with pressure being the sixth most important variable for the leaching of Cu. The effectiveness of the sensitivity analyses is illustrated by comparing the differences in the averages for the pressure in the data sets for Ni and Cu, 37.3 kPa and 5.7 kPa, respectively. This is only a relative measure that gives an indication of how strongly the variable is correlated with the output.

6.6.3.3 Iron

The two variables that affect the leaching of Fe the most is the pulp density in tanks 1102 (P_7) and 1506 (P_2) (see Fig. 6.25). The averages of these two variables (Table 6.8) indicate that significant differences exist, which could point to the importance of

these variables, as well as the fact that for higher pulp densities in tanks 1506 and 1102 less leaching of Fe will occur. The third and fourth most important variables for the leaching of Fe are the acid concentration ($[H_2SO_4]$) and the oxygen flowrate (F_{ox}). An interesting aspect that was noticed from the averages of the acid concentration was that for higher acid concentrations less Fe was leached, which is the opposite of what is expected and what has been stated in the literature for the leaching of Fe. This is most probably due to the interaction of the various components or variables with one another, which give an indication of the complexity of the process. The averages for the oxygen flowrate on the other hand, produce results which are expected, where higher oxygen flowrates will reduce the leaching of Fe. Another important variable is the level in tank 1102 (h_1) which gives an indication of the approximate residence time of the pulp in this tank. From the average tank levels for tank 1102 it seems that a longer residence time will increase the leaching of Fe (which is expected).

Comparing the six most important variables for the Ni, Cu and Fe leaching, it is evident that the tank levels and pulp densities of tanks 1506 (h, P_2) and 1102 (h_1, P_7) consist of three of the six most important variables for each output. This implies that the control of the preleach section as a whole is very important in obtaining a stable process (Chapter 5, Rademan, *et al.*, 1995). Furthermore, by choosing the correct operating conditions for the preleach section the probability of obtaining the desired output concentration of Ni, Cu and Fe will be increased.

6.6.4 Process analysis techniques

The statistical techniques are either linear operations (correlation coefficients and multiple linear regression) or require *a priori* information which is not available for a fundamentally poorly understood process. The advantage of these evaluations is that it is simple and fast to use and it gives a good indication of what could be expected when a non-linear or truly inductive technique is used. Conventional statistical calculations (mean and variance) can be used in conjunction with other techniques to obtain more informative results.

The learning vector quantization (LVQ) neural network models are good for predicting the process performance, because it uses a nearest neighbour classification approach. It does not learn a pattern but rather characterises the input vectors to a certain output class. The sensitive nature of the LVQ models to variations in the training data sets could be viewed as both a positive and a negative characteristic. The sensitivity of these models are of advantage when it enables the identification of the influence of the different variables on the process, i.e. to determine the most important variables for an output parameter of the process. It also identifies the influence of delay times and the different time representations of the input data sets, i.e. determining the correct time representation of the input variables. The negative aspect of the sensitive nature of the LVQ models is that it is a cumbersome and a time consuming operation to obtain the optimum data representation. Therefore, it is assumed that the procedure of determining the most important variables with the LVQ neural network models is more reliable than the other techniques discussed. (The induced decision tree obtained approximately the same classification results with the original data set as the LVQ and back propagation neural net models, Fig. 6.19.)

The inductive learning by decision trees produced good classification results with both data sets A and B and yielded classification rates comparable to those of neural network models (Fig. 6.19). The induced decision trees are less sensitive to variations in the input data sets and therefore this technique is not as suitable to perform sensitivity analyses with as the LVQ models. The inductive learning procedure produces a slightly more robust process model (or decision tree) than the LVQ neural network model. The main advantage of developing a decision tree of a process is that a set of induced rules is obtained which can be directly interpreted for a better understanding of the process or the rules can be used in an expert or knowledge based system (KBS).

6.7 SUMMARY

The methodology described in this chapter can be applied to any ill-defined and poorly understood process to interpret the data and to determine the correct representation so that an effective model can be developed. All the techniques used to analyse the data supplied bits of information of the process that helped to form a better understanding of the process.

Classification results of the learning vector quantization (LVQ) neural network models (as well as the back propagation neural network models) and the inductive learning by decision trees of the process were able to obtain comparable results of 79.6% and 79.5% for Ni, 82.0% and 78.2% for Cu and 75.4% and 74.7% for Fe, respectively. These results are exceptionally good if it is taken into consideration that noisy process (plant) data were used. These LVQ neural network models were used to determine the relative importance of the different variables for each output and are substantiated by the *Chi square* test (χ^2 -test) employed by decision trees and the correlation coefficients. Knowledge of the process is obtained by analysing the influence of the most important variables together with the statistical means of these variables to determine the effect of a specific variable on the output variable. The LVQ neural network models and the inductive learning by decision trees both have their positive and negative characteristics for analysing an ill-defined process. Therefore, the choice of the technique that must be used will depend on what type of information is needed of the process. For example, use (i) decision trees when the process requires easily interpretable rules, so that the operator can have an indication of the control action that must be taken, or (ii) LVQ neural network models (together with statistical mean) to obtain a more detailed investigation of the influence of various parameters on the process, so that the operating conditions of the process could be adjusted to improve the efficiency of the process. Both the LVQ neural network and decision tree modelling techniques are robust techniques that can be used to model and analyse complex and ill-defined processes.

The investigations performed in Chapters 5 and 6 identified and discussed all the influences that affect the "external" (intrinsic characteristics not known) performance

of the first stage leach process. Therefore, with the macro influences identified and qualitatively quantified the intrinsic behaviour (reaction mechanism) of the leaching process can be determined. This information can theoretically validate the results obtained in the two previous chapters and it will also help to obtain a complete understanding of the whole first stage leach process (external and intrinsic behaviour).

Table 6.1 - The approximate variations in the matte and spent electrolyte solution compositions

	Matte **%**	**Spent electrolyte solution** **g/L**
Nickel (Ni)	49-51	28-31
Copper (Cu)	27-29	19-22
Iron (Fe)	0.3-0.7	0.4-0.7
Acid (H_2SO_4)	-	80-110

Table 6.2 - Time series expansion example

Input variable no. 1	**Input variable no. 2**
$x_1(t)$	$x_2(t) = x_1(t-1)$
$x_1(t+1)$	$x_2(t+1) = x_1(t)$
$x_1(t+2)$	$x_2(t+2) = x_1(t+1)$

Table 6.3 - Data representation for the LVQ neural net model for Ni

Variables	**Ni**	
	Time delay [h]	Time series expansion
Level in tank 1506 (h)	0	2
Pulp density in tank 1506 (P_2)	0	2
Level in tank 1102 (h_1)	1	2
Pulp density in tank 1102 (P_7)	1	2
Pulp flowrate to autoclave (F_7)	3	1
Spent electrolyte solution flowrate (F_{Acid})	3	1
Acid concentration ($[H_2SO_4]$)	4	2
Pressure (p_1)	4	1
Temperature (T_1)	2	1
Oxygen flowrate (F_{ox})	4	2
pH in compartment no. 1 (pH_1) of autoclave	4	1
pH in compartment no. 4 (pH_4) of autoclave	4	1
Concentration of Cu in compartment no. 1 ($[Cu]_1$) of autoclave	4	2

Table 6.4 - Data representation for the LVQ neural net model for Cu

Variables	**Cu**	
	Time delay [h]	Time series expansion
Level in tank 1506 (h)	0	2
Pulp density in tank 1506 (P_2)	0	2
Level in tank 1102 (h_1)	1	2
Pulp density in tank 1102 (P_7)	1	2
Pulp flowrate to autoclave (F_7)	4	2
Spent electrolyte solution flowrate (F_{Acid})	3	1
Acid concentration ($[H_2SO_4]$)	Excluded	-
Pressure (p_1)	4	1
Temperature (T_1)	4	1
Oxygen flowrate (F_{ox})	3	1
pH in compartment no. 1 (pH_1) of autoclave	4	1
pH in compartment no. 4 (pH_4) of autoclave	4	1
Concentration of Cu in compartment no. 1 ($[Cu]_1$) of autoclave	4	2

Table 6.5 - Data representation for the LVQ neural net model for Fe

Variables	**Fe**	
	Time delay [h]	Time series expansion
Level in tank 1506 (h)	0	2
Pulp density in tank 1506 (P_2)	0	2
Level in tank 1102 (h_1)	1	1
Pulp density in tank 1102 (P_7)	1	1
Pulp flowrate to autoclave (F_7)	4	1
Spent electrolyte solution flowrate (F_{Acid})	4	1
Acid concentration ($[H_2SO_4]$)	4	1
Pressure (p_1)	4	1
Temperature (T_1)	4	1
Oxygen flowrate (F_{ox})	4	1
pH in compartment no. 1 (pH_1) of autoclave	4	1
pH in compartment no. 4 (pH_4) of autoclave	4	1
Concentration of Cu in compartment no. 1 ($[Cu]_1$) of autoclave	Excluded	-

Table 6.6 - Ranking of the attributes for the process outputs of Ni and Cu

Variables/Attributes	**Ranking**	
	Ni	**Cu**
Level in tank 1506 (h)	3	7
Pulp density in tank 1506 (P_2)	12	9
Level in tank 1102 (h_1)	10	5
Pulp density in tank 1102 (P_7)	8	4
Pulp flowrate to autoclave (F_7)	4	10
Spent electrolyte solution flowrate (F_{Acid})	13	8
Acid concentration ($[H_2SO_4]$)	1	11
Pressure (p_1)	2	3
Temperature (T_1)	6	12
Oxygen flowrate (F_{ox})	7	13
pH in compartment no. 1 (pH_1)	5	6
pH in compartment no. 4 (pH_4)	9	2
Concentration of Cu in compartment no. 1 ($[Cu]_1$) of autoclave	11	1

Table 6.7 - The four highest ranked variables for the process outputs of Ni and Cu obtained by the correlation coefficients, LVQ models and decision trees.

Ranking	Correlation coefficients	LVQ models Sensitivity analyses	Decision tree χ^2 -test
Ni			
1	Acid concentration	Acid concentration	Acid concentration
2	Pulp flowrate	Level tank 1506	Pressure
3	Level tank 1506	Pressure	Level tank 1506
4	Temperature	Oxygen flowrate	Pulp flowrate
Cu			
1	pH in compartment no. 4	pH in compartment no. 4	Cu concentration in compartment no.1
2	Cu concentration in compartment no.1	Cu concentration in compartment no.1	pH in compartment no. 4
3	Spent electrolyte flowrate	Level tank 1102	Pressure
4	Temperature	Pulp density tank 1506	Pulp density tank 1102

Table 6.8 - The statistical mean (averages) for the six most important variables for Ni, Cu and Fe

No.	Variables	Output class	
		High	Low
	Ni:		
1	Acid concentration [g/L]	87.5	81.8
2	Level in tank 1506 [%]	60.4	59.5
3	Pressure [kPa]	610	573
4	Oxygen flowrate [kg/h]	165	136
5	Pulp density in tank 1506 [kg/L]	1.537	1.528
6	Pulp density in tank 1102 [kg/L]	1.558	1.545
	Cu:		
1	pH in compartment no. 4 (autoclave)	1.87	2.39
2	Concentration of Cu in compartment no. 4 [g/L]	14.6	6.0
3	Level in tank 1102 [%]	60.9	57.4
4	Pulp density in tank 1506 [kg/L]	1.475	1.498
5	Pulp density in tank 1102 [kg/L]	1.525	1.521
6	Pressure [kPa]	551	556
	Fe:		
1	Pulp density in tank 1102 [kg/L]	1.543	1.564
2	Pulp density in tank 1506 [kg/L]	1.526	1.545
3	Acid concentration [g/L]	82.4	84.6
4	Oxygen flowrate [kg/h]	132	175
5	Level in tank 1102 [%]	60.3	59.5
6	Spent electrolyte solution flowrate [L/min]	11939	14333

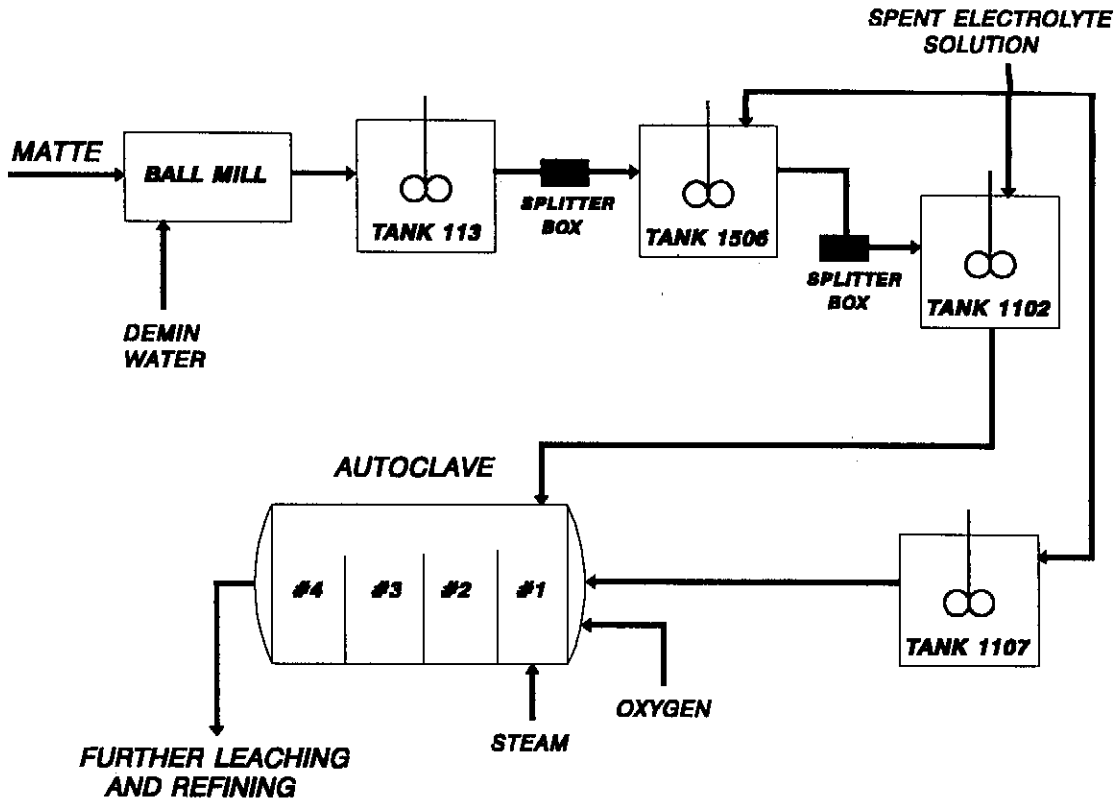

Figure 6.1 - Flow diagram of the first stage leaching section of the plant

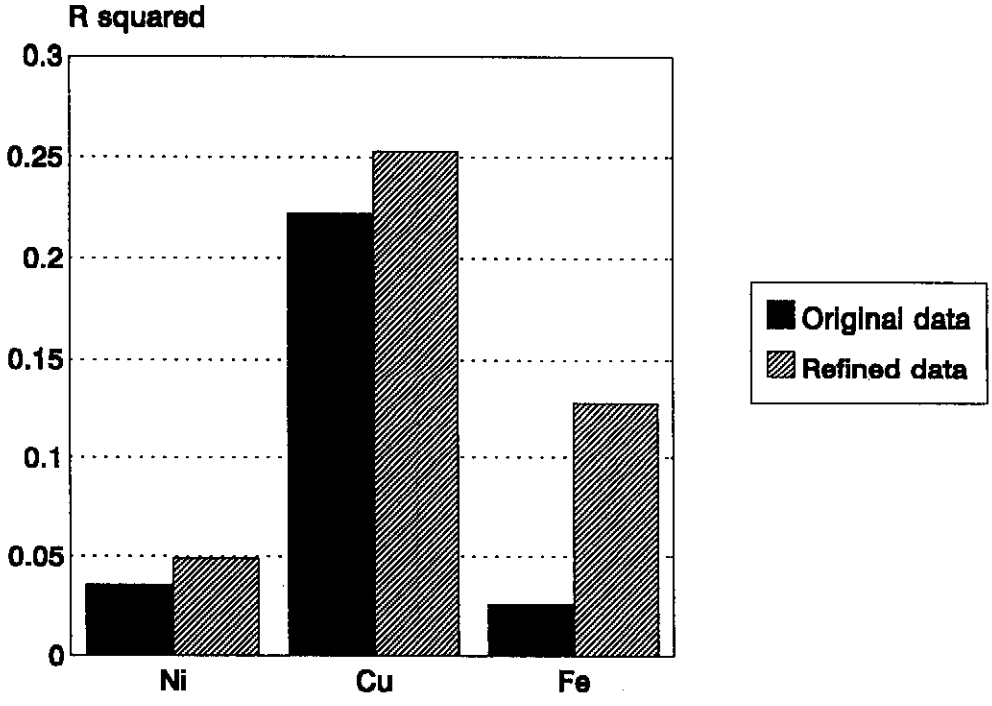

Figure 6.2 - R squared values of multiple linear regression on the original data (set A) and the refined data (set B)

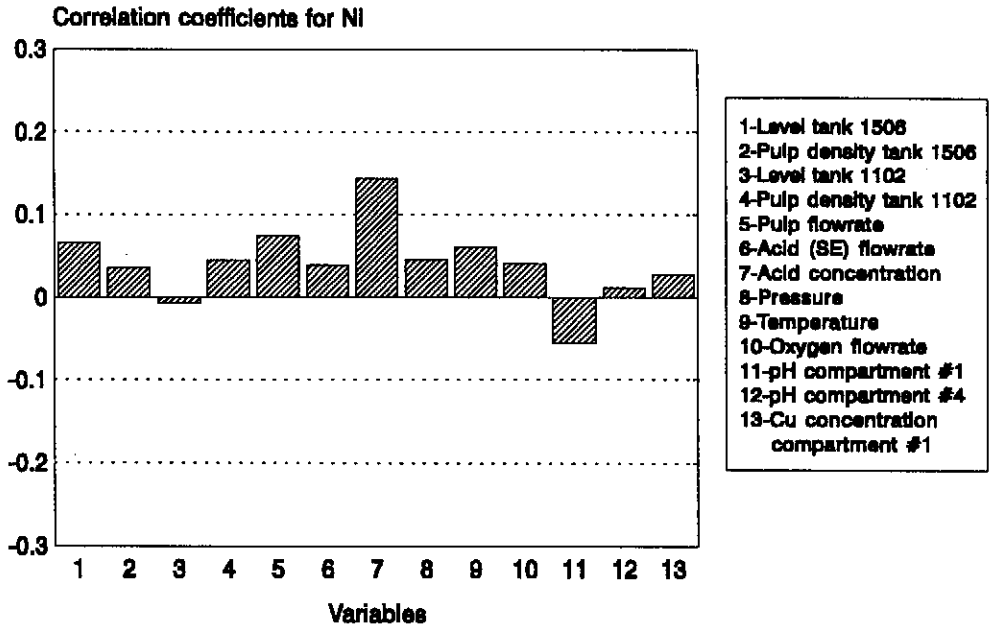

Figure 6.3 - Correlation coefficients of the different variables to Ni

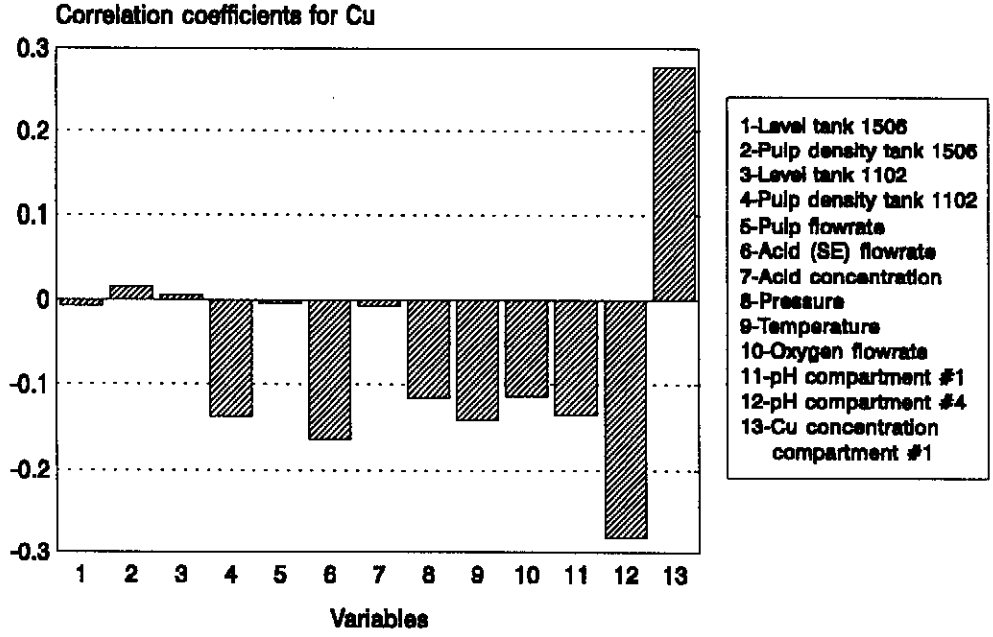

Figure 6.4 - Correlation coefficients of the different variables to Cu

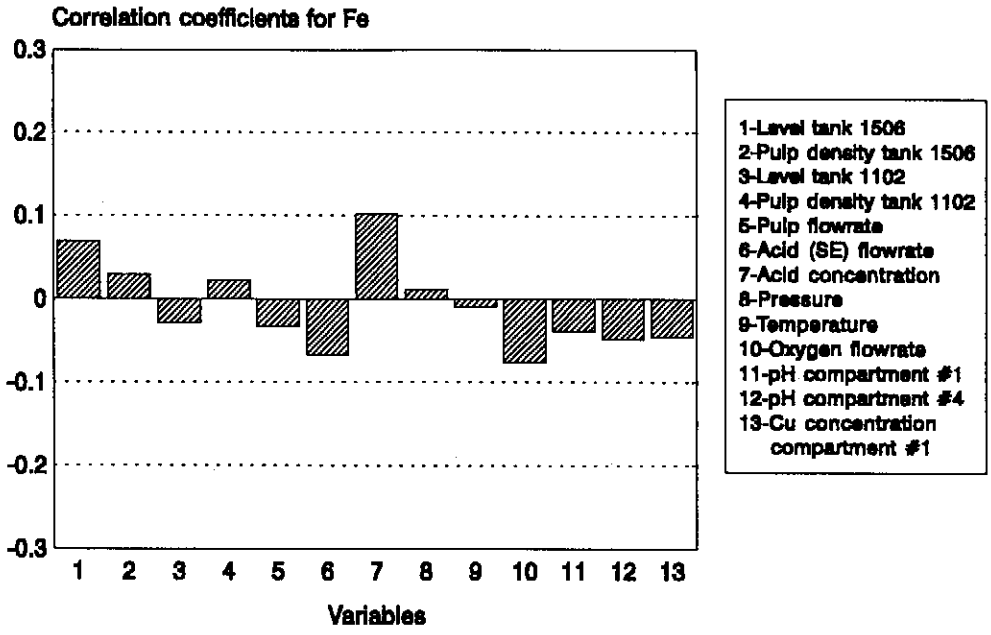

Figure 6.5 - Correlation coefficients of the different variables to Fe

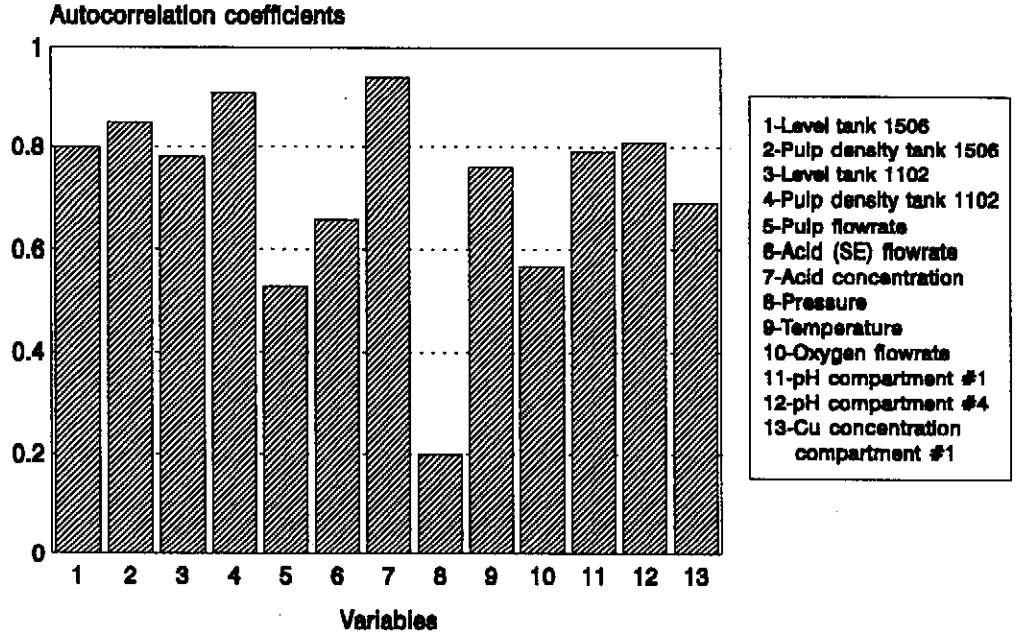

Figure 6.6 - Autocorrelation coefficients of the different variables

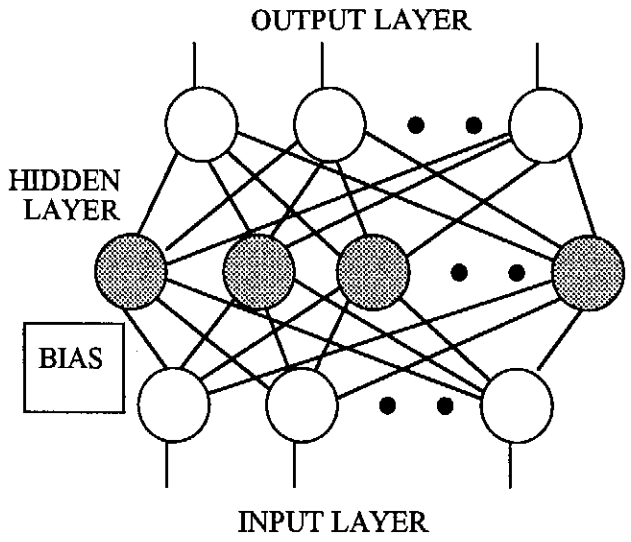

Figure 6.7 - The general structure of an artificial neural network (ANN)

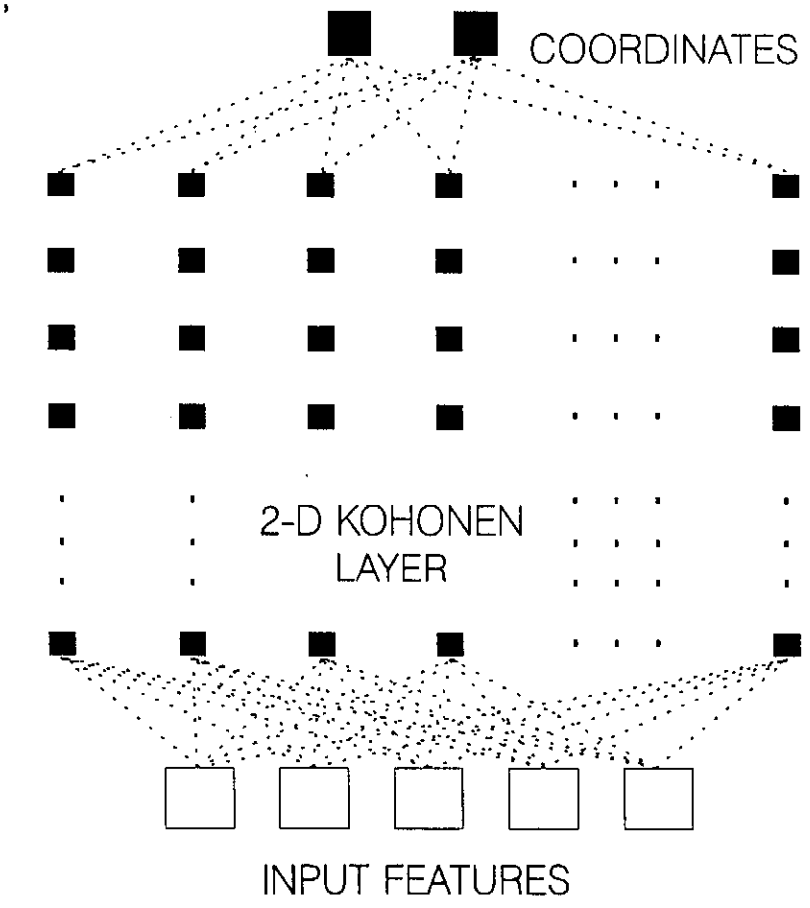

Figure 6.8 - Generic structure of a self-organising map (SOM) neural network

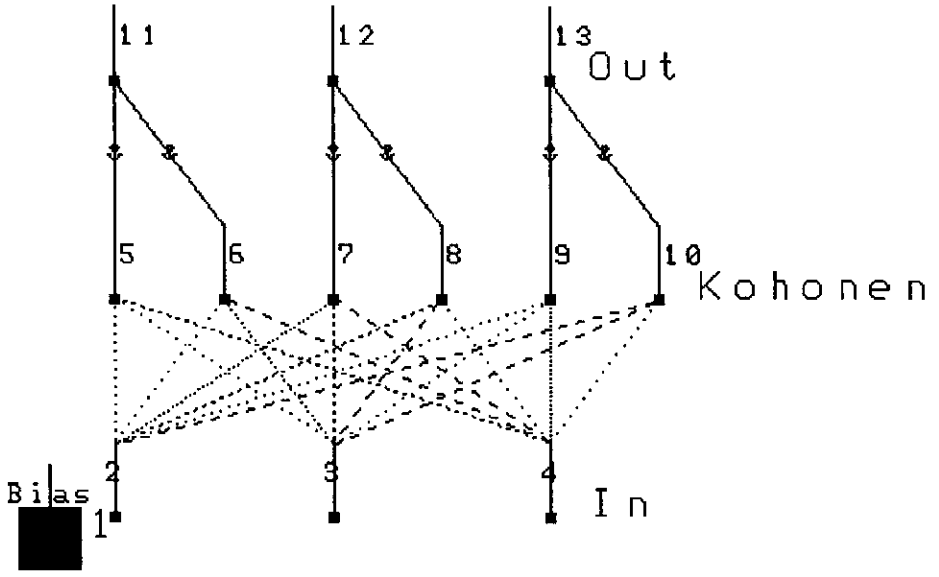

Figure 6.9 - A typical LVQ neural net with 3 input nodes, a Kohonen layer of 2 nodes per input, and an output layer of 3 nodes

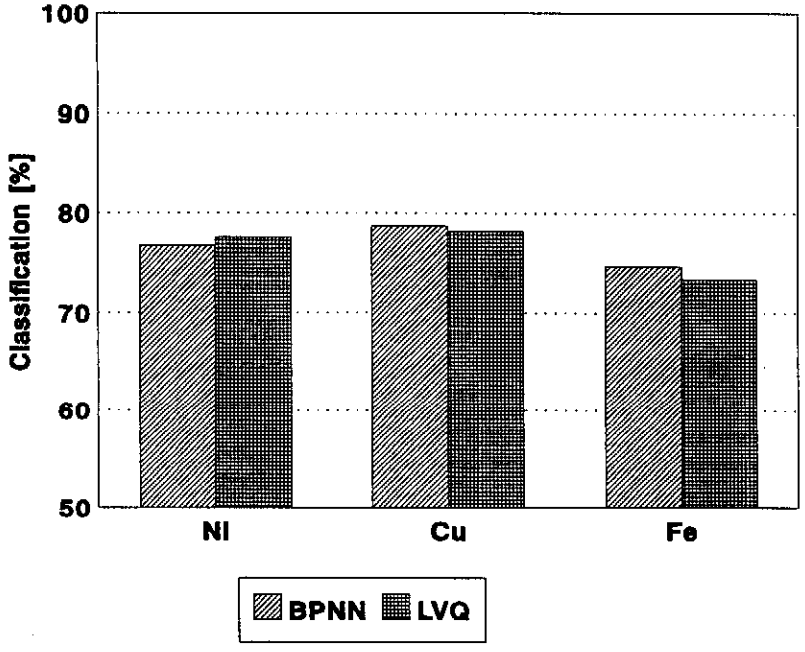

Figure 6.10 - The classification results, with data set A, for the back propagation neural net (BPNN) and the LVQ neural net models

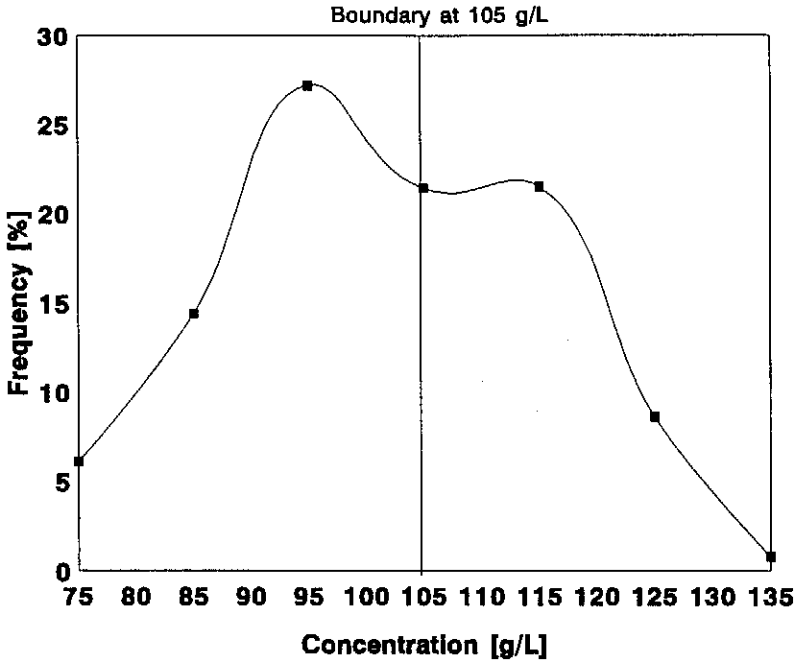

Figure 6.11 - The frequency distribution of the concentration of Ni (process output)

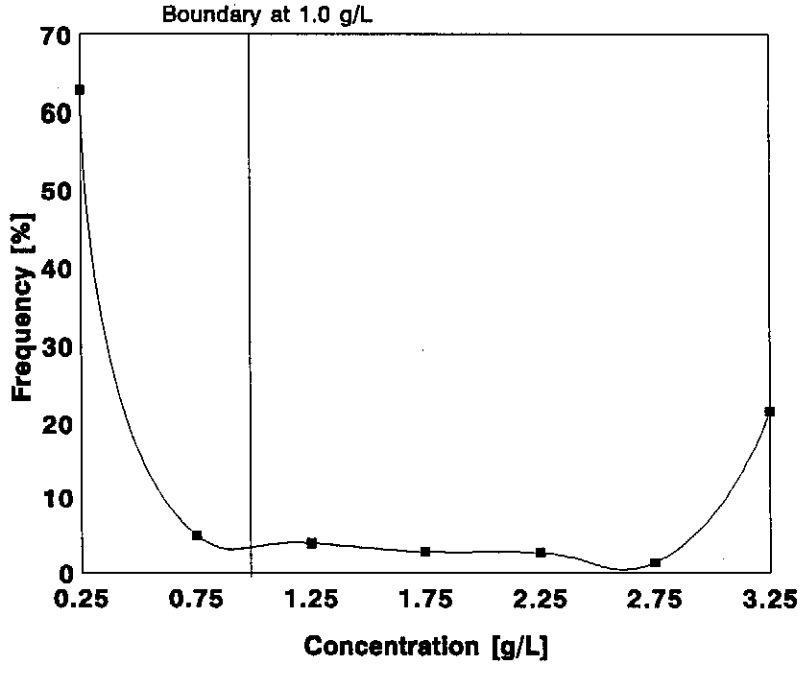

Figure 6.12 - The frequency distribution of the concentration of Cu (process output)

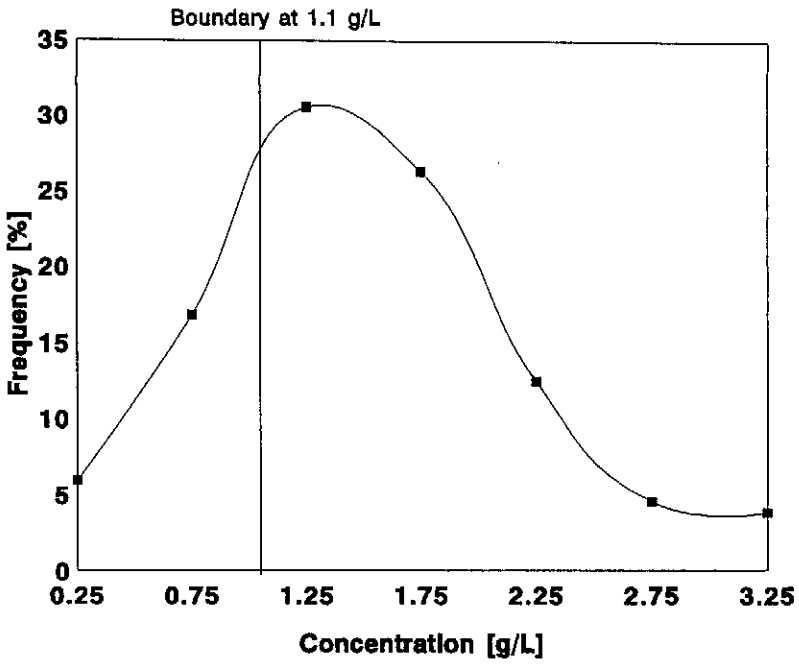

Figure 6.13 - The frequency distribution of the concentration of Fe (process output)

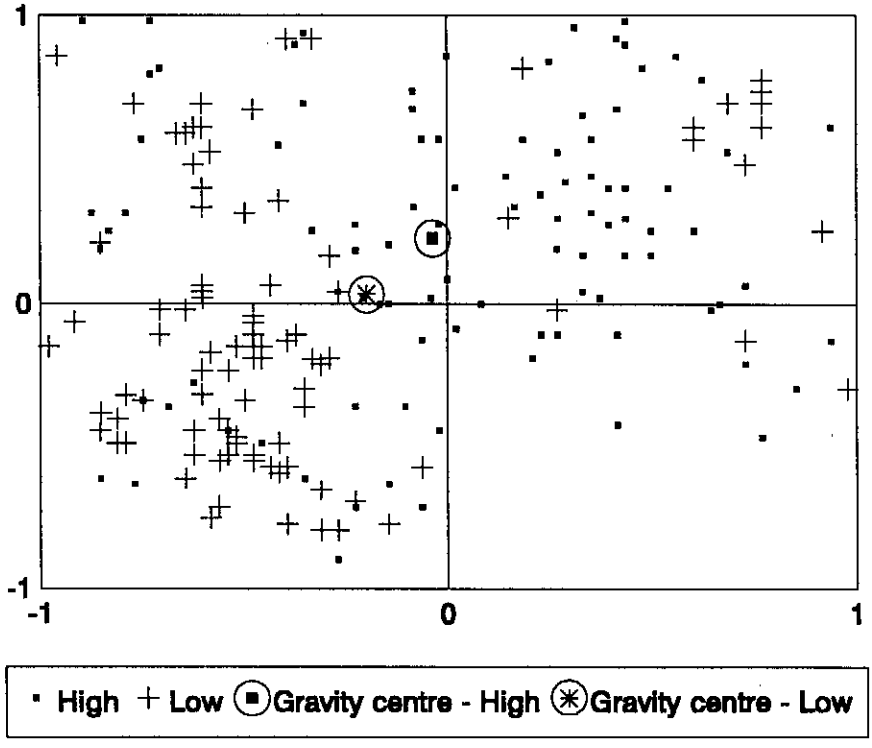

Figure 6.14 - The self-organising map (SOM) representation for the high and low classes (concentrations) for the process output, Ni

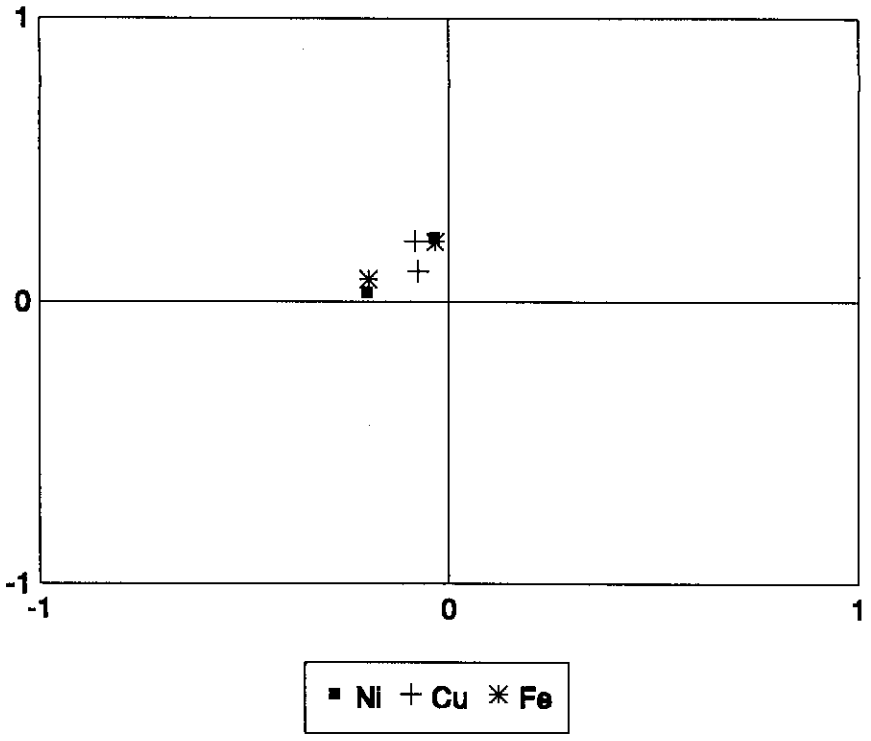

Figure 6.15 - The centres of gravity of the self-organising maps (SOM) clusters for the high and low output parameters of the process

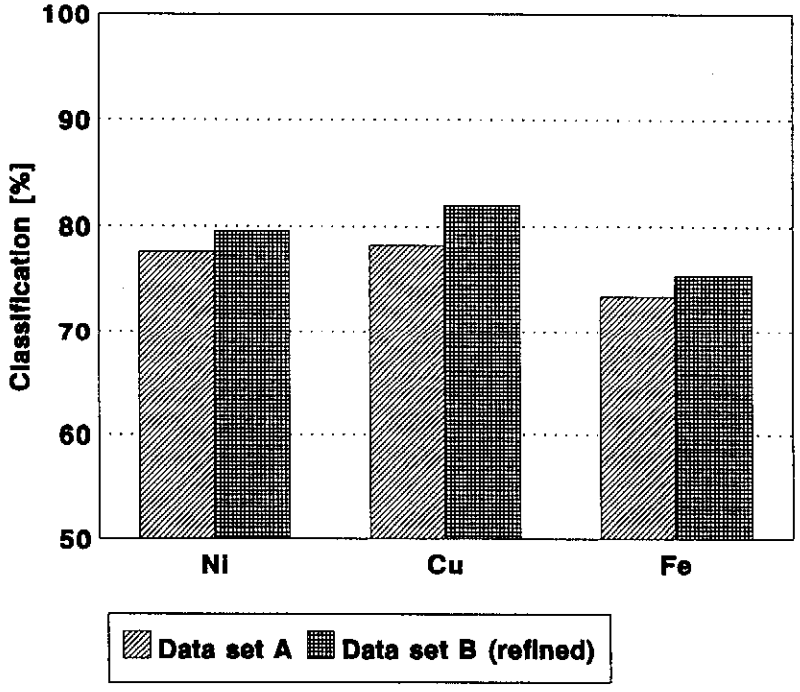

Figure 6.16 - The classification results of the LVQ neural network models with data sets A (original) and B (refined)

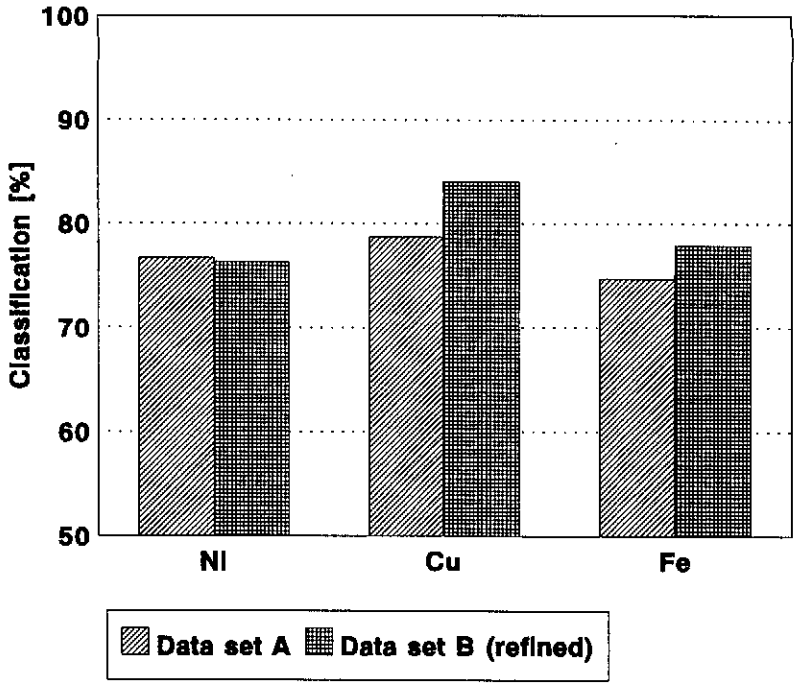

Figure 6.17 - The classification results of the back propagation neural network models with data sets A (original) and B (refined)

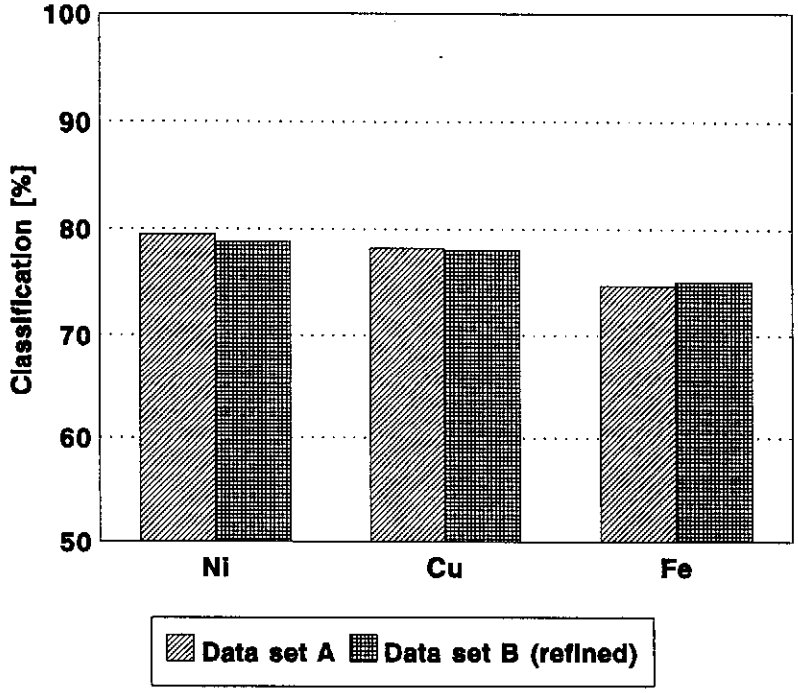

Figure 6.18 - The classification results of the decision trees with data sets A (original) and B (refined)

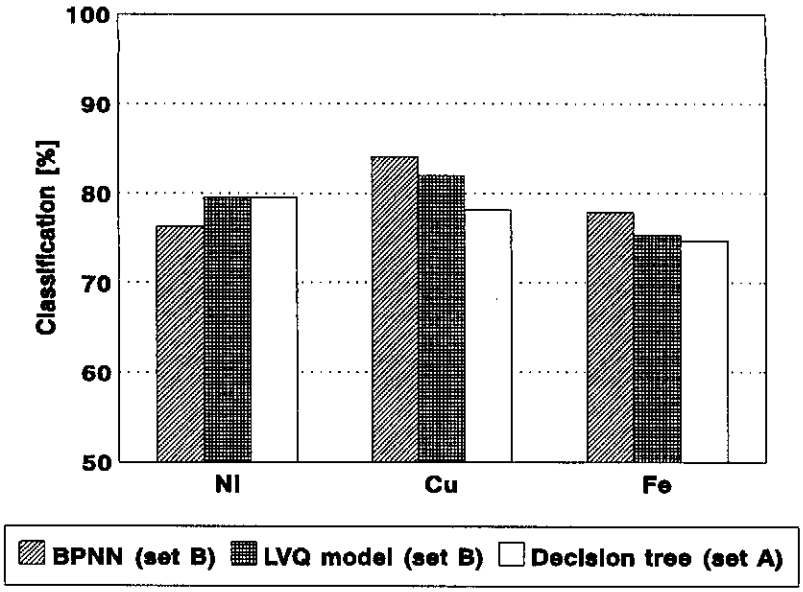

Figure 6.19 - The comparison of the classification results for the back propagation neural net (BPNN) - data set B, the LVQ neural net - data set B and the decision tree - data set A

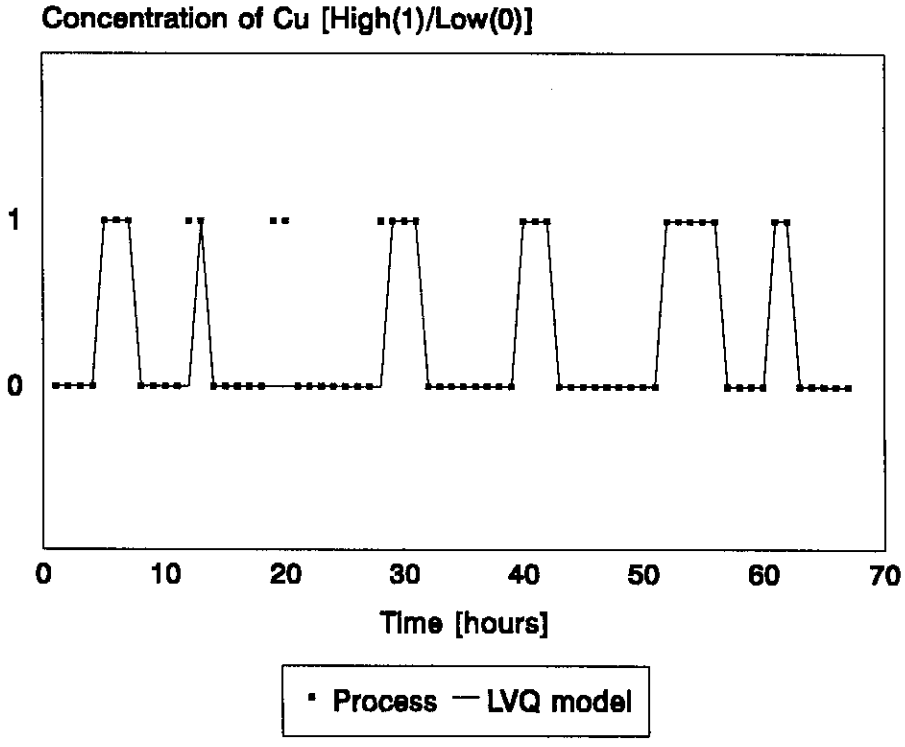

Figure 6.20 - An illustration of the LVQ neural net model for Cu simulating the actual output of the process

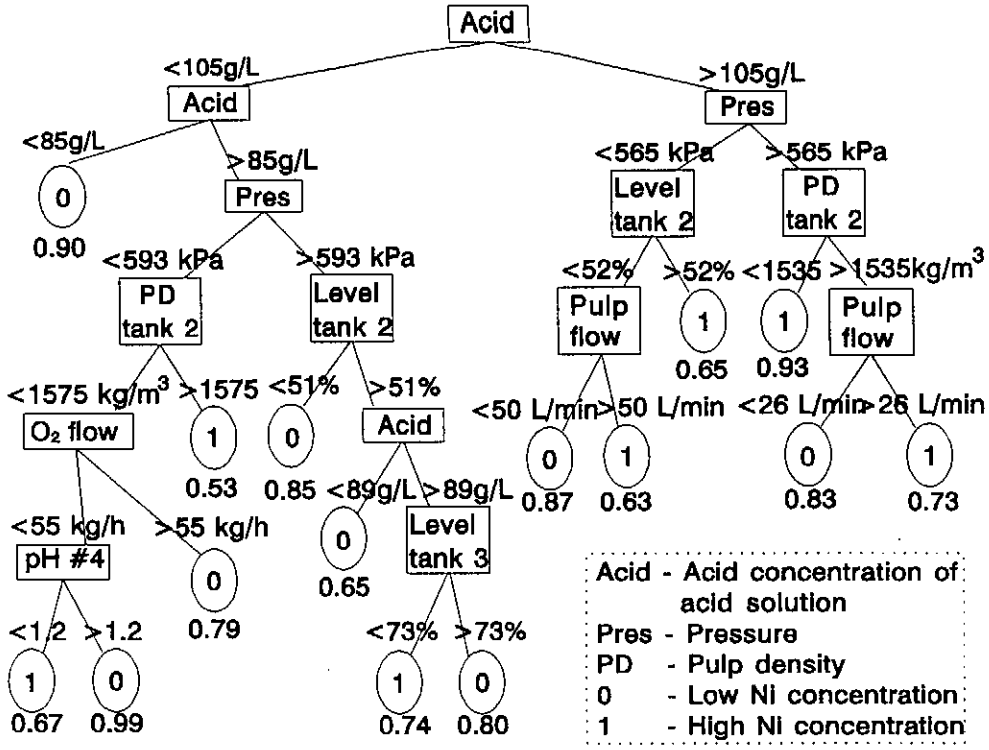

Figure 6.21 - The induced decision tree for the process output Ni, which obtained a classification result of 79.5%

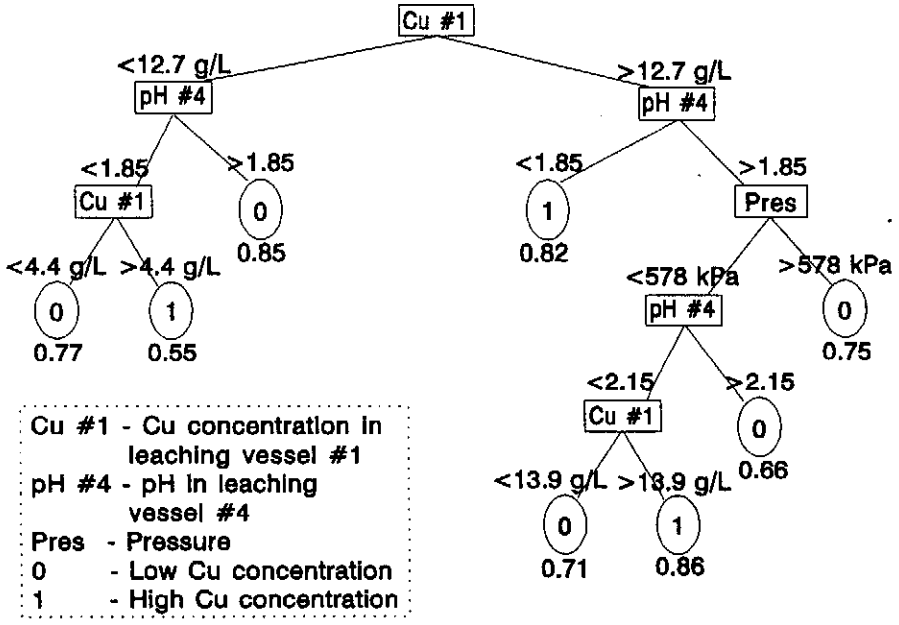

Figure 6.22 - The induced decision tree for the process output Cu, which obtained a classification result of 78.2%

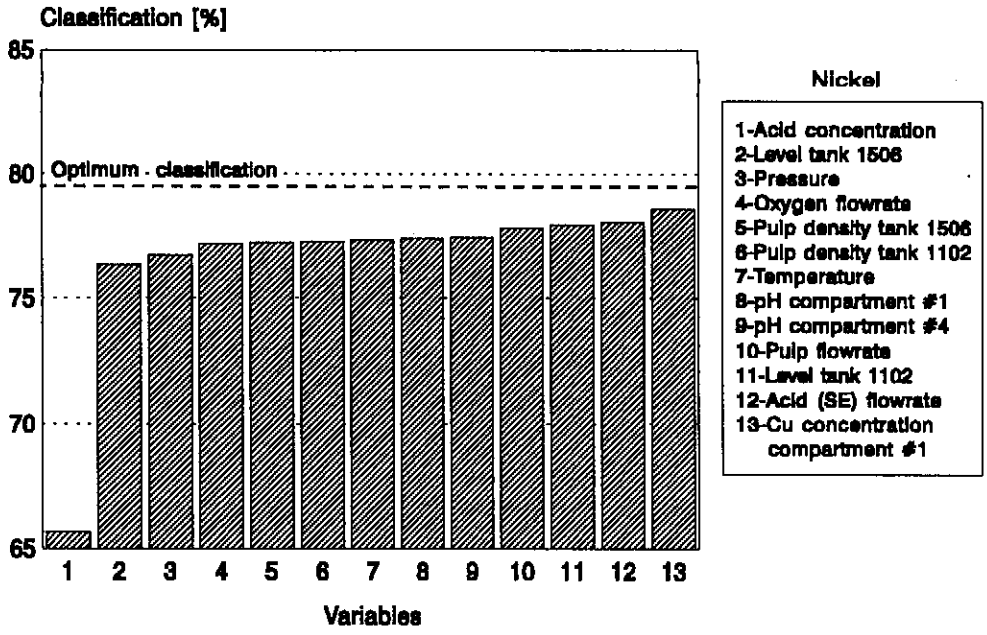

Figure 6.23 - Ranking of the importance of the different variables for Ni, as determined by sensitivity analyses

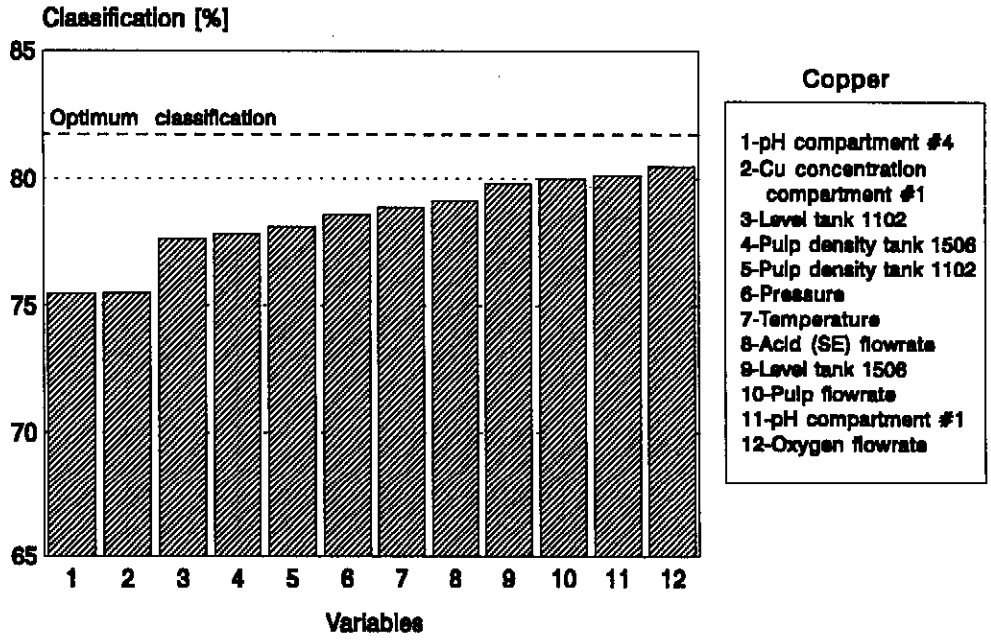

Figure 6.24 - Ranking of the importance of the different variables for Cu, as determined by sensitivity analyses

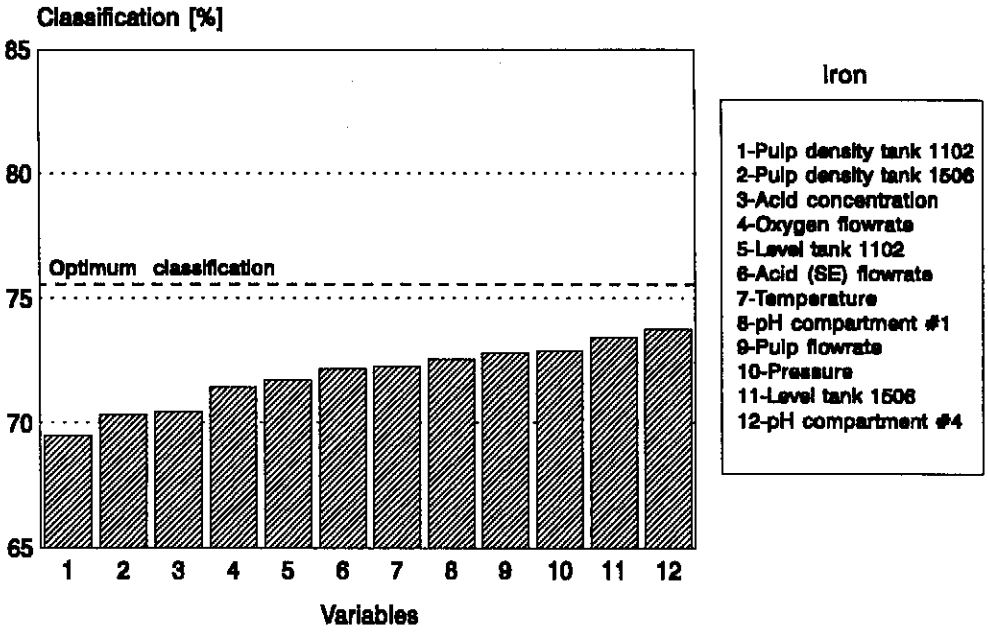

Figure 6.25 - Ranking of the importance of the different variables for Fe, as determined by sensitivity analyses

Chapter 7

LEACHING MECHANISM

Generally the kinetics of leaching reactions are described in terms of concentrations temperature, pressure and the rate of agitation, while the transformation of the mineral structure is usually neglected. In the specific leaching mechanism discussed here, it is obvious that the physical changes in the solids (matte), for example, the crystal structure, specific gravity and the type of anion lattice (sulphide lattice), play an important role in the leaching kinetics of the base metals from the Ni-Cu matte. The influence of changes in the mineral phase characteristics (i.e. symmetry of crystal structure and specific gravity) on the leaching mechanism of the leaching process is also discussed. The different leaching reactions proposed in this chapter are substantiated by XRD analysis and mole balance calculations (Appendix F), as well as information from the literature (see Chapter 2).

7.1 MINERALOGICAL CHANGES IN THE SOLIDS

In the determination of the mineral phases present it was assumed that the only relevant elements (with high enough concentration) present in the solid samples were nickel, copper and sulphur, with the other species comprising less than 1% (weight/weight) of the original matte. The nickel alloy, nickel sulphides and copper sulphides are shown in Table 7.1 and Table 7.2 in the order that they appear and disappear during the course of the leaching experiment. The methodology used in obtaining the mineral compositions of the phases in each sample as well as the calculations performed on the original data are discussed in Appendix F.

The mineral structure of the nickel and copper sulphides can be visualised as layers of sulphide anions with nickel and copper cations filling some of the spaces in this layers, where the filling of the nickel and copper cations in the sulphide lattice will determine the crystal structure of the mineral, and hence it's properties. The mineral

phase changes occurring in the samples produced by the leaching process are shown in Table 7.1 and were determined by XRD analyses. The nickel sulphides leach from heazlewoodite (Ni_3S_2) to millerite (NiS), with godlevskite (Ni_7S_6) forming as an intermediate product. The millerite (NiS) leaches further to form polydymite (Ni_3S_4). The mechanism for the leaching of the copper sulphides is slightly more complex with chalcocite (Cu_2S) being leached and formed in the beginning of the experiment. The chalcocite (Cu_2S) is leached to form digenite ($Cu_{1.8}S$), with djurleite ($Cu_{31}S_{16}$) forming as an intermediate product. The digenite ($Cu_{1.8}S$) leaches further to form covellite (CuS). From the composition of these minerals (Table 7.2) it is evident that nickel and copper are gradually leached out of the sulphide lattice to form minerals with a lower nickel and copper to sulphur ratio. The nickel in the alloy phase leaches out of the matte fairly quickly and no mineral change was detected in the alloy phase. The leaching of the nickel alloy out of the heazlewoodite (Ni_3S_2) matrix is evident from Fig. 7.1(a) and (b). During the leaching of the nickel alloy, veins and cracks start to form in the Ni_3S_2 matrix and a thin layer of Cu_2S is deposited on the rims (or edges) of the veins (barely visible) and on the outside of the particle (Fig. 7.1(b)). The cracks and veins increase as the leaching process continues until the particles are completely porous (Fig. 7.1(e)). This is illustrated by the range of SEM (scanning electron microscope) photographs in Fig. 7.1(a)-(e).

An intermediate mineral product in the leaching mechanism is defined as a mineral species which occurs only for a short period in the reaction and does not exceed approximately 5% (w/w) of the sample composition.

7.1.1 Nickel sulphides

The Ni-S system has been studied systematically by Kullerud and Yund (1962) from 200° to 1030°C and the compounds in the system were found to be Ni_3S_2, Ni_7S_6, NiS, Ni_3S_4 and NiS_2.

The most obvious change in the mineral is the gradual decrease in the specific gravity of each mineral species that is formed (Table 7.1). The decrease in specific gravity goes hand in hand with the gradual decrease in the nickel content in each of

the mineral species (Table 7.2). This indicates that the nickel is leached out of the mineral structure with the sulphide lattice staying intact. Another interesting aspect of the order in which the minerals are formed is the fact that as the nickel concentration decreases in the sulphide lattice (nickel diffusion out of the lattice), the mineral that is formed tends to have a higher degree of symmetry (see Table 7.3). For example, looking at Ni_3S_2 (rhombohedral), Ni_7S_6 (orthorhombic), NiS (rhombohedral) and Ni_3S_4 (cubic), the only mineral structure that does not fit this rule is that of Ni_7S_6. This can be explained by the fact that Ni_7S_6 is formed as an intermediate product. Ni_7S_6 (orthorhombic) is formed as an intermediate product in the leaching process because the crystal class is of a lower order of symmetry than Ni_3S_2 (rhombohedral). Therefore, the structural driving force for the formation of this crystal structure is less than that for the formation of NiS. This will then have the effect of nickel being leached out more easily from Ni_7S_6 with a orthorhombic structure to form NiS with a rhombohedral structure.

7.1.2 Copper sulphides

The mineralogy of the copper sulphides is a bit more complex than that of the nickel sulphides, because (chemically) nickel in the solids can be replaced with copper from the solution. Therefore, with the reacting solution being spent electrolyte which originally contains a high concentration of copper, the copper in the solution is cemented as a copper sulphide while at the same time nickel is leached out of the solids. Thus the copper sulphides increase in the beginning of the experiment. Copper is also leached simultaneously with the cementation of copper, because sufficient conditions exist for the leaching of copper out of the solids (Cu_2S). Because the chemical driving force for the cementation of copper with nickel sulphide (Ni_3S_2) is higher, copper in the solution is preferably cemented (Cu_2S or $Cu_{1.96}S$) while nickel is leached. The minerals of Cu_2S and $Cu_{1.96}S$ are transformed to $Cu_{1.8}S$ phase during the leaching of copper out of these minerals. Table 7.2 shows that $Cu_{1.8}S$ is present in the solids from approximately 5 minutes after the start of the experiment. This indicates that the minerals of Cu_2S and $Cu_{1.96}S$ have been leached to form $Cu_{1.8}S$ to a minor extent, and Cu_2S and $Cu_{1.96}S$ were formed again from the cementation of copper, because no increase (in fact a decrease) in the copper

concentration in the solution was detected. A factor that complicates the determination of the chalcocite (Cu_2S) and chalcocite-Q ($Cu_{1.96}S$) mineral species is that both species have XRD patterns with relatively small peaks that overlap. Due to this, and the fact that the chemical compositions of Cu_2S and $Cu_{1.96}S$ are very close, these copper sulphide species are referred to as Cu_2S until it is possible at a latter stage to separately detect the two species.

It is again noticed that the copper sulphide minerals forming in the leaching process follow the same basic crystallographic rules as the nickel sulphide minerals. It should be kept in mind that the chemical driving force for the leaching reactions (which leach out the nickel and copper from the sulphide structure) is the main driving force for the transformations occurring in the solids. The mineral species forming first have a high specific gravity and as the other copper sulphide minerals are detected in the order that they appear and disappear the specific gravity decreases. The indication is that the most stable minerals are the minerals with the highest degree of symmetry (Table 7.3). For example, Cu_2S with an orthorhombic structure forms $Cu_{31}S_{16}$ with a monoclinic structure as an intermediate product as the copper is leached out of the sulphide lattice, which then forms $Cu_{1.8}S$ with a rhombohedral structure (Table 7.1). The rhombohedral structure of $Cu_{1.8}S$ then leaches to the hexagonal structure of CuS. The fact that $Cu_{31}S_{16}$ (monoclinic) is only an intermediate product is justified because it is of a lower order of symmetry than Cu_2S (orthorhombic) where naturally the mineral structure will tend to change to a structure of higher symmetry. This also explains the compositional difference between $Cu_{1.96}S$ and Cu_2S at times 120 and 160 minutes (Table 7.2), because $Cu_{1.96}S$ (tetragonal) is of higher symmetry than Cu_2S (orthorhombic) and therefore its resistance to be transformed from a structural point of view is slightly higher than Cu_2S. This explains why $Cu_{1.96}S$ is still present in significant concentrations while Cu_2S has already been leached or transformed.

From the leaching sequence of the minerals in the solids it could be said that certain basic crystallographic rules exist by which the crystal structure and mineral species are being modified in this leaching process, excluding the chemical driving forces.

These rules are:

(i) The mineral species present will be determined mainly by the specific gravity of the mineral, which in the case of the sulphide minerals indirectly means the concentration of the metal cations present in the sulphide lattice.

(ii) The mineral with the highest degree of symmetry will preferentially form, thus the mineral with the highest symmetry is the most stable species with the lowest free energy for formation (most resistance to the leaching process).

Independent research conducted by Lourens (1993) of the Gencor Laboratories and by Dutrizac and Chen (1987) generally obtained similar findings on the mineralogy of the leaching process (see Chapter 2). These findings agree with the major mineral phases identified from the experimental samples. One of the differences in the mineralogy of the leaching experiment to the actual plant is that NiS_2 was identified (Lourens, 1993) as a minor phase in the autoclave, while only a trace quantity was detected in the experiments. Furthermore, what is interesting to note is that the same phases are present in the solids of the autoclave in compartment no. 1 and 4, with CuS present in higher concentrations in the 4^{th} compartment, which indicates that most of the reactions have already occurred in the first compartment of the autoclave. The reason why Ni_3S_2 is still present in the first stage leach residue is because some of the material in the autoclave will pass through the autoclave faster than other material in the autoclave (residence time distribution of particles in the autoclave is not that of a perfectly mixed reactor).

7.2 THE MECHANISM OF LEACHING BASED ON THE OBSERVED REACTION RATES

The leaching mechanism for the Sherritt Gordon acid-oxygen pressure leach was determined from the phase changes identified in the reaction process and the analytical results, as well as knowledge gained from the literature. These reactions identified were confirmed by calculating the mole increases or decreases indicated by the stoichiometry of the reactions and comparing it to the analytical results (see Appendix F). All the reactions identified for the leaching mechanism were

electrochemical of nature, therefore the reactions can also be written as half cell reactions (anodic and cathodic half cell reactions).

The first 10 minutes of the autoclave acid-oxygen pressure leach experiment was omitted in the discussion because it is part of the start-up procedure of the experiment (reaction conditions have not yet stabilised). The experiment only starts to simulate the actual plant (autoclave) process after approximately 10 to 20 minutes (see Appendix B). In the determination of the reaction mechanism care was taken to stay with the main reactions occurring in the leaching process, therefore cobalt was omitted from this investigation, while less attention was paid to the role of iron.

The overall reaction mechanism could roughly be divided into three stages (according to the batch experiment) where the major reactions occurring in each stage of the leaching process differ (Fig. 7.2 - Fig. 7.5), i.e.:

(i) Stage I (10 - 40 minutes) - the cementation of copper and the leaching of nickel from the alloy phase and out of the Ni_3S_2 phase.

(ii) Stage II (40 - 160 minutes) - the selective leaching of nickel to form various Ni-S mineral phases and the simultaneous leaching and cementation of copper to form the various Cu-S mineral phases.

(iii) Stage III (160 - 300 minutes) - the simultaneous leaching of nickel (to form NiS and Ni_3S_4) and copper (to form and CuS).

The variation in the reaction mechanism for each stage is due to the formation of different mineral species that determine the reactions, and subsequently influence the reaction kinetics.

(i) Stage I (10 - 40 minutes)

The major reactions occurring in this time period for the leaching process are the leaching of nickel from the alloy phase (see Fig. 7.1(b) and Fig. 7.2). Figure 7.2 shows that the Ni alloy phase is almost completely leached out of the solid phase after 40 minutes in the experiment, which indicates fast reaction kinetics for the leaching of Ni alloy.

$$Ni + 2H^+ + {}^1/_2O_2 \rightarrow Ni^{2+} + H_2O \qquad (7.1)$$

The fast kinetics for the leaching of nickel alloy could also be due to the galvanic couple that exists between the nickel metal and the nickel and copper sulphides. Therefore, nickel metal must have a lower rest potential than the sulphide minerals present in the matte. Galvanic interaction is possible between Ni alloy and the other mineral phases because they are highly intergrown. The transformation of Ni_3S_2 to form NiS and the cementation of copper to form Cu_2S occur simultaneously with the leaching of nickel (eqs. 7.2 - 7.4).

$$Ni_3S_2 + 2H^+ + {}^1/_2O_2 \rightarrow Ni^{2+} + 2NiS + H_2O \qquad (7.2)$$

The reaction proposed in equation (7.2) is substantiated by Fig. 7.2 where it is evident that the leaching of Ni_3S_2 coincides with the formation of NiS at this stage of the leaching process.

$$Ni + Ni_3S_2 + 4Cu^{2+} \rightarrow 4Ni^{2+} + 2Cu_2S \qquad (7.3)$$

Nickel alloy is leached together with Ni_3S_2 according to equation (7.3) due to the catalytic effect of cupric ions (Cu^{2+}) on the Ni alloy and Ni_3S_2, and where the Cu^{2+} ions are cemented as Cu_2S.

$$Ni_3S_2 + 2Cu^{2+} \rightarrow 2Ni^{2+} + NiS + Cu_2S \qquad (7.4)$$

The cementation of copper to form Cu_2S is evident from Fig. 7.3 where the chalcocite (Cu_2S) concentration increases and the Cu^{2+} ion concentration in solution decreases (Fig. 7.4) in this stage of the leaching process. Figure 7.4 also shows that the cementation of Cu^{2+} according to equations (7.3) and (7.4) has fast reaction kinetics (the Cu^{2+} in the spent electrolyte is cemented in the first 40 minutes of the experiment). The cementation of copper is confirmed by the increase in the copper concentration in the solids (Fig. 7.5). Copper is also leached from Cu_2S by H_2SO_4 and O_2 to form $Cu_{1.8}S$ as follows:

$$5Cu_2S + 2H^+ + {}^1/_2O_2 \rightarrow Cu^{2+} + 5Cu_{1.8}S + H_2O \qquad (7.5)$$

Some of the Cu^{2+} ions that are leached by reaction (7.5) will immediately be cemented by reactions (7.3) and (7.4). Several authors (Hofirek and Kerfoot, 1992, Symens *et al*, 1979 and Dutrizac and Chen, 1987) stated that Cu^{2+} ions act as a catalyst for leaching of Ni_3S_2 (see Chapter 2). The tendency of the Cu^{2+} ions to be cemented by Ni_3S_2 (with fast kinetics) to Cu_2S is one explanation why Ni_3S_2 is leached instead of Cu_2S in the initial stages of the leaching process. Otherwise the reactions of Ni_3S_2 and Cu_2S with H^+ and O_2 occur at approximately the same rate. Another explanation why Ni_3S_2 is leached before Cu_2S is that a galvanic couple exist between these minerals, with Ni_3S_2 having a lower rest potential than Cu_2S.

Iron is leached, to a minor extent (see Fig. 7.4), together with Ni_3S_2 according to equation (7.6) and the metallic iron in the nickel-copper alloy dissolves together with the metallic nickel in this stage of the leach, to form ferrous sulphate (eq. 7.7).

$$Ni_3S_2.FeS + 2H^+ + {}^1/_2O_2 \rightarrow 3NiS + Fe^{2+} + H_2O \qquad (7.6)$$

$$Fe + 2H^+ + {}^1/_2O_2 \rightarrow Fe^{2+} + H_2O \qquad (7.7)$$

It is evident from Fig. 7.2 that the leaching rate of Ni_3S_2 (formation rate of NiS) decreased dramatically after 20 minutes in the experiment. This is due to hydrogen sulphide (H_2S) that was detected in the experiment in the time period 20 to 80 minutes (with an O_2 partial pressure of 1.8 bar). The formation of H_2S occurs through the oxidation (anodic half cell) reaction of the cementation of copper with Ni_3S_2 and Ni alloy (eqs. 7.3a and 7.4a). The electrochemical half cell reactions for equations (7.3) and (7.4) are as follows:

$$Ni + Ni_3S_2 + 4H^+ \leftrightarrow 2H_2S + 4Ni^{2+} + 4e^- \qquad (7.3a)$$

$$4Cu^{2+} + 2H_2S + 4e^- \leftrightarrow 2Cu_2S + 4H^+ \qquad (7.3b)$$

$$Ni + Ni_3S_2 + 4Cu^{2+} \rightarrow 4Ni^{2+} + 2Cu_2S \qquad (7.3)$$

$$Ni_3S_2 + 2H^+ \leftrightarrow H_2S + NiS + 2Ni^{2+} + 2e^- \quad (7.4a)$$

$$2Cu^{2+} + H_2S + 2e^- \leftrightarrow Cu_2S + 2H^+ \quad (7.4b)$$

$$Ni_3S_2 + 2Cu^{2+} \rightarrow 2Ni^{2+} + NiS + Cu_2S \quad (7.4)$$

The reason why H_2S was detected was due to the Cu^{2+} ion concentration becoming very low in the solution and reactions (7.3b) and (7.4b) could not proceed at a sufficient rate to consume the H_2S produced in reactions (7.3a) and (7.4a). (H_2S is also detected in the plant operations.) The production of H_2S stopped when the Ni alloy content of the solid phase was depleted. It is therefore assumed that reaction (7.3) is more dominant than reaction (7.4) in the production of H_2S. A slight decrease in the acid consumption rate was also noticed (see Fig. 7.4) in the time period from 20 to 80 minutes, indicating that the H_2S possibly reacted to cement nickel again as a nickel sulphide. This is substantiated (Fig. 7.2) by looking at the gradual decrease in the leaching rate of Ni alloy in comparison with the decrease in the Ni_3S_2 leaching rate for this time period (20 to 80 minutes). Figure 7.3 indicates that the formation of H_2S (eqs. 7.3a and 7.4a) also inhibits the leaching of Cu_2S to produce Cu^{2+} ions (eq. 7.5) and the subsequent formation of $Cu_{1.8}S$ for this leaching period. Noticing the still fast leaching rate of Ni alloy in relation to Ni_3S_2 from 20 to 80 minutes (Fig. 7.2) it can be concluded that reaction (7.3) is more prominent than reaction (7.4). Therefore, this explains why H_2S is formed until all the Ni alloy is leached at time = 80 minutes (Fig. 7.2).

(ii) Stage II (40 - 160 minutes)

During this stage of the leaching experiment the composition of the solids is a mixture of major mineral phases and intermediate phases (Fig. 7.2 and Fig. 7.3). Therefore, many slow phase transformations occurred, which indicates that the reaction rate must have decreased or that the conditions prevailing were not kinetically favourable to produce complete reactions. The major reactions occurring are the transformation of the mineral phases, to phases of lower Ni:S and Cu:S ratios. These transformations occur through leaching reactions extracting the nickel and copper out of the mineral structure to form a new mineral phase (structure). In

all these reactions where copper is leached (eqs. 7.5, 7.8, 7.9 and 7.10) the dissolved Cu^{2+} ions are cemented by reactions (7.3) and (7.4). The cementation reaction in equation (7.3) ceases when all the Ni alloy has been leached. It is evident from Fig. 7.5 that the overall cementation of copper terminates (decreases), at 120 minutes, as the Ni_3S_2 concentration becomes low in the solids (Fig. 7.2). The copper cementation in reaction (7.4) ceases when all the Ni_3S_2 has been leached. The constant leaching rate of Ni_3S_2 during this stage is due to the leaching of Cu_2S (eqs. 7.8 and 7.9) and the simultaneous cementation of Cu^{2+} ions (eqs. 7.3 and 7.4). From Table 7.2 (at time 120 to 160 minutes) it is evident that reaction (7.8) occurs at a slower rate than reaction (7.5) in the latter part of this stage (more stable mineral phase, i.e. higher symmetry of crystal structure).

$$25Cu_{1.96}S + 8H^+ + 2O_2 \rightarrow 4Cu^{2+} + 25Cu_{1.8}S + 4H_2O \qquad (7.8)$$

$$16Cu_2S + 2H^+ + {}^1/_2O_2 \rightarrow Cu^{2+} + Cu_{31}S_{16} + H_2O \qquad (7.9)$$

$$5Cu_{31}S_{16} + 22H^+ + {}^{11}/_2O_2 \rightarrow 11Cu^{2+} + 80Cu_{1.8}S + 11H_2O \qquad (7.10)$$

The complete reaction of equations (7.9) and (7.10) is given as equation (7.5).

The $Cu_{31}S_{16}$ forming in reaction (7.9) is an intermediate product that forms from the leaching of copper out of the structure of Cu_2S (orthorhombic) to the lower symmetry structure of $Cu_{31}S_{16}$ (monoclinic). This reaction occurs because of the inhibiting effect of H_2S on the leaching of Cu_2S, therefore the leaching rate of Cu_2S is decreased which results in the formation of $Cu_{31}S_{16}$ as an intermediate product. The leaching rate of reactions (7.5), (7.8) and (7.10) increases significantly (Fig. 7.3) from 80 to 160 minutes, because of the disappearance of Ni alloy out of the solids. This indicates the possibility of a galvanic effect existing between Ni alloy and Cu_2S which indirectly has an effect on the leaching of Ni_3S_2. For example, if the leaching of Cu^{2+} ions into solution decreases (eq. 7.5) the leaching of Ni_3S_2 according to equation (7.4) decreases. The increase in the leaching rate of the transformation reaction (eq. 7.10) of $Cu_{31}S_{16}$ (monoclinic) to $Cu_{1.8}S$ (rhombohedral) can also be due to the fact that it is mineralogically more viable (tendency of the mineral structure to form a product of higher symmetry, which is more stable). The leaching reactions of

Cu_2S (eq. 7.5), $Cu_{1.96}S$ (eq. 7.8) and $Cu_{31}S_{16}$ (eq. 7.10) to form $Cu_{1.8}S$ are confirmed by the simultaneous decrease in the reacting minerals and the increase in $Cu_{1.8}S$ according to Fig. 7.3.

The nickel that is leached is mostly leached from Ni_3S_2 according to reactions (7.2) and (7.4). The leaching of Ni^{2+} with H_2SO_4 and O_2 (eq. 7.2) occurs through the formation of an intermediate product Ni_7S_6 (eq. 7.11) which reacts further to form NiS (eq. 7.12). The formation of the intermediate product occurs because of the incomplete leaching reaction which is due to the inhibiting effect of the formation of H_2S (until Ni alloy is leached) and the possible cementation of nickel by H_2S to form nickel sulphide. Another reason why Ni_7S_6 is formed as an intermediate product is because the mineral structure of Ni_7S_6 (orthorhombic) is of a lower order of symmetry than NiS (rhombohedral), therefore it will rather tend to form NiS.

$$3Ni_3S_2 + 4H^+ + O_2 \rightarrow 2Ni^{2+} + Ni_7S_6 + 2H_2O \qquad (7.11)$$

$$Ni_7S_6 + 2H^+ + {}^1/_2O_2 \rightarrow Ni^{2+} + 6NiS + H_2O \qquad (7.12)$$

The complete reactions (7.11) and (7.12) are shown as reaction (7.2).

Figure 7.2 indicates that the increase in the leaching rate of Ni_7S_6 according to equation (7.12) at 80 minutes occurs simultaneously with the increase in the formation of NiS. This increase in NiS is also due to the direct leaching of Ni_3S_2 according equation (7.2). In Fig. 7.2 it is evident that the leaching rate of Ni_3S_2 stayed constant in this time period (40 to 160 minutes), indicating that the leaching of the Ni_3S_2 mineral (to NiS and Ni_7S_6) continued at a constant rate even with the formation of the Ni_7S_6 as an intermediate product. With the leaching of nickel from Ni_3S_2 and Ni_7S_6, NiS is formed which is then leached to a certain extent according to equation (7.13) to form Ni_3S_4.

$$4NiS + 2H^+ + {}^1/_2O_2 \rightarrow Ni^{2+} + Ni_3S_4 + H_2O \qquad (7.13)$$

Figures 7.2 and 7.3 indicate that Ni_3S_4 and CuS are formed when the concentrations of NiS and $Cu_{1.8}S$ start to increase significantly. From Fig. 7.2 and Fig. 7.3 it is

noticed that NiS and $Cu_{1.8}S$ reached their peaks when the intermediate Ni-S (Ni_7S_6) and Cu-S ($Cu_{31}S_{16}$) have disappeared, respectively. Nickel is leached from NiS in reaction (7.13) to form Ni_3S_4 which is evident from Fig. 7.2.

Figure 7.4 shows that the rate of decrease of acid was nearly constant during this stage of the leaching process. Part of the increase in the iron concentration shown in Fig. 7.4 is due to the acid-oxygen attack of the stainless steel autoclave shell. Another reason for the decrease in the leaching rate (in this stage of the leach) could be that, with all the mineral phases and specifically the intermediate phases ("impure" phases) present, the electrical conductivity of the solids could have decreased, therefore decreasing the reaction rate.

(iii) Stage III (160 - 300 minutes)

Nickel and copper are leached simultaneously during this stage of the leaching process. Copper starts leaching when all the Ni_3S_2 has been leached (compare Fig. 7.2 and Fig. 7.3) and when all the Cu_2S and $Cu_{1.96}S$ have been converted to $Cu_{1.8}S$ (eqs. 7.5 and 7.8) and CuS (eqs. 7.14, 7.15 and 7.17). Copper is leached from $Cu_{1.8}S$ mineral to form CuS in reaction (7.14) and (7.15), respectively. In reaction (7.14), H_2SO_4 and O_2 are the oxidising agents and in reaction (7.15) Fe^{3+} ion is the oxidising agent. These leaching reactions are substantiated by the evidence in Fig. 7.3 where the $Cu_{1.8}S$ concentration decreases with a significant increase in the CuS concentration. It has also been stated by Hofirek and Kerfoot (1992) that iron acts as an electron carrier in the leaching of base metals (see Chapter 2).

$$5Cu_{1.8}S + 8H^+ + 2O_2 \rightarrow 4Cu^{2+} + 5CuS + 4H_2O \qquad (7.14)$$

$$5Cu_{1.8}S + 8Fe^{3+} \rightarrow 4Cu^{2+} + 5CuS + 8Fe^{2+} \qquad (7.15)$$

Nickel is leached from NiS to form Ni_3S_4, which is then leached further according to equation (7.16) and converted to Ni^{2+} and SO_4^{2-} with H_2O and O_2 as the reactants. In reaction (7.17) nickel is leached from Ni_3S_4 and copper is cemented as CuS with the subsequent formation of acid.

$$Ni_3S_4 + H_2O + {}^{15}/_2O_2 \rightarrow 3Ni^{2+} + 2H^+ + 4SO_4^{2-} \quad (7.16)$$

$$Ni_3S_4 + 3Cu^{2+} + H_2O + {}^{3}/_2O_2 \rightarrow 3Ni^{2+} + 3CuS + 2H^+ + 4SO_4^{2-} \quad (7.17)$$

CuS is oxidised by O_2 (eq. 7.18) to form Cu^{2+} and SO_4^{2-}.

$$CuS + 2O_2 \rightarrow Cu^{2+} + SO_4^{2-} \quad (7.18)$$

The transformation of sulphide (S^{2-}) to sulphate (SO_4^{2-}) in reactions (7.16), (7.17) and (7.18) is substantiated by the decrease in the sulphur concentration in the solids, as indicated by Fig. 7.5. The sulphur concentration stayed reasonably constant in stages I and II with a noticeable decrease only occurring in stage III.

The iron in the leaching process acts as an electron carrier where the ferric (Fe^{3+}) ions are reduced to ferrous (Fe^{2+}) ions by reaction (7.15) and the Fe^{2+} ions are re-oxidised to Fe^{3+} ions by reaction (7.19). Therefore, iron is continually precipitated and redissolved in the leaching process. The Fe^{3+} ions react further to regenerate acid (H^+) and precipitate haematite (eq. 7.20) and jarosite (eq. 7.21) when the pH range of the solution reaches a pH of approximately 1.3 - 2.5 (Plasket and Dunn, 1986) for the prevailing reaction conditions (temperature and pressure).

$$2Fe^{2+} + 2H^+ + {}^{1}/_2O_2 \rightarrow 2Fe^{3+} + H_2O \quad (7.19)$$

$$2Fe^{3+} + 3H_2O \rightarrow Fe_2O_3 + 6H^+ \quad (7.20)$$

$$6Fe^{3+} + 2NH_4^+ + 12H_2O \rightarrow 2NH_4Fe_3(SO_4)_2(OH)_6 + 12H^+ \quad (7.21)$$

The occurrence of reaction (7.21) is dependent on the concentration of ammonium (NH_4^+) ions in the spent electrolyte solution (see Chapter 3). Therefore, the degree of reaction existing between reactions (7.20) and (7.21) depends on the presence of NH_4^+ and the prevailing reaction conditions. The formation of acid (H^+) by reactions (7.16), (7.17), (7.20) and (7.21) is evident in Fig. 7.4 where it can be seen that the H^+ consumption is almost non-existent in the time period 200 to 300 minutes, while the

leaching of the nickel and copper sulphides continues. Figure 7.4 also confirms the precipitation of iron out of the solution (eqs. 7.20 and 7.21). The precipitation of iron occurs because the pH of the solution increased to 1.3 between 160 and 200 minutes, which is the required pH for iron cementation at the reaction conditions (Plasket and Dunn, 1986). The overall leaching rate of nickel decreases noticeably in stage III of the leaching experiment as indicated by Fig. 7.5, which is possibly due to the low acid concentration prevailing in the reactor at this stage.

It seems that the effect of galvanic interactions subsided in this period because leaching of the nickel and copper sulphides occurs simultaneously, without one sulphide mineral inhibiting the leaching of another. This decrease in the galvanic effect can also be due to the increase in porosity of the particles (see Fig. 7.1(c) and (e)), therefore effectively reducing the galvanic couple between minerals.

Elemental sulphur was not detected in any noticeable quantities during the leaching process, which is possibly due to the high redox potentials existing in the process. Plasket and Romanchuk (1978) as well as Dutrizac and Chen (1987) did not detect the formation of elemental sulphur in their investigations for the acid-oxygen pressure leach of Ni-Cu matte. Some of the literature for the leaching of Ni-Cu matte where sulphur was formed were for the atmospheric leach process at temperatures of between 70-90°C.

7.3 SUMMARY

The reaction mechanism developed for the leaching of Ni-Cu matte is shown to be very complex, with the various minerals species interacting with one another. The mineral species being leached also have some crystallographic rules by which the leaching mechanism is determined. The most important rule is that the mineral with the structure with the highest degree of symmetry will have the lowest free energy of formation and therefore the highest resistance to further leaching. Nickel and copper are leached from the sulphide lattice to form nickel and copper sulphides with a decreasing Ni:S and Cu:S ratio. The kinetics for the cementation of copper in the first 40 minutes of the experiment were very fast, as well as the leaching of Ni alloy

out of the matte. Hydrogen sulphide (H_2S) was detected to form in the experiment from 20 to 80 minutes, even under an oxygen partial pressure of 1.8 bar. The H_2S had the effect of decreasing the reaction rate of the Ni_3S_2 and Cu_2S, which led to the formation of intermediate nickel and copper sulphides, i.e. Ni_7S_6 and $Cu_{31}S_{16}$. The leaching of copper (Cu^{2+}) into the solution only started when all the Ni_3S_2 had been depleted and when Cu_2S, $Cu_{1.96}S$ and $Cu_{31}S_{16}$ had been leached to $Cu_{1.8}S$ (and CuS to some extent). The acid (H^+) consumption rate was nearly constant for the first 200 minutes of the experiment, i.e. until the pH reaches approximately 1.3, after which it stabilised. The acid consumption rate levelled out because H^+ was formed from the precipitation reaction of iron, as well as by the oxidation of Ni_3S_4 by O_2 and H_2O. Furthermore, the leaching rates of the nickel and copper sulphides decreased at this stage of the experiment.

Having determined the leaching mechanism it is possible to develop a fundamental kinetic model of the leaching process (Chapter 8).

Table 7.2 - Mineral phase composition of the samples in the leaching experiment

Mineral	**Composition [%]**										
Time [min]	**0**	**5**	**10**	**20**	**40**	**80**	**120**	**160**	**200**	**240**	**300**
Ni	9.9	6.6	5.0	3.0	1.2	-	-	-	-	-	-
Ni_3S_2	57.0	50.7	45.4	36.7	35.2	25.5	12.8	trace	-	-	-
Ni_7S_6	-	-	trace	trace	trace	3.6	trace	-	-	-	-
NiS	-	1.5	2.4	7.0	7.6	9.5	16.7	11.4	6.2	4.9	2.0
Ni_3S_4	-	-	-	-	-	trace	6.7	21.1	22.1	22.3	22.8
NiS_2	trace	trace	trace	trace	trace	trace	trace	-	-	trace	-
Cu_2S	33.1	38.2	41.9	45.0	46.3	46.6	15.3	-	-	-	-
$Cu_{1.96}S$							23.4	2.3	-	-	-
$Cu_{31}S_{16}$	-	-	-	-	-	3.1	2.2	-	-	-	-
$Cu_{1.8}S$	-	3.0	5.3	8.3	9.7	11.7	22.9	53.6	42.1	29.5	29.0
CuS	-	-	-	-	-	-	trace	11.6	29.6	43.3	46.2
$Cu(Ni,Co)_2S_4$	-	-	-	-	-	trace	trace	trace	trace	trace	trace

Table 7.3 - The symmetry in crystal structures, in the order from high symmetry to low symmetry

Order	**Crystal structure**	**Ni mineral**	**Cu mineral**
1	Isometric (cubic)	Ni_3S_4, NiS_2	-
2	Tetragonal	-	$Cu_{1.96}S$
3	Hexagonal (rhombohedral)	Ni_3S_2, NiS	$Cu_{1.8}S$, CuS
4	Orthorhombic	Ni_7S_6	Cu_2S
5	Monoclinic	-	$Cu_{31}S_{16}$
6	Triclinic	-	-

Figure 7.1(a)

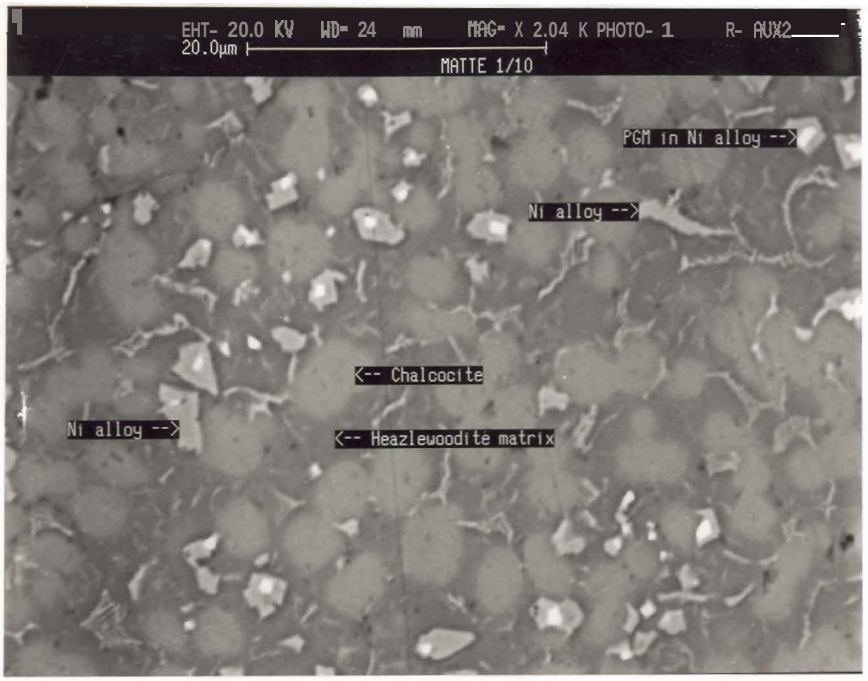

Figure 7.1**(b)**

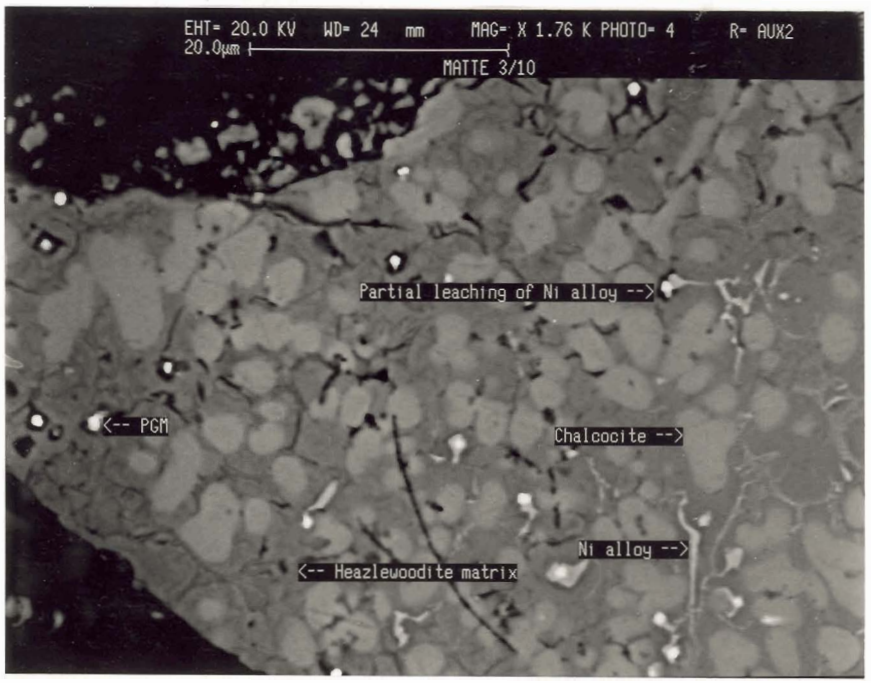

Figure 7.1(c)

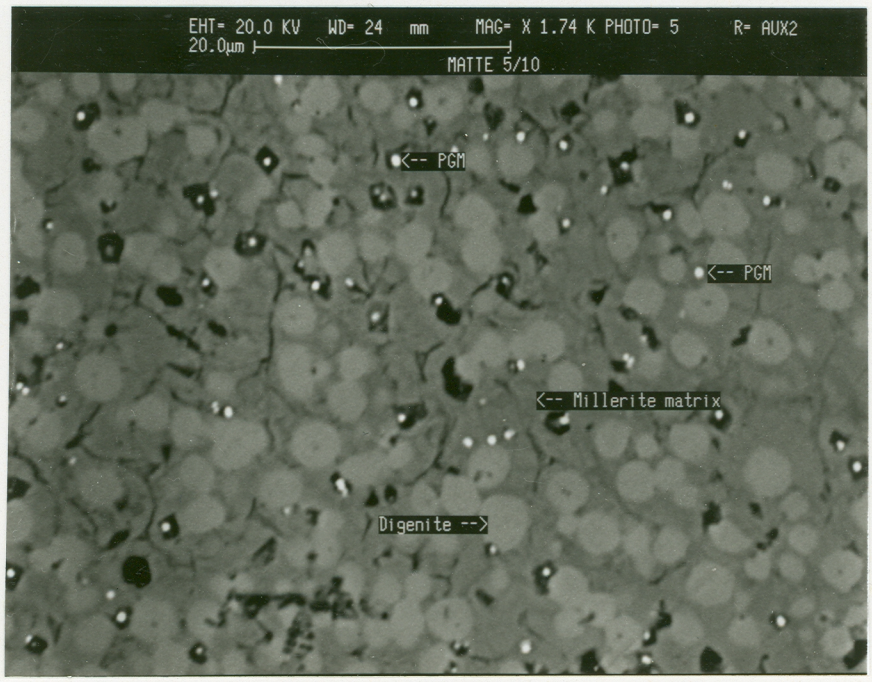

,

Figure 7.1(d)

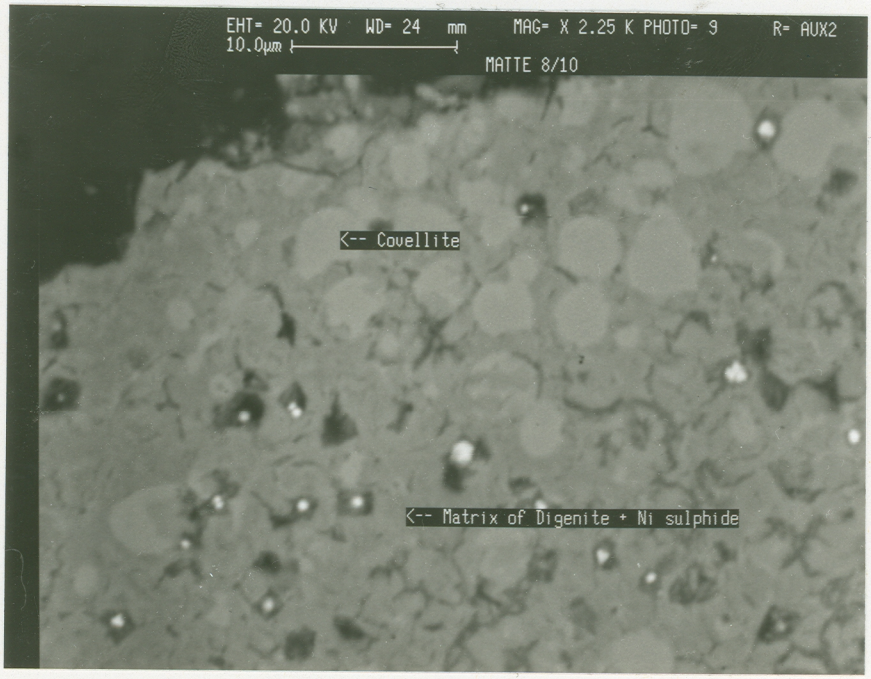

Figure 7.1(e)

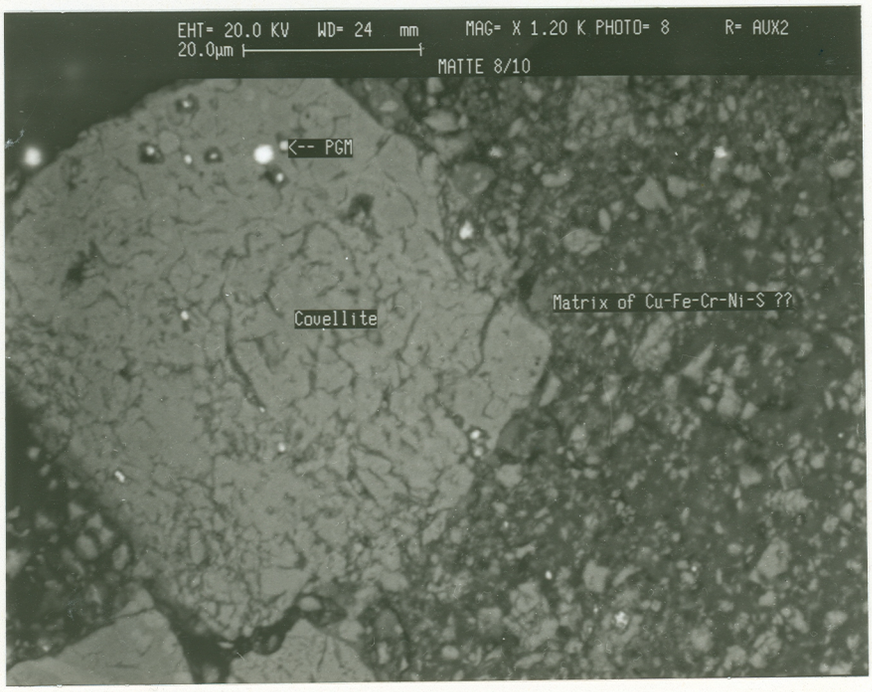

,

Figure 7.1 - SEM photographs of the samples from the leaching experiment at (a) time = 0, (b) time = 40, (c) time = 120, (d) time = 240 and (e) time = 240 (example of porous particle) minutes, respectively

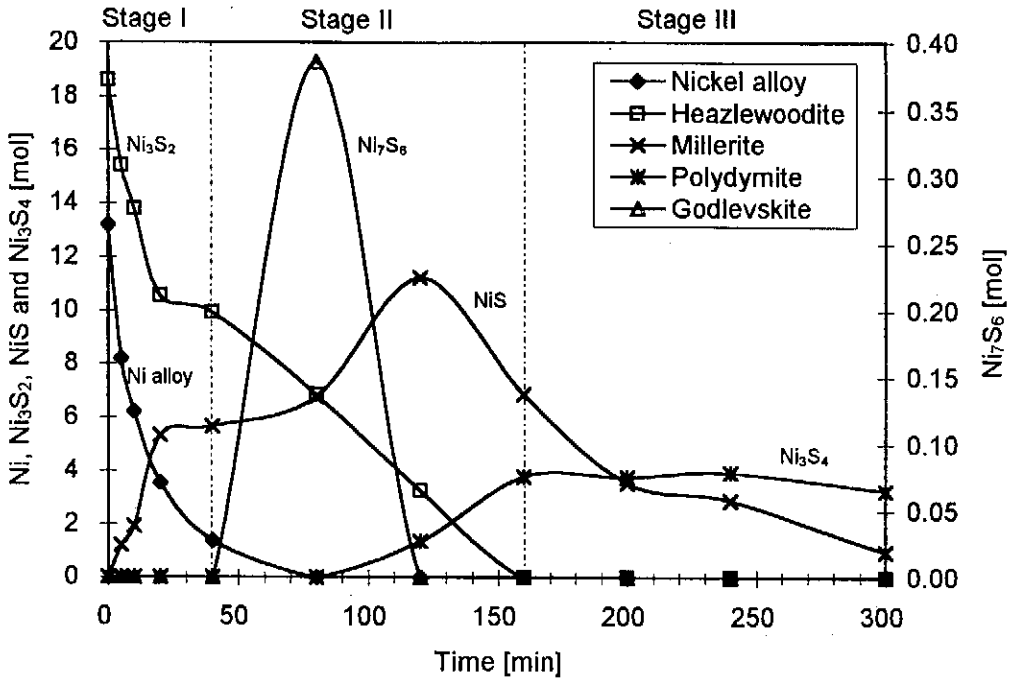

Figure 7.2 - The variation in the composition of the nickel sulphide minerals during the leaching experiment

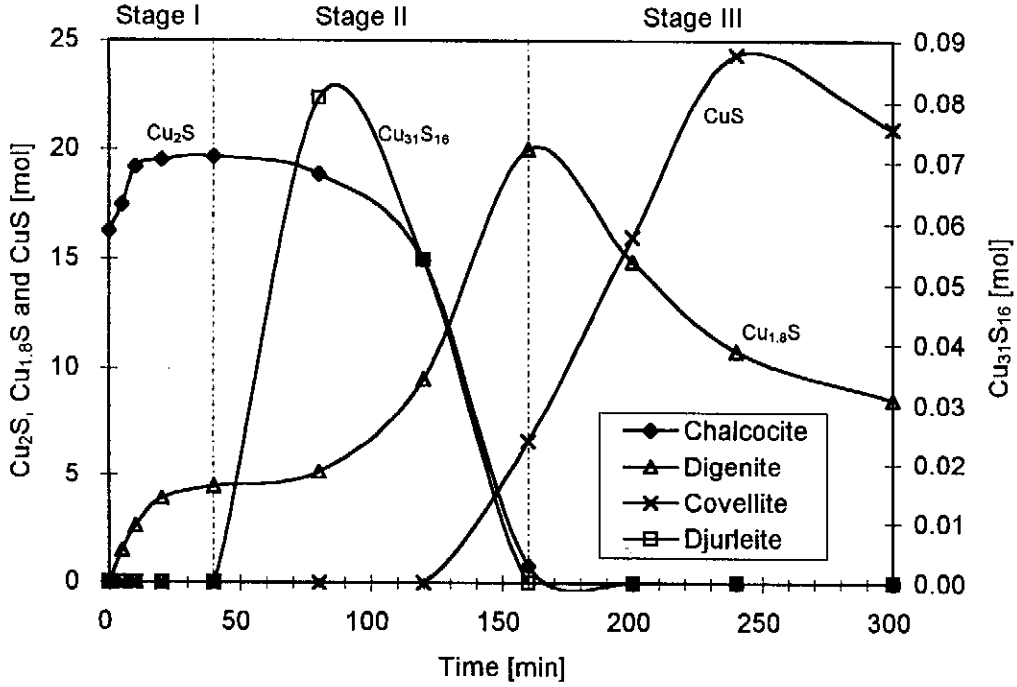

Figure 7.3 - The variation in the composition of the copper sulphide minerals during the leaching experiment

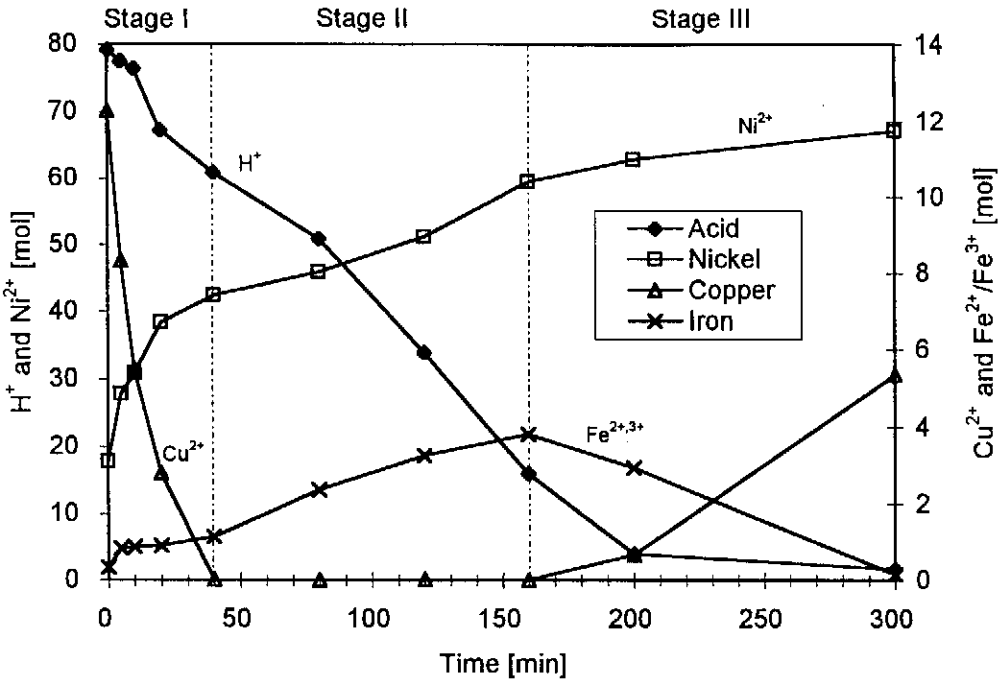

Figure 7.4 - The variation in the sulphuric acid, nickel, copper and iron concentration in the solution during the leaching experiment

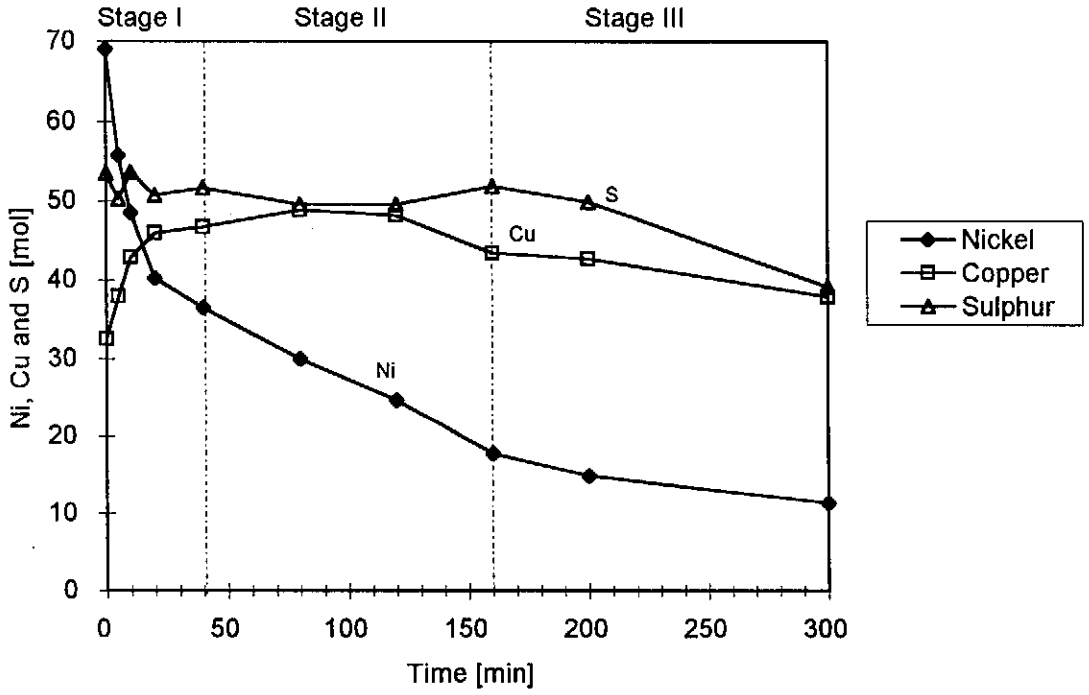

Figure 7.5 - The variation in the nickel, copper and total sulphur concentration in the solids during the leaching experiment

Chapter 8

KINETIC MODEL

In this chapter a semi-empirical kinetic model is developed based on the chemical reaction rates of the different reactions and the mechanism explained in Chapter 7. The model also makes provision for variations in the O_2 partial pressure, O_2 flowrate, temperature, initial acid concentration and particle size variations. The kinetic model for the batch experiments is then evaluated by experimental results.

The effectiveness of the model is evaluated by the ability of the model to predict the leaching and formation of the mineral species in the solid phase, as well as the nickel, copper, total iron and acid concentration in the solution and the nickel, copper and total sulphur concentration in the solids.

In determining the leaching mechanism in Chapter 7, it was concluded that the macro effects of the leaching kinetics can be assumed to be of a chemical reaction nature. Therefore this model is a macro model that includes electrochemical (galvanic influences) and mass transfer effects empirically and not fundamentally. SEM photographs (Fig. 7.1) of the samples in the leaching experiment indicate that the particles leach to a porous structure with macro pores, minimising solid diffusion effects. The composition of the particles with a nickel sulphide matrix and copper sulphide grains imbedded in this matrix enables all the minerals to be exposed to the leaching solution as the pores are developed. Furthermore, no ash layer is formed on the particle surface, excluding diffusion control through a product layer.

8.1 REPRESENTATION OF REACTION KINETICS

The reaction rate equations based on the unit volume of the reacting fluid are presented in terms of the change in moles of the species of the element in solution per time (Levenspiel, 1972),

$$r_s = \frac{1}{V_r}\frac{dN_s}{dt} = \frac{\text{moles } s \text{ formed in solution}}{(\text{volume of solution})(\text{time})} \tag{8.1}$$

$$V_r r_s = \frac{dN_s}{dt} \tag{8.2}$$

and the reaction rate equations of the solid products are based on the unit mass of the solid in the solution-solid system.

$$r_s' = \frac{1}{W}\frac{dN_s}{dt} = \frac{\text{moles } s \text{ formed in solid}}{(\text{mass of solid})(\text{time})} \tag{8.3}$$

$$W r_s' = \frac{dN_s}{dt} \tag{8.4}$$

This definition also includes the effects of pressure, temperature, composition, etc. and may be written for the reaction rate of species *s*:

$$r_s = f(pressure, temperature, composition, etc.) \tag{8.5}$$

Considering a single elementary homogeneous reaction with stoichiometric equation as in reaction (8.6),

$$A + B \rightarrow R \tag{8.6}$$

the rate of disappearance of A is given by equation (8.7),

$$-r_A = kC_A C_B \tag{8.7}$$

where k is the reaction rate constant and C_s is the concentration of reactant species s (A, B) in the solution.

In nonelementary reaction systems the reaction rate does not correspond with the stoichiometry of the reaction (reaction 8.6 is an elementary reaction because it

produces a reaction rate expression which corresponds to the stoichiometry of the reaction). Let us assume that first order relations of the reactants for describing the reaction rate are usually a good starting point in developing reaction rate expressions. Therefore, the reaction rate expressions developed for the leaching mechanism described in Chapter 7, were based on the first order relation of the reactants. The order relations of the reactants, in the expressions, were adjusted by a method of trail-and-error to improve the accuracy (performance) of the model and in some instances according to models published in literature for the leaching of a specific base metal.

The reaction rate expressions for this model are expressed in terms of the mole change of species *s* per time, i.e. $\frac{dN_s}{dt}$, where the subscript *s* indicating if it is a solution or solid component.

8.2 REACTION RATE EXPRESSIONS FOR LEACHING MECHANISM

The reaction rate expressions were derived from the leaching mechanism as described in the previous chapter. In developing the mathematical model from the rate expressions certain assumptions were made corresponding to the explanations given in the discussion of the leaching mechanism. The variables a_s^c, b_s^c,..., r_s^c are the stoichiometric constants of the different reactions in relation to the solid mineral species in the reactants (or else to the metal species in solution). Thus for reaction (7.1):

$$Ni + 2H^+ + {}^1/_2O_2 \rightarrow Ni^{2+} + H_2O \qquad (7.1)$$

$$\frac{dN_s}{dt} = a_s^c k_1 C_{H^+} p_{O_2} \qquad (8.8)$$

For example equation 8.8 is as follows for the different species:

(i) for Ni alloy, $\frac{dN_{\text{Ni alloy}}}{dt} = -k_1 C_{H^+} p_{O_2}$, with $a_s^c = -1$ (the negative sign indicates to the disappearance of Ni alloy and the 1 is the stoichiometric constant),

(ii) for the acid (H^+), $\frac{dN_{H^+}}{dt} = -2k_1 C_{H^+} p_{O_2}$, with $a_s^c = -2$ (the negative sign indicates to the disappearance of H^+ and the 2 is the stoichiometric constant in relation to the Ni alloy), and

(iii) for Ni^{2+}, $\frac{dN_{Ni^{2+}}}{dt} = k_1 C_{H^+} p_{O_2}$, with $a_s^c = +1$ (the positive sign indicates to the increase in Ni^{2+} and the 1 is the stoichiometric constant in relation to the Ni alloy).

The leaching rate constant (k_1) for the leaching of Ni alloy with H^+ and O_2 was adjusted to incorporate a term for the shrinking core leaching effect (Levenspiel, 1972). This term was added because, although the leaching of the Ni alloy is very fast, the Ni alloy occurs as small inclusions randomly distributed throughout the matte particles. Therefore pores have to form for the reactants to reach the Ni alloy particles, and the pores are formed initially by the leaching of the Ni alloy out of the matte particles (see Fig. 7.1(a)-(c), Chapter 7). The reaction rate constant is as follows:

$$k_1 = k_1' \left(\frac{N_{\text{Ni alloy}}(t)}{N_{\text{Ni alloy}}(t=0)} \right)^{\frac{2}{3}} \qquad (8.9)$$

The conditional restriction for equation (8.8) to occur is that sufficient Ni alloy must be present ($\frac{N_{\text{Ni alloy}}(t)}{N_{\text{Ni alloy}}(t=0)} > 0$).

Equation (8.10) is subject to the conditional restrictions that the Cu^{2+} ionic concentration in the solution must be higher than approximately 0.3 mol (or 0.0078 mol/L) or the $\frac{N_{\text{Ni alloy}}(t)}{N_{\text{Ni alloy}}(t=0)} < 0.02$. These restrictions are necessary because, when the leaching rate is inhibited by the formation of H_2S, reaction (7.2) does not react to completion, but the reaction rather occurs through two intermediate reactions (reactions 7.11 and 7.12). Furthermore, H_2S is formed by reaction (7.3) when the copper concentration in the solution becomes low (see also reactions 7.3a and b). Sufficient Ni_3S_2 ($\frac{N_{Ni_3S_2}(t)}{N_{Ni_3S_2}(t=0)} > 0$) must be available for equation (8.10) to occur.

$$Ni_3S_2 + 2H^+ + {}^1/_2O_2 \rightarrow Ni^{2+} + 2NiS + H_2O \quad (7.2)$$

$$\frac{dN_s}{dt} = b_s^c k_2 C_{H^+}^2 p_{O_2} \quad (8.10)$$

The exponent for the acid concentration in equation 8.10 is an empirical value determined by a trail-and-error method. The exponents for the rest of the expressions were determined on the same principle. The stoichiometric constants for the rate expressions (equations 8.8 and 8.10 - 8.26) are shown in equations 8.50 - 8.63.

Ni alloy and Ni_3S_2 must be present for reaction (7.3) to occur (eq. 8.11).

$$Ni + Ni_3S_2 + 4Cu^{2+} \rightarrow 4Ni^{2+} + 2Cu_2S \quad (7.3)$$

$$\frac{dN_s}{dt} = c_s^c k_3 C_{Cu^{2+}}^{\frac{1}{2}} \quad (8.11)$$

It is assumed that reaction (7.3) occurs preferentially to reaction (7.4) while Ni alloy is still available in the solid phase, thus when the Ni alloy has been leached out, reaction (7.4) will be the major reaction. Therefore, equation (8.12) will only be applicable when the Ni alloy concentration becomes very low.

$$Ni_3S_2 + 2Cu^{2+} \rightarrow 2Ni^{2+} + NiS + Cu_2S \quad (7.4)$$

$$\frac{dN_s}{dt} = d_s^c k_4 C_{Cu^{2+}} \quad (8.12)$$

The reactions (7.5) and (7.8) occurring are assumed to be similar, therefore, only reaction (7.5) is considered for modelling purposes, ignoring the compositional difference between $Cu_{1.96}S$ and Cu_2S.

Equation (8.13) is also subject to the conditional restriction that $\frac{N_{Ni\ alloy}(t)}{N_{Ni\ alloy}(t=0)} < 0.02$ or the Cu^{2+} ionic content must be higher than approximately 0.008 mol/L, because reaction

(7.5) will not occur to completion while the leaching rate is inhibited by the formation of H_2S. The leaching of Cu_2S will then rather occur through the intermediate reactions (7.9) and (7.10). H_2S is formed mainly by reaction (7.3) when the Cu^{2+} ionic concentration becomes very low, and this reaction will stop when the Ni alloy content becomes very low. Also, equation (8.13) will only be relevant in the calculations while the Cu_2S concentration is still sufficient ($\frac{N_{Cu_2S}(t)}{N_{Cu_2S}(t=0)} > 0$).

$$5Cu_2S + 2H^+ + {}^1/_2O_2 \rightarrow Cu^{2+} + 5Cu_{1.8}S + H_2O \qquad (7.5)$$

$$\frac{dN_s}{dt} = e_s^c \frac{k_5 p_{O_2}}{C_{H^+}^2} \qquad (8.13)$$

The unexpected form of the rate expression (eq. 8.13) is consistent with previously reported models (Verbaan and Grundwell, 1986) for the oxidation of ferrous ions by dissolved oxygen and acid, which the authors were unable to explain. This form of the rate expression could be due to the redox potential or redox couple that exists between Cu_2S and H^+.

In the development of the kinetic model reaction (7.6) was omitted and reaction (7.7) accounted for the leaching of iron. It was assumed that the majority of the iron is situated in the alloy phase in the matte. Therefore, the iron is leached according to reaction (7.7). Leaching of iron out of the alloy phase (reaction 7.7) continues until copper starts being leached into the solution phase (eq. 8.14).

$$Fe + 2H^+ + {}^1/_2O_2 \rightarrow Fe^{2+} + H_2O \qquad (7.7)$$

$$\frac{dN_s}{dt} = f_s^c k_7 C_{H^+} p_{O_2} \qquad (8.14)$$

Reaction (7.9) occurs due to the inhibiting effect of H_2S, which implicates that equation (8.15) is relevant when the Cu^{2+} ionic content is approximately less than 0.008 mol/L and sufficient Ni alloy, $\frac{N_{Ni\ alloy}(t)}{N_{Ni\ alloy}(t=0)} > 0.02$ (conditions for the formation of

H_2S). For equation (8.15) to be calculated the conditional statement that the Cu_2S content is still sufficient ($\frac{N_{Cu_2S}(t)}{N_{Cu_2S}(t=0)} > 0$) must also be met.

$$16Cu_2S + 2H^+ + {}^1/_2O_2 \rightarrow Cu^{2+} + Cu_{31}S_{16} + H_2O \qquad (7.9)$$

$$\frac{dN_s}{dt} = g_s^c k_9 C_{H^+} p_{O_2} \qquad (8.15)$$

Reaction (7.10) will occur (eq. 8.16) while $Cu_{31}S_{16}$ is present in the solid phase.

$$5Cu_{31}S_{16} + 22H^+ + {}^{11}/_2O_2 \rightarrow 11Cu^{2+} + 80Cu_{1.8}S + 11H_2O \qquad (7.10)$$

$$\frac{dN_s}{dt} = h_s^c k_{10} C_{H^+} p_{O_2} \qquad (8.16)$$

Reaction (7.11) occurs due to the inhibiting effect of H_2S, the same as reaction (7.9), therefore, equation (8.17) is relevant when the Cu^{2+} ionic content is less than approximately 0.008 mol/L and the Ni alloy content is still sufficient, $\frac{N_{Ni\ alloy}(t)}{N_{Ni\ alloy}(t=0)} > 0.02$. Furthermore, the Ni_3S_2 content must also be sufficient ($\frac{N_{Ni_3S_2}(t)}{N_{Ni_3S_2}(t=0)} > 0$) for reaction (7.11) to continue.

$$3Ni_3S_2 + 4H^+ + O_2 \rightarrow 2Ni^{2+} + Ni_7S_6 + 2H_2O \qquad (7.11)$$

$$\frac{dN_s}{dt} = i_s^c k_{11} C_{H^+} p_{O_2} \qquad (8.17)$$

The conditional restriction for equation (8.18) is that Ni_7S_6 must be present in the solid phase.

$$Ni_7S_6 + 2H^+ + {}^1/_2O_2 \rightarrow Ni^{2+} + 6NiS + H_2O \qquad (7.12)$$

$$\frac{dN_s}{dt} = j_s^c k_{12} C_{H^+} p_{O_2} \qquad (8.18)$$

From the leaching mechanism it is evident that the leaching of NiS to Ni_3S_4 (reaction 7.13) is possibly inhibited galvanically by the Ni alloy. Therefore, equation (8.19) is only occurring to any significant extent when the Ni alloy content is very low ($\frac{N_{Ni\ alloy}(t)}{N_{Ni\ alloy}(t=0)} < 0.02$). It was also assumed that the galvanic influence of Ni_7S_6 will slow down the leaching of NiS, thus incorporating a higher reaction rate constant (×4) when Ni_7S_6 is not present in the solid phase.

$$4NiS + 2H^+ + {}^1/_2O_2 \rightarrow Ni^{2+} + Ni_3S_4 + H_2O \qquad (7.13)$$

$$\frac{dN_s}{dt} = k_s^c k_{13} C_{H^+} p_{O_2} \qquad (8.19)$$

The leaching of $Cu_{1.8}S$ to CuS (reaction 7.14 and 7.15) is also possibly galvanically inhibited by the Ni alloy. Therefore, the Ni alloy content must become very low and a sufficient content of $Cu_{1.8}S$ ($N_{Cu_{1.8}S}(t) > 0$) must be available before these reactions could occur. As for equation (8.19) it was assumed that the galvanic influence of $Cu_{31}S_{16}$ will slow down the leaching of $Cu_{1.8}S$ by reaction (7.14). A higher reaction rate constant (×7) was incorporated for this reaction when $Cu_{31}S_{16}$ is not present in the solid phase (eq. 8.20). For reaction (7.15) to occur ferric ions should be available in the solution (eq. 8.21).

$$5Cu_{1.8}S + 8H^+ + 2O_2 \rightarrow 4Cu^{2+} + 5CuS + 4H_2O \qquad (7.14)$$

$$\frac{dN_s}{dt} = l_s^c k_{14} C_{H^+} p_{O_2} \qquad (8.20)$$

$$5Cu_{1.8}S + 8Fe^{3+} \rightarrow 4Cu^{2+} + 5CuS + 8Fe^{2+} \qquad (7.15)$$

$$\frac{dN_s}{dt} = m_s^c k_{15} C_{Fe^{3+}} \qquad (8.21)$$

For reaction (7.16) to occur Ni_3S_4 must be present in the solid phase (eq. 8.22) and for reaction (7.17) to occur Ni_3S_4 must be present in the solid phase, as well as Cu^{2+} ions in the solution (eq. 8.23).

$$Ni_3S_4 + H_2O + {}^{15}/_2O_2 \rightarrow 3Ni^{2+} + 2H^+ + 4SO_4^{2-} \quad (7.16)$$

$$\frac{dN_s}{dt} = n_s^c k_{16} p_{O_2} \quad (8.22)$$

$$Ni_3S_4 + 3Cu^{2+} + H_2O + {}^{3}/_2O_2 \rightarrow 3Ni^{2+} + 3CuS + 2H^+ + 4SO_4^{2-} \quad (7.17)$$

$$\frac{dN_s}{dt} = o_s^c \frac{k_{17} p_{O_2}}{C_{Cu^{2+}}^{\frac{1}{2}}} \quad (8.23)$$

The unexpected form of equation (8.23) where the copper concentration is under the line and which is inconsistent with the actual reaction (eq. 7.17) can be explained by the possible existence of redox couples. A similar form of this equation (for sphalerite leaching in an acidic ferric sulphate solution) for ferrous ion oxidation was presented by Verbaan and Grundwell, 1986 (as well as by Keenan, 1969 and Mathews and Robins, 1973 cited in Chmielewski and Charewicz, 1984). The exponents in the equation were empirically determined.

The reaction for the oxidation of CuS to Cu^{2+} and SO_4^{2-} will occur when CuS is present in the solid phase (eq. 8.24).

$$CuS + 2O_2 \rightarrow Cu^{2+} + SO_4^{2-} \quad (7.18)$$

$$\frac{dN_s}{dt} = p_s^c k_{18} p_{O_2} \quad (8.24)$$

The oxidation of ferrous ions to ferric ions (reaction 7.19) starts when copper is being leached into the solution phase or when the acid concentration is becoming low (eq. 8.25). Equation (8.25) compares with models developed for the oxidation of ferrous ions to ferric ions by Verbaan and Grundwell (1986) and those cited in Chmielewski and Charewicz (1984). These authors were unable to explain the reason for this type of form of the equation.

$$2Fe^{2+} + 2H^{+} + {}^{1}/_{2}O_2 \rightarrow 2Fe^{3+} + H_2O \quad (7.19)$$

$$\frac{dN_s}{dt} = q_s^c \frac{k_{19} C_{Fe^{2+}} p_{O_2}}{C_{H^+}} \quad (8.25)$$

The cementation reactions (7.20) and (7.21) causes the same effect in the leaching process, i.e. cementing ferric ions and forming acid (H^+), the only difference is that the ferric ions are cemented as haematite and jarosite, respectively. To keep the kinetic model as simple as possible only reaction (7.20) was used for the cementation of ferric ions.

$$2Fe^{3+} + 3H_2O \rightarrow Fe_2O_3 + 6H^{+} \quad (7.20)$$

$$\frac{dN_s}{dt} = r_s^c k_{20} C_{Fe^{3+}} \quad (8.26)$$

The cementation of iron, by reaction (7.20), and the production of acid occur as long as ferric ions are available in the solution.

8.2.1 Kinetic parameters and reaction rate constants

The reaction rate constants used in equations (8.8) and (8.10) - (8.26) incorporate kinetic expressions that can predict variations caused by changes in the temperature (T), average particle size ($d_{p,i}$) and initial acid concentration (C_{i,H_2SO_4}). Furthermore, an empirical term accounts for variations in the oxygen partial pressure (p_{O_2}) and oxygen flowrate (F_{O_2}).

Oxygen partial pressure (p_{O_2})

An interesting aspect that was noticed in the determination of the effect of O_2 partial pressure on the reaction system is that for lower partial pressures (lower than the standard O_2 partial pressure of 1.8 bar) the model is very sensitive to small variations. For O_2 partial pressures higher than the standard O_2 partial pressure the

model is less sensitive to variations. Papangelakis and Demopoulos (1991) studied the acid pressure oxidation of pyrite and found that a change of order in the O_2 partial pressure occurs from a fraction of 0.5 at high O_2 partial pressures to unity at lower oxygen partial pressures. With only three experiments conducted with varying O_2 partial pressures it is not possible to accurately determine the change in the order of this parameter (two trendlines with two data points each). Therefore, the best solution to account for these O_2 partial pressure changes was using two different scaling factors, for higher and lower O_2 partial pressures than the standard O_2 pressure. The modification of the O_2 partial pressure for modelling purposes is shown in equation (8.27),

$$p_{O_2}^{P} = 1.8 + S_P^A (p_{O_2} - 1.8) \qquad (8.27)$$

where S_P^A is the scaling factor ($p_{O_2} < 1.8$ bar: $S_P^L = 0.10$; $p_{O_2} > 1.8$ bar: $S_P^H = 0.75$).

Oxygen flowrate (F_{O_2})

The increase in the oxygen flowrate (flowrate through the reacting pulp) has the effect of increasing the rate of mass transfer of oxygen (O_2) to the solution and maintaining a high level of solubilised O_2 in the solution. A higher oxygen flowrate results in more O_2 bubbles to pass through the slurry increasing the contact of O_2 with the solution and the solids, hence enhancing mass transfer. In general, for all the reactions that are O_2 dependent an increase in the O_2 flowrate will have the effect of increasing the level of O_2 whereas an increase in the O_2 partial pressure will increase the equilibrium solubility of O_2 in the solution. Both these effects result in an increased O_2 content but to a varying degree (the same argument holds for lower O_2 flowrates). Therefore the conversion calculation for the O_2 flowrate to its equivalent O_2 partial pressure is as follows:

$$p_{O_2}^{F} = S_F (F_{O_2} - 0.59) \qquad (8.28)$$

where S_F is the conversion factor ($S_F = 0.70$). The O_2 flowrate of the standard or reference test is 0.59 kg/h.

The calculated O_2 partial pressure that is used in the model calculations is determined according to equation (8.29).

$$\begin{aligned} p_{O_2}^{C} &= p_{O_2}^{P} + p_{O_2}^{F} \\ &= 1.8 + S_P(p_{O_2} - 1.8) + S_F(F_{O_2} - 0.59) \end{aligned} \tag{8.29}$$

Temperature (T)

In determining the temperature dependency of the leaching reactions it was found that only reactions (7.1), (7.3) - (7.5), (7.7) and (7.15) - (7.17) were temperature dependent in the temperature range from 120 to 158°C. These reactions were identified to be temperature dependent by determining the sensitivity of the different reactions to variations in the temperature. The leaching rate of the other reactions was not noticeably affected by the variations in the temperature (for this range). The temperature relations have been found to be well represented by Arrhenius' law (Levenspiel, 1972),

$$k_i = k_i^0 \exp\left(-\frac{E_{a,i}}{RT}\right) \tag{8.30}$$

where k_i^0 is the frequency factor for reaction i, $E_{a,i}$ the activation energy for reaction i and R the ideal gas law constant.

The frequency factors and activation energies are determined from Fig. 8.1 to Fig. 8.8 for the relevant reactions and are as follows:

Reaction (7.1): $k_1^0 = 0.284108$; $E_{a,1} = 5.24$ kJ/mol

Reaction (7.3): $k_3^0 = 5.368239$; $E_{a,3} = 10.88$ kJ/mol

Reaction (7.4): $k_4^0 = 9.622460$; $E_{a,4} = 2.26$ kJ/mol

Reaction (7.5): $k_5^0 = 0.004243$; $E_{a,5} = -10.41$ kJ/mol

Reaction (7.7): $k_7^0 = 603.5929$; $E_{a,7} = 38.21$ kJ / mol

Reaction (7.15): $k_{15}^0 = 0.000630$; $E_{a,15} = -14.93$ kJ / mol

Reaction (7.16): $k_{16}^0 = 3.534246$; $E_{a,16} = 25.46$ kJ / mol

Reaction (7.17): $k_{17}^0 = 437.1166$; $E_{a,17} = 44.25$ kJ / mol

Generally the apparent activation energies give an indication whether the rate controlling steps are of a liquid-phase diffusion or chemical reaction nature. For reactions controlled by liquid-phase diffusion the activation energies are approximately between 8 and 25 kJ/mol and for chemical controlled reactions it is generally higher than 25 kJ/mol. Activation energies higher than 25 kJ/mol could also indicate to reactions controlled by mixed mechanisms. From the activation energies it is noticed that the activation energy for reactions (7.5) and (7.15) are negative (reactions (7.5) and (7.15) are the reactions for the leaching of copper out of Cu_2S and $Cu_{1.8}S$, respectively). This indicates that these reactions will have the effect of slowing the reaction rate when the temperature increases, and accelerating the reaction rate when the temperature decreases. The reason for the negative apparent activation energies could be due to electrochemical nature of these reactions (redox potentials). The other reactions are accelerated by an increase in the temperature and *vice versa* for a decrease in temperature, but to a varying degree depending on the activation energy. From the activation energies it is not possible to clearly define the rate controlling mechanism for the reaction system because the activation energies are influenced by the interaction of the different rate controlling mechanisms. It could be concluded that these activation energies include the mixed effects of the different rate controlling mechanisms.

Average particle size ($d_{p,i}$)

The effect of the variation in the average particle size of the matte was accounted for by adjusting the reaction rate constant by a factor derived from the increase or decrease in the effective surface area of the particle. It was again noticed that not all the reactions are affected by the average particle size variations. The reactions that are sensitive to particle size variations are reactions (7.1) - (7.5), (7.9) - (7.13) and (7.17), respectively. The derivation is based on the assumption that the particles are

spherical and that the reaction rate is directly related to the initial surface area of the particles. With the reaction rate constants based on the reference (plant particle size distribution) average particle size the area factor (A_s) is,

$$A_s = \left(\left(\frac{A_{p,i}}{V_{p,i}} \right) \Big/ \left(\frac{A_{p,ref}}{V_{p,ref}} \right) \right)^{\frac{2}{3}} = \left(\frac{d_{p,ref}}{d_{p,i}} \right)^{\frac{2}{3}} \qquad (8.31)$$

where $d_{p,ref}$ is the average particle size diameter used in the development of the model and $d_{p,i}$ is the average particle size diameter of size fraction i. The area factor also has the same format (power of $^2/_3$) as the reaction rate expression for shrinking spherical particles (Levenspiel, 1972).

The average particle size of a specific particle size fraction is the geometric mean of the size fraction, e.g. the geometric mean particle size for the fraction +75μm - 106μm is $\sqrt{75 \times 106} = 89.2\mu m$. The average particle size for the plant size distribution (Table 4.1) of the matte is determined by calculating the sum of the geometric mean for each size fraction multiplied by the mass distribution percentage (%). This calculates to an average particle size of the matte of 120.3μm ($d_{p,ref}$). The average particle sizes of the particle size fractions investigated are:

i = *ref*: plant $\Rightarrow d_{p,ref}$ = 120.3μm
i = 1: +150 -300 $\Rightarrow d_{p,1}$ = 212.0μm
i = 2: +75 -106 $\Rightarrow d_{p,2}$ = 89.2μm
i = 3: +45 -75 $\Rightarrow d_{p,3}$ = 58.1μm
i = 4: -45 $\Rightarrow d_{p,4}$ = 37.8μm

Initial acid concentration (C_{i,H_2SO_4})

The variation in the initial acid concentration has two distinct effects on the mechanism and kinetics of the leaching reactions. These two effects on the leaching reactions can be divided into high and low initial acid concentrations. For high initial acid concentrations (assumed to be approximately C_{i,H_2SO_4}>0.92 mol/L) the formation of H_2S was more prominent than for the reactions with the lower acid concentrations. Therefore, the reaction rate of the initial reactions (affected by the H_2S formation) in the high initial acid concentration system will be slower (inhibiting effect of H_2S), and *vice versa* for the lower initial acid concentration systems. The reactions affected by the variation in the initial acid concentration are reactions (7.1), (7.2), (7.5) and (7.9) - (7.12). These effects indicate that different reaction rate constants apply for the high and low initial acid concentrations. The reaction rate constants for the high and low initial acid concentrations are,

	High $[H^+]$	Low $[H^+]$
Reaction (7.1):	$k_1^{0,H} = 0.284108$;	$k_1^{0,L} = 0.390108$
Reaction (7.2):	$k_2^{H} = 0.0213$;	$k_2^{L} = 0.0303$
Reaction (7.5):	$k_5^{0,H} = 0.004243$;	$k_5^{0,L} = 0.002043$
Reaction (7.9):	$k_9^{H} = 0.015$;	$k_9^{L} = 0.022$
Reaction (7.10):	$k_{10}^{H} = 0.00068$;	$k_{10}^{L} = 0.00368$
Reaction (7.11):	$k_{11}^{H} = 0.025$;	$k_{11}^{L} = 0.075$
Reaction (7.12):	$k_{12}^{H} = 0.0045$;	$k_{12}^{L} = 0.0215$

where $k_i^{0,A}$ is the reaction rate constant for high (A=H) and low (A=L) initial acid concentrations, respectively, of reaction i.

Reaction rate constants

The reaction rate constants for the rate equations with all the combined effects are as follows (k_i is the reaction rate constants for reactions i, and i represents reactions (7.1) to (7.20), i.e. $k_1 = k_{7.1}$):

$$k_1 = A_s k_1^{0,A} \left(\frac{N_{\text{Ni alloy}}(t)}{N_{\text{Ni alloy}}(t=0)} \right)^{\frac{2}{3}} \exp\left(-\frac{E_{a,1}}{RT} \right) \tag{8.32}$$

$$k_2 = A_s k_2^A \tag{8.33}$$

$$k_3 = A_s k_3^0 \exp\left(-\frac{E_{a,3}}{RT} \right) \tag{8.34}$$

$$k_4 = A_s k_4^0 \exp\left(-\frac{E_{a,4}}{RT} \right) \tag{8.35}$$

$$k_5 = A_s k_5^{0,A} \exp\left(-\frac{E_{a,5}}{RT} \right) \tag{8.36}$$

$$k_7 = k_7^{0,} \exp\left(-\frac{E_{a,7}}{RT} \right) \tag{8.37}$$

$$k_9 = A_s k_9^A \tag{8.38}$$

$$k_{10} = A_s k_{10}^A \tag{8.39}$$

$$k_{11} = A_s k_{11}^A \tag{8.40}$$

$$k_{12} = A_s k_{12}^A \tag{8.41}$$

$$k_{13} = A_s k_{13}^{*}$$
$$k_{13}^{*} = 0.0500 \tag{8.42}$$

$$k_{14} = 0.0400 \tag{8.43}$$

$$k_{15} = k_{15}^0 \exp\left(-\frac{E_{a,15}}{RT} \right) \tag{8.44}$$

$$k_{16} = k_{16}^{0} \exp\left(-\frac{E_{a,16}}{RT}\right) \tag{8.45}$$

$$k_{17} = A_s k_{17}^{0} \exp\left(-\frac{E_{a,17}}{RT}\right) \tag{8.46}$$

$$k_{18} = 0.0144 \tag{8.47}$$

$$k_{19} = 0.4000 \tag{8.48}$$

$$k_{20} = 1.2000 \tag{8.49}$$

These expressions for the rate constants (eqs. 8.32 - 8.49) are used in the calculations of the rate equations.

8.2.2 Mathematical rate equations

The combined reaction rate equations for the ionic and mineral species describing the increase and decrease in the various components are presented by equations (8.50) - (8.63). The different terms in each rate equation are subject to the conditional restrictions as described in the explanation of the rate expressions. In all these equations (eqs. 8.50 - 8.63) the reaction rate constants must be substituted by equations (8.32) - (8.49).

Ni^{2+}:
$$\frac{dN_{Ni^{2+}}}{dt} = k_1 C_{H^+} p_{O_2}^{C} + k_2 C_{H^+}^{2} p_{O_2}^{C} + 4k_3 C_{Cu^{2+}}^{\frac{1}{2}} + 2k_4 C_{Cu^{2+}} + \frac{2}{3} k_{11} C_{H^+} p_{O_2}^{C} + k_{12} C_{H^+} p_{O_2}^{C} + \frac{1}{4} k_{13} C_{H^+} p_{O_2}^{C} + 3k_{16} p_{O_2}^{C} + 3k_{17} \frac{p_{O_2}^{C}}{C_{Cu^{2+}}^{\frac{1}{2}}} \tag{8.50}$$

Cu^{2+}:
$$\frac{dN_{Cu^{2+}}}{dt} = -4k_3 C_{Cu^{2+}}^{\frac{1}{2}} - 2k_4 C_{Cu^{2+}} + \frac{1}{5} k_5 \frac{p_{O_2}^{C}}{C_{H^+}^{2}} + \frac{1}{16} k_9 C_{H^+} p_{O_2}^{C} + \frac{11}{5} k_{10} C_{H^+} p_{O_2}^{C} + \frac{4}{5} k_{14} C_{H^+} p_{O_2}^{C} + \frac{4}{5} k_{15} C_{Fe^{3+}} - 3k_{17} \frac{p_{O_2}^{C}}{C_{Cu^{2+}}^{\frac{1}{2}}} + k_{18} p_{O_2}^{C} \tag{8.51}$$

Fe^{2+}: $$\frac{dN_{Fe^{2+}}}{dt} = k_7 C_{H^+} p_{O_2}^C + \frac{8}{5} k_{15} C_{Fe^{3+}} - k_{19} \frac{C_{Fe^{2+}} p_{O_2}^C}{C_{H^+}} \tag{8.52}$$

Fe^{3+}: $$\frac{dN_{Fe^{3+}}}{dt} = -\frac{8}{5} k_{15} C_{Fe^{3+}} + k_{19} \frac{C_{Fe^{2+}} p_{O_2}^C}{C_{H^+}} - k_{20} C_{Fe^{3+}} \tag{8.53}$$

H^+:
$$\begin{aligned}\frac{dN_{H^+}}{dt} = & -2k_1 C_{H^+} p_{O_2}^C - 2k_2 C_{H^+}^2 p_{O_2}^C - \frac{2}{5} k_5 \frac{p_{O_2}^C}{C_{H^+}^2} - \frac{1}{2} k_7 C_{H^+} p_{O_2}^C - \frac{2}{16} k_9 C_{H^+} p_{O_2}^C \\ & - \frac{22}{5} k_{10} C_{H^+} p_{O_2}^C - \frac{4}{3} k_{11} C_{H^+} p_{O_2}^C - 2k_{12} C_{H^+} p_{O_2}^C - \frac{1}{2} k_{13} C_{H^+} p_{O_2}^C \\ & - \frac{8}{5} k_{14} C_{H^+} p_{O_2}^C + 2k_{16} p_{O_2}^C + 2k_{17} \frac{p_{O_2}^C}{C_{Cu^{2+}}^{\frac{1}{2}}} - k_{19} \frac{C_{Fe^{2+}} p_{O_2}^C}{C_{H^+}} + k_{20} C_{Fe^{3+}}\end{aligned} \tag{8.54}$$

Ni alloy: $$\frac{dN_{\text{Ni alloy}}}{dt} = -k_1 C_{H^+} p_{O_2}^C - k_3 C_{Cu^{2+}}^{\frac{1}{2}} \tag{8.55}$$

Ni_3S_2: $$\frac{dN_{Ni_3S_2}}{dt} = -k_2 C_{H^+}^2 p_{O_2}^C - k_3 C_{Cu^{2+}}^{\frac{1}{2}} - k_4 C_{Cu^{2+}} - k_{11} C_{H^+} p_{O_2}^C \tag{8.56}$$

Ni_7S_6: $$\frac{dN_{Ni_7S_6}}{dt} = \frac{1}{3} k_{11} C_{H^+} p_{O_2}^C - k_{12} C_{H^+} p_{O_2}^C \tag{8.57}$$

NiS: $$\frac{dN_{NiS}}{dt} = 2k_2 C_{H^+}^2 p_{O_2}^C + k_4 C_{Cu^{2+}} + 6k_{12} C_{H^+} p_{O_2}^C - k_{13} C_{H^+} p_{O_2}^C \tag{8.58}$$

Ni_3S_4: $$\frac{dN_{Ni_3S_4}}{dt} = \frac{1}{4} k_{13} C_{H^+} p_{O_2}^C - k_{16} p_{O_2}^C - k_{17} \frac{p_{O_2}^C}{C_{Cu^{2+}}^{\frac{1}{2}}} \tag{8.59}$$

Cu_2S: $$\frac{dN_{Cu_2S}}{dt} = 2k_3 C_{Cu^{2+}}^{\frac{1}{2}} + k_4 C_{Cu^{2+}} - k_5 \frac{p_{O_2}^C}{C_{H^+}^2} - k_9 C_{H^+} p_{O_2}^C \tag{8.60}$$

$Cu_{31}S_{16}$: $$\frac{dN_{Cu_{31}S_{16}}}{dt} = \frac{1}{16} k_9 C_{H^+} p_{O_2}^C - k_{10} C_{H^+} p_{O_2}^C \tag{8.61}$$

$$Cu_{1.8}S: \frac{dN_{Cu_{1.8}S}}{dt} = k_5 \frac{p_{O_2}^C}{C_{H^+}^2} + \frac{80}{5} k_{10} C_{H^+} p_{O_2}^C - k_{14} C_{H^+} p_{O_2}^C - k_{15} C_{Fe^{3+}} \quad (8.62)$$

$$CuS: \frac{dN_{CuS}}{dt} = k_{14} C_{H^+} p_{O_2}^C + k_{15} C_{Fe^{3+}} + 3k_{17} \frac{p_{O_2}^C}{C_{Cu^{2+}}^{\frac{1}{2}}} - k_{18} p_{O_2}^C \quad (8.63)$$

The mole balances for the separate elements (Ni, Cu and S - total sulphur) in the solids are obtained from the different mineral phases (eqs. 8.64 -8.66).

$$\text{Ni (solids):} \quad N_{Ni\ (solids)} = N_{Ni\ alloy} + 3N_{Ni_3S_2} + 7N_{Ni_7S_6} + N_{NiS} + 3N_{Ni_3S_4} \quad (8.64)$$

$$\text{Cu (solids):} \quad N_{Cu\ (solids)} = 2N_{Cu_2S} + 31N_{Cu_{31}S_{16}} + 1.8N_{Cu_{1.8}S} + N_{CuS} \quad (8.65)$$

$$\text{S (solids):} \quad \begin{aligned} N_{S\ (solids)} = {} & 2N_{Ni_3S_2} + 6N_{Ni_7S_6} + N_{NiS} + 4N_{Ni_3S_4} \\ & + N_{Cu_2S} + 16N_{Cu_{31}S_{16}} + N_{Cu_{1.8}S} + N_{CuS} \end{aligned} \quad (8.66)$$

The simultaneous calculation of these ordinary differential equations (eqs. 8.50 - 8.63) are conducted by the fourth order Runge-Kutta procedure (see Appendix G).

8.3 EVALUATION OF KINETIC MODEL

The kinetic model is evaluated by fitting the model predictions of the nickel and copper sulphides, the nickel, copper, total iron and acid content in the solution, as well as the nickel, copper and total sulphur content in the solids, to batch experimental data. The preliminary evaluation is based on the data of one experiment, therefore the objective of this part of the discussion is rather to illustrate that the kinetic model is able to simulate the change in the mineral species (nickel and copper sulphides). This is necessary because the leaching mechanism (Chapter 7) and kinetics (discussed in this chapter) are dependent on the change in the mineral species and mineral composition. The changes in the solution and solid concentration of the metal species are a direct consequence of the leaching of the mineral species. Therefore, the main factor that determines if the model is able to

simulate the leaching mechanism is that the model must be able to accurately predict the leaching and formation of the mineral species.

The results of the same experiment (test 9), that was used to discuss the leaching mechanism (Chapter 7), are used for the evaluation of the kinetic model. The initial values and parameter values used in the kinetic model are presented in Table 8.1 and 8.2. The reaction conditions for the experiment are as indicated by Table 4.5 (for test 9), with the only difference from the standard experiment being that the oxygen flowrate (F_{O_2}) is 0.48 kg/h.

Nickel and copper sulphides

Figure 8.9 shows that the model is able to predict the leaching of the nickel sulphides reasonably accurate. The greatest variation of the model prediction for the nickel sulphides is for NiS during the time interval 30 to 110 minutes. This variation and the slight variation of the predicted Ni_3S_4 content from the experimental results, could possibly be ascribed to less accurate determinations of mineral composition. The copper sulphides are also predicted accurately by the model (Fig. 8.10). The greatest deviation of the model prediction from the experimental results is for the time interval 230 to 300 minutes for $Cu_{1.8}S$ and CuS, respectively. This deviation is due to possibly inaccurate determinations of mineral composition (see mole balances in Appendix F, Tables F.15 - F.17).

Solution and solids

The leaching of nickel and iron into the solution is predicted accurately by the kinetic model (Fig. 8.11). The iron in the solution is indicated as the total iron (Fe^{2+} and Fe^{3+}). The consumption of the acid (H^+) is also predicted reasonably accurately. The cementation of copper in the initial stages is simulated accurately until the copper is being leached again (160 minutes), when the predicted copper content in the solution is higher than the experimental results. The reason is that in the model development (the performance of the model concentrated on the change in mineral phases), a compromise was made between the amount of $Cu_{1.8}S$ leaching (and

formation of CuS) and the copper content in the solution. This was necessary because of the discrepancies that exist in the mass balances of the copper (see Table F.4, Appendix F), which resulted in an inaccurate determination of the mineral phases. Therefore, the reaction rate constants determined on the basis of the variations in the mineral phases are not necessarily accurate. On the other hand, the determination of copper concentrations in the solution could also be inaccurate in the later stages of the leach due to the high metal concentrations existing in the solution, so that copper could precipitate out of solution with the decrease in temperature occurring during the filtration of the sample (solution highly concentrated and the solubility of $CuSO_4$ is less than that of $NiSO_4$ at temperatures below approximately 100°C, Habashi, 1992).

The model simulated the decreasing trend of the nickel content in the solids reasonably well (see Fig. 8.12). Furthermore, the trends of increase and decrease in the copper and total sulphur (in the solids) are predicted satisfactorily. The nickel, copper and total sulphur content in the solids are based on the mineral composition, therefore, it could be concluded (from Fig. 8.10 and 8.12) that the mass (mole) balance of the nickel, copper and sulphur in the mineral species, reconciles with the mass (mole) balance of the nickel, copper and sulphur in the solids.

Emperical restrictions in model

The complex nature of the reaction mechanism and the inability of the chemical rate equations to fundamentally quantifying the leaching process necessitated the addition of conditional restrictions. The fact that the reactions are of an electrochemical nature led to the assumption that all the reactions have an equal weight in the reaction process, but with varying kinetics. Explaining what is meant by 'the reactions having an equal weight in the model' is that with a decrease in the mass of a specific mineral species the rate of the reaction of that species does not necessarily slow down (characteristic of electrochemical reactions). Therefore the reactions do not slowly terminate as the mass decreases of the mineral species and the reactions must be terminated artificially. In the model the reactions are terminated (artificially) when the mineral species are less than or equal to zero. The

effect of these restrictions are evident on Fig. 8.9 and 8.10 as sharp changes in the differential equation calculations.

The effect of the change in the reaction mechanism for variations in the Ni alloy content in the solids and the copper concentration in the solution were identified and discussed in Chapter 7 and in the explanation of the reaction rate expressions. Figures 8.13 and 8.14 indicate that the reaction trends of the model still simulate the experimental results even without the Ni alloy and copper concentration restrictions on the model, but it is necessary to include these restrictions to obtain a more correct representation (artificially) of the actual leaching kinetics.

8.4 SUMMARY

In this chapter it was shown that the leaching mechanism for the acid-oxygen pressure leaching of base metal sulphides from converter matte can be modelled accurately by the chemical reaction rate approach. For the mathematical model to be able to correctly calculate the multitude of chemical reaction rates, it was necessary to incorporate the knowledge obtained from the analysis of the leaching mechanism (Chapter 7).

It was also shown that the effect of the variation in the oxygen partial pressure, oxygen flowrate, temperature, initial acid concentration and average particle size can be mathematically incorporated in the model. The oxygen flowrate was incorporated in the oxygen partial pressure, because it was argued that the oxygen flowrate has a similar effect on the oxygen level as the oxygen pressure. The temperature variations can be accounted for by Arrhenius' law. The effect of the variation in the average particle size was found to influence the kinetic rate of some of the reactions, therefore a factor that accounts for the variation in the surface area was added. The variation in the initial acid concentration changes the leaching mechanism. This is due to less H_2S that forms as a result of lower acid concentrations and thus the reaction rates are generally faster. The model evaluation where these variations in conditions are tested is discussed in the next chapter.

Table 8.1 - The values for the initial conditions used in the kinetic model, t = 0 (10 min after the start of the experiment)

Condition	**Value**
Calculated solid mass (after 10 min of experiment)	7300 g
Mineral composition:	
Ni alloy	5.0 %
Ni_3S_2	45.4 %
NiS	2.4 %
Cu_2S	41.9 %
$Cu_{1.8}S$	5.3 %
Solution volume (V_r)	38.6 L
Initial acid concentration (C_{i,H_2SO_4})	0.99 mol/L
Initial nickel (Ni^{2+}) concentration	0.80 mol/L
Initial copper (Cu^{2+}) concentration	0.14 mol/L
Initial iron (Fe^{2+}) concentration	0.023 mol/L
Average particle size ($d_{p,ref}$) for plant distribution (see Table 4.5)	120.3 μm

Table 8.2 - The model parameter values

Reaction rate constant	Value	Activation energy	Value
$k_1^{0,H}$	0.284108	$E_{a,1}$	5.24
$k_1^{0,L}$	0.390108	$E_{a,1}$	5.24
k_2^H	0.021300	-	-
k_2^L	0.030300	-	-
k_3^0	5.368239	$E_{a,3}$	10.88
k_4^0	9.622460	$E_{a,4}$	2.26
$k_5^{0,H}$	0.004243	$E_{a,5}$	-10.41
$k_5^{0,L}$	0.002043	$E_{a,5}$	-10.41
k_7^0	603.5929	$E_{a,7}$	38.21
k_9^H	0.015000	-	-
k_9^L	0.022000	-	-
k_{10}^H	0.000680	-	-
k_{10}^L	0.003680	-	-
k_{11}^H	0.025000	-	-
k_{11}^L	0.075000	-	-
k_{12}^H	0.004500	-	-
k_{12}^L	0.021500	-	-
k_{13}^*	0.050000	-	-
k_{14}	0.040000	-	-
k_{15}^0	0.000630	$E_{a,15}$	-14.93
k_{16}^0	3.534246	$E_{a,16}$	25.46
k_{17}^0	437.1166	$E_{a,17}$	44.25
k_{18}	0.014400	-	-
k_{19}	0.400000	-	-
k_{20}	1.200000	-	-

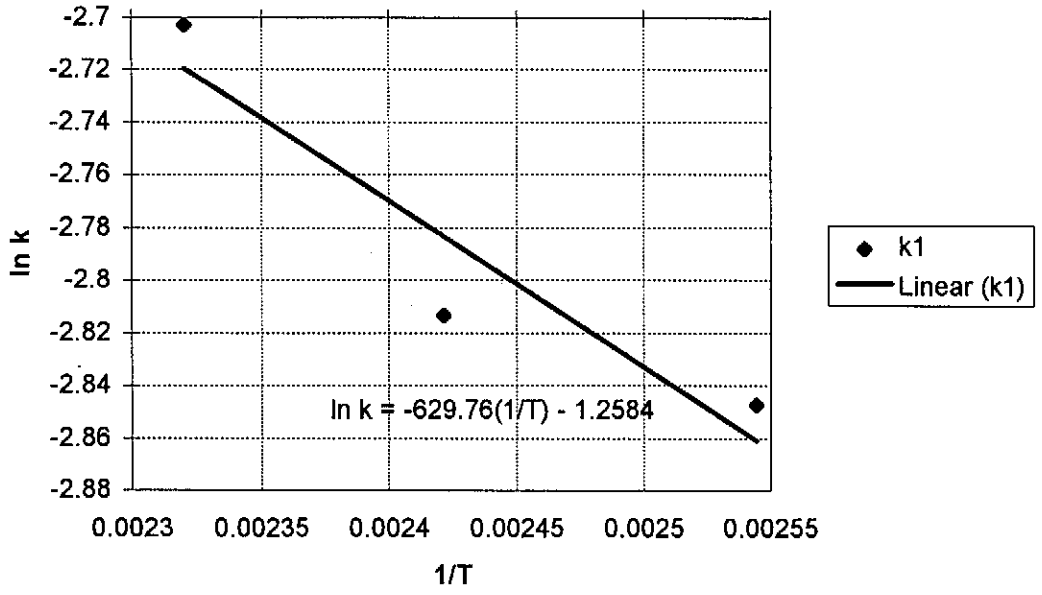

Figure 8.1 - Arrhenius plot of the natural logarithm of the apparent rate constant, k_1, against 1/T for reaction (7.1)

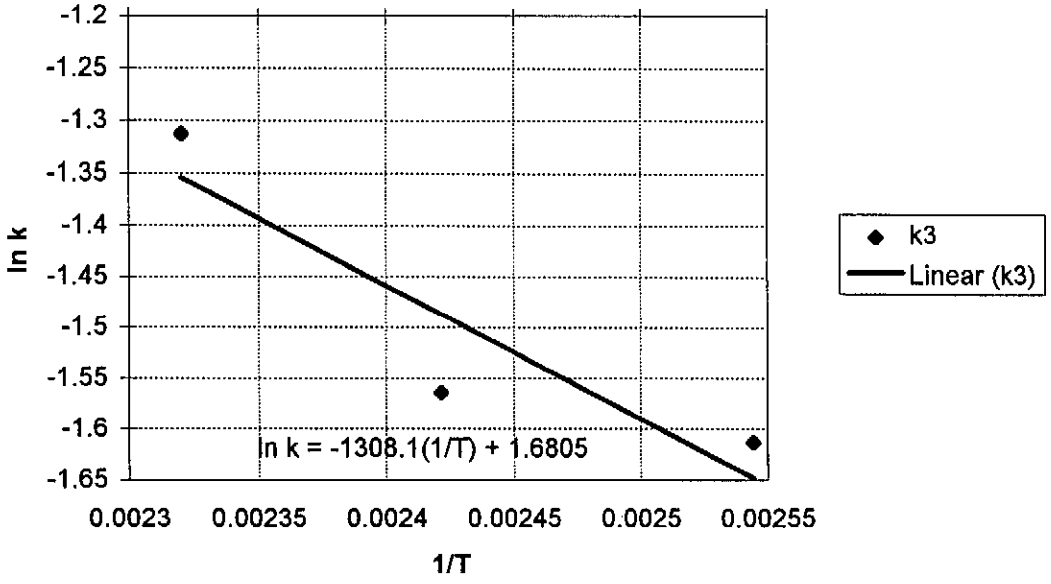

Figure 8.2 - Arrhenius plot of the natural logarithm of the apparent rate constant, k_3, against 1/T for reaction (7.3)

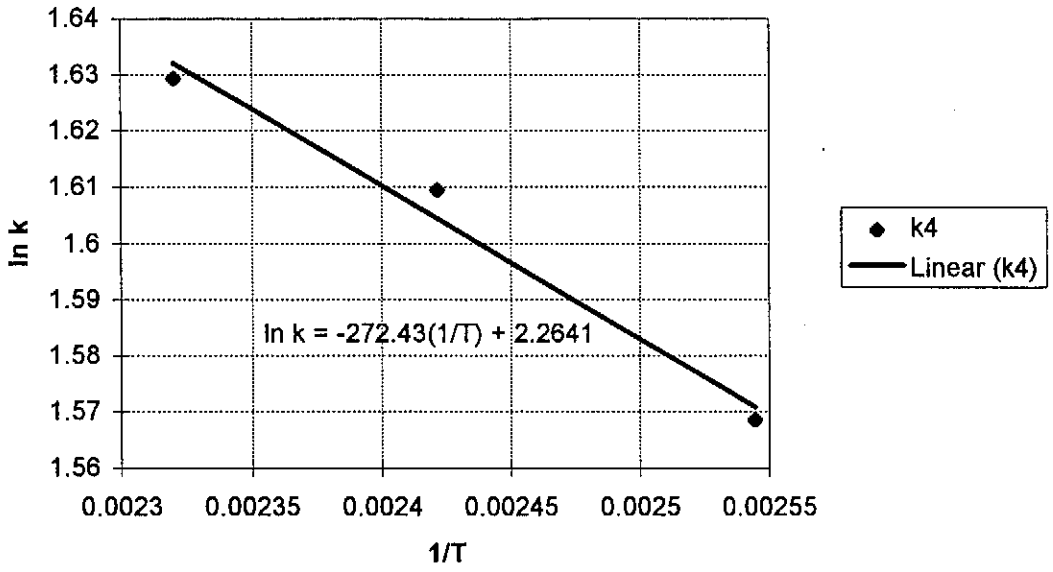

Figure 8.3 - Arrhenius plot of the natural logarithm of the apparent rate constant, k_4, against 1/T for reaction (7.4)

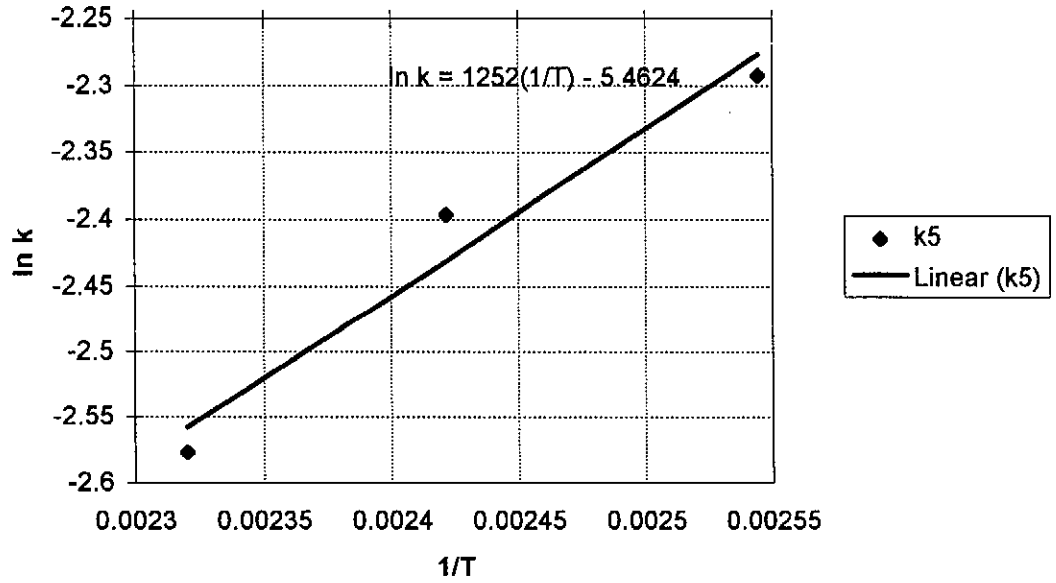

Figure 8.4 - Arrhenius plot of the natural logarithm of the apparent rate constant, k_5, against 1/T for reaction (7.5)

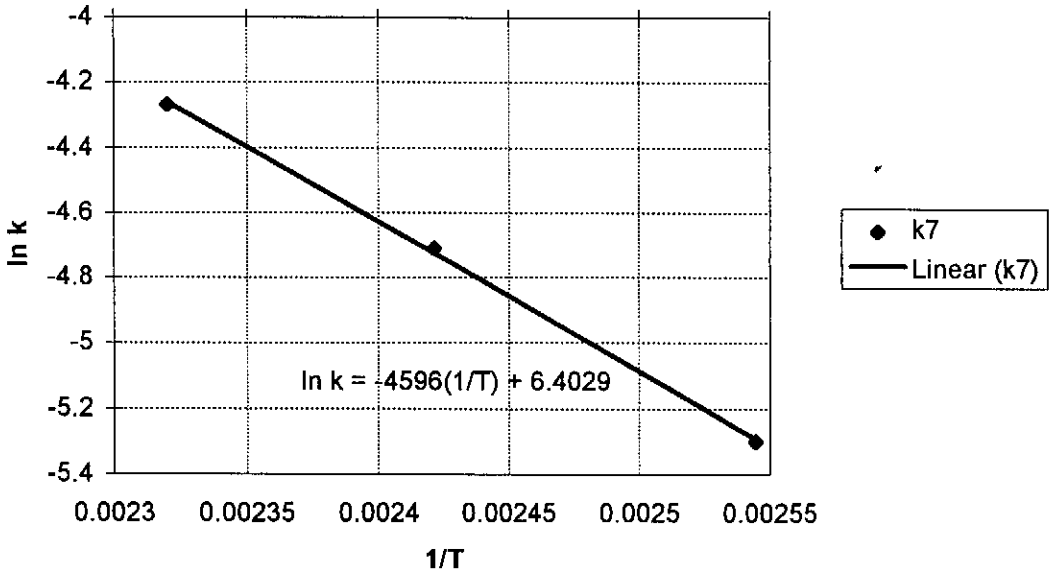

Figure 8.5 - Arrhenius plot of the natural logarithm of the apparent rate constant, k_7, against 1/T for reaction (7.7)

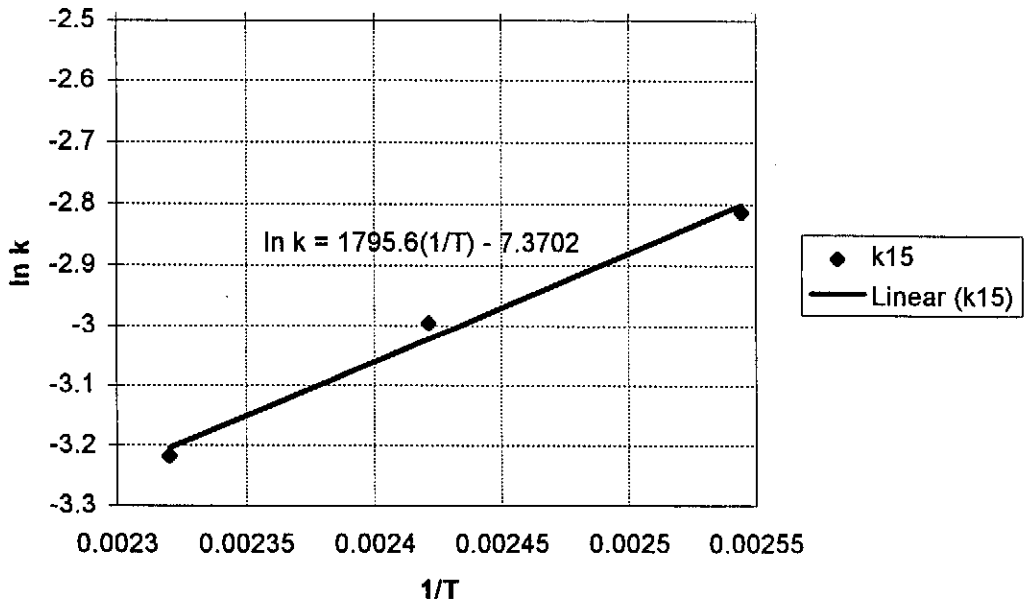

Figure 8.6 - Arrhenius plot of the natural logarithm of the apparent rate constant, k_{15}, against 1/T for reaction (7.15)

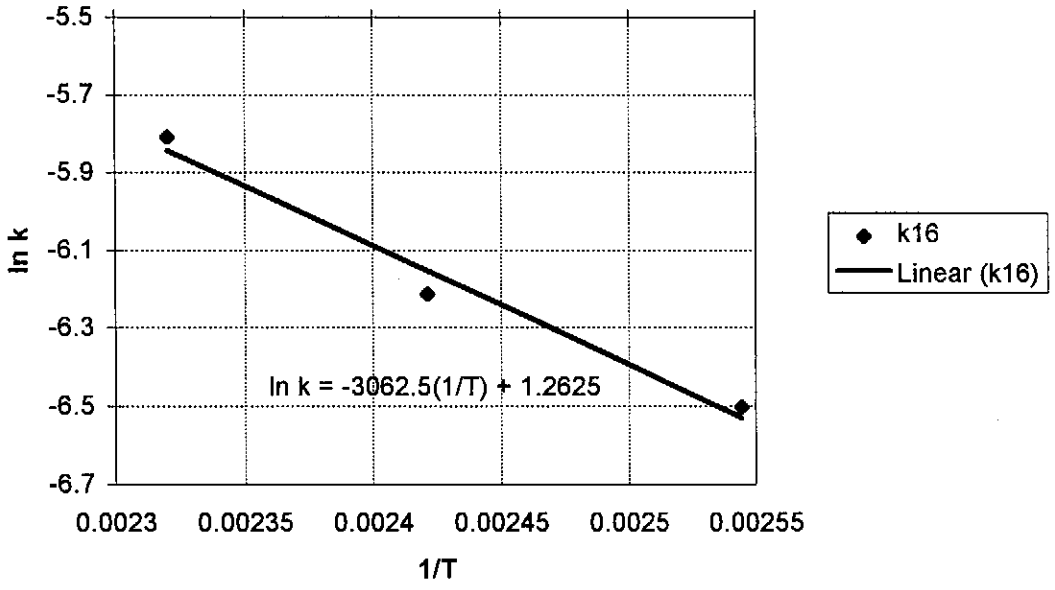

Figure 8.7 - Arrhenius plot of the natural logarithm of the apparent rate constant, k_{16}, against 1/T for reaction (7.16)

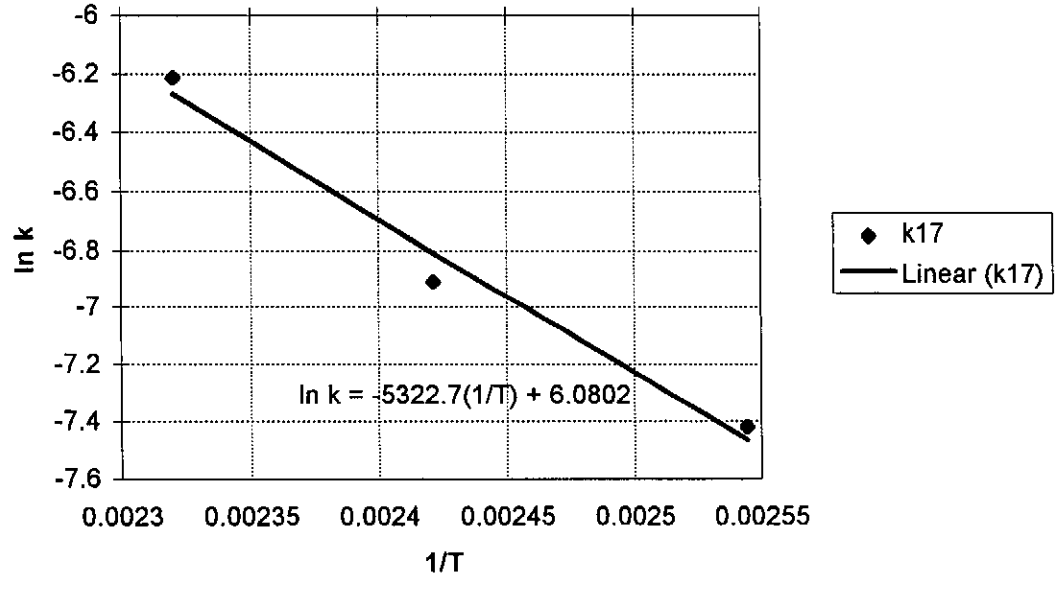

Figure 8.8 - Arrhenius plot of the natural logarithm of the apparent rate constant, k_{17}, against 1/T for reaction (7.17)

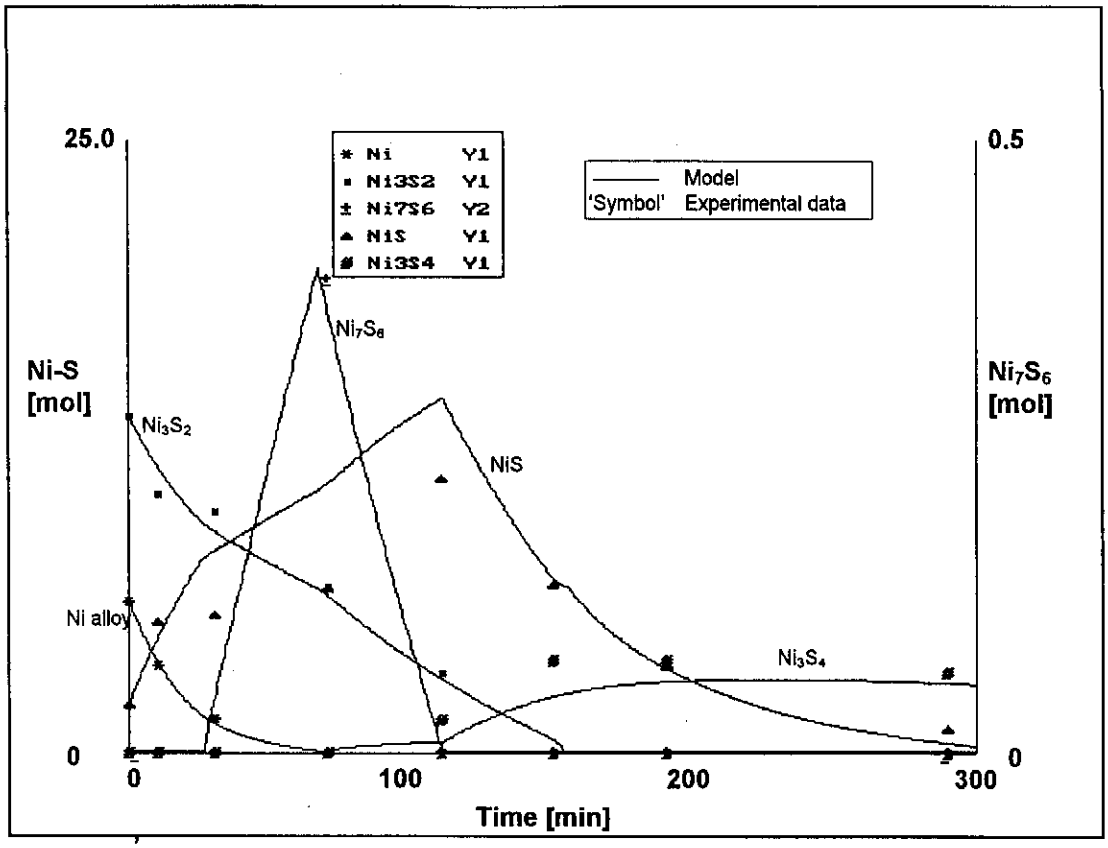

Figure 8.9 - The comparison of the kinetic model predictions for the leaching rates of the nickel sulphides with the experimental results (test 9)

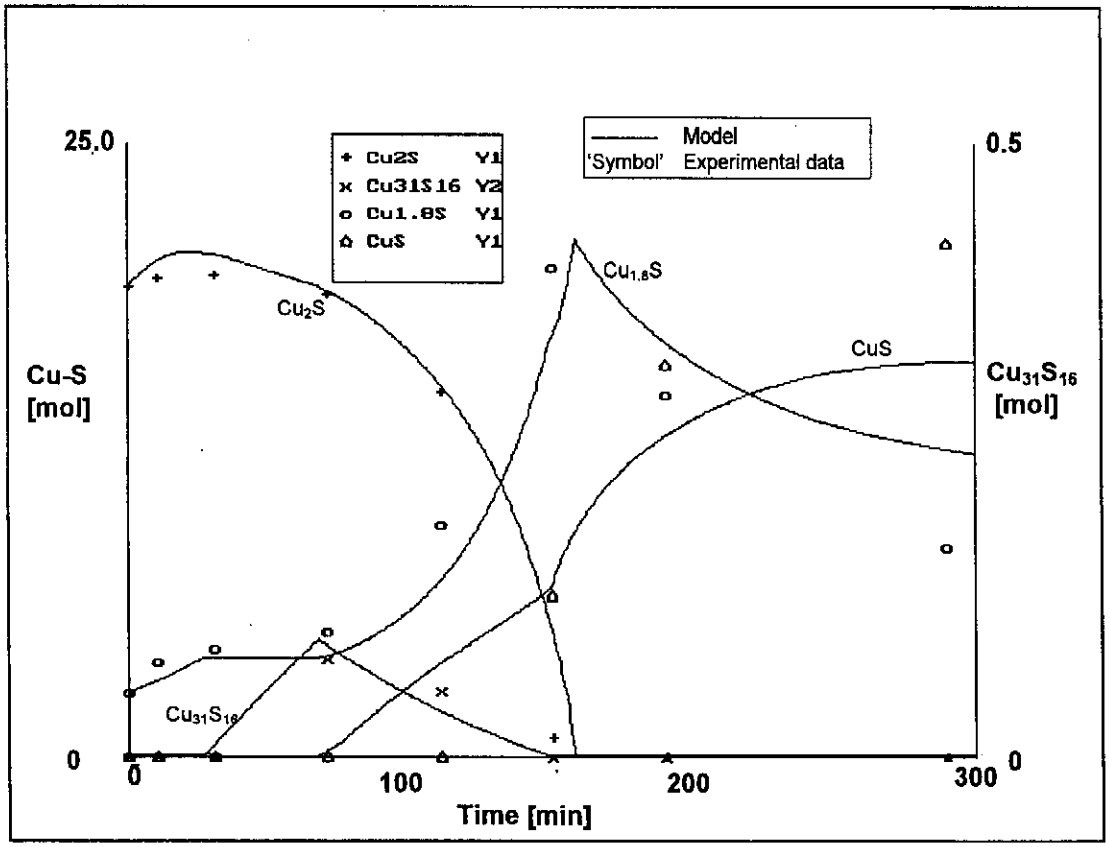

Figure 8.10 - The comparison of the kinetic model predictions for the leaching rate of the copper sulphides with the experimental results (test 9)

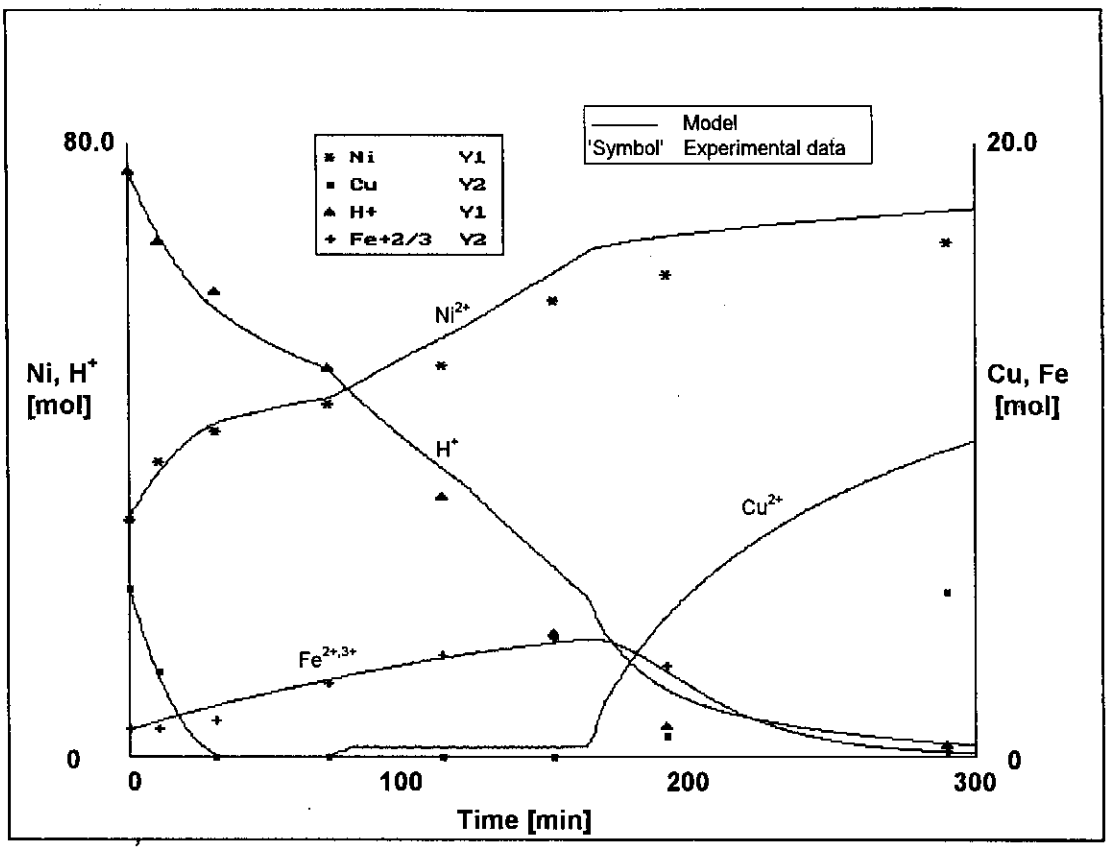

Figure 8.11 - The comparison of the kinetic model predictions of the acid, nickel, copper and iron content with the experimental results (test 9)

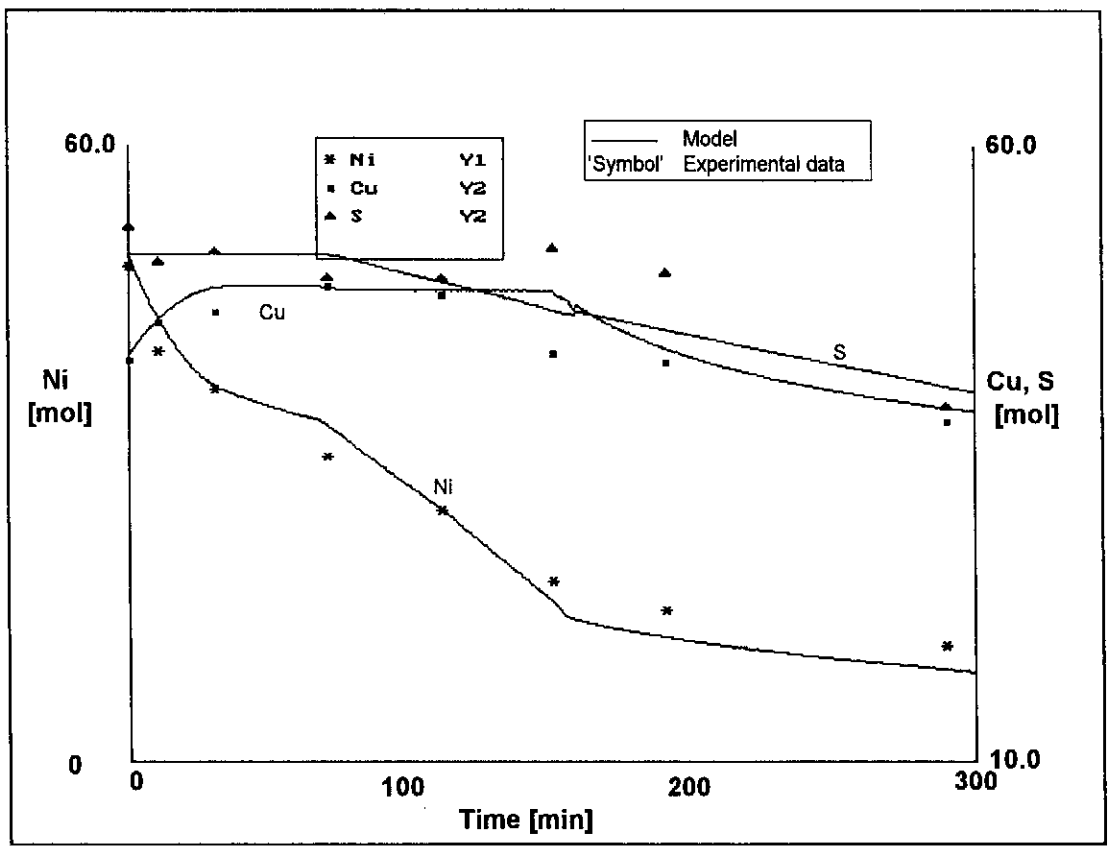

Figure 8.12 - The comparison of the kinetic model predictions of the nickel, copper and total sulphur leaching rates with the experimental results (test 9)

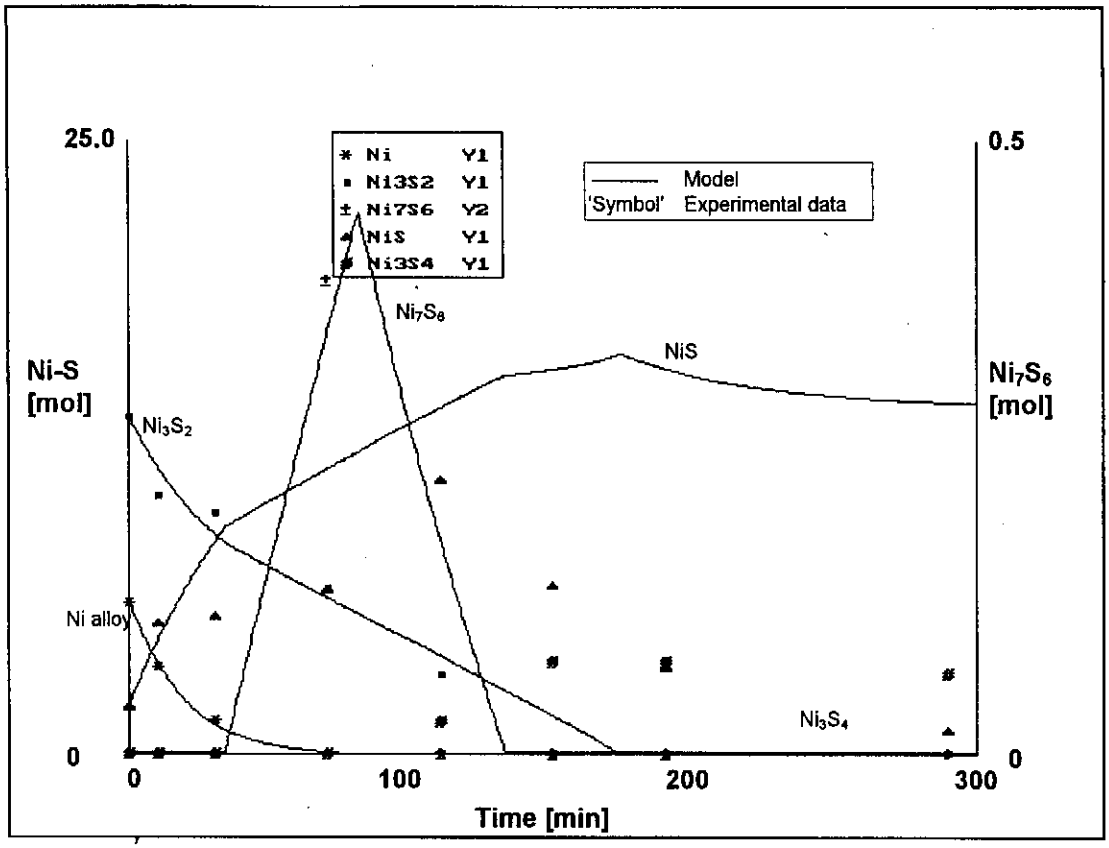

Figure 8.13 - The comparison of the kinetic model predictions for the leaching rate of the nickel sulphides, without the copper and nickel alloy content restrictions

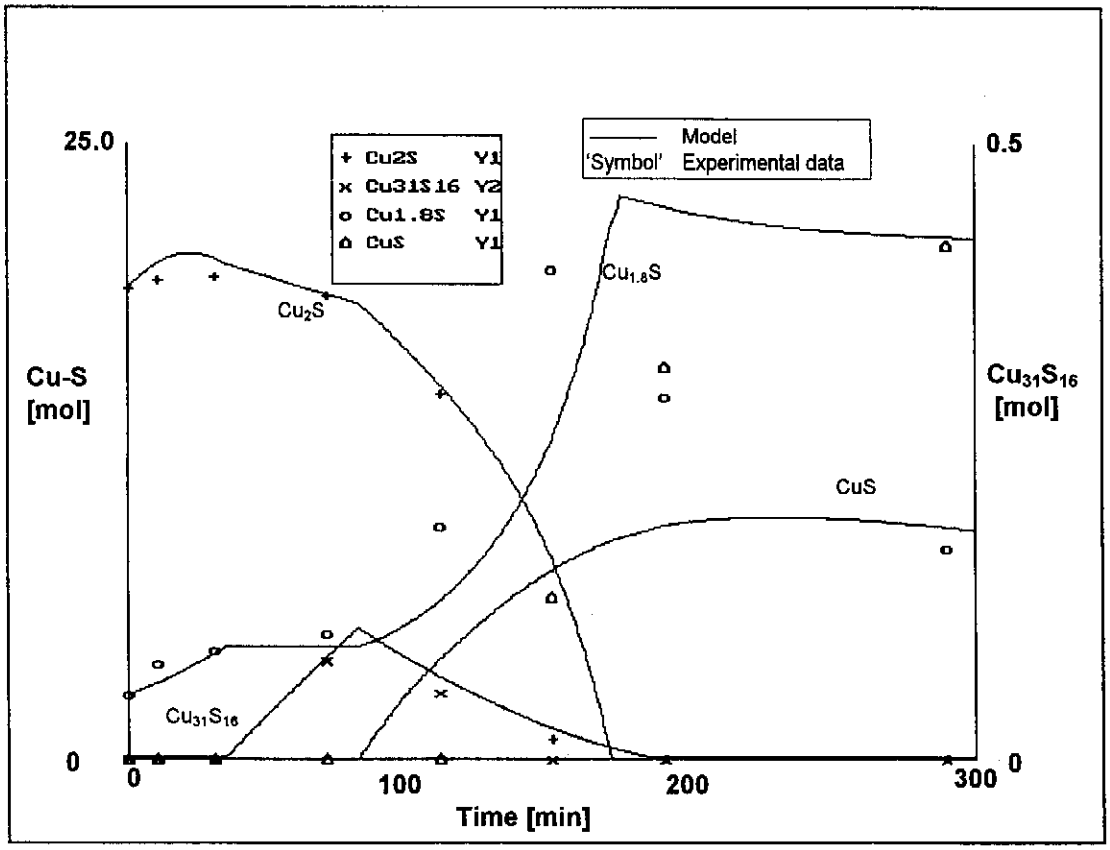

Figure 8.14 - The comparison of the kinetic model predictions for the leaching rate of the copper sulphides, without the copper and nickel alloy content restrictions

Chapter 9

MODEL EVALUATION AND PRACTICAL IMPLICATIONS OF PARAMETER SENSITIVITY

The effectiveness of the model is determined by comparing the model predictions for variations in the oxygen flowrate (F_{O_2}), oxygen partial pressure (p_{O_2}), temperature (T_r), particle size ($d_{p,i}$), initial acid concentration (C_{i,H_2SO_4}) and pulp density with experimental results. The practical implications and the sensitive nature of the various parameters are discussed simultaneously. The reason for combining the discussions is to quantify the behaviour of the process and at the same time relating this behaviour to the model performance. The findings observed in the experiments are further substantiated by results obtained from Chapter 6 (analysis of plant data). Sensitivity analyses with the model were conducted also for variations in the initial copper and iron concentrations (initial nickel concentration has no effect on the model predictions) and composition of the matte, because it had not been tested for in the experiments.

The kinetic model (Chapter 8) was developed to start simulating the batch experiments 10 minutes after the actual start-up, thus, ensuring that stable reaction conditions exist. It is also assumed that the extent of the reaction after the start-up period is the same for all the experiments (the start-up procedure is the same for all the experiments). Therefore the initial values and parameters used in the evaluation of the model for all the variations are presented in Table 8.1, except when otherwise stated. The values for the reaction conditions (in the model) are the same as that of the specific experiment that is simulated by the model (see Table 4.5). The results are presented in graphs of the mole content of the solution versus time, where the mole content is related to the concentration by:

$$C_s = \frac{N_s \text{ (mole content of species } s)}{V_r \text{ (reaction volume)}} \qquad (9.1)$$

The experimental results given in the graphs start at 0 minutes which is actually 10 minutes after the start of the experiments to comply with graphs produced by the model.

9.1 OXYGEN FLOWRATE

Model evaluation

The model is able to accurately predict the variations in the solution concentrations for varying oxygen flowrates, i.e. 0.48 kg/h: test 9 (Fig. 8.11), 0.59 kg/h: test 10 (Fig. 9.1), 0.30 kg/h: test 6 (Fig. 9.2), 0.96 kg/h: test 27 (Fig. 9.3) and 3.12 kg/h: test 1 (Fig. 9.4). Figure 8.11 illustrates that the concentrations of nickel, iron and acid are simulated accurately by the model, with only the copper concentration from 200 minutes onwards being predicted significantly higher than the experimental results (explained in Chapter 8). Figure 9.1 indicates that the model prediction for test 10 with an oxygen flowrate of 0.59 kg/h is very accurate for all the elements. It is noticed in Fig. 9.3 that the model prediction for the experiment where the oxygen flowrate is 0.30 kg/h (test 6) is good except for the copper concentration in the latter stages of the experiment, where it is higher than the experimental results. For the oxygen flowrates of 0.96 kg/h (test 27) and 3.12 kg/h (test 1), Fig. 9.3 and 9.4 respectively, it is evident that the model predictions are very good. The possible reason why the experimental nickel concentration, for an oxygen flowrate of 3.12 kg/h (Fig. 9.4), is higher than the predicted nickel concentration can be due to evaporation of the solution which occurred during this experiment (to obtain this high oxygen flowrate a high through flow of gas is required necessitating the vent valve to be nearly completely open). From Fig. 8.11 and Fig. 9.1 - Fig. 9.4 it can be concluded that the model can accurately simulate the experiments for the variation in the oxygen flowrates by implementing an emperical conversion factor for the oxygen flowrate, relating the oxygen flowrate to the increased level of oxygen solubility and therefore to the oxygen partial pressure (see Chapter 8).

Practical implications

An increase in the oxygen flowrate increases the acid consumption rate significantly (Fig. 9.5) with a corresponding increase in the leaching rate of nickel (Fig. 9.6). Therefore, an increase in the oxygen flowrate increases the reaction rate of the leaching mechanism and in effect shortening the time that copper stays cemented (Fig. 9.7) in the solids (which is unwanted in the process). The increased oxygen flowrate also decreases the leaching of iron and its subsequent precipitation (Fig. 9.8). For higher oxygen flowrates the acid consumption is much faster, which causes the ferrous ions to be oxidised to ferric ions (oxidising conditions exist, as well as a low acid concentration) which are then precipitated as either, haematite or jarosite. Therefore, for plant purposes the optimum oxygen flowrate will be where the leaching of nickel and iron is high, while the copper is still cemented in the solid product. Taking into account that the approximate residence time of the plant autoclave is ,90 minutes, the optimum oxygen flowrate for the plant seems to be around 0.96 kg/h (per 40 L of pulp).

The analysis of the plant data (Chapter 6) indicated that the oxygen flowrate is an important parameter for the leaching of nickel and iron. From that investigation it was concluded that a higher oxygen flowrate resulted in increased leaching of nickel, on the other hand, the higher oxygen flowrate resulted in a decrease in the leaching of iron (Table 6.8). Therefore, the analysis of the plant data agrees with the experimental and model findings for the variation in the oxygen flowrate.

9.2 OXYGEN PARTIAL PRESSURE

Model evaluation

The model predictions for the variations in the oxygen partial pressures are satisfactory, as indicated by Fig. 9.9 (p_{O_2} = 0.7 bar: test 16) and Fig. 9.10 (p_{O_2} = 4.4 bar: test 21). The only significant discrepancy of the model prediction is for the oxygen partial pressure of 0.7 bar, where the copper concentration prediction is higher than the experimental results (from 180 minutes on). This could be due to the

inaccurate reaction rate constants determination as explained in Chapter 8 (The evaluation of the kinetic model).

Practical implications

It is evident from Fig. 9.11 that the variation of the oxygen partial pressure from 0.7 (test 16) to 1.8 bar (test 10) does not significantly affect either the consumption of acid, or the leaching rate of nickel (Fig. 9.12). But, increasing the oxygen partial pressure to 4.4 bar (test 21) the consumption rate of acid increased considerably (Fig. 9.11), while only the initial leaching rate of nickel is increased (Fig. 9.12). The initial leaching rate of nickel is faster for the oxygen partial pressure of 4.4 bar up until all the acid is consumed. An increase in the oxygen partial pressure slightly increases the initial cementation of copper (0 to 30 minutes, see Fig. 9.13). Increasing the oxygen partial pressure also has the effect of decreasing the time that copper stays cemented in the solids (and the subsequent increase in the leaching rate of copper), which is due to the overall increase in the leaching rate or kinetics. Therefore, the concentration of Ni alloy and Ni_3S_2 is depleted more rapidly (the Ni alloy and Ni_3S_2 are the reactants needed to cement the Cu^{2+} ions, see reactions 7.3 and 7.4). The increase in the leaching rate can be substantiated by the fact that H_2S was detected in the experiment (test 21) from 10 - 30 minutes (20 - 40 minutes in experiment) for an oxygen partial pressure of 4.4 bar and from 30 - 110 minutes in the experiment (test 16) for an oxygen partial pressure of 0.7 bar. Furthermore, the increase in the oxygen partial pressure from 0.7 to 1.8 bar has a noticeable effect on the leaching of copper and iron in the later stages (from 150 minutes) of the experiments (Fig. 9.13 and 9.14), whereas the effects on the acid consumption and the initial leaching of nickel are insignificant. The increase in the oxygen partial pressure to 4.4 bar significantly influenced final leaching of copper, and the precipitation of iron.

By comparing the experimental results of the tests for the variations in the oxygen flowrates to the variations in the oxygen partial pressures for the acid content (Fig. 9.5 and 9.11), the nickel content (Fig. 9.6 and 9.12), the copper content (Fig. 9.7 and

9.13) and the iron content (Fig. 9.8 and 9.14), it is evident that an increase in the oxygen flowrate has a similar effect as an increase in the oxygen partial pressure.

The analysis of the plant data indicated that an increase in the total pressure (effectively an increase in oxygen partial pressure) results in higher concentrations of nickel and lower concentrations of copper in the fourth compartment of the plant autoclave. The lower concentration of copper in the plant for higher pressures can be explained by the fact that (i) higher oxygen partial pressures result in the faster cementation of copper (Fig. 9.13) as shown in the initial stages of the experiment, and (ii) the residence time of the autoclave is approximately 90 minutes, which is a period during the experiment (test 10: simulating the plant conditions) where the copper is still cemented in the solids.

9.3 TEMPERATURE

Model evaluation

Figure 9.15 (T_r = 120°C: test 14) illustrates that the model predicted the trends of the nickel and iron content accurately, but discrepancies occur for the acid and copper content. The deviation of the acid concentration in the model prediction from the experimental results is due to the fact that a slightly different leaching mechanism may be occurring at this low temperature. During the experiment (test 14) it was noticed that the reactions were almost exothermic for the first 200 minutes of the experiment (almost no steam, heating, was required for this time period, after the desired reaction temperature was obtained). The formation of H_2S was also not as prominently detected as for the standard test (test 10). Therefore, the higher acid concentration prevailing (as predicted by the model) when the copper starts to leach, causes the model to predict higher copper concentrations than those obtained by the experimental results. The model prediction for the temperature, T_r = 158°C (test 15) is reasonable, as can be seen in Fig. 9.16. Therefore, from Fig. 9.15 and 9.16 it is evident that the temperature effects can be simulated in the model using Arrhenius' law (Chapter 8).

Practical implications

From Fig. 9.17 and 9.18 it seems that the decrease in the temperature from 140°C (test 10) to 120°C (test 14) has the effect of changing the leaching mechanism to faster initial kinetics (consumption of acid and the leaching of nickel). But at this lower temperature (120°C) the final concentration of nickel leached (Fig. 9.18) is less than that obtained for the leach conducted at a higher temperature, 158°C (test 15). An interesting aspect that was noticed, was that the acid consumption and nickel content trends of the two experiments, i.e. at 140°C and 158°C, are almost identical, especially in the initial stages of the experiments. Faster initial kinetics occur at a temperature of 120°C, because the intermediate reactions (reactions 7.9 - 7.12) which could slow down the leaching process (at this stage) are less prominent (less H_2S detected in experiment). The reason why less H_2S is formed is due to a decrease in the temperature which decreases the initial rate of copper cementation out of the solution (Fig. 9.19). Therefore, the copper concentration in the solution (Cu^{2+}) does not become too low for reactions (7.3) and (7.4) to be inhibited (see Chapter 7). On the other hand, the decrease in the temperature results in the early start of copper leaching at higher temperatures. Some explanations for the earlier start in the leaching of copper into the solution, are that less of the intermediate products ($Cu_{31}S_{16}$ and Ni_7S_6) are formed (galvanic influence slows down the leaching of $Cu_{1.8}S$) and the subsequent increase in the copper concentration of the solution. Another explanation is that the activation energies (E_a) calculated in Chapter 8 for the leaching of Cu_2S (reaction 7.5) and $Cu_{1.8}S$ (reaction 7.15) are negative, indicating that the reaction rates of these reactions increase with a decrease in the temperature. As was expected, for lower temperatures the amount of iron leached is less (Fig. 9.20) up to a point where the acid concentration becomes too low and iron oxidation starts.

Temperature was not initially identified as a parameter, from the analysis of the plant data (Chapter 6), that will significantly influence the performance of the process. This observation was due to the fact that the temperature range on the plant only varied between 130 and 155°C. In Fig. 9.17 and Fig. 9.18 one can see that the variation in the temperature from 140 to 158°C does not significantly influence the

acid consumption or the leaching of nickel. The correlation coefficients (Fig. 6.3 and 6.4) indicated that a noticeable linear relation exists between the temperature and the nickel and copper concentrations in the fourth compartment of the autoclave. A positive linear relation is indicated for the nickel concentration, $[Ni]_4$ (Fig. 6.3), implying that for higher temperatures more nickel is leached. The opposite was observed for the copper concentration, $[Cu]_4$ (a negative relation), where lower temperatures resulted in more copper being leached (Fig. 6.4). These results from the plant data also substantiate the results obtained by the experiments.

9.4 PARTICLE SIZE

The effect of the variation in the particle size was experimentally tested with the following particle size fractions, i.e. -45 μm ($d_{p,1}$ = 37.8 μm: test 22), +45 -75 μm ($d_{p,2}$ = 58.1 μm: test 19), +75-106 μm ($d_{p,3}$ = 89.2 μm: test 20) and +150 -300 μm ($d_{p,4}$ = 212.0 μm: test 18). The other reaction conditions were the same as for the standard (or reference) experiment (test 10).

Model evaluation

The prediction of the acid and iron content by the model for the particle size fraction of -45 μm ($d_{p,1}$ = 37.8 μm) is satisfactory. This is also true for the nickel and copper content in the initial stages of the experiment (Fig. 9.21). From Fig. 9.22 ($d_{p,2}$ = 58.1 μm) it is evident that the model prediction follows the same trends as in Fig. 9.21, but it is less accurate. This could possibly be ascribed to the slight variation in the initial values of the experiment from the values used in the model (initial values for the model is given in Table 8.1). The model prediction for the particle size fraction +75 -106 μm ($d_{p,3}$ = 89.2 μm) is again accurate except for the copper content from 120 minutes onwards (Fig. 9.23). The relatively low concentration of the copper that is leached in the end of the experiments is not generally expected. The amount of copper being leached at the end of the 300 minutes is higher for the plant particle size distribution with an average particle size of 120.3 μm ($d_{p,ref}$). The reason for this observation is that for smaller particles a greater contact area is available for the solution to preferentially react with nickel and nickel sulphides, consuming acid more

rapidly, therefore, less acid is available for the leaching of the copper sulphides. The model prediction for the particle size fraction +150 -300 μm ($d_{p,4}$ = 212.0 μm) is not accurate at all (Fig. 9.24), indicating that the reactions for the bigger particle size fraction do not follow the same particle leaching effects as described in Chapter 7. Thus, for the bigger particle size fractions the Ni alloy is unable to be leached out of the particle to such an extent that a uniform porosity is created throughout the particle, as is obtained with the smaller size fractions. The results from Fig. 9.21 to 9.23 and Fig. 9.1 show that the variation of the average particle size (37.8 to 120.3 μm) can be accounted for in the model by an area factor based on the average diameter of the particles in the size fraction (or distribution). The model is unable to simulate the leaching process when the size fraction is such that the postulated surface reaction effects are not valid. The postulated surface reaction effect is that the rate determining step of the reactions is chemically controlled and the reaction rate is proportional to the initial surface area of the particle. Furthermore, it was determined in Chapter 7 that the particles leach to a porous state which effectively increases the surface area of the particle (the effects of film diffusion and pore diffusion are negligible). It was already shown that the model gives comparable predictions for experiments where the plant particle size distribution was used (Fig. 9.1). In practice an average particle size of 212 μm will lead to poor metal recoveries and inefficient leaching.

Practical implications

It is evident from Fig. 9.25 and Fig. 9.26 that the smaller the particle the higher the leaching rate of nickel and subsequent consumption of acid (greater surface area for reaction). Figure 9.27 indicates that for the particle size fraction +150 -300 μm, the copper is not completely cemented out of the solution. This could be ascribed to the fact that the effective surface area of the particles are coated by the copper sulphide (Cu_2S) formed by reactions (7.3) and (7.4), see Fig. 7.1b. Therefore, less surface area is available for the contact of Cu^{2+} ions with Ni alloy and Ni_3S_2. From Fig 9.27 it can also be observed that the initial cementation of copper is faster for smaller particles and the subsequent leaching of these smaller particle size fractions is slightly faster (for size fraction -45 μm copper starts to leach at approximately 100

minutes and for the size fraction +75 -106 μm the copper only starts to leach at 150 minutes). The fact that almost no iron is leached in the particle size fraction +150 - 300 μm substantiates the conclusion that pore formation does not occur to the same extent for larger particle size fractions (bigger particles) as for smaller particle size fractions, Fig. 9.28 (Fe occurs mostly in the alloy phase with Ni). Pores are not readily formed for this particle size fraction ($d_{p,4}$ = 212.0 μm) due to the initially less available surface area and the subsequent coating of the surfaces with Cu_2S. Figure 9.28 also indicates that the smaller the particle the faster iron starts to precipitate, because acid is consumed faster (more leaching of nickel, Fig. 9.25).

9.5 INITIAL ACID CONCENTRATION

Experiments were conducted to determine the effect of variations in the initial acid concentrations (from that of the standard test). Only lower concentrations were tested, because the corrosion effects on the plant are too severe for concentrations higher than approximately 1.0 mol/L H_2SO_4. The lower initial acid concentrations for the spent electrolyte solution investigated were 86 g/L (10 minutes after start of experiment, test 24, it was C_{i,H_2SO_4} = 0.82 mol/L) and 76 g/L (10 minutes after start of experiment, test 25, it was C_{i,H_2SO_4} = 0.73 mol/L). The conditions for the model are similar to that of the standard test, except for the oxygen flowrate which was 0.84 kg/h for these two test (the other initial values are as in Table 8.1). The practical difficulty of obtaining the correct oxygen flowrate was discussed in Chapter 4.

Model evaluation

Figures 9.29 and 9.30 illustrate that the model predictions for initial acid concentrations of 0.82 mol/L and 0.73 mol/L are satisfactory. Slight deviations from the experimental data are visible (Fig. 9.29) for the acid concentration in the early stages, and as before, for the copper concentration in the later stages of the model predictions. For an acid concentration of 0.73 mol/L (Fig. 9.30) the model prediction is not very good for the time period 40 to 100 minutes, but the nickel and copper concentration predictions are satisfactory. It is therefore evident that the change in the reaction mechanism as proposed in Chapter 8 is validated by Fig. 9.29 and 9.30,

where faster kinetics prevail for reactions (7.1), (7.2) and (7.9) - (7.12) (higher reaction rate constants, see Chapter 8).

Practical implications

Due to the higher oxygen flowrates obtained for tests 24 and 25 (0.84 kg/h), test 27 with an oxygen flowrate of 0.96 kg/h was used as the reference test. Figure 9.31 shows that the consumption of acid is very fast for the lower acid concentrations (almost similar for the concentrations of 0.82 and 0.73 mol/L). The slower consumption of the acid for C_{i,H_2SO_4} = 0.94 mol/L (test 27), is due to the production of H_2S (inhibit reactions, see Chapter 7) which leads to the formation of the intermediate products, Ni_7S_6 and $Cu_{31}S_{16}$, (reactions 7.9 and 7.11). The initial reaction rate for the nickel leaching (Fig. 9.32) for the experiment with the C_{i,H_2SO_4} = 0.94 mol/L (test 27), during the period 10 to 150 minutes, is slower than those tests with initial acid concentrations of 0.82 (test 24) and 0.73 mol/L (test 25). This result validates the assumption made in Chapter 8 that a certain critical initial acid concentration exists, and depending if it is higher or lower than this concentration (0.92 mol/L), the reaction rate constants for the affected reactions will be higher or lower. From Fig. 9.32 it is also evident that for the experiments with lower acid concentrations, the experiment with the initial acid concentration of 0.82 mol/L leads to slightly faster kinetics and higher nickel concentrations than the experiment where the initial acid concentration was 0.73 mol/L. The lower initial acid concentrations have the effect of increasing the cementation rate of the copper, as well as decreasing the time that copper stays cemented in the solid phase (Fig. 9.33). The reason for the earlier start of the leaching of copper, i.e. at 70 minutes for the lower acid concentrations (0.82 and 0.73 mol/L) and at 110 minutes for the higher acid concentration (0.94 mol/L), is that the formation of the intermediate products (because of H_2S) is less for the lower acid concentrations (less H_2S was detected for the experiments with the lower acid concentrations). The intermediate products have the effect of galvanically inhibiting the leaching rate of copper (see Chapter 7). Therefore, for the higher initial acid concentration the leaching of copper starts at a later stage, because of the presence of Ni_7S_6 and $Cu_{31}S_{16}$ in the solid phase at that

stage. Furthermore, the precipitation of the leached iron is related to the presence of acid in the solution (compare Fig. 9.34 with Fig. 9.31).

The data analysis investigation in Chapter 6 showed that the acid concentration of the spent electrolyte is the most important parameter that will influence the leaching of nickel. Results in Table 6.8 indicate that the average (or mean) acid concentration of the spent electrolyte must be approximately 87.5 g/L to ensure sufficient leaching of nickel in the autoclave, which compares with the experimental results of test 24. On the other hand, for lower acid concentrations (81.8 g/L) the leaching of nickel is insufficient. The results of the learning vector quantization (LVQ) neural network indicated (Table 9.1) that for outputs (of $[Ni]_4$) that were wrongly classified as high (which is actually low) the average acid concentration is 100.1 g/L. This also substantiates the findings of the experiments where it was determined that for a high initial acid concentration (>100 g/L), the initial leaching rate of nickel is slower (for the first 150 minutes, Fig. 9.32). This will then result in a lower output concentration of nickel (in compartment no. 4 of the autoclave), because the autoclave has an approximate residence time of 90 minutes. Therefore, the optimum acid concentration for the plant operations will be a compromise between the maximum leaching of nickel desired and the minimum leaching of copper in the residence time available, which should probably be between the approximate values of 80 to 90 g/L.

It was noticed for all the experiments thus far, that precipitation of the leached iron starts simultaneously with the leaching of copper (after it had been cemented originally). This could either be due to the fact that the conditions for copper leaching to start are exactly the same as that for iron precipitation to occur, or because of the interacting catalytic effect of the copper and the iron, where the oxidation of ferrous to ferric ions is catalysed by the Cu^{2+} ions.

9.6 PULP DENSITY

Two variations in the pulp density were tested for, other than the standard experiment (test 10: pulp density = 1.35 kg/L, V_r = 38.6 L, calculated solid mass 10 minutes after start of experiment, W = 7300 g and initial acid concentration of 0.99

mol/L). A pulp density of 1.30 kg/L (solution volume, V_r = 39.1 L, calculated solid mass 10 minutes after start of experiment, W = 4713 g and initial acid concentration of 1.02 mol/L: test 12) and a pulp density of 1.40 kg/L (solution volume, V_r = 37.7 L, calculated solid mass 10 minutes after start of experiment, W = 9942 g and initial acid concentration of 0.92 mol/L: test 13) were used. Variations in the initial acid concentrations, after 10 minutes of the experiment, were due to the variation in the starting conditions (different solution:solid ratios), i.e. the reactions were not occurring to the same extent, because different quantities of matte and solution were present.

Model evaluation

Figure 9.35 indicates that the nickel concentrations are predicted accurately by the model, but that the predicted acid consumption is faster than the experimental results. The faster consumption of acid results in the faster prediction of the leaching rate of copper, initially. The model prediction for the pulp density of 1.40 kg/L is overall very good (Fig. 9.36).

Practical implications

The results presented in Fig. 9.37 to Fig. 9.40 are in the form of concentration versus time curves to compare the different experiments with each other (test 12: V_r = 39.1 L, test 10: V_r = 38.6 L, test 13: V_r = 37.7 L).

An interesting aspect that is observed from Fig. 9.37 and 9.38 is that in the experiment for the low pulp density of 1.30 kg/L, the acid consumption rate is initially faster than for the experiment where the pulp density was 1.35 kg/L, even with the difference in the solution:solid ratio (H_2S formation is expected for the low pulp density because of the high initial acid concentration). Furthermore, no H_2S was detected during the experiment for the low pulp density, indicating that a different leaching mechanism or reaction kinetics exists, because the inhibiting effect of the H_2S and the possible formation of the intermediate Ni_7S_6 and $Cu_{31}S_{16}$ phases, do not occur. The reason why no H_2S was detected (pulp density 1.30 kg/L: test 12) is because the copper concentration in relation to the solids is sufficient for reactions

(7.3) and (7.4) to occur without the formation of H_2S (Cu^{2+} ions in solution are sufficient while Ni alloy is still present in the solid phase, see Chapter 7). Therefore, the change in the reaction kinetics for the experiment with the low pulp density of 1.30 kg/L, is the main reason why the model is unable to make good predictions for acid and copper concentration (Fig. 9.35). Figure 9.39 illustrates that the cementation of copper is faster as the pulp density increases. The leaching of the cemented copper, on the other hand, starts earlier for the lower pulp density, because less solids are present and therefore less Ni alloy and Ni_3S_2 are present to keep cementing the leached copper (Fig 9.39). The leaching effect of iron (Fig. 9.40) is determined by the acid concentration, therefore, the iron of test 13 (pulp density of 1.40 kg/L) starts to precipitate before (in time) the iron of test 10 (pulp density of 1.35 kg/L) because acid is consumed faster in test 13. The iron leached in test 12 (pulp density of 1.30 kg/L) is not precipitated to any significant degree, because the acid concentration had not been depleted enough at the end of the experiment to create the right conditions for iron to precipitate.

The plant data analysis in Chapter 6 indicated that the pulp densities in the preleach tanks are important parameters in the performance of the autoclave, because it influences the extent of the reactions that occur in the preleach tanks (before the pulp enters the autoclave).

9.7 SENSITIVITY ANALYSIS

Sensitivity analyses were also conducted for the variations in the initial copper and iron concentration and mineral composition (Ni alloy, Ni_3S_2 and Cu_2S). The values used for the model are the same as in Table 8.1 (except for when the sensitivity of the parameter is investigated) and the conditions are similar as for the standard experiment, test 10 (oxygen flowrate of 0.59 kg/h, oxygen partial pressure of 1.8 bar and temperature of 140°C).

9.7.1 Initial concentrations

Initial copper concentration

The sensitivity analyses conducted for the variation in the initial copper concentration are for a lower concentration of 0.12 mol/L, Fig. 9.41, (reference copper concentration 0.14 mol/L, Fig. 9.42) and for a higher concentration of 0.16 mol/L (Fig. 9.43). From Fig. 9.41 to Fig. 9.43 it is evident that for a higher initial copper concentration more copper is leached in the later stages. A higher initial copper concentration also has the effect of decreasing the time that copper stays cemented in the solid phase.

Initial iron concentration

Sensitivity analyses were conducted for a lower (0.013 mol/L, Fig. 9.44) and higher (0.032 mol/L, Fig. 9.45) initial iron concentration (reference initial iron concentration is 0.023 mol/L). The variation in the initial iron concentration had no significant effect on the leaching characteristics of the matte, except that slightly more copper is leached in the latter stages (compare Fig. 9.44, 9.42 and 9.44).

9.7.2 Mineral composition

Ni alloy

The variations tested in the sensitivity analysis of the mineral composition had to be chosen in such a way that the total composition of the matte stayed 100%. Therefore, it was decided that for a decrease in the Ni alloy content the Ni_3S_2 content will increase with the corresponding percentage (w/w). The variations in the Ni alloy composition are given in Table 9.2 and are illustrated in Fig. 9.46 and 9.47. Comparing Fig. 9.46, 9.42 and 9.47 it is evident that for a lower Ni alloy (higher Ni_3S_2) content in the matte (Fig. 9.46), the reaction rate for the leaching of nickel will be much faster, and the subsequent leaching of copper will start earlier. Therefore, the model illustrates the inhibiting (galvanic) effect that the Ni alloy has on the

leaching kinetics of this process. Therefore, the less Ni alloy present in the matte, the faster the reaction kinetics will be.

Ni_3S_2 and Cu_2S

The variations in the composition for Ni_3S_2 and Cu_2S were tested simultaneously, because for a decrease in the Ni_3S_2 content, the Cu_2S content was increased to keep the composition of the matte at 100% (see Table 9.2). Comparing Fig. 9.48 (low Ni_3S_2), 9.42 (reference) and 9.49 (high Ni_3S_2) it is shown that for a higher Ni_3S_2 (lower Cu_2S) content more nickel is leached, and for a lower Cu_2S content less copper is leached in the later stages. The acid consumption is not significantly influenced by these variations, and no variation in the leaching of iron is noticed.

9.8 SUMMARY

This chapter validates the effectiveness of the kinetic model and its ability to account for the variations in the oxygen partial pressure, oxygen flowrate, temperature, average particle size, initial acid concentration and pulp density (as discussed in Chapter 8), by comparison of the model predictions with experimental results. The most significant variations of the model predictions from the experimental results for experiments with a low temperature (120°C, test 14) and a low pulp density of 1.30 kg/L (test 12) could be explained by a change in the reaction kinetics. The deviation of the model prediction from the experimental results for the experiment with an average particle size of 212.0 μm (test 18) is due to a change in the postulated particle leaching method (particles are initially leached to a porous state) to a particle leaching method where the available surface area of the particle becomes rate controlling.

The increase in the oxygen flowrate and the oxygen partial pressure leads to more efficient nickel extractions and to the faster leaching rate of the cemented copper. A higher initial leaching rate for nickel and a slower initial copper cementation rate are obtained for a lower temperature of 120°C. The reason for the initially higher leaching rate is that the formation of H_2S is less (H_2S inhibits reactions) because

Cu^{2+} ions are present in solution for a longer period. This effect was also noticed for a lower pulp density of 1.30 kg/L, where the high solution to solid ratio is such that sufficient copper is available in the solution to prevent the formation of H_2S. The smaller the average particle size the more nickel is leached and the faster the initial cementation of copper. It is also evident from the experiments for the variation in the initial acid concentration that an initial acid concentration exists that will inhibit some of the reactions in the initial stages, if the initial acid concentration is too high. This fact is also substantiated by the results of the data analysis of Chapter 6. For the initial acid concentrations less than this critical concentration the initial leaching rate of nickel is faster, as well as the initial cementation rate of copper. Furthermore, the findings from the experimental results (for the oxygen flowrate, oxygen partial pressure, temperature and initial acid concentration) and the data analysis investigation of Chapter 6 substantiate each other.

The sensitivity analyses with the kinetic model indicated that for lower initial Ni alloy content in the matte the leaching kinetics of both the nickel and copper are significantly higher. This illustrates the galvanic effect that the Ni alloy has on the leaching of the nickel and copper sulphides.

The results of the experiments illustrate the complexity of the reaction mechanism and reaction kinetics for the variation in the reaction conditions. Taking these complexity effects into consideration the model obtained satisfactory predictive results.

Table 9.1 - The statistical mean values of the output for the nickel concentration in the fourth compartment of the autoclave produced by the learning vector quantization (LVQ) neural network for the acid concentration of the spent electrolyte solution

LVQ output class	**Mean [g/L]**
Classed high = Actual high	91.0
Classed high = Actual low	100.1
Classed low = Actual low	80.4
Classed low = Actual high	85.8
Actual acid concentrations for HIGH $[Ni]_4$	87.5
Actual acid concentrations for LOW $[Ni]_4$	81.8

Table 9.2 - The initial values used in the sensitivity analysis with the kinetic model for the variations in the initial mineral composition

Mineral composition	**Standard conditions [%]** (Fig. 9.42)	**Low initial Ni alloy [%]** (Fig. 9.46)	**High initial Ni alloy [%]** (Fig. 9. 47)	**Low initial Ni_3S_2 [%]** (Fig. 9.48)	**High initial Ni_3S_2 [%]** (Fig. 9.49)
Ni alloy	5.0	3.0	7.0	5.0	5.0
Ni_3S_2	45.4	47.4	43.4	40.4	50.4
NiS	2.4	2.4	2.4	2.4	2.4
Cu_2S	41.9	41.9	41.9	46.9	36.9
$Cu_{1.8}S$	5.3	5.3	5.3	5.3	5.3

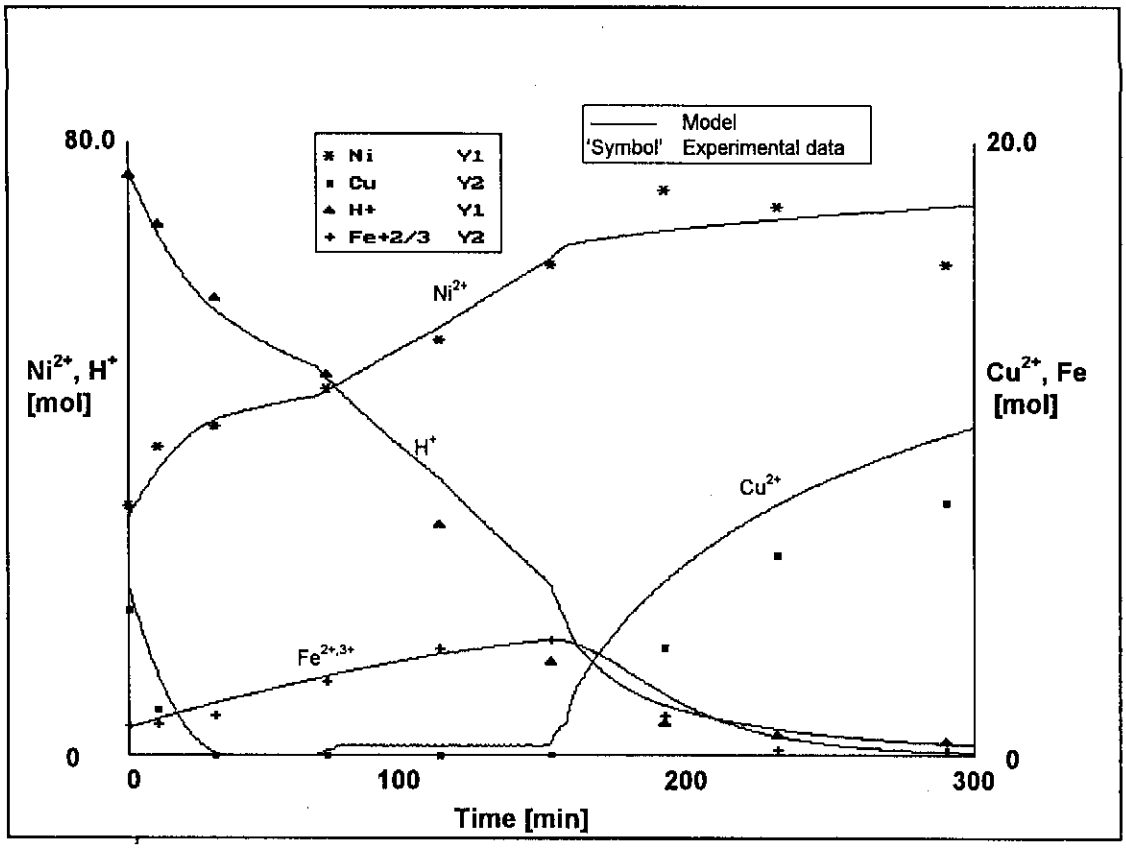

Figure 9.1 - The comparison of the kinetic model prediction with the experimental data for test 10 (standard or reference experiment), with F_{O_2} = 0.59 kg/h

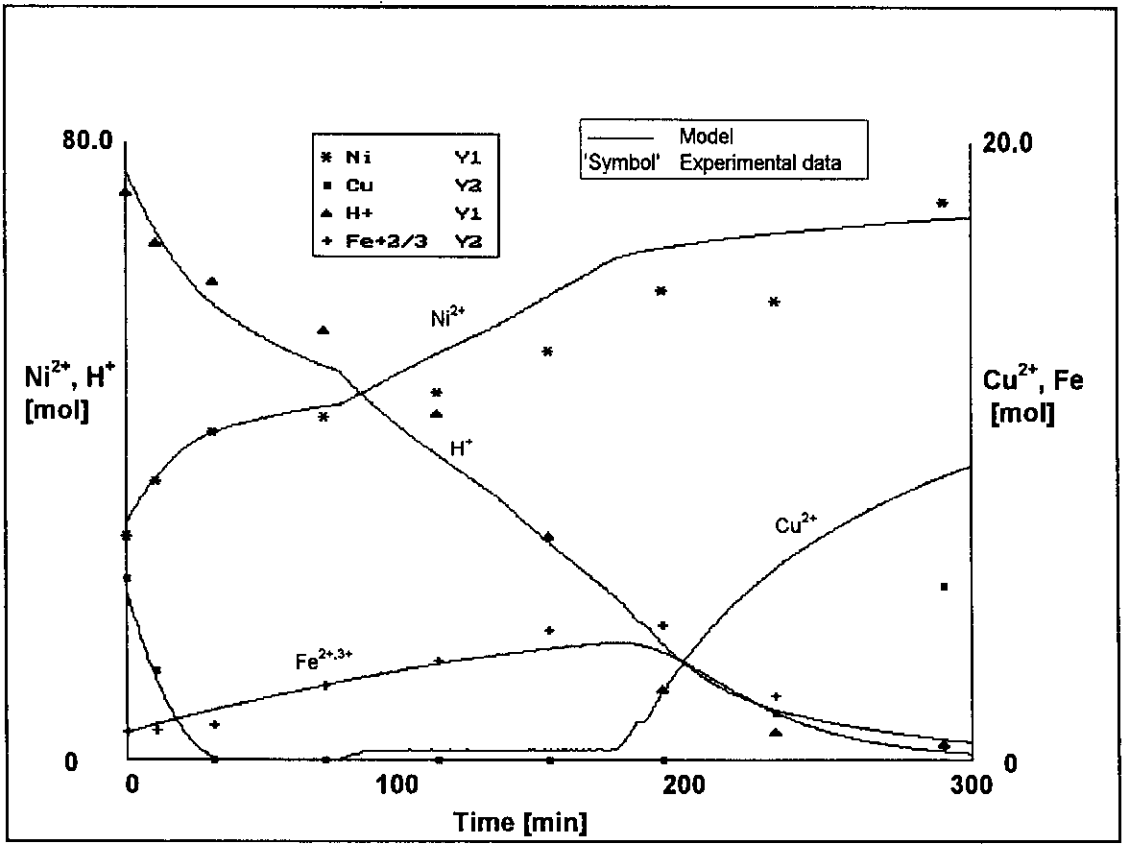

Figure 9.2 - The comparison of the kinetic model prediction with the experimental data for test 6, with F_{O_2} = 0.30 kg/h

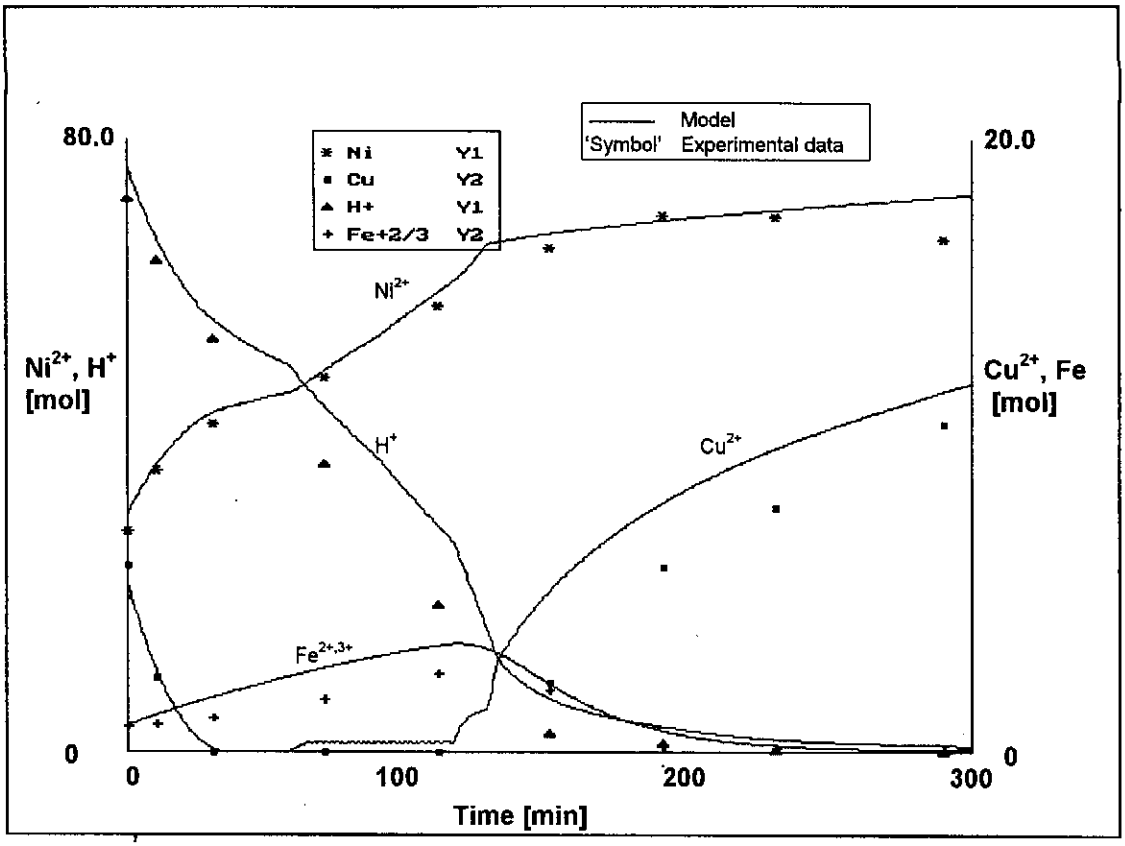

Figure 9.3 - The comparison of the kinetic model prediction with the experimental data for test 27, with F_{O_2} = 0.96 kg/h

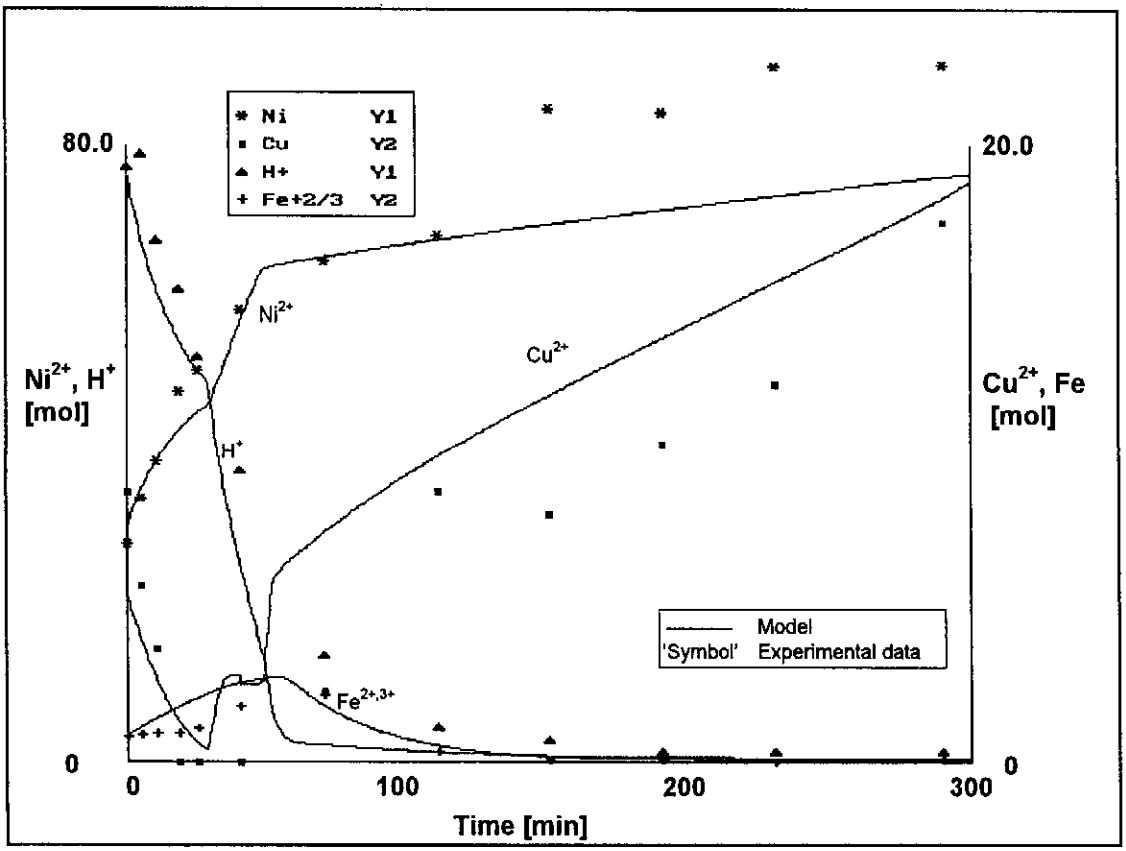

Figure 9.4 - The comparison of the kinetic model prediction with the experimental data for test 1, with F_{O_2} = 3.12 kg/h

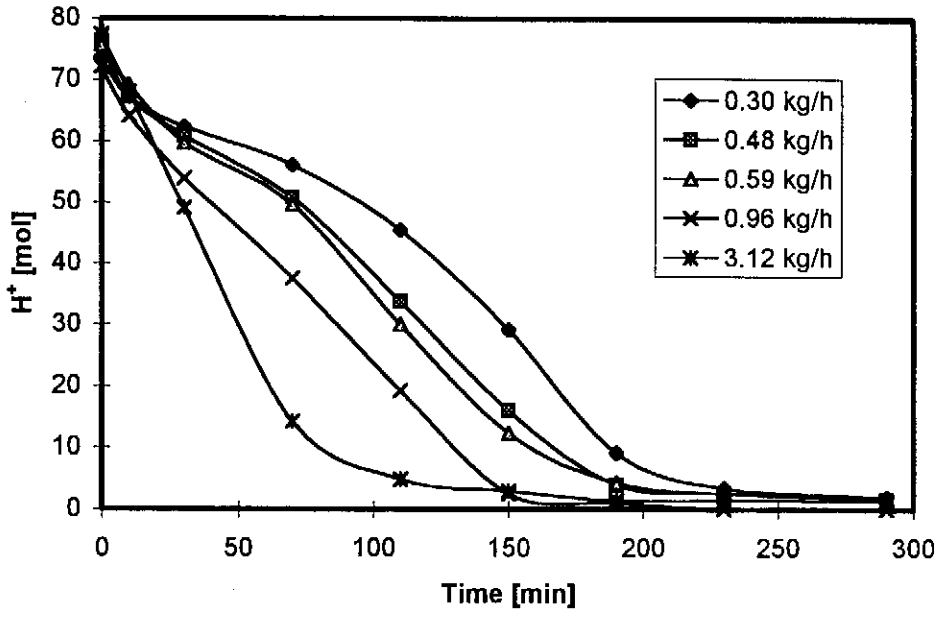

Figure 9.5 - Experimental results of the acid (H^+) content versus time for the variations in the oxygen flowrate (test 6: F_{O_2} = 0.30 kg/h, test 9: F_{O_2} = 0.48 kg/h, test 10: F_{O_2} = 0.59 kg/h, test 27: F_{O_2} = 0.96 kg/h and test 1: F_{O_2} = 3.12 kg/h)

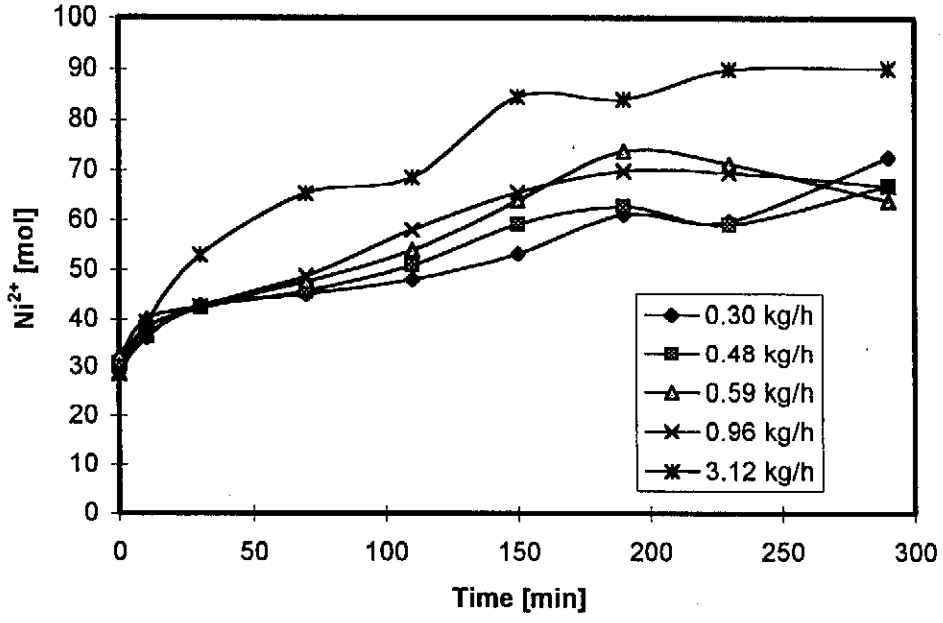

Figure 9.6 - Experimental results of the nickel (Ni^{2+}) content versus time for the variations in the oxygen flowrate (test 6: F_{O_2} = 0.30 kg/h, test 9: F_{O_2} = 0.48 kg/h, test 10: F_{O_2} = 0.59 kg/h, test 27: F_{O_2} = 0.96 kg/h and test 1: F_{O_2} = 3.12 kg/h)

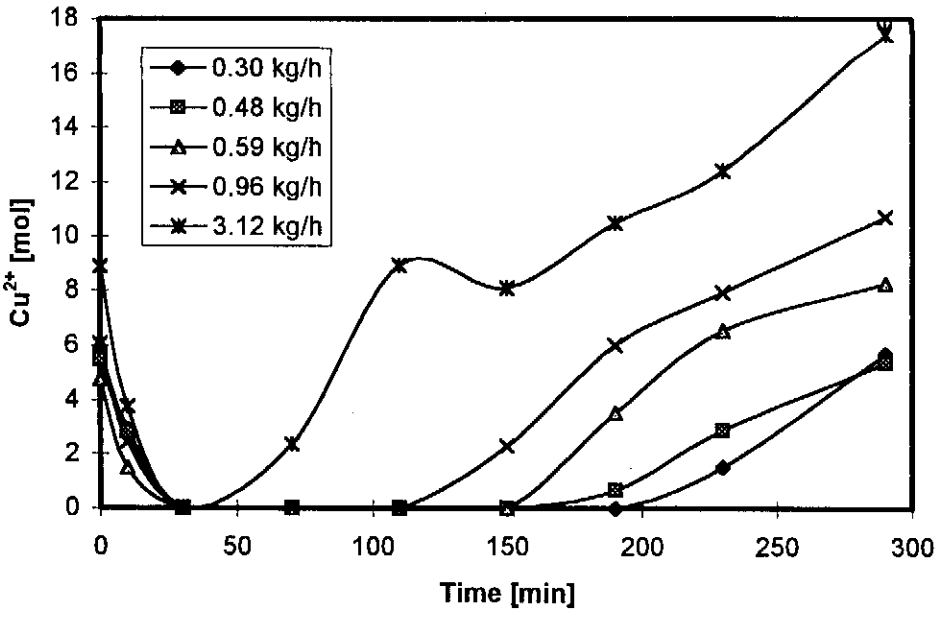

Figure 9.7 - Experimental results of the copper (Cu^{2+}) content versus time for the variations in the oxygen flowrate (test 6: F_{O_2} = 0.30 kg/h, test 9: F_{O_2} = 0.48 kg/h, test 10: F_{O_2} = 0.59 kg/h, test 27: F_{O_2} = 0.96 kg/h and test 1: F_{O_2} = 3.12 kg/h)

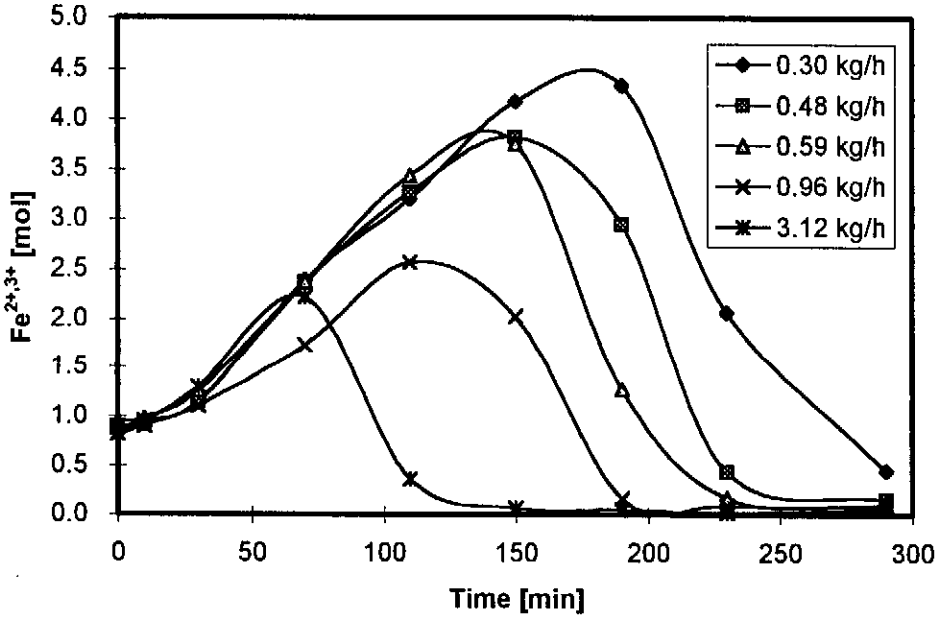

Figure 9.8 - Experimental results of the total iron (Fe^{2+} and Fe^{3+}) content versus time for the variations in the oxygen flowrate (test 6: F_{O_2} = 0.30 kg/h, test 9: F_{O_2} = 0.48 kg/h, test 10: F_{O_2} = 0.59 kg/h, test 27: F_{O_2} = 0.96 kg/h and test 1: F_{O_2} = 3.12 kg/h)

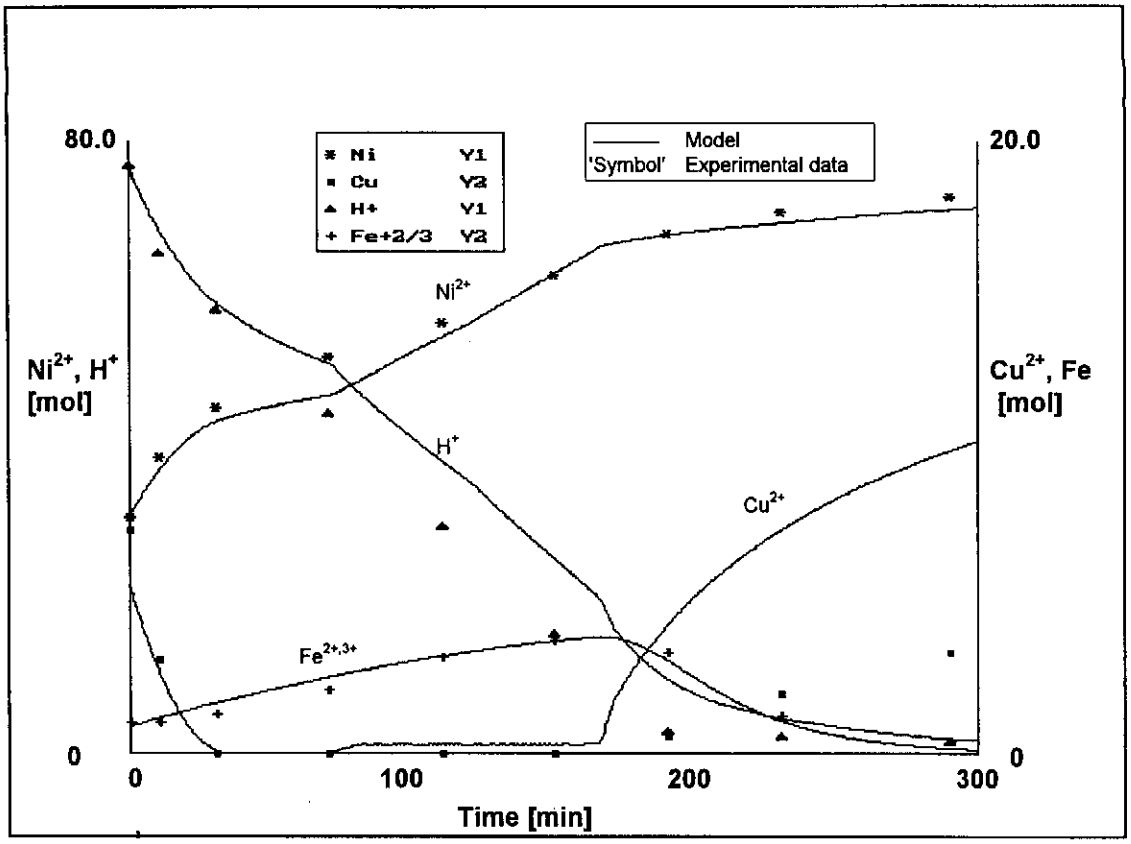

Figure 9.9 - The comparison of the kinetic model prediction with the experimental data for test 16, with p_{O_2} = 0.7 bar

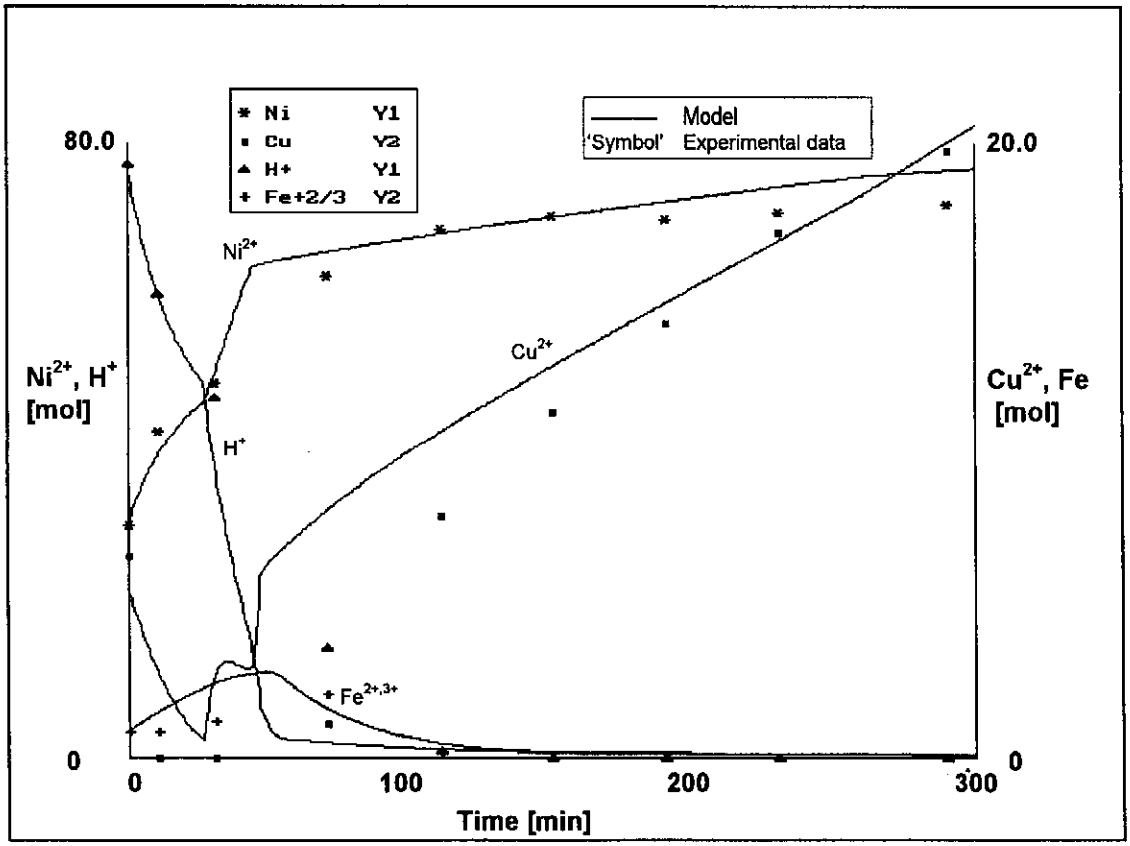

Figure 9.10 - The comparison of the kinetic model prediction with the experimental data for test 21, with p_{O_2} = 4.4 bar

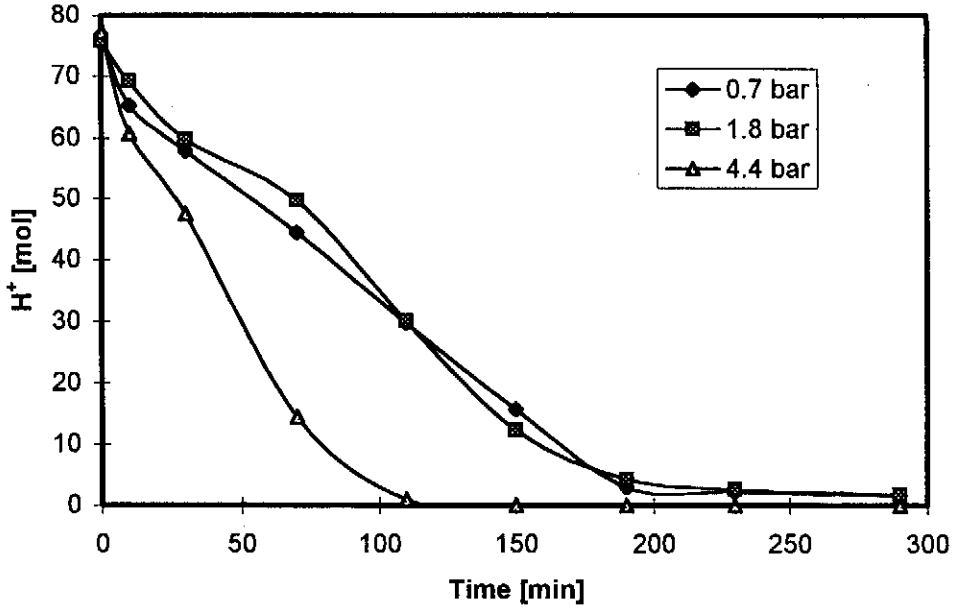

Figure 9.11 - Experimental results of the acid (H^+) content versus time for the variations in the oxygen partial pressure (test 16: p_{O_2} = 0.7 bar, test 10: p_{O_2} = 1.8 bar and test 21: p_{O_2} = 4.4 bar)

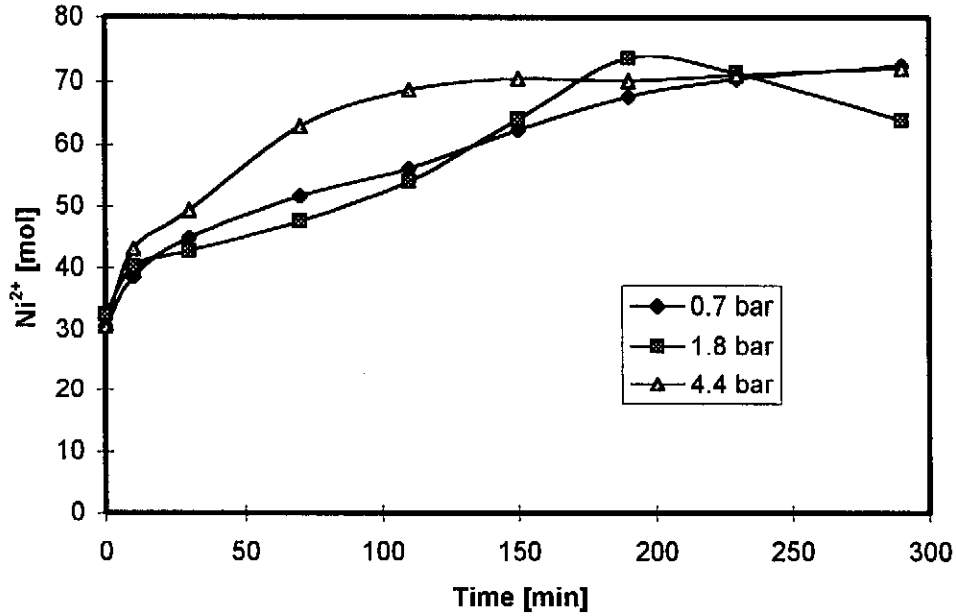

Figure 9.12 - Experimental results of the nickel (Ni^{2+}) content versus time for the variations in the oxygen partial pressure (test 16: p_{O_2} = 0.7 bar, test 10: p_{O_2} = 1.8 bar and test 21: p_{O_2} = 4.4 bar)

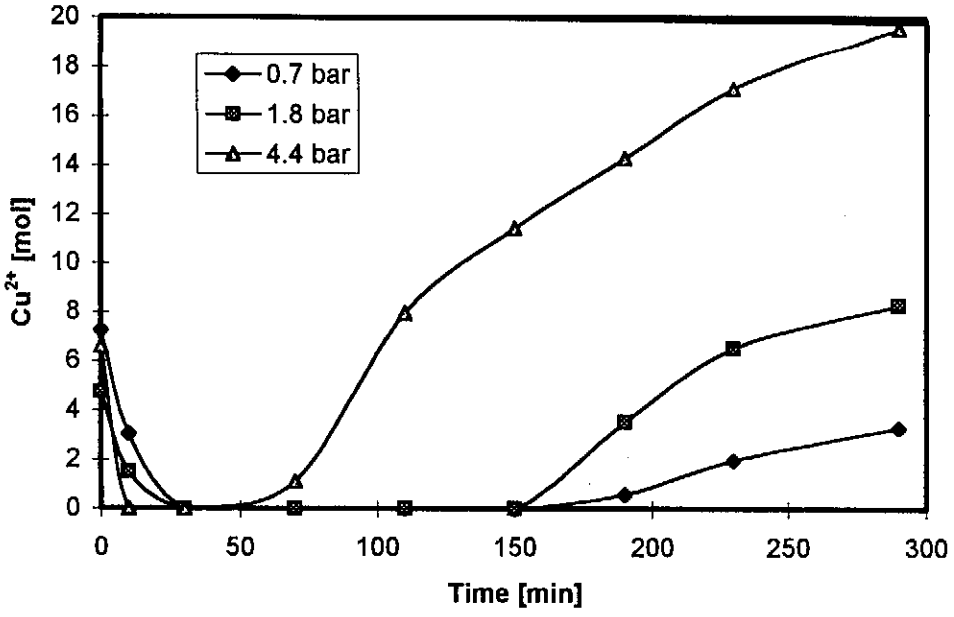

Figure 9.13 - Experimental results of the copper (Cu^{2+}) content versus time for the variations in the oxygen partial pressure (test 16: p_{O_2} = 0.7 bar, test 10: p_{O_2} = 1.8 bar and test 21: p_{O_2} = 4.4 bar)

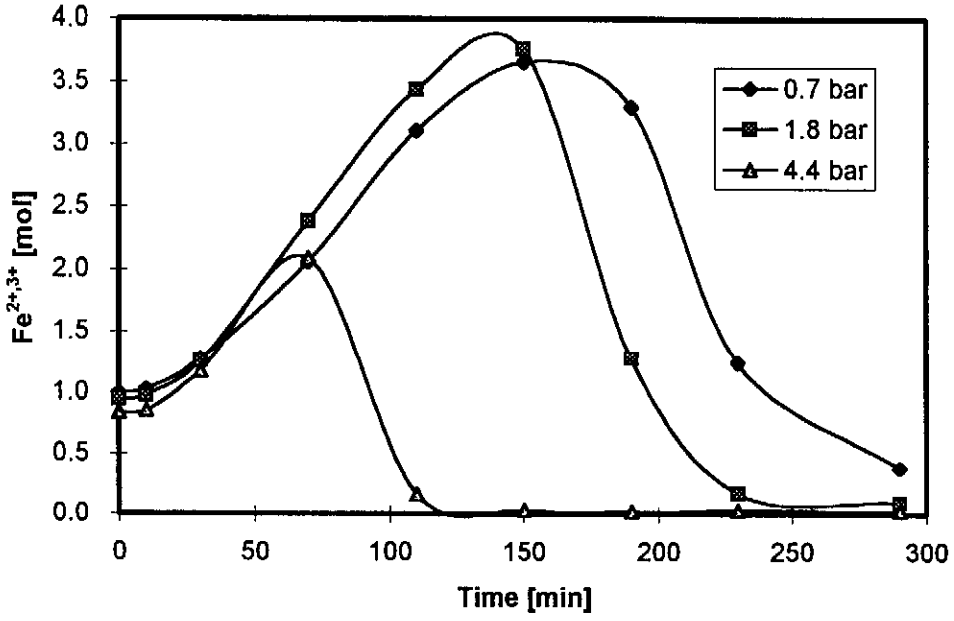

Figure 9.14 - Experimental results of the total iron (Fe^{2+} and Fe^{3+}) content versus time for the variations in the oxygen partial pressure (test 16: p_{O_2} = 0.7 bar, test 10: p_{O_2} = 1.8 bar and test 21: p_{O_2} = 4.4 bar)

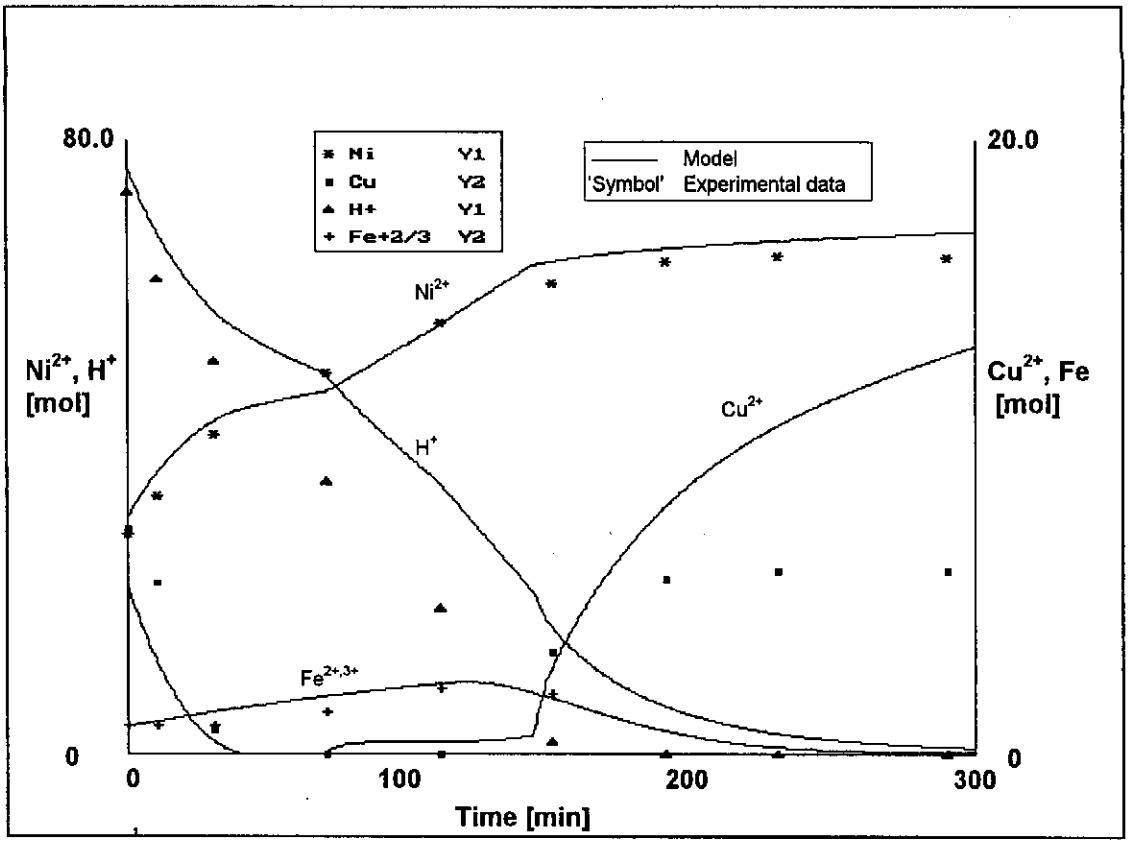

Figure 9.15 - The comparison of the kinetic model prediction with the experimental data for test 14, with T_r = 120°C

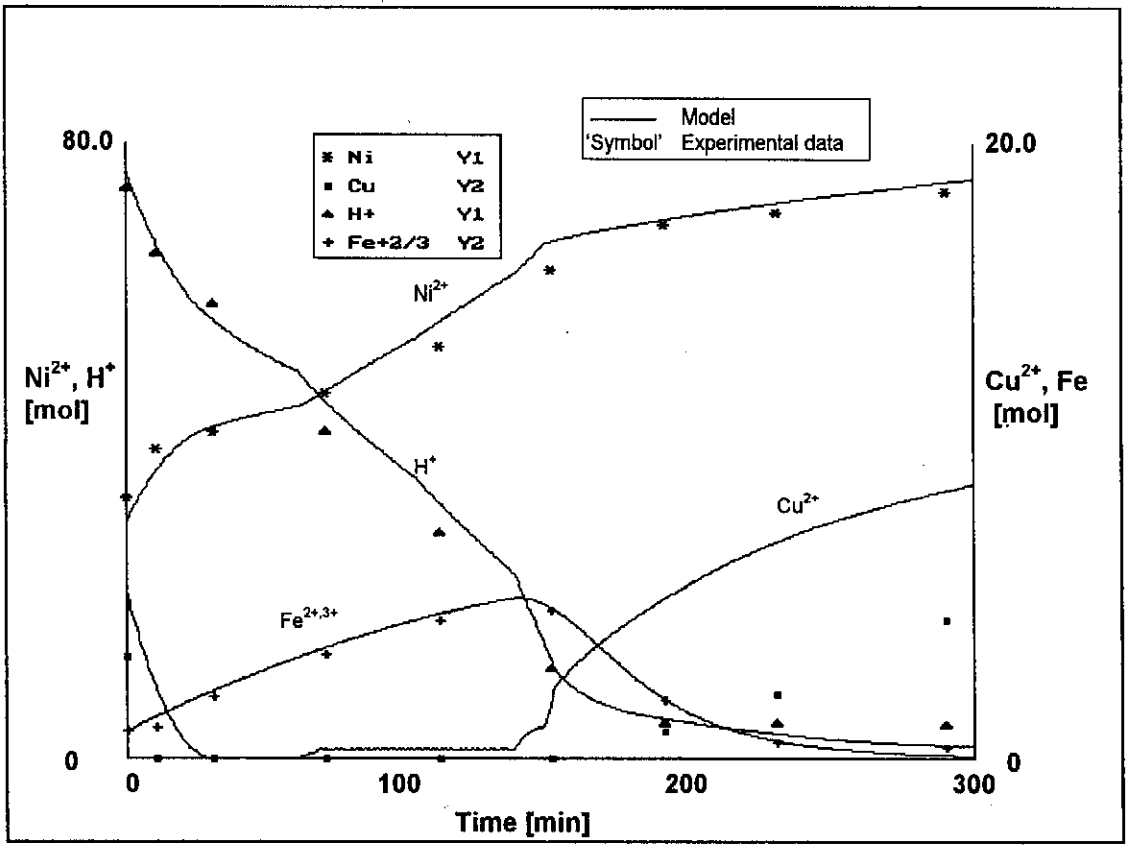

Figure 9.16 - The comparison of the kinetic model prediction with the experimental data for test 14, with T_r = 158°C

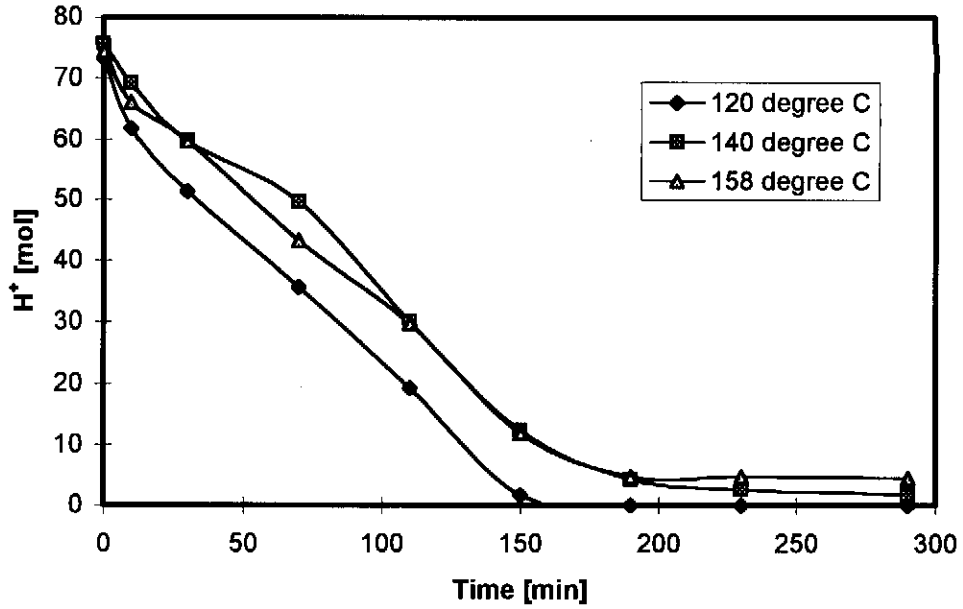

Figure 9.17 - Experimental results of the acid (H^+) content versus time for the variations in the temperature (test 14: T_r = 120°C, test 10: T_r = 140°C and test 15: T_r = 158°C)

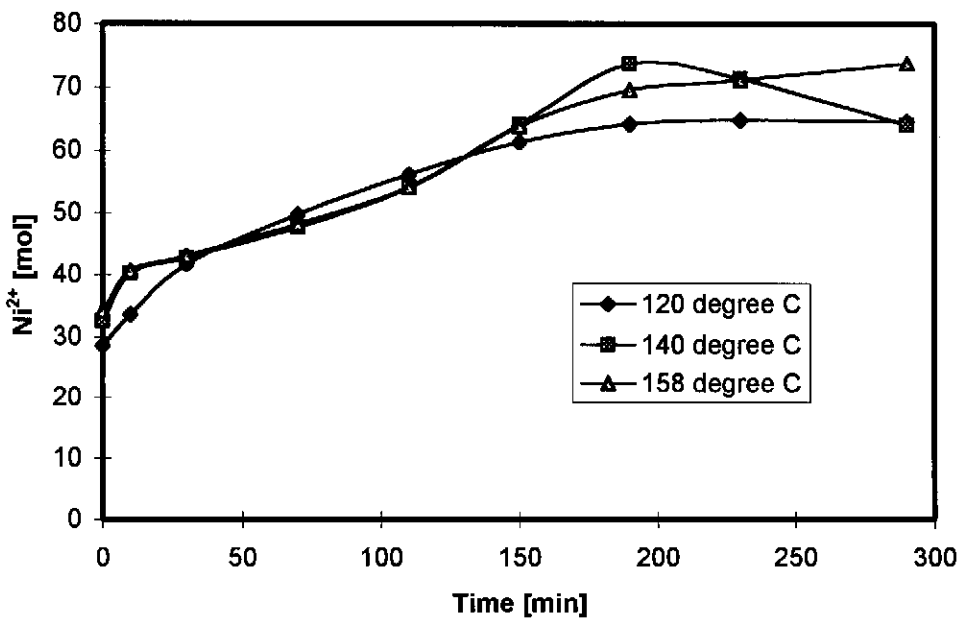

Figure 9.18 - Experimental results of the nickel (Ni^{2+}) content versus time for the variations in the temperature (test 14: T_r = 120°C, test 10: T_r = 140°C and test 15: T_r = 158°C)

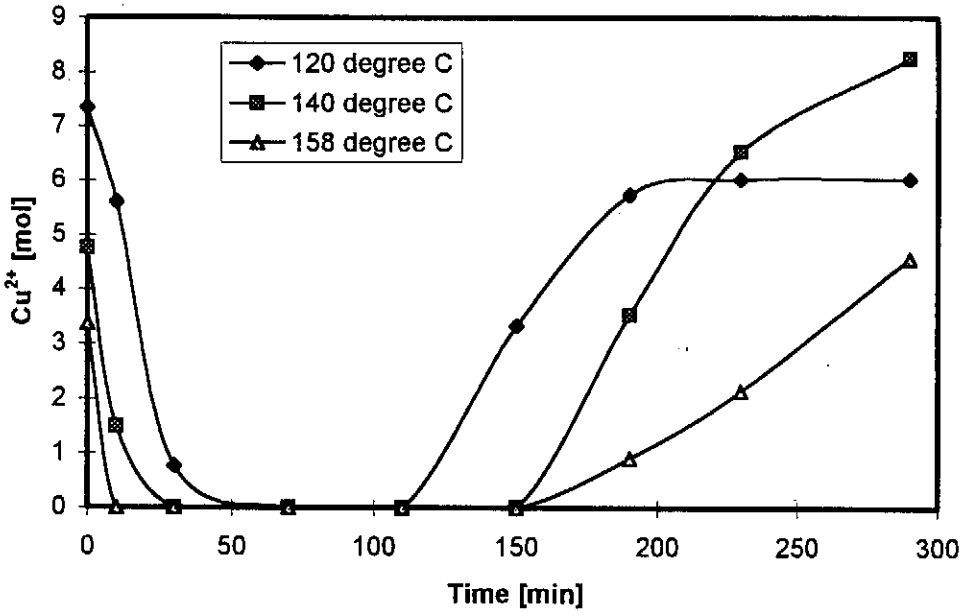

Figure 9.19 - Experimental results of the copper (Cu^{2+}) content versus time for the variations in the temperature (test 14: T_r = 120°C, test 10: T_r = 140°C and test 15: T_r = 158°C)

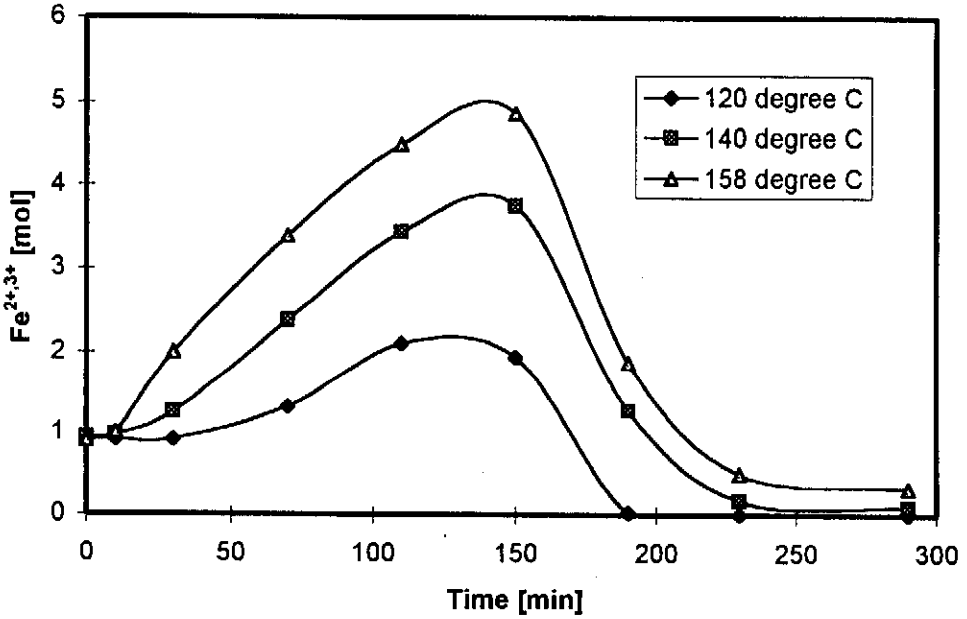

Figure 9.20 - Experimental results of the total iron (Fe^{2+} and Fe^{3+}) content versus time for the variations in the temperature (test 14: T_r = 120°C, test 10: T_r = 140°C and test 15: T_r = 158°C)

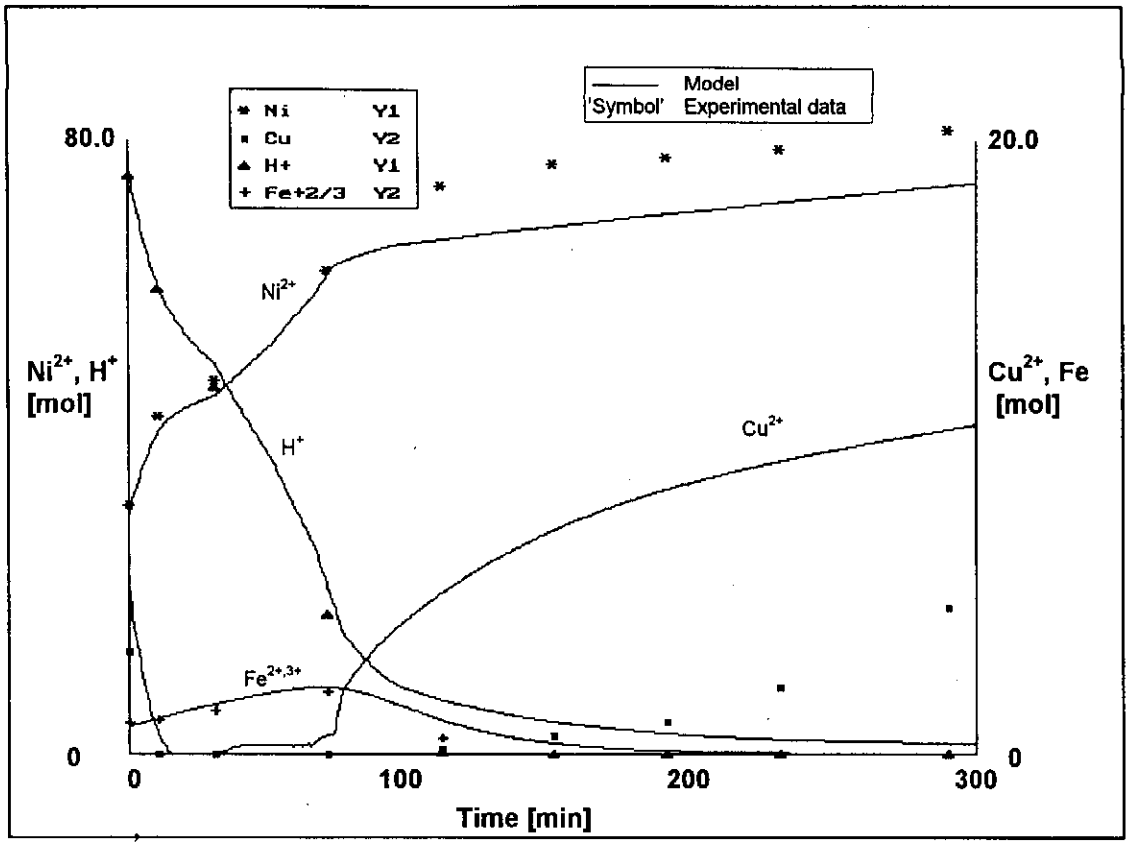

Figure 9.21 - The comparison of the kinetic model prediction with the experimental data for test 22, with $d_{p,1}$ = 37.8 μm

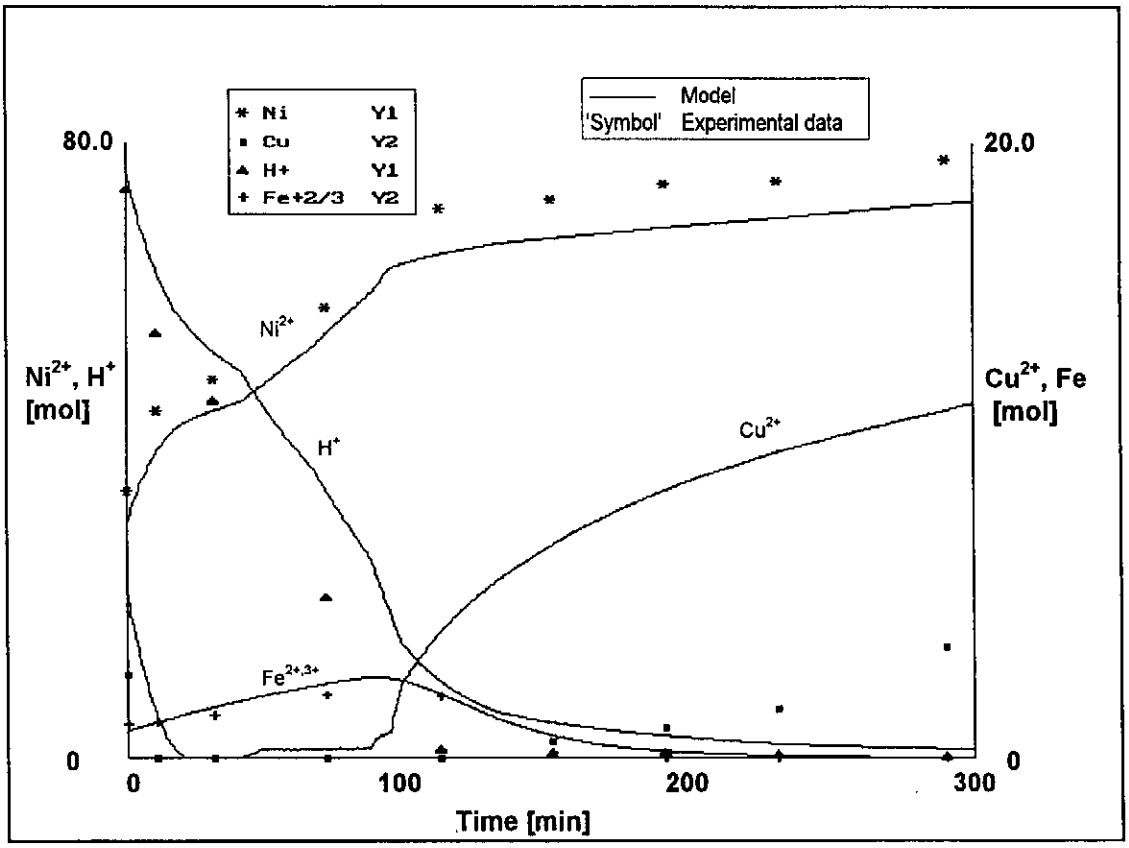

Figure 9.22 - The comparison of the kinetic model prediction with the experimental data for test 19, with $d_{p,2}$ = 58.1 μm

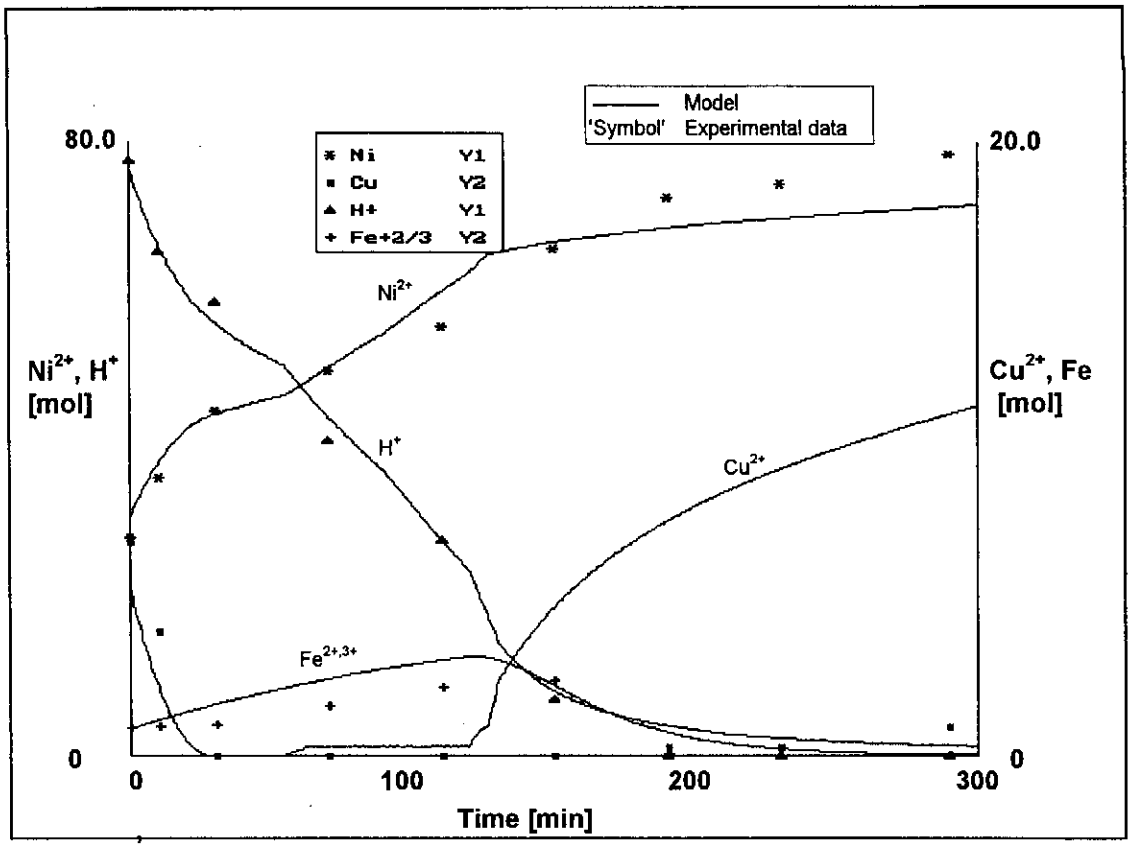

Figure 9.23 - The comparison of the kinetic model prediction with the experimental data for test 20, with $d_{p,3}$ = 89.2 μm

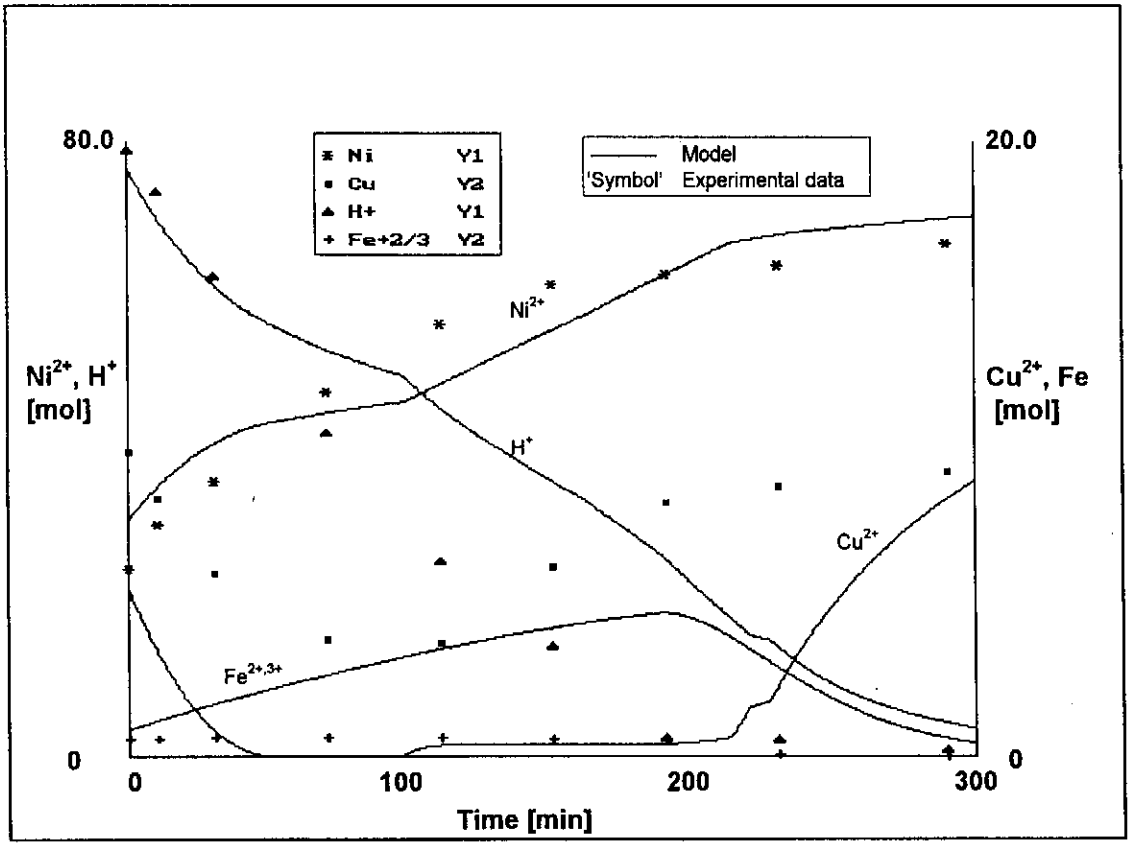

Figure 9.24 - The comparison of the kinetic model prediction with the experimental data for test 18, with $d_{p,4}$ = 212.0 μm

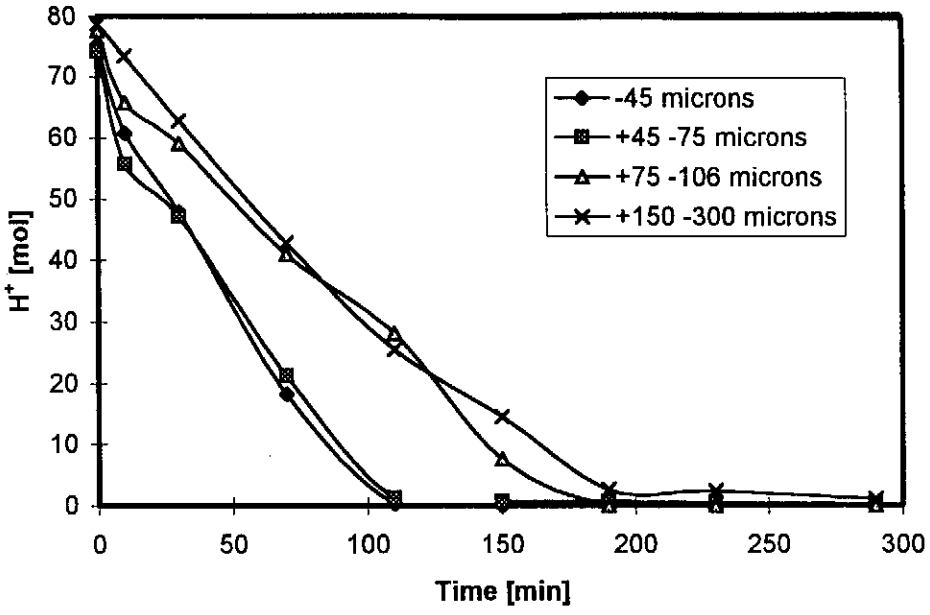

Figure 9.25 - Experimental results of the acid (H^+) content versus time for the variations in the (average) particle size fractions (test 22: $d_{p,1}$ = 37.8 μm, test 19: $d_{p,2}$ = 58.1 μm, test 20: $d_{p,3}$ = 89.2 μm and test 18: $d_{p,4}$ = 212.0 μm)

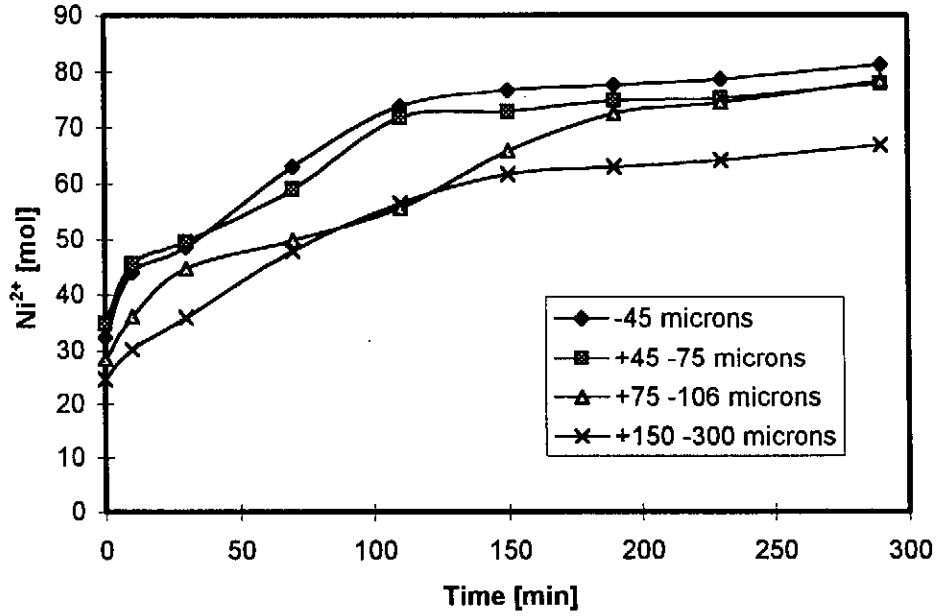

Figure 9.26 - Experimental results of the nickel (Ni^{2+}) content versus time for the variations in the (average) particle size fractions (test 22: $d_{p,1}$ = 37.8 μm, test 19: $d_{p,2}$ = 58.1 μm, test 20: $d_{p,3}$ = 89.2 μm and test 18: $d_{p,4}$ = 212.0 μm)

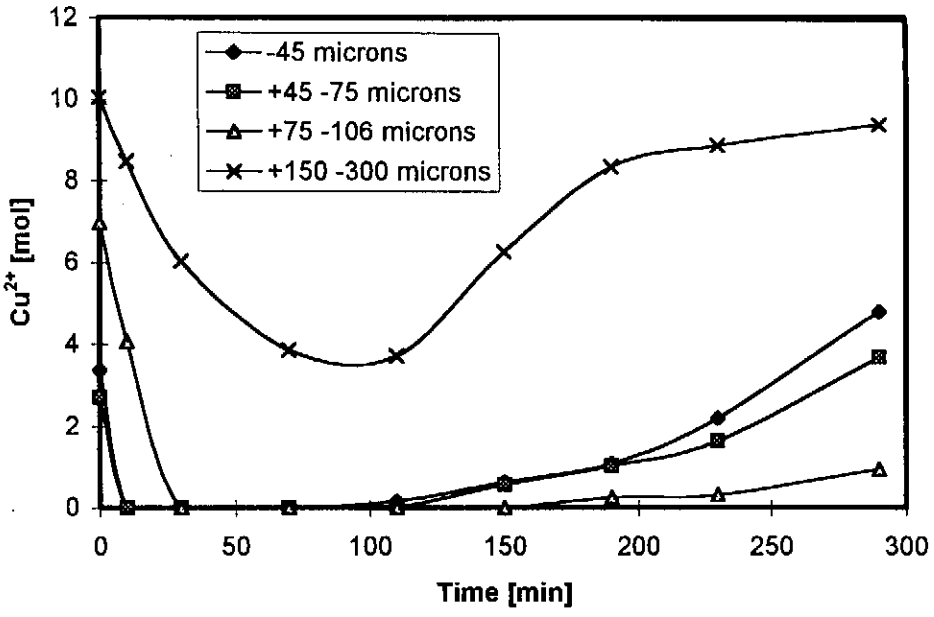

Figure 9.27 - Experimental results of the copper (Cu^{2+}) content versus time for the variations in the (average) particle size fractions (test 22: $d_{p,1}$ = 37.8 μm, test 19: $d_{p,2}$ = 58.1 μm, test 20: $d_{p,3}$ = 89.2 μm and test 18: $d_{p,4}$ = 212.0 μm)

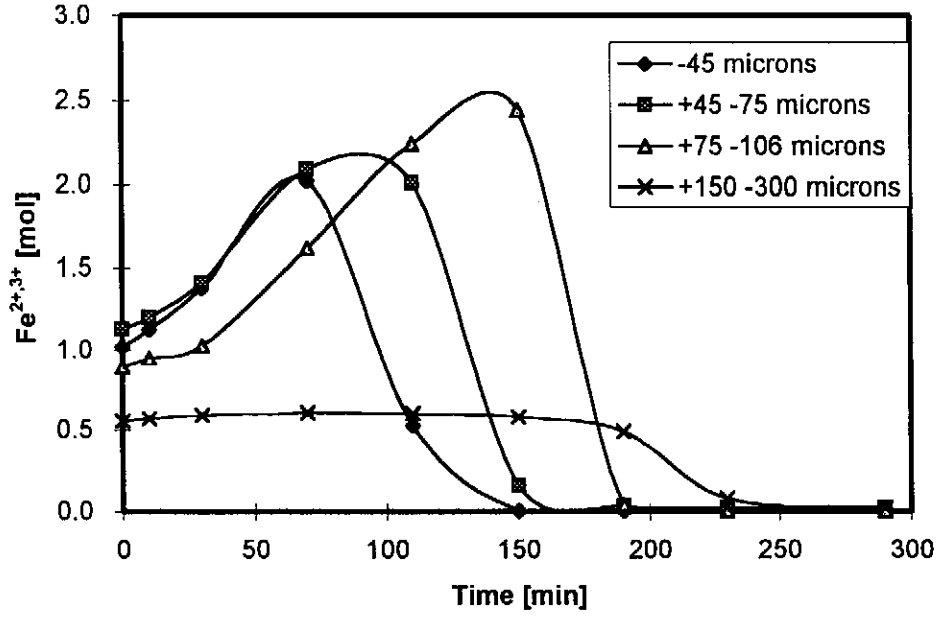

Figure 9.28 - Experimental results of the total iron (Fe^{2+} and Fe^{3+}) content versus time for the variations in the (average) particle size fractions (test 22: $d_{p,1}$ = 37.8 μm, test 19: $d_{p,2}$ = 58.1 μm, test 20: $d_{p,3}$ = 89.2 μm and test 18: $d_{p,4}$ = 212.0 μm)

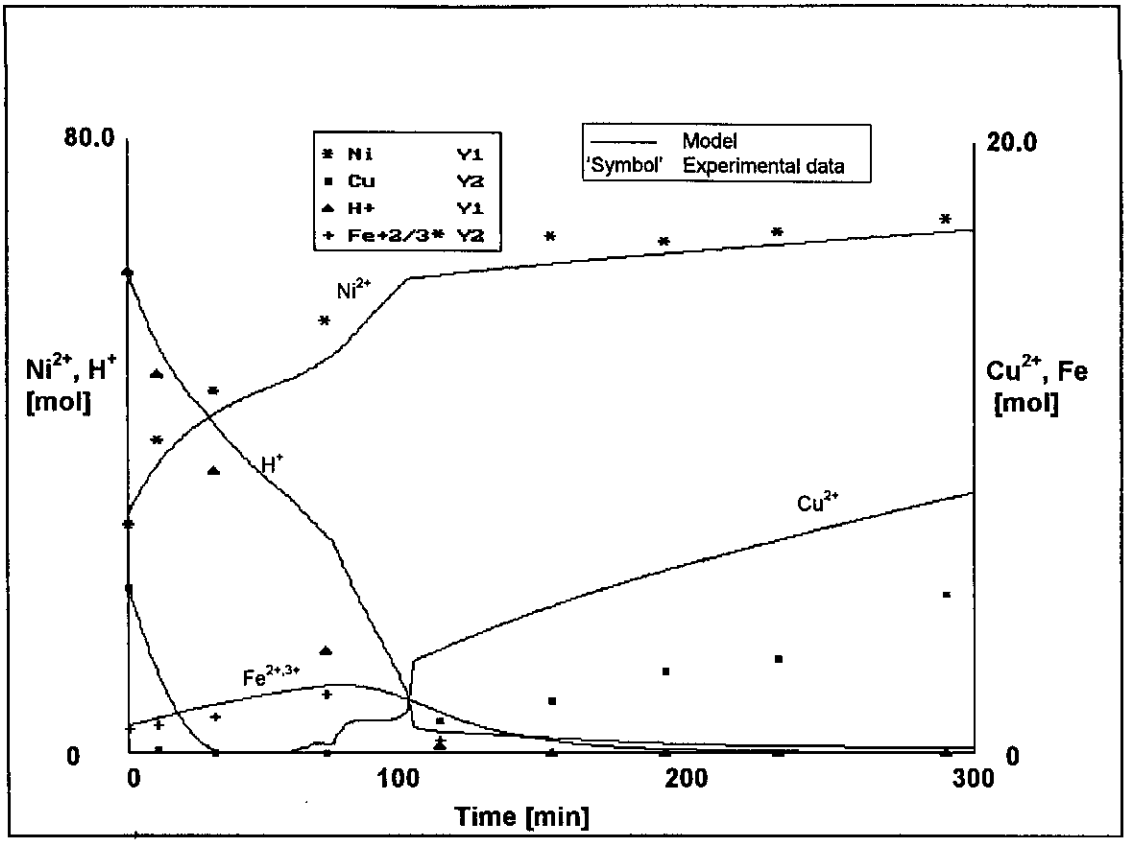

Figure 9.29 - The comparison of the kinetic model prediction with the experimental data for test 24, with C_{i,H_2SO_4} = 0.82 mol/L

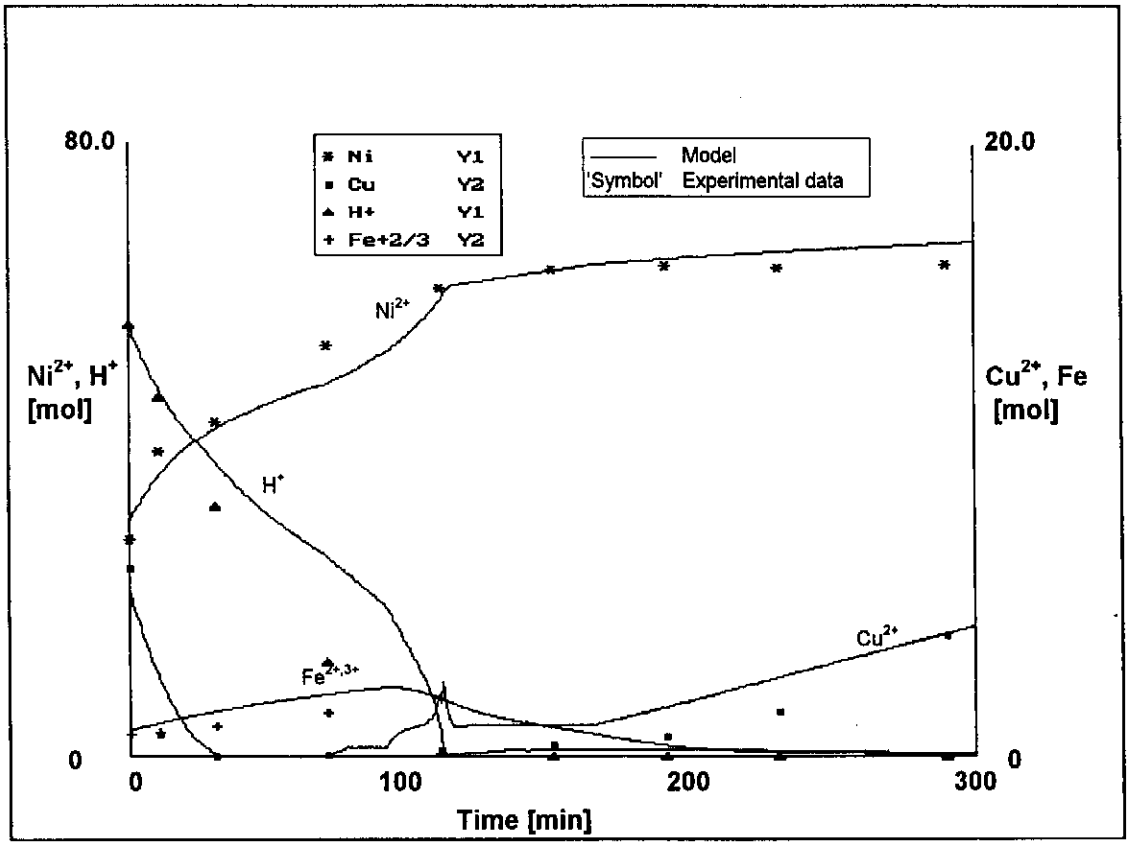

Figure 9.30 - The comparison of the kinetic model prediction with the experimental data for test 25, with C_{i,H_2SO_4} = 0.73 mol/L

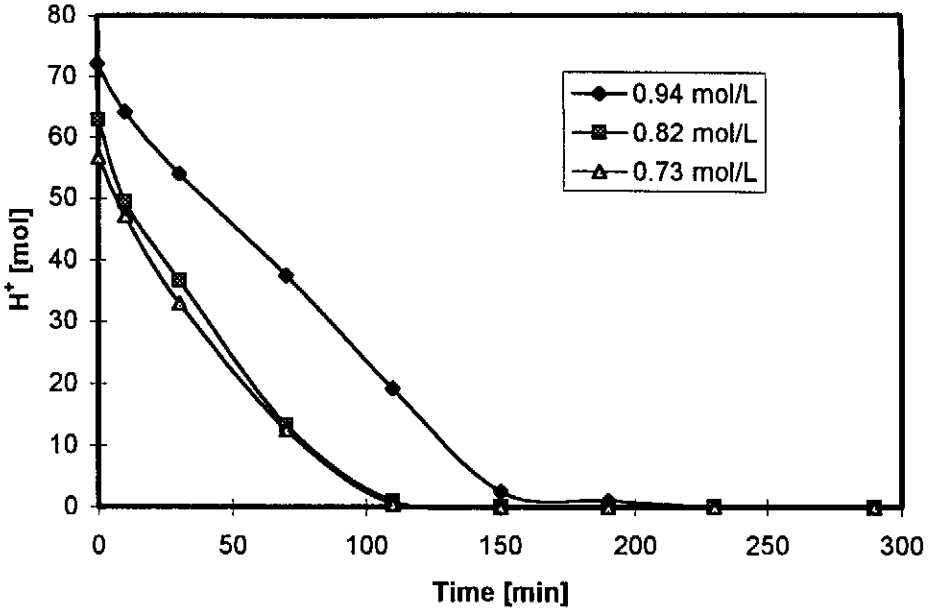

Figure 9.31 - Experimental results of the acid (H^+) content versus time for the variations in the initial acid concentrations (test 27: C_{i,H_2SO_4} = 0.94 mol/L, test 24: C_{i,H_2SO_4} = 0.82 mol/L and test 25: C_{i,H_2SO_4} = 0.73 mol/L)

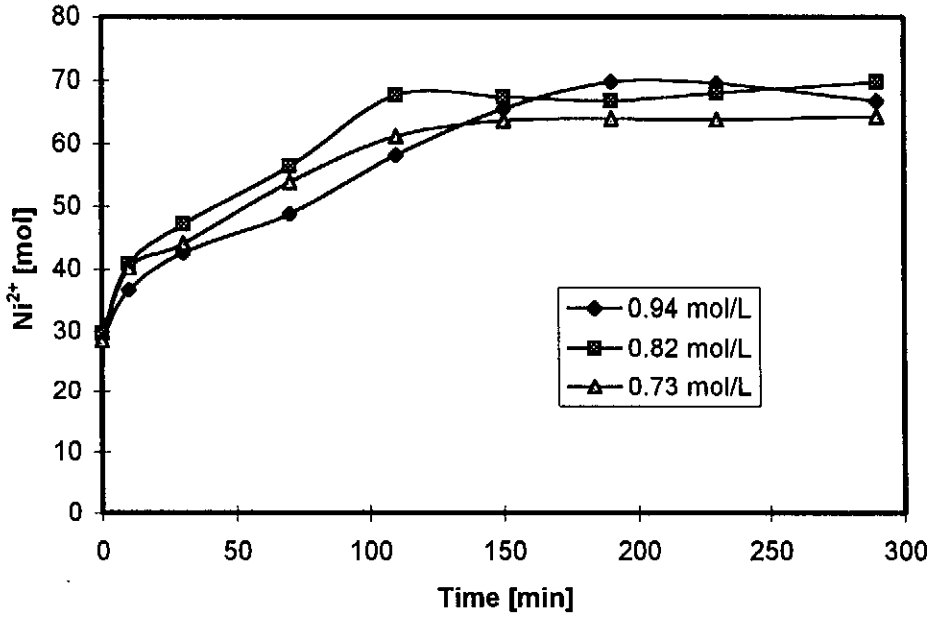

Figure 9.32 - Experimental results of the nickel (Ni^{2+}) content versus time for the variations in the initial acid concentrations (test 27: C_{i,H_2SO_4} = 0.94 mol/L, test 24: C_{i,H_2SO_4} = 0.82 mol/L and test 25: C_{i,H_2SO_4} = 0.73 mol/L)

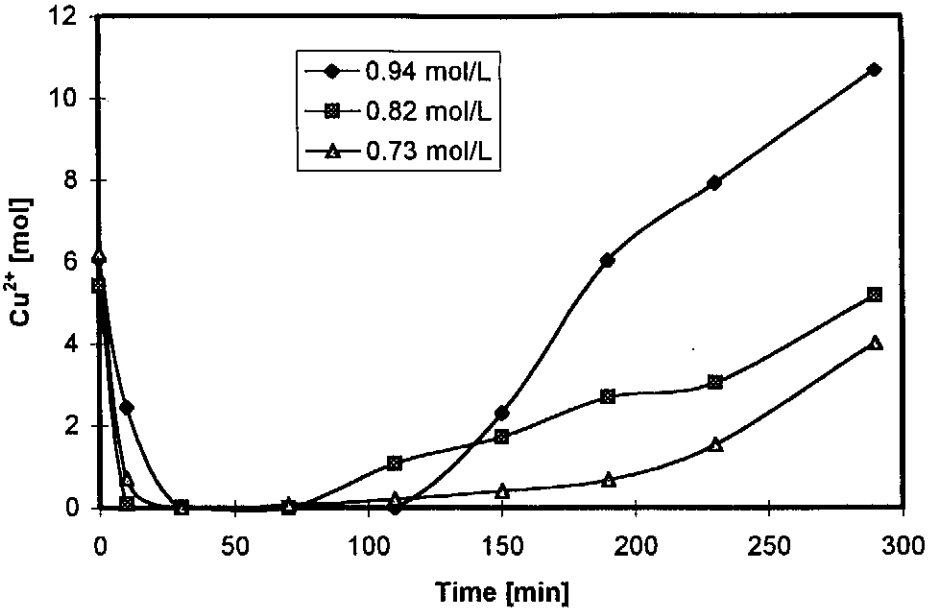

Figure 9.33 - Experimental results of the copper (Cu^{2+}) content versus time for the variations in the initial acid concentrations (test 27: C_{i,H_2SO_4} = 0.94 mol/L, test 24: C_{i,H_2SO_4} = 0.82 mol/L and test 25: C_{i,H_2SO_4} = 0.73 mol/L)

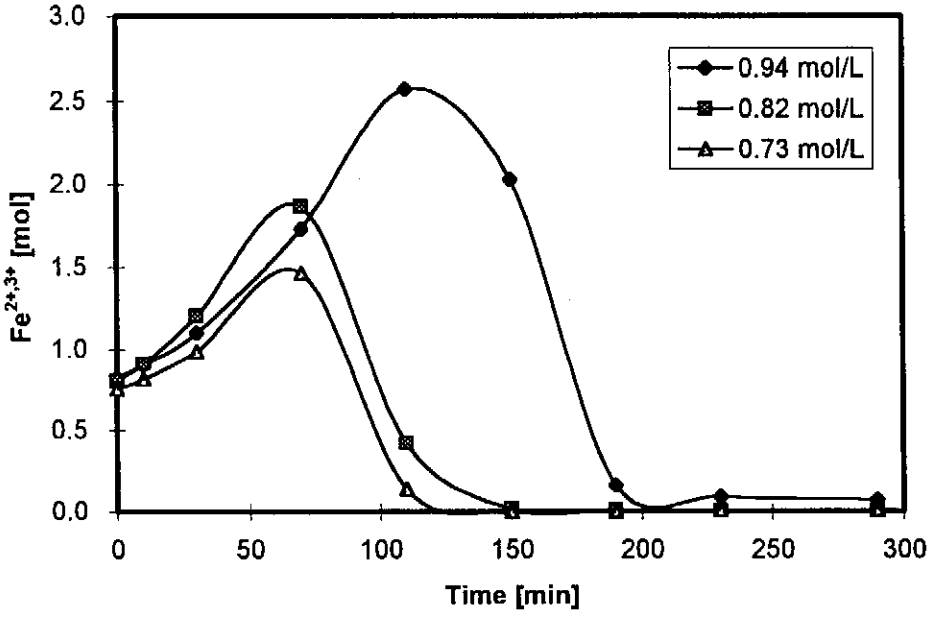

Figure 9.34 - Experimental results of the total iron (Fe^{2+} and Fe^{3+}) content versus time for the variations in the initial acid concentrations (test 27: C_{i,H_2SO_4} = 0.94 mol/L, test 24: C_{i,H_2SO_4} = 0.82 mol/L and test 25: C_{i,H_2SO_4} = 0.73 mol/L)

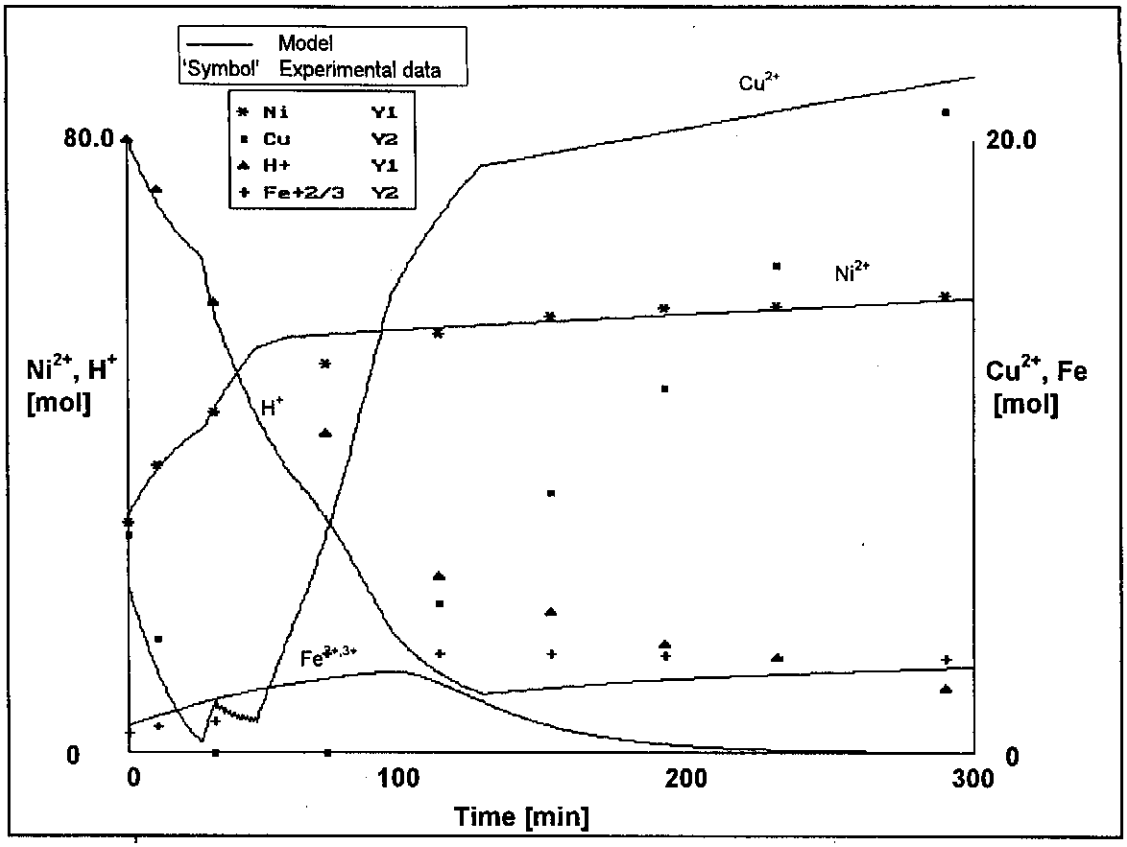

Figure 9.35 - The comparison of the kinetic model prediction with the experimental data for test 12, with the pulp density = 1.30 kg/L

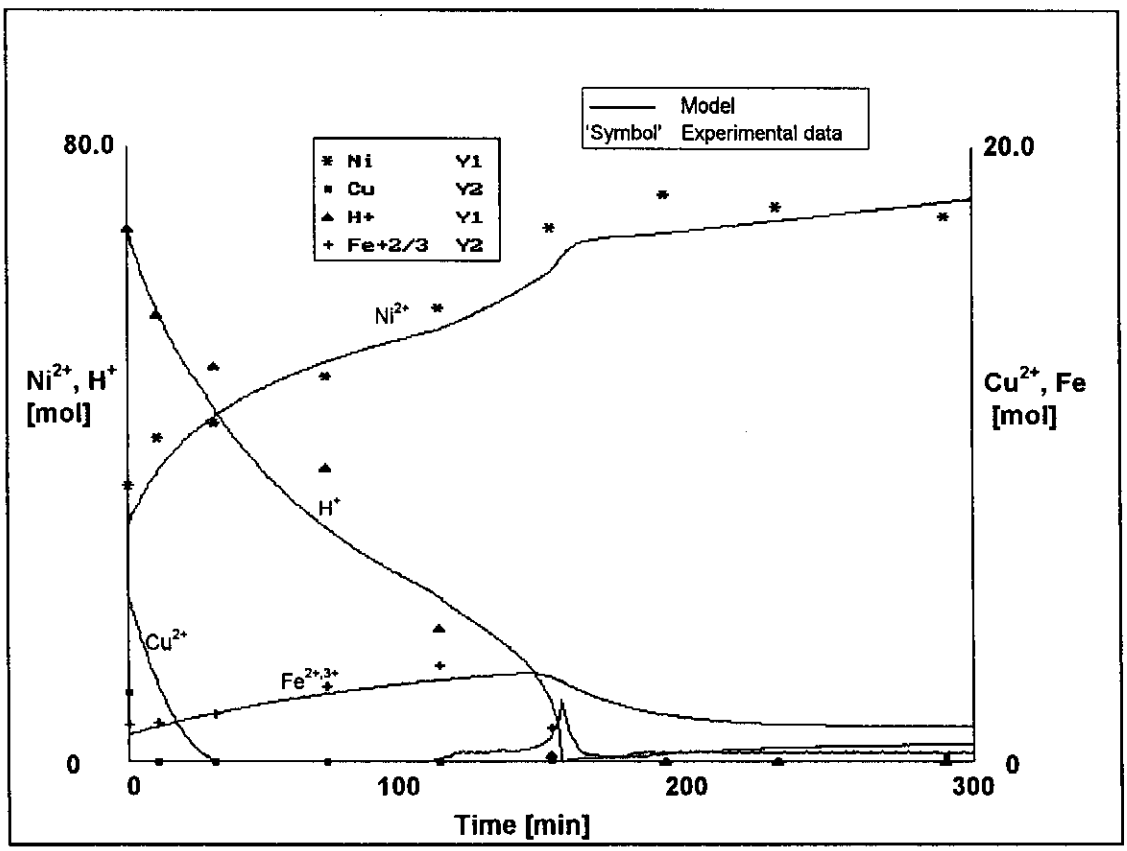

Figure 9.36 - The comparison of the kinetic model prediction with the experimental data for test 13, with the pulp density = 1.40 kg/L

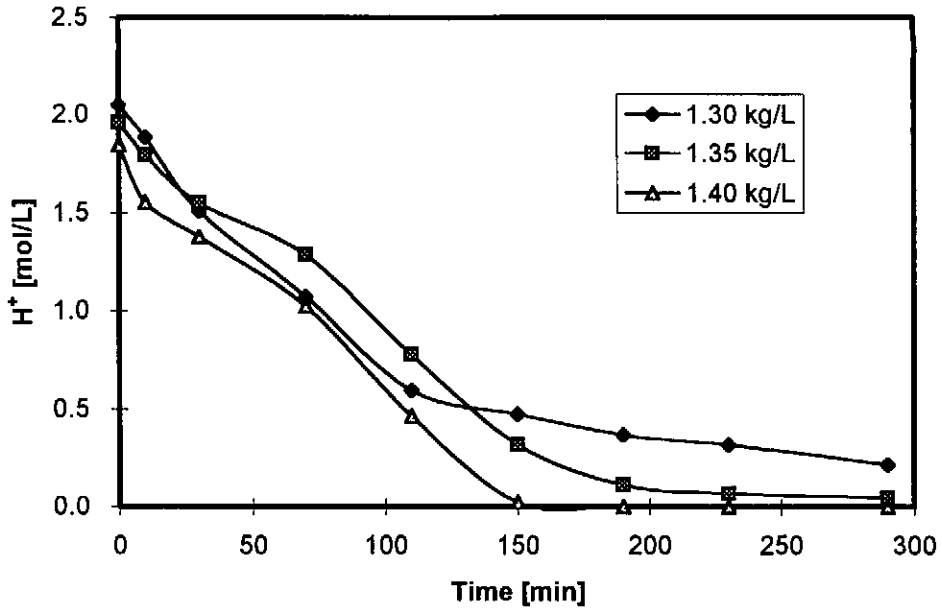

Figure 9.37 - Experimental results of the acid (H^+) concentration versus time for the variations in the pulp densities (test 12: pulp density = 1.30 kg/L, test 10: pulp density = 1.35 kg/L and test 13: pulp density = 1.40 kg/L)

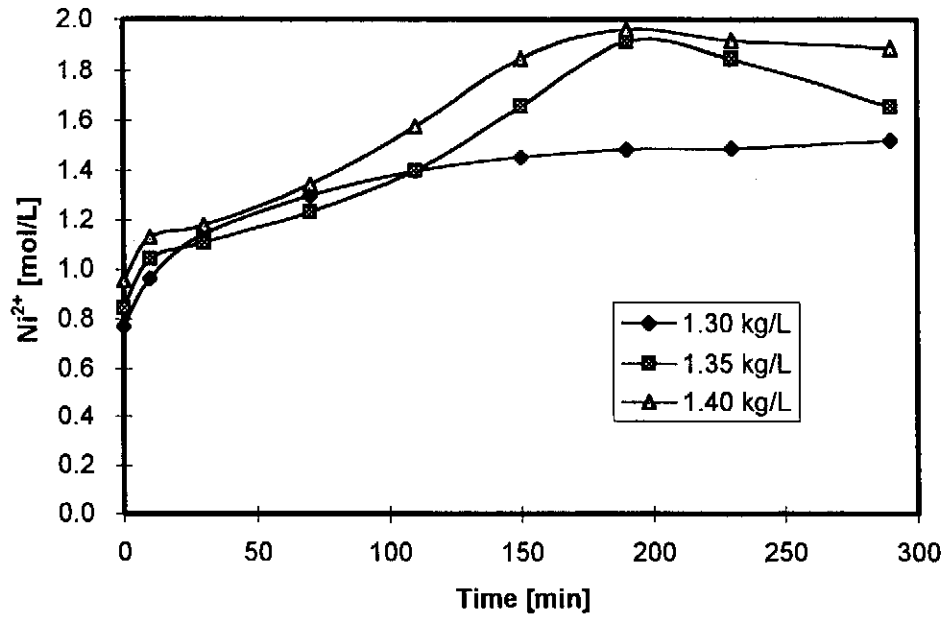

Figure 9.38 - Experimental results of the nickel (Ni^{2+}) concentration versus time for the variations in the pulp densities (test 12: pulp density = 1.30 kg/L, test 10: pulp density = 1.35 kg/L and test 13: pulp density = 1.40 kg/L)

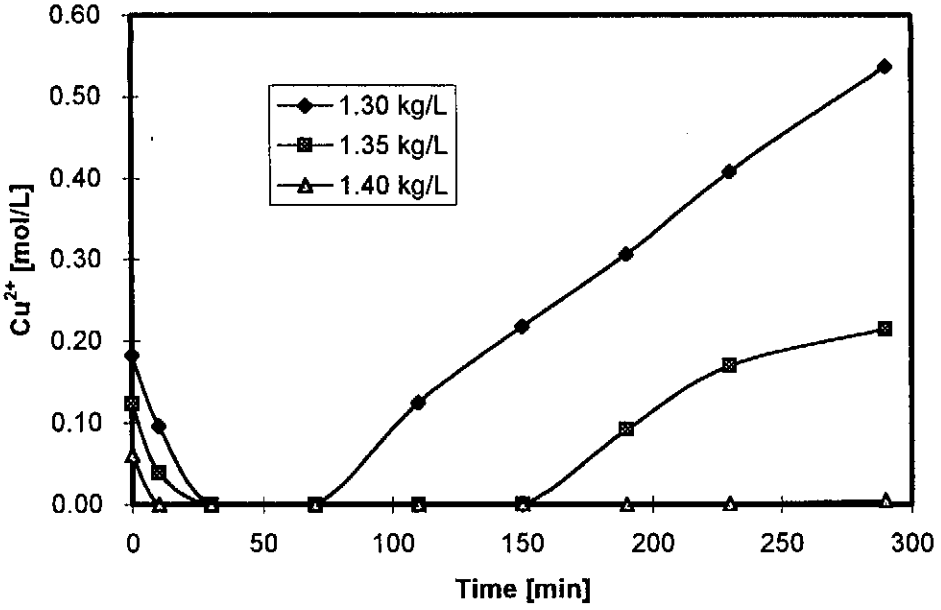

Figure 9.39 - Experimental results of the copper (Cu^{2+}) concentration versus time for the variations in the pulp densities (test 12: pulp density = 1.30 kg/L, test 10: pulp density = 1.35 kg/L and test 13: pulp density = 1.40 kg/L)

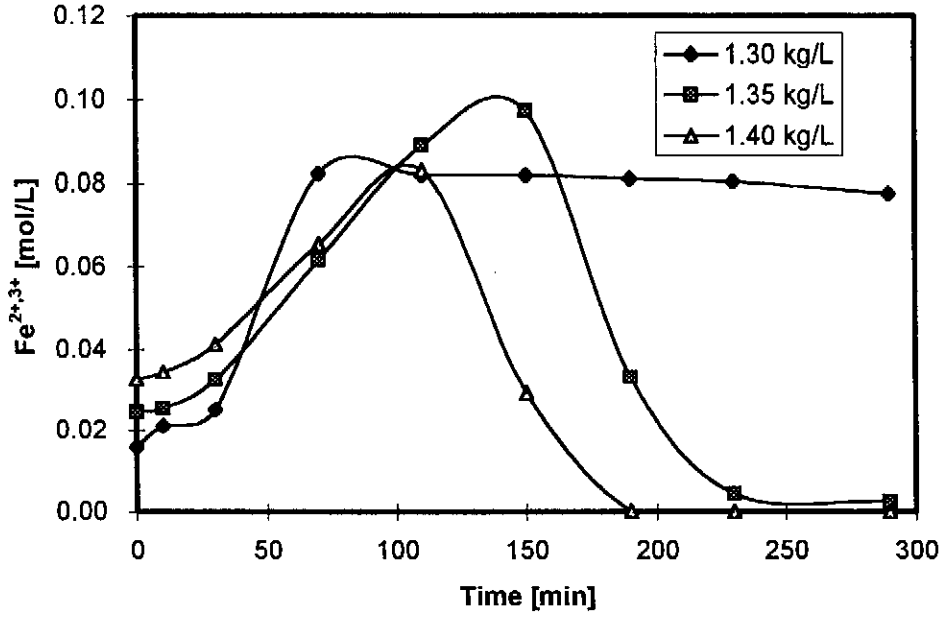

Figure 9.40 - Experimental results of the total iron (Fe^{2+} and Fe^{3+}) concentration versus time for the variations in the pulp densities (test 12: pulp density = 1.30 kg/L, test 10: pulp density = 1.35 kg/L and test 13: pulp density = 1.40 kg/L)

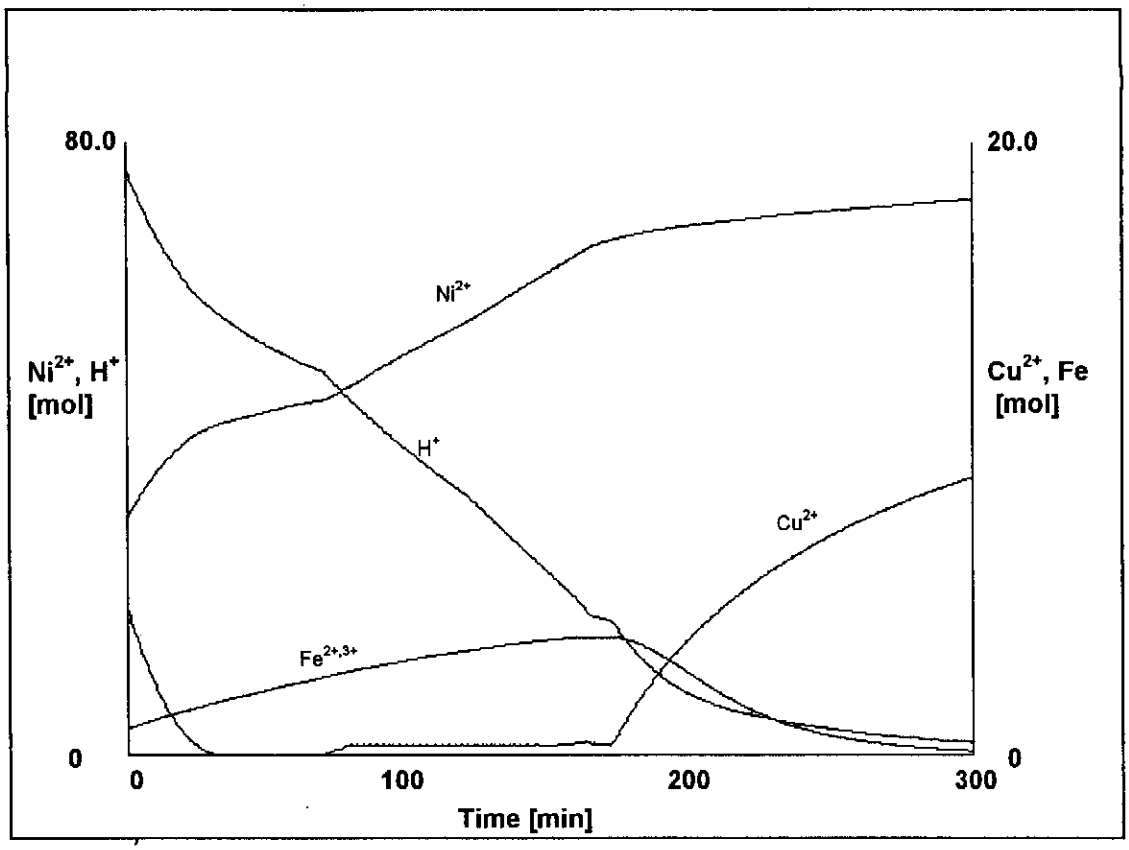

Figure 9.41 - Sensitivity analysis with the model for the lower initial copper concentration of 0.12 mol/L

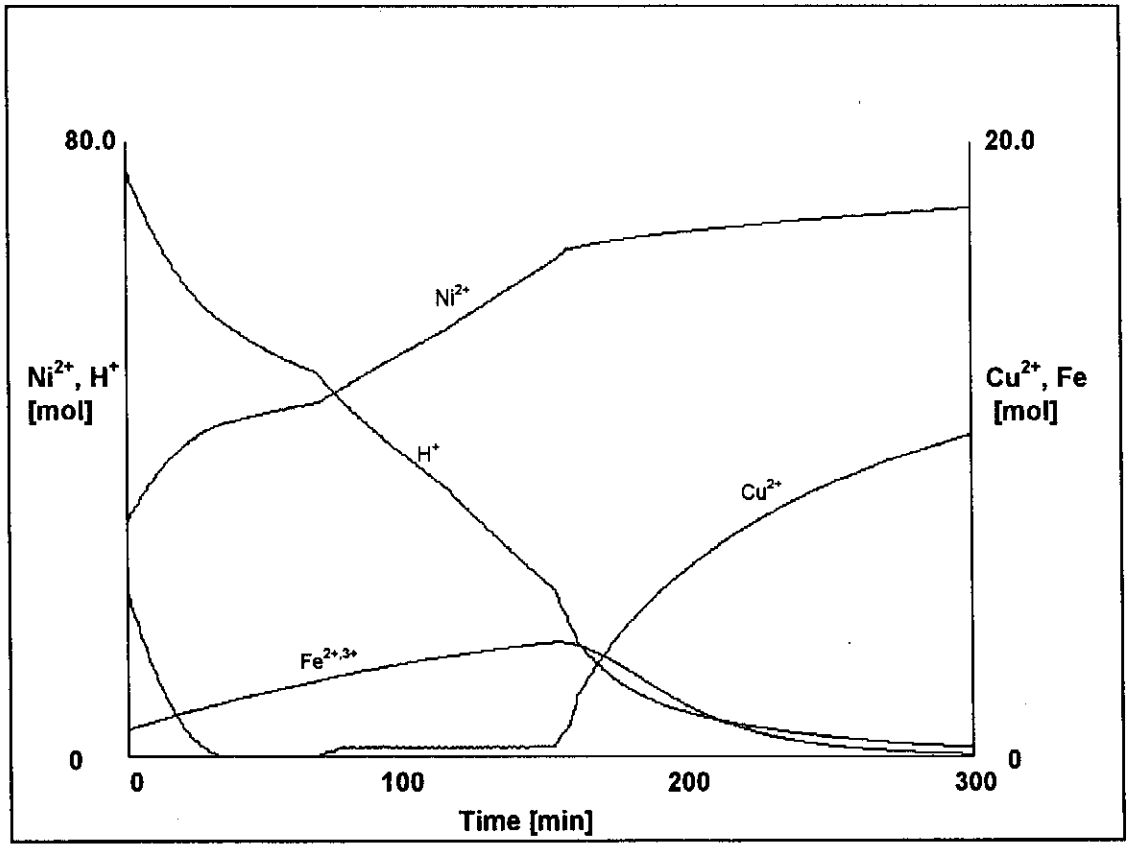

Figure 9.42 - Sensitivity analysis with the model for the reference values as indicated by Table 8.1 and with F_{O_2} = 0.59 kg/h, p_{O_2} = 1.8 bar and T_r = 140°C

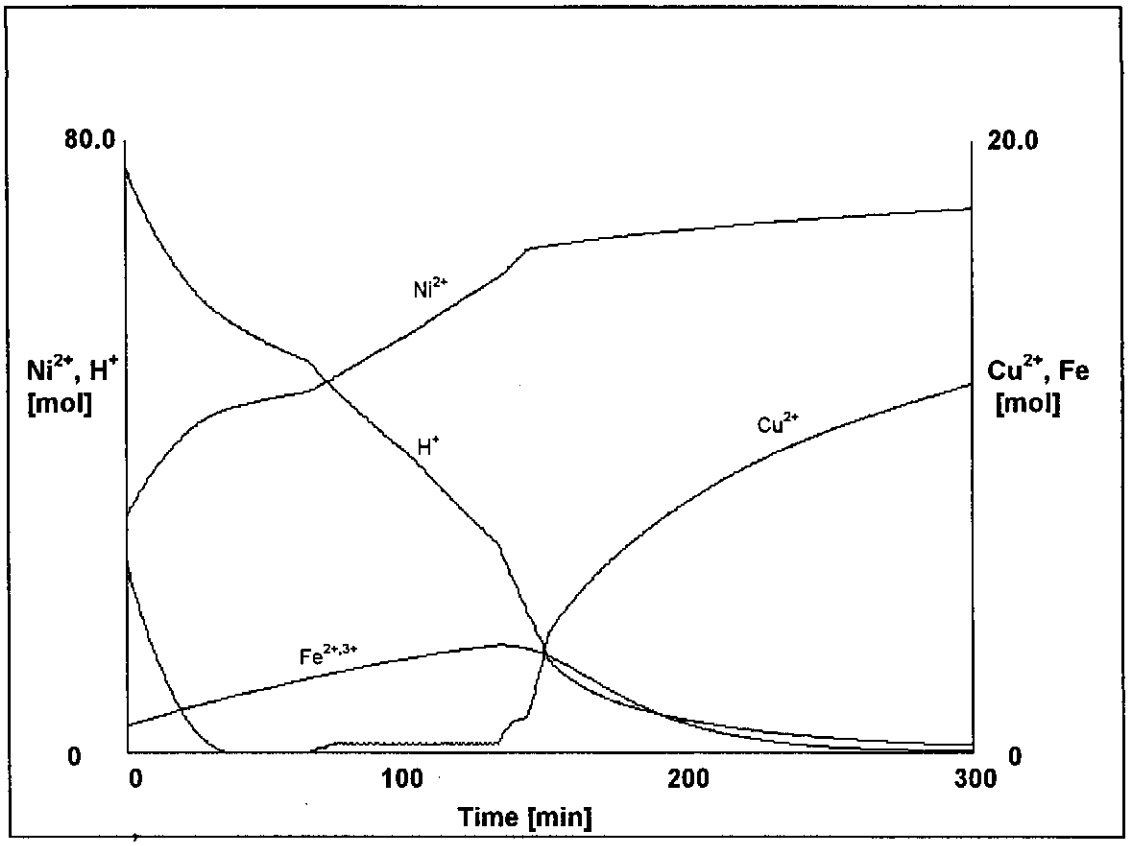

Figure 9.43 - Sensitivity analysis with the model for the higher initial copper concentration of 0.16 mol/L

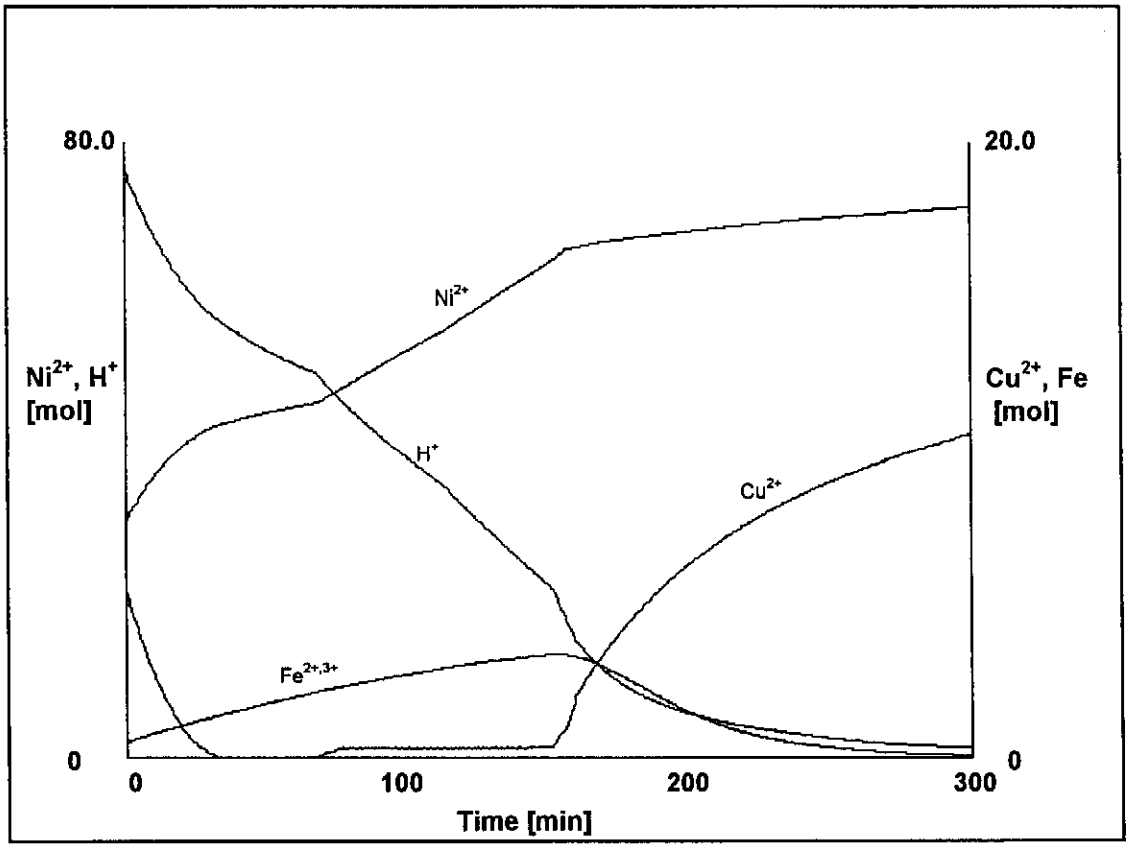

Figure 9.44 - Sensitivity analysis with the model for the lower initial iron concentration of 0.013 mol/L

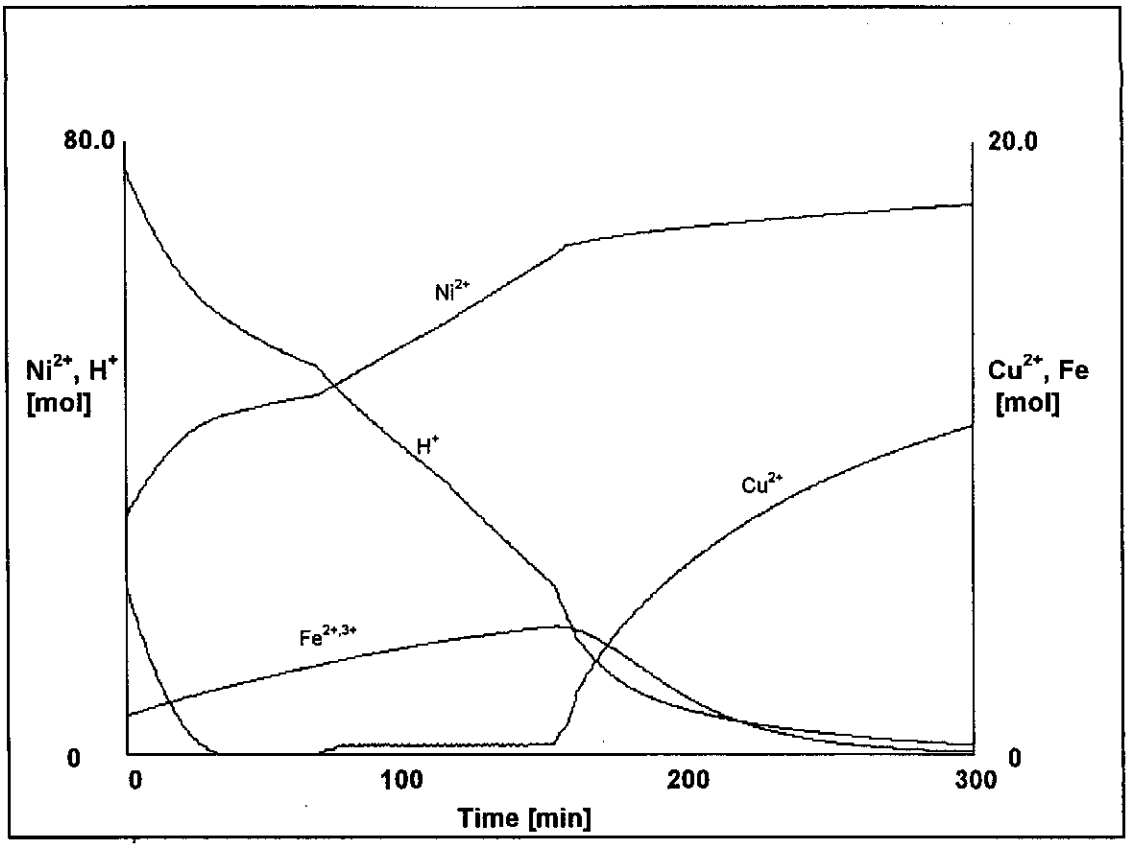

Figure 9.45 - Sensitivity analysis with the model for the higher initial iron concentration of 0.032 mol/L

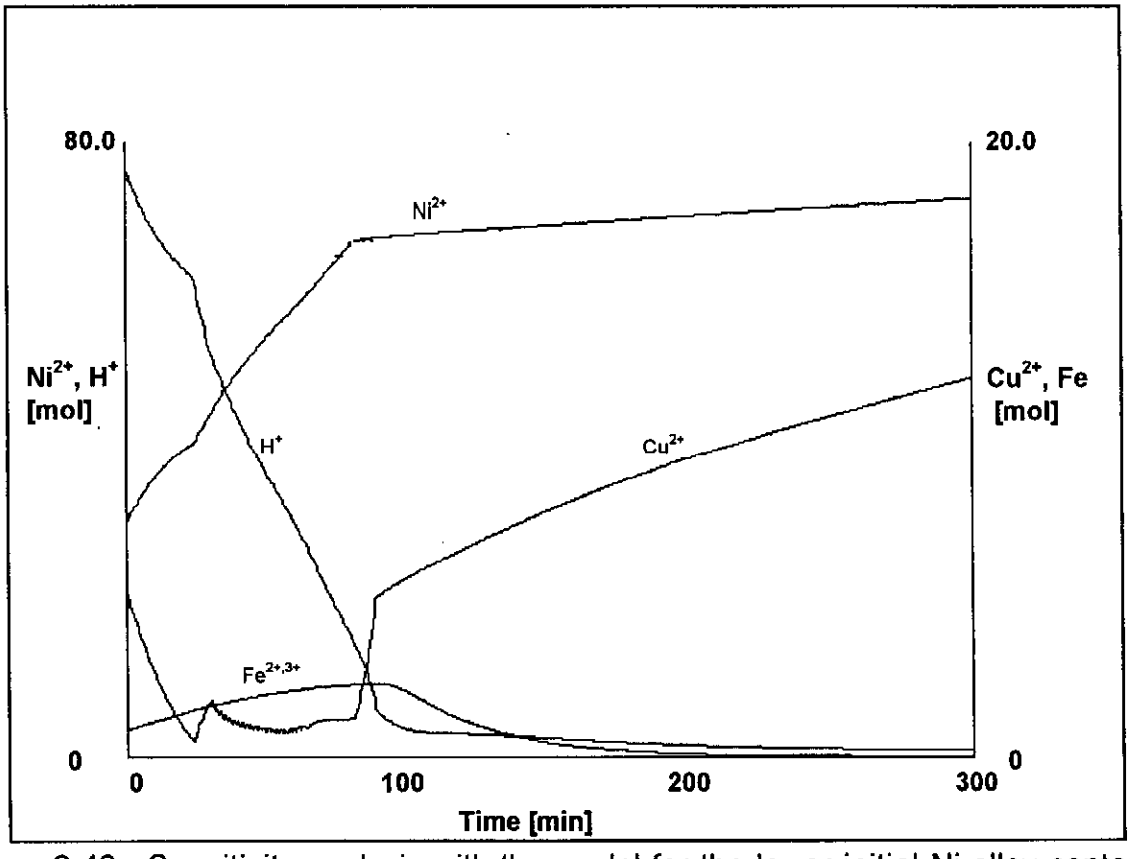

Figure 9.46 - Sensitivity analysis with the model for the lower initial Ni alloy content in the matte of 3.0 % (w/w)

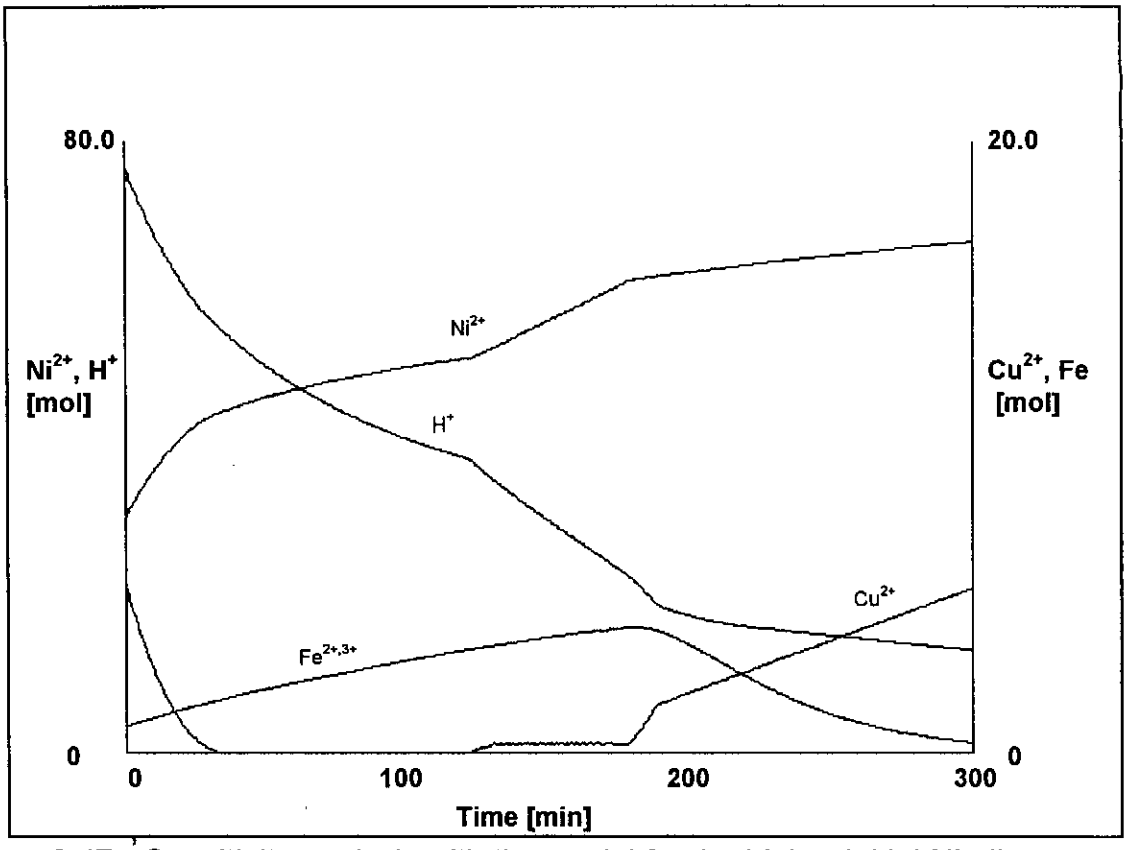

Figure 9.47 - Sensitivity analysis with the model for the higher initial Ni alloy content in the matte of 7.0 % (w/w)

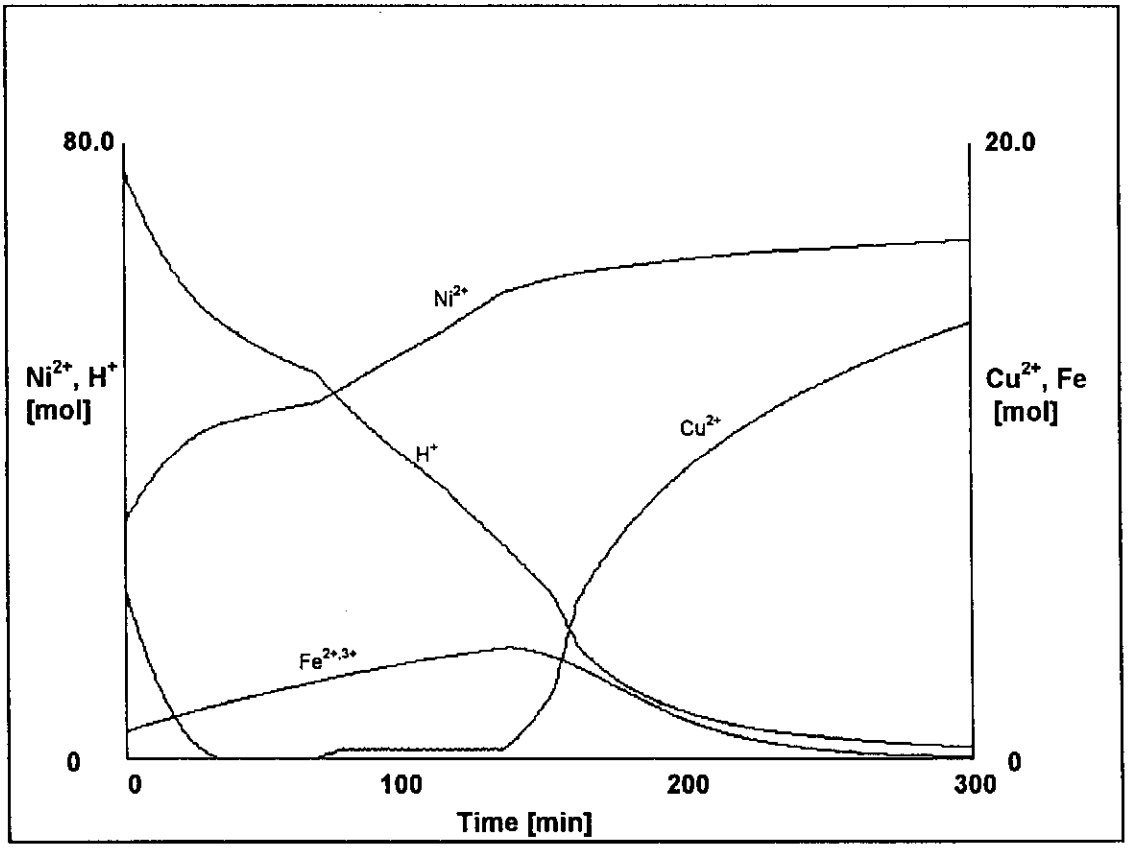

Figure 9.48 - Sensitivity analysis with the model for the lower initial Ni_3S_2 (40.4 %) content and the higher Cu_2S (46.9 %) content in the matte

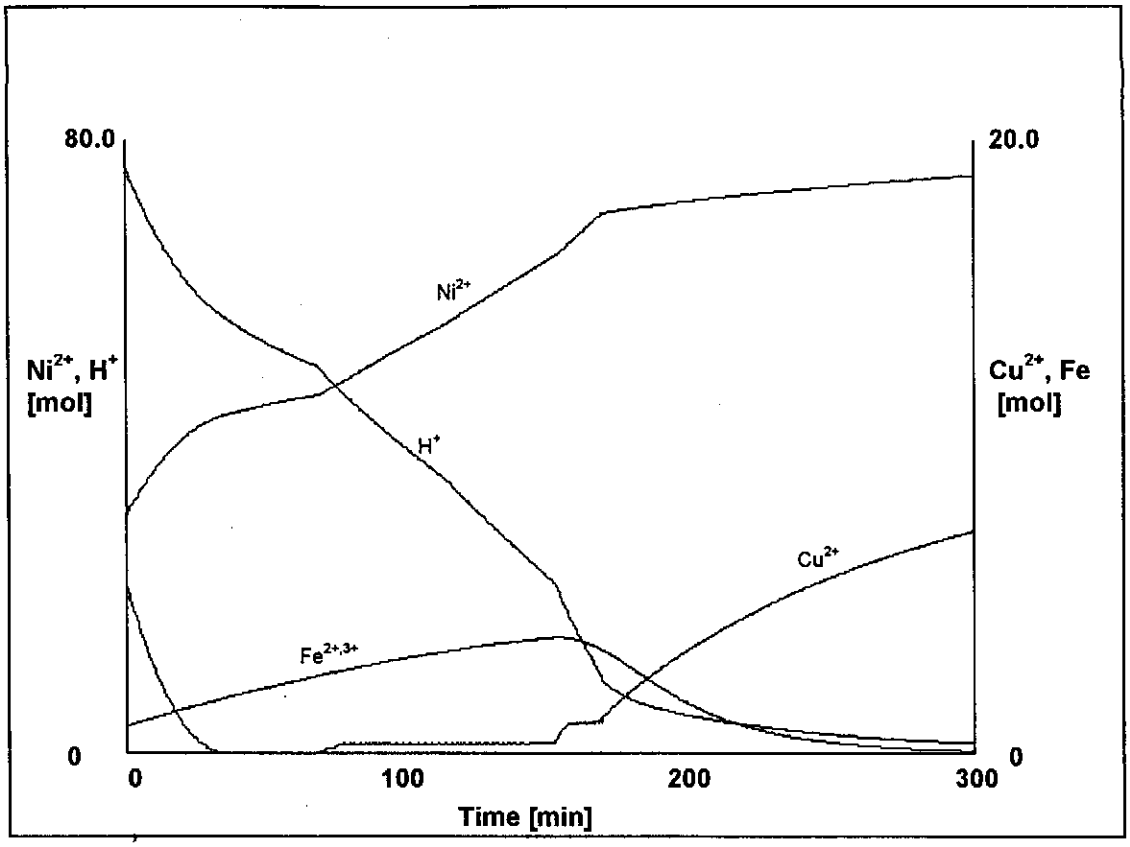

Figure 9.49 - Sensitivity analysis with the model for the higher initial Ni_3S_2 (50.4 %) content and the lower Cu_2S (36.9 %) content in the matte

Chapter 10

CONCLUSIONS

From the results presented in this dissertation it can be concluded that the control of the plant process can be improved with an off-line simulation program and that valuable knowledge can be obtained from the analysis of the historical data with artificial neural networks and inductive learning by decision trees. The intrinsic leaching mechanism of the reaction system is determined and a fundamental kinetic model is developed from the mechanism, that explains the behaviour of the leaching kinetics under different conditions.

10.1 CONCLUSIONS AND SIGNIFICANCE

1) The compiled off-line computer simulation program of the repulping (or preleach) section of the plant gives reasonable predictions of the pulp densities and tank levels of the actual process, in spite of the various practical problems (mainly the inaccurate settings of splitter box). Better and more accurate plant control can be obtained with the simulation program if more advanced control equipment are used and installed.

1.1) The calculation of the dynamic mass balances of the mathematical model for simulation purposes indicated that the numerical fourth order Runge-Kutta method, which incorporates the Golden Section search optimisation procedure, is better than the Laplace transformation calculations for this type of control. The Runge-Kutta method was chosen because it obtained the higher accuracy required for this specific control problem. The less accurate determination of the manipulated variables by the Laplace method is because this method inherently linearises around the steady state conditions of the process.

2) The learning vector quantization (LVQ) neural network, back propagation neural network (BPNN) and inductive decision tree process models developed from the historical data of the plant are able to classify the output concentrations of nickel, copper and iron of the plant autoclave accurately. The LVQ neural net models correctly classified the output concentrations for nickel, copper and iron at 79.6%, 82.0% and 75.4%, respectively. The back propagation neural net models classified the outputs for nickel, copper and iron at 76.3%, 84.1% and 77.9%, respectively. The inductive decision trees also obtained comparable classification results of 79.5% for nickel, 78.2% for copper and 74.7% for iron. These results from the three different modelling techniques are exceptionally good if it is taken into consideration that noisy plant data was used. The knowledge obtained from the different models can be compared and substantiated with each other, because all three these artificial intelligence techniques obtained good comparable classification results.

2.1) The LVQ neural network models were used to determine the relative importance of the different variables for each output and are substantiated by the *Chi square* test (χ^2 -test) employed by decision trees and the correlation coefficients.

2.2) The conventional statistical parameter, i.e. the mean (or average), is used in conjunction with the LVQ neural net models to quantify the influence of a specific variable on the process. The effect a variation of a specific variable has, is qualitatively determined by calculating the average of the specific variable for the high and low output concentrations (class), respectively, for nickel, copper and iron.

2.3) The most important variable in the process for the leaching of nickel, as determined by the process models, is the acid concentration of the spent electrolyte solution. The influence of the variation in acid concentrations indicated that for higher average acid concentrations (85 g/L in relation to 82

g/L) of the spent electrolyte solution a higher leaching efficiency of nickel is obtained.

2.4) The two most important variables in the determination of the copper concentration in the fourth compartment of the autoclave are the pH in this compartment and the copper concentration in the first compartment. A low pH (compartment no. 4) and a high copper concentration (compartment no. 1) in the autoclave produce a high concentration of copper.

2.5) The different modelling and data analysis techniques used constantly indicated that the tank levels (relative indication of residence time) and pulp densities of tanks 1506 and 1102 significantly influence the leaching performance of nickel, copper and iron in the autoclave. The reasons for these significant influences (tank levels and pulp densities) on the leaching performance of the process are due to the different conditions (temperatures and acid concentrations) existing in the two preleach tanks. Thus, for varying residence times (tank levels) and pulp densities in tank 1506 and 1102, the pulp stream entering the autoclave is of a varying composition. The short residence time (90 minutes) and the sensitive nature of the autoclave causes the inconsistent performance of the autoclave. This again confirms the need for control of the preleach or repulp section (conclusion 1).

2.6) The LVQ neural network models and the inductive learning by decision trees both have certain advantages for modelling and analysing ill-defined processes. Therefore, in general the choice of the technique that must be used will depend on what type of information is needed of the process. Decision trees should be used when easy interpretable rules are required of the process, so that the operator can have an indication of the type of control action that must be taken (increase or decrease flowrate, etc.). LVQ neural network models (together with the statistical mean) should be used to obtain a more detailed investigation of the influence of the different parameters on the efficiency of the process, so that the operating conditions of the process could be adjusted to improve the efficiency of the process.

3) The leaching sequence of the nickel sulphides and copper sulphides (as the leaching process continues) is as follows: Ni_3S_2-Ni_7S_6-NiS-Ni_3S_4, and Cu_2S-$Cu_{31}S_{16}$-$Cu_{1.8}S$-CuS, respectively. Ni_7S_6 and $Cu_{31}S_{16}$ are intermediate nickel and copper sulphide products that form during the leaching process.

3.1) The reaction mechanism developed for the leaching of Ni-Cu matte is very complex, with the interaction of the various mineral species influencing the kinetics of the leaching process. It was determined that in the leaching of the mineral species basic crystallographic rules exist by which the crystal structure and mineral species are modified in the leaching process. These two rules are, that (i) the mineral with the crystal structure with the higher degree of symmetry will preferentially form and is more stable, therefore, a lower free energy for formation (more resistant to the leaching process), and (ii) the sequence of the mineral species (with sulphide lattices) present in the leaching process are determined by the specific gravity of the mineral (indirectly meaning the concentration of the metal cations present in the sulphide lattice). Therefore, a lower specific gravity of the mineral in the leaching process (from its initial specific gravity), indicates that the mineral has undergone leaching.

3.2) The reactions proposed for the complex leaching mechanism in Chapter 7 are substantiated by the comparable values obtained by the analytical results and by the mole balances (for the mole increase or decrease according to the stoichiometry of the reactions of the mineral species and the acid, nickel and copper concentrations, see Appendix F).

3.3) The leaching mechanism is divided into three stages, i.e. stage I - the cementation of copper and the leaching of nickel from the alloy phase and out of the Ni_3S_2 phase, stage II - the selective leaching of nickel to form various Ni-S mineral phases and the simultaneous leaching and cementation of copper to form the various Cu-S mineral phases, and stage III - the simultaneous leaching of nickel (to form NiS and Ni_3S_4) and copper (to form CuS). Depending on the reaction conditions, the leaching rate in the different stages varies.

3.4) The fast leaching kinetics of the Ni alloy phase could be ascribed to the galvanic couple that exists between the nickel metal and the nickel and copper sulphides (nickel metal has a lower rest potential than the nickel and copper sulphides).

3.5) Sequential scanning electron microscope (SEM) photographs of the leaching process indicated that the matte particle systematically leaches to a porous state and eventually to crumbly particles. This occurs because of the fast leaching rate of the Ni alloy out of the Ni_3S_2 matrix. Ni alloy occurs in the Ni_3S_2 matrix as small inclusions, randomly distributed throughout the particle. As the nickel is leached the pores are formed. This is the basis for the assumption that the particle leaching kinetics are chemically controlled with negligible surface area, film diffusion or pore diffusion (for the plant particle size distribution). Copper in the solution is initially cemented as Cu_2S on the surface of the particles. Therefore, for larger particle size fractions (effectively less surface area) the leaching rate of nickel and the cementation rate of copper are reduced, due to the decrease in the effective surface area. This implies that for larger particle size fractions (greater than the plant particle size distribution mentioned in this dissertation) the surface area influences the leaching kinetics.

3.6) The reason for the selective leaching of nickel into the solution during the initial stages of the leaching process is that the copper leached by H_2SO_4 and O_2, is cemented (with fast reaction kinetics) by Ni alloy and Ni_3S_2. Therefore, the copper will stay cemented in the solid phase as long as either Ni alloy or Ni_3S_2 is still present in the matte.

3.7) H_2S formation occurs even under oxidising conditions (oxygen partial pressure of 1.8 bar) if the initial acid concentration of the spent electrolyte is higher than approximately 90 g/L. H_2S inhibits the leaching rate and leads to the formation of the intermediate mineral products of Ni_7S_6 and $Cu_{31}S_{16}$. H_2S is formed when the copper concentration in the solution becomes low, resulting in the incomplete reaction of copper with mostly Ni alloy, and to some extent Ni_3S_2. Therefore, H_2S occurs in systems where the initial acid concentration is

high and Ni alloy is still present when the copper in solution has been depleted.

3.8) Iron acts as an electron carrier and the precipitation of iron to form, either jarosite or haematite, releases acid into the solution, creating conditions for the reactions to continue.

4) The proposed semi-emperical kinetic model of the batch leach process, based on the chemical reaction rate expressions, is shown to accurately describe the leaching and formation of the various mineral species, as well as the trends in the nickel, copper, total iron and acid content in the solution phase and the nickel, copper and total sulphur content in the solid phase.

4.1) In the kinetic model a shrinking core mechanism was used in describing the pore forming effect due to the leaching of Ni alloy. The effects of variations in the oxygen partial pressure, oxygen flowrate, temperature, average particle size and the initial acid concentration were incorporated in the kinetic model. It was evident that for a lower oxygen partial pressure (less than 1.8 bar) the leaching kinetics are not influenced to the same extent as for higher oxygen partial pressures. The same effect on the leaching rate is observed for variations in the oxygen flowrate (oxygen mass transfer) and oxygen partial pressure (oxygen equilibrium solubility), although it is with two different mechanisms. Therefore in the semi-emperical model it is justifiable to incorporate the oxygen flowrate as a scaled factor in the oxygen partial pressure. The temperature effects are accurately modelled by using Arrhenius' law. An area factor relating the initial average particle size to the reference average particle size is used in the model to account for the variation in the particle size fractions. It is also concluded that for different initial acid concentrations different leaching rate constants and therefore, kinetics exists. For higher initial acid concentrations (assumed to be > 0.92 mol/L or 90 g/L H_2SO_4) the leaching rate is slower due to the formation of H_2S than for a lower initial acid concentration where the acid concentration is too low for the formation of H_2S under the present oxidising conditions.

4.2) An increase in the oxygen flowrate increases the reaction rate of the leaching mechanism (stages I - III), increasing the acid consumption rate and the rate of nickel leaching significantly, and simultaneously shortening the time that copper stays cemented in the solid phase. It is therefore evident that the optimum oxygen flowrate for the plant will be approximately 0.96 kg/h per 40 L of pulp to obtain effective leaching of nickel while keeping copper cemented. Results from the analysis of the plant data (with the artificial intelligence techniques and statistical calculations) substantiated this observation.

4.3) Exactly the same effects are noticed for the variation in the oxygen partial pressure as for the variation in the oxygen flowrate (a higher oxygen partial pressure has the same effect as a higher oxygen flowrate and *vice versa*). The analysis of the plant data substantiated these findings. For a higher pressure in the autoclave more nickel is leached and less copper is present in the fourth compartment of the autoclave. The reason for the lower copper concentration obtained for a higher pressure in the plant is that the residence time of the autoclave (effectively 90 minutes) is less than that of the experimental autoclave and the range of pressures in the plant varies from 4.5 bar to 6.5 bar (maximum oxygen partial pressure of 2.9 bar). If these factors are taken into consideration the results compare with the experimental findings.

4.4) It was found that at a lower temperature of 120°C (in relation to 140°C) the initial reaction rate (for the leaching of nickel and consumption of acid) of the leaching process is faster, but the cementation of copper is slower, therefore, less H_2S is formed (see conclusion 3.7). The copper also starts to leach earlier at this lower temperature, because less intermediate products, i.e. Ni_7S_6 and $Cu_{31}S_{16}$ are formed that will galvanically inhibit the leaching of copper, as well as the fact that Ni_3S_2 is leached out of the solid phase more quickly (higher initial leaching kinetics).

4.5) For smaller particle size fractions the leaching of nickel is faster, resulting in less acid being available for the copper to leach, therefore, less copper is leached. The model indicated that for larger particle size fractions the Ni alloy

is not leached out to such an extent that a uniform porosity is created (see conclusion 3.5). The kinetic model also showed that the variation in the initial average particle size of the matte can be incorporated in the model using an area factor based on the initial average particle size (for average particle sizes less than 120.3 μm).

4.6) It was determined that higher initial acid concentrations (> 0.92 mol/L) lead to slower initial reaction kinetics. This is substantiated by the results from the learning vector quantization (LVQ) neural network model (plant data analysis), which indicated that for high average acid concentrations in the spent electrolyte (approximately 100 g/L) nickel is not leached effectively (see Chapter 9).

4.7) For a lower pulp density of 1.30 kg/L, less H_2S is formed (which is the opposite of the expected result because of the higher acid content in the solution), because the ratio of copper in solution to the solids is higher for a lower pulp density. Therefore, while copper is still present in the solution the reaction for the formation of H_2S will not occur (see conclusion 3.7). For lower pulp densities the initial cementation of copper is slower, but leaching of copper starts earlier due to the initial faster leaching kinetics (leaching of nickel and acid consumption, thus, Ni_3S_2 is consumed faster).

5) The sensitivity analyses with the kinetic model indicated that for lower initial Ni alloy content in the matte the leaching rate of nickel is much faster and the subsequent leaching of copper will start earlier. Therefore, the inhibiting effect (possible galvanic effect and H_2S formation) that Ni alloy has on the reaction is illustrated by the model. The less Ni alloy present, the faster the overall leaching kinetics will be.

10.2 RECOMMENDATIONS

10.2.1 Practical implementation

1) The computer simulation program for the preleach (repulping) section of the plant should be used as an off-line tool to help the operator to control the tank levels and pulp densities of this section. The importance of controlling the tank levels and pulp densities is clearly shown in this dissertation.

2) As a first step the control of the process can be improved by using the knowledge obtained in this study to develop a knowledge base (KBS) or expert system, that (i) can indicate to the operator what control action he must take during certain situations on the plant, and (ii) at the same time the control procedures are standardised for the different operators (control the process on the same principles).

3) The kinetic model developed for the batch experiments must be converted to a continuous model which can be tested on the plant to evaluate its performance. If the performance is satisfactory this model can be incorporated in the expert (fuzzy logic) or knowledge base (KBS) system to develop a complete control system that takes the practical variations qualitatively into account with the knowledge base. The fundamental reaction kinetic aspect is then accounted for in the control system by the kinetic model.

10.2.2 Future research

4) The effect that the initial acid and copper concentrations have on the formation of H_2S and the inhibiting effect thereof, should be investigated further to quantify this behaviour in the leaching process.

5) The galvanic effects of the various nickel and copper sulphide mineral species on each other should be determined and quantified, if possible, to obtain a more complete understanding of the interaction of these mineral

phases with each other. The first step could be to undertake a complete electrochemical study of the leaching process.

6) The semi-emperical model can be improved to a more fundamental model by incorporating the intrinsic rate determining effects more fundamentally, such as mass transfer, in the model and possibly by including redox potentials.

REFERENCES

Bakshi, B.R. and Stephanopoulos, G., 1994, Representation of Process Trends - IV. Induction of Real-Time Patterns from Operating Data for Diagnosis and Supervisory Control, *Computers and Chemical Engineering*, **18**(4), 303-332.

Barriga Mateos, F., Palencia Pérez, I. and Carranza Mora, F., 1987, The passivation of chalcopyrite subjected to ferric sulphate leaching and its reactivation with metal sulphides, *Hydrometallurgy*, **19**, 159-167.

Bhat, N. and McAvoy, T.J., 1990, Use of Neural Nets for Dynamic Modeling and Control of Chemical Process Systems, *Computers and Chemical Engineering*, **14**(4/5), 573-583.

Boldt, J.R., jr., 1967, The Winning of Nickel - Its Geology, Mining, and Extractive Metallurgy, Methuen and Co. Ltd, 487 pages.

Bratko, I., 1993, Machine learning in artificial intelligence, *Artificial Intelligence in Engineering*, **8**, 159-164.

Brugman, C.F. and Kerfoot, D.G., 1986, Treatment of Nickel-Copper Matte at Western Platinum by the Sherritt Acid Leach Process, *C.I.M.*, Proceedings of Nickel Metallurgy, **1**, 512-531.

Burkin, A.R., 1966, The Chemistry of Hydrometallurgical Processes, E. & F. N. Spon Ltd., London, 157 pages.

Chen, H., Fu, C. and Zheng, D., 1992, Reduction leaching of manganese nodules by nickel matte in hydrochloric acid solution, *Hydrometallurgy*, **28**, 269-275.

Chitra, S.P., 1993, Use Neural Networks for Problem Solving, *Chemical Engineering Progress*, **89**(4), 44-52.

Chmielewski, T. and Charewicz, W.A., 1984, The oxidation of Fe(II) in aqueous sulphuric acid under oxygen pressure, *Hydrometallurgy*, **12**, 21-30.

Chu Yong Cheng and Lawson, F., 1991a, The kinetics of leaching chalcocite in acidic oxygenated sulphate-chloride solutions, *Hydrometallurgy*, **27**, 249-268.

Chu Yong Cheng and Lawson, F., 1991b, The kinetics of leaching covelite in acidic oxygenated sulphate-chloride solutions, *Hydrometallurgy*, **27**, 269-284.

Dobrokhotov, G.N., 1959, Chemistry of acid autoclave leaching of the monosulphides of nickel, cobalt and iron, *Journal of Applied Chemistry USSR*, **32**, 775-789.

Dry, M.J. and Bryson, A.W., 1987, Kinetics of leaching of a low-grade Fe-Ni-Cu-Co matte in ferric sulphate solution, *Hydrometallurgy*, **18**, 155-181.

Dutrizac, J.E. and Chen, T.T., 1987, A mineralogical study of the phases formed during the $CuSO_4$-H_2SO_4-O_2 leaching of nickel-copper matte, *Canadian Metallurgical Quarterly*, **26**, 265-276.

Dutrizac, J.E. and MacDonald, R.J.C., 1973, The effect of some impurities on the rate of chalcopyrite dissolution, *Canadian Metallurgical Quarterly*, **12**(4), 409.

Dutrizac, J.E. and MacDonald, R.J.C., 1974, Ferric ion as a leaching medium, *Minerals Science and Engineering*, **6**(2), 59-100.

Edgar, T.F. and Himmelblau, D.M., 1989, Optimization of Chemical Processes, McGraw-Hill Book Company, 171-175.

Fleet, M.E., 1977, The crystal structure of heazlewoodite, and metallic bonds in the sulfide minerals, *American Mineralogist*, **62**, 341-345.

Frye, K., 1974, Modern Mineralogy, Prentice-Hall, Inc., New Jersey, 1-51 & 153-170.

Gerald, C.F. and Wheatley, P.O., 1984, Applied Numerical Analysis, Third edition, Addison-Wesley, 299-333.

Grewal, I., Dreisinger, D.B., Krueger, D., Tyroler, P.M., Krause, E. and Nissen, N.C., 1992, Total oxidative leaching of Cu_2S-containing residue at INCO Ltd.'s copper refinery: laboratory studies on the reaction pathways, *Hydrometallurgy*, **29**, 319-333.

Habashi, F., 1992, A Textbook of Hydrometallurgy, Métallurgie Extractive Québec, Enr., Québec, 689 pages.

Haung, H.-H. and Bernal, J.E., 1984, Kinetic study on direct leaching of sphalerite in sulphuric acid solution using ferrous sulphate as the catalyst, Electrochemistry in Mineral and Metal processing (*Proceedings of the International Symposium*), Richardson, P.E., Srinivasan, S. and Woods, R. (Eds.), The Electrochemical Society, Inc., 469-485.

Hinton, G.E., 1992, How Neural Networks Learn from Experience, *Scientific American*, **267**(3), 105-127.

Hochreiter, R.C., Kennedy, D.C., Muir, W. and Wood, A.I., 1985, Platinum in South Africa (Metals Review Series no. 3), *Journal of the South African Institute of Mining and Metallurgy*, **85**, 165-185.

Hofirek, Z. and Kerfoot, D.G.E., 1992, The chemistry of the nickel-copper matte leach and its application to process control and optimisation, *Hydrometallurgy*, **29**, 357-381.

Hong-Te Su, McAvoy, T.J. and Werbos, P., 1992, Long-Term Prediction of Chemical Processes Using Recurrent Neural Networks: A Parallel Training Approach, *Industrial and Engineering Chemistry Research*, **31**, 1338-1352.

Hoskins, J.C. and Himmelblau, D.M., 1992, Process control via artificial neural networks and reinforcement learning, *Computers and Chemical Engineering*, **16**(4), 241-251.

Kanome, O., Abe, H., Okuwaki, A. and Okabe, T., 1987, Sulphuric acid oxygen-pressure leaching of Ni_3S_2 prepared by a wet process, *Hydrometallurgy*, **19**, 1-9.

Karim, M.N. and Rivera, S.L., 1992, Comparison of Feed-Forward and Recurrent Neural Networks for Bioprocess State Estimation, *European Symposium on Computer Aided Process Engineering-1*, ESCAPE-1 (Supplement to Computers & Chemical Engineering), Elsinore, Denmark, S369-S377.

Kattan, M., 1994, Inductive Expert Systems vs. Human Experts, *AI Expert*, 32-38.

Kramer, M.A. and Leonard, J.A., 1990, Diagnosis Using Backpropagation Neural Networks - Analysis and Criticism, *Computers and Chemical Engineering*, **14**(12) (1990), 1323-1338.

Kullerud, G. and Yund, R.A., 1962, The Ni-S System and Related Minerals, *Journal of Petrology*, **3**(1), 126-175.

Levenspiel, O., 1972, Chemical Reaction Engineering, Second edition, John Wiley & Sons, New York, 1-34 & 349-400.

Lippmann, R.P., 1987, An Introduction to Computing with Neural Nets, IEEE *ASSP Magazine*, **35**, 4-22.

Lippmann, R.P., 1989, Pattern classification using neural networks, IEEE *Communications Magazine*, **35**, 4-21.

Llanos, Z.R., Queneau, P.B. and Rickard, R.S., 1974, Atmospheric leaching of matte at the Port Nickel Refinery, *CIM Bulletin*, **67**, 74-81.

Lourens, E., 1993, Mineralogical investigation of NCR Process Stream Samples, Report no. R30/93-ICR25, Project no. DL1895 and DL1969, GENCOR Laboratories, Mineralogical Department (Confidential), 12.

Ma, Z. and Ek, C., 1991, Rate processes and mathematical modelling of the acid leaching of a manganese carbonate ore, *Hydrometallurgy*, **27**, 125-139.

Mao, M.H. and Peters, E., 1982, Acid pressure leaching of chalcocite, Hydrometallurgy - Research, Development and Plant Practice, Osse-Asare, K. and Miller, J.D. (Eds.), The Metallurgical Society of AIME, 243-260.

Maren, A., Harston, C.T. and Pap, R.M., 1990, Handbook of Neural Computing Applications, Academic Press, 448 pages.

Mehta, A.P. and Murr, L.E., 1983, Fundamental studies of the contribution of galvanic interaction to acid-bacterial leaching of mixed metal sulphides, *Hydrometallurgy*, **9**, 235-256.

Moolman, D.W., Aldrich, C. and Van Deventer, J.S.J., 1995, The videographic characterization of flotation froths using neural networks, *Neural Networks for Chemical Engineers*, Ed. A. B. Bulsari, Elsevier Science B.V., Amsterdam, 525-545.

Mulak, W., 1985, Kinetics of dissolution of synthetic heazlewoodite (Ni_3S_2) in nitric acid solutions, *Hydrometallurgy*, **14**, 67-81.

Mulak, W., 1987, The catalytic action of cupric and ferric ions in nitric acid leaching of Ni_3S_2, *Hydrometallurgy*, **17**, 201-214.

Mulak, W., 1992, Kinetics of dissolution of Ni_3S_2 in acidic potassium dichromate solutions, *Hydrometallurgy*, **28**, 309-322.

Náray-Szabó, I., 1969, Inorganic Crystal Chemistry, Akadémiai Kiadó, Budapest, 46-186.

Narita, E., Lawson, F. and Han, K.N., 1983, Solubility of oxygen in aqueous electrolyte solutions, *Hydrometallurgy*, **10**, 21-37.

Nicol, J.N., 1984, An electrochemical study of the interaction of copper(II) ions with sulphide minerals, Electrochemistry in Mineral and Metal processing (*Proceedings of the International Symposium*), Richardson, P.E., Srinivasan, S. and Woods, R. (Eds.), The Electrochemical Society, Inc., 152-168.

Nuffield, E.W., 1966, X-Ray Diffraction Methods, John Wiley & Sons, Inc., New York, 1-86 & 137-147.

Pandit, S.M. and Wu, S-M., 1983, Time Series and System Analysis with Applications, John Wiley and Sons, New York, 1-4, 112-115.

Papangelakis, V.G. and Demopoulos, G.P., 1991, Acid pressure oxidation of pyrite: reaction kinetics, *Hydrometallurgy*, **26**, 309-325.

Pawlek, F., 1969, Research in pressure leaching, *Journal of the South African Institute of Mining and Metallurgy*, **69**, 632-654.

Peters, E., 1984, Electrochemical mechanisms for decomposing sulphide minerals, Electrochemistry in Mineral and Metal processing (Proceedings of the International Symposium), Richardson, P.E., Srinivasan, S. and Woods, R. (Eds.), The Electrochemical Society, Inc., 343-361.

Plasket, R.P. and Dunn, G.M., 1986, Iron rejection and impurity removal from nickel leach liquor at Impala Platinum Limited, *Iron Control In Hydrometallurgy*, Symposium in Toronto, Canada, 695-718.

Plasket, R.P. and Romanchuk, S., 1978, Recovery of Nickel and Copper from high-grade matte at Impala Platinum by the Sherritt Process, *Hydrometallurgy*, **3**, 135-151.

Quinlan, J.R., 1986, Induction of decision trees, *Machine Learning*, **1**, 81-106.

Quinlan, J.R., 1990, Decision Trees and Decisionmaking, IEEE *Transactions on Systems, Man, and Cybernetics*, **20**(2), 339-346.

Rademan, J.A.M., Lorenzen, L. and Van Deventer, J.S.J., 1995, An off-line computer simulation for controlling the repulp section in a plant, *Minerals Engineering*, **8**(6), 679-696.

Rao, C.N.R. and Rao, K.J., 1978, Phase Transitions in Solids, McGraw-Hill Inc., 1-80.

Rao, S.R. and Finch, J.A., 1987, Galvanic interaction studies on sulphide minerals, *Canadian Metallurgical Quarterly*, **27**(4), 253-259.

Reuter, M.A., Van der Walt, T.J. and Van Deventer, J.S.J., 1992, Modeling of Metal-Slag Equilibrium Processes Using Neural Nets, *Metallurgical Transactions B*, **23B**, 643-650.

Shieh, D. S.-S. and Joseph, B., 1992, Exploratory data analysis using inductive partitioning and regression trees, *Industrial and Engineering Chemistry Research*, **31**, 1989-1998.

Sinkankas, J., 1966, Mineralogy: A first course, D. van Nostrand Company, Inc., Princeton, New Jersey, 1-56 & 157-192.

Snyder, R.L. and Bish, D.L., 1989, Modern Powder Diffraction, Reviews in Mineralogy, **20**, Bish, D.L. and Post, J.E. (Eds.), The Mineralogical Society of America, Washington, 101-144.

Stephanopoulos, G., 1984, Chemical Process Control: An Introduction to Theory and Practice, Prentice-Hall International, 1-79 & 128-158.

Subrahmanyam, T.V. and Forssberg, K.S.E., 1993, Mineral solution-interface chemistry in minerals engineering, *Minerals Engineering*, **6**(5), 439-454.

Symens, R.D., Queneau, P.B., Chou, E.C. and Clark, F.F., 1979, Leaching of Iron-containing Copper-Nickel Matte at Atmospheric Pressure, *Canadian Metallurgical Quaterly*, **18**, 145-153.

Van der Walt, T.J. and Van Deventer, J.S.J., 1992, The simulation of ill-defined metallurgical processes using a neural net training program based on conjugate-gradient optimization, *IFAC Workshop on Expert Systems in Mineral and Metal Processing*, Helsinki University of Technology, Espoo, Finland, 26-28 August.

Van der Walt, T.J., Van Deventer, J.S.J. and Barnard, E., 1992, The Dynamic Modeling of Ill-defined Processing Operations Using Connectionist Networks, *Chemical Engineering Science*, **28**(11), 1945-1958.

Verbaan, B. and Crundwell, F.K., 1986, An electrochemical model for the leaching of a sphalerite concentrate, *Hydrometallurgy*, **16**, 345-359.

Veltman, H. and Robert Weir, D., 1981, Sherritt Gordon's pressure leaching technology - its industrial application, *Hydrometallurgy 81, Proceedings of a Society of Chemical Industry symposium*, University of Manchester Institute of Science and Technology, Manchester, England, London, ^{B1}/1 - ^{B1}/13.

Walpole, R.E. and Myers, R.H., 1989, Probability and Statistics for Engineers and Scientists, Fourth edition, New York, 79-104 & 391-397.

Wasserman, P.D., 1989, Neural Computing - Theory and Practice, Van Nostrand Reinhold, New York, 230 pages.

Yester, M., 1991, Using Turbo Pascal 6.0, Second edition, Que Corporation, 896 pages.

Neural Computing, 1993, Neural Computing - A technology handbook for Professional II/PLUS and NeuralWorks Explorer, NeuralWare, Pittsburgh, 181 pages.

NOMENCLATURE

$a_s^c, b_s^c, \ldots, r_s^c$	stoichiometric constants of the different reactions in relation to the reactant mineral species [-]
a^k	upper boundary of the interval in the k'th stage of the golden section search [-]
A_s	the area factor for the variation in the average particle size in the kinetic model [-]
b^k	lower boundary of the interval in the k'th stage of the golden section search [-]
C_1	iteration limit (tank 1506) for Golden Section Search procedure [-]
C_2	iteration limit (tank 1102) for Golden Section Search procedure [-]
C_{i,H_2SO_4}	the initial acid concentration [mol/L]
cov(X,Y)	covariance between X and Y in determining the correlation coefficients [-]
C_s	concentration of the reactant species *s* in solution [mol/L]
$[Cu]_i$	concentration of copper in the i'th compartment of the autoclave [g/L]
$d_{p,i}$	the average particle size diameter for the i'th size fraction [μm]
E	information entropy [-]
$E_{a,i}$	the activation energy for the i'th reaction [kJ/mol]
F_1	volumetric flowrate of spent electrolyte solution to tank 1506 [L/min]
F_2	volumetric flowrate of pulp from tank 1506 to tank 1102 [L/min]
F_3	volumetric flowrate of pulp from the mill to tank 1506 [L/min]
F_4	volumetric flowrate of recycled solids to tank 1506 [L/min]
F_5	volumetric flowrate of spent electrolyte solution used to wash the recycled solids into tank 1506 [L/min]
F_6	volumetric flowrate of spent electrolyte to tank 1102 [L/min]
F_7	volumetric flowrate of pulp from tank 1102 to the autoclave [L/min]
F_{1MIN}	minimum volumetric flowrate of spent electrolyte solution to tank 1506 [L/min]

F_{1MAX} maximum volumetric flowrate of spent electrolyte solution to tank 1506 [L/min]

F_{2MIN} minimum volumetric flowrate of pulp from tank 1506 to tank 1102 [L/min]

F_{2MAX} maximum volumetric flowrate of pulp from tank 1506 to tank 1102 [L/min]

F_{6MIN} minimum volumetric flowrate of spent electrolyte solution to tank 1102 [L/min]

F_{6MAX} maximum volumetric flowrate of spent electrolyte solution to tank 1102 [L/min]

F_{Acid} volumetric flowrate of spent electrolyte solution to the autoclave [L/min]

$[Fe]_4$ concentration of iron in the 4th compartment of the autoclave [g/L]

F_M matte feedrate to the mill [t/h]

F_{O_2} mass flowrate of oxygen (kinetic model) [kg/h]

F_{ox} mass flowrate of oxygen to the autoclave [kg/h]

F_W Demineralised water flowrate to the mill [L/min]

h pulp level in tank 1506 [%]

h_1 pulp level in tank 1102 [%]

$[H_2SO_4]$ acid concentration of spent electrolyte solution [g/L]

k_i reaction rate constant for the i'th reaction [mol^a.L^b.min^{-1}]*

k_i' pseudo reaction rate constant for the i'th reaction [mol^a.L^b.min^{-1}]*

k_i^0 the frequency factor for the i'th reaction in the Arrhenius equation [mol^a.L^b.min^{-1}]*

$k_i^{0,A}$ the combined frequency factor and reaction rate constant for the i'th reaction for high (A=H) and low (A=L) initial acid concentrations [mol^a.L^b.min^{-1}]*

k_i^A reaction rate constant for the i'th reaction for high (A=H) and low (A=L) initial acid concentrations [mol^a.L^b.min^{-1}]*

L^k any particular interval in the k'th stage of the golden section search [-]

n^- the probability of a negative instance of a class given a certain set of attribute values [-]

$[Ni]_4$ concentration of nickel in the 4th compartment of the autoclave [g/L]

N_s mole quantity of species s [mol]

p^+	the probability of a positive instance of a class given a certain set of attribute values [-]
p_1	pressure in compartment no 1 of autoclave [kPa]
$P_{1,5,6}$	pulp density of the spent electrolyte solution [kg/L]
P_2	pulp density in tank 1506 [kg/L]
P_3	desired pulp density of the mixture leaving the mill [kg/L]
P_4	pulp density of the recycled solids to tank 1506 [kg/L]
P_7	pulp density in tank 1102 [kg/L]
$p_{O_2}^C$	the calculated oxygen partial pressure [bar]
$p_{O_2}^F$	the equivalent oxygen partial pressure of the oxygen flowrate [bar]
pH_i	pH of pulp in the i'th compartment of the autoclave [-]
P_M	density of the matte [kg/L]
p_{O_2}	oxygen partial pressure [bar]
$p_{O_2}^P$	the modified actual partial pressure [bar]
P_r	pulp density of the reaction mixture [kg/L]
P_s	pulp density of the slurry after the milling section in the plant [kg/L]
P_T	the desired pulp density in tank 1506 [kg/L]
P_{T1}	the desired pulp density in tank 1102 [kg/L]
P_W	density of the demineralised water [kg/L]
R	the ideal gas law constant [8.314 J/(mol.K)]
r_s	reaction rate of species s based on the unit volume of the solution [mol/L.min^{-1}]
r_s'	reaction rate of species s based on the unit mass of the solids [mol/g.min^{-1}]
S_P^A	oxygen partial pressure scaling factor for the higher (A=H) and the lower (A=L) partial pressures [-]
S_F	the conversion factor for the oxygen flowrate to its equivalent oxygen partial pressure [bar.h/kg]
t	time or iteration step [h or min]#
T	reaction temperature [K]
T_1	temperature in the 1st compartment of the autoclave [°C]
T_r	reaction temperature [°C]

V	volume of the pulp in tank 1506 [L]
V_1	volume of the pulp in tank 1102 [L]
V_{1MAX}	MAXIMUM volume of the pulp in tank 1102 [L]
V_{1MIN}	MINIMUM volume of the pulp in tank 1102 [L]
V_M	volume of matte [L]
V_{MIN}	MINIMUM volume of the pulp in tank 1506 [L]
VOL	initial volume of the pulp in tank 1506 [L]
$VOL1$	initial volume of the pulp in tank 1102 [L]
V_r	volume of reaction mixture [L]
V_s	volume of the slurry after the mill [L]
V_{se}	volume of spent electrolyte solution [L]
V_{T1}	desired volume of the pulp in tank 1102 [L]
V_{TOT}	The MAXIMUM volume of the pulp in tank 1506 [L]
V_W	volume of demineralised water [L]
W	weight of solids in reaction mixture [g]
$w_{ij}(t)$	weight associated with the connection between the i'th and j'th nodes of a neural net at time t [-]
$w_{ij,new}$	updated weight associated with the connection between the i'th and j'th nodes of a neural net [-]
$w_{ij,old}$	weight prior to modification associated with the connection between the i'th and j'th nodes of a neural net [-]
$\Delta w_{ij}(t)$	change in weight associated with the connection between the i'th and j'th nodes of a neural net at time t [-]
x_1^k	upper interior point of the interval in the k'th stage of the golden section search [-]
x_2^k	lower interior point of the interval in the k'th stage of the golden section search [-]
x_i	the i'th input variable to the data analysis and modelling techniques [-]
$\boldsymbol{x}_j$	the j'th input vector to a neural net [-]
X_s	the fraction known as the "golden section" [-]
$z_i(t)$	output or state of the i'th neuron in a neural net at time t [-]

Greek letters

α	momentum term used during training of a neural net [-]
β	time-dependent learning coefficient used in the training of the self-organising neural nets [-]
δ	error gradient associated with the output of the i'th node in a neural net [-]
σ_X	standard deviation of parameter X in determining the correlation coefficients [-]
σ_Y	standard deviation of parameter Y in determining the correlation coefficients [-]
ρ_{XY}	correlation coefficient of variable X in relation to variable Y [-]
τ	learning parameter which defines the step size during training of a neural net [-]

* The coefficients a and b depend on the reaction rate expression.

The unit of time (t) is [h] for the data analysis and [min] for the kinetic model.

THE SIMULATION OF A TRANSIENT LEACHING CIRCUIT

JOHAN ANDRIES MÜLLER RADEMAN

Dissertation presented for the Degree of

Doctor of Philosophy
in Engineering

at the University of Stellenbosch.

Promoters: Prof. L. Lorenzen
Prof. J.S.J. van Deventer

September 1995

Volume II

Contents

List of Figures

Appendix F:

List of Tables

Appendix A

CALCULATION OF THE EXPERIMENTAL CONDITIONS

A computer program was compiled in Borland Turbo Pascal 7.0 to execute the calculations for the variations in the experimental conditions, especially for changes in the pulp density and temperature. These calculations were necessary to determine the various ratios of matte, spent electrolyte solution and demineralized water which have to be added together for the variation in the pulp density. With the variations in temperature the program calculates the oxygen partial pressure for a given total pressure and a partial steam pressure at that specific temperature. The calculation of the steam pressure is done through interpolation from the steam table data that the user has to enter.

The inputs for the calculations are (the variable is indicated in brackets):

(i) the reaction mixture volume (V_r),

(ii) density of the matte (P_M),

(iii) specific gravity of demineralized water (P_W),

(iv) the actual pulp density of the slurry after the milling section in the plant (P_s),

(v) the pulp density of the spent electrolyte solution (P_{se}), and

(vi) the pulp density of the final reaction mixture (P_r).

The calculation is divided into two sections, firstly it will determine the composition of the slurry just after the milling section and secondly, the composition of the final reaction mixture, which will simulate the conditions in the autoclave (plant). In order to solve the set of equations the two sections will be calculated simultaneously.

V_M : volume of matte [L]

V_W : volume of water [L]

V_s : volume of slurry after the mill [L]

V_{se} : volume of spent electrolyte solution [L]

V_r : reaction mixture volume [L]

P_M : density of the matte [kg/L]

P_W : specific gravity of demineralized water [-]

P_s : actual pulp density of the slurry after the milling section in the plant [kg/L]

P_{se} : pulp density of the spent electrolyte solution [kg/L]

P_r : pulp density of the final reaction mixture [kg/L]

$$V_s = V_M + V_W \tag{A.1}$$

$$P_s = \frac{V_M \times P_M + V_W \times P_W}{V_M + V_W} \tag{A.2}$$

$$V_r = V_s + V_{se} \tag{A.3}$$

$$P_r = \frac{V_s \times P_s + V_{se} \times P_{se}}{V_s + V_{se}} \tag{A.4}$$

Substitute equation A.1 into A.3.

$$V_r = V_M + V_W + V_{se} \tag{A.5}$$

Substitute equation A.1 into A.4.

$$P_r = \frac{(V_M + V_W)P_s + V_{se} \times P_{se}}{V_M + V_W + V_{se}} \tag{A.6}$$

Equation A.2 changes to:

$$V_M = \frac{P_s - P_W}{P_M - P_s} \times V_W \tag{A.7}$$

$$a = \frac{P_s - P_W}{P_M - P_s} \tag{A.8}$$

The simplified form of equation A.7.

$$V_M = a \times V_W \tag{A.7}$$

Substitute equation A.7 into A.5.

$$V_W = \frac{V_r - V_{se}}{1+a} \tag{A.9}$$

Substitute equation A.7 into A.6.

$$V_{se} = \frac{(P_r - P_s)(1+a)V_W}{P_{se} - P_r} \tag{A.10}$$

Substitute equation A.9 into A.10.

$$V_{se} = \frac{\left(\frac{P_r - P_s}{P_{se} - P_r}\right)}{\left(\frac{P_r - P_s}{P_{se} - P_r}\right)+1} \times V_r \tag{A.11}$$

The value of V_W is determined with equation A.9 and then the value of V_M will be determined by equation A.7. Therefore, with the volumes calculated and the pulp densities of the matte known, spent electrolyte and demineralized water, the mass of each component necessary for the different experiments could be calculated. As already mentioned the program also calculates the partial oxygen pressure from the difference between the partial steam pressure and the total pressure which will be applied on the reaction mixture in the experiment. The partial steam pressure is determined from steam table data entered by the user, through interpolation.

As output the program gives the volume, mass and % weight/weight of matte, spent electrolyte and demineralized water that have to be added to obtain the correct pulp density. It also calculates the oxygen partial pressure at the given total pressure.

Appendix B

TESTS TO DETERMINE VIABILITY OF EXPERIMENTS IN SIMULATING PLANT OPERATIONS

In order to conduct useful experiments in the laboratory scale autoclave the most important aspect is to simulate conditions in the plant. The amount of leaching occurring in the two preleach tanks (degree of leaching in tanks 1506 and 1102) must be investigated because: (i) the bulk sample of matte was taken just after the milling section, and (ii) the batch experiment can not simulate the preleach step together with the pressure leach step in one experiment. The reasons for taking the bulk sample from just after the milling section are: (i) that the process is not very consistent, so when a bulk sample is taken from tank 1102 for example this would not necessarily represent the optimum or desirable pulp mixture, (ii) to obtain a complete reaction mechanism of the process it is better to perform the leaching experiments with the fresh (unreacted) matte, and (iii) one of the parameters that was investigated, was the effect of the variation in the initial particle size distribution.

Three preleach tests were conducted simulating conditions in tank 1506 (test 7: using fresh matte), tank 1102 (test 8: using fresh matte) and tank 1102 where pulp from tank 1506 was used for the experiment (test 23). There was also one test (test 11 with conditions the same as test 10) conducted by using pulp from tank 1102 in the oxygen pressure leach experiments to determine the difference in the leaching reactions and kinetics of the pulp from the plant and the fresh matte.

B.1 PRELEACH TESTS

The conditions present in the preleach section and then in the autoclave, could not be simulated by the experiment in only one run. Therefore, tests were conducted to determine the extent of reactions taking place in the preleach tanks. These tests were then used to determine if it is a valid assumption to assume that the reactions

taking place in the preleach tanks will be completed in the first few minutes of the leaching process in the batch laboratory experiments. (Results on cobalt in the solution and solid are omitted, because the leaching rate of cobalt is consistent, and of minor importance relative to nickel, copper and iron.)

B.1.1 Tank 1506

From Fig. B.1 and Fig. B.2 it can be seen that a reasonable degree of leaching occurs in tank 1506. For example, the leaching efficiency of nickel in this tank, with a pulp density of 1.90 kg/L, an approximate residence time of 300 minutes and temperature of 75°C, at the current operating conditions, is 7.2%. Fig. B.1 shows that there is a consistent increase in the pH of the solution indicating that reactions must be occurring in the pulp. It is also evident that nickel (Ni) and iron (Fe) are leached and copper (Cu) cemented quickly in the first 40 minutes of this experiment. The leaching of especially Ni and Fe continues until 300 minutes when it gradually starts precipitating again. This effect was not investigated further because the residence time in the tank is approximately 300 minutes and the precipitation rate is assumed to be insignificant. Therefore, it could be concluded that good and consistent leaching of Ni and Fe and cementation of Cu occur in tank 1506, furthermore the reaction trends comply with the reaction trends of the experimental autoclave leaching tests. This indicates that the reactions occurring in tank 1506 would be occurring in the experimental autoclave as well, but with faster kinetics due to the temperature, pressure and chemical solution conditions.

B.1.2 Tank 1102

Two preleach tests were conducted simulating conditions in tank 1102, i.e. a test using pulp from tank 1506 in the process (test 23) and a test using fresh matte (test 8). These two tests were conducted to make sure that the actual conditions and reactions occurring in this tank in the process could be simulated. From Fig. B.3 to Fig. B.6 it can be seen that the basic reaction trends are again the same as for tank 1506 but with different kinetics. The leaching efficiency for Ni in the test using pulp from tank 1506 is 6.5% (Fig. B.4) and for the test using fresh matte it is

approximately 9.6% (Fig. B.6). The different kinetics in tank 1102 compared with tank 1506 can be ascribed to the different conditions present, i.e. a pulp density of 1.60 kg/L, an approximate residence time of 180 minutes and a temperature of 60°C. The basic reaction trends in tank 1102 are the same as in tank 1506.

From Fig. B.1, B.3 and B.5 it is evident that Cu precipitation is faster in tank 1506 than in tank 1102. This fact is attributed to the higher temperature (75°C) and higher pulp density (1.90 kg/L) in tank 1506, than the temperature (60°C) and pulp density (1.60 kg/L) in tank 1102, respectively.

B.2 ACID-OXYGEN PRESSURE LEACH TEST

The acid-oxygen pressure leach test which compared fresh matte (test 10) to the test using pulp from tank 1102 (test 11) was conducted to confirm the assumption that the condition of the pulp entering the autoclave in the plant will be reached quickly in the experiment. Figures B.7 and B.8 show that the reactions of the tests in the experimental autoclave, with pulp from tank 1102 and with fresh matte, follow each other reasonably closely. The only obvious difference in the two experiments is the difference in the acid concentration which stayed consistent throughout the experiments. The lower acid concentration of the experiment using pulp from tank 1102 (Fig. B.7) could be ascribed to the possible dilution with water in tank 1506 when the solids are recycled from the Cu cementation circuit and to the leaching which has already occurred in tanks 1506 and 1102.

It is possible to approximate the reactions occurring in the preleach tanks with the experiment where fresh matte was used in the pressure leach experiment, so that the possible reactions in the preleach tanks have been simulated in the first 10 to 20 minutes of the pressure leach experiment. Therefore this investigation confirmed that the acid-oxygen pressure leach tests can be conducted with fresh (unreacted) matte to produce results which simulate the actual plant autoclave leach process.

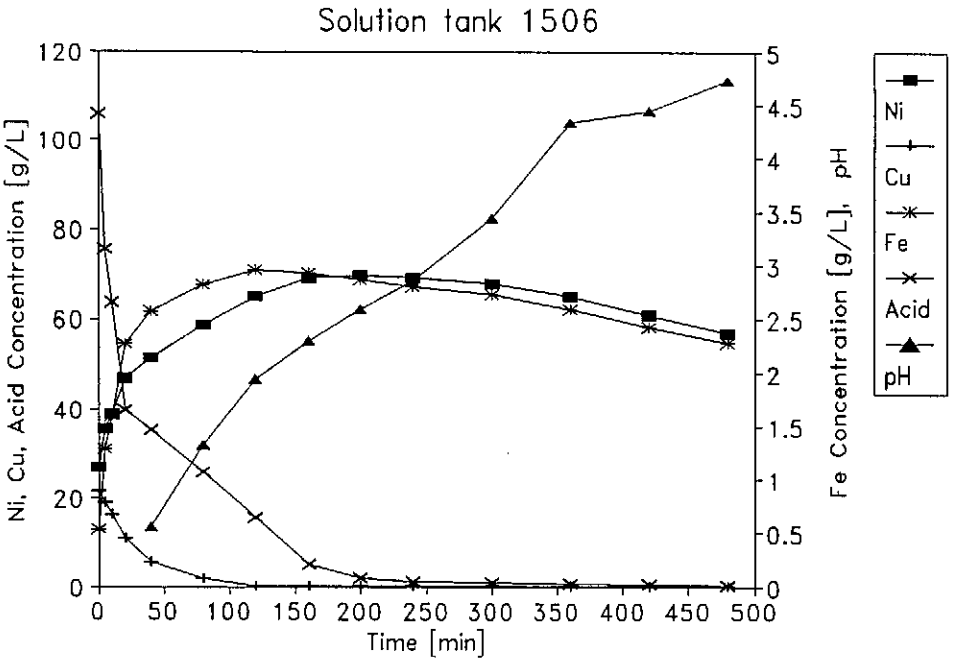

Figure B.1 - Solution analysis of experiment simulating tank 1506 (test 7) versus leaching time

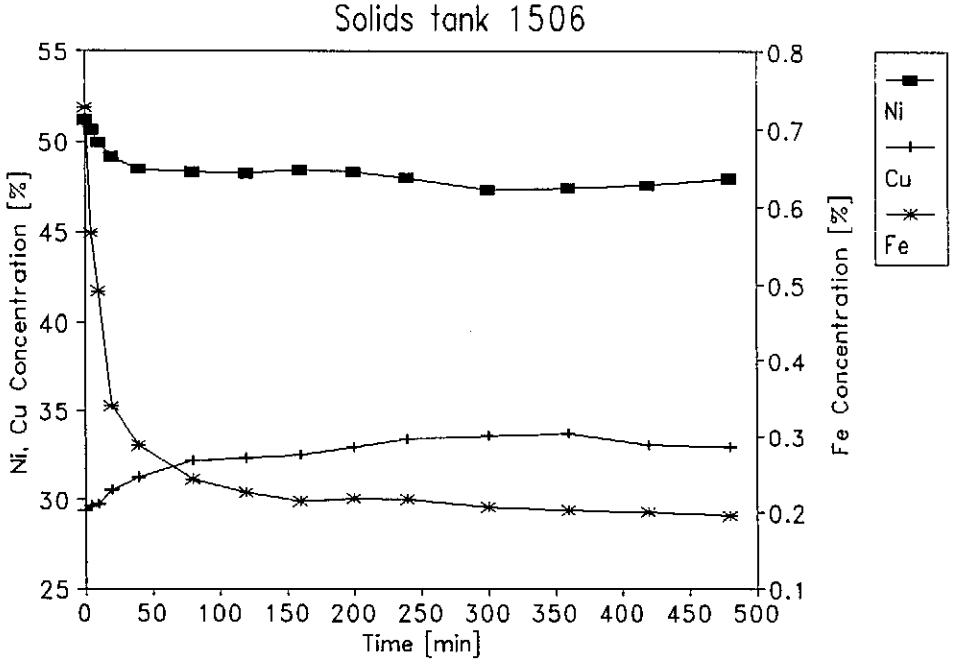

Figure B.2 - Solids analysis of experiment simulating tank 1506 (test 7) versus leaching time

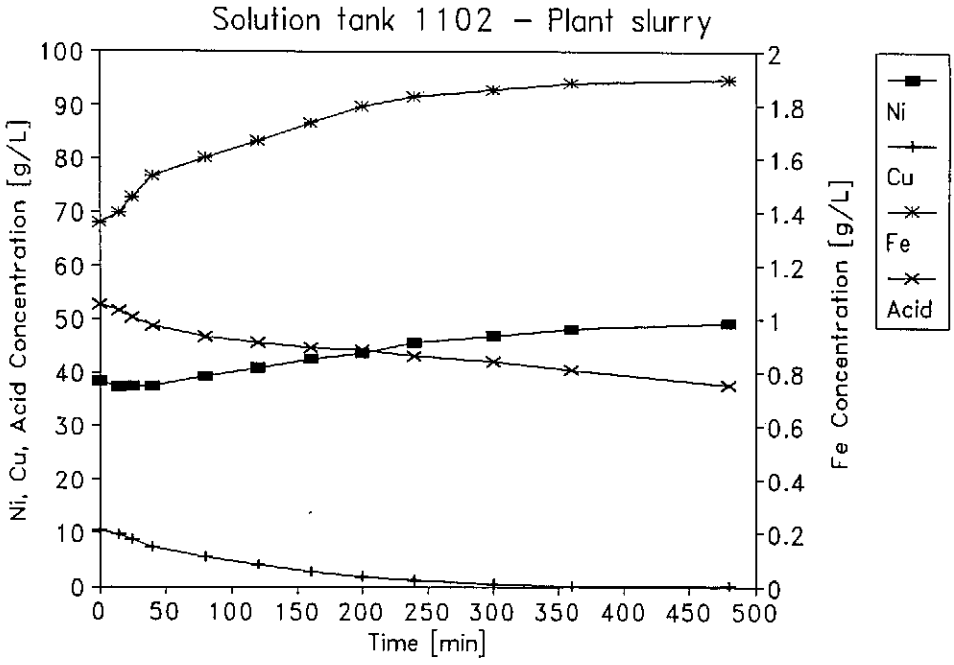

Figure B.3 - Solution analysis of experiment simulating tank 1102 (test 23: using pulp from tank 1506) versus leaching time

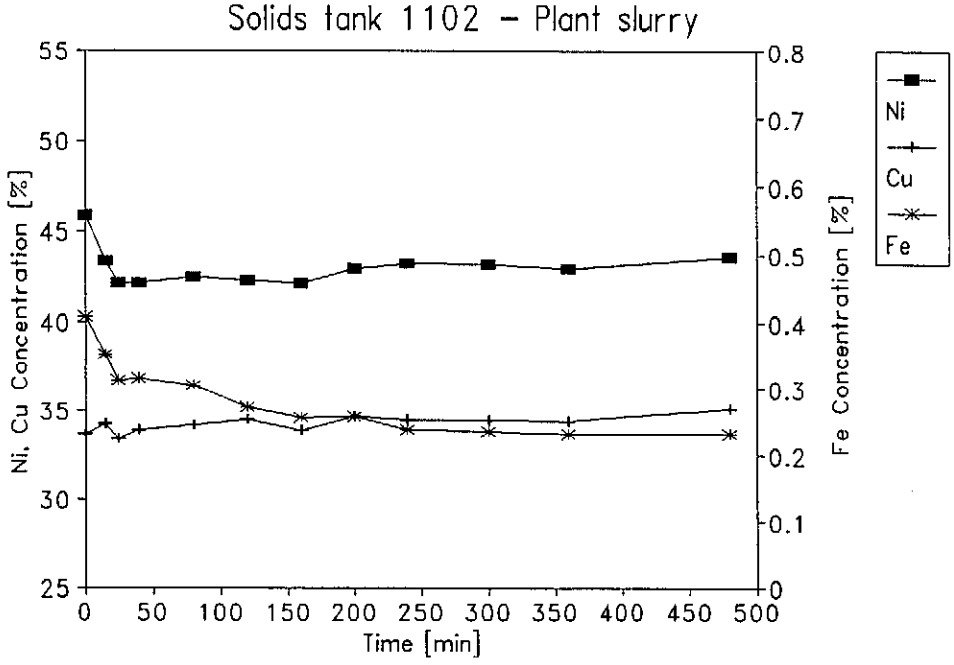

Figure B.4 - Solids analysis of experiment simulating tank 1102 (test 23: using pulp from tank 1506) versus leaching time

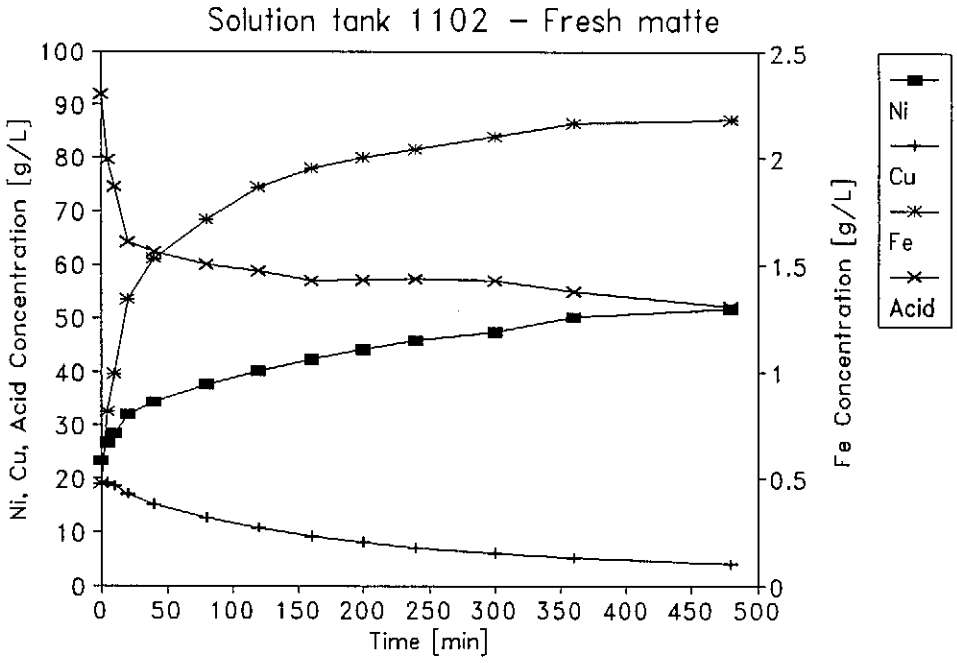

Figure B.5 - Solution analysis of experiment simulating tank 1102 (test 8: using fresh matte) versus leaching time

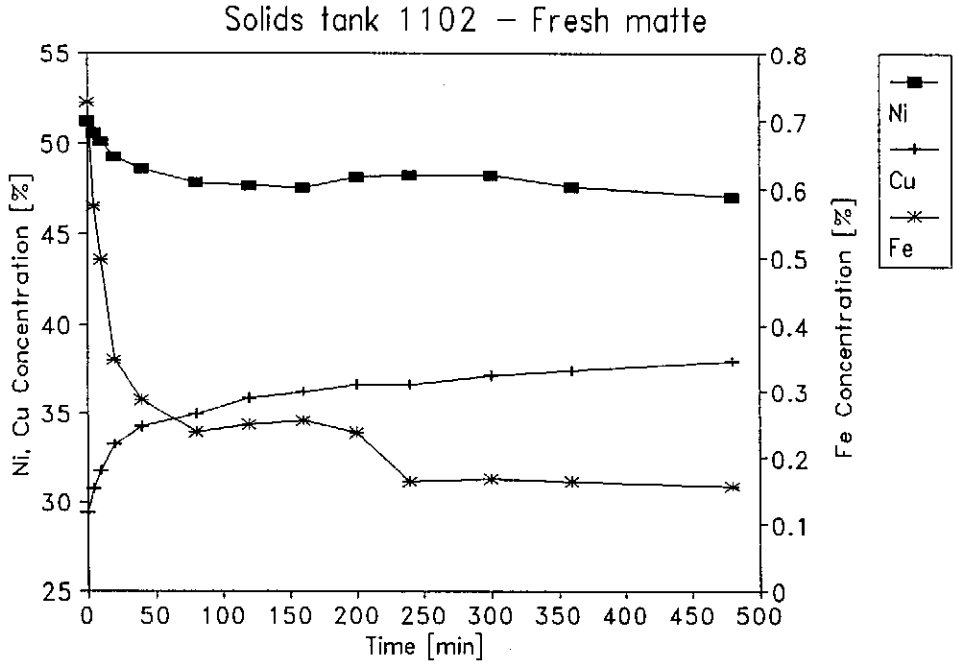

Figure B.6 - Solids analysis of experiment simulating tank 1102 (test 8: using fresh matte) versus leaching time

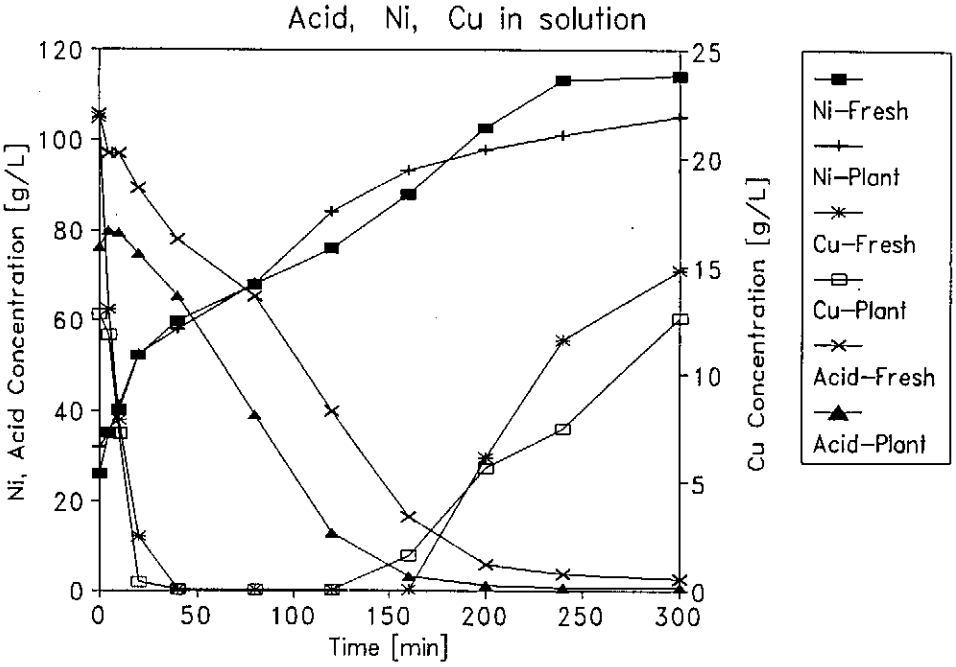

Figure B.7 - Solution analysis comparing the oxygen pressure leach experiment, by using fresh matte (test 10) and by using pulp from tank 1102 (test 11), versus leaching time. (O_2 flowrate = 0.59 kg/h)

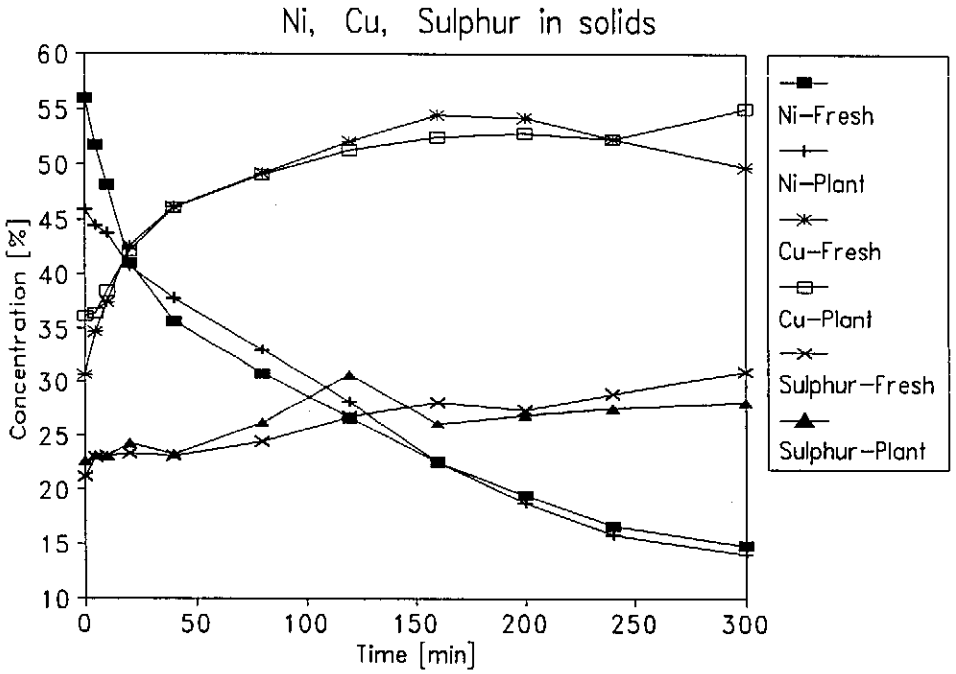

Figure B.8 - Solids analysis comparing the oxygen pressure leach experiment, by using fresh matte (test 10) and by using pulp from tank 1102 (test 11), versus leaching time. (O_2 flowrate = 0.59 kg/h)

Appendix C

PROCEDURES FOR SOLUTION ANALYSIS

The procedures used for solution analysis described in telegraph style are as follows:

Iron (Fe), Cobalt (Co) and low concentration Copper (Cu):

* Pipette 10 mL of the sample into a 100 mL volumetric flask, fill the flask with distilled water and mix it thoroughly (10 dilution).
* Pipette 10 mL of the first diluted sample into a 100 mL flask, fill the flask with distilled water and mix it thoroughly (100 dilution).
* Pipette 10 mL of the second diluted sample into 100 mL flask, fill the flask with distilled water and mix it thoroughly (1000 dilution).
* Analyse the diluted samples on the AA.

Total metals (TM):

* Pipette 10 mL of 10 dilution sample into a beaker for the auto titrator and add 50 mL of distilled water.
* Add 1 mL 2.94 *M* H_2SO_4 (sulphuric acid) to the beaker.
* Start to titrate the mixture in the beaker with 0.17 *M* Na_2CO_3 (soda carb) in the auto titrator till it stop (fill burette).
* Add 30 mL of 0.11*N* (42 g/L) EDTA to the titrated mixture, then start to titrate it again till the auto titrator stop.
* The reading on the auto titrator x10 = TM concentration.

The principle on which the total metals (TM) titration is based is that a sulphate solution pH is normal at 4.5, therefore Na_2CO_3 is added to neutralise all the acids with the first auto titration (the solution is originally acid). When the Na_2CO_3 is added

it will form mainly two products i.e. Na_2SO_4 and H_2CO_3. EDTA is then added to replace the remaining sulphates to couple with the metals to form metal complexes. The sulphates that had been replaced by the EDTA are now titrated quantitatively with Na_2CO_3.

Copper (high Cu concentration):

* Measure 20 mL of 20% KI (potassium iodide) into a conical flask.
* Add 5 mL of starch (10 g/L) into the flask.
* Add 5 mL of the sample into the flask.
* Titrate with 19.7 g/L $Na_2S_2O_3$ (Thio) till end point white.
* Direct burette reading = Cu concentration (g/L).

Free acid (FA = H_2SO_4):

* Continue with the same sample used for the copper titration.
* Add a few drops of Congo Red (2 g/L).
* Titrate with 1.02 *M* Na_2CO_3 (soda carb) till end point red.
* Burette reading x10 = FA (g/L H_2SO_4).

Sulphur (S):

* Pipette 10 mL of the 10 dilution sample into a 250 mL conical flask.
* Add a spatula tip of pure NH_4Cl (ammonium chloride), followed by 10 mL of 0.2 *M* $BaCl_2$ (barium chloride).
* Heat the sample to approximately 50°C and leave it to cool to room temperature.
* Add 5-10 drops of freshly prepared sodium rhodizonate indicator (3 g/L) and mix thoroughly.
* Add 3 drops of 10% HCl and 7 mL of ethanol.
* Titrate the mixture slowly with 0.2 *M* $(NH_4)_2SO_4$ (ammonium sulphate) until the colour begins to fade.
* The volume $(NH_4)_2SO_4$ titrated = T mL.
* The volume $(NH_4)_2SO_4$ titrated for standardisation = A mL.
* (A-T) x 32.064 x 0.2 x dilution factor = S (total sulphur) concentration (g/L).

Standardisation of the $BaCl_2$ solution:

* 10 mL of the 0.2 *M* $BaCl_2$ solution is pipetted into a conical flask and 1 g of NH_4Cl is added.
* Heat the sample to approximately 50°C and leave it to cool to room temperature.
* Add 5-10 drops of freshly prepared sodium rhodizonate indicator (3 g/L) and mix thoroughly.
* Add 3 drops of 10% HCl and 7 mL of ethanol.
* Titrate the mixture slowly with 0.2 *M* $(NH_4)_2SO_4$ (ammonium sulphate) until the colour begins to fade.
* The volume $(NH_4)_2SO_4$ titrated = A mL.

The principle of the total sulphur titration is that a known volume of 0.2 *M* $BaCl_2$ is added in excess, and the insoluble $BaSO_4$ is formed. The barium left in solution forms a red complex with the indicator (sodium rhodizonate in a weak HCl solution). $BaSO_4$ is much less soluble than the red complex, and when back-titrated with a sulphate solution, the barium will be completely precipitated when the red colour disappears.

Appendix D

COMPUTER CODE OF THE SIMULATION PROGRAM FOR THE REPULPING SECTION OF THE PLANT

The computer code was compiled in Borland, Turbo Pascal 7.0.

```
PROGRAM CONTROL;

USES
CRT,FastTTT,DOS,WinTTT,MenuTTT,VARIABLE,INPUT_MENU,RK_GOLD,TRIAL,OUTPUT_MEN
U,GRAPHICS;

VAR Main_choice,Error:INTEGER;
   M1:MENU_RECORD;

PROCEDURE WAIT;
BEGIN
 SOUND(400);DELAY(150);NOSOUND;
 WriteCenter(25,white+blink,RED,'*************** PRESS ANY KEY TO PROCEED ***************');
 READKEY;
END;

PROCEDURE TITEL;
BEGIN
 ClrScr;
 Offcursor;
 Speed:=1000;
 GrowFBox(10,4,70,16,WHITE,GREEN,2);
 WriteCenter(6,blue,green,'UNIVERSITY OF STELLENBOSCH');
 WriteCenter(7,blue,green,'DEPARTMENT OF METALLURGICAL ENGINEERING');
 WriteCenter(9,red,green,'DENSITY AND VOLUME (RESIDENCE TIME) CONTROLLER ');
 WriteCenter(10,red,GREEN,'FOR TANK 1100/1506 AND 1102');
 WriteCenter(12,blue,green,'PROGRAMMER: J.A.M. RADEMAN');
 WriteCenter(14,blue,green,'DATE: SEPTEMBER 1993');
 WAIT;
END;
```

```
PROCEDURE Define_Menu;
Begin
 With M1 do
  Begin
  Offcursor;
   Heading1:='OUTPUTS';
   Heading2:='Choose option';
   Topic[1]:='   Mill, Tanks 1506 and 1102';
   Topic[2]:='   Mill';
   Topic[3]:='   Tanks 1100/1506 and 1102';
   Topic[4]:='   Graph of PD change';
   Topic[5]:='   Graph of VOLUME change';
   Topic[6]:='   Repeat the PROGRAM';
   Topic[7]:='   Quit the PROGRAM';
   TotalPicks:=7;
   PicksPerLine:=1;
   Addprefix:=1;
   TopleftXY[1]:=0;
   TopleftXY[2]:=5;
   Boxtype:=5;
    IF BaseOfScreen = $B800 THEN
     Begin
      Colors[1] := white;
      Colors[2] := red;
      Colors[3] := lightgray;
      Colors[4] := blue;
      Colors[5] := lightcyan;
     End
    ELSE
     Begin
      Colors[1] := white;
      Colors[2] := black;
      Colors[3] := black;
      Colors[4] := lightgray;
      Colors[5] := white;
     End;
    AllowEsc := false;
    Margins := 5;
   End;
 End;
```

```
FUNCTION HERHAAL:BOOLEAN;
VAR ANSW:CHAR;
BEGIN
 REPEAT
  FBox(12,8,68,14,YELLOW,3,2);
  WRITEAT(17,11,4,3,'Do you want to repeat the INPUT section [Y,N] ? ');
  ANSW:=UPCASE(READKEY);
 UNTIL ANSW In['Y','N'];
 CASE ANSW OF
  'Y':HERHAAL:=TRUE;
  'N':HERHAAL:=FALSE;
 END;
END;

PROCEDURE CHOICE1;
BEGIN
 MILL;
 TANKS;
END;

PROCEDURE CHOICE2;
BEGIN
 REP:=TRUE;
END;

PROCEDURE CHOICE3;
BEGIN
 PD:=TRUE;
 GRAPH_D;
END;

PROCEDURE CHOICE4;
BEGIN
 PD:=FALSE;
 GRAPH_D;
END;

PROCEDURE OUTPUT_ORDER;
Begin
 Case Main_Choice of
 1 :CHOICE1;
 2 :MILL;
```

```
  3 :TANKS;
  4 :CHOICE3;
  5 :CHOICE4;
  6 :CHOICE2;
  7 :Finish;
  End;
End;

PROCEDURE OUTPUT;
BEGIN
  REPEAT
    MAIN_CHOICE:=1;
    DEFINE_MENU;
    DisplayMenu(M1,false,Main_choice,Error);
    OUTPUT_ORDER;
  UNTIL REP;
END;

PROCEDURE BUSY;
BEGIN
  CLRSCR;
  FBox(12,9,68,13,YELLOW,3,2);
  WRITEAT(17,11,4,3,'Busy with calculation. Please be patient ! ');
END;

BEGIN
  TITEL;
  CLRSCR;
  REPEAT
    REP:=FALSE;
    REPEAT
      INPUT;
    UNTIL NOT(HERHAAL);
    BUSY;
    IF CHOICE THEN OPERATOR
    ELSE TANK_1102_CALC;
    SOUND(400);DELAY(150);NOSOUND;
    OUTPUT;
  UNTIL NOT(REP);
END.
```

```
UNIT VARIABLE;

INTERFACE

VAR F6,P6,F2,P2,F7,DENS1,VOL1,VT1,PT1:REAL;
   MATTE,PM,PW,F1,P1,P3,P4,P5,F4,F5,VOL,DENS,PT:REAL;
   F1MIN,F1MAX,VTOT,VMIN,F2MIN,F2MAX,F6MIN,F6MAX,V1MAX,V1MIN:REAL;
   C1,C2,H,T,MTB,MTE,MILL_Y_N:INTEGER;
   REP,CHOICE,RK:BOOLEAN;
   S15,S16,S13,S14:STRING;

IMPLEMENTATION

END.
```

```
UNIT INPUT_MENU;

INTERFACE

USES CRT,VARIABLE,FastTTT,DOS,WinTTT,KeyTTT,IOTTT,MenuTTT,StrngTTT;

PROCEDURE INPUT;
PROCEDURE FINISH;

IMPLEMENTATION

VAR S10,S12:STRING;
   YES,HOUR,MIN,I,C,Main_choice,Error:INTEGER;
   M1:MENU_RECORD;
   TIMER:BOOLEAN;

PROCEDURE TEST_TIME;
BEGIN
 IF ((HOUR>=0) AND (HOUR<=23) AND (MIN>=0) AND (MIN<=59)) THEN TIMER:=TRUE
 ELSE
 BEGIN
  TIMER:=FALSE;
  I:=I+1;
 END;
END;
```

```
PROCEDURE SIMPLE1;
VAR S21,S22,S23,S24,S25,S26,S27,S28,S29,S30,S31,S32,S33:STRING;
   RETCODE:INTEGER;
BEGIN
{ ClrScr;}
 FBox(1,1,80,25,yellow,1,2);
 Horizline(2,79,5,yellow,1,1);
 WriteCenter(3,yellow,1,'MILL, TANK 1506 & TANK 1102');
 WriteAt(5,7,white,1,'Matte feedrate to the mill [t/h]]');
 WriteAt(5,8,white,1,'Desired pulp density (PD) of mixture leaving the mill [kg/l]');
 WriteAt(5,10,white,1,'Pulp density (PD) of the spent electrolyte (SE) [kg/l]');
 WriteAt(5,11,white,1,'The actual pulp density (PD) in tank 1506 [kg/l]');
 WriteAt(5,12,white,1,'The desired pulp density (PD) in tank 1506 [kg/l]');
 WriteAt(5,13,white,1,'The actual level of the pulp in tank 1506 [%]');
 WriteAt(5,14,white,1,'Amount of times the solids from press 1407 will be washed');
 WriteAt(5,15,white,1,'SE flowrate used to wash solids to tank 1506 [l/min]');
 WriteAt(5,17,white,1,'Pulp flowrate from tank 1102 to the autoclave 1110A [l/min]');
 WriteAt(5,18,white,1,'Pulp flowrate from tank 1102 to the autoclave 1110B [l/min]');
 WriteAt(5,19,white,1,'The actual pulp density (PD) in tank 1102 [kg/l]');
 WriteAt(5,20,white,1,'The desired pulp density (PD) in tank 1102 [kg/l]');
 WriteAt(5,21,white,1,'The actual level of the pulp in tank 1102 [%]');
 WriteAt(5,22,white,1,'The desired level of the pulp in tank 1102 [%]');
 S21:='3.3';
 S22:='3.4';
 S33:='1.20';
 S23:='2.0';
 S24:='75';
 S25:='1';
 S26:='7.5';
 S27:='0';
 S28:='43';
 S29:='1.6';
 S30:='1.6';
 S31:='80';
 S32:='80';
 IO_SetFields(14);
 IO_Soundbeeper(false);
 IO_AllowEsc(true);
 IO_DefineStr(1,14,2,14,2,70,7,S21,'####');
 IO_DefineStr(2,1,3,1,3,70,8,S22,'#####');
 IO_DefineStr(3,2,4,2,4,70,10,S33,'#####');
 IO_DefineStr(4,3,5,3,5,70,11,S10,'#####');
```

```
IO_DefineStr(5,4,6,4,6,70,12,S23,'#####');
IO_DefineStr(6,5,7,5,7,70,13,S24,'#####');
IO_DefineStr(7,6,8,6,8,70,14,S25,'#####');
IO_DefineStr(8,7,9,7,9,70,15,S26,'#####');
IO_DefineStr(9,8,10,8,10,70,17,S27,'#####');
IO_DefineStr(10,9,11,9,11,70,18,S28,'#####');
IO_DefineStr(11,10,12,10,12,70,19,S29,'#####');
IO_DefineStr(12,11,13,11,13,70,20,S30,'#####');
IO_DefineStr(13,12,14,12,14,70,21,S31,'#####');
IO_DefineStr(14,13,1,13,1,70,22,S32,'#####');
IO_DefineMsg(1,23,25,' *** Press "END" to continue *** ');
IO_DefineMsg(2,23,25,' *** Press "END" to continue *** ');
IO_DefineMsg(3,23,25,' *** Press "END" to continue *** ');
IO_DefineMsg(4,23,25,' *** Press "END" to continue *** ');
IO_DefineMsg(5,23,25,' *** Press "END" to continue *** ');
IO_DefineMsg(6,23,25,' *** Press "END" to continue *** ');
IO_DefineMsg(7,23,25,' *** Press "END" to continue *** ');
IO_DefineMsg(8,23,25,' *** Press "END" to continue *** ');
IO_DefineMsg(9,23,25,' *** Press "END" to continue *** ');
IO_DefineMsg(10,23,25,' *** Press "END" to continue *** ');
IO_DefineMsg(11,23,25,' *** Press "END" to continue *** ');
IO_DefineMsg(12,23,25,' *** Press "END" to continue *** ');
IO_DefineMsg(13,23,25,' *** Press "END" to continue *** ');
IO_DefineMsg(14,23,25,' *** Press "END" to continue *** ');
OnCursor;
IO_Edit(Retcode);
Offcursor;
IO_Resetfields;
MATTE:=Str_to_real(S21);
P3:=Str_to_real(S22);
P1:=Str_to_real(S33);
P6:=P1;
P5:=P1;
PT:=Str_to_real(S23);
VOL:=Str_to_real(S24);
VOL:=VOL/100*10800;
F5:=Str_to_real(S25);
F4:=119.6/60*F5;
F5:=Str_to_real(S26)*F5;
F7:=Str_to_real(S27)+Str_to_real(S28);
DENS1:=Str_to_real(S29);
PT1:=Str_to_real(S30);
```

```
  VOL1:=Str_to_real(S31);
  VOL1:=VOL1/100*9970;
  VT1:=Str_to_real(S32);
  VT1:=VT1/100*9970;
END;

PROCEDURE TIME1;
VAR S2:STRING;
   RETCODE:INTEGER;
BEGIN
{ ClrScr;}
  FBox(6,3,74,17,YELLOW,5,2);
  Horizline(7,73,7,YELLOW,5,1);
  WriteCenter(5,WHITE,5,'SET CALCULATION TIME');
  WriteAt(10,10,WHITE,5,'What is the TIME right now ? (00:00 to 23:59)          :');
  WriteAt(10,11,WHITE,5,'When are you going to take your next readings ?        :');
  Horizline(7,73,13,YELLOW,5,1);
  WriteCenter(13,WHITE+BLINK,5,'OPTION');
  WriteAt(10,15,WHITE,5,'Do you want to change some of the OTHER PARAMETERS [YES=1]');
  S2:='2';
  REPEAT
    I:=0;
    IO_SetFields(5);
    IO_soundbeeper(false);
    IO_AllowEsc(true);
    IO_DefineStr(1,5,2,5,2,67,10,S15,'##');
    IO_DefineStr(2,1,3,1,3,70,10,S16,'##');
    IO_DefineStr(3,2,4,2,4,67,11,S13,'##');
    IO_DefineStr(4,3,5,3,5,70,11,S14,'##');
    IO_DefineStr(5,4,1,4,1,70,15,S2,'#');
    IO_DefineMsg(1,23,17,' *** Press "END" to continue *** ');
    IO_DefineMsg(2,23,17,' *** Press "END" to continue *** ');
    IO_DefineMsg(3,23,17,' *** Press "END" to continue *** ');
    IO_DefineMsg(4,23,17,' *** Press "END" to continue *** ');
    IO_DefineMsg(5,23,17,' *** Press "END" to continue *** ');
    Oncursor;
    IO_Edit(Retcode);
    Offcursor;
    IO_Resetfields;
    HOUR:=Str_to_int(S15);
    MIN:=Str_to_int(S16);
    TEST_TIME;
```

```
   HOUR:=Str_to_int(S13);
   MIN:=Str_to_int(S14);
   TEST_TIME;
   IF I>0 THEN
   BEGIN
    TIMER:=FALSE;
    OnCursor;
    TempMessage(6,8,yellow+blink,red,'******** THE TIME ENTERED MUST BE IN THE FORM
00:00 TO 23:59 ********');
   END;
  UNTIL TIMER;
  HOUR:=(Str_to_int(S13)-Str_to_int(S15));
  MIN:=(Str_to_int(S14)-Str_to_int(S16));
  IF ((HOUR>=0) AND (MIN<0)) THEN MIN:=MIN+60;
  IF ((HOUR<0) AND (MIN<0)) THEN
  BEGIN
   HOUR:=HOUR+23;
   MIN:=MIN+60;
  END;
  IF ((HOUR<0) AND (MIN>=0)) THEN HOUR:=HOUR+24;
  HOUR:=HOUR*60;
  T:=HOUR+MIN;
  YES:=Str_to_Int(S2);
END;

PROCEDURE SIMPLE2;
VAR S21,S22,S23,S24,S25,S26,S27,S28,S29,S30,S31,S32,S33,S34:STRING;
   RETCODE:INTEGER;
   MILLING:BOOLEAN;
BEGIN
{ ClrScr;}
  FBox(1,1,80,25,yellow,1,2);
  Horizline(2,79,5,yellow,1,1);
  WriteCenter(3,yellow,1,'MILL, TANK 1506 & TANK 1102');
  WriteAt(5,7,white,1,'Are you busy milling/are you going to mill now ? [YES=1/NO=2]');
  WriteAt(5,8,white,1,'Matte feedrate to the mill [t/h]]');
  WriteAt(5,9,white,1,'Desired pulp density (PD) of mixture leaving the mill [kg/l]');
  WriteAt(5,11,white,1,'Pulp density (PD) of the spent electrolyte (SE) [kg/l]');
  WriteAt(5,12,white,1,'The actual pulp density (PD) in tank 1506 [kg/l]');
  WriteAt(5,13,white,1,'The desired pulp density (PD) in tank 1506 [kg/l]');
  WriteAt(5,14,white,1,'The actual level of the pulp in tank 1506 [%]');
  WriteAt(5,15,white,1,'Amount of times the solids from press 1407 will be washed');
```

```
WriteAt(5,16,white,1,'SE flowrate used to wash solids to tank 1506 [l/min]');
WriteAt(5,18,white,1,'Pulp flowrate from tank 1102 to the autoclave 1110A [l/min]');
WriteAt(5,19,white,1,'Pulp flowrate from tank 1102 to the autoclave 1110B [l/min]');
WriteAt(5,20,white,1,'The actual pulp density (PD) in tank 1102 [kg/l]');
WriteAt(5,21,white,1,'The desired pulp density (PD) in tank 1102 [kg/l]');
WriteAt(5,22,white,1,'The actual level of the pulp in tank 1102 [%]');
WriteAt(5,23,white,1,'The desired level of the pulp in tank 1102 [%]');
S34:='1';
S21:='3.3';
S22:='3.4';
S33:='1.20';
S23:='2.0';
S24:='75';
S25:='1';
S26:='7.5';
S27:='0';
S28:='43';
S29:='1.6';
S30:='1.6';
S31:='80';
S32:='80';
REPEAT
  IO_SetFields(15);
  IO_soundbeeper(false);
  IO_AllowEsc(true);
  IO_DefineStr(1,15,2,15,2,70,7,S34,'#');
  IO_DefineStr(2,1,3,1,3,70,8,S21,'####');
  IO_DefineStr(3,2,4,2,4,70,9,S22,'#####');
  IO_DefineStr(4,3,5,3,5,70,11,S33,'#####');
  IO_DefineStr(5,4,6,4,6,70,12,S10,'#####');
  IO_DefineStr(6,5,7,5,7,70,13,S23,'#####');
  IO_DefineStr(7,6,8,6,8,70,14,S24,'#####');
  IO_DefineStr(8,7,9,7,9,70,15,S25,'#####');
  IO_DefineStr(9,8,10,8,10,70,16,S26,'#####');
  IO_DefineStr(10,9,11,9,11,70,18,S27,'#####');
  IO_DefineStr(11,10,12,10,12,70,19,S28,'#####');
  IO_DefineStr(12,11,13,11,13,70,20,S29,'#####');
  IO_DefineStr(13,12,14,12,14,70,21,S30,'#####');
  IO_DefineStr(14,13,15,13,15,70,22,S31,'#####');
  IO_DefineStr(15,14,1,14,1,70,23,S32,'#####');
  IO_DefineMsg(1,23,25,' *** Press "END" to continue *** ');
  IO_DefineMsg(2,23,25,' *** Press "END" to continue *** ');
```

```
  IO_DefineMsg(3,23,25,' *** Press "END" to continue *** ');
  IO_DefineMsg(4,23,25,' *** Press "END" to continue *** ');
  IO_DefineMsg(5,23,25,' *** Press "END" to continue *** ');
  IO_DefineMsg(6,23,25,' *** Press "END" to continue *** ');
  IO_DefineMsg(7,23,25,' *** Press "END" to continue *** ');
  IO_DefineMsg(8,23,25,' *** Press "END" to continue *** ');
  IO_DefineMsg(9,23,25,' *** Press "END" to continue *** ');
  IO_DefineMsg(10,23,25,' *** Press "END" to continue *** ');
  IO_DefineMsg(11,23,25,' *** Press "END" to continue *** ');
  IO_DefineMsg(12,23,25,' *** Press "END" to continue *** ');
  IO_DefineMsg(13,23,25,' *** Press "END" to continue *** ');
  IO_DefineMsg(14,23,25,' *** Press "END" to continue *** ');
  IO_DefineMsg(15,23,25,' *** Press "END" to continue *** ');
  OnCursor;
  IO_Edit(Retcode);
  Offcursor;
  IO_Resetfields;
  MILL_Y_N:=Str_to_INT(S34);
  IF ((MILL_Y_N=1) OR (MILL_Y_N=2)) THEN MILLING:=TRUE
  ELSE
  BEGIN
    MILLING:=FALSE;
    OnCursor;
    TempMessage(8,8,yellow+blink,red,'*************** ENTER EITHER YES [1] OR NO [2]
*******************');
   END;
 UNTIL MILLING;
 MATTE:=Str_to_real(S21);
 P3:=Str_to_real(S22);
 P1:=Str_to_real(S33);
 P6:=P1;
 P5:=P1;
 PT:=Str_to_real(S23);
 VOL:=Str_to_real(S24);
 VOL:=VOL/100*10800;
 F5:=Str_to_real(S25);
 F4:=119.6/60*F5;
 F5:=Str_to_real(S26)*F5;
 F7:=Str_to_real(S27)+Str_to_real(S28);
 DENS1:=Str_to_real(S29);
 PT1:=Str_to_real(S30);
 VOL1:=Str_to_real(S31);
```

```
 VOL1:=VOL1/100*9970;
 VT1:=Str_to_real(S32);
 VT1:=VT1/100*9970;
END;

PROCEDURE TIME2;
VAR S2,S3,S4,S6,S7:STRING;
   RETCODE:INTEGER;
BEGIN
 IF MILL_Y_N=1 THEN
 BEGIN
{   ClrScr;}
   FBox(6,3,74,21,YELLOW,5,2);
   Horizline(7,73,7,YELLOW,5,1);
   WriteCenter(5,WHITE,5,'SET CALCULATION TIME');
   WriteAt(10,9,WHITE,5,'What is the TIME right now ? (00:00 to 23:59)          :');
   WriteAt(10,10,WHITE,5,'When are you going to take your next readings ?        :');
   Horizline(7,73,12,YELLOW,5,1);
   WriteCenter(12,WHITE+BLINK,5,'MILLING TIME');
   WriteAt(10,14,WHITE,5,'When are you going to START milling ? (00:00 to 23:59)   :');
   WriteAt(10,15,WHITE,5,'When are you going to STOP milling ?                    :');
   Horizline(7,73,17,YELLOW,5,1);
   WriteCenter(17,WHITE+BLINK,5,'OPTION');
   WriteAt(10,19,WHITE,5,'Do you want to change some of the OTHER PARAMETERS [YES=1]');
   S2:='2';
   S3:='12';
   S4:='00';
   S6:='13';
   S7:='00';
   REPEAT
    I:=0;
    IO_SetFields(9);
    IO_soundbeeper(false);
    IO_AllowEsc(true);
    IO_DefineStr(1,9,2,9,2,67,9,S15,'##');
    IO_DefineStr(2,1,3,1,3,70,9,S16,'##');
    IO_DefineStr(3,2,4,2,4,67,10,S13,'##');
    IO_DefineStr(4,3,5,3,5,70,10,S14,'##');
    IO_DefineStr(5,4,6,4,6,67,14,S3,'##');
    IO_DefineStr(6,5,7,5,7,70,14,S4,'##');
    IO_DefineStr(7,6,8,6,8,67,15,S6,'##');
    IO_DefineStr(8,7,9,7,9,70,15,S7,'##');
```

```
 IO_DefineStr(9,8,1,8,1,70,19,S2,'#');
 IO_DefineMsg(1,23,21,' *** Press "END" to continue *** ');
 IO_DefineMsg(2,23,21,' *** Press "END" to continue *** ');
 IO_DefineMsg(3,23,21,' *** Press "END" to continue *** ');
 IO_DefineMsg(4,23,21,' *** Press "END" to continue *** ');
 IO_DefineMsg(5,12,21,' ** If you are already milling enter the CURRENT TIME ** ');
 IO_DefineMsg(6,23,21,' *** Press "END" to continue *** ');
 IO_DefineMsg(7,6,21,' ** If you are milling the whole time enter calculation END TIME ** ');
 IO_DefineMsg(8,23,21,' *** Press "END" to continue *** ');
 IO_DefineMsg(9,23,21,' *** Press "END" to continue *** ');
 Oncursor;
 IO_Edit(Retcode);
 Offcursor;
 IO_Resetfields;
 HOUR:=Str_to_int(S15);
 MIN:=Str_to_int(S16);
 TEST_TIME;
 HOUR:=Str_to_int(S13);
 MIN:=Str_to_int(S14);
 TEST_TIME;
 HOUR:=Str_to_int(S3);
 MIN:=Str_to_int(S4);
 TEST_TIME;
 HOUR:=Str_to_int(S6);
 MIN:=Str_to_int(S7);
 TEST_TIME;
 IF I>0 THEN
 BEGIN
   TIMER:=FALSE;
   OnCursor;
   TempMessage(6,8,yellow+blink,red,'******** THE TIME ENTERED MUST BE IN THE FORM
   00:00 TO 23:59 ********');
 END;
UNTIL TIMER;
HOUR:=(Str_to_int(S13)-Str_to_int(S15));
MIN:=(Str_to_int(S14)-Str_to_int(S16));
IF ((HOUR>=0) AND (MIN<0)) THEN MIN:=MIN+60;
IF ((HOUR<0) AND (MIN<0)) THEN
BEGIN
  HOUR:=HOUR+23;
  MIN:=MIN+60;
END;
```

```
  IF ((HOUR<0) AND (MIN>=0)) THEN HOUR:=HOUR+24;
  HOUR:=HOUR*60;
  T:=HOUR+MIN;
  HOUR:=(Str_to_int(S3)-Str_to_int(S15));
  MIN:=(Str_to_int(S4)-Str_to_int(S16));
  IF ((HOUR>=0) AND (MIN<0)) THEN MIN:=MIN+60;
  IF ((HOUR<0) AND (MIN<0)) THEN
  BEGIN
   HOUR:=HOUR+23;
   MIN:=MIN+60;
  END;
  IF ((HOUR<0) AND (MIN>=0)) THEN HOUR:=HOUR+24;
  HOUR:=HOUR*60;
  MTB:=HOUR+MIN;
  HOUR:=(Str_to_int(S6)-Str_to_int(S3));
  MIN:=(Str_to_int(S7)-Str_to_int(S4));
  IF ((HOUR>=0) AND (MIN<0)) THEN MIN:=MIN+60;
  IF ((HOUR<0) AND (MIN<0)) THEN
  BEGIN
   HOUR:=HOUR+23;
   MIN:=MIN+60;
  END;
  IF ((HOUR<0) AND (MIN>=0)) THEN HOUR:=HOUR+24;
  HOUR:=HOUR*60;
  MTE:=HOUR+MIN;
  MTE:=MTE+MTB;
  YES:=Str_to_Int(S2);
 END
 ELSE
 BEGIN
{  ClrScr;}
  FBox(6,3,74,17,YELLOW,5,2);
  Horizline(7,73,7,YELLOW,5,1);
  WriteCenter(5,WHITE,5,'SET CALCULATION TIME');
  WriteAt(10,9,WHITE,5,'What is the TIME right now ? (00:00 to 23:59)          :');
  WriteAt(10,10,WHITE,5,'When are you going to take your next readings ?        :');
  Horizline(7,73,12,YELLOW,5,1);
  WriteCenter(12,WHITE+BLINK,5,'OPTION');
  WriteAt(10,14,WHITE,5,'Do you want to change some of the OTHER PARAMETERS [YES=1]');
  S2:='2';
  REPEAT
   I:=0;
```

```
 IO_SetFields(5);
 IO_soundbeeper(false);
 IO_AllowEsc(true);
 IO_DefineStr(1,5,2,5,2,67,9,S15,'##');
 IO_DefineStr(2,1,3,1,3,70,9,S16,'##');
 IO_DefineStr(3,2,4,2,4,67,10,S13,'##');
 IO_DefineStr(4,3,5,3,5,70,10,S14,'##');
 IO_DefineStr(5,4,1,4,1,70,14,S2,'#');
 IO_DefineMsg(1,23,17,' *** Press "END" to continue *** ');
 IO_DefineMsg(2,23,17,' *** Press "END" to continue *** ');
 IO_DefineMsg(3,23,17,' *** Press "END" to continue *** ');
 IO_DefineMsg(4,23,17,' *** Press "END" to continue *** ');
 IO_DefineMsg(5,23,17,' *** Press "END" to continue *** ');
 Oncursor;
 IO_Edit(Retcode);
 Offcursor;
 IO_Resetfields;
 HOUR:=Str_to_int(S15);
 MIN:=Str_to_int(S16);
 TEST_TIME;
 HOUR:=Str_to_int(S13);
 MIN:=Str_to_int(S14);
 TEST_TIME;
 IF I>0 THEN
 BEGIN
   TIMER:=FALSE;
   OnCursor;
   TempMessage(6,8,yellow+blink,red,'******** THE TIME ENTERED MUST BE IN THE FORM
   00:00 TO 23:59 ********');
 END;
UNTIL TIMER;
HOUR:=(Str_to_int(S13)-Str_to_int(S15));
MIN:=(Str_to_int(S14)-Str_to_int(S16));
IF ((HOUR>=0) AND (MIN<0)) THEN MIN:=MIN+60;
IF ((HOUR<0) AND (MIN<0)) THEN
BEGIN
 HOUR:=HOUR+23;
 MIN:=MIN+60;
END;
IF ((HOUR<0) AND (MIN>=0)) THEN HOUR:=HOUR+24;
HOUR:=HOUR*60;
T:=HOUR+MIN;
```

```
   YES:=Str_to_Int(S2);
  END;
END;

PROCEDURE SIMPLE3;
VAR S21,S22,S23,S25,S26,S27,S28,S29,S30,S31,S32,S33,S34:STRING;
   RETCODE:INTEGER;
   MILLING:BOOLEAN;
BEGIN
{ ClrScr;}
  FBox(1,1,80,25,yellow,1,2);
  Horizline(2,79,5,yellow,1,1);
  WriteCenter(3,yellow,1,'MILL, TANK 1506 & TANK 1102');
  WriteAt(5,7,white,1,'Are you busy milling/are you going to mill now ? [YES=1/NO=2]');
  WriteAt(5,8,white,1,'Matte feedrate to the mill [t/h]]');
  WriteAt(5,9,white,1,'Desired pulp density (PD) of mixture leaving the mill [kg/l]');
  WriteAt(5,11,white,1,'Pulp density (PD) of the spent electrolyte (SE) [kg/l]');
  WriteAt(5,12,white,1,'The flowrate of spent electrolyte (SE) to tank 1506 [l/min]');
  WriteAt(5,13,white,1,'The actual pulp density (PD) in tank 1506 [kg/l]');
  WriteAt(5,14,white,1,'The pulp flowrate from tank 1506 to tank 1102 [l/min]');
  WriteAt(5,15,white,1,'The actual level of the pulp in tank 1506 [%]');
  WriteAt(5,16,white,1,'Amount of times the solids from press 1407 will be washed');
  WriteAt(5,17,white,1,'SE flowrate used to wash solids to tank 1506 [l/min]');
  WriteAt(5,19,white,1,'Pulp flowrate from tank 1102 to the autoclave 1110A [l/min]');
  WriteAt(5,20,white,1,'Pulp flowrate from tank 1102 to the autoclave 1110B [l/min]');
  WriteAt(5,21,white,1,'The actual pulp density (PD) in tank 1102 [kg/l]');
  WriteAt(5,22,white,1,'The spent electrolyte (SE) flowrate to tank 1102 [l/min]');
  WriteAt(5,23,white,1,'The actual level of the pulp in tank 1102 [%]');
  S34:='1';
  S21:='3.3';
  S22:='3.4';
  S33:='1.20';
  S23:='48.7';
  S25:='75';
  S26:='1';
  S27:='7.5';
  S28:='0';
  S29:='43';
  S30:='1.6';
  S31:='22.3';
  S32:='80';
  REPEAT
```

```
IO_SetFields(15);
IO_soundbeeper(false);
IO_AllowEsc(true);
IO_DefineStr(1,15,2,15,2,70,7,S34,'#');
IO_DefineStr(2,1,3,1,3,70,8,S21,'####');
IO_DefineStr(3,2,4,2,4,70,9,S22,'#####');
IO_DefineStr(4,3,5,3,5,70,11,S33,'#####');
IO_DefineStr(5,4,6,4,6,70,12,S23,'#####');
IO_DefineStr(6,5,7,5,7,70,13,S10,'#####');
IO_DefineStr(7,6,8,6,8,70,14,S12,'#####');
IO_DefineStr(8,7,9,7,9,70,15,S25,'#####');
IO_DefineStr(9,8,10,8,10,70,16,S26,'#####');
IO_DefineStr(10,9,11,9,11,70,17,S27,'#####');
IO_DefineStr(11,10,12,10,12,70,19,S28,'#####');
IO_DefineStr(12,11,13,11,13,70,20,S29,'#####');
IO_DefineStr(13,12,14,12,14,70,21,S30,'#####');
IO_DefineStr(14,13,15,13,15,70,22,S31,'#####');
IO_DefineStr(15,14,1,14,1,70,23,S32,'#####');
IO_DefineMsg(1,23,25,' *** Press "END" to continue *** ');
IO_DefineMsg(2,23,25,' *** Press "END" to continue *** ');
IO_DefineMsg(3,23,25,' *** Press "END" to continue *** ');
IO_DefineMsg(4,23,25,' *** Press "END" to continue *** ');
IO_DefineMsg(5,23,25,' *** Press "END" to continue *** ');
IO_DefineMsg(6,23,25,' *** Press "END" to continue *** ');
IO_DefineMsg(7,23,25,' *** Press "END" to continue *** ');
IO_DefineMsg(8,23,25,' *** Press "END" to continue *** ');
IO_DefineMsg(9,23,25,' *** Press "END" to continue *** ');
IO_DefineMsg(10,23,25,' *** Press "END" to continue *** ');
IO_DefineMsg(11,23,25,' *** Press "END" to continue *** ');
IO_DefineMsg(12,23,25,' *** Press "END" to continue *** ');
IO_DefineMsg(13,23,25,' *** Press "END" to continue *** ');
IO_DefineMsg(14,23,25,' *** Press "END" to continue *** ');
IO_DefineMsg(15,23,25,' *** Press "END" to continue *** ');
OnCursor;
IO_Edit(Retcode);
Offcursor;
IO_Resetfields;
MILL_Y_N:=Str_to_INT(S34);
IF ((MILL_Y_N=1) OR (MILL_Y_N=2)) THEN MILLING:=TRUE
ELSE
BEGIN
  MILLING:=FALSE;
```

```
    OnCursor;
    TempMessage(8,8,yellow+blink,red,'*************** ENTER EITHER YES [1] OR NO [2]
*****************');
   END;
  UNTIL MILLING;
  MATTE:=Str_to_real(S21);
  P3:=Str_to_real(S22);
  P1:=Str_to_real(S33);
  P6:=P1;
  P5:=P1;
  F1:=Str_to_real(S23);
  VOL:=Str_to_real(S25);
  VOL:=VOL/100*10800;
  F5:=Str_to_real(S26);
  F4:=119.6/60*F5;
  F5:=Str_to_real(S27)*F5;
  F7:=Str_to_real(S28)+Str_to_real(S29);
  DENS1:=Str_to_real(S30);
  F6:=Str_to_real(S31);
  VOL1:=Str_to_real(S32);
  VOL1:=VOL1/100*9970;
END;

PROCEDURE PROCESS;
VAR S1,S2,S3,S4,S5,S6:STRING;
    RETCODE:INTEGER;
BEGIN
{ ClrScr;}
  FBox(1,3,80,21,YELLOW,0,2);
  Horizline(2,79,7,YELLOW,0,1);
  WriteCenter(5,WHITE,0,'INFORMATION FOR THE MILL, TANK 1506 AND TANK 1102');
  WriteAt(5,9,WHITE,0,'Density of the matte (PD) [kg/l]');
  WriteAt(5,10,WHITE,0,'Density of the demineralised water added to the mill [kg/l]');
  WriteAt(5,12,WHITE,0,'The pulp density (PD) of solids from press 1407 [kg/l]');
  Horizline(2,79,14,YELLOW,0,1);
  WriteCenter(14,WHITE+BLINK,0,'CALCULATION OPTIONS');
  WriteAt(5,16,WHITE,0,'Step size in minutes for the Runga-Kutta calculation [min]');
  WriteAt(5,17,WHITE,0,'Iteration limit (tank 1506) for Golden Section Search procedure');
  WriteAt(5,18,WHITE,0,'Iteration limit (tank 1102) for Golden Section Search procedure');
  S1:='5.3';
  S2:='1.0';
  S3:='4.5';
```

```
 S4:='20';
 S5:='20';
 S6:='5';
 IO_SetFields(6);
 IO_soundbeeper(false);
 IO_AllowEsc(true);
 IO_DefineStr(1,6,2,6,2,70,9,S1,'####');
 IO_DefineStr(2,1,3,1,3,70,10,S2,'#####');
 IO_DefineStr(3,2,4,2,4,70,12,S3,'#####');
 IO_DefineStr(4,3,5,3,5,70,16,S4,'####');
 IO_DefineStr(5,4,6,4,6,70,17,S5,'####');
 IO_DefineStr(6,5,1,5,1,70,18,S6,'####');
 IO_DefineMsg(1,23,21,' *** Press "END" to continue *** ');
 IO_DefineMsg(2,23,21,' *** Press "END" to continue *** ');
 IO_DefineMsg(3,23,21,' *** Press "END" to continue *** ');
 IO_DefineMsg(4,23,21,' *** Press "END" to continue *** ');
 IO_DefineMsg(5,23,21,' *** Press "END" to continue *** ');
 IO_DefineMsg(6,23,21,' *** Press "END" to continue *** ');
 OnCursor;
 IO_Edit(Retcode);
 Offcursor;
 IO_Resetfields;
 PM:=Str_to_real(S1);
 PW:=Str_to_real(S2);
 P4:=Str_to_real(S3);
 H:=Str_to_int(S4);
 C1:=Str_to_int(S5);
 C2:=Str_to_int(S6);
END;

PROCEDURE LIMIT;
VAR S1,S2,S3,S4,S5,S6,S7,S8,S9,S11:STRING;
   RETCODE:INTEGER;
BEGIN
{ ClrScr;}
 FBox(3,2,78,24,YELLOW,1,2);
 Horizline(4,77,6,YELLOW,1,1);
 WriteCenter(4,YELLOW,1,'LIMITING CONDITIONS');
 WriteAt(8,9,WHITE,1,'The MINIMUM flowrate of spent(SE) to tank 1506 [l/min]');
 WriteAt(8,10,WHITE,1,'The MAXIMUM flowrate of spent(SE) to tank 1506 [l/min]');
 WriteAt(8,12,WHITE,1,'The MINIMUM level of tank 1506 [%]');
 WriteAt(8,13,WHITE,1,'The MAXIMUM level of tank 1506 [%]');
```

```
WriteAt(8,15,WHITE,1,'The MINIMUM pulp flowrate from tank 1506 to 1102 [l/min]');
WriteAt(8,16,WHITE,1,'The MAXIMUM pulp flowrate from tank 1506 to 1102 [l/min]');
WriteAt(8,18,WHITE,1,'The MINIMUM flowrate of spent(SE) to tank 1102 [l/min]');
WriteAt(8,19,WHITE,1,'The MAXIMUM flowrate of spent(SE) to tank 1102 [l/min]');
WriteAt(8,21,WHITE,1,'The MINIMUM level of tank 1102 [%]');
WriteAt(8,22,WHITE,1,'The MAXIMUM level of tank 1102 [%]');
S1:='0';
S2:='116';
S3:='50';
S4:='95';
S5:='0';
S6:='218';
S7:='0';
S8:='228';
S9:='45';
S11:='100';
IO_SetFields(10);
IO_soundbeeper(false);
IO_AllowEsc(true);
IO_DefineStr(1,10,2,10,2,70,9,S1,'###');
IO_DefineStr(2,1,3,1,3,70,10,S2,'###');
IO_DefineStr(3,2,4,2,4,70,12,S3,'####');
IO_DefineStr(4,3,5,3,5,70,13,S4,'####');
IO_DefineStr(5,4,6,4,6,70,15,S5,'###');
IO_DefineStr(6,5,7,5,7,70,16,S6,'###');
IO_DefineStr(7,6,8,6,8,70,18,S7,'###');
IO_DefineStr(8,7,9,7,9,70,19,S8,'###');
IO_DefineStr(9,8,10,8,10,70,21,S9,'####');
IO_DefineStr(10,9,1,9,1,70,22,S11,'####');
IO_DefineMsg(1,23,24,' *** Press "END" to continue *** ');
IO_DefineMsg(2,23,24,' *** Press "END" to continue *** ');
IO_DefineMsg(3,23,24,' *** Press "END" to continue *** ');
IO_DefineMsg(4,23,24,' *** Press "END" to continue *** ');
IO_DefineMsg(5,23,24,' *** Press "END" to continue *** ');
IO_DefineMsg(6,23,24,' *** Press "END" to continue *** ');
IO_DefineMsg(7,23,24,' *** Press "END" to continue *** ');
IO_DefineMsg(8,23,24,' *** Press "END" to continue *** ');
IO_DefineMsg(9,23,24,' *** Press "END" to continue *** ');
IO_DefineMsg(10,23,24,' *** Press "END" to continue *** ');
Oncursor;
IO_Edit(Retcode);
Offcursor;
```

```
 IO_Resetfields;
 F1MIN:=Str_to_real(S1);
 F1MAX:=Str_to_real(S2);
 VMIN:=Str_to_real(S3);
 VMIN:=VMIN/100*10800;
 VTOT:=Str_to_real(S4);
 VTOT:=VTOT/100*10800;
 F2MIN:=Str_to_real(S5);
 F2MAX:=Str_to_real(S6);
 F6MIN:=Str_to_real(S7);
 F6MAX:=Str_to_real(S8);
 V1MIN:=Str_to_real(S9);
 V1MIN:=V1MIN/100*9970;
 V1MAX:=Str_to_real(S11);
 V1MAX:=V1MAX/100*9970;
END;

PROCEDURE TEST;
BEGIN
 IF F2<F2MIN THEN F2:=F2MIN;
 IF F2>F2MAX THEN F2:=F2MAX;
 IF F6<F6MIN THEN F6:=F6MIN;
 IF F6>F6MAX THEN F6:=F6MAX;
 IF F1<F1MIN THEN F1:=F1MIN;
 IF F1>F1MAX THEN F1:=F1MAX;
END;

PROCEDURE Define_Menu;
Begin
 With M1 do
  Begin
  Offcursor;
   Heading1:='INPUTS FOR CONTROL';
   Heading2:='Choose option';
   Topic[1]:='   Determine SETTINGS - Mill time UNKNOWN';
   Topic[2]:='   Determine SETTINGS - Mill time KNOWN';
   Topic[3]:='   PREDICT input SETTINGS';
   Topic[4]:='   Quit the PROGRAM';
   TotalPicks:=4;
   PicksPerLine:=1;
   Addprefix:=1;
   TopleftXY[1]:=0;
```

```
  TopleftXY[2]:=5;
  Boxtype:=5;
   IF BaseOfScreen = $B800 THEN
    Begin
     Colors[1] := white;          {hi forground}
     Colors[2] := red;           {hi background}
     Colors[3] := lightgray;      {lo foreground}
     Colors[4] := blue;          {lo background}
     Colors[5] := lightcyan;      {box color}
    End
   ELSE
    Begin
     Colors[1] := white;          {hi forground}
     Colors[2] := black;          {hi background}
     Colors[3] := black;          {lo foreground}
     Colors[4] := lightgray;      {lo background}
     Colors[5] := white;          {box color}
    End;
   AllowEsc := false;           {inactivate the escape key}
   Margins := 5;
  End;
End;

PROCEDURE CONSTANTS;
BEGIN
  PM:=5.3;
  PW:=1.0;
  P4:=4.5;
  H:=5;
  C1:=20;
  C2:=20;
  F1MIN:=0;
  F1MAX:=116;
  VMIN:=50/100*10800;
  VTOT:=95/100*10800;
  F2MIN:=0;
  F2MAX:=218;
  F6MIN:=0;
  F6MAX:=228;
  V1MIN:=45/100*9970;
  V1MAX:=100/100*9970;
END;
```

```
PROCEDURE CHOICE1;
BEGIN
 CHOICE:=FALSE;
 RK:=TRUE;
 S10:='2.0';
 S15:='12';
 S16:='00';
 S13:='13';
 S14:='00';
 SIMPLE1;
 TIME1;
 IF YES=1 THEN
 BEGIN
  PROCESS;
  LIMIT;
 END
 ELSE CONSTANTS;
 DENS:=Str_to_Real(S10);
 P2:=DENS;
END;

PROCEDURE CHOICE2;
BEGIN
 CHOICE:=FALSE;
 RK:=FALSE;
 S10:='2.0';
 S15:='12';
 S16:='00';
 S13:='13';
 S14:='00';
 SIMPLE2;
 TIME2;
 IF YES=1 THEN
 BEGIN
  PROCESS;
  LIMIT;
 END
 ELSE CONSTANTS;
 DENS:=Str_to_Real(S10);
 P2:=DENS;
END;
```

```
PROCEDURE CHOICE3;
BEGIN
 CHOICE:=TRUE;
 S10:='2.0';
 S12:='29.4';
 S15:='12';
 S16:='00';
 S13:='13';
 S14:='00';
 SIMPLE3;
 TIME2;
 IF YES=1 THEN
 BEGIN
  PROCESS;
  LIMIT;
 END
 ELSE CONSTANTS;
 DENS:=Str_to_Real(S10);
 P2:=DENS;
 F2:=Str_to_real(S12);
 TEST;
END;

PROCEDURE Finish;
VAR ANSW:CHAR;
Begin
 REPEAT
 ClrScr;
 FBox(12,8,68,14,YELLOW,3,2);
 WriteAt(15,10,yellow+blink,red,'***************** END OF PROGRAM ******************');
 WRITEAT(16,12,4,3,'Are you sure you want to quit the program [Y,N] ? ');
 ANSW:=UPCASE(READKEY);
 UNTIL ANSW In['Y','N'];
 CASE ANSW OF
  'Y':REP:=TRUE;
  'N':REP:=FALSE;
 END;
 IF REP THEN
 BEGIN
  Oncursor; Halt;
 END;
END;
```

```
PROCEDURE Input_ORDER;
Begin
 Case Main_Choice of
 1 :CHOICE1;
 2 :CHOICE2;
 3 :CHOICE3;
 4 :Finish;
 End;
End;

PROCEDURE INPUT;
BEGIN
{ CLRSCR;}
 MAIN_CHOICE:=1;
 DEFINE_MENU;
 DisplayMenu(M1,false,Main_choice,Error);
 INPUT_ORDER;
END;

END.
```

```
UNIT RK_GOLD;

INTERFACE

USES CRT,VARIABLE;

VAR P7,V1,V,MF,WF,F3,P7_T,P2_T,V1_T,V_T,F3_T:REAL;
   F1_T,F2_T,F6_T:REAL;
   TB,TE:INTEGER;
   TT2:BOOLEAN;

PROCEDURE TANK_1102_CALC;
PROCEDURE RUNGA2_1102;
PROCEDURE RUNGA1_1102;
PROCEDURE RUNGA2_1100;
PROCEDURE RUNGA1_1100;
PROCEDURE MILL_CALC;

IMPLEMENTATION
```

```
VAR P,X,FX,P0,X0,FX0:REAL;
   TYD:INTEGER;
   TT1:BOOLEAN;

PROCEDURE MILL_CALC;
BEGIN
 MF:=MATTE*1000/60;
 WF:=MF*(1-(P3/PM))/(P3-PW);
 F3:=WF+MF/PM;
END;

PROCEDURE VERGELYK2(X0,V:REAL);   {*Differential equation tank 1506*}
BEGIN
 P0:=(F1*(P1-X0)+F3*(P3-X0)+F4*(P4-X0)+F5*(P5-X0))/V;
END;

PROCEDURE RUNGA2_1100;
BEGIN
 V:=V+(F1+F3+F4+F5-F2)*H;
END;

PROCEDURE RUNGA1_1100;
VAR X1,X2,k0,k1,k2,k3:REAL;
BEGIN
 X0 := P2;
 VERGELYK2(X0,V);
 k0 := H*P0;
 X1 := X0+k0/2;
 VERGELYK2(X1,V);
 k1 := H*P0;
 k2 := k1;
 X2 := X0+k2;
 VERGELYK2(X2,V);
 k3 := H*P0;
 P2 := P2+((k0+2*k1+2*k2+k3)/6);
END;

PROCEDURE RUNGA_1100;          {*Runga-Kutta procedure for tank 1506*}
BEGIN
 V:=VOL;
 P2:=DENS;
```

```
TYD:=H;
IF RK THEN                {*Mill time UNKNOWN*}
BEGIN       {*Program will only calculate for one milling cycle*}
 IF VOL<=VMIN THEN
 BEGIN
  MILL_CALC;
  REPEAT
   RUNGA2_1100;
   RUNGA1_1100;
   IF V>=VTOT THEN F3:=0;
   TYD := TYD+H;
  UNTIL (TYD>T);
 END
 ELSE
 BEGIN
  F3:=0;
  MF:=0;
  WF:=0;
  REPEAT
   RUNGA2_1100;
   RUNGA1_1100;
   IF V<=VMIN THEN MILL_CALC;
   IF V>=VTOT THEN F3:=0;
   TYD := TYD+H;
  UNTIL (TYD>T);
 END;
END
ELSE                {*Mill time KNOWN*}
BEGIN       {*Program will only calculate for one milling cycle*}
 IF MILL_Y_N=1 THEN
 BEGIN
  REPEAT
   IF ((TYD>MTB) AND (TYD<=MTE)) THEN MILL_CALC
   ELSE F3:=0;
   RUNGA2_1100;
   RUNGA1_1100;
   TYD := TYD+H;
  UNTIL (TYD>T);
 END;
 IF MILL_Y_N=2 THEN
 BEGIN
  F3:=0;
```

```
    MF:=0;
    WF:=0;
    REPEAT
     RUNGA2_1100;
     RUNGA1_1100;
     TYD := TYD+H;
    UNTIL (TYD>T);
   END;
 END;
END;

PROCEDURE GOLDEN_1100; {*Determine optimum F1 (SE) flow to tank 1506*}
VAR AK0,BK0,FS0,LK0,L00,DEL0,F110,F120,FX10,FX20:REAL;
   K0:INTEGER;
BEGIN              {*Golden Section search (GSS) procedure*}
 K0:=0;
 AK0:=F1MIN;       {*Minimum value for interval*}
 BK0:=(VTOT-VOL)/T+F2-(F3+F4+F5); {*Maximum value for interval (F1)*}
 IF ((BK0>F1MAX) OR (BK0<F1MIN)) THEN BK0:=F1MAX;
 L00:=BK0-AK0;
 FS0:=(3-SQRT(5))/2;
 LK0:=L00;
 F110:=AK0+FS0*LK0;
 F1:=F110;
 RUNGA_1100;
 FX10:=P2;
 F120:=BK0-FS0*LK0;
 F1:=F120;
 RUNGA_1100;
 FX20:=P2;
 REPEAT
  K0:=K0+1;
  LK0:=EXP(K0*LN(1-FS0))*L00;
  IF (ABS(PT-FX10)>ABS(PT-FX20)) THEN
  BEGIN
   FX0:=FX20;
   IF (ABS(PT-FX0)<0.0005) THEN
   BEGIN
    F1:=F120;
    EXIT;
   END;
   AK0:=F110;
```

```
    F110:=F120;
    FX10:=FX20;
    F120:=BK0-FS0*LK0;
    F1:=F120;
    RUNGA_1100;
    FX20:=P2;
   END
   ELSE
   BEGIN
    FX0:=FX10;
    IF (ABS(PT-FX0)<0.0005) THEN
    BEGIN
     F1:=F110;
     EXIT;
    END;
    BK0:=F120;
    F120:=F110;
    FX20:=FX10;
    F110:=AK0+FS0*LK0;
    F1:=F110;
    RUNGA_1100;
    FX10:=P2;
   END;
  UNTIL K0>C1;
END;

PROCEDURE VERGELYK1(X,V:REAL);   {*Differential equation for tank 1102*}
BEGIN
  P:=(F6/V1*(P6-X)+F2/V1*(P2-X));
END;

PROCEDURE RUNGA2_1102;
BEGIN
  V1:=V1+(F6+F2-F7)*H;
END;

PROCEDURE RUNGA1_1102;       {*Runga-Kutta procedure for tank 1102*}
VAR X1,X2,k0,k1,k2,k3:REAL;
BEGIN
  X := P7;
  VERGELYK1(X,V1);
  k0 := H*P;
```

```
 X1 := X+k0/2;
 VERGELYK1(X1,V1);
 k1 := H*P;
 k2 := k1;
 X2 := X+k2;
 VERGELYK1(X2,V1);
 k3 := H*P;
 P7 := P7+((k0+2*k1+2*k2+k3)/6);
END;

PROCEDURE RUNGA_1102;  {*Runga-Kutta procedure for tank 1102 and 1506*}
BEGIN
 P7:=DENS1;
 V1:=VOL1;
 V:=VOL;
 P2:=DENS;
 TYD:=H;
 TT1:=TRUE;
 TT2:=TRUE;
 IF RK THEN          {*Milling time UNKNOWN*}
 BEGIN
  IF VOL<=VMIN THEN   {*Start milling immediately*}
  BEGIN
   TT1:=FALSE;
   TB:=0;
   MILL_CALC;
   REPEAT      {*Do Runga-Kutta calculation for each time step*}
    RUNGA2_1102;
    RUNGA1_1102;
    RUNGA2_1100;
    RUNGA1_1100;
    IF V>=VTOT THEN
    BEGIN
     F3:=0;
     IF TT2 THEN TE:=TYD;
     TT2:=FALSE;
    END;
    TYD := TYD+H;
   UNTIL (TYD>T);
  END
  ELSE         {*Start milling during time period*}
  BEGIN
```

```
  F3:=0;
  MF:=0;
  WF:=0;
  REPEAT
    RUNGA2_1102;
    RUNGA1_1102;
    RUNGA2_1100;
    RUNGA1_1100;
    IF V<=VMIN THEN
    BEGIN
      MILL_CALC;
      IF TT1 THEN TB:=TYD;
      TT1:=FALSE;
    END;
    IF V>=VTOT THEN
    BEGIN
      F3:=0;
      IF TT2 THEN TE:=TYD;
      TT2:=FALSE;
    END;
    TYD := TYD+H;
  UNTIL (TYD>T);
 END;
END
ELSE                {*Mill time KNOWN*}
BEGIN
 IF MILL_Y_N=1 THEN
 BEGIN
  REPEAT
    RUNGA2_1102;
    RUNGA1_1102;
    IF ((TYD>MTB) AND (TYD<=MTE)) THEN MILL_CALC
    ELSE F3:=0;
    RUNGA2_1100;
    RUNGA1_1100;
    TYD := TYD+H;
  UNTIL (TYD>T);
 END;
 IF MILL_Y_N=2 THEN
 BEGIN
  F3:=0;
  MF:=0;
```

```
    WF:=0;
    REPEAT
      RUNGA2_1102;
      RUNGA1_1102;
      RUNGA2_1100;
      RUNGA1_1100;
      TYD := TYD+H;
    UNTIL (TYD>T);
  END;
 END;
END;

PROCEDURE TEST;      {*Test values given from GSS to F2 and F6*}
BEGIN
 IF F2<F2MIN THEN F2:=F2MIN;
 IF F2>F2MAX THEN F2:=F2MAX;
END;

PROCEDURE GOLDEN_1102; {*Golden Section search procedure for tank 1102*}
VAR AK,BK,FS,LK,L0,DEL,F11,F12,F21,F22,FX1,FX2:REAL;
   K:INTEGER;
BEGIN         {*Determine optimum settings for F2 and F6*}
 K:=0;
 AK:=F6MIN;   {*Minimum value for interval*}
 BK:=F6MAX;   {*Maximum value for interval*}
 L0:=BK-AK;
 FS:=(3-SQRT(5))/2;
 DEL:=(VT1-VOL1)/T+F7;  {*Maximum value for F2+F6*}
 LK:=L0;
 F11:=AK+FS*LK;
 F21:=DEL-F11;
 F6:=F11;
 F2:=F21;
 TEST;
 GOLDEN_1100;
 RUNGA_1102;
 FX1:=P7;
 F12:=BK-FS*LK;
 F22:=DEL-F12;
 F6:=F12;
 F2:=F22;
 TEST;
```

```
GOLDEN_1100;
RUNGA_1102;
FX2:=P7;
REPEAT
 K:=K+1;
 LK:=EXP(K*LN(1-FS))*L0;
 IF (ABS(PT1-FX1)>ABS(PT1-FX2)) THEN
 BEGIN
  FX:=FX2;
  IF (ABS(PT1-FX)<0.0005) THEN
  BEGIN
   F6:=F12;
   F2:=F22;
   TEST;
   EXIT;
  END;
  AK:=F11;
  F11:=F12;
  FX1:=FX2;
  F12:=BK-FS*LK;
  F22:=DEL-F12;
  F6:=F12;
  F2:=F22;
  TEST;
  GOLDEN_1100;
  RUNGA_1102;
  FX2:=P7;
 END
 ELSE
 BEGIN
  FX:=FX1;
  IF (ABS(PT1-FX)<0.0005) THEN
  BEGIN
   F6:=F11;
   F2:=F21;
   TEST;
   EXIT;
  END;
  BK:=F12;
  F12:=F11;
  FX2:=FX1;
  F11:=AK+FS*LK;
```

```
    F21:=DEL-F11;
    F6:=F11;
    F2:=F21;
    TEST;
    GOLDEN_1100;
    RUNGA_1102;
    FX1:=P7;
   END;
 UNTIL K>C2;
END;

PROCEDURE TANK_1102_CALC;
BEGIN
 GOLDEN_1102;
 P7:=FX;
 P2:=FX0;
 P7_T:=P7;
 P2_T:=P2;
 V1_T:=V1;
 V_T:=V;
 F1_T:=F1;
 F3_T:=F3;
 F2_T:=F2;
 F6_T:=F6;
END;

END.
```

```
UNIT TRIAL;

INTERFACE

USES CRT,VARIABLE,RK_GOLD;

VAR VMIN_1100,VMAX_1100,VMIN_1102,VMAX_1102:BOOLEAN;
   TMIN,TMAX,T1MIN,T1MAX:INTEGER;

PROCEDURE OPERATOR;

IMPLEMENTATION
```

```
VAR TYD:INTEGER;
   N1,N2,N3,N4:BOOLEAN;

PROCEDURE MINMAX;
BEGIN
 IF N1 THEN
 BEGIN
  IF V>VTOT THEN
  BEGIN
   VMAX_1100:=TRUE;
   TMAX:=TYD-H;
   N1:=FALSE;
  END;
 END;
 IF N2 THEN
 BEGIN
  IF V<VMIN THEN
  BEGIN
   VMIN_1100:=TRUE;
   TMIN:=TYD-H;
   N2:=FALSE;
  END;
 END;
 IF N3 THEN
 BEGIN
  IF V1>V1MAX THEN
  BEGIN
   VMAX_1102:=TRUE;
   T1MAX:=TYD-H;
   N3:=FALSE;
  END;
 END;
 IF N4 THEN
 BEGIN
  IF V1<V1MIN THEN
  BEGIN
   VMIN_1102:=TRUE;
   T1MIN:=TYD-H;
   N4:=FALSE;
  END;
 END;
END;
```

```
PROCEDURE OPERATOR; {*Use predicted values to determine end conditions*}
BEGIN
 TT2:=TRUE;
 N1:=TRUE;
 N2:=TRUE;
 N3:=TRUE;
 N4:=TRUE;
 P7:=DENS1;
 V1:=VOL1;
 V:=VOL;
 P2:=DENS;
 TYD:=H;
 IF MILL_Y_N=1 THEN
 BEGIN
  REPEAT
   RUNGA2_1102;
   RUNGA1_1102;
   IF ((TYD>MTB) AND (TYD<=MTE)) THEN MILL_CALC
   ELSE F3:=0;
   RUNGA2_1100;
   RUNGA1_1100;
   MINMAX;
   TYD := TYD+H;
  UNTIL (TYD>T);
 END;
 IF MILL_Y_N=2 THEN
 BEGIN
  F3:=0;
  MF:=0;
  WF:=0;
  REPEAT
   RUNGA2_1102;
   RUNGA1_1102;
   RUNGA2_1100;
   RUNGA1_1100;
   MINMAX;
   TYD := TYD+H;
  UNTIL (TYD>T);
 END;
 P2_T:=P2;
 P7_T:=P7;
 V_T:=V;
```

```
 V1_T:=V1;
 F1_T:=F1;
 F3_T:=F3;
 F2_T:=F2;
 F6_T:=F6;
END;

END.
```

```
UNIT GRAPHICS;

INTERFACE

USES VARIABLE,CRT,RK_GOLD,TRIAL;

VAR PD:BOOLEAN;

PROCEDURE GRAPH_D;

IMPLEMENTATION

USES GRAPH;

VAR Y_1,Y1_1,X_1,Y,Y1,X:INTEGER;
   Ymax,Xmax:WORD;
   TYD:REAL;

PROCEDURE GRAPH_INITIAL;
VAR grDriver,grMode,YP,YP1:INTEGER;
   Xmid,Ymid:WORD;
   S:STRING[3];
BEGIN
 ClrScr;
 grDriver:=Detect;
 Initgraph(grDriver,grMode,'BGI');
 Xmax:=GetMaxX;
 Xmid:=(Round(Xmax*(1-40/640)) div 2);
 Ymax:=GetMaxY;
 Ymid:=(Ymax div 2);
 SetColor(3);
```

```
 SetLineStyle(0,0,3);
 Rectangle(Round(20/640*Xmax),Round(60/480*Ymax),Round(Xmax*(1-20/640)),Round(Ymax*(1-
20/480)));
  SetColor(7);
  SetLineStyle(0,0,1);
  Line(Round(80/640*Xmax),Round(Ymax*(1-40/480)),Round(Xmax*(1-40/640)),Round(Ymax*(1-
40/480)));
  Line(Round(80/640*Xmax),Round(Ymax*(1-40/480)),Round(80/640*Xmax),Round(80/480*Ymax));
  OutTextXY(Round(80/640*Xmax),Round(Ymax*(1-35/480)),'0');
  IF NOT(TT2) THEN Str(TE:5,S)
  ELSE Str(T:5,S);
  IF CHOICE THEN Str(T:5,S);
  OutTextXY(Round(Xmax*(1-65/640)),Round(Ymax*(1-35/480)),S);
  OutTextXY(Xmid,Round(Ymax*(1-32/480)),'Time [min]');
  IF PD THEN
  BEGIN
    OutTextXY(Round(45/640*Xmax),Ymid-5,'PD');
    OutTextXY(Round(30/640*Xmax),Ymid+5,'[kg/l]');
    OutTextXY(Round(50/640*Xmax),Round(Ymax*(1-40/480)),'1.2');
    OutTextXY(Round(50/640*Xmax),Round(80/480*Ymax),'2.2');
    YP:=ROUND(Ymax-(PT-1.2)/(2.2-1.2)*(Ymax*(1-120/480))-40/480*Ymax);
    YP1:=ROUND(Ymax-(PT1-1.2)/(2.2-1.2)*(Ymax*(1-120/480))-40/480*Ymax);
    SetLineStyle(1,0,1);
    Line(Round(80/640*Xmax),YP,Round(Xmax*(1-40/640)),YP);
    Line(Round(80/640*Xmax),YP1,Round(Xmax*(1-40/640)),YP1);
  END
  ELSE
  BEGIN
    OutTextXY(Round(45/640*Xmax),Ymid-5,'Vol');
    OutTextXY(Round(45/640*Xmax),Ymid+5,'[l]');
    OutTextXY(Round(30/640*Xmax),Round(Ymax*(1-40/480)),'3 000');
    OutTextXY(Round(30/640*Xmax),Round(80/480*Ymax),'10 800');
    YP1:=ROUND(Ymax-(VT1-3000)/(7000)*(Ymax*(1-120/480))-40/480*Ymax);
    SetLineStyle(1,0,1);
    Line(Round(80/640*Xmax),YP1,Round(Xmax*(1-40/640)),YP1);
  END;
END;

PROCEDURE GRAPH_HEADING;
BEGIN
  SetColor(WHITE);
  SetTextStyle(1,0,3);
```

```
 IF PD THEN OutTextXY(Round(230/640*Xmax),Round(15/480*Ymax),'PD 1506 & 1102')
 ELSE OutTextXY(Round(210/640*Xmax),Round(15/480*Ymax),'VOLUME 1506 & 1102');
 SetLineStyle(0,0,2);
 Rectangle(Round(Xmax*(1-360/640)),Round(75/480*Ymax),Round(Xmax*(1-
250/640)),Round(130/480*Ymax));
 SetLineStyle(0,0,1);
 SetColor(YELLOW);
 SetTextStyle(0,0,0);
 OutTextXY(Round(Xmax*(1-325/640)),Round(89/480*Ymax),'Tank 1506');
 Line(Round(Xmax*(1-355/640)),Round(94/480*Ymax),Round(Xmax*(1-
330/640)),Round(94/480*Ymax));
 SetLineStyle(3,0,1);
 SetColor(WHITE);
 Line(Round(Xmax*(1-355/640)),Round(112/480*Ymax),Round(Xmax*(1-
330/640)),Round(112/480*Ymax));
 OutTextXY(Round(Xmax*(1-325/640)),Round(107/480*Ymax),'Tank 1102');
END;

PROCEDURE GRAPH_DRAW;
BEGIN
 SetLineStyle(0,0,1);
 SetColor(YELLOW);
 Line(X_1,Y_1,X,Y);
 SetColor(white);
 SetLineStyle(3,0,1);
 Line(X_1,Y1_1,X,Y1);
END;

PROCEDURE EQUATION;
BEGIN
 IF PD THEN
 BEGIN
  Y:=ROUND(Ymax-(P2-1.2)/(2.2-1.2)*(Ymax*(1-120/480))-40/480*Ymax);
  Y1:=ROUND(Ymax-(P7-1.2)/(2.2-1.2)*(Ymax*(1-120/480))-40/480*Ymax);
 END
 ELSE
 BEGIN
  Y:=ROUND(Ymax-(V-3000)/(7000)*(Ymax*(1-120/480))-40/480*Ymax);
  Y1:=ROUND(Ymax-(V1-3000)/(7000)*(Ymax*(1-120/480))-40/480*Ymax);
 END;
END;
```

```
PROCEDURE GRAPH_CALC1;
VAR TC:INTEGER;
BEGIN
 P7:=DENS1;
 V1:=VOL1;
 V:=VOL;
 P2:=DENS;
 IF PD THEN
 BEGIN
  Y_1:=ROUND(Ymax-(P2-1.2)/(2.2-1.2)*(Ymax*(1-120/480))-40/480*Ymax);
  Y1_1:=ROUND(Ymax-(P7-1.2)/(2.2-1.2)*(Ymax*(1-120/480))-40/480*Ymax);
 END
 ELSE
 BEGIN
  Y_1:=ROUND(Ymax-(V-3000)/(7000)*(Ymax*(1-120/480))-40/480*Ymax);
  Y1_1:=ROUND(Ymax-(V1-3000)/(7000)*(Ymax*(1-120/480))-40/480*Ymax);
 END;
 X_1:=Round(80/640*Xmax);
 TYD:=H;
 IF NOT(TT2) THEN TC:=TE
 ELSE TC:=T;
 IF VOL<=VMIN THEN
 BEGIN
  MILL_CALC;
  REPEAT
   RUNGA2_1102;
   RUNGA1_1102;
   RUNGA2_1100;
   RUNGA1_1100;
   EQUATION;
   X:=ROUND(TYD/TC*(Xmax*(1-120/640))+80/640*Xmax);
   GRAPH_DRAW;
   IF V>=VTOT THEN F3:=0;
   TYD := TYD+H;
   Y_1:=Y;
   Y1_1:=Y1;
   X_1:=X;
  UNTIL (TYD>TC);
 END
 ELSE
 BEGIN
  F3:=0;
```

```
  MF:=0;
  WF:=0;
  REPEAT
    RUNGA2_1102;
    RUNGA1_1102;
    RUNGA2_1100;
    RUNGA1_1100;
    EQUATION;
    X:=ROUND(TYD/TC*(Xmax*(1-120/640))+80/640*Xmax);
    GRAPH_DRAW;
    IF V<=VMIN THEN MILL_CALC;
    IF V>=VTOT THEN F3:=0;
    TYD := TYD+H;
    Y_1:=Y;
    Y1_1:=Y1;
    X_1:=X;
  UNTIL (TYD>TC);
 END;
 X_1:=ROUND(T/TC*(Xmax*(1-120/640))+80/640*Xmax);
 SetColor(7);
 SetLineStyle(1,0,1);
 Line(X_1,Round(Ymax*(1-40/480)),X_1,Round(80/480*Ymax));
 OutTextXY(Round(X_1+5/640*Xmax),Round(Ymax*(1-55/480)),'Calc. Time');
END;

PROCEDURE GRAPH_CALC2;
BEGIN
 P7:=DENS1;
 V1:=VOL1;
 V:=VOL;
 P2:=DENS;
 IF PD THEN
 BEGIN
  Y_1:=ROUND(Ymax-(P2-1.2)/(2.2-1.2)*(Ymax*(1-120/480))-40/480*Ymax);
  Y1_1:=ROUND(Ymax-(P7-1.2)/(2.2-1.2)*(Ymax*(1-120/480))-40/480*Ymax);
 END
 ELSE
 BEGIN
  Y_1:=ROUND(Ymax-(V-3000)/(7000)*(Ymax*(1-120/480))-40/480*Ymax);
  Y1_1:=ROUND(Ymax-(V1-3000)/(7000)*(Ymax*(1-120/480))-40/480*Ymax);
 END;
 X_1:=Round(80/640*Xmax);
```

```
TYD:=H;
IF MILL_Y_N=1 THEN
BEGIN
 REPEAT
  RUNGA2_1102;
  RUNGA1_1102;
  IF ((TYD>MTB) AND (TYD<=MTE)) THEN MILL_CALC
  ELSE F3:=0;
  RUNGA2_1100;
  RUNGA1_1100;
  EQUATION;
  X:=ROUND(TYD/T*(Xmax*(1-120/640))+80/640*Xmax);
  GRAPH_DRAW;
  TYD := TYD+H;
  Y_1:=Y;
  Y1_1:=Y1;
  X_1:=X;
 UNTIL (TYD>T);
END;
IF MILL_Y_N=2 THEN
BEGIN
 F3:=0;
 MF:=0;
 WF:=0;
 REPEAT
  RUNGA2_1102;
  RUNGA1_1102;
  RUNGA2_1100;
  RUNGA1_1100;
  EQUATION;
  X:=ROUND(TYD/T*(Xmax*(1-120/640))+80/640*Xmax);
  GRAPH_DRAW;
  TYD := TYD+H;
  Y_1:=Y;
  Y1_1:=Y1;
  X_1:=X;
 UNTIL (TYD>T);
END;
END;
```

```
PROCEDURE GRAPH_D;
BEGIN
 F1:=F1_T;
 F3:=F3_T;
 F2:=F2_T;
 F6:=F6_T;
 GRAPH_INITIAL;
 SetBkColor(1);
 GRAPH_HEADING;
 IF (CHOICE OR NOT(RK)) THEN GRAPH_CALC2
 ELSE GRAPH_CALC1;
 SetTextStyle(0,0,0);
 OutTextXY(Round(30/640*Xmax),Round(Ymax*(1-12/480)),'Press <ENTER> to continue ...');
 READLN;
 CloseGraph;
END;

END.
```

```
UNIT OUTPUT_MENU;

INTERFACE

USES CRT, TURBO3, FastTTT, DOS, WinTTT, KeyTTT, IOTTT, MenuTTT, StrngTTT, VARIABLE,
RK_GOLD, TRIAL;

PROCEDURE MILL;
PROCEDURE TANKS;

IMPLEMENTATION

VAR ZERO:BOOLEAN;
   SS:STRING;

PROCEDURE ZEROS(S:INTEGER);
BEGIN
 IF S<10 THEN
 BEGIN
   ZERO:=TRUE;
   CASE S OF
```

```
    0:SS:='00';
    1:SS:='01';
    2:SS:='02';
    3:SS:='03';
    4:SS:='04';
    5:SS:='05';
    6:SS:='06';
    7:SS:='07';
    8:SS:='08';
    9:SS:='09';
   END;
  END
  ELSE ZERO:=FALSE;
END;

PROCEDURE MILL;
VAR S1,S2,S3,S4,S5,S6,S7:STRING;
   HOUR,MIN,TH,TM,TH1,TM1,RETCODE:INTEGER;
   V_1:REAL;
BEGIN
  IF (CHOICE OR NOT(RK)) THEN
  BEGIN
   ClrScr;
   FBox(1,5,80,19,YELLOW,1,2);
   Horizline(2,79,9,YELLOW,1,1);
   WriteCenter(7,WHITE,1,'SETTINGS FOR THE MILL');
   WriteAt(5,11,WHITE,1,'Demin water flowrate to the Mill [l/min]');
   Horizline(2,79,13,YELLOW,1,1);
   WriteCenter(13,WHITE,1,'CALCULATED CONDITIONS AT END OF TIME PERIOD !');
   WriteAt(5,15,WHITE,1,'Pulp flowrate from Mill to tank 1506 [l/min]');
   WriteAt(5,16,WHITE,1,'Pulp density of stream from Mill to tank 1506 [kg/l]');
   S1:=Real_to_Str(WF,1);
   S2:=Real_to_Str(F3_T,1);
   S3:=Real_to_Str(P3,3);
   IO_SetFields(3);
   IO_soundbeeper(false);
   IO_AllowEsc(true);
   IO_DefineStr(1,3,2,3,2,70,11,S1,'###');
   IO_DefineStr(2,1,3,1,3,70,15,S2,'####');
   IO_DefineStr(3,2,1,2,1,70,16,S3,'#####');
   IO_DefineMsg(1,23,19,' *** Press "END" to continue *** ');
   IO_DefineMsg(2,23,19,' *** Press "END" to continue *** ');
```

```
  IO_DefineMsg(3,23,19,' *** Press "END" to continue *** ');
  Writeln;writeln;Writeln('        THIS CALCULATED SETTINGS ARE VALID UNTIL ... ',S13,':',S14,'
HOURS !');
  OffCursor;
  IO_Edit(Retcode);
  IO_Resetfields;
 END
 ELSE
 BEGIN
  ClrScr;
  V_1:=V_T/10800*100;
  FBox(1,5,80,20,YELLOW,1,2);
  Horizline(2,79,9,YELLOW,1,1);
  WriteCenter(7,WHITE,1,'SETTINGS FOR THE MILL');
  WriteAt(5,11,WHITE,1,'START MILLING at this TIME (below required level)              :');
  WriteAt(5,12,WHITE,1,'STOP MILLING at this TIME (maximum level reached)              :');
  WriteAt(5,13,WHITE,1,'Demin water flowrate to the Mill [l/min]');
  Horizline(2,79,15,YELLOW,1,1);
  WriteCenter(15,WHITE,1,'CALCULATED CONDITIONS AT THE END OF TIME PERIOD');
  WriteAt(5,17,WHITE,1,'Pulp flowrate from Mill to tank 1506 [l/min]');
  WriteAt(5,18,WHITE,1,'The level of tank 1506 [%]');
  IF TT2 THEN
  BEGIN
   S4:=' ';
   S5:=' ';
   S6:=' ';
   S7:=' ';
  END
  ELSE
  BEGIN
   ZERO:=FALSE;
   HOUR:=Str_to_Int(S15);
   MIN:=Str_to_Int(S16);
   TH:=TB DIV 60;
   IF TH>0 THEN TM:=TB-TH*60
   ELSE TM:=TB;
   TH:=HOUR+TH;
   TM:=MIN+TM;
   IF TM>=60 THEN
   BEGIN
    TM:=TM-60;
    TH:=TH+1;
```

```
 END;
 IF TH>=24 THEN TH:=TH-24;
 TH1:=TE DIV 60;
 IF TH1>0 THEN TM1:=TE-TH1*60
 ELSE TM1:=TE;
 TH1:=HOUR+TH1;
 TM1:=MIN+TM1;
 IF TM1>=60 THEN
 BEGIN
  TM1:=TM1-60;
  TH1:=TH1+1;
 END;
 IF TH1>=24 THEN TH1:=TH1-24;
 ZEROS(TH);
 IF ZERO THEN S4:=SS
 ELSE S4:=Int_to_Str(TH);
 ZEROS(TM);
 IF ZERO THEN S5:=SS
 ELSE S5:=Int_to_Str(TM);
 ZEROS(TH1);
 IF ZERO THEN S6:=SS
 ELSE S6:=Int_to_Str(TH1);
 ZEROS(TM1);
 IF ZERO THEN S7:=SS
 ELSE S7:=Int_to_Str(TM1);
END;
S1:=Real_to_Str(WF,1);
S2:=Real_to_Str(F3_T,1);
S3:=Real_to_Str(V_1,1);
IO_SetFields(10);
IO_soundbeeper(false);
IO_AllowEsc(true);
IO_DefineStr(1,7,2,7,2,70,11,S4,'##');
IO_DefineStr(2,1,3,1,3,73,11,S5,'##');
IO_DefineStr(3,2,4,2,4,70,12,S6,'##');
IO_DefineStr(4,3,5,3,5,73,12,S7,'##');
IO_DefineStr(5,4,6,4,6,70,13,S1,'###');
IO_DefineStr(6,5,7,5,7,70,17,S2,'####');
IO_DefineStr(7,6,1,6,1,70,18,S3,'#####');
IO_DefineMsg(1,23,20,' *** Press "END" to continue *** ');
IO_DefineMsg(2,12,20,'*** REMEMBER the time mode ranges from 00:00 to 23:59 ***');
IO_DefineMsg(3,10,20,'** Assuming all the flowrates are constant for time period **');
```

```
   IO_DefineMsg(4,23,20,' *** Press "END" to continue *** ');
   IO_DefineMsg(5,23,20,' *** Press "END" to continue *** ');
   IO_DefineMsg(6,23,20,' *** Press "END" to continue *** ');
   IO_DefineMsg(7,23,20,' *** Press "END" to continue *** ');
   Writeln;Writeln('        THIS CALCULATED SETTINGS ARE VALID UNTIL ... ',S13,':',S14,'
   HOURS !');
   OffCursor;
   IO_Edit(Retcode);
   IO_Resetfields;
  END;
END;

PROCEDURE MINMAX_1100;
VAR KEY:CHAR;
BEGIN
  CLRSCR;
  IF (VMIN>VOL) THEN
  BEGIN
   FBox(12,9,68,13,YELLOW,RED,2);
   WRITEAT(20,11,YELLOW+BLINK,RED,'TANK 1506 IS BELOW ITS MINIMUM LEVEL !');
   SOUND(400);DELAY(150);NOSOUND;
   IF VMIN_1100 THEN
   BEGIN

WRITELN;WRITELN;WRITELN;WRITELN;WRITELN;WRITELN;WRITELN;WRITELN;WRITELN;
WRITELN;WRITELN;WRITELN;WRITELN;WRITELN;
     WRITELN('          THE MINIMUM LEVEL WILL BE REACHED IN ',TMIN:3,' MINUTES');
   END;
   WriteCenter(25,white+blink,RED,'************** PRESS ANY KEY TO PROCEED **************');
   READ(Kbd,KEY);
  END;
  IF ((VMIN>V_T) AND (VMIN<VOL)) THEN
  BEGIN
   FBox(12,9,68,13,YELLOW,RED,2);
   WRITEAT(19,11,YELLOW+BLINK,RED,'TANK 1506 WILL REACH ITS MINIMUM LEVEL !');
   SOUND(400);DELAY(150);NOSOUND;
   IF VMIN_1100 THEN
   BEGIN
    WRITELN;WRITELN;WRITELN;WRITELN;WRITELN;WRITELN;WRITELN;WRITELN;
    WRITELN;WRITELN;WRITELN;WRITELN;WRITELN;WRITELN;
    WRITELN('          THE MINIMUM LEVEL WILL BE REACHED IN ',TMIN:3,' MINUTES');
   END;
```

```
  WriteCenter(25,white+blink,RED,'********** PRESS ANY KEY TO PROCEED **********');
  READ(Kbd,KEY);
 END;
 IF VMAX_1100 THEN
 BEGIN
  ClrScr;
  FBox(12,9,68,13,YELLOW,RED,2);
  WRITEAT(19,11,YELLOW+BLINK,RED,'TANK 1506 WILL REACH ITS MAXIMUM LEVEL !');
  SOUND(400);DELAY(150);NOSOUND;
  WRITELN;WRITELN;WRITELN;WRITELN;WRITELN;WRITELN;WRITELN;WRITELN;
  WRITELN;WRITELN;WRITELN;WRITELN;WRITELN;WRITELN;WRITELN;
  WRITELN('          THE MAXIMUM LEVEL WILL BE REACHED IN ',TMAX:3,' MINUTES');
  WriteCenter(25,white+blink,RED,'********** PRESS ANY KEY TO PROCEED **********');
  READ(Kbd,KEY);
 END;
END;

PROCEDURE MINMAX_1102;
VAR KEY:CHAR;
BEGIN
 ClrScr;
 IF (V1MIN>VOL1) THEN
 BEGIN
  FBox(12,9,68,13,YELLOW,RED,2);
  WRITEAT(20,11,YELLOW+BLINK,RED,'TANK 1102 IS BELOW ITS MINIMUM LEVEL !');
  SOUND(400);DELAY(150);NOSOUND;
  IF VMIN_1102 THEN
  BEGIN
   WRITELN;WRITELN;WRITELN;WRITELN;WRITELN;WRITELN;WRITELN;WRITELN;
   WRITELN;WRITELN;WRITELN;WRITELN;WRITELN;WRITELN;
   WRITELN('          THE MINIMUM LEVEL WILL BE REACHED IN ',T1MIN:3,' MINUTES');
  END;
  WriteCenter(25,white+blink,RED,'********** PRESS ANY KEY TO PROCEED **********');
  READ(Kbd,KEY);
 END;
 IF ((V1MIN>V1) AND (V1MIN<VOL1)) THEN
 BEGIN
  FBox(12,9,68,13,YELLOW,RED,2);
  WRITEAT(19,11,YELLOW+BLINK,RED,'TANK 1102 WILL REACH ITS MINIMUM LEVEL !');
  SOUND(400);DELAY(150);NOSOUND;
  IF VMIN_1102 THEN
  BEGIN
```

```
    WRITELN;WRITELN;WRITELN;WRITELN;WRITELN;WRITELN;WRITELN;WRITELN;
    WRITELN;WRITELN;WRITELN;WRITELN;WRITELN;WRITELN;
    WRITELN('            THE MINIMUM LEVEL WILL BE REACHED IN ',T1MIN:3,' MINUTES');
   END;
   WriteCenter(25,white+blink,RED,'************** PRESS ANY KEY TO PROCEED **************');
   READ(Kbd,KEY);
  END;
  IF VMAX_1102 THEN
  BEGIN
   ClrScr;
   FBox(12,9,68,13,YELLOW,RED,2);
   WRITEAT(19,11,YELLOW+BLINK,RED,'TANK 1102 WILL REACH ITS MAXIMUM LEVEL !');
   SOUND(400);DELAY(150);NOSOUND;
   WRITELN;WRITELN;WRITELN;WRITELN;WRITELN;WRITELN;WRITELN;WRITELN;
   WRITELN;WRITELN;WRITELN;WRITELN;WRITELN;WRITELN;WRITELN;
   WRITELN('            THE MAXIMUM LEVEL WILL BE REACHED IN ',T1MAX:3,' MINUTES');
   WriteCenter(25,white+blink,RED,'************** PRESS ANY KEY TO PROCEED **************');
   READ(Kbd,KEY);
  END;
END;

PROCEDURE TANKS;
VAR S1,S2,S3,S4,S5,S6,S7:STRING;
   RETCODE:INTEGER;
   V_1,V1_1:REAL;
   KEY:CHAR;
BEGIN
  IF CHOICE THEN
  BEGIN
   MINMAX_1100;
   MINMAX_1102;
  END;
  IF NOT(RK) THEN
  BEGIN
   IF (VMIN>VOL) THEN
   BEGIN
    FBox(12,9,68,13,YELLOW,RED,2);
    WRITEAT(20,11,YELLOW+BLINK,RED,'TANK 1506 IS BELOW ITS MINIMUM LEVEL !');
    SOUND(400);DELAY(150);NOSOUND;
    WriteCenter(25,white+blink,RED,'************** PRESS ANY KEY TO PROCEED **************');
    READ(Kbd,KEY);
   END;
```

```
 IF ((VMIN>V_T) AND (VMIN<VOL)) THEN
 BEGIN
   FBox(12,9,68,13,YELLOW,RED,2);
   WRITEAT(19,11,YELLOW+BLINK,RED,'TANK 1506 WILL REACH ITS MINIMUM LEVEL !');
   SOUND(400);DELAY(150);NOSOUND;
   WriteCenter(25,white+blink,RED,'*************** PRESS ANY KEY TO PROCEED ***************');
   READ(Kbd,KEY);
 END;
END;
V_1:=V_T/10800*100;
V1_1:=V1_T/9970*100;
ClrScr;
FBox(1,2,80,25,YELLOW,0,2);
Horizline(2,79,6,YELLOW,0,1);
WriteCenter(4,WHITE,0,'SETTINGS FOR TANKS 1506 AND 1102');
WriteCenter(6,YELLOW+BLINK,0,'TANK 1506 !');
WriteAt(5,8,WHITE,0,'Pulp flowrate from tank 1506 to tank 1102 [l/min]');
WriteAt(5,9,WHITE,0,'Spent Electrolyte (SE) flowrate to tank 1506 [l/min]');
Horizline(2,79,'11,YELLOW,0,1);
WriteCenter(11,YELLOW,0,'CALCULATED CONDITIONS FOR TANK 1506');
WriteAt(5,13,WHITE,0,'The pulp density (PD) of mixture in tank 1506 [kg/l]');
WriteAt(5,14,WHITE,0,'The level in tank 1506  [%]');
Horizline(2,79,16,YELLOW,0,1);
WriteCenter(16,YELLOW+BLINK,0,'TANK 1102');
WriteAt(5,18,WHITE,0,'Spent Electrolyte (SE) flowrate to tank 1102 [l/min]');
Horizline(2,79,20,YELLOW,0,1);
WriteCenter(20,YELLOW,0,'CALCULATED CONDITIONS FOR TANK 1102');
WriteAt(5,22,WHITE,0,'The pulp density (PD) of mixture in tank 1102 [kg/l]');
WriteAt(5,23,WHITE,0,'The level in tank 1102  [%]');
S1:=Real_to_Str(F2_T,1);
S2:=Real_to_Str(F1_T,1);
S3:=Real_to_Str(P2_T,3);
S4:=Real_to_Str(V_1,1);
S5:=Real_to_Str(F6_T,1);
S6:=Real_to_Str(P7_T,3);
S7:=Real_to_Str(V1_1,1);
IO_SetFields(7);
IO_soundbeeper(false);
IO_AllowEsc(true);
IO_DefineStr(1,7,2,7,2,70,8,S1,'####');
IO_DefineStr(2,1,3,1,3,70,9,S2,'####');
IO_DefineStr(3,2,4,2,4,70,13,S3,'#####');
```

```
 IO_DefineStr(4,3,5,3,5,70,14,S4,'#####');
 IO_DefineStr(5,4,6,4,6,70,18,S5,'#####');
 IO_DefineStr(6,5,7,5,7,70,22,S6,'#####');
 IO_DefineStr(7,6,1,6,1,70,23,S7,'#####');
 IO_DefineMsg(1,23,25,' *** Press "END" to continue *** ');
 IO_DefineMsg(2,23,25,' *** Press "END" to continue *** ');
 IO_DefineMsg(3,23,25,' *** Press "END" to continue *** ');
 IO_DefineMsg(4,23,25,' *** Press "END" to continue *** ');
 IO_DefineMsg(5,23,25,' *** Press "END" to continue *** ');
 IO_DefineMsg(6,23,25,' *** Press "END" to continue *** ');
 IO_DefineMsg(7,23,25,' *** Press "END" to continue *** ');
 Writeln('        THIS CALCULATED SETTINGS ARE VALID UNTIL ... ',S13,':',S14,' HOURS !');
 OffCursor;
 IO_Edit(Retcode);
 IO_Resetfields;
END;

END.
```

END END END END END END END END

Appendix E

IDENTIFICATION OF PROCESS VARIABLES

In order to develop a model from historical data that will give an accurate simulation of the first stage acid oxygen leach process, it is necessary to identify all the possible variables that could cause perturbations in the process. The identification of the variables as such is not that difficult, but to make the model account for all the perturbations caused by the variables, seemed to be a problem. The data showed great variations in basically all the variables, such as mill grading, pulp densities, spent electrolyte flowrates, pH's and concentrations which all have a significant effect on the leaching efficiency of the matte in the autoclave.

E.1 MODELLING STRATEGY

As the first step, to start modelling the process, it was necessary to analyse the data to gain more experience in the behaviour of the process and to extract all valuable information, such as the dependencies of the different variables on each other, etc., from the data. The process characteristics as such will then be extracted by means of artificial neural networks (ANN), statistical methods and inductive learning techniques, in order to obtain the optimum set of independent variables for the model that will simulate the process.

E.1.1 Problems with plant data

As with any plant data a certain error percentage is present in the data. The errors in the data, from experience in the plant, could be attributed to:

(a) the data on the logsheet does not include some of the essential data, such as the acid concentration and temperature in tank 1102, as well as at least hourly chemical analysis of the base metals in solution in the different compartments,

(b) the logsheet entries which are not recorded exactly on the hour by the operators,
(c) the different operating procedures by different operators under the same circumstances,
(d) the process assistants and operators have different sampling methods,
(e) the process helpers do not take the samples at the exact time,
(f) instrumental errors, and
(g) errors made by the analysts.

Furthermore, the major problem with the data is that not sufficient data is available, because the process must be modelled on at least an hourly basis to be useful. Therefore data of the daily composite samples will not be representative of the process from a modelling point of view. A contradiction that arises from this situation is that when a model is developed it should be as accurate as possible, and hence should include as many variables as possible. But on the other hand, because of the cost involved in obtaining and monitoring this information, the model must include as few as possible variables.

E.2 PROCESS VARIABLES

The different types of variables that will influence the process are discussed.

(i) *Matte composition* is expected to have a small effect on the leaching process (due to relatively small variations in its components).

(ii) *Mill grading* (particle size distribution) will influence the leaching in the sense that the finer the grind the more liberated the particles will be and a more efficient contact area with the solution is produced.

(iii) *Pulp density* will have the effect that the lower the pulp density the more solution is present and the more metals could be dissolved into solution.

(iv) *Residence time* will determine the time that is available for reactions to occur in the process.

(v) *Composition of the recycle streams*, which include the streams coming from Cu cementation (press 1407) and spent electrolyte from copper winning (tank 313). In the spent electrolyte solution the free acid (H_2SO_4) concentration will determine the pH of the reaction system. The Ni, Cu, Fe, etc. content will have the effect that the higher the concentration of metals in the solution, the less metals will be leached, due to the fact that the solution might be saturated more quickly.

(vi) *pH* will create the right conditions for specific reactions to take place.

(vii) *Oxygen* will increase the oxidising conditions.

(viii) *Temperature and pressure* will determine the overall reaction kinetics.

E.2.1 Measurement of the efficiency of the process

The ideal situation would be the determination of the process efficiency on an hourly basis by the analysis of the solids from the autoclave. As already mentioned, the daily analysis of the solids will not give representative results of the process due to the relatively short residence times of tanks 1506 and 1102 and the autoclave.

Therefore, the analysis of the solution in the autoclave for Cu in the first and fourth compartment, Fe in the fourth compartment and total metals (TM) in the fourth compartment will be used as second best measure of the efficiency of the process. The total metals concentration includes the concentration of all the metals in the solution, which basically indicates the concentration of Ni because the concentration of the other metals are relatively low, except maybe the Cu concentration which could become significant at times. But, for the purpose of this investigation, the TM concentration will be directly assumed as the Ni concentration.

E.3 CORRELATION COEFFICIENTS

The correlation coefficients (Walpole and Myers, 1989) of the different independent variables in relation to the dependent variables were determined by equation E.1, with the data for the period 01/02/1992 to 30/04/1992.

$$\rho_{XY} = \frac{cov(X,Y)}{\sqrt{\sigma_X . \sigma_Y}} \qquad (E.1)$$

ρ - correlation coefficient

cov - covariance

σ - standard deviation

These correlation coefficients are a relative measure of the association between random variables. For example if ρ_{XY} = 1, X and Y are perfectly positively correlated and the possible values of X and Y will all be on a straight line with a positive slope in the (X,Y) plane.

From the correlation coefficients (Fig. E.1) of the Cu in the first compartment of the autoclave, it is evident, that the Cu in the first and fourth compartment are strongly related. This in effect will mean that a high Cu concentration in compartment no. 1 will give rise to a high Cu concentration in compartment no. 4. Furthermore, the effect of the pH in compartment no. 1, the pulp density in tank 1102, the pulp flowrate to the autoclave and the temperature and pressure in the autoclave have no significant effect on the amount of Cu that is leached in the first compartment.

A higher spent electrolyte flowrate introduces more Cu into the autoclave due to the high Cu concentration in the spent electrolyte solution. A low free acid (H_2SO_4) concentration in the spent electrolyte solution will result in better Cu leaching, which could also be due to the fact that the solution is less saturated and therefore more metals could be dissolved. High oxygen addition will also increase the leaching of Cu.

From Fig. E.2 it could be seen that a high pH, as well as a high temperature and pressure will result in better precipitation of the Cu in the fourth compartment. It also seems that the other variables would not have such a significant effect on the leaching/precipitation characteristics of the Cu in compartment no. 4.

The correlation coefficients of Fe (Fig. E.3) show that Fe is a very "sensitive" variable to disturbances in the system. Low pH's, therefore a high acid concentration in the spent electrolyte solution and low pulp density in tank 1102 will give rise to a higher Fe concentration in solution. The low pulp density in 1102 will have the effect of increasing the contact area between the solids and liquids, therefore increasing the degree of leaching in this tank.

A higher spent electrolyte flowrate to the autoclave will dilute the Fe concentration in solution. Oxygen will have the effect that the higher the oxygen addition the more Fe will be oxidised from the ferrous to the ferric state which will be precipitated. A higher temperature and lower pressure will increase the saturation point of the solution, therefore more Fe could be dissolved.

According to Fig. E.4 a low pulp density and a high acid concentration will increase the total metals (TM) leaching efficiency. The fact that the TM (or Ni) concentration is dependent on the pulp flowrate could possibly indicate to the degree of reaction taking place in the repulping tanks. This factor together with the fact that the higher the oxygen addition the higher the TM concentration, could also indicate the fast reaction occurring in the first compartment of the autoclave. From Fig. E.4 it could also be said that TM leaching is not very pH dependent in the autoclave.

E.3.1 pH Data

An interesting observation that was made from the pH data (Fig. E.5) in compartments no. 1 and 4 of the autoclave, is that the average and the mode (the value of the sample that occurs most often or with the highest frequency) of the pH

of the system are lower in compartment no. 4 (2.1 and 1.75 respectively) than in compartment no. 1 (2.2 and 2.25 respectively). This is quite opposite of what is expected.

The possible reason for this is due to the cementation of Cu or due to the formation of antlerite and/or beaverite (Plasket and Dunn, 1986). The precipitation of basic copper sulphate, antlerite (eq. E.2), occurs by hydrolysis if the pH increases above 3.

$$3CuSO_4 + 4H_2O \rightarrow 2Cu(OH)_2CuSO_4\downarrow + H_2SO_4 \qquad (E.2)$$

It could also be due to the formation of beaverite (eq. E.3) or jarosite (eq. E.4). The formation of beaverite usually goes hand in hand with a decrease in Cu and Pb concentrations in compartment no. 4. Both reactions produce acid in the cementation process.

$$PbSO_4 + CuSO_4 + Fe_2(SO_4)_3 + 6H_2O \rightarrow PbCuFe_2(SO_4)_2(OH)_6 + 3H_2SO_4 \qquad (E.3)$$

$$(NH_4)_2SO_4 + 3Fe_2(SO_4)_3 + 12H_2O \leftrightarrow 2NH_4Fe_3(SO_4)_2(OH)_6 + 6H_2SO_4 \qquad (E.4)$$

The possible reason for the tail in Fig. E.5 (from pH 3 and higher) where the pH in the fourth compartment is higher than in the first compartment is because the leaching reaction has consumed most of the acid in the previous compartments. Therefore if some unreacted products end up in the fourth compartment due to non-ideal flow patterns in the autoclave, acid is consumed in the leaching of these unreacted products.

E.4 CONCLUSIONS

With this knowledge obtained from the process and the process data it is possible to analyse the process with artificial neural network (ANN) models and decision trees (inductive learning). Although artificial neural networks are "black box" models of the

process, more knowledge of the process can be obtained by performing sensitivity analyses with these models. Analysing the data with decision trees, will be more desirable from a practical (operating) point of view, because physically interpretable rules are developed of the process, which can be used as guidelines for operating the process.

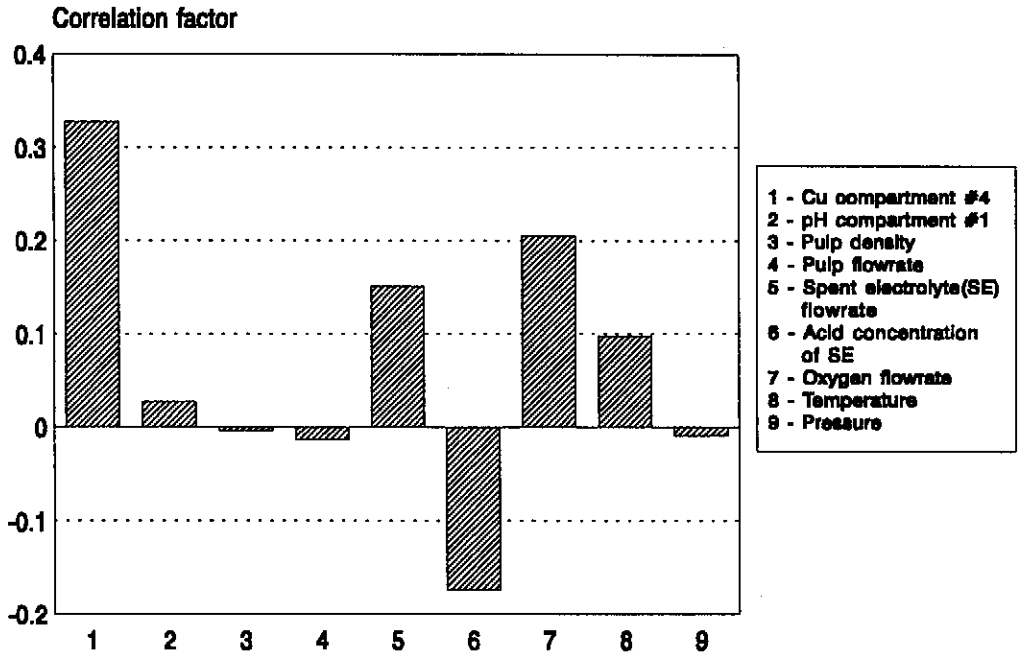

Figure E.1 - Correlation coefficients of Cu in the first compartment of the autoclave

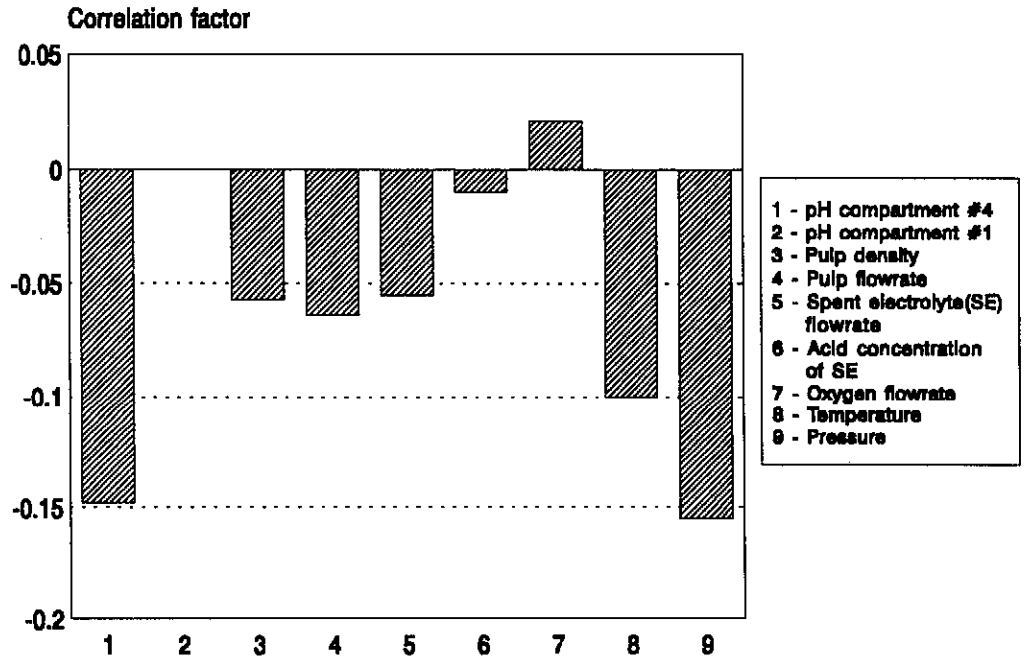

Figure E.2 - Correlation coefficients of Cu in the fourth compartment of the autoclave

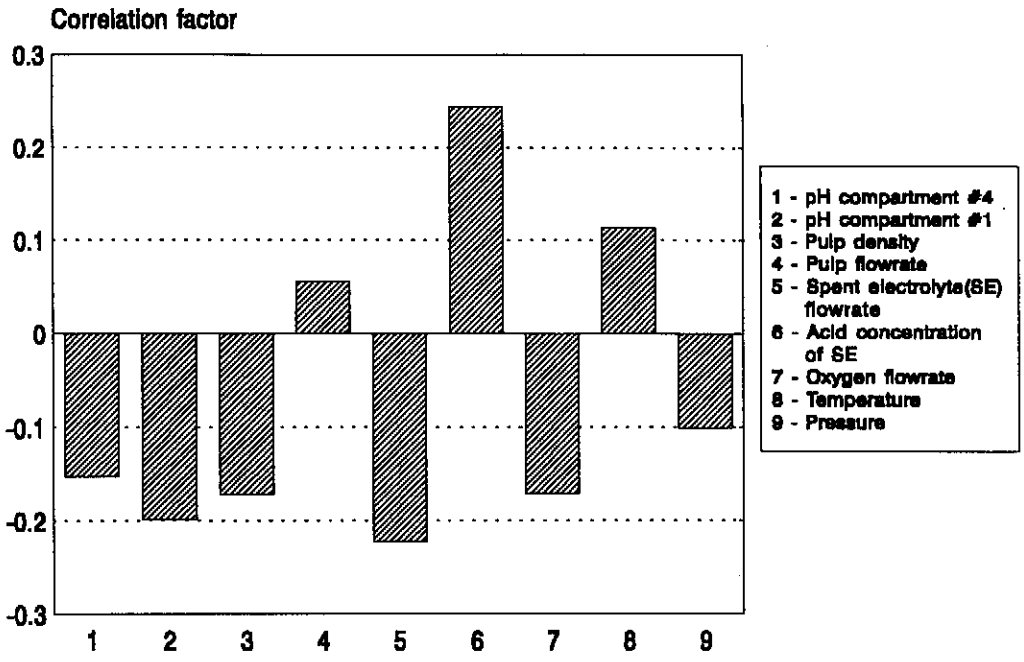

Figure E.3 - Correlation coefficients of Fe in the fourth compartment of the autoclave

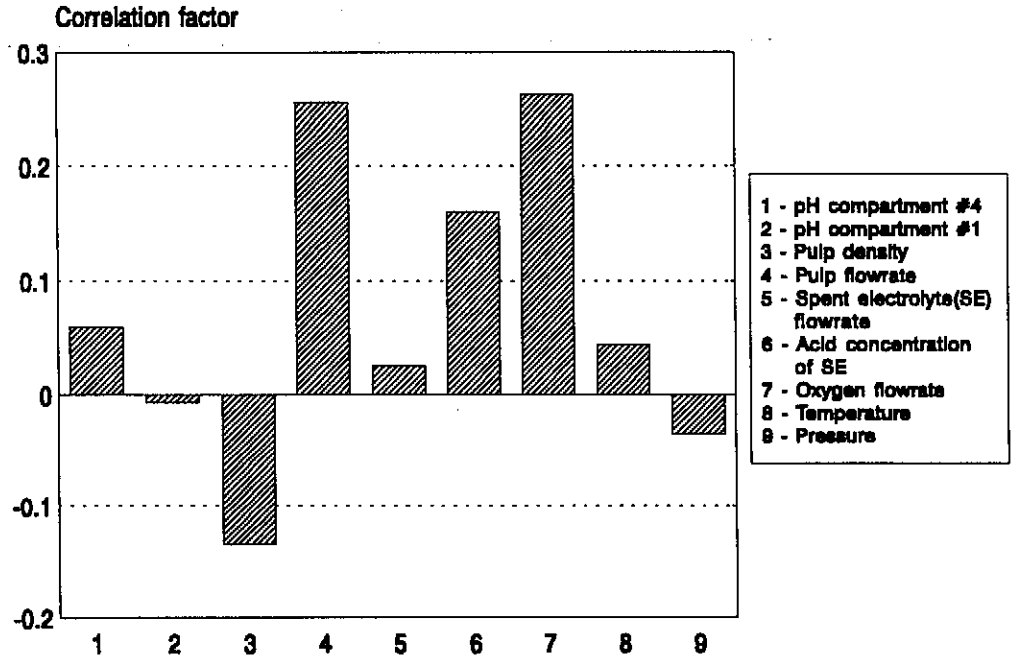

Figure E.4 - Correlation coefficients of TM (or Ni) in the fourth compartment of the autoclave

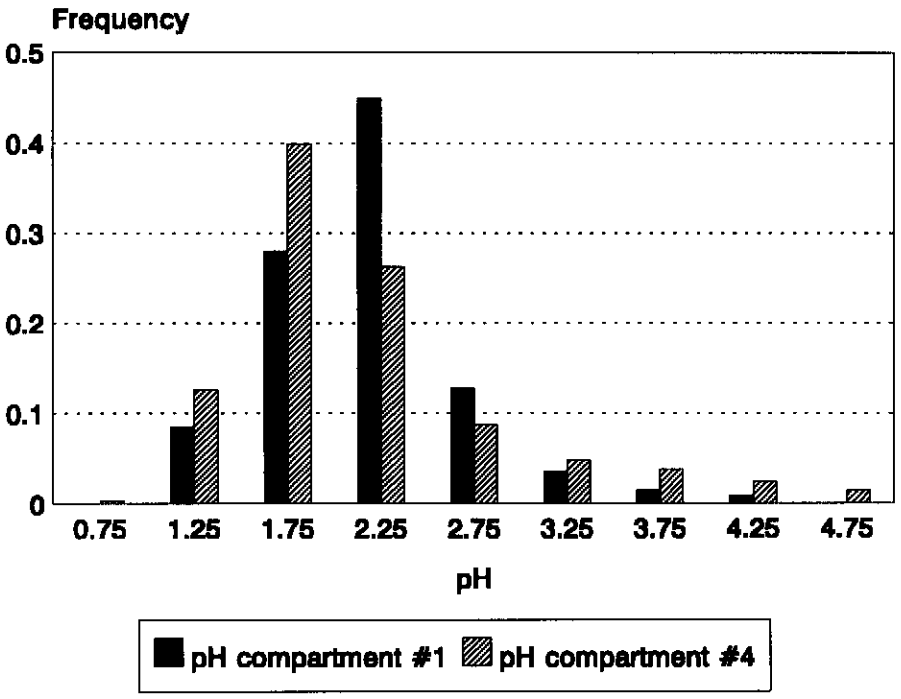

Figure E.5 - Frequency distribution of the pH in compartments no. 1 and no. 4 of the autoclave

Appendix F

MANIPULATIONS PERFORMED ON THE EXPERIMENTAL RESULTS (Chapter 7)

The experimental results of the tests that were conducted had to be transformed into a more interpretable form before they could be used. Therefore, calculations were performed on the data to take into account the extent of the variations in the solid mass throughout the experiment. These variations were caused by the leaching of the elements out of the solid phase into the solution and by the loss of material through sampling and separation methods. The analysis errors made on the data have already been mentioned (data smoothing) in Chapter 4. These transformed results were then used further in the calculation of the mineral composition of each sample with the help of XRD analyses. The rationale for the calculations performed on the results is discussed in this section, as well as the rationale behind the technique used to determine the mineral composition of the phases present in each sample. The reaction mechanism is also verified, by calculating the mole balances from the stoichiometry of the reactions.

F.1 PRESENTATION OF DATA

The first important aspect of the experimental results is to define a meaningful way to present the data. The solution results of the tests could be presented in either concentration (g/L), or in mass (g or mol), but the solids results can not be presented in concentration (%) because during the leaching reaction the effective mass of the solids in the mixture decrease significantly. The decrease of mass in the solids is due to leaching of the metal ions out of the solid into the solution, which necessitates that the solids results are presented in mass (g or mol).

The calculations performed on the experimental data, in order to obtain the various types of presentations of the results that will be used in this dissertation, are

discussed on the basis of the results of one experiment (test 9), as an example. The experimental conditions for this specific test are: plant particle size distribution, a pulp density of 1.35 kg/L, a temperature of 140°C, a total pressure of 5.5 bar, an oxygen flowrate of 0.48 kg/h and an initial H_2SO_4 concentration of 104 g/L. The calculations will be explained on the basis of the nickel (Ni) in the solution and solids (Table F.1) for the sample at the time = 40 minutes (Table F.2 and Table F.3). The amount of sample taken during each sampling period was 350 mL of pulp, thus the volume of solution reclaimed was approximately 350 mL (0.35 L) and the mass of solids reclaimed was approximately 40g per sample. In this experiment the volume of solution added to the 7900g of matte (solids) is 38.6 L, which consists of 37.3 L spent electrolyte and 1.3 L demineralised water. In all tests the first sample (time = 0 min) is of the original matte and spent electrolyte solution, therefore 10 samples are taken during each test which amounts to acceptable losses through sample taking (8.8% solution loss and 5.1% solids loss). The effect of the formation of H_2O by the different reactions was ignored because less than 1 liter of H_2O was formed as well as the fact that some of the solution will be lost due to evaporation.

The nickel in solution is indicated as Ni^{2+}, as it is the most common (acceptable) ionic form of nickel in solution. The columns for sample loss in Tables F.2 and F.3 give the amount of nickel lost through sample-taking in the solution and solids, respectively.

The following sample calculations are based on the solution results (3rd sample of the experiment) of Table F.2:

Mass of Ni^{2+} in solution [g] = 66.3(38.6 - 3×0.35)
= 2490.1 g

Sample loss [g] = 66.3×0.35
= 23.2 g

Mass increase/decrease [g] = 2490.1 - 2249.7
= 263.6 g

Mole increase/decrease [mol] = 263.6/58.7 (molecular weight of Ni)

= 4.490 mol

Rate of change [mol/min] = 4.490/(40-20)

= 0.224 mol/min

The incremental mass decrease in the solids was calculated from the mass increase/decrease of nickel, copper (Table F.4), iron (Table F.5), cobalt (Table F.6) and total sulphur (Table F.7) in the solution. The incremental mass decrease in the solids for each time step is shown in Table F.8. The acid consumption during the experiment is shown in Table F.9. (The iron being dissolved in the solution from time = 80 minutes was not added to the incremental mass decrease because this iron presumably originated from another source.)

Incremental mass decrease [g] = 263.6 + [g] Cu + [g] Fe + [g] Co + [g] S

= 134.8 g

From the incremental mass decrease the total mass decrease in the solids up to that time is calculated (Table F.8) by taking the sum of the incremental mass decreases in the solids up to time = 40 minutes (for this example).

Total mass decrease in solids [g] = ... + 388.1 + 134.8

= 1109.8 g

The following sample calculations are based on the solids results of Table F.3:

$$\text{Mass of nickel in solids [g]} = \frac{31.6}{100}(7900 - 1109.8)$$

= 2144.0 g

$$\text{Sample loss [g]} = \frac{31.6}{100} \times 40$$

= 15.8 g

Mass increase/decrease [g] = 2144.0 - 2363.6

= -203.8 g

Mole increase/decrease [mol] = -203.8/58.7 (molecular weight of Ni)

= -3.472 mol

Rate of change [mol/min] = -3.472/(40-20)

= -0.174 mol/min

The mass balance of nickel is calculated by adding the mass of nickel in the solution to the mass of nickel left in the solids (see highlighted text in Table F.1). The variations in the mass balances of all the different elements could be ascribed to the following experimental problems:

(i) Inaccurate solids analysis results which have been addressed by data smoothing (Chapter 4).

(ii) During filtering of the samples (with a vacuum filter) the samples cooled down significantly, which could have led to the precipitation of metal sulphates out of the solution into the solids. Therefore, a lower concentration of the metal species in the solution will be analysed. These metal sulphates which have precipitated on the filter cake would then be dissolved and washed out of the filter cake to a certain extent (filter cake is washed with 500 ml water). Therefore, in this case the precipitated metal species would not be detected in either the solution or solids which then accounts for the decrease in the mass balance for the specific metal.

(iii) Because of the harsh nature of the reaction conditions employed the 304L stainless steel shell of the experimental autoclave was attacked by the acidic-oxidising conditions which led to the increase of iron in the system (see Table F.5).

The overall decrease in the mass balance of the nickel (Table F.1) could be due to the factor mentioned in point (ii) above where the decrease in temperature of the pulp being filtered causes discrepancies, especially for nickel which has the highest concentration in the solution throughout the experiment. The noticeable increase in the mass balance of the copper (Table F.4) could be explained by point (i), because

the mass balance indicated the highest values in the mass balance at the stages where the analysis of the copper concentration was the highest in the solids (in comparison to the other elements). The increase in the mass of iron (Table F.5) as the experiment progresses is explained by the above mentioned point (iii). The mass balance for cobalt (Table F.6) stayed reasonably constant throughout the experiment. The variation in the mass balance of sulphur (Table F.7) could be ascribed to the problem given in point (ii) which explains why a decrease in the SO_4^{2-} ion concentration in the solution could also occur. Considering the above mentioned factors the discrepancies in the mass balances of the different elements are explained.

F.2 DETERMINATION OF MINERAL COMPOSITION

One of the most effective and well known techniques of identifying crystal structures are the X-ray diffraction (XRD) technique. The principles of XRD analysis (Nuffield, 1966, Frye, 1974) are given briefly and are as follows: A crystal is a complex, although orderly, arrangement of atoms. All atoms in the path of an X-ray beam scatter X-rays simultaneously. In general, the scattered waves interfere with and destroy one another, but in certain specific directions they combine to form new wave fronts. This cooperative scattering is known as diffraction. The directions of possible diffraction depend only on the size and shape of the unit cell. An electron in the path of an unpolarised X-ray beam vibrates with the frequency of the incident radiation, periodically absorbing energy and emitting it as x-radiation of the same frequency. The original X-rays are unmodified in wavelength by the interaction, but are radiated in all directions. The electron has the effect of scattering the incident radiation and acts as a source of secondary X-rays. The nucleus, because of its high mass, makes a negligible contribution to the radiation scattered by an atom. The X-rays diffracted by the electrons in a crystal and emitted at different angles are detected by the apparatus, producing a continuous graph of the intensity of the detected X-rays at the angles of 0-90°. The intensity of the emitted X-rays at specific angles are a characteristic of each mineral species.

The mineral compositions of the different samples were determined by means of a semi-quantitative technique combining the XRD results with the analytical chemical composition of the solids. The reason why the most general quantitative technique for phase analysis was not used, i.e. the principles of the internal standard method (Snyder and Bish, 1989), is because the required modern equipment was not available and secondly, because of the difficulties involved in the standardisation of the equipment and obtaining representative reference ratios for each sample (approximately 11 samples with different mineral phases and varying mineral compositions). The accuracy of the results did not justify the time that would have been spent on such problems. Thus, a different method was developed using some of the principles of the internal standard method and simple mass balances.

For the purpose of the determination of the mineral composition, only nickel, copper and sulphur in the samples were considered. Iron and cobalt were ignored (because of its low concentration) in order to simplify the determinations, and due to the fact that in the XRD analysis the iron and cobalt mineral species will not be detected because they are present in such low concentrations. The mineral phases were identified by means of XRD analyses (see Fig. F.1 to Fig. F.11). The mineral composition for the phases of the first sample at time = 0 minutes (the original matte sample) was calculated from the chemical analysis results. It was possible to determine the composition of this sample because only three major mineral phases were present which consisted of mainly three elements (Ni, Cu and S), therefore three unknown compositions with three known quantities of their constituent elements, resulting in three equations which could be solved simultaneously. The principles for determining the phase compositions of the rest of the samples (time 5 to 300 minutes) are as follows:

(i) that the previous sample is used as the reference for the composition determination of the next sample (the sample at time = 0 min is the reference for the sample at time = 5 min),

(ii) the average percentage increase or decrease of the major intensity peaks (with least overlapping) of each specific mineral in this sample, in comparison with the previous sample, serves as a relative indication (it is not a linear relation) of the increase or decrease in concentration of the mineral phase (Nuffield, 1966), and

(iii) the phase compositions of the samples are then calculated and adjusted by means of mass balances obtained from the chemical analyses of the solid samples.

The mineral compositions of the different samples were calculated by following the above mentioned rules and the results are presented in Table F.10. In this table 'traces' refer to minerals which could be detected on the XRD graph but which could not be quantified due to their small concentration, usually less than 3%. The accuracy of the calculated mineral composition of each sample can be compared to the mass of nickel, copper and total sulphur chemically analysed in the solids. Some discrepancies are present in the comparison of the elemental mass balances for the elements analysed with the mass balances of the elements from the proposed mineral composition. Most of these variations can be ascribed to reasons mentioned above in preparing the presentation of the data, but the significant variations in the mass balances can be specifically explained.

The variation of the sulphur mass balances at times 160, 240 and 300 minutes with more than 50g, is explained on the basis of the sample at time 160 min. For this sample the sulphur (in the solids) was analysed too high which can be substantiated by looking at the significant increase in the sulphur content in the solution (Table F.7) but at the same time no decrease in the sulphur content in the solids occurred indicating that either the solution or solids analysis for the sulphur content was incorrect. Independent tests were conducted on the solution samples (on a Dionex analyser) to determine the sulphate (SO_4^{2-}) concentration in the solution. These tests confirmed an increase in the SO_4^{2-} concentration for this specific sample which substantiates the fact that the solution analysis is more accurate. Therefore, it is acceptable that the mass of sulphur calculated from the mineral composition is lower than the sulphur mass analysed for, in the solids. The same argument holds for the samples at times 240 and 300 minutes. The copper mass balance at time 240 minutes shows a significant variation which can be ascribed to the incorrect analysis of the copper in the solids for this specific sample. Looking at Table F.4 for this specific sample it is evident that the copper concentration in the solution increased, but the copper concentration analysed for in the solids did not decrease. Therefore,

this explains the lower calculated copper mass balance obtained from the mineral composition.

F.3 VERIFICATION OF LEACHING MECHANISM

The reaction mechanism proposed for this leaching process is substantiated with comparisons of the mole increases or decreases of the mineral species in the solids and by H^+, Ni^{2+} and Cu^{2+} ionic increases or decreases in the solution. The mole increase or decrease from the mineral composition (solids) and analytical results (solution) are compared with the stoichiometric prediction from the reaction mechanism. The method for calculating the mole increases or decreases are explained on the basis of an example for the reactions occurring in the experiment from time 20 minutes to 40 minutes (see Table F.11).

The reaction'mechanisms, which are of an electrochemical nature, for the leaching process are as follows:

$$Ni + 2H^+ + {}^1/_2O_2 \rightarrow Ni^{2+} + H_2O \qquad (F.1)$$

$$Ni_3S_2 + 2Cu^{2+} \rightarrow 2Ni^{2+} + NiS + Cu_2S \qquad (F.2)$$

$$5Cu_2S + 2H^+ + {}^1/_2O_2 \rightarrow Cu^{2+} + 5Cu_{1.8}S + H_2O \qquad (F.3a)$$

$$25Cu_{1.96}S + 8H^+ + 2O_2 \rightarrow 4Cu^{2+} + 25Cu_{1.8}S + 4H_2O \qquad (F.3b)$$

$$Ni + Ni_3S_2 + 4Cu^{2+} \rightarrow 4Ni^{2+} + 2Cu_2S \qquad (F.4)$$

$$3Ni_3S_2 + 4H^+ + O_2 \rightarrow 2Ni^{2+} + Ni_7S_6 + 2H_2O \qquad (F.5a)$$

$$Ni_7S_6 + 2H^+ + {}^1/_2O_2 \rightarrow Ni^{2+} + 6NiS + H_2O \qquad (F.5b)$$

Combining reactions (F.5a) and (F.5b) produces reaction (F.6):

$$Ni_3S_2 + 2H^+ + {}^1/_2O_2 \rightarrow Ni^{2+} + 2NiS + H_2O \quad \text{(F.6)}$$

$$4NiS + 2H^+ + {}^1/_2O_2 \rightarrow Ni^{2+} + Ni_3S_4 + H_2O \quad \text{(F.7)}$$

$$16Cu_2S + 2H^+ + {}^1/_2O_2 \rightarrow Cu^{2+} + Cu_{31}S_{16} + H_2O \quad \text{(F.8)}$$

$$5Cu_{31}S_{16} + 22H^+ + {}^{11}/_2O_2 \rightarrow 11Cu^{2+} + 80Cu_{1.8}S + 11H_2O \quad \text{(F.9)}$$

$$5Cu_{1.8}S + 8H^+ + 2O_2 \rightarrow 4Cu^{2+} + 5CuS + 4H_2O \quad \text{(F.10a)}$$

$$5Cu_{1.8}S + 8Fe^{3+} \rightarrow 4Cu^{2+} + 5CuS + 8Fe^{2+} \quad \text{(F.10b)}$$

$$Ni_3S_4 + H_2O + {}^{15}/_2O_2 \rightarrow 3Ni^{2+} + 2H^+ + 4SO_4^{2-} \quad \text{(F.11)}$$

$$Ni_3S_4 + 3Cu^{2+} + H_2O + {}^3/_2O_2 \rightarrow 3Ni^{2+} + 3CuS + 2H^+ + SO_4^{2-} \quad \text{(F.12)}$$

$$2Fe^{2+} + 2H^+ + {}^1/_2O_2 \rightarrow 2Fe^{3+} + H_2O \quad \text{(F.13a)}$$

$$2Fe^{3+} + 3H_2O \rightarrow Fe_2O_3 + 6H^+ \quad \text{(F.13b)}$$

$$6Fe^{3+} + 2NH_4^+ + 12H_2O \rightarrow 2NH_4Fe_3(SO_4)_2(OH)_6 + 12H^+ \quad \text{(F.13c)}$$

$$Fe + 2H^+ + {}^1/_2O_2 \rightarrow 2Fe^{2+} + H_2O \quad \text{(F.14)}$$

$$CuS + 2O_2 \rightarrow Cu^{2+} + SO_4^{2-} \quad \text{(F.15)}$$

The reactions occurring in the time period of 20-40 minutes are reactions (F.1) - (F.3a), (F.4) and (F.6). Firstly, the mole increase or decrease of each mineral species is determined which will be used to compare with the mole increase or decrease in the mineral according to the stoichiometry of the reactions occurring at this stage of the leaching process. The method of determining the mole quantities

used in each of the different reactions is a random method where the procedure is repeated until the optimum balance is achieved for the different mineral species. The increase or decrease of the mineral species from the mineral composition of the two samples can be compared with the increase or decrease in the mineral species due to the stoichiometry of the reactions occurring in the leaching process, as shown in Table F.11 (by the "Difference: Mole" column and "Mineral +/- by reaction" column). At the same time the increase or decrease in the H^+, Ni^{2+} and Cu^{2+} ions in the solution is calculated (from the stoichiometry) and compared with the analytically determined amounts of these ions in the solution and the solids.

The final mole balances for the reaction mechanism for the leaching reactions from time 10-300 minutes are shown in Table F.11 to Table F.17. The mole balances for the reactions occurring from time 0 to 10 minutes are omitted because the first 10 minutes are part of the start-up time for the experiment and the pressure leach experiment only starts to simulate the plant conditions after 10 to 20 minutes of the experiment.

Satisfactory mole balances were obtained for the mineral species as well as for the ionic species for the reaction mechanisms proposed for the times 10-20 minutes (Table F.12) and 20-40 minutes (Table F.11).

The mole balance of NiS for the reaction mechanism at time 40-80 minutes (Table F.13) shows a discrepancy which could be ascribed to the inaccurate compositional determination of NiS or to earlier experimental or analytical errors. The difference of approximately 2.4 mol in the H^+ mole balance is probably due to the fact that excessive iron is being leached presumably from the stainless steel shell of the experimental autoclave. The Ni^{2+} and Cu^{2+} mole balances are in between the values analysed for these metal species in the solution and solids.

The reaction mechanism proposed for the time period 80-120 minutes (Table F.14) shows that the mole balances for the mineral species are very accurate. It could again be argued here that the compositional determination of NiS is not accurate. The difference in the H^+ mole balance is because iron is leached and because a

small amount of Ni alloy may still be present in the solids at this stage which the XRD analysis was not able to identify due to its low concentration.

The difference for the time period of 120-160 minutes (Table F.15) differences in the mole balances of $Cu_{1.8}S$ and CuS for the proposed reaction mechanism which are due to errors that were propagated with the determinations of composition which were caused by experimental or analytical errors.

The reaction mechanism proposed for the time period 160-200 minutes (Table F.16) produced reasonably accurate mole balances for the mineral species. It should also be noticed that from this table onwards the mole decrease of iron (Fe^{2+} or Fe^{3+}) in solution (due to reactions (E.13b) and (E.13c)) is given in comparison to the amount of iron actually analysed for in the solution.

The sample at time 240 minutes was omitted because of irregularities in the data for this sample. The reason for the differences in the mole balances for the mineral species of $Cu_{1.8}S$ and CuS for the reaction mechanism proposed for time 200-300 minutes (Table F.17) could be explained by propagated errors in the calculation procedures.

Table F.1 - Nickel concentrations and mass balances for the kinetic experimental run, test 9

	Solution				Solids				
Time	$[Ni^{2+}]$	Ni^{2+}	Increase/ decrease	Rate of change	[Ni]	Ni	Increase/ decrease	Rate of change	Mass of Ni
min	g/L	g	mol	mol/min	%	g	mol	mol/min	g
0	28.0	1043.5			51.3	4049.4			5092.9
5	42.3	1633.9	10.058	2.012	44.7	3273.0	-13.227	-2.645	4906.9
10	47.3	1810.8	3.294	0.659	38.9	2847.8	-6.913	-1.383	4658.5
20	59.4	2249.7	7.832	0.783	34.1	2363.6	-7.958	-0.796	4613.3
40	66.3	**2490.1**	4.490	0.224	31.6	**2144.0**	-3.472	-0.174	**4634.0**
80	72.3	2691.1	3.856	0.096	27.3	1762.5	-6.266	-0.157	4453.6
120	81.4	3000.2	5.750	0.144	23.8	1455.9	-5.021	-0.126	4456.0
160	95.5	3485.5	8.838	0.221	19.1	1044.6	-6.843	-0.171	4530.2
200	102.0	3686.9	4.039	0.101	16.7	873.9	-2.766	-0.069	4560.8
240	97.2	3480.8	-2.931	-0.073	15.4	868.8	0.044	0.001	4349.6
300	111.1	3937.8	8.447	0.141	14.6	671.5	-3.236	-0.054	4609.3

Table F.2 - Part of the results used to explain the sample calculations of the solution samples (sample at time = 40 min)

Sampl no.	Time	$[Ni^{2+}]$	Ni^{2+}	Sample loss	Increase/ decrease		Rate of change	Incrementa mass decrease in Solids	Total Mass decrease
	min	g/L	g	g	g	mol	mol/min	g	g
...	...							...	...
2	20	59.4	2249.7					388.1	...
3	40	66.3	2490.1	23.2	263.6	4.490	0.224	134.8	1109.8
...	...							...	...

Table F.3 - Part of the results used to explain the sample calculations of the solid samples (sample at time = 40 min)

Sampl no.	Time	[Ni]	Ni	Sample loss	Increase/ decrease		Rate of change	Mass of Ni
	min	%	g	g	g	mol	mol/min	g
...	...							
2	20	34.1	2363.6					
3	40	31.6	2144.0	15.8	-203.8	-3.472	-0.174	4634.0
...	...							

Table F.4 - Copper concentrations and mass balances for the kinetic experimental run, test 9

	Solution				Solids				
Time	$[Cu^{2+}]$	Cu^{2+}	Increase/ decrease	Rate of change	[Cu]	Cu	Increase/ decrease	Rate of change	Mass of Cu
min	g/L	g	mol	mol/min	%	g	mol	mol/min	g
0	20.900	779.6			26.2	2069.5			2849.1
5	13.700	528.8	-3.946	-0.789	32.9	2409.0	5.342	1.068	2937.8
10	9.100	348.1	-2.794	-0.559	37.3	2727.2	5.300	1.060	3075.2
20	4.700	178.1	-2.648	-0.265	42.2	2920.1	3.368	0.337	3098.2
40	0.036	1.4	-2.782	-0.139	43.7	2967.1	1.083	0.054	2968.4
80	0.008	0.3	-0.017	0.000	48.0	3105.0	2.549	0.064	3105.3
120	0.015	0.5	0.004	0.000	50.1	3059.7	-0.319	-0.008	3060.2
160	0.006	0.2	-0.005	0.000	50.4	2761.9	-4.289	-0.107	2762.1
200	1.170	42.3	0.669	0.017	52.0	2717.1	-0.296	-0.007	2759.4
240	5.100	182.6	2.236	0.056	51.7	2913.7	3.500	0.087	3096.3
300	9.600	340.3	2.535	0.042	52.3	2413.5	-7.460	-0.124	2753.8

Table F.5 - Iron concentrations and mass balances for the kinetic experimental run, test 9

	Solution				Solids				
Time	$[Fe^{2+}]$ $[Fe^{3+}]$	$Fe^{2+/3+}$	Increase/ decrease	Rate of change	[Fe]	Fe	Increase/ decrease	Rate of change	Mass of Fe
min	g/L	g	mol	mol/min	%	g	mol	mol/min	g
0	0.514	19.2			0.51	40.1			59.3
5	1.210	46.7	0.493	0.099	0.13	9.4	-0.549	-0.110	56.2
10	1.270	48.6	0.041	0.008	0.09	6.7	-0.049	-0.010	55.2
20	1.340	50.8	0.048	0.005	0.07	4.8	-0.033	-0.003	55.6
40	1.710	64.2	0.251	0.013	0.27	18.6	0.250	0.012	82.8
80	3.560	132.4	1.244	0.031	0.05	3.1	-0.277	-0.007	135.6
120	4.950	182.4	0.926	0.023	0.05	3.2	0.001	0.000	185.6
160	5.850	213.5	0.594	0.015	0.04	2.3	-0.015	0.000	215.8
200	4.560	164.8	-0.843	-0.021	0.67	34.9	0.589	0.015	199.8
240	0.690	24.7	-2.505	-0.063	4.69	264.8	4.158	0.104	289.5
300	0.240	8.5	-0.288	-0.005	5.77	266.1	0.075	0.001	274.6

Table F.6 - Cobalt concentrations and mass balances for the kinetic experimental run, test 9

	Solution				Solids				
Time	$[Co^{2+}]$	Co^{2+}	Increase/ decrease	Rate of change	[Co]	Co	Increase/ decrease	Rate of change	Mass of Co
min	g/L	g	mol	mol/min	%	g	mol	mol/min	g
0	0.210	7.8			0.33	25.9			33.7
5	0.460	17.8	0.168	0.034	0.19	13.7	-0.207	-0.041	31.4
10	0.490	18.7	0.020	0.004	0.17	12.2	-0.025	-0.005	30.9
20	0.600	22.7	0.071	0.007	0.12	8.4	-0.062	-0.006	31.2
40	0.740	27.8	0.090	0.005	0.05	3.1	-0.091	-0.005	30.8
80	0.790	29.4	0.032	0.001	0.03	1.8	-0.022	-0.001	31.2
120	0.820	30.2	0.019	0.000	0.04	2.1	0.007	0.000	32.4
160	0.850	31.0	0.019	0.000	0.04	2.4	0.005	0.000	33.4
200	0.880	31.8	0.019	0.000	0.04	2.3	-0.002	0.000	34.1
240	0.780	27.9	-0.061	-0.002	0.04	2.1	-0.002	0.000	30.1
300	0.880	31.2	0.061	0.001	0.04	1.7	-0.007	0.000	32.9

Table F.7 - Total sulphur concentrations and mass balances for the kinetic experimental run, test 9

	Solution				Solids				
Time	Total S	S	Increase/ decrease	Rate of change	Total S	S	Increase/ decrease	Rate of change	Mass of Sulphur
min	g/L	g	mol	mol/min	%	g	mol	mol/min	g
0	67.2	2506.6			21.7	1714.3			4220.9
5	69.1	2667.3	5.012	1.002	22.0	1610.9	-3.226	-0.645	4278.1
10	67.8	2593.4	-1.565	-0.313	23.5	1718.6	3.725	0.745	4311.9
20	69.1	2618.9	1.551	0.155	23.5	1627.4	-2.478	-0.248	4246.3
40	68.8	2583.4	-0.355	-0.018	24.4	1656.8	1.299	0.065	4240.3
80	70.4	2618.9	1.874	0.047	24.6	1589.9	-1.704	-0.043	4208.8
120	69.7	2568.4	-0.812	-0.020	26.0	1588.6	0.366	0.009	4157.1
160	71.7	2617.1	2.299	0.057	30.4	1665.0	2.855	0.071	4282.0
200	71.0	2566.7	-0.797	-0.020	30.6	1600.0	-1.549	-0.039	4166.7
240	63.3	2266.1	-8.682	-0.217	28.2	1590.7	0.148	0.004	3856.8
300	72.9	2584.3	10.720	0.179	27.3	1259.2	-9.912	-0.165	3843.5

Table F.8 - The incremental and total mass decrease in the solids for each time step

Time min	Incremental mass decrease in solids g	Total Mass decrease g
0		
5	577.8	577.8
10	9.1	587.0
20	388.1	975.0
40	134.8	1109.8
80	327.3	1437.0
120	352.9	1789.9
160	633.3	2423.2
200	248.1	2671.2
240	-411.9	2259.4
300	1028.1	3287.4

Table F.9 - Results of the acid (H_2SO_4) concentration for the kinetic experimental run, test 9

Time min	pH 25 °C	$[H_2SO_4]$ g/L	H_2SO_4 g	Increase/ decrease mol $[H^+]$	Rate of change mol/min
0		104.0	3879.2		
5		98.5	3802.1	-1.572	-0.314
10		98.0	3748.5	-0.394	-0.079
20		87.0	3297.3	-8.580	-0.858
40		79.5	2985.2	-5.797	-0.290
80		67.0	2492.4	-9.572	-0.239
120		45.0	1658.3	-16.689	-0.417
160	1.10	21.5	784.8	-17.659	-0.441
200	1.47	5.4	195.2	-11.984	-0.300
240	1.75	3.6	128.9	-1.327	-0.033
300	2.01	2.2	78.0	-1.022	-0.017

Table F.10 - Mineral compositions and mass balances of the samples of kinetic experiment, test 9

Time [min]	**0**	**5**	**10**	**20**	**40**	**80**	**120**
Ni [%]	9.9	6.6	5.0	3.0	1.2	0	0
Ni_3S_2 [%]	57.0	50.7	45.4	36.7	35.2	25.5	12.8
Ni_7S_6 [%]	0	0	trace	trace	trace	3.6	trace
NiS [%]	0	1.5	2.4	7.0	7.6	9.5	16.7
Ni_3S_4 [%]	0	0	0	0	0	trace	6.7
Cu_2S [%]	33.1	38.2	41.9	45.0	46.3	46.6	15.3
$Cu_{1.96}S$ [%]	-	-	-	-	-	-	23.4
$Cu_{31}S_{16}$ [%]	0	0	0	0	0	3.1	2.2
$Cu_{1.8}S$ [%]	0	3.0	5.3	8.3	9.7	11.7	22.9
CuS [%]	0	0	0	0	0	0	trace
$Cu(Ni,Co)_2S_4$		Traces were detected at certain stages					
NiS_2'		Traces were detected at certain stages					
Total [%]	100	100	100	100	100	100	100
Ni analysed [g]	4049.4	3273.0	2847.8	2363.6	2144.0	1762.5	1455.9
Ni in mineral composition [g]	4049.4	3262.6	2905.3	2379.6	2160.3	1762.2	1468.7
Cu analysed [g]	2069.5	2409.0	2727.2	2920.1	2967.1	3105.0	3059.7
Cu in mineral composition [g]	2069.6	2395.6	2742.3	2931.3	3015.0	3151.9	3080.1
S analysed [g]	1714.3	1610.9	1718.6	1627.4	1656.8	1589.9	1588.6
S in mineral composition [g]	1714.3	1634.7	1645.9	1599.9	1592.5	1543.3	1555.3
Mass of elements analysed [g]	7833.3	7292.9	7293.5	6911.0	6767.8	6457.4	6104.2
Mass balance of mineral composition	7833.3	7292.9	7293.5	6911.0	6767.8	6457.4	6104.2
True calculated mass of solids [g]	7900.0	7322.2	7313.0	6925.0	6790.2	6463.0	6110.1

Table F.10 (continue)

Time [min]	160	200	240	300
Ni [%]	0	0	0	0
Ni_3S_2 [%]	trace	0	0	0
Ni_7S_6 [%]	0	0	0	0
NiS [%]	11.4	6.2	4.9	2.0
Ni_3S_4 [%]	21.1	22.1	22.3	22.8
Cu_2S [%]	0	0	0	0
$Cu_{1.96}S$ [%]	2.3	0	0	0
$Cu_{31}S_{16}$ [%]	0	0	0	0
$Cu_{1.8}S$ [%]	53.6	42.1	29.5	29.0
CuS [%]	11.6	29.6	43.3	46.2
$Cu(Ni,Co)_2S_4$	Traces were detected			
NiS_2	Traces were detected			
Total [%]	100	100	100	100
Ni analysed [g]	1044.6	873.9	868.8	671.5
Ni in mineral composition [g]	1071.4	872.0	863.6	629.3
Cu analysed [g]	2761.9	2717.1	2913.7	2413.5
Cu in mineral composition [g]	2812.6	2728.3	2784.5	2318.1
S analysed [g]	1665.0	1600.0	1590.7	1259.2
S in mineral composition [g]	1587.5	1590.8	1725.1	1396.9
Mass of elements analysed [g]	5471.5	5191.1	5373.2	4344.3
Mass balance of mineral composition	5471.5	5191.1	5373.2	4344.3
True calculated mass of solids [g]	5476.8	5228.8	5640.6	4612.6

Table F.11 - An example of the mole balances performed on the reactions occurring from time 20 to 40 minutes in the experiment (test 9)

	20 minutes		40 minutes		Difference		
Mineral	Composition [%]	Weight [g]	Composition [%]	Weight [g]	Weight [g]	Mole [mol]	Mineral +/- by reaction
Ni	3.0	207.3	1.2	81.2	-126.1	-2.148	-2.148
Ni_3S_2	36.7	2536.3	35.2	2382.3	-154.1	-0.641	-0.641
Ni_7S_6	-	0.0	-	0.0	0.0	0.000	0.000
NiS	7.0	483.8	7.6	514.4	30.6	0.337	0.571
Ni_3S_4	-	0.0	-	0.0	0.0	0.000	0.000
Cu_2S	45.0	3110.0	46.3	3133.5	23.5	0.148	0.145
$Cu_{1.96}S$	-	0.0	-	0.0	0.0	0.000	0.000
$Cu_{31}S_{16}$	-	0.0	-	0.0	0.0	0.000	0.000
$Cu_{1.8}S$	8.3	573.6	9.7	656.5	82.9	0.566	0.566
CuS	-	0.0	-	0.0	0.0	0.000	0.000
Total	100.0	6911.0	100.0	6767.8			

Table F.11 (continue)

		Increase/decrease of ion in the solution according to the reactions					
Mineral reacting	[mol]	Reactions	H^+ [mol]	Ni^{2+} [mol]	Cu^{2+} [mol]	Mineral formed	[mol]
Ni	-2.048	F.1	-4.097	2.048	-		
Ni_3S_2	-0.511	F.2	-	1.023	-1.023	$NiS=Cu_2S$	0.511
Cu_2S	-0.566	F.3a	-0.226	-	0.113	$Cu_{1.8}S$	0.566
$Ni_3S_2 = Ni$	-0.100	F.4	-	0.400	-0.400	$2Cu_2S$	0.200
Ni_3S_2	-0.030	F.6	-	-	-	2NiS	0.060
Fe	-0.120	F.14	-0.240			Fe^{2+}	0.120
		Total	-4.623	3.501	-1.310		
	Analytical results	Solution Solids	-5.797 -	4.490 3.472	-2.782 -1.083		

Table F.12 - Mole balances performed on the reactions occurring from time 10 to 20 minutes in the experiment (test 9)

Mineral increase/decrease			Reaction mechanism				
Mineral	by composition	by reaction	Mineral reacting	[mol]	Reactions	Mineral formed	[mol]
Ni	-2.680	-2.680	Ni	-2.480	F.1		
Ni_3S_2	-3.226	-3.226	Ni_3S_2	-0.926	F.2	$NiS=Cu_2S$	0.926
Ni_7S_6	0.000	0.000	Cu_2S	-1.010	F.3a	$Cu_{1.8}S$	1.010
NiS	3.402	5.126	$Ni_3S_2 = Ni$	-0.200	F.4	$2Cu_2S$	0.400
Ni_3S_4	0.000	0.000	Ni_3S_2	-2.100	F.6	2NiS	4.200
Cu_2S	0.339	0.316	Fe	-0.050	F.14	Fe^{2+}	0.050
$Cu_{1.96}S$	0.000	0.000					
$Cu_{31}S_{16}$	0.000	0.000			H^+ [mol]	Ni^{2+} [mol]	Cu^{2+}[mol]
$Cu_{1.8}S$	1.277	1.010	Reactions	Solution	-9.665	7.232	-2.450
CuS	0.000	0.000	Analytical results	Solution	-8.585	7.832	-2.648
				Solids	-	7.958	-3.368

Table F.13 - Mole balances performed on the reactions occurring from time 40 to 80 minutes in the experiment (test 9)

Mineral increase/decrease			Reaction mechanism				
Mineral	by composition	by reaction	Mineral reacting	[mol]	Reactions	Mineral formed	[mol]
Ni	-1.384	-1.384	Ni	-1.384	F.1		
Ni_3S_2	-3.062	-3.062	Ni_3S_2	-0.862	F.2	$NiS=Cu_2S$	0.862
Ni_7S_6	0.385	0.333	Cu_2S	-1.200	F.3a	$Cu_{1.8}S$	0.676
NiS	1.092	3.262	$Ni_3S_2 = Ni$	-0.000	F.4	$2Cu_2S$	0.000
Ni_3S_4	0.000	0.000	$3Ni_3S_2$	-2.200	F.5a	Ni_7S_6	0.733
Cu_2S	-0.781	-1.628	Ni_7S_6	-0.400	F.5b	6NiS	2.400
$Cu_{1.96}S$	0.000	0.000	$16Cu_2S$	-1.290	F.8	$Cu_{31}S_{16}$	0.081
$Cu_{31}S_{16}$	0.081	0.080	$5Cu_{31}S_{16}$	-0.001	F.9	$80Cu_{1.8}S$	0.016
$Cu_{1.8}S$	0.676	0.692	Fe	-1.100	F.14	Fe^{2+}	1.100
CuS	0.000	0.000			**H^+ [mol]**	**Ni^{2+} [mol]**	**Cu^{2+}[mol]**
			Reactions	Solution	-9.346	4.975	-1.402
			Analytical results	Solution	-9.572	3.856	-0.017
				Solids	-	6.266	-2.549

Table F.14 - Mole balances performed on the reactions occurring from time 80 to 120 minutes in the experiment (test 9)

Mineral increase/decrease			Reaction mechanism				
Mineral	by composition	by reaction	Mineral reacting	[mol]	Reactions	Mineral formed	[mol]
Ni	0.000	0.000	Ni_3S_2	-0.302	F.2	$NiS=Cu_2S$	0.302
Ni_3S_2	-3.602	-3.602	Cu_2S	-4.200	F.3a	$Cu_{1.8}S$	4.200
Ni_7S_6	-0.385	-0.360	$Cu_{1.96}S$	-0.487	F.3b	$Cu_{1.8}S$	0.487
NiS	4.473	3.687	$3Ni_3S_2$	-3.300	F.5a	Ni_7S_6	1.100
Ni_3S_4	1.344	1.344	Ni_7S_6	-1.460	F.5b	6NiS	8.760
Cu_2S	-3.585	-3.898	4NiS	-5.375	F.7	Ni_3S_4	1.344
$Cu_{1.96}S$	-0.487	-0.487	$16Cu_2S$	-0.000	F.8	$Cu_{31}S_{16}$	0.000
$Cu_{31}S_{16}$	-0.027	-0.025	$5Cu_{31}S_{16}$	-0.025	F.9	$80Cu_{1.8}S$	0.400
$Cu_{1.8}S$	4.386	5.087	Fe	-1.800	F.14	Fe^{2+}	1.800
CuS	0.000	0.000			**H^+ [mol]**	**Ni^{2+} [mol]**	**Cu^{2+}[mol]**
			Reactions	Solution	-15.553	5.608	0.369
			Analytical results	Solution	-16.689	5.750	0.004
				Solids	-	5.021	0.319

Table F.15 - Mole balances performed on the reactions occurring from time 120 to 160 minutes in the experiment (test 9)

Mineral increase/decrease			Reaction mechanism				
Mineral	by composition	by reaction	Mineral reacting	[mol]	Reactions	Mineral formed	[mol]
Ni	0.000	0.000	Ni_3S_2	-2.853	F.2	$NiS=Cu_2S$	2.853
Ni_3S_2	-3.253	-3.253	Cu_2S	-8.000	F.3a	$Cu_{1.8}S$	8.000
Ni_7S_6	0.000	0.000	$Cu_{1.96}S$	-8.000	F.3b	$Cu_{1.8}S$	8.000
NiS	-4.359	-5.347	$3Ni_3S_2$	-0.400	F.5a	Ni_7S_6	0.133
Ni_3S_4	2.450	2.130	Ni_7S_6	-0.133	F.5b	6NiS	0.800
Cu_2S	-5.868	-5.277	4NiS	-9.200	F.7	Ni_3S_4	2.300
$Cu_{1.96}S$	-8.317	-8.000	$16Cu_2S$	-0.130	F.8	$Cu_{31}S_{16}$	0.008
$Cu_{31}S_{16}$	-0.054	-0.072	$5Cu_{31}S_{16}$	-0.080	F.9	$80Cu_{1.8}S$	1.280
$Cu_{1.8}S$	10.481	12.032	$Cu_{1.8}S$	-4.948	F.10a	CuS	4.948
CuS	6.639	5.098	$5Cu_{1.8}S$ $8Fe^{3+}$	-0.300	F.10b	5CuS $8Fe^{2+}$	0.600
			Ni_3S_4	-0.120	F.11		
			$2Fe^{2+}$	-0.480	F.13a	$2Fe^{3+}$	0.480
			Fe	-0.050	F.14	Fe^{2+}	0.050
			CuS	-0.150	F.15		
Total Fe in solution:		[mol]			**H^+ [mol]**	**Ni^{2+} [mol]**	**Cu^{2+}[mol]**
by reactions		3.270	Reactions	Solution	-19.685	8.715	1.707
by analytical results		3.823	Analytical results	Solution Solids	-17.659 -	8.838 6.843	-0.005 4.289

Table F.16 - Mole balances performed on the reactions occurring from time 160 to 200 minutes in the experiment (test 9)

Mineral increase/decrease			Reaction mechanism				
Mineral	by composition	by reaction	Mineral reacting	[mol]	Reactions	Mineral formed	[mol]
Ni	0.000	0.000	$Cu_{1.96}S$	-0.804	F.3b	$Cu_{1.8}S$	0.804
Ni_3S_2	0.000	0.000	4NiS	-3.326	F.7	Ni_3S_4	0.832
Ni_7S_6	0.000	0.000	$Cu_{1.8}S$	-5.450	F.10a	CuS	5.540
NiS	-3.326	-3.326	$5Cu_{1.8}S$ $8Fe^{3+}$	-0.550	F.10b	5CuS $8Fe^{2+}$	0.550
Ni_3S_4	-0.024	-0.038	Ni_3S_4	-0.150	F.11		
Cu_2S	0.000	0.000	Ni_3S_4	-0.720	F.12	3CuS	2.160
$Cu_{1.96}S$	-0.804	-0.804	$2Fe^{2+}$	-0.880	F.13a	$2Fe^{3+}$	0.880
$Cu_{31}S_{16}$	0.000	0.000	$2Fe^{3+}$	-0.200	F.13b	Fe_2O_3	0.200
$Cu_{1.8}S$	-5.103	-5.196	CuS	-0.100	F.15		
CuS	9.433	8.060					
Fe decrease in solution:		[mol]			**H^+ [mol]**	**Ni^{2+} [mol]**	**Cu^{2+}[mol]**
by hydrolysis reactions (total)		-0.200 (3.070)	Reactions	Solution	-9.180	3.442	2.869
by analytical results of solution (total)		-0.843 (2.980)	Analytical results	Solution Solids	-11.984 -	4.039 2.766	0.669 0.296

Table F.17 - Mole balances performed on the reactions occurring from time 200 to 300 minutes in the experiment (test 9)

Mineral increase/decrease			Reaction mechanism				
Mineral	by composition	by reaction	Mineral reacting	[mol]	Reactions	Mineral formed	[mol]
Ni	0.000	0.000	4NiS	-2.700	F.7	Ni_3S_4	0.675
Ni_3S_2	0.000	0.000	$Cu_{1.8}S$	-5.400	F.10a	CuS	5.400
Ni_7S_6	0.000	0.000	$5Cu_{1.8}S$ $8Fe^{3+}$	-1.300	F.10b	5CuS $8Fe^{2+}$	1.300
NiS	-2.362	-2.700	Ni_3S_4	-0.300	F.11		
Ni_3S_4	0.256	0.225	Ni_3S_4	-0.300	F.12	3CuS	0.900
Cu_2S	0.000	0.000	$2Fe^{2+}$	-2.080	F.13a	$2Fe^{3+}$	2.080
$Cu_{1.96}S$	0.000	0.000	$2Fe^{3+}$	-2.400	F.13b	Fe_2O_3	
$Cu_{31}S_{16}$	0.000	0.000	$6Fe^{3+}$	-0.400	F.13c	$2NH_4Fe_3(SO_4)_2(OH)_6$	
$Cu_{1.8}S$	-4.283	-6.700	CuS	-0.250	F.15		
CuS	9.893	7.350					
Fe increase in solution:		[mol]			**H^+ [mol]**	**Ni^{2+} [mol]**	**Cu^{2+} [mol]**
by hydrolysis reactions (total)		-2.800 (0.270)	Reactions	Solution	-2.870	2.475	4.710
by analytical results of solution (total)		-2.799 (0.181)	Analytical results	Solution Solids	-2.349	4.274 3.448	4.689 4.778

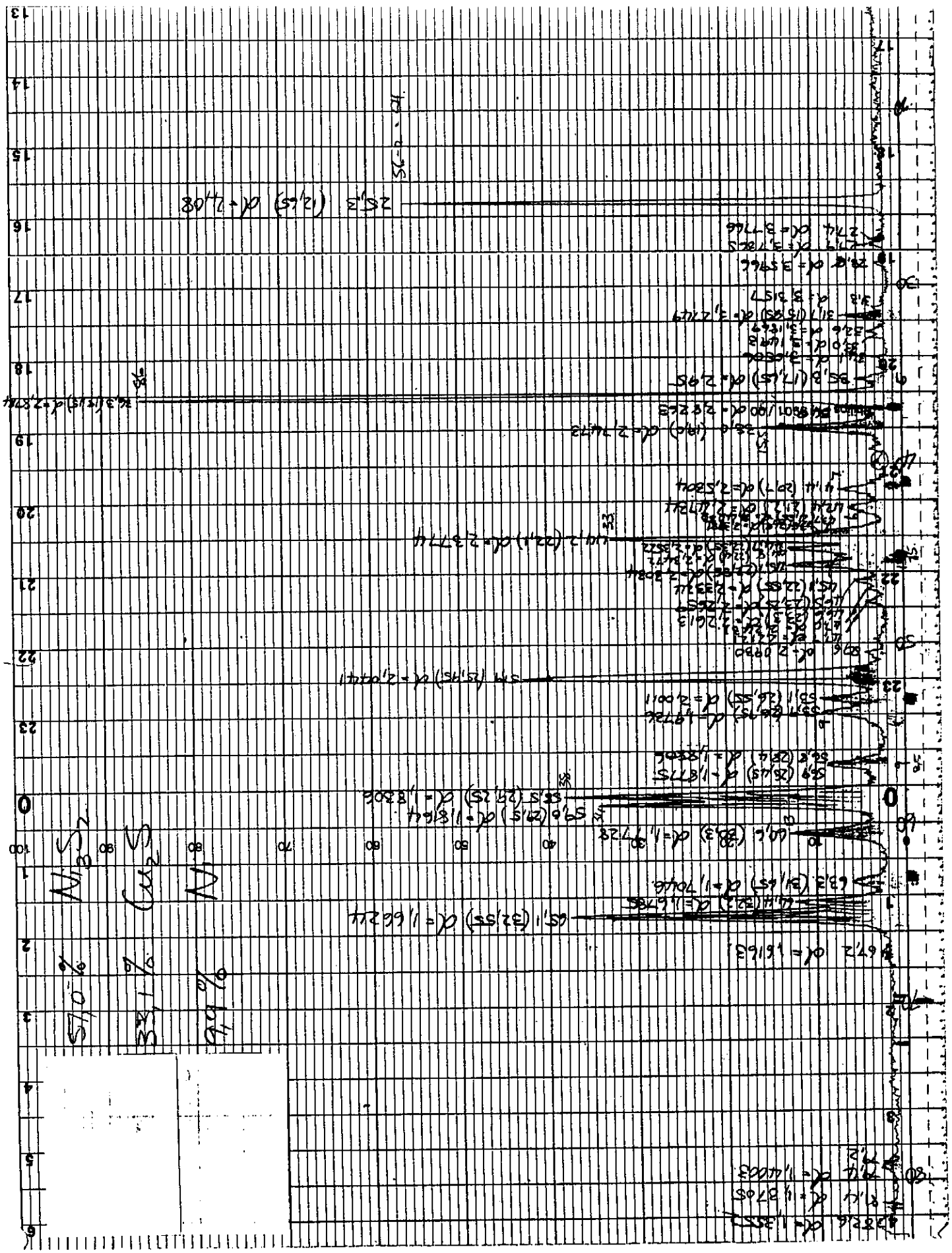

Figure F.1 - Original XRD graph at time = 0 minutes

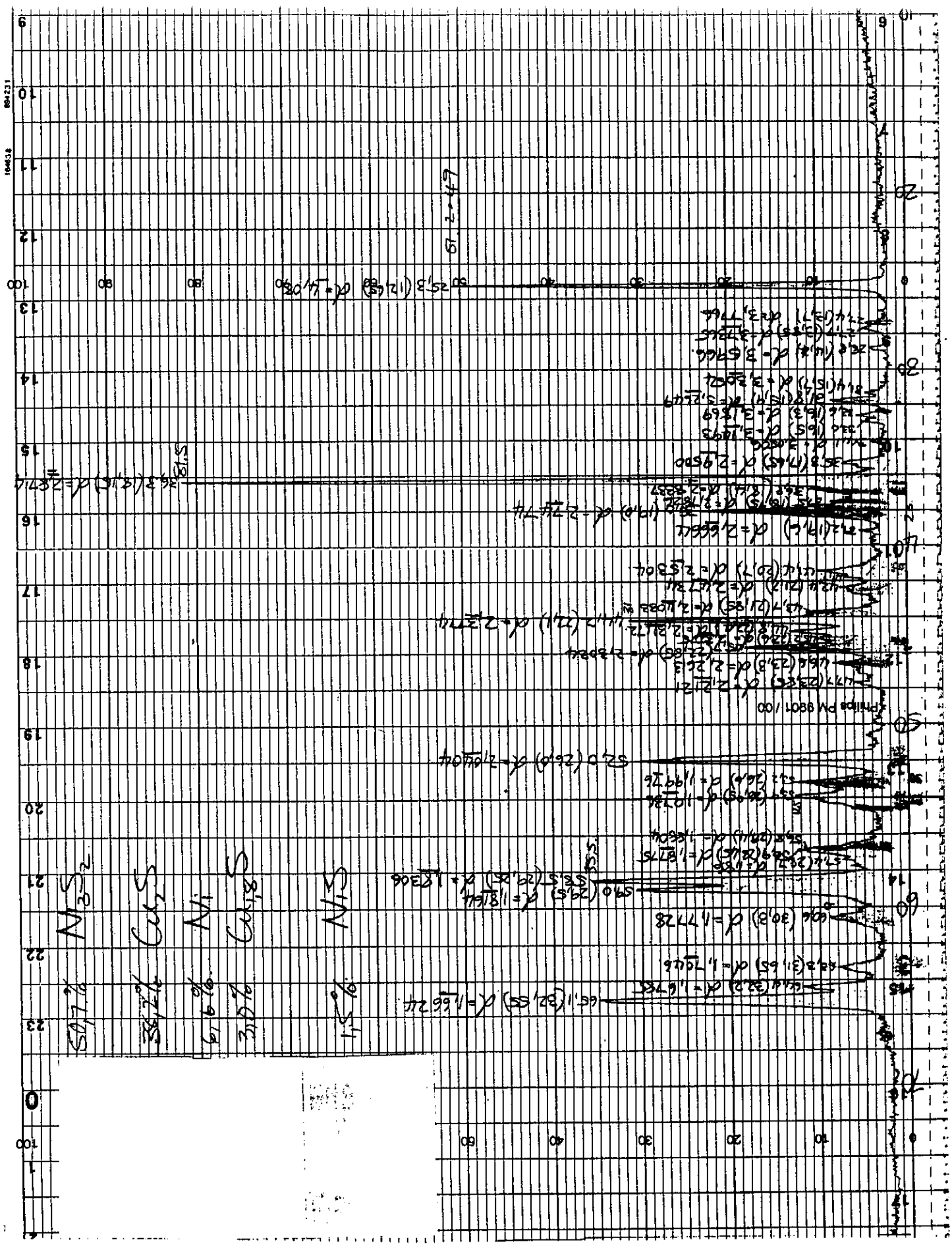

Figure F.2 - Original XRD graph at time = 5 minutes

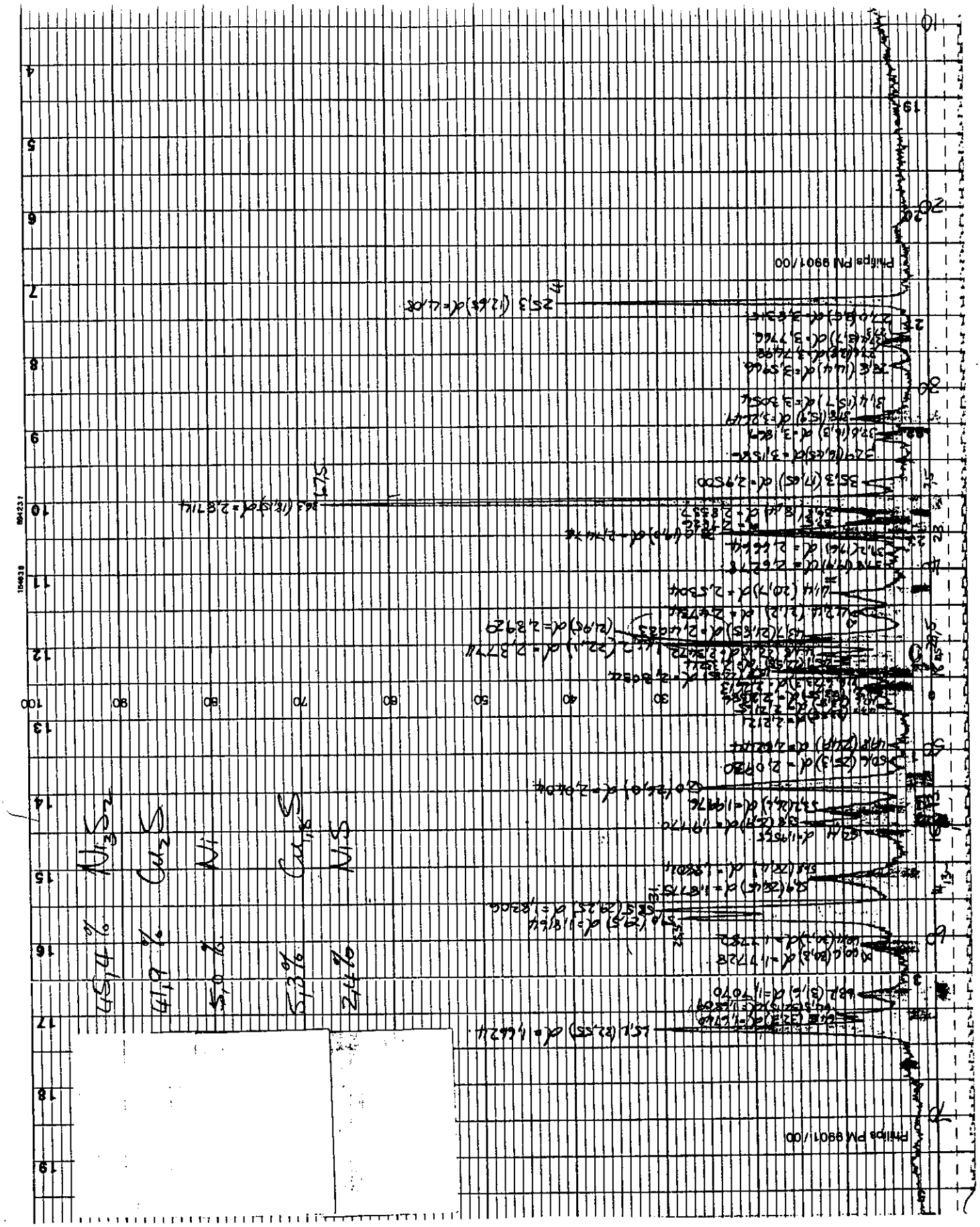

Figure F.3 - Original XRD graph at time = 10 minutes

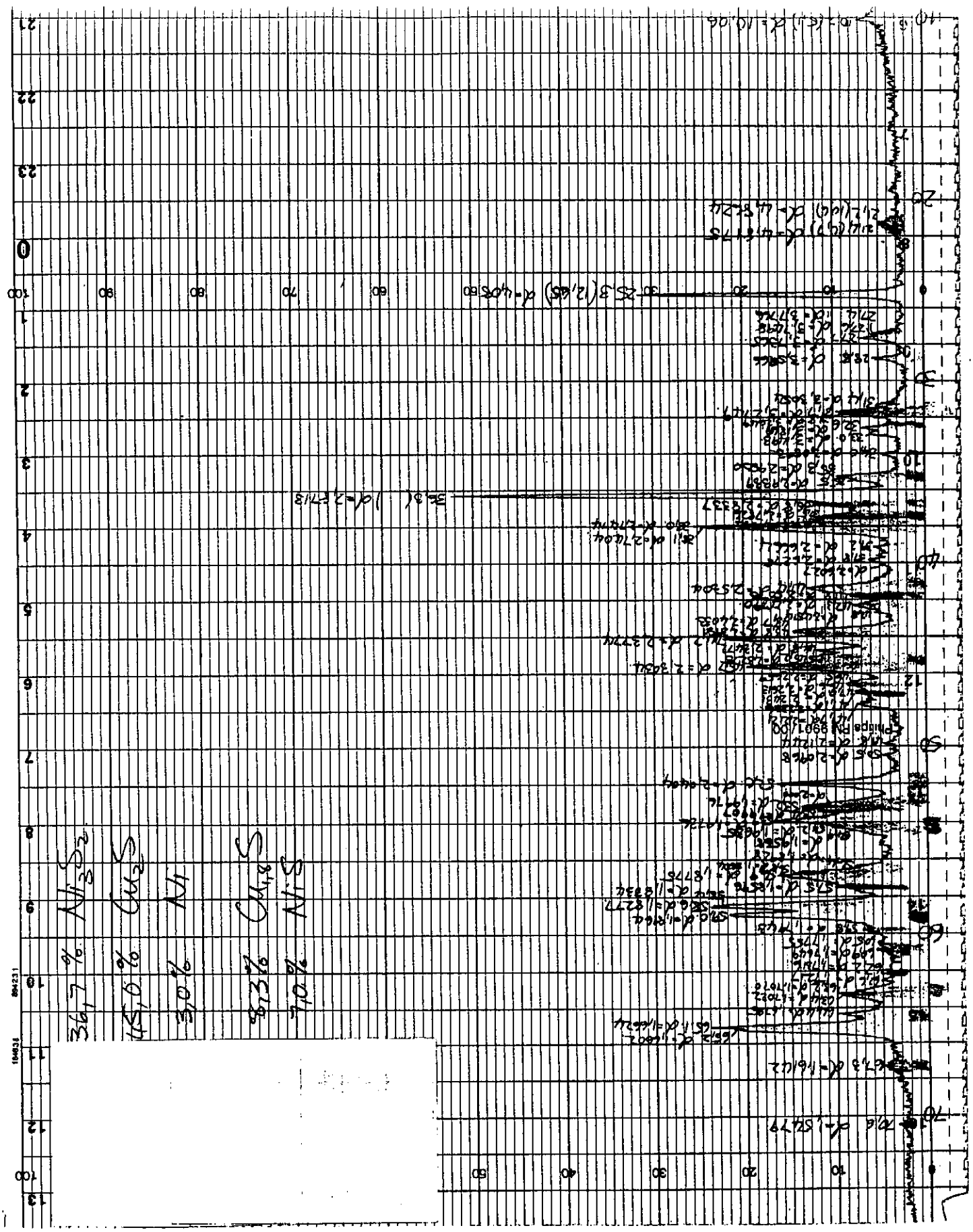

Figure F.4 - Original XRD graph at time = 20 minutes

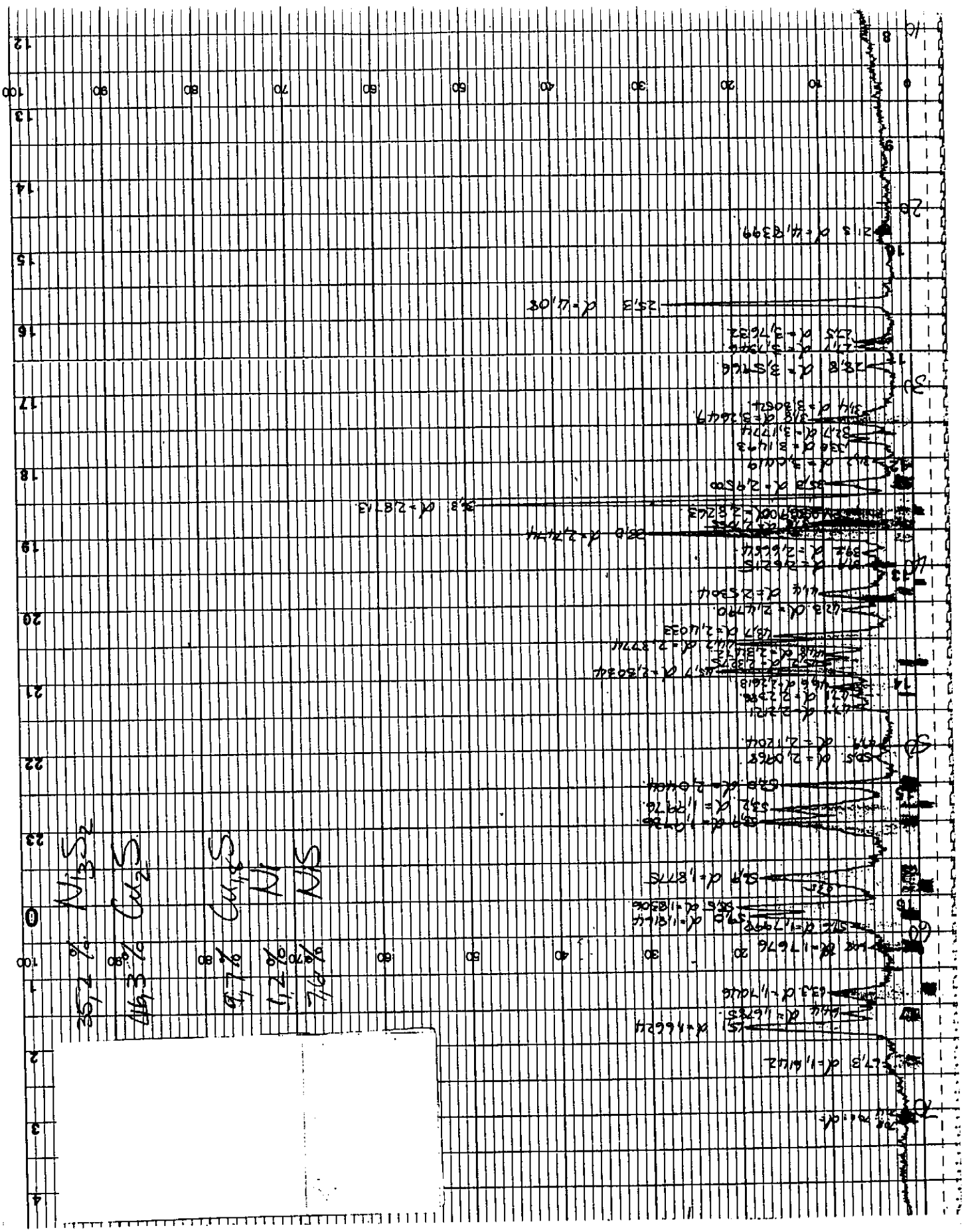

Figure F.5 - Original XRD graph at time = 40 minutes

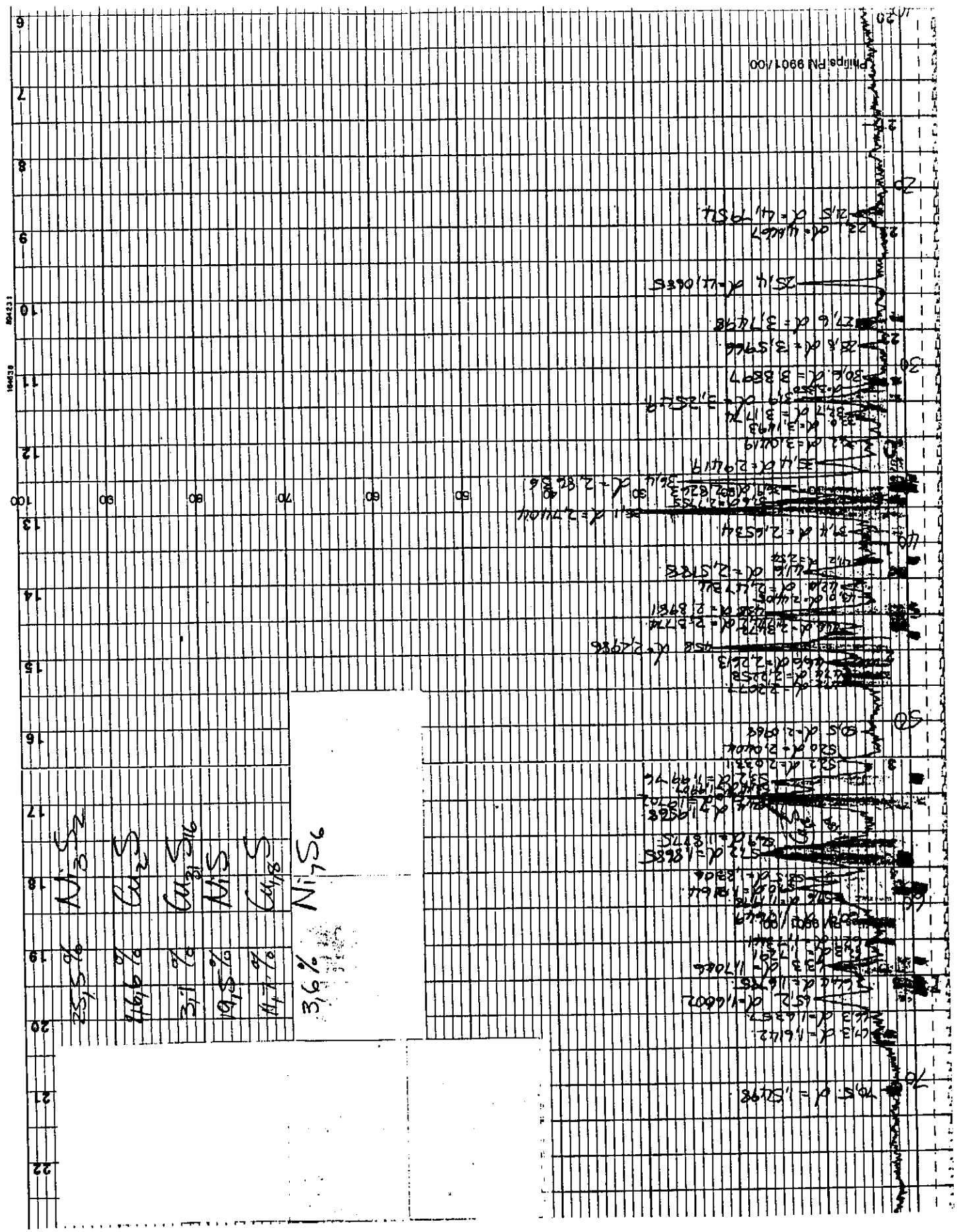

Figure F.6 - Original XRD graph at time = 80 minutes

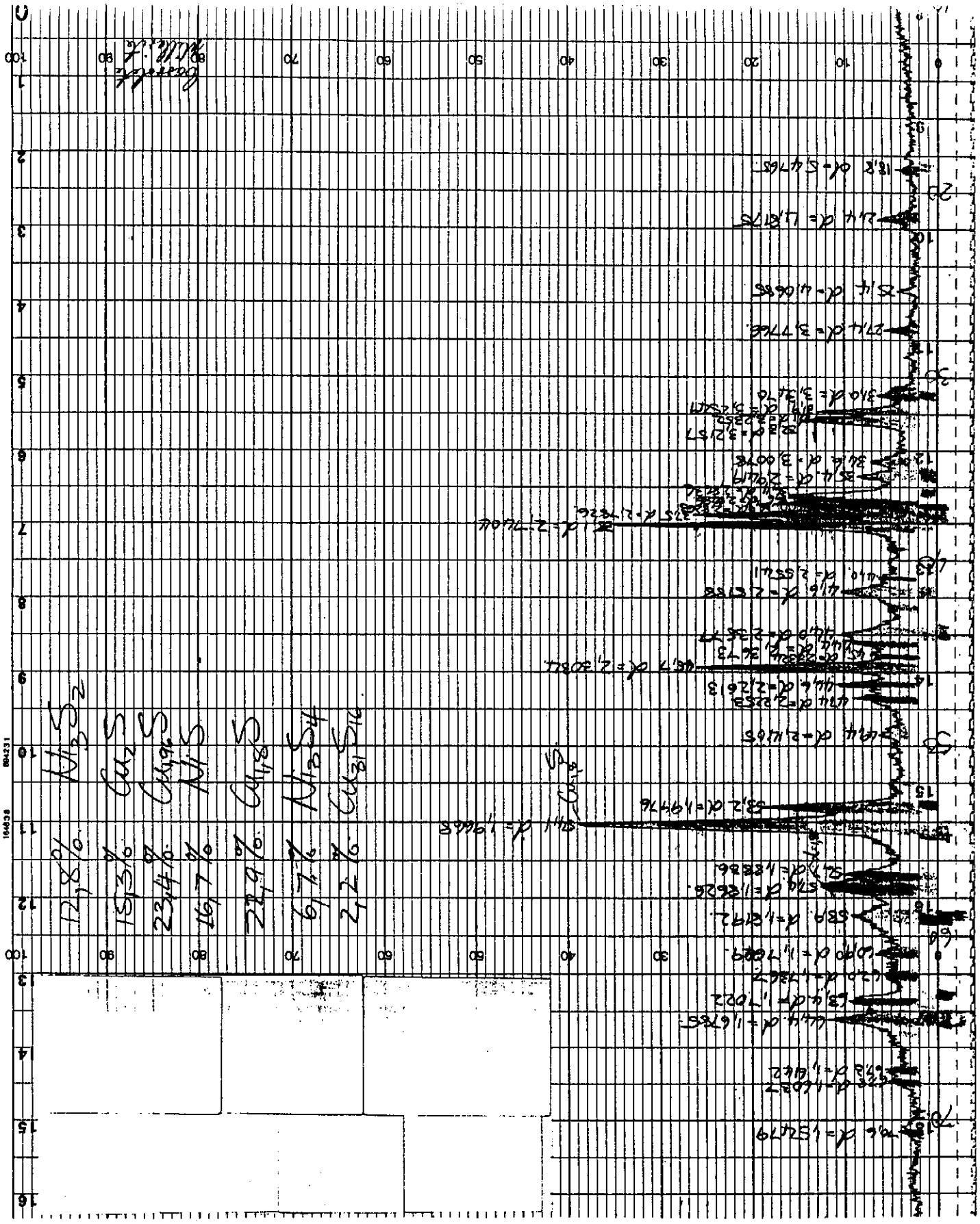

Figure F.7 - Original XRD graph at time = 120 minutes

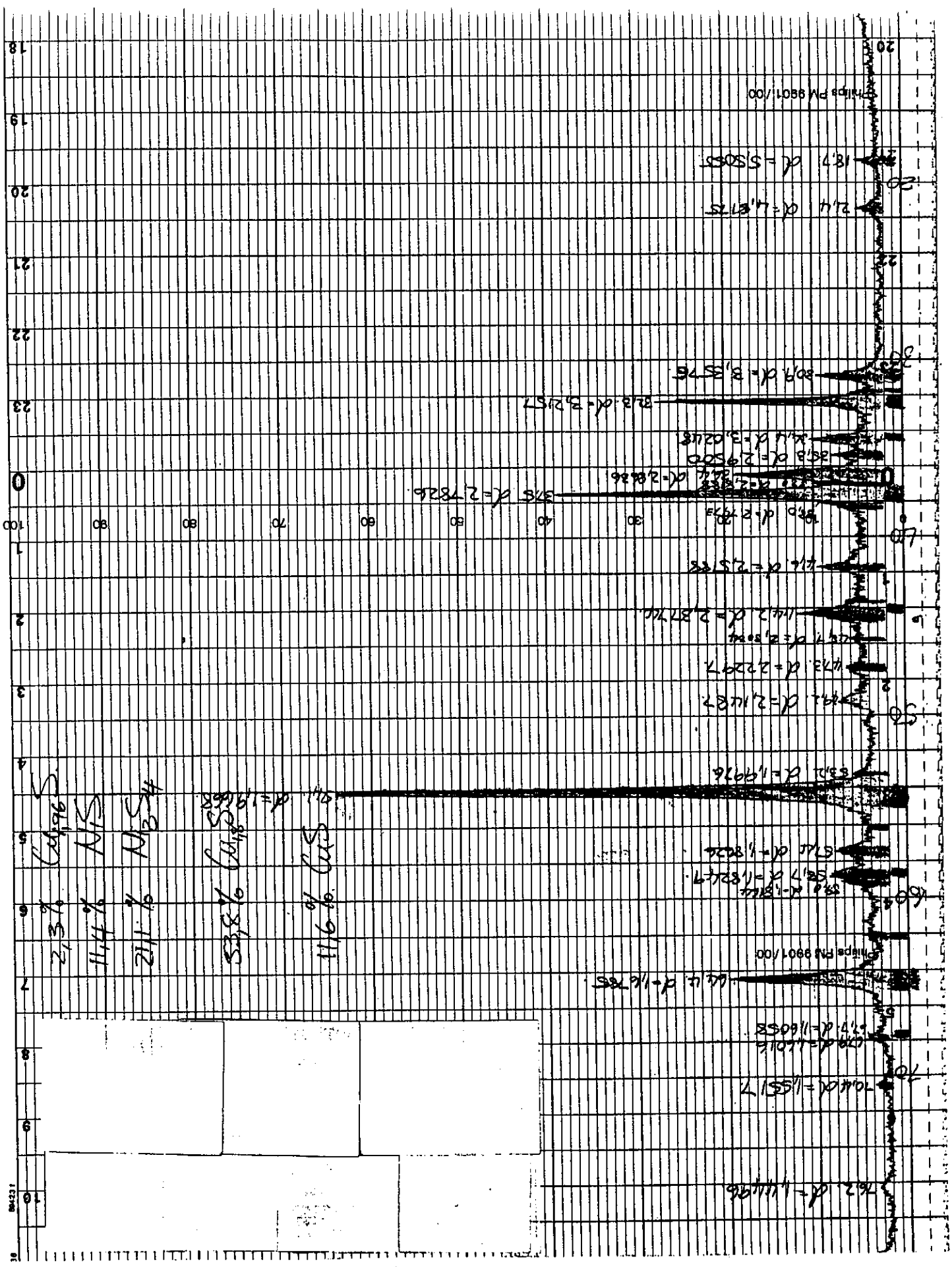

Figure F.8 - Original XRD graph at time = 160 minutes

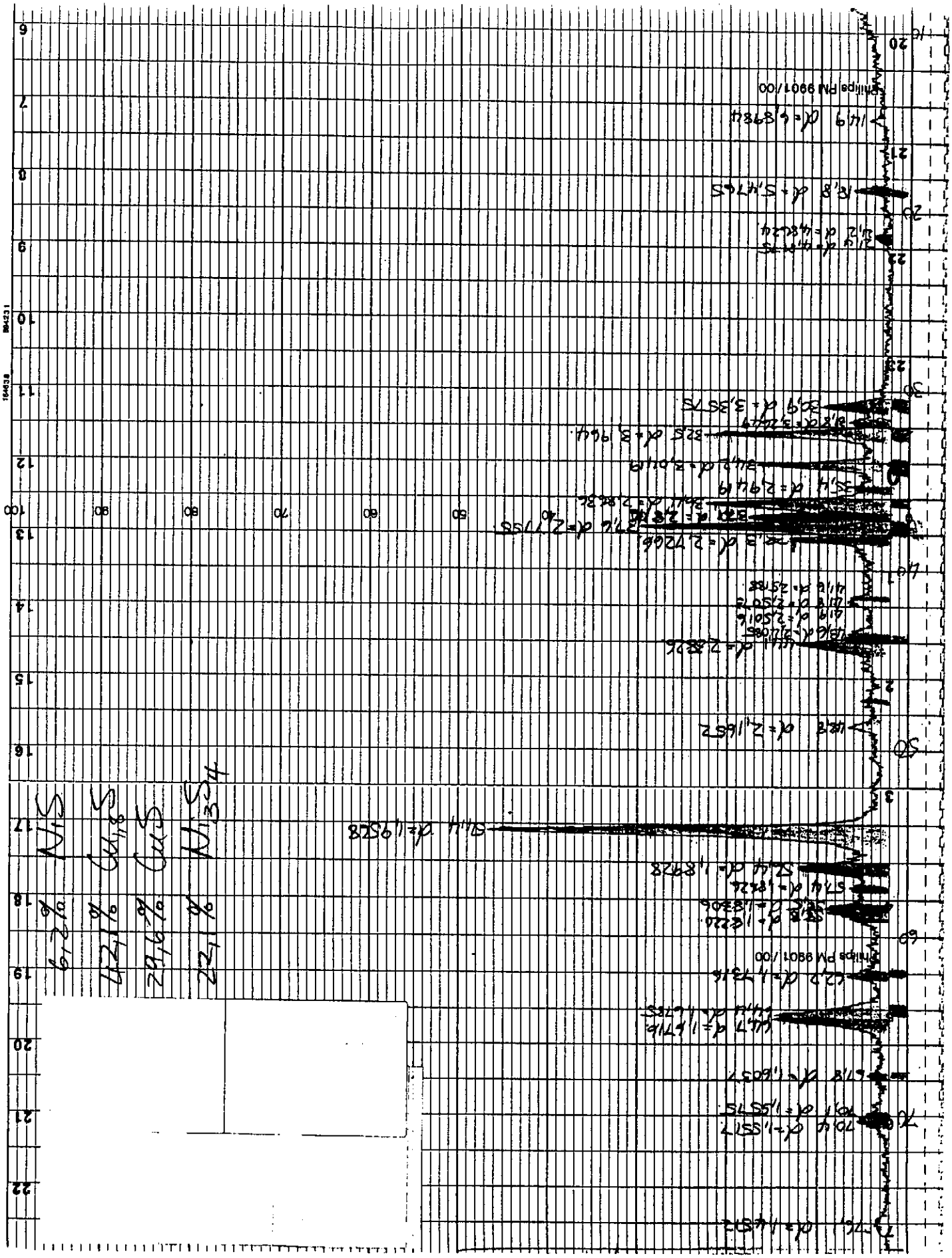

Figure F.9 - Original XRD graph at time = 200 minutes

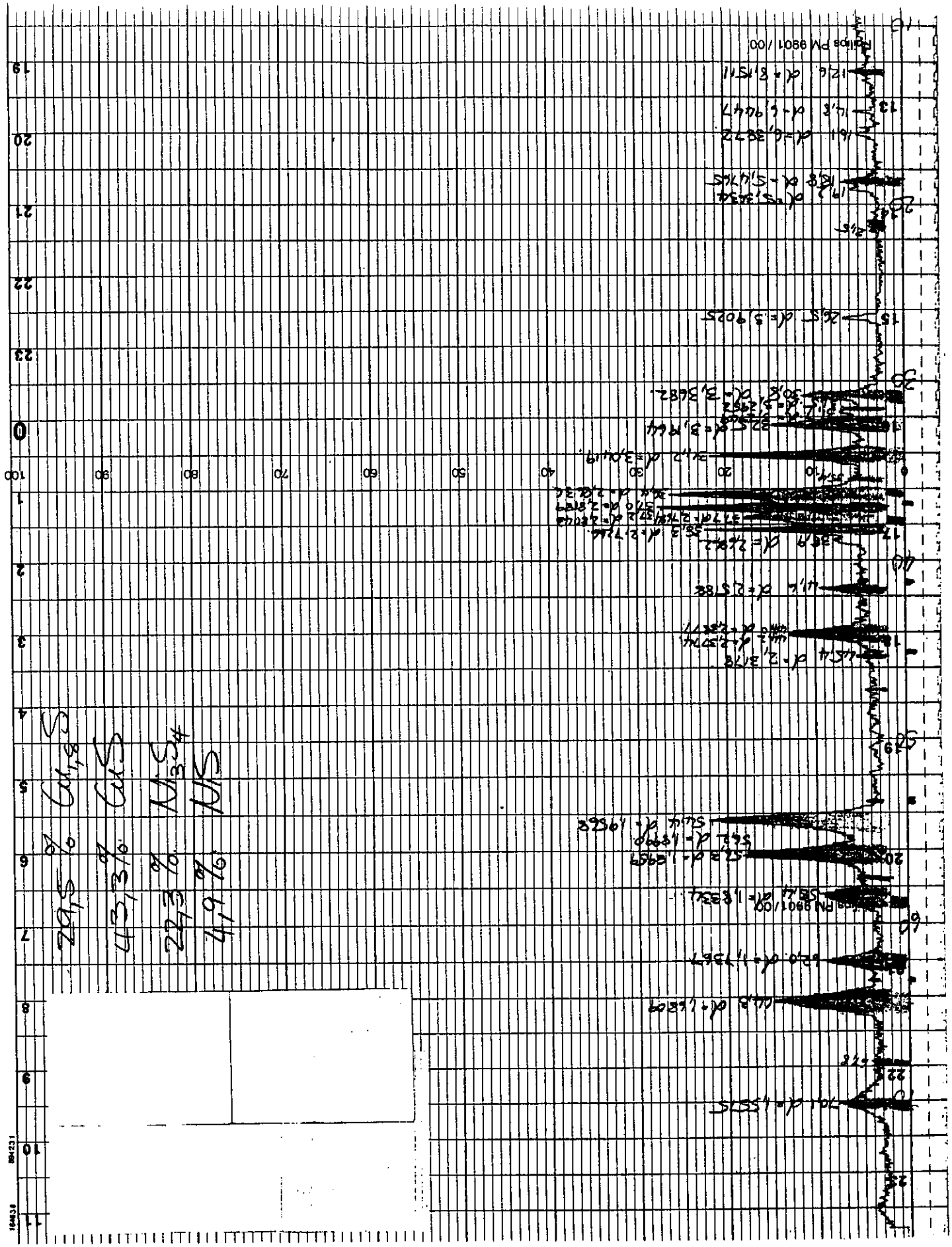

Figure F.10 - Original XRD graph at time = 240 minutes

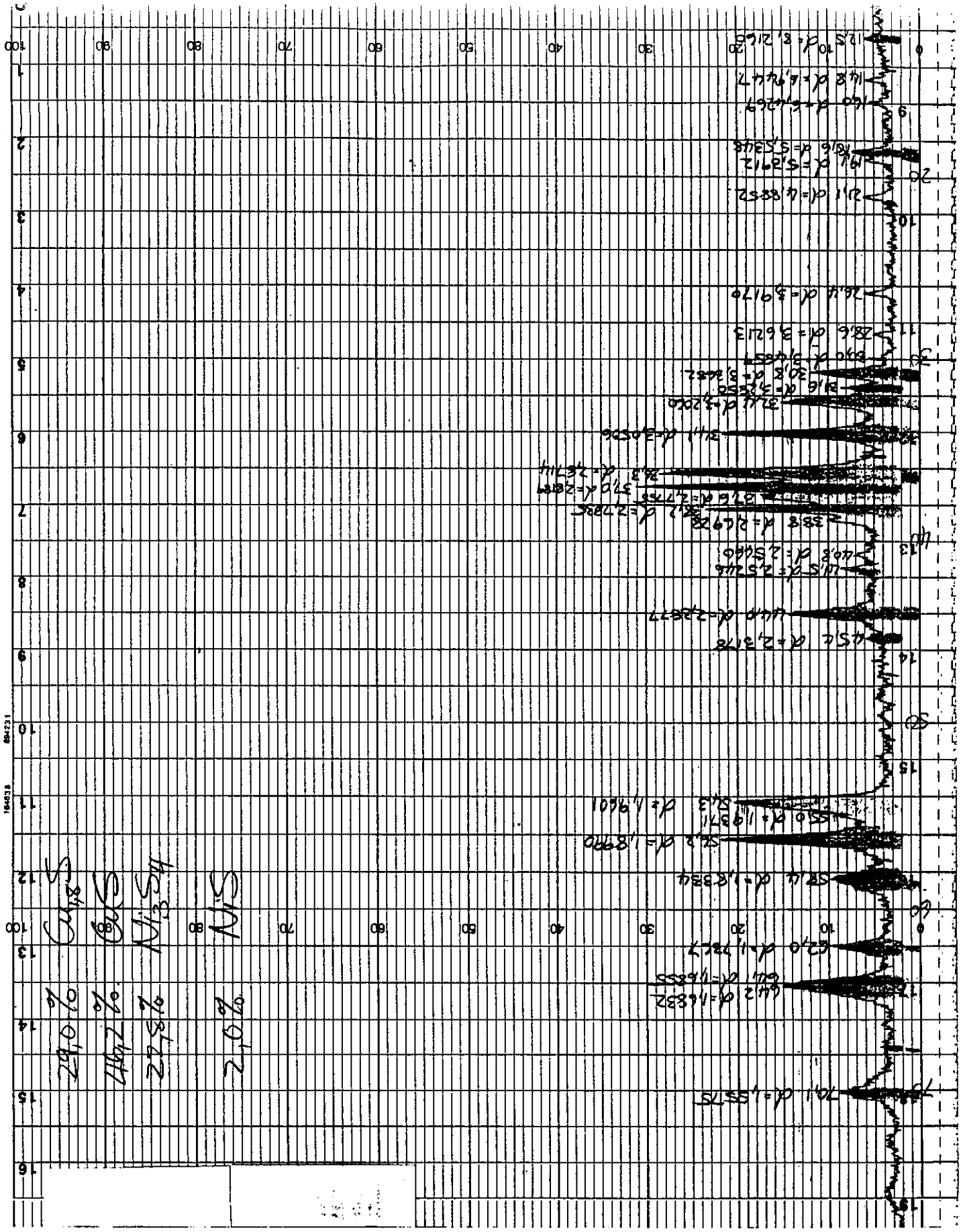

Figure F.11 - Original XRD graph at time = 300 minutes

Appendix G

COMPUTER CODE OF THE KINETIC MODEL PROGRAM

The computer code was compiled in Borland, Turbo Pascal 7.0.

```
PROGRAM MODEL;

USES
CRT,FastTTT,DOS,WinTTT,MenuTTT,VARIABLE,INPUT_MENU,CALCULATIONS,GRAPHICS;

VAR Main_choice,Error:INTEGER;
   M1:MENU_RECORD;

PROCEDURE WAIT;
BEGIN
 SOUND(400);DELAY(150);NOSOUND;
 WriteCenter(25,white+blink,RED,
 '************** PRESS ANY KEY TO PROCEED **************');
 READKEY;
END;

PROCEDURE TITEL;
BEGIN
 ClrScr;
 Offcursor;
 Speed:=1000;
 GrowFBox(10,4,70,16,WHITE,GREEN,2);
 WriteCenter(6,blue,green,'UNIVERSITY OF STELLENBOSCH');
 WriteCenter(7,blue,green,'DEPARTMENT OF CHEMICAL ENGINEERING');
 WriteCenter(9,red,green,'KINETIC MODEL FOR THE SHERRITT-GORDON');
 WriteCenter(10,red,green,'ACID-OXYGEN PRESSURE LEACH');
 WriteCenter(12,blue,green,'PROGRAMMER: J.A.M. RADEMAN');
 WriteCenter(14,blue,green,'DATE: JUNE 1995');
 WAIT;
END;
```

```
PROCEDURE Define_Menu;
Begin
 With M1 do
  Begin
  Offcursor;
   Heading1:='OUTPUTS';
   Heading2:='Choose option';
   Topic[1]:='   Solution';
   Topic[2]:='   Solids';
   Topic[3]:='   Ni-sulphide minerals';
   Topic[4]:='   Cu-sulphide minerals';
   Topic[5]:='   Display data';
   Topic[6]:='   Repeat the PROGRAM';
   Topic[7]:='   Quit the PROGRAM';
   TotalPicks:=7;
   PicksPerLine:=1;
   Addprefix:=1;
   TopleftXY[1]:=0;
   TopleftXY[2]:=5;
   Boxtype:=5;
    IF BaseOfScreen = $B800 THEN
     Begin
      Colors[1] := white;
      Colors[2] := red;
      Colors[3] := lightgray;
      Colors[4] := blue;
      Colors[5] := lightcyan;
     End
    ELSE
     Begin
      Colors[1] := white;
      Colors[2] := black;
      Colors[3] := black;
      Colors[4] := lightgray;
      Colors[5] := white;
     End;
    AllowEsc := false;
    Margins := 5;
  End;
End;
```

```
FUNCTION HERHAAL:BOOLEAN;
VAR ANSW:CHAR;
BEGIN
 REPEAT
{   CLRSCR;}
   FBox(12,8,68,14,white,1,2);
   WRITEAT(17,11,white,1,'Do you want to repeat the INPUT section [Y,N] ? ');
   ANSW:=UPCASE(READKEY);
 UNTIL ANSW In['Y','N'];
 CASE ANSW OF
   'Y':HERHAAL:=TRUE;
   'N':HERHAAL:=FALSE;
 END;
END;

PROCEDURE GRAPH_CHOICE1;
BEGIN
 GRAPH_option:=true;
 CHOICE:=TRUE;
 Soln_Solid_GRAPH;
END;

PROCEDURE GRAPH_CHOICE2;
BEGIN
 GRAPH_option:=true;
 CHOICE:=FALSE;
 Soln_Solid_GRAPH;
END;

PROCEDURE GRAPH_CHOICE3;
BEGIN
 GRAPH_option:=false;
 Choice_Ni_Cu:=true;
 Soln_Solid_GRAPH;
END;

PROCEDURE GRAPH_CHOICE4;
BEGIN
 GRAPH_option:=false;
 Choice_Ni_Cu:=false;
 Soln_Solid_GRAPH;
END;
```

```
PROCEDURE REPEAT_PROGRAM;
BEGIN
 REP:=TRUE;
END;

PROCEDURE OUTPUT_ORDER;
Begin
 Case Main_Choice of
 1 :GRAPH_CHOICE1;
 2 :GRAPH_CHOICE2;
 3 :GRAPH_CHOICE3;
 4 :GRAPH_CHOICE4;
 5 :RUNGE_KUTTA;
 6 :REPEAT_PROGRAM;
 7 :FINISH;
 End;
End;

PROCEDURE OUTPUT;
BEGIN
 REPEAT
{   CLRSCR;}
   MAIN_CHOICE:=1;
   DEFINE_MENU;
   DisplayMenu(M1,false,Main_choice,Error);
   OUTPUT_ORDER;
 UNTIL REP;
END;

BEGIN
{ TITEL;
 } CLRSCR;
 REPEAT
    REP:=FALSE;
    INPUT;
    OUTPUT;
 UNTIL NOT(REP);
END.
```

```
UNIT INPUT_MENU;

INTERFACE

USES
CRT,VARIABLE,FastTTT,DOS,WinTTT,KeyTTT,IOTTT,MenuTTT,StrngTTT,EXP_DATA_INPUT;

PROCEDURE INPUT;
PROCEDURE FINISH;

IMPLEMENTATION

CONST Ave_PI_P=120.0;

VAR Main_choice,Error:INTEGER;
   M1:MENU_RECORD;
   CREATE:BOOLEAN;

PROCEDURE PRESSURE;
VAR A,B:REAL;
BEGIN
 IF pO2<1.8 THEN A:=0.1*(pO2-1.8);
 IF pO2>1.8 THEN A:=0.75*(pO2-1.8);
 IF NOT(flow_O2=0.59) THEN B:=0.7*(flow_O2-0.59);
 pO2:=1.8+A+B;
END;

PROCEDURE INIT_ACID;
BEGIN
 Acid:=1;
 k1:=0.39010824;
 k2:=0.0303;
 k5a:=0.00204336;
 k6:=0.022;
 k7:=0.00368;
 k8a:=0.075;
 k8b:=0.0215;
END;

PROCEDURE PARTICLE;
VAR Area_factor:REAL;
BEGIN
```

```
  Area_factor:=exp(2/3*ln(Ave_Pl_P/Ave_P));
  k1:=Area_factor*k1;
  k2:=Area_factor*k2;
  k3:=Area_factor*k3;
  k4:=Area_factor*k4;
  k5a:=Area_factor*k5a;
  k6:=Area_factor*k6;
  k7:=Area_factor*k7;
  k8a:=Area_factor*k8a;
  k8b:=Area_factor*k8b;
  k9:=Area_factor*k9;
  k11:=Area_factor*k11;
END;

PROCEDURE SIMPLE2;
VAR S1,S2,S3,S4,S5,S6,S7,S8,S9,S10,S11,S12:STRING;
    RETCODE:INTEGER;
BEGIN
  ClrScr;
  FBox(1,1,80,25,yellow,1,2);
  Horizline(2,79,5,yellow,1,1);
  WriteCenter(3,yellow,1,'REACTION RATE CONSTANTS');
  WriteAt(5,7,white,1,'Oxygen partial pressure, pO2 [bar]');
  WriteAt(5,8,white,1,'Oxygen flow rate, O2 [kg/h]');
  WriteAt(5,9,white,1,'Reaction temperature, [degree C]');
  WriteAt(5,10,white,1,'Initial H2SO4 concentration (after 10 min), [mol/L]');
  WriteAt(5,11,white,1,'Initial mass of matte (after 10 min), [g]');
  WriteAt(5,12,white,1,'Solution volume in reactor, [L]');
  WriteAt(5,13,white,1,'Approximate average particle size, [microns]');
  WriteAt(5,15,white,1,'Runge-Kutta calculation step size, [min]');
  WriteAt(5,16,white,1,'Calculation time, [min]');
  WriteAt(5,18,white,1,'Data file, experimental results solution, [Time,Cu,H+,Ni]');
  WriteAt(5,19,white,1,'Data file, experimental results solids, [Time,Ni,Cu,S]');
  WriteAt(5,20,white,1,'Data file, mineral composition, [Time,Ni,Ni3S2,NiS,Cu2S,Cu1.8S]');
  S1:='1.8';
  S2:='0.59';
  S3:='140';
  S4:='0.99';
  S5:='7300.0';
  S6:='38.6';
  S7:='120.3';
  S8:='0.5';
```

```
S9:='300';
S10:='soln.dat';
S11:='solid.dat';
S12:='min.dat';
IO_SetFields(12);
IO_Soundbeeper(false);
IO_AllowEsc(true);
IO_DefineStr(1,12,2,12,2,65,7,S1,'########');
IO_DefineStr(2,1,3,1,3,65,8,S2,'########');
IO_DefineStr(3,2,4,2,4,65,9,S3,'########');
IO_DefineStr(4,3,5,3,5,65,10,S4,'########');
IO_DefineStr(5,4,6,4,6,65,11,S5,'########');
IO_DefineStr(6,5,7,5,7,65,12,S6,'########');
IO_DefineStr(7,6,8,6,8,65,13,S7,'########');
IO_DefineStr(8,7,9,7,9,65,15,S8,'########');
IO_DefineStr(9,8,10,8,10,65,16,S9,'########');
IO_DefineStr(10,9,11,9,11,65,18,S10,'############');
IO_DefineStr(11,10,12,10,12,65,19,S11,'############');
IO_DefineStr(12,11,1,11,1,65,20,S12,'############');
IO_DefineMsg(1,23,25,' *** Press "END" to continue *** ');
IO_DefineMsg(2,23,25,' *** Press "END" to continue *** ');
IO_DefineMsg(3,23,25,' *** Press "END" to continue *** ');
IO_DefineMsg(4,23,25,' *** Press "END" to continue *** ');
IO_DefineMsg(5,23,25,' *** Press "END" to continue *** ');
IO_DefineMsg(6,23,25,' *** Press "END" to continue *** ');
IO_DefineMsg(7,23,25,' *** Press "END" to continue *** ');
IO_DefineMsg(8,23,25,' *** Press "END" to continue *** ');
IO_DefineMsg(9,23,25,' *** Press "END" to continue *** ');
IO_DefineMsg(10,23,25,' *** Press "END" to continue *** ');
IO_DefineMsg(11,23,25,' *** Press "END" to continue *** ');
IO_DefineMsg(12,23,25,' *** Press "END" to continue *** ');
OnCursor;
IO_Edit(Retcode);
Offcursor;
IO_Resetfields;
pO2:=Str_to_real(S1);
flow_O2:=Str_to_real(S2);
Tp:=Str_to_real(S3);
Tp:=Tp+273;
N_H_0:=Str_to_real(S4);
IF N_H_0<0.92 THEN INIT_ACID
ELSE Acid:=0.001;
```

```
 W0:=Str_to_real(S5);
 V:=Str_to_real(S6);
 N_H_0:=N_H_0*2*V;
 Ave_P:=Str_to_real(S7);
 h_step:=Str_to_real(S8);
 T:=Str_to_real(S9);
 NAME_SOLN:=S10;
 NAME_SOLID:=S11;
 NAME_MIN:=S12;
 PRESSURE;
 PARTICLE;
END;

PROCEDURE SIMPLE1;
VAR S1,S2,S3,S4,S5,S6,S7,S8,S9,S10,S11,S12,S13,S14,S15,S16,S17,S18:STRING;
   RETCODE:INTEGER;
BEGIN
{ ClrScr;}
 CREATE:=TRUE;
 FBox(1,1,80,25,yellow,1,2);
 Horizline(2,79,5,yellow,1,1);
 WriteCenter(3,yellow,1,'REACTION RATE CONSTANTS');
 WriteAt(5,7,white,1,'Reaction 1, Ni+H+ - k1 (thesis k1)');
 WriteAt(5,8,white,1,'Reaction 2, Ni3S2+H+ - k2 (thesis k2)');
 WriteAt(5,9,white,1,'Reaction 3, Ni+Ni3S2+Cu2+ - k3 (thesis k3)');
 WriteAt(5,10,white,1,'Reaction 4, Ni3S2+Cu2+ - k4 (thesis k4)');
 WriteAt(5,11,white,1,'Reaction 5a, Cu2S+H+ - k5a (thesis k5)');
 WriteAt(5,12,white,1,'Reaction 15, CuS+O2 -  k15 (thesis k18)');
 WriteAt(5,13,white,1,'Reaction 6, Cu2S+H+ - k6 (thesis k9)');
 WriteAt(5,14,white,1,'Reaction 7, Cu31S16+H+ - k7 (thesis k10)');
 WriteAt(5,15,white,1,'Reaction 8a, Ni3S2+H+ - k8a (thesis k11)');
 WriteAt(5,16,white,1,'Reaction 8b, Ni7S6+H+ - k8b (thesis k12)');
 WriteAt(5,17,white,1,'Reaction 9, NiS+H+ - k9 (thesis k13)');
 WriteAt(5,18,white,1,'Reaction 10, Ni3S4+H2O - k10 (thesis k16)');
 WriteAt(5,19,white,1,'Reaction 11, Ni3S4+Cu2+ +H2O - k11 (thesis k17)');
 WriteAt(5,20,white,1,'Reaction 12a, Cu1.8S+H+ - k12a (thesis k14)');
 WriteAt(5,21,white,1,'Reaction 12b, Cu1.8S+Fe3+ - k12b (thesis k15)');
 WriteAt(5,22,white,1,'Reaction 13a, Fe2+ +H+ - k13a (thesis k19)');
 WriteAt(5,23,white,1,'Reaction 13b, Fe3+ +H2O - k13b (thesis k20)');
 WriteAt(5,24,white,1,'Reaction 14, Fe+H+ - k14 (thesis k7)');
 S1:='0.28410824';      {k1}
 S2:='0.0213';          {k2}
```

```
S3:='5.3682394';      {k3}
S4:='9.6224605';      {k4}
S5:='0.00424336';     {k5a}
S6:='0.0144';         {k15}
S7:='0.015';          {k6}
S8:='0.00068';        {k7}
S9:='0.025';          {k8a}
S10:='0.0045';        {k8b}
S11:='0.050';         {k9}
S12:='3.53424607';    {k10}
S13:='437.11661';     {k11}
S14:='0.04';          {k12a}
S15:='0.00062974';    {k12b}
S16:='0.4';           {k13a}
S17:='1.2';           {k13b}
S18:='603.59292';     {k14}
IO_SetFields(18);
IO_Soundbeeper(false);
IO_AllowEsc(true);
IO_DefineStr(1,18,2,18,2,65,7,S1,'########');
IO_DefineStr(2,1,3,1,3,65,8,S2,'########');
IO_DefineStr(3,2,4,2,4,65,9,S3,'########');
IO_DefineStr(4,3,5,3,5,65,10,S4,'########');
IO_DefineStr(5,4,6,4,6,65,11,S5,'########');
IO_DefineStr(6,5,7,5,7,65,12,S6,'########');
IO_DefineStr(7,6,8,6,8,65,13,S7,'########');
IO_DefineStr(8,7,9,7,9,65,14,S8,'########');
IO_DefineStr(9,8,10,8,10,65,15,S9,'########');
IO_DefineStr(10,9,11,9,12,65,16,S10,'########');
IO_DefineStr(11,10,12,10,12,65,17,S11,'########');
IO_DefineStr(12,11,13,11,13,65,18,S12,'########');
IO_DefineStr(13,12,14,12,14,65,19,S13,'########');
IO_DefineStr(14,13,15,13,15,65,20,S14,'########');
IO_DefineStr(15,14,16,14,16,65,21,S15,'########');
IO_DefineStr(16,15,17,15,17,65,22,S16,'########');
IO_DefineStr(17,16,18,16,18,65,23,S17,'########');
IO_DefineStr(18,17,1,17,1,65,24,S18,'########');
IO_DefineMsg(1,23,25,' *** Press "END" to continue *** ');
IO_DefineMsg(2,23,25,' *** Press "END" to continue *** ');
IO_DefineMsg(3,23,25,' *** Press "END" to continue *** ');
IO_DefineMsg(4,23,25,' *** Press "END" to continue *** ');
IO_DefineMsg(5,23,25,' *** Press "END" to continue *** ');
```

```
IO_DefineMsg(6,23,25,' *** Press "END" to continue *** ');
IO_DefineMsg(7,23,25,' *** Press "END" to continue *** ');
IO_DefineMsg(8,23,25,' *** Press "END" to continue *** ');
IO_DefineMsg(9,23,25,' *** Press "END" to continue *** ');
IO_DefineMsg(10,23,25,' *** Press "END" to continue *** ');
IO_DefineMsg(11,23,25,' *** Press "END" to continue *** ');
IO_DefineMsg(12,23,25,' *** Press "END" to continue *** ');
IO_DefineMsg(13,23,25,' *** Press "END" to continue *** ');
IO_DefineMsg(14,23,25,' *** Press "END" to continue *** ');
IO_DefineMsg(15,23,25,' *** Press "END" to continue *** ');
IO_DefineMsg(16,23,25,' *** Press "END" to continue *** ');
IO_DefineMsg(17,23,25,' *** Press "END" to continue *** ');
IO_DefineMsg(18,23,25,' *** Press "END" to continue *** ');
 OnCursor;
 IO_Edit(Retcode);
 Offcursor;
 IO_Resetfields;
 k1:=Str_to_real(S1);
 k2:=Str_to_real(S2);
 k3:=Str_to_real(S3);
 k4:=Str_to_real(S4);
 k5a:=Str_to_real(S5);
 k15:=Str_to_real(S6);
 k6:=Str_to_real(S7);
 k7:=Str_to_real(S8);
 k8a:=Str_to_real(S9);
 k8b:=Str_to_real(S10);
 k9:=Str_to_real(S11);
 k10:=Str_to_real(S12);
 k11:=Str_to_real(S13);
 k12a:=Str_to_real(S14);
 k12b:=Str_to_real(S15);
 k13a:=Str_to_real(S16);
 k13b:=Str_to_real(S17);
 k14:=Str_to_real(S18);
 SIMPLE2;
END;

PROCEDURE DATA_FILE;
BEGIN
 CREATE_DATA_FILE;
 CREATE:=FALSE;
```

```
END;

PROCEDURE FINISH;
VAR ANSW:CHAR;
Begin
 REPEAT
 ClrScr;
 FBox(12,8,68,14,white,1,2);
 WriteAt(15,10,white+blink,red,'********** END OF PROGRAM **********');
 WRITEAT(16,12,white,1,'Are you sure you want to quit the program [Y,N] ? ');
 ANSW:=UPCASE(READKEY);
 UNTIL ANSW In['Y','N'];
 CASE ANSW OF
  'Y':REP:=TRUE;
  'N':REP:=FALSE;
 END;
 IF REP THEN
 BEGIN
  Oncursor;
  Halt;
 END;
END;

PROCEDURE Define_Menu;
Begin
 With M1 do
  Begin
  Offcursor;
   Heading1:='INPUTS FOR CONTROL';
   Heading2:='Choose option';
   Topic[1]:='   Rate constants and data file names';
   Topic[2]:='   Create or display data file';
   Topic[3]:='   Quit the PROGRAM';
   TotalPicks:=3;
   PicksPerLine:=1;
   Addprefix:=1;
   TopleftXY[1]:=0;
   TopleftXY[2]:=5;
   Boxtype:=5;
    IF BaseOfScreen = $B800 THEN
     Begin
      Colors[1] := white;          {hi foreground}
```

```
    Colors[2] := red;          {hi background}
    Colors[3] := lightgray;    {lo foreground}
    Colors[4] := blue;         {lo background}
    Colors[5] := lightcyan;    {box color}
   End
  ELSE
   Begin
    Colors[1] := white;        {hi forground}
    Colors[2] := black;        {hi background}
    Colors[3] := black;        {lo foreground}
    Colors[4] := lightgray;    {lo background}
    Colors[5] := white;        {box color}
   End;
  AllowEsc := false;           {inactivate the escape key}
  Margins := 5;
 End;
End;

PROCEDURE Input_ORDER;
Begin
 Case Main_Choice of
 1 :SIMPLE1;
 2 :DATA_FILE;
 3 :FINISH;
 End;
End;

PROCEDURE INPUT;
BEGIN
 REPEAT
 { CLRSCR;}
  MAIN_CHOICE:=1;
  DEFINE_MENU;
  DisplayMenu(M1,false,Main_choice,Error);
  INPUT_ORDER;
 UNTIL CREATE;
END;

END.
```

```
UNIT CALCULATIONS;

INTERFACE

USES CRT,VARIABLE;

PROCEDURE INITIAL_VALUE;
PROCEDURE RUNGE_KUTTA;
PROCEDURE GRAPH_RUNGE_Soln;
PROCEDURE GRAPH_RUNGE_Solid;

IMPLEMENTATION

CONST Mr_Ni=58.7;
      Mr_Ni3S2=240.22;
      Mr_NiS=90.76;
      Mr_Cu2S=159.152;
      Mr_Cu18S=146.4428;
      Mr_Cu=63.546;
      Mr_Fe=55.847;
      Mr_O2=31.9988;
      Mr_O=15.9994;
      Mr_S=32.06;
      Mr_H=1.0079;
      Mr_H2SO4=98.0734;
      wNim_0=0.05;
      wNi3S2_0=0.454;
      wCu2S_0=0.419;
      wNiS_0=0.024;
      wCu18S_0=0.053;
      N_Ni_0=30.85;
      N_Cu_0=5.48;
      N_Fe_0=0.87;
      ER1=-629.76;     {-Ea/R}
      ER3=-1308.1;
      ER5a=1252;
      ER11=-5322.7;
      ER14=-4596;
      ER4=-272.43;
      ER10=-3062.5;
      ER12b=1795.6;
```

```
VAR N_Nim_0,N_Ni3S2_0,N_Ni7S6_0,N_NiS_0,N_Ni3S4_0,N_Cu2S_0,N_Cu31S16_0,
   N_Cu18S_0,N_CuS_0:REAL;
   N_Ni_s0,N_Cu_s0,N_S_s0:REAL;
   Y,N0_Ni,N0_Cu,N0_H,N0_Nim,N0_Ni3S2,N0_Ni7S6,N0_NiS,N0_Ni3S4,N0_Cu2S,
   N0_Cu31S16,N0_Cu18S,N0_CuS,N0_Fe3,N0_Fe2,N0_Fe:REAL;
   Cu_low,H_High:BOOLEAN;

PROCEDURE CALCS;
BEGIN
 N_Nim_0:=(wNim_0*W0)/Mr_Ni;
 N_Ni3S2_0:=(wNi3S2_0*W0)/Mr_Ni3S2;
 N_Ni7S6_0:=0;
 N_NiS_0:=(wNiS_0*W0)/Mr_NiS;
 N_Ni3S4_0:=0;
 N_Cu2S_0:=(wCu2S_0*W0)/Mr_Cu2S;
 N_Cu31S16_0:=0;
 N_Cu18S_0:=(wCu18S_0*W0)/Mr_Cu18S;
 N_CuS_0:=0;
 N_Cu_s0:=N_Cu2S_0*2+N_Cu31S16_0*31+N_Cu18S_0*1.8+N_CuS_0;
 N_Ni_s0:=N_Nim_0+N_Ni3S2_0*3+N_Ni7S6_0*7+N_NiS_0;
 N_S_s0:=N_Ni3S2_0*2+N_Ni7S6_0*6+N_NiS_0+N_Ni3S4_0*4+N_Cu2S_0+N_Cu31S16_0*16
         +N_Cu18S_0+N_CuS_0;
END;

PROCEDURE CHECK;
BEGIN
 IF N0_Ni<=0.001 THEN N0_Ni:=0.001;
 IF N0_Cu<=0.001 THEN N0_Cu:=0.001;
 IF N0_H<=0.001 THEN N0_H:=0.001;
 IF N0_Nim<=0.001 THEN N0_Nim:=0.001;
 IF N0_Ni3S2<=0.001 THEN N0_Ni3S2:=0.001;
 IF N0_Ni7S6<=0.001 THEN N0_Ni7S6:=0.001;
 IF N0_NiS<=0.001 THEN N0_NiS:=0.001;
 IF N0_Ni3S4<=0.001 THEN N0_Ni3S4:=0.001;
 IF N0_Cu2S<=0.001 THEN N0_Cu2S:=0.001;
 IF N0_Cu31S16<=0.001 THEN N0_Cu31S16:=0.001;
 IF N0_Cu18S<=0.001 THEN N0_Cu18S:=0.001;
 IF N0_CuS<=0.001 THEN N0_CuS:=0.001;
 IF N0_Fe3<=0.001 THEN N0_Fe3:=0.001;
 IF N0_Fe2<=0.001 THEN N0_Fe2:=0.001;
END;
```

```
PROCEDURE RATE_Ni;
VAR A,B,C,D,H,I,J,K,L,RN_Ni:REAL;
BEGIN
 IF ((N_Nim/N_Nim_0)>0.001) THEN
  A:=k1*exp(ER1/Tp)*(exp(2/3*ln(N_Nim/N_Nim_0)))*(exp(1*ln(N_H/V)))*pO2
 ELSE A:=0;
 IF ((N_Ni3S2/N_Ni3S2_0)>0.001) THEN
 BEGIN
  IF ((N_Cu>0.3) OR (N_Nim<=0.1)) THEN
   B:=k2*(exp(2*ln(N_H/V)))*pO2
  ELSE B:=0;
  IF ((N_Nim/N_Nim_0)>0.001) THEN
   C:=4*k3*exp(ER3/Tp)*(exp(1/2*ln(N_Cu/V)))
  ELSE C:=0;
  IF N_Nim<=0.1 THEN
   D:=2*k4*exp(ER4/Tp)*(exp(1*ln(N_Cu/V)))
  ELSE D:=0;
  IF ((N_Cu<=0.3) AND (N_Nim>0.1)) THEN
   H:=2/3*k8a*(exp(1*ln(N_H/V)))*pO2
  ELSE H:=0;
 END
 ELSE
 BEGIN
  B:=0;
  C:=0;
  D:=0;
  H:=0;
 END;
 IF ((N_Ni7S6>0.001){ AND (N_Nim<=0.1)}) THEN
  I:=k8b*(exp(1*ln(N_H/V)))*pO2
 ELSE I:=0;
 IF ((N_NiS>0.001) AND (N_Nim<=0.1)) THEN
 BEGIN
  IF N_Ni7S6<=0.001 THEN
   J:=4*1/4*k9*(exp(1*ln(N_H/V)))*pO2
  ELSE J:=1/4*k9*(exp(1*ln(N_H/V)))*pO2;
 END
 ELSE J:=0;
 IF N_Ni3S4>0.001 THEN
 BEGIN
  K:=3*k10*exp(ER10/Tp)*pO2;
  IF ((N_Nim<=0.1) AND (N_Cu>0.3)) THEN
```

```
    L:=3*k11*exp(ER11/Tp)*(exp(-1/2*ln(N_Cu/V)))*pO2
   ELSE L:=0;
  END
  ELSE
  BEGIN
   K:=0;
   L:=0;
  END;
  RN_Ni:=A+B+C+D+H+I+J+K+L;
  N0_Ni:=N_Ni+h_step*RN_Ni;
  CHECK;
END;

FUNCTION RATE_Cu(Y:REAL):REAL;
VAR C,D,E,F,G,L,M,N,R:REAL;
BEGIN
  IF Y<=0 THEN Y:=0.001;
  IF ((N_Ni3S2/N_Ni3S2_0)>0.001) THEN
  BEGIN
   IF ((N_Nim/N_Nim_0)>0.001) THEN
    C:=-4*k3*exp(ER3/Tp)*(exp(1/2*ln(Y/V)))
   ELSE C:=0;
   IF N_Nim<=0.1 THEN
    D:=-2*k4*exp(ER4/Tp)*(exp(1*ln(Y/V)))
   ELSE D:=0;
  END
  ELSE
  BEGIN
   C:=0;
   D:=0;
  END;
  IF ((N_Cu2S/N_Cu2S_0)>0.001) THEN
  BEGIN
   IF H_High THEN
   BEGIN
    IF N_H>Acid THEN
    BEGIN
     IF ((N_Cu>0.3) OR (N_Nim<=0.1)) THEN
      E:=1/5*k5a*exp(ER5a/Tp)/(exp(2*ln(N_H/V)))*pO2
     ELSE E:=0;
    END
    ELSE E:=0;
```

```
 END
 ELSE E:=100*1/5*k5a*exp(ER5a/Tp)*(exp(1*ln(N_H/V)))*pO2;
 IF ((N_Cu<=0.3) AND (N_Nim>0.1)) THEN
  F:=1/16*k6*(exp(1*ln(N_H/V)))*pO2
 ELSE F:=0;
END
ELSE
BEGIN
 E:=0;
 F:=0;
END;
IF ((N_Cu31S16>0.001) AND (N_Nim<=0.1)) THEN
 G:=11/5*k7*(N_H/V)*pO2
ELSE G:=0;
IF N_Nim<=0.1 THEN
BEGIN
 IF ((N_Ni3S4>0.001) AND (N_Cu>0.3)) THEN
  L:=-3*k11*exp(ER11/Tp)*(exp(-1/2*ln(Y/V)))*pO2
 ELSE L:=0;
 IF ((N_Cu18S>0.001)) THEN
 BEGIN
  IF N_Cu31S16>0.001 THEN
   M:=4/5*k12a*(exp(1*ln(N_H/V)))*pO2
  ELSE M:=7*4/5*k12a*(exp(1*ln(N_H/V)))*pO2;
  IF N_Fe3>0.001 THEN
   N:=4/5*k12b*exp(ER12b/Tp)*(exp(1*ln(N_Fe3/V)))
  ELSE N:=0;
 END
 ELSE
 BEGIN
  M:=0;
  N:=0;
 END;
END
ELSE
BEGIN
 L:=0;
 M:=0;
 N:=0;
END;
IF N_CuS>0.1 THEN
 R:={(N_CuS18/V)*}k15*pO2
```

```
 ELSE R:=0;
 RATE_Cu:=C+D+E+F+G+L+M+N+R;
END;

FUNCTION RATE_H(Y:REAL):REAL;
VAR A,B,E,F,G,H,I,J,K,L,M,O,P,Q:REAL;
BEGIN
 IF Y<=0 THEN Y:=0.001;
 IF ((N_Nim/N_Nim_0)>0.001) THEN
  A:=-1.5*2*k1*exp(ER1/Tp)*(exp(2/3*ln(N_Nim/N_Nim_0)))*(exp(1*ln(Y/V)))*pO2
 ELSE A:=0;
 IF ((N_Cu2S/N_Cu2S_0)>0.001) THEN
 BEGIN
  IF H_High THEN
  BEGIN
   IF N_H>Acid THEN
   BEGIN
    IF ((N_Cu>0.3) OR (N_Nim<=0.1)) THEN
     E:=-2/5*k5a*exp(ER5a/Tp)/(exp(2*ln(Y/V)))*pO2
    ELSE E:=0;
   END
   ELSE E:=0;
  END
  ELSE E:=-100*2/5*k5a*exp(ER5a/Tp)*(exp(1*ln(Y/V)))*pO2;
  IF ((N_Cu<=0.3) AND (N_Nim>0.1)) THEN
   F:=-2/16*k6*(exp(1*ln(Y/V)))*pO2
  ELSE F:=0;
 END
 ELSE
 BEGIN
  E:=0;
  F:=0;
 END;
 IF ((N_Cu31S16>0.001) AND (N_Nim<=0.1)) THEN
  G:=-22/5*k7*(Y/V)*pO2
 ELSE G:=0;
 IF ((N_Ni3S2/N_Ni3S2_0)>0.001) THEN
 BEGIN
  IF ((N_Cu>0.3) OR (N_Nim<=0.1)) THEN
   B:=-2*k2*(exp(2*ln(Y/V)))*pO2
  ELSE B:=0;
  IF ((N_Cu<=0.3) AND (N_Nim>0.1)) THEN
```

```
   H:=-4/3*k8a*(exp(1*ln(Y/V)))*pO2
  ELSE H:=0;
END
ELSE
BEGIN
  B:=0;
  H:=0;
END;
IF ((N_Ni7S6>0.001){ AND (N_Nim<=0.1)}) THEN
  I:=-2*k8b*(exp(1*ln(Y/V)))*pO2
ELSE I:=0;
IF ((N_NiS>0.001) AND (N_Nim<=0.1)) THEN
BEGIN
  IF N_Ni7S6<=0.001 THEN
    J:=-4*1/2*k9*(exp(1*ln(Y/V)))*pO2
  ELSE J:=-1/2*k9*(exp(1*ln(Y/V)))*pO2;
END
ELSE J:=0;
IF N_Ni3S4>0.001 THEN
BEGIN
  K:=2*k10*exp(ER10/Tp)*pO2;
  IF ((N_Nim<=0.1) AND (N_Cu>0.3)) THEN
    L:=2*k11*exp(ER11/Tp)*(exp(-1/2*ln(N_Cu/V)))*pO2
  ELSE L:=0;
END
ELSE
BEGIN
  K:=0;
  L:=0;
END;
IF ((N_Cu18S>0.001) AND (N_Nim<=0.1)) THEN
BEGIN
  IF N_Cu31S16>0.001 THEN
    M:=-8/5*k12a*(exp(1*ln(Y/V)))*pO2
  ELSE M:=-7*8/5*k12a*(exp(1*ln(Y/V)))*pO2;
END
ELSE M:=0;
IF (N_Cu>0.4) THEN
BEGIN
  IF (Cu_low OR ((N_Cu2S/N_Cu2S_0)<0.001)) THEN
  BEGIN
    Q:=0;
```

```
    IF N_H>Acid THEN
      O:=-k13a*(N_Fe2/V)/(exp(1*ln(Y/V)))*pO2
    ELSE O:=0;
  END
  ELSE
  BEGIN
    Q:=-1/2*k14*exp(ER14/Tp)*(Y/V)*pO2;
    O:=0;
  END;
 END
 ELSE
 BEGIN
   Q:=-1/2*k14*exp(ER14/Tp)*(Y/V)*pO2;
   O:=0;
 END;
 P:=k13b*(N_Fe3/V);
 RATE_H:=A+B+E+F+G+H+I+J+K+L+M+O+P+Q;
END;

FUNCTION RATE_Nim(Y:REAL):REAL;
VAR A,C:REAL;
BEGIN
  IF Y<=0 THEN Y:=0.001;
  IF ((N_Nim/N_Nim_0)>0.001) THEN
  BEGIN
    A:=-k1*exp(ER1/Tp)*(exp(2/3*ln(Y/N_Nim_0)))*(exp(1*ln(N_H/V)))*pO2;
    IF ((N_Ni3S2/N_Ni3S2_0)>0.001) THEN
      C:=-k3*exp(ER3/Tp)*(exp(1/2*ln(N_Cu/V)))
    ELSE C:=0;
  END
  ELSE
  BEGIN
    A:=0;
    C:=0;
  END;
  RATE_Nim:=A+C;
END;

FUNCTION RATE_Ni3S2(Y:REAL):REAL;
VAR B,C,D,H:REAL;
BEGIN
  IF ((N_Ni3S2/N_Ni3S2_0)>0.001) THEN
```

```
 BEGIN
  IF ((N_Cu>0.3) OR (N_Nim<=0.1)) THEN
   B:=-k2*(exp(2*ln(N_H/V)))*pO2
  ELSE B:=0;
  IF ((N_Cu<=0.3) AND (N_Nim>0.1)) THEN
   H:=-k8a*(exp(1*ln(N_H/V)))*pO2
  ELSE H:=0;
  IF ((N_Nim/N_Nim_0)>0.001) THEN
   C:=-k3*exp(ER3/Tp)*(exp(1/2*ln(N_Cu/V)))
  ELSE C:=0;
  IF N_Nim<=0.1 THEN
   D:=-k4*exp(ER4/Tp)*(exp(1*ln(N_Cu/V)))
  ELSE D:=0;
 END
 ELSE
 BEGIN
  B:=0;
  H:=0;
  C:=0;
  D:=0;
 END;
 RATE_Ni3S2:=B+H+C+D;
END;

FUNCTION RATE_Ni7S6(Y:REAL):REAL;
VAR H,I:REAL;
BEGIN
 IF ((N_Ni3S2/N_Ni3S2_0)>0.001) THEN
 BEGIN
  IF ((N_Cu<=0.3) AND (N_Nim>0.1)) THEN
   H:=1/3*k8a*(exp(1*ln(N_H/V)))*pO2
  ELSE H:=0;
 END
 ELSE H:=0;
 IF ((N_Ni7S6>0.001){ AND (N_Nim<=0.1)}) THEN
  I:=-k8b*(exp(1*ln(N_H/V)))*pO2
 ELSE I:=0;
 RATE_Ni7S6:=H+I;
END;

FUNCTION RATE_NiS(Y:REAL):REAL;
VAR B,D,I,J:REAL;
```

```
BEGIN
 IF ((N_Ni3S2/N_Ni3S2_0)>0.001) THEN
 BEGIN
  IF ((N_Cu>0.3) OR (N_Nim<=0.1)) THEN
   B:=2*k2*(exp(2*ln(N_H/V)))*pO2
  ELSE B:=0;
  IF N_Nim<=0.1 THEN
   D:=k4*exp(ER4/Tp)*(exp(1*ln(N_Cu/V)))
  ELSE D:=0;
 END
 ELSE
 BEGIN
  B:=0;
  D:=0;
 END;
 IF ((N_Ni7S6>0.001){ AND (N_Nim<=0.1)}) THEN
  I:=6*k8b*(exp(1*ln(N_H/V)))*pO2
 ELSE I:=0;
 IF ((N_NiS>0.001) AND (N_Nim<=0.1)) THEN
 BEGIN
  IF N_Ni7S6<=0.001 THEN
   J:=-4*k9*(exp(1*ln(N_H/V)))*pO2
  ELSE J:=-k9*(exp(1*ln(N_H/V)))*pO2;
 END
 ELSE J:=0;
 RATE_NiS:=B+D+I+J;
END;

FUNCTION RATE_Ni3S4(Y:REAL):REAL;
VAR J,K,L:REAL;
BEGIN
 IF ((N_NiS>0.001) AND (N_Nim<=0.1)) THEN
 BEGIN
  IF N_Ni7S6<=0.001 THEN
   J:=4*1/4*k9*(exp(1*ln(N_H/V)))*pO2
  ELSE J:=1/4*k9*(exp(1*ln(N_H/V)))*pO2;
 END
 ELSE J:=0;
 IF N_Ni3S4>0.001 THEN
 BEGIN
  K:=-k10*exp(ER10/Tp)*pO2;
  IF ((N_Nim<=0.1) AND (N_Cu>0.3)) THEN
```

```
    L:=-k11*exp(ER11/Tp)*(exp(-1/2*ln(N_Cu/V)))*pO2
   ELSE L:=0;
  END
  ELSE
  BEGIN
   K:=0;
   L:=0;
  END;
  RATE_Ni3S4:=J+K+L;
END;

FUNCTION RATE_Cu2S(Y:REAL):REAL;
VAR C,D,E,F:REAL;
BEGIN
  IF ((N_Ni3S2/N_Ni3S2_0)>0.001) THEN
  BEGIN
   IF ((N_Nim/N_Nim_0)>0.001) THEN
    C:=2*k3*exp(ER3/Tp)*(exp(1/2*ln(N_Cu/V)))
   ELSE C:=0;
   IF N_Nim<=0.1 THEN
    D:=k4*exp(ER4/Tp)*(exp(1*ln(N_Cu/V)))
   ELSE D:=0;
  END
  ELSE
  BEGIN
   C:=0;
   D:=0;
  END;
  IF ((N_Cu2S/N_Cu2S_0)>0.001) THEN
  BEGIN
   IF H_High THEN
   BEGIN
    IF N_H>Acid THEN
    BEGIN
     IF ((N_Cu>0.3) OR (N_Nim<=0.1)) THEN
      E:=-k5a*exp(ER5a/Tp)/(exp(2*ln(N_H/V)))*pO2
     ELSE E:=0;
    END
    ELSE E:=0;
   END
   ELSE E:=-100*k5a*exp(ER5a/Tp)*(exp(1*ln(N_H/V)))*pO2;
   IF ((N_Cu<=0.3) AND (N_Nim>0.1)) THEN
```

```
    F:=-k6*(exp(1*ln(N_H/V)))*pO2
   ELSE F:=0;
  END
  ELSE
  BEGIN
   E:=0;
   F:=0;
  END;
  RATE_Cu2S:=C+D+E+F;
END;

FUNCTION RATE_Cu31S16(Y:REAL):REAL;
VAR F,G:REAL;
BEGIN
  IF ((N_Cu2S/N_Cu2S_0)>0.001) THEN
  BEGIN
   IF ((N_Cu<=0.3) AND (N_Nim>0.1)) THEN
    F:=1/16*k6*(exp(1*ln(N_H/V)))*pO2
   ELSE F:=0;
  END
  ELSE F:=0;
  IF ((N_Cu31S16>0.001) AND (N_Nim<=0.1)) THEN G:=-k7*N_H/V*pO2
  ELSE G:=0;
  RATE_Cu31S16:=F+G;
END;

FUNCTION RATE_Cu18S(Y:REAL):REAL;
VAR E,G,M,N:REAL;
BEGIN
  IF ((N_Cu2S/N_Cu2S_0)>0.001) THEN
  BEGIN
   IF H_High THEN
   BEGIN
    IF N_H>Acid THEN
    BEGIN
     IF ((N_Cu>0.3) OR (N_Nim<=0.1)) THEN
      E:=k5a*exp(ER5a/Tp)/(exp(2*ln(N_H/V)))*pO2
     ELSE E:=0;
    END
    ELSE E:=0;
   END
   ELSE E:=100*k5a*exp(ER5a/Tp)*(exp(1*ln(N_H/V)))*pO2;
```

```
 END
 ELSE E:=0;
 IF ((N_Cu31S16>0.001) AND (N_Nim<=0.1)) THEN
  G:=80/5*k7*(N_H/V)*pO2
 ELSE G:=0;
 IF ((N_Cu18S>0.001) AND (N_Nim<=0.1)) THEN
 BEGIN
  IF N_Cu31S16>0.001 THEN
   M:=-k12a*(exp(1*ln(N_H/V)))*pO2
  ELSE M:=-7*k12a*(exp(1*ln(N_H/V)))*pO2;
  IF N_Fe3>0.001 THEN
   N:=-k12b*exp(ER12b/Tp)*(exp(1*ln(N_Fe3/V)))
  ELSE N:=0;
 END
 ELSE
 BEGIN
  M:=0;
  N:=0;
 END;
 RATE_Cu18S:=E+G+M+N;
END;

FUNCTION RATE_CuS(Y:REAL):REAL;
VAR L,M,N,R:REAL;
BEGIN
 IF N_Nim<=0.1 THEN
 BEGIN
  IF ((N_Ni3S4>0.001) AND (N_Cu>0.3)) THEN
   L:=3*k11*exp(ER11/Tp)*(exp(-1/2*ln(N_Cu/V)))*pO2
  ELSE L:=0;
  IF ((N_Cu18S>0.001)) THEN
  BEGIN
   IF N_Cu31S16>0.001 THEN
    M:=k12a*(exp(1*ln(N_H/V)))*pO2
   ELSE M:=7*k12a*(exp(1*ln(N_H/V)))*pO2;
   IF N_Fe3>0.001 THEN
    N:=k12b*exp(ER12b/Tp)*(exp(1*ln(N_Fe3/V)))
   ELSE N:=0;
  END
  ELSE
  BEGIN
   M:=0;
```

```
    N:=0;
   END;
  END
  ELSE
  BEGIN
   L:=0;
   M:=0;
   N:=0;
  END;
  IF N_CuS>0.1 THEN
   R:=-{(Y18/V)*}k15*pO2
  ELSE R:=0;
  RATE_CuS:=L+M+N+R;
END;

FUNCTION RATE_Fe3(Y:REAL):REAL;
VAR N,O,P:REAL;
BEGIN
  IF Y<=0 THEN Y:=0.001;
  IF N_H>Acid THEN
  BEGIN
   IF (N_Cu>0.4) THEN
   BEGIN
    IF (Cu_low OR ((N_Cu2S/N_Cu2S_0)<0.001)) THEN
     O:=k13a*(N_Fe2/V)/(exp(1*ln(N_H/V)))*pO2
    ELSE O:=0;
   END
   ELSE O:=0;
  END
  ELSE O:=0;
  IF ((N_Nim<=0.1) AND (N_Fe3>0.001)) THEN
   N:=-8/5*k12b*exp(ER12b/Tp)*(exp(1*ln(Y/V)))
  ELSE N:=0;
  P:=-k13b*(Y/V);
  RATE_Fe3:=N+O+P;
END;

FUNCTION RATE_Fe2(Y:REAL):REAL;
VAR N,O,Q:REAL;
BEGIN
  IF Y<=0 THEN Y:=0.001;
  IF ((N_Nim<=0.1) AND (N_Fe3>0.001)) THEN
```

```
  N:=8/5*k12b*exp(ER12b/Tp)*(exp(1*ln(N_Fe3/V)))
 ELSE N:=0;
 IF (N_Cu>0.4) THEN
 BEGIN
  IF (Cu_low OR ((N_Cu2S/N_Cu2S_0)<0.001)) THEN
  BEGIN
   Q:=0;
   IF N_H>Acid THEN
    O:=-k13a*(Y/V)/(exp(1*ln(N_H/V)))*pO2
   ELSE O:=0;
  END
  ELSE
  BEGIN
   Q:=k14*exp(ER14/Tp)*(N_H/V)*pO2;
   O:=0;
  END;
 END
 ELSE
 BEGIN
  Q:=k14*exp(ER14/Tp)*(N_H/V)*pO2;
  O:=0;
 END;
 RATE_Fe2:=N+O+Q;
END;

PROCEDURE RUNGE_Cu;
VAR RK1,RK2,RK3,RK4,Y1,Y2,Y3,Y4:REAL;
BEGIN
 Y1:=N_Cu;
 RK1:=h_step*RATE_Cu(Y1);
 Y2:=Y1+RK1/2;
 RK2:=h_step*RATE_Cu(Y2);
 Y3:=Y1+RK2/2;
 RK3:=h_step*RATE_Cu(Y3);
 Y4:=Y1+RK3;
 RK4:=h_step*RATE_Cu(Y4);
 N0_Cu:=N_Cu+(RK1+2*RK2+2*RK3+RK4)/6;
 CHECK;
END;

PROCEDURE RUNGE_H;
VAR RK1,RK2,RK3,RK4,Y1,Y2,Y3,Y4:REAL;
```

```
BEGIN
 Y1:=N_H;
 RK1:=h_step*RATE_H(Y1);
 Y2:=Y1+RK1/2;
 RK2:=h_step*RATE_H(Y2);
 Y3:=Y1+RK2/2;
 RK3:=h_step*RATE_H(Y3);
 Y4:=Y1+RK3;
 RK4:=h_step*RATE_H(Y4);
 N0_H:=N_H+(RK1+2*RK2+2*RK3+RK4)/6;
 CHECK;
END;

PROCEDURE RUNGE_Nim;
VAR RK1,RK2,RK3,RK4,Y1,Y2,Y3,Y4:REAL;
BEGIN
 Y1:=N_Nim;
 RK1:=h_step*RATE_Nim(Y1);
 Y2:=Y1+RK1/2;
 RK2:=h_step*RATE_Nim(Y2);
 Y3:=Y1+RK2/2;
 RK3:=h_step*RATE_Nim(Y3);
 Y4:=Y1+RK3;
 RK4:=h_step*RATE_Nim(Y4);
 N0_Nim:=N_Nim+(RK1+2*RK2+2*RK3+RK4)/6;
 CHECK;
END;

PROCEDURE RUNGE_Ni3S2;
VAR RK1,RK2,RK3,RK4,Y1,Y2,Y3,Y4:REAL;
BEGIN
 Y1:=N_Ni3S2;
 RK1:=h_step*RATE_Ni3S2(Y1);
 Y2:=Y1+RK1/2;
 RK2:=h_step*RATE_Ni3S2(Y2);
 Y3:=Y1+RK2/2;
 RK3:=h_step*RATE_Ni3S2(Y3);
 Y4:=Y1+RK3;
 RK4:=h_step*RATE_Ni3S2(Y4);
 N0_Ni3S2:=N_Ni3S2+(RK1+2*RK2+2*RK3+RK4)/6;
 CHECK;
END;
```

```
PROCEDURE RUNGE_Ni7S6;
VAR RK1,RK2,RK3,RK4,Y1,Y2,Y3,Y4:REAL;
BEGIN
 Y1:=N_Ni7S6;
 RK1:=h_step*RATE_Ni7S6(Y1);
 Y2:=Y1+RK1/2;
 RK2:=h_step*RATE_Ni7S6(Y2);
 Y3:=Y1+RK2/2;
 RK3:=h_step*RATE_Ni7S6(Y3);
 Y4:=Y1+RK3;
 RK4:=h_step*RATE_Ni7S6(Y4);
 N0_Ni7S6:=N_Ni7S6+(RK1+2*RK2+2*RK3+RK4)/6;
 CHECK;
END;

PROCEDURE RUNGE_NiS;
VAR RK1,RK2,RK3,RK4,Y1,Y2,Y3,Y4:REAL;
BEGIN
 Y1:=N_NiS;
 RK1:=h_step*RATE_NiS(Y1);
 Y2:=Y1+RK1/2;
 RK2:=h_step*RATE_NiS(Y2);
 Y3:=Y1+RK2/2;
 RK3:=h_step*RATE_NiS(Y3);
 Y4:=Y1+RK3;
 RK4:=h_step*RATE_NiS(Y4);
 N0_NiS:=N_NiS+(RK1+2*RK2+2*RK3+RK4)/6;
 CHECK;
END;

PROCEDURE RUNGE_Ni3S4;
VAR RK1,RK2,RK3,RK4,Y1,Y2,Y3,Y4:REAL;
BEGIN
 Y1:=N_Ni3S4;
 RK1:=h_step*RATE_Ni3S4(Y1);
 Y2:=Y1+RK1/2;
 RK2:=h_step*RATE_Ni3S4(Y2);
 Y3:=Y1+RK2/2;
 RK3:=h_step*RATE_Ni3S4(Y3);
 Y4:=Y1+RK3;
 RK4:=h_step*RATE_Ni3S4(Y4);
 N0_Ni3S4:=N_Ni3S4+(RK1+2*RK2+2*RK3+RK4)/6;
```

```
 CHECK;
END;

PROCEDURE RUNGE_Cu2S;
VAR RK1,RK2,RK3,RK4,Y1,Y2,Y3,Y4:REAL;
BEGIN
 Y1:=N_Cu2S;
 RK1:=h_step*RATE_Cu2S(Y1);
 Y2:=Y1+RK1/2;
 RK2:=h_step*RATE_Cu2S(Y2);
 Y3:=Y1+RK2/2;
 RK3:=h_step*RATE_Cu2S(Y3);
 Y4:=Y1+RK3;
 RK4:=h_step*RATE_Cu2S(Y4);
 N0_Cu2S:=N_Cu2S+(RK1+2*RK2+2*RK3+RK4)/6;
 CHECK;
END;

PROCEDURE RUNGE_Cu31S16;
VAR RK1,RK2,RK3,RK4,Y1,Y2,Y3,Y4:REAL;
BEGIN
 Y1:=N_Cu31S16;
 RK1:=h_step*RATE_Cu31S16(Y1);
 Y2:=Y1+RK1/2;
 RK2:=h_step*RATE_Cu31S16(Y2);
 Y3:=Y1+RK2/2;
 RK3:=h_step*RATE_Cu31S16(Y3);
 Y4:=Y1+RK3;
 RK4:=h_step*RATE_Cu31S16(Y4);
 N0_Cu31S16:=N_Cu31S16+(RK1+2*RK2+2*RK3+RK4)/6;
 CHECK;
END;

PROCEDURE RUNGE_Cu18S;
VAR RK1,RK2,RK3,RK4,Y1,Y2,Y3,Y4:REAL;
BEGIN
 Y1:=N_Cu18S;
 RK1:=h_step*RATE_Cu18S(Y1);
 Y2:=Y1+RK1/2;
 RK2:=h_step*RATE_Cu18S(Y2);
 Y3:=Y1+RK2/2;
 RK3:=h_step*RATE_Cu18S(Y3);
```

```
 Y4:=Y1+RK3;
 RK4:=h_step*RATE_Cu18S(Y4);
 N0_Cu18S:=N_Cu18S+(RK1+2*RK2+2*RK3+RK4)/6;
 CHECK;
END;

PROCEDURE RUNGE_CuS;
VAR RK1,RK2,RK3,RK4,Y1,Y2,Y3,Y4:REAL;
BEGIN
 Y1:=N_CuS;
 RK1:=h_step*RATE_CuS(Y1);
 Y2:=Y1+RK1/2;
 RK2:=h_step*RATE_CuS(Y2);
 Y3:=Y1+RK2/2;
 RK3:=h_step*RATE_CuS(Y3);
 Y4:=Y1+RK3;
 RK4:=h_step*RATE_CuS(Y4);
 N0_CuS:=N_CuS+(RK1+2*RK2+2*RK3+RK4)/6;
 CHECK;
END;

PROCEDURE RUNGE_Fe3;
VAR RK1,RK2,RK3,RK4,Y1,Y2,Y3,Y4:REAL;
BEGIN
 Y1:=N_Fe3;
 RK1:=h_step*RATE_Fe3(Y1);
 Y2:=Y1+RK1/2;
 RK2:=h_step*RATE_Fe3(Y2);
 Y3:=Y1+RK2/2;
 RK3:=h_step*RATE_Fe3(Y3);
 Y4:=Y1+RK3;
 RK4:=h_step*RATE_Fe3(Y4);
 N0_Fe3:=N_Fe3+(RK1+2*RK2+2*RK3+RK4)/6;
 CHECK;
END;

PROCEDURE RUNGE_Fe2;
VAR RK1,RK2,RK3,RK4,Y1,Y2,Y3,Y4:REAL;
BEGIN
 Y1:=N_Fe2;
 RK1:=h_step*RATE_Fe2(Y1);
 Y2:=Y1+RK1/2;
```

```
 RK2:=h_step*RATE_Fe2(Y2);
 Y3:=Y1+RK2/2;
 RK3:=h_step*RATE_Fe2(Y3);
 Y4:=Y1+RK3;
 RK4:=h_step*RATE_Fe2(Y4);
 N0_Fe2:=N_Fe2+(RK1+2*RK2+2*RK3+RK4)/6;
 CHECK;
END;

PROCEDURE WRITE_DATA;
BEGIN
 WRITELN('Time = ',Time:2:1,' min');
 WRITELN(' ',N_Cu:5:3,'  ',N_H:5:3,'    ',N_Ni:5:3,'    ',N_Fe:5:3);
 READLN;
END;

PROCEDURE INITIAL_VALUE;
BEGIN
 CALCS;
 Cu_low:=FALSE;
 H_High:=TRUE;
 Time:=h_step;
 N_Cu:=N_Cu_0;
 N_H:=N_H_0;
 N_Ni:=N_Ni_0;
 N_Fe3:=0;
 N_Fe2:=N_Fe_0;
 N_Fe:=N_Fe_0;
 N_Nim:=N_Nim_0;
 N_Ni3S2:=N_Ni3S2_0;
 N_Ni7S6:=N_Ni7S6_0;
 N_NiS:=N_NiS_0;
 N_Ni3S4:=N_Ni3S4_0;
 N_Cu2S:=N_Cu2S_0;
 N_Cu31S16:=N_Cu31S16_0;
 N_Cu18S:=N_Cu18S_0;
 N_CuS:=N_CuS_0;
 N_Ni_s:=N_Ni_s0;
 N_Cu_s:=N_Cu_s0;
 N_S_s:=N_S_s0;
END;
```

```
PROCEDURE Cu;
BEGIN
 IF N_Cu<=0.3 THEN
 BEGIN
  Cu_low:=TRUE;
 END;
END;

PROCEDURE Low_H;
BEGIN
 IF N_H<=0.001 THEN H_High:=FALSE;
END;

PROCEDURE RUNGE_KUTTA;
BEGIN
 INITIAL_VALUE;
 CLRSCR;
 WRITELN('  Cu2+   ,  H+     ,  Ni2+   , Fe    ');
 REPEAT
  Cu;
  Low_H;
  RATE_Ni;
  RUNGE_Cu;
  RUNGE_H;
  RUNGE_Nim;
  RUNGE_Ni3S2;
  RUNGE_Ni7S6;
  RUNGE_NiS;
  RUNGE_Ni3S4;
  RUNGE_Cu2S;
  RUNGE_Cu31S16;
  RUNGE_Cu18S;
  RUNGE_CuS;
  RUNGE_Fe3;
  RUNGE_Fe2;
  N_Ni:=N0_Ni;
  N_Cu:=N0_Cu;
  N_H:=N0_H;
  N_Nim:=N0_Nim;
  N_Ni3S2:=N0_Ni3S2;
  N_Ni7S6:=N0_Ni7S6;
  N_NiS:=N0_NiS;
```

```
  N_Ni3S4:=N0_Ni3S4;
  N_Cu2S:=N0_Cu2S;
  N_Cu31S16:=N0_Cu31S16;
  N_Cu18S:=N0_Cu18S;
  N_CuS:=N0_CuS;
  N_Fe3:=N0_Fe3;
  N_Fe2:=N0_Fe2;
  N_Fe:=N0_Fe3+N0_Fe2;
  IF ((Time=10) OR (Time=30) OR (Time=70) OR (Time=110)) THEN
    WRITE_DATA;
  IF ((Time=150) OR (Time=190) OR (Time=230) OR (Time=290)) THEN
    WRITE_DATA;
  Time:=Time+h_step;
 Until (Time>T);
END;

PROCEDURE GRAPH_RUNGE_Soln;
BEGIN
 Cu;
 Low_H;
 RATE_Ni;
 RUNGE_Cu;
 RUNGE_H;
 RUNGE_Nim;
 RUNGE_Ni3S2;
 RUNGE_Ni7S6;
 RUNGE_NiS;
 RUNGE_Ni3S4;
 RUNGE_Cu2S;
 RUNGE_Cu31S16;
 RUNGE_Cu18S;
 RUNGE_CuS;
 RUNGE_Fe3;
 RUNGE_Fe2;
 N_Ni:=N0_Ni;
 N_Cu:=N0_Cu;
 N_H:=N0_H;
 N_Nim:=N0_Nim;
 N_Ni3S2:=N0_Ni3S2;
 N_Ni7S6:=N0_Ni7S6;
 N_NiS:=N0_NiS;
 N_Ni3S4:=N0_Ni3S4;
```

```
  N_Cu2S:=N0_Cu2S;
  N_Cu31S16:=N0_Cu31S16;
  N_Cu18S:=N0_Cu18S;
  N_CuS:=N0_CuS;
  N_Fe3:=N0_Fe3;
  N_Fe2:=N0_Fe2;
  N_Fe:=N0_Fe3+N0_Fe2;
END;

PROCEDURE GRAPH_RUNGE_Solid;
BEGIN
  Cu;
  Low_H;
  RATE_Ni;
  RUNGE_Cu;
  RUNGE_H;
  RUNGE_Nim;
  RUNGE_Ni3S2;
  RUNGE_Ni7S6;
  RUNGE_NiS;
  RUNGE_Ni3S4;
  RUNGE_Cu2S;
  RUNGE_Cu31S16;
  RUNGE_Cu18S;
  RUNGE_CuS;
  RUNGE_Fe3;
  RUNGE_Fe2;
  N_Ni:=N0_Ni;
  N_Cu:=N0_Cu;
  N_H:=N0_H;
  N_Nim:=N0_Nim;
  N_Ni3S2:=N0_Ni3S2;
  N_Ni7S6:=N0_Ni7S6;
  N_NiS:=N0_NiS;
  N_Ni3S4:=N0_Ni3S4;
  N_Cu2S:=N0_Cu2S;
  N_Cu31S16:=N0_Cu31S16;
  N_Cu18S:=N0_Cu18S;
  N_CuS:=N0_CuS;
  N_Fe3:=N0_Fe3;
  N_Fe2:=N0_Fe2;
  N_Cu_s:=N_Cu2S*2+N_Cu31S16*31+N_Cu18S*1.8+N_CuS;
```

```
 N_Ni_s:=N_Nim+N_Ni3S2*3+N_Ni7S6*7+N_NiS+N_Ni3S4*3;
 N_S_s:=N_Ni3S2*2+N_Ni7S6*6+N_NiS+N_Ni3S4*4+N_Cu2S+N_Cu31S16*16+N_Cu18S+N_CuS;
END;

END.
```

```
UNIT GRAPHICS;

INTERFACE

USES CRT,VARIABLE,CALCULATIONS;

PROCEDURE Soln_Solid_GRAPH;

IMPLEMENTATION

USES GRAPH;

TYPE DATA=ARRAY[1..30] OF REAL;
    REC=RECORD
      PTS:INTEGER;
      DATA_X:DATA;
      DATA_Y:DATA;
      DATA_Y1:DATA;
      DATA_Y2:DATA;
      DATA_Y3:DATA;
      DATA_Y4:DATA;
      DATA_Y5:DATA;
      DATA_Y6:DATA;
      DATA_Y7:DATA;
      DATA_Y8:DATA;
      DATA_Y9:DATA;
    END;
    DATAFILE=FILE OF REC;

 VAR DATA_R:REC;
    DATA_F:DATAFILE;
    NUMBER,X,Y,Y1,Y2,Y3,Y4,Y5,Y6,Y7,Y8,Y9,X_1,Y_1,Y1_1,Y2_1,Y3_1,Y4_1,Y5_1,Y6_1,Y7_1,
    Y8_1,Y9_1:INTEGER;
    Xscale,Yscale,Xconst,Yconst:REAL;
```

```
   Ymax,Xmax:WORD;

PROCEDURE GRAPH_INITIAL;
VAR grDriver,grMode:INTEGER;
   Xmid,Ymid:WORD;
   S:STRING[4];
BEGIN
  ClrScr;
  grDriver:=Detect;
  Initgraph(grDriver,grMode,'BGI');
  Xmax:=GetMaxX;
  Xmid:=(Round(Xmax*(1-20/640)) div 2);
  Ymax:=GetMaxY;
  Ymid:=(Ymax div 2);
  SetColor(white);
  SetLineStyle(0,0,1);
  Line(Round(70/640*Xmax),Round(Ymax*(1-40/480)),Round(Xmax*(1-70/640)),
       Round(Ymax*(1-40/480)));
  Line(Round(70/640*Xmax),Round(Ymax*(1-40/480)),Round(70/640*Xmax),Round(80/480*Ymax));
  Line(Round(Xmax*(1-70/640)),Round(Ymax*(1-40/480)),Round(Xmax*(1-70/640)),
       Round(80/480*Ymax));
  OutTextXY(Round(70/640*Xmax),Round(Ymax*(1-35/480)),'0');
  Str(T:4:0,S);
  OutTextXY(Round(Xmax*(1-100/640)),Round(Ymax*(1-35/480)),S);
  OutTextXY(Xmid,Round(Ymax*(1-32/480)),'Time [min]');
  IF GRAPH_option THEN
  BEGIN
   IF CHOICE THEN
   BEGIN
    OutTextXY(Round(20/640*Xmax),Ymid-5,'Ni,H+');
    OutTextXY(Round(20/640*Xmax),Ymid+5,'[mol]');
    OutTextXY(Round(40/640*Xmax),Round(Ymax*(1-40/480)),'0');
    OutTextXY(Round(30/640*Xmax),Round(80/480*Ymax),'80.0');
    OutTextXY(Round((1-68/640)*Xmax),Ymid-5,'Cu,Fe');
    OutTextXY(Round((1-68/640)*Xmax),Ymid+5,'[mol]');
    OutTextXY(Round((1-65/640)*Xmax),Round(Ymax*(1-40/480)),'0');
    OutTextXY(Round((1-68/640)*Xmax),Round(80/480*Ymax),'20.0');
   END
   ELSE
   BEGIN
    OutTextXY(Round(20/640*Xmax),Ymid-5,'Ni');
    OutTextXY(Round(20/640*Xmax),Ymid+5,'[mol]');
```

```
    OutTextXY(Round(40/640*Xmax),Round(Ymax*(1-40/480)),'0');
    OutTextXY(Round(30/640*Xmax),Round(80/480*Ymax),'60.0');
    OutTextXY(Round((1-68/640)*Xmax),Ymid-5,'Cu,S');
    OutTextXY(Round((1-68/640)*Xmax),Ymid+5,'[mol]');
    OutTextXY(Round((1-65/640)*Xmax),Round(Ymax*(1-40/480)),'10.0');
    OutTextXY(Round((1-68/640)*Xmax),Round(80/480*Ymax),'60.0');
  END;
 END
 ELSE
 BEGIN
  OutTextXY(Round(20/640*Xmax),Ymid-5,'Ni-S');
  OutTextXY(Round(20/640*Xmax),Ymid+5,'Cu-S');
  OutTextXY(Round(20/640*Xmax),Ymid+15,'[mol]');
  OutTextXY(Round(40/640*Xmax),Round(Ymax*(1-40/480)),'0');
  OutTextXY(Round(30/640*Xmax),Round(80/480*Ymax),'25.0');
  OutTextXY(Round((1-68/640)*Xmax),Ymid-5,'Ni7S6');
  OutTextXY(Round((1-68/640)*Xmax),Ymid+5,'Cu31S16');
  OutTextXY(Round((1-68/640)*Xmax),Ymid+15,'[mol]');
  OutTextXY(Round((1-65/640)*Xmax),Round(Ymax*(1-40/480)),'0');
  OutTextXY(Round((1-68/640)*Xmax),Round(80/480*Ymax),'0.5');
 END;
 Xscale:=Xmax*(1-140/640);
 Xconst:=70/640*Xmax;
 Yscale:=Ymax*(1-120/480);
 Yconst:=40/480*Ymax;
END;

PROCEDURE GRAPH_HEADING1;
BEGIN
  SetColor(white);
{  SetTextStyle(1,0,3);
  IF CHOICE THEN OutTextXY(Round(230/640*Xmax),Round(15/480*Ymax),'SOLUTION')
  ELSE OutTextXY(Round(230/640*Xmax),Round(15/480*Ymax),'SOLIDS');
 } SetLineStyle(0,0,2);
  Rectangle(Round(Xmax*(1-460/640)),Round(75/480*Ymax),Round(Xmax*(1-
350/640)),Round(145/480*Ymax));
  SetTextStyle(0,0,0);
  SetLineStyle(0,0,1);
  SetColor(white);
  IF CHOICE THEN OutTextXY(Round(Xmax*(1-455/640)),Round(85/480*Ymax),'* Ni      Y1')
  ELSE OutTextXY(Round(Xmax*(1-455/640)),Round(85/480*Ymax),'* Ni      Y1');
  IF CHOICE THEN OutTextXY(Round(Xmax*(1-455/640)),Round(101/480*Ymax),'þ Cu      Y2')
```

```
 ELSE OutTextXY(Round(Xmax*(1-455/640)),Round(101/480*Ymax),'þ Cu      Y2');
 IF CHOICE THEN OutTextXY(Round(Xmax*(1-455/640)),Round(117/480*Ymax),'- H+      Y1')
 ELSE OutTextXY(Round(Xmax*(1-455/640)),Round(117/480*Ymax),'- S      Y2');
 IF CHOICE THEN OutTextXY(Round(Xmax*(1-455/640)),Round(133/480*Ymax),'+ Fe+2/3  Y2')
END;

PROCEDURE GRAPH_HEADING2;
BEGIN
 SetColor(white);
{ SetTextStyle(1,0,3);
 OutTextXY(Round(230/640*Xmax),Round(15/480*Ymax),'MINERAL COMPOSITION');
 } SetLineStyle(0,0,2);
 Rectangle(Round(Xmax*(1-450/640)),Round(75/480*Ymax),Round(Xmax*(1-
350/640)),Round(160/480*Ymax));
 SetTextStyle(0,0,0);
 If Choice_Ni_Cu then
 Begin
  OutTextXY(Round(Xmax*(1-445/640)),Round(85/480*Ymax),'* Ni     Y1');
  OutTextXY(Round(Xmax*(1-445/640)),Round(101/480*Ymax),'þ Ni3S2  Y1');
  OutTextXY(Round(Xmax*(1-445/640)),Round(117/480*Ymax),'ñ Ni7S6  Y2');
  OutTextXY(Round(Xmax*(1-445/640)),Round(133/480*Ymax),'- NiS    Y1');
  OutTextXY(Round(Xmax*(1-445/640)),Round(149/480*Ymax),'# Ni3S4  Y1');
 End
 Else
 Begin
  OutTextXY(Round(Xmax*(1-445/640)),Round(85/480*Ymax),'+ Cu2S    Y1');
  OutTextXY(Round(Xmax*(1-445/640)),Round(101/480*Ymax),'x Cu31S16 Y2');
  OutTextXY(Round(Xmax*(1-445/640)),Round(117/480*Ymax),'o Cu1.8S  Y1');
  OutTextXY(Round(Xmax*(1-445/640)),Round(133/480*Ymax),'□ CuS     Y1');
 End;
END;

PROCEDURE GRAPH_DRAW1;
BEGIN
 SetLineStyle(0,0,1);
 SetColor(white);
 Line(X_1,Y_1,X,Y);
 Line(X_1,Y1_1,X,Y1);
 Line(X_1,Y2_1,X,Y2);
 IF (CHOICE) THEN
 BEGIN
  Line(X_1,Y3_1,X,Y3);
```

```
{   Line(X_1,Y4_1,X,Y4);
 } END;
END;

PROCEDURE GRAPH_DRAW2;
BEGIN
 SetLineStyle(0,0,1);
 If Choice_Ni_Cu then
 Begin
   SetColor(white);
   Line(X_1,Y_1,X,Y);
   Line(X_1,Y1_1,X,Y1);
   Line(X_1,Y2_1,X,Y2);
   Line(X_1,Y3_1,X,Y3);
   Line(X_1,Y4_1,X,Y4);
 End
 Else
 Begin
   SetColor(white);
   Line(X_1,Y5_1,X,Y5);
   Line(X_1,Y6_1,X,Y6);
   Line(X_1,Y7_1,X,Y7);
   Line(X_1,Y8_1,X,Y8);
 End;
END;

PROCEDURE EQUATION1;
BEGIN
  Y:=ROUND(Ymax-(N_Ni-0)/(80-0)*Yscale-Yconst);
  Y1:=ROUND(Ymax-(N_Cu-0)/(20-0)*Yscale-Yconst);
  Y2:=ROUND(Ymax-(N_H-0)/(80-0)*Yscale-Yconst);
  Y3:=ROUND(Ymax-(N_Fe-0)/(20-0)*Yscale-Yconst);
  Y4:=ROUND(Ymax-(N_Fe2-0)/(20-0)*Yscale-Yconst);
END;

PROCEDURE EQUATION2;
BEGIN
  Y:=ROUND(Ymax-(N_Ni_s-0)/(60-0)*Yscale-Yconst);
  Y1:=ROUND(Ymax-(N_Cu_s-10)/(60-10)*Yscale-Yconst);
  Y2:=ROUND(Ymax-(N_S_s-10)/(60-10)*Yscale-Yconst);
END;
```

```
PROCEDURE EQUATION3;
BEGIN
 Y:=ROUND(Ymax-(N_Nim-0)/(25-0)*Yscale-Yconst);
 Y1:=ROUND(Ymax-(N_Ni3S2-0)/(25-0)*Yscale-Yconst);
 Y2:=ROUND(Ymax-(N_Ni7S6-0)/(0.5-0)*Yscale-Yconst);
 Y3:=ROUND(Ymax-(N_NiS-0)/(25-0)*Yscale-Yconst);
 Y4:=ROUND(Ymax-(N_Ni3S4-0)/(25-0)*Yscale-Yconst);
 Y5:=ROUND(Ymax-(N_Cu2S-0)/(25-0)*Yscale-Yconst);
 Y6:=ROUND(Ymax-(N_Cu31S16-0)/(0.5-0)*Yscale-Yconst);
 Y7:=ROUND(Ymax-(N_Cu18S-0)/(25-0)*Yscale-Yconst);
 Y8:=ROUND(Ymax-(N_CuS-0)/(25-0)*Yscale-Yconst);
END;

PROCEDURE GRAPH_CALC1;
BEGIN
 INITIAL_VALUE;
 Y_1:=ROUND(Ymax-(N_Ni-0)/(80.0-0)*Yscale-Yconst);
 Y1_1:=ROUND(Ymax-(N_Cu-0)/(20.0-0)*Yscale-Yconst);
 Y2_1:=ROUND(Ymax-(N_H-0)/(80.0-0)*Yscale-Yconst);
 Y3_1:=ROUND(Ymax-(N_Fe-0)/(20.0-0)*Yscale-Yconst);
 Y4_1:=ROUND(Ymax-(N_Fe2-0)/(20.0-0)*Yscale-Yconst);
 X_1:=Round(Xconst);
 Time:=h_step;
 REPEAT
  GRAPH_RUNGE_Soln;
  EQUATION1;
  X:=ROUND(Time/T*Xscale+Xconst);
  GRAPH_DRAW1;
  Time:=Time+h_step;
  X_1:=X;
  Y_1:=Y;
  Y1_1:=Y1;
  Y2_1:=Y2;
  Y3_1:=Y3;
  Y4_1:=Y4;
 UNTIL (Time>T);
END;
```

```
PROCEDURE GRAPH_CALC2;
BEGIN
 INITIAL_VALUE;
 Y_1:=ROUND(Ymax-(N_Ni_s-0)/(60-0)*Yscale-Yconst);
 Y1_1:=ROUND(Ymax-(N_Cu_s-10)/(60-10)*Yscale-Yconst);
 Y2_1:=ROUND(Ymax-(N_S_s-10)/(60-10)*Yscale-Yconst);
 X_1:=Round(Xconst);
 Time:=h_step;
 REPEAT
  GRAPH_RUNGE_Solid;
  EQUATION2;
  X:=ROUND(Time/T*Xscale+Xconst);
  GRAPH_DRAW1;
  Time:=Time+h_step;
  X_1:=X;
  Y_1:=Y;
  Y1_1:=Y1;
  Y2_1:=Y2;
 UNTIL (Time>T);
END;

PROCEDURE GRAPH_CALC3;
BEGIN
 INITIAL_VALUE;
 Y_1:=ROUND(Ymax-(N_Nim-0)/(25-0)*Yscale-Yconst);
 Y1_1:=ROUND(Ymax-(N_Ni3S2-0)/(25-0)*Yscale-Yconst);
 Y2_1:=ROUND(Ymax-(N_Ni7S6-0)/(0.5-0)*Yscale-Yconst);
 Y3_1:=ROUND(Ymax-(N_NiS-0)/(25-0)*Yscale-Yconst);
 Y4_1:=ROUND(Ymax-(N_Ni3S4-0)/(25-0)*Yscale-Yconst);
 Y5_1:=ROUND(Ymax-(N_Cu2S-0)/(25-0)*Yscale-Yconst);
 Y6_1:=ROUND(Ymax-(N_Cu31S16-0)/(0.5-0)*Yscale-Yconst);
 Y7_1:=ROUND(Ymax-(N_Cu18S-0)/(25-0)*Yscale-Yconst);
 Y8_1:=ROUND(Ymax-(N_CuS-0)/(25-0)*Yscale-Yconst);
 X_1:=Round(Xconst);
 Time:=h_step;
 REPEAT
  GRAPH_RUNGE_Soln;
  EQUATION3;
  X:=ROUND(Time/T*Xscale+Xconst);
  GRAPH_DRAW2;
  Time:=Time+h_step;
  X_1:=X;
```

```
  Y_1:=Y;
  Y1_1:=Y1;
  Y2_1:=Y2;
  Y3_1:=Y3;
  Y4_1:=Y4;
  Y5_1:=Y5;
  Y6_1:=Y6;
  Y7_1:=Y7;
  Y8_1:=Y8;
 UNTIL (Time>T);
END;

PROCEDURE PLOT_DATA;
BEGIN
 IF GRAPH_option THEN
 BEGIN
  IF CHOICE THEN ASSIGN(DATA_F,NAME_SOLN)
  ELSE ASSIGN(DATA_F,NAME_SOLID);
 END
 ELSE ASSIGN(DATA_F,NAME_MIN);
 RESET(DATA_F);
 READ(DATA_F,DATA_R);
 IF GRAPH_option THEN
 BEGIN
  WITH DATA_R DO
  BEGIN
   IF CHOICE THEN
   BEGIN
    FOR NUMBER:=1 TO PTS DO
    BEGIN
     SetColor(white);
     OutTextXY(ROUND(DATA_X[NUMBER]/T*Xscale+Xconst-3),
               ROUND(Ymax-(DATA_Y[NUMBER]-0)/(80-0)*Yscale-Yconst-3),'*');
     OutTextXY(ROUND(DATA_X[NUMBER]/T*Xscale+Xconst-3),
               ROUND(Ymax-(DATA_Y1[NUMBER]-0)/(20-0)*Yscale-Yconst-3),'þ');
     OutTextXY(ROUND(DATA_X[NUMBER]/T*Xscale+Xconst-3),
               ROUND(Ymax-(DATA_Y2[NUMBER]-0)/(80-0)*Yscale-Yconst-3),'-');
     OutTextXY(ROUND(DATA_X[NUMBER]/T*Xscale+Xconst-3),
               ROUND(Ymax-(DATA_Y3[NUMBER]-0)/(20-0)*Yscale-Yconst-3),'+');
    END;
   END
   ELSE
```

```
  BEGIN
   FOR NUMBER:=1 TO PTS DO
   BEGIN
    SetColor(white);
    OutTextXY(ROUND(DATA_X[NUMBER]/T*Xscale+Xconst-3),
              ROUND(Ymax-(DATA_Y[NUMBER]-0)/(60-0)*Yscale-Yconst-3),'*');
    OutTextXY(ROUND(DATA_X[NUMBER]/T*Xscale+Xconst-3),
              ROUND(Ymax-(DATA_Y1[NUMBER]-10)/(60-10)*Yscale-Yconst-3),'þ');
    OutTextXY(ROUND(DATA_X[NUMBER]/T*Xscale+Xconst-3),
              ROUND(Ymax-(DATA_Y2[NUMBER]-10)/(60-10)*Yscale-Yconst-3),'-');
   END;
  END;
 END;
END
ELSE
BEGIN
 WITH DATA_R DO
 BEGIN
  FOR NUMBER:=1 TO PTS DO
  BEGIN
   If Choice_Ni_Cu then
   Begin
    SetColor(white);
    OutTextXY(ROUND(DATA_X[NUMBER]/T*Xscale+Xconst-3),
              ROUND(Ymax-(DATA_Y[NUMBER]-0)/(25-0)*Yscale-Yconst-3),'*');
    OutTextXY(ROUND(DATA_X[NUMBER]/T*Xscale+Xconst-3),
              ROUND(Ymax-(DATA_Y1[NUMBER]-0)/(25-0)*Yscale-Yconst-3),'þ');
    OutTextXY(ROUND(DATA_X[NUMBER]/T*Xscale+Xconst-3),
              ROUND(Ymax-(DATA_Y2[NUMBER]-0)/(0.5-0)*Yscale-Yconst-3),'ñ');
    OutTextXY(ROUND(DATA_X[NUMBER]/T*Xscale+Xconst-3),
              ROUND(Ymax-(DATA_Y3[NUMBER]-0)/(25-0)*Yscale-Yconst-3),'-');
    OutTextXY(ROUND(DATA_X[NUMBER]/T*Xscale+Xconst-3),
              ROUND(Ymax-(DATA_Y4[NUMBER]-0)/(25-0)*Yscale-Yconst-3),'#');
   End
   Else
   Begin
    SetColor(white);
    OutTextXY(ROUND(DATA_X[NUMBER]/T*Xscale+Xconst-3),
              ROUND(Ymax-(DATA_Y5[NUMBER]-0)/(25-0)*Yscale-Yconst-3),'+');
    OutTextXY(ROUND(DATA_X[NUMBER]/T*Xscale+Xconst-3),
              ROUND(Ymax-(DATA_Y6[NUMBER]-0)/(0.5-0)*Yscale-Yconst-3),'x');
    OutTextXY(ROUND(DATA_X[NUMBER]/T*Xscale+Xconst-3),
```

```
                ROUND(Ymax-(DATA_Y7[NUMBER]-0)/(25-0)*Yscale-Yconst-3),'o');
      OutTextXY(ROUND(DATA_X[NUMBER]/T*Xscale+Xconst-3),
                ROUND(Ymax-(DATA_Y8[NUMBER]-0)/(25-0)*Yscale-Yconst-3),'□');
     End;
    END;
  END;
 END;
 CLOSE(DATA_F);
END;

PROCEDURE Soln_Solid_GRAPH;
BEGIN
 GRAPH_INITIAL;
 SetBkColor(black);
 IF GRAPH_option THEN
 BEGIN
  GRAPH_HEADING1;
  PLOT_DATA;
  IF CHOICE THEN GRAPH_CALC1
  ELSE GRAPH_CALC2;
 END
 ELSE
 BEGIN
  GRAPH_HEADING2;
  PLOT_DATA;
  GRAPH_CALC3;
 END;
{ SetColor(white);
 SetTextStyle(0,0,0);
 OutTextXY(Round(30/640*Xmax),Round(Ymax*(1-12/480)),'Press <ENTER> to continue ...');
} READLN;
 CloseGraph;
END;

END.
```

```
UNIT EXP_DATA_INPUT;

INTERFACE
```

```
USES CRT,StrngTTT;

PROCEDURE CREATE_DATA_FILE;

IMPLEMENTATION

TYPE DATA=ARRAY[1..30] OF REAL;

   REC=RECORD
   POINTS:INTEGER;
    DATA_X:DATA;
    DATA_Y:DATA;
    DATA_Y1:DATA;
    DATA_Y2:DATA;
    DATA_Y3:DATA;
    DATA_Y4:DATA;
    DATA_Y5:DATA;
    DATA_Y6:DATA;
    DATA_Y7:DATA;
    DATA_Y8:DATA;
    DATA_Y9:DATA;
   END;

   DATAFILE=FILE OF REC;

VAR DATA_R:REC;
   DATA_F:DATAFILE;
   FILENAME:STRING[12];
   NUMBER,Y_VALUE:INTEGER;

PROCEDURE Y_VALUES;
VAR D:CHAR;
   A:INTEGER;
BEGIN
  WRITELN('Enter the number of Y-series (1 - 10) [10=0]: ');
  WRITELN;
  REPEAT
    D:=READKEY;
  UNTIL D IN ['1','2','3','4','5','6','7','8','9','0'];
  CASE D OF
  '1':Y_VALUE:=1;
  '2':Y_VALUE:=2;
```

```
 '3':Y_VALUE:=3;
 '4':Y_VALUE:=4;
 '5':Y_VALUE:=5;
 '6':Y_VALUE:=6;
 '7':Y_VALUE:=7;
 '8':Y_VALUE:=8;
 '9':Y_VALUE:=9;
 '0':Y_VALUE:=10;
 END;
END;

PROCEDURE READ_DATA;
BEGIN
 WITH DATA_R DO
 BEGIN
  WRITE('Enter number of data points: ');
  READLN(POINTS);
  WRITELN;
  WRITELN;
  FOR NUMBER:=1 TO POINTS DO
  BEGIN
   WRITELN('Data points ',NUMBER:2,':');
   WRITELN('----------');
   WRITE('Time : ');
   READLN(DATA_X[NUMBER]);
   WRITE('    Y value [mol] : ');
   READLN(DATA_Y[NUMBER]);
   IF Y_VALUE>1 THEN
   BEGIN
    WRITE('    Y1 value [mol] : ');
    READLN(DATA_Y1[NUMBER]);
   END;
   IF Y_VALUE>2 THEN
   BEGIN
    WRITE('    Y2 value [mol] : ');
    READLN(DATA_Y2[NUMBER]);
   END;
   IF Y_VALUE>3 THEN
   BEGIN
    WRITE('    Y3 value [mol] : ');
    READLN(DATA_Y3[NUMBER]);
   END;
```

```
    IF Y_VALUE>4 THEN
    BEGIN
     WRITE('    Y4 value [mol] : ');
     READLN(DATA_Y4[NUMBER]);
    END;
    IF Y_VALUE>5 THEN
    BEGIN
     WRITE('    Y5 value [mol] : ');
     READLN(DATA_Y5[NUMBER]);
    END;
    IF Y_VALUE>6 THEN
    BEGIN
     WRITE('    Y6 value [mol] : ');
     READLN(DATA_Y6[NUMBER]);
    END;
    IF Y_VALUE>7 THEN
    BEGIN
     WRITE('    Y7 value [mol] : ');
     READLN(DATA_Y7[NUMBER]);
    END;
    IF Y_VALUE>8 THEN
    BEGIN
     WRITE('    Y8 value [mol] : ');
     READLN(DATA_Y8[NUMBER]);
    END;
    IF Y_VALUE>9 THEN
    BEGIN
     WRITE('    Y9 value [mol] : ');
     READLN(DATA_Y9[NUMBER]);
    END;
    WRITELN;
   END;
  END;
  WRITE(DATA_F,DATA_R);
END;

PROCEDURE CREATE_DATA_FILE;
VAR ANSWER:CHAR;
BEGIN
  CLRSCR;
  WRITELN;
  WRITELN('          The following options are available :');
```

```
WRITELN('          ------------------------------------');
WRITELN;
WRITELN('          Do you want to <C>reate a data file ?');
WRITELN('          <D>isplay data file ?');
WRITELN('          <E>xit !');
WRITELN;
WRITELN('          Use the option in <brackets>');
REPEAT
 ANSWER:=UPCASE(READKEY);
UNTIL ANSWER IN ['C','D','E'];
CASE ANSWER OF
'C':
BEGIN
 WRITELN;
 Y_VALUES;
 WRITE('Enter the name of the file to create (example - file****.dat) : ');
 READLN(FILENAME);
 ASSIGN(DATA_F,{'SOLN.DAT'}FILENAME);
 REWRITE(DATA_F);
 READ_DATA;
 CLOSE(DATA_F);
 CREATE_DATA_FILE;
END;
'D':
BEGIN
 writeln;
 WRITE('   Enter the name of the file to show (example - file****.dat) : ');
 READLN(FILENAME);
 ASSIGN(DATA_F,{'SOLN.DAT'}FILENAME);
 RESET(DATA_F);
 READ(DATA_F,DATA_R);
 WITH DATA_R DO
 BEGIN
  FOR NUMBER:=1 TO POINTS DO
  BEGIN
   WRITE(DATA_X[NUMBER]:3:0,' ',DATA_Y[NUMBER]:2:3,' ',DATA_Y1[NUMBER]:2:3,'
',DATA_Y2[NUMBER]:2:3,' ');
   WRITE(DATA_Y3[NUMBER]:2:3,' ',DATA_Y4[NUMBER]:2:3,' ',DATA_Y5[NUMBER]:2:3,'
',DATA_Y6[NUMBER]:2:3);
   WRITELN(DATA_Y7[NUMBER]:2:3,' ',DATA_Y8[NUMBER]:2:3,' ',DATA_Y9[NUMBER]:2:3);
  END;
 END;
```

```
    CLOSE(DATA_F);
    readln;
    CREATE_DATA_FILE;
  END;
  'E':EXIT;
  END;
END;

END.
```

```
UNIT VARIABLE;

INTERFACE

VAR N_Ni,N_Cu,N_H,N_Nim,N_Ni3S2,N_Ni7S6,N_NiS,N_Ni3S4,N_Cu2S,N_Cu31S16,N_Cu18S,
      N_CuS,N_Fe3,N_Fe2,N_Fe:REAL;
    N_Ni_s,N_Cu_s,N_S_s:REAL;
    k1,k2,k3,k4,k5a,k5b,k6,k7,k8a,k8b,k9,k10,k11,k12a,k12b,k13a,k13b,k13c,k14,k15,pO2,h_step,
    T,Time:REAL;
    GRAPH_option,CHOICE,Choice_Ni_Cu,REP:BOOLEAN;
    NAME_SOLN,NAME_SOLID,NAME_MIN:STRING[12];
    W0,V,Tp,N_H_0,Acid,flow_O2,Ave_P:REAL;

IMPLEMENTATION

END.
```

END END END END END END END END

Appendix H

PAPERS BASED ON THIS DISSERTATION

Rademan, J.A.M., Lorenzen, L. and Van Deventer, J.S.J., 1995, An off-line computer simulation for controlling the repulp section in a plant, Minerals Engineering, 8(6), 679-696.

Rademan, J.A.M., Moolman, D.W., Lorenzen, L., Van Deventer, J.S.J. and Aldrich, C., 1995, Neural net based knowledge extraction from historical data of an industrial leaching plant, *Hydrometallurgy*, (provisionally accepted for publication).

Rademan, J.A.M., Moolman, D.W., Lorenzen, L., Van Deventer, J.S.J. and Aldrich, C., Analysing an ill-defined leaching process with ANN's and Decision trees, *Journal of Systems Engineering*, (submitted for publication).

Rademan, J.A.M., Moolman, D.W., Lorenzen, L., Van Deventer, J.S.J. and Aldrich, C., 1995, A methodology for modelling and analysing an ill-defined leaching process from historical data, Engineering Applications of Artificial Neural Networks, Eds. Bulsari, A.B. and Kallio, S., *Proceedings of the International Conference EANN '95*, Helsinki, Finland, 21-23 August 1995, 209 -212.